UNIVERSITY OF SOUTHAMPTON

HIGH-RESOLUTION ENVIRONMENTAL CHANGE IN THE LATE JURASSIC KIMMERIDGE CLAY FORMATION

By

Sarah Jane Pearson

This thesis was submitted in partial fulfillment of the requirements for the degree of Doctor of Philosophy. It does not necessarily represent the final form of the thesis deposited in the University after examination.

School of Ocean and Earth Science

June 2000

UNIVERSITY OF SOUTHAMPTON

ABSTRACT

FACULTY OF SCIENCE

SCHOOL OF OCEAN AND EARTH SCIENCE

Doctor of Philosophy

HIGH-RESOLUTION ENVIRONMENTAL CHANGE IN THE LATE JURASSIC KIMMERIDGE CLAY FORMATION

By Sarah Jane Pearson

Several discrete intervals of the Late Jurassic Kimmeridge Clay Formation were analyzed to assess the high-resolution environmental change, which occurs within laminated lithologies. The material was from new boreholes drilled in Dorset, southern England, for the Rapid Global Geological Events (RGGE) project. Complementary techniques of back scattered electron microscopy, palynology, total organic carbon and atomic H/C ratios were used to determine the fabric structure and composition and the character of the organic matter component. The sampling resolution was higher than for previous studies, based on two scales, a lower resolution 5cm point sample scale and a high-resolution lamina scale.

Modern day water column, benthic and sedimentary processes were applied to explain fabric composition and structure. This shows the KCF to have been a complex marine system. All lithologies were dominated by three major components of organic matter, carbonate and clays/silts, the flux of which was a primary control on both the lithology and microfabric, together with water column oxygenation levels and terrestrial input. Sedimentation rates, based on a yearly assumption for organic-rich and coccolith-rich laminae couplets, ranged from 4.5cm per 1000 years for the oil shales to 30-118cm per 1000 years for the coccolith limestone.

TOC % ranged from 3-51%, while an average atomic H/C ratio of 1.5 indicated type I to type II kerogens. Optical microscopy found the organic matter to be dominated by amorphous forms (AOM). Palynological analysis of structured organic particles revealed a close correlation between the marine and terrestrial environments and significant variability between lithologies. Oil shales were charcterized by very low particle abundances, while coccolith-rich lithologies showed high frequency and high-amplitude pulses of organic particles. These pulses are interpreted as the result of storms causing re-suspension and transportation of organic material, clays and nutrients from the proximal shelf into the distal basin. These storm events occur at the beginning and end of the coccolith limestones and thus, are suggested to have been linked to the initiation and cessation of coccolith limestone deposition. An intensification of the palaeo-Atlantic storm track due to an increase in climate humidity and instability is postulated to have resulted in these high frequency and high intensity storms. The frequency of these storm episodes was calculated to represent periods of 60 to 100 years, and possibly up to 200-400 years.

Environmental and climatic reconstructions were made for the intervals by combining the fabric, geochemical and palynological results and interpretations. High-resolution change below the Milankovitch frequency was found to be present within the intervals on a number of scales. These changes ranged from yearly 'varve couplet' alternations of organic-rich and coccolith-rich fabric, to 60-100 year and perhaps 200-400 year storm events and larger scale events of the order of several 1000 years. The later represent changes in climatic humidity over the limestone lithologies.

For

My grandfathers Vernon Hinkley and Peter Pearson
My Love Always

The modern Jurassic,
North Island, New Zealand

CONTENTS

LIST OF TABLES

LIST OF FIGURES

LIST OF ELEMENTAL MAPS

ACKNOWLEDGEMENTS

This research was supported by the Natural Environmental Research Council (NERC), which is gratefully acknowledged.

I would firstly like to thank my supervisors John Marshall and Alan Kemp for their supervision, support and guidance throughout. My thanks also go to Ramues Gallois for imparting his knowledge and fascination of the Kimmeridge Clay during the many cold months we spent on site, and to the Soil Mechanics team for their drilling expertise. Thanks are also extended to the many other colleagues and friends within the Rapid Global Geological Events (RGGE) project, for the numerous discussions, support and encouragement they have provided. Within the Southampton Oceanography Centre, I would also like to thank Andy Roberts from my advisory panel, Richard Pearce for his patient guidance on the scanning electron microscope and Ian West for his discussions and broadening of my knowledge of the Jurassic Southern England.

I am grateful to the following people for providing invaluable technical assistance and support:- Bob Jones, John Ford, Shir Akbari, Barbara Cressey, Barry Marsh, Kate Davis, and last but by no means least, Ross Williams, without whom the core would not have been available.

This project has also benefited from discussion with Richard Pearce, Jenny Pike and Carl Jenkins. In particular, I would like to thank Jean Dean for all her helpful discussions and support throughout this project.

These acknowledgements would not be complete without thanking all my friends who have made the last three and a half years so enjoyable; Mia, Darryl, Ruth, Duncan, Jon, Barbs, Tim, Ang, Mark, Tracy, Steve, Rachel, Dave, Richard, Ivailo and Jean. I would also like to thank Elco Rohling and his family for the pleasurable task of dog sitting!

Finally, I would like to thank my parents and sister for their unfailing faith in me and continual support, and to my fiancée Craig, without whom I could not have achieved this.

1.0 INTRODUCTION

The Kimmeridge Clay Formation (KCF) has been the focus of numerous scientific and commercial investigations due to its exceptional organic richness and highly varied lithological nature (Table 1.1). It is the richest oil-source rock in Europe, providing much of the North Sea oil (Barnard and Cooper, 1981), but has also provided an unrivalled insight into the palaeoenvironment and palaeoclimate of the Late Jurassic Period. However, despite this commercial and climatological importance, the intensive study of this Formation has resulted in more questions than answers. Considerable disagreement exists as to the mechanisms and processes that resulted in the KCF deposition and consequently the KCF is under continuing review.

This study forms part of an interdisciplinary research program, the Rapid Global Geological Events Project (RGGE) special topic "Anatomy of a Source Rock", which aims to address questions on both the environmental and climatological aspects of the KCF. The RGGE project is funded by the Natural Environmental Research Council (NERC) and a consortium of oil companies (Arco British, Conoco Norway, Enterprise, Fina, Phillips, Saga Petroleum, Shell, Statoil and Texaco). It involves eight British Universities (Southampton, Luton, Reading, Newcastle, Leeds, Open, University College London and Oxford), the British Museum and the British Geological Survey (BGS), which are coordinated by Oxford University. Within the RGGE project the KCF has been examined at a variety of scales, using a multidisciplinary approach, with the purpose of enhancing our present knowledge on the environmental and climatic processes that resulted in the KCF deposition. This in turn has enabled increased understanding of climate change mechanisms during the Jurassic Period and provided further insight into organic matter accumulation and preservation in ancient marine environments.

1.1 BACKGROUND

The KCF was deposited during the Late Jurassic Period, a time when continental positions, oceanography and climate were very different from today (Chapter 2). The KCF lithological variation has been shown to reflect climatic and environmental changes occurring on several scales (Oschmann, 1990; Wignall and Ruffell, 1990). Sedimentary cycles on a meter scale have been shown to correspond to Milankovitch orbital forcing rhythmicity in the obliquity and precessional bands (Waterhouse, 1992, 1995; Weedon *et al.*, 1999). However, discrete laminated intervals within these orbital forced sedimentary cycles also indicate environmental variability at a far higher resolution, and are the focus of this study. Thus, the KCF provides a valuable high-resolution record of the Earth's natural cycles during this period.

PREVIOUS STUDY TOPICS	REFERENCES
General geology and sequence stratigraphy	Arkell, 1933, 1947; Cope, 1978, 1980; Cox & Gallois, 1981; Wignall, 1991; Herbin *et al.*, 1995; Tyson, 1996; Macquaker *et al.*, 1998.
Milankovitch orbital forcing	Waterhouse, 1992, 1995, 1999; Weedon *et al.*, 1999.
Palaeoecology and biofacies	Aigner, 1980; Myers and Wignall, 1987; Oschmann, 1988a, 1993, 1994; Wignall, 1990.
Micropalaeontology and palynology	Gitmez and Sarjeant, 1972; Ioannides *et al.*, 1976; Riding and Thomas, 1988; Barron, 1989; Tyson, 1989; Hart and Fitzpatrick, 1995; Bailey, Milner and Varney, 1997.
Sedimentology, diagenesis and pyrite formation	Irwin, Curtis and Coleman, 1977; Irwin, 1979, 1980, 1981; Sladen and Batten, 1980; Scotchman, 1987, 1989; Shaw and Primmer, 1991; Macquaker and Gawthorpe, 1993; Baudin *et al.*, 1994; Desprairies *et al.*, 1995; Wilkin, Barnes and Brantley, 1996; Macquaker, Curtis and Coleman, 1997; Wignall and Newton, 1998.
Geochemistry	Farnimond *et al.*, 1984; Ebukanson and Kinghorn, 1985; Baird, 1986; Williams, 1986; Nøhr-Hansen, 1989; Scotchman, 1991; Tribovillard *et al.*, 1994; Saelen *et al.*, 1998; Van Kaam-Peters *et al.*, 1998.
Scanning electron microscopy fabric analyses	Feistner, 1989; Bertrand *et al.*, 1990; Belin, 1992; Bishop, Kearsley and Patience, 1992; Boussafir *et al.*, 1995, 1995a.
Environmental reconstruction	Gallois, 1976; Gallois and Medd, 1979; Tyson *et al.*, 1979; Oschmann, 1988b, 1990; Miller, 1990; Wignall and Ruffel, 1990; Wignall, 1989, 1991, 1994; Wignall and Hallam, 1991; Baudin *et al.*, 1992 Bertrand and Lallier-Verges, 1993; Herbin and Geyssant, 1993; Lallier-Verges *et al.*, 1993, 1995; Desprairies *et al.*, 1995; Disnar and Ramanampisoa, 1995; Moore *et al.*, 1995.
Organic matter - preservation	Demaison and Moore, 1980; Allison *et al.*, 1995.
Organic matter - productivity	Bertrand and Lallier-Verges, 1993; Lalier-Verges *et al.*, 1993; Ramanampisoa and Disnar, 1994; Disnar and Ramanampisoa, 1995; Lallier-Verges *et al.*, 1997.

Table 1.1 Previous studies on the Kimmeridge Clay Formation are numerous and of a multidisciplinary nature, though a large number have focused on the formation of the KCF and it's environmental reconstruction.

1.1.1 DORSET, KCF TYPE SECTION

The KCF was deposited extensively over the Northwestern European Basin, which outcrops in Northern France (Boulonnais), Yorkshire and Southern England (Dorset) (Figure 1.1). The focus of this study is the Dorset coastal section (Figure 1.2), located in the Wessex Basin, and is the stratotype for the Jurassic Kimmeridgian Stage (154.7 – 152.1 Ma (Harland *et al.*, 1989)). The thickness of the KCF in Southern England varies from 300m in western Dorset to more than 500m in the Isle of Purbeck (Cox and Gallois, 1981). The tectonic evolution of the Wessex Basin and subsequent erosional episodes have led to this thickness variability. During the Late Jurassic, the Wessex Basin sedimentary evolution was controlled by extensional tectonics, which resulted in a series of E-W trending grabens and half-grabens, defined by zones of major, predominately south facing, syn-depositional normal faults (Chadwick, 1986). Thus, fault controlled differential subsidence contemporaneous with sedimentation had a marked influence on stratigraphic thickness and facies (Brown, 1990).

Detailed stratigraphic descriptions of the KCF include those of Arkell (1933), Cope (1978) and Cox and Gallois (1981) (Figure 1.3a and b). The KCF of Dorset displays rhythmic sedimentation of brownish-grey bituminous mudrock or oil shales, passing into pale grey calcareous mudstones (Cox and Gallois, 1981). Dolomitic cementstones and coccolith limestones frequently interrupt this sequence and provide convenient marker horizons (House, 1995). Within the oil shales and coccolith limestones, millimeter to sub-millimeter scale lamination has been preserved. This laminated record provides an ideal opportunity to study high-resolution palaeoenvironmental and climatic change during discrete periods of the Kimmeridgian Stage.

1.2 RATIONALE, RESEARCH AIMS AND OBJECTIVES

Within the RGGE project, this study is the high-resolution examination of several discrete intervals of the KCF, focusing on the nature of, and controls on the depositional system. Two scales of analysis have been applied, a millimeter/sub-millimeter scale and a lower resolution of point samples every 5cm (Section 1.4.2), which have provided a higher resolution record of these intervals than previous studies. This has facilitated more specific inferences about environmental processes and mechanisms occurring during the deposition of these intervals and indicated high-resolution environmental and climatic change within the KCF.

Both the organic richness and the lithological variation of the KCF make this formation important in the understanding of organic-rich ancient marine sediments and to the identification of climatic influence on such lithologies. However, as previously mentioned, debate surrounds the mechanisms which resulted in the deposition of the KCF. Organic-rich sediments from

modern marine environments are known to be the result of two mechanisms, one productivity controlled, the other preservation controlled, which may either act separately or together. This productivity/preservation debate is a key issue in the reconstruction of ancient marine environments and thus is central to the understanding of the KCF (Section 2.3). This study aims to reconstruct the depositional environment of several specific intervals within the KCF at a high-resolution, by applying an understanding of the mechanisms and processes occurring in comparable but modern marine systems.

Specific objectives are,

1) The determination of sediment fabrics, in particular laminae composition and structure.
2) To relate the genesis of sediment fabrics to surface processes and benthic responses.
3) To identify changes in organic matter as close to lamina scale as possible.
4) To relate organic matter variations to sediment fabric.
5) Establish high-resolution environmental reconstructions for the KCF intervals.

1.2.1 METHODOLOGY

Complementary techniques of back-scattered electron microscopy (BSEM), palynology and geochemical analyses of total organic carbon (TOC) and atomic H/C ratios have been applied in this study. The high-resolution BSEM is used to determine sediment fabric and composition. Lamina scale palynology and the geochemical techniques provide environmental information from palynofacies analysis and bulk rock geochemistry. An integration of these techniques enables an assessment of local environmental conditions and the processes that took place, both in the water column and in the sediment, during and after deposition.

1.3 SITE LOCATION

During the winter of 1996 and spring of 1997, three new boreholes were drilled through the Dorset Kimmeridge Clay, specifically for the RGGE project. During the first six months of this project, the author spent on well site assisting Dr R. Gallois of the BGS, in core logging, handling and over seeing shipment of core back to the Southampton Oceanography Centre. Situated within the Isle of Purbeck, two boreholes (Swanworth 1 and 2) were drilled near Worth Matravers, while the third (Metherhills) was drilled on the cliff top above Kimmeridge Bay, the type section locality (Figure 1.2). The Swanworth 1 and 2 boreholes were drilled in parallel and encompassed the Lower Portlandian into the Lower Kimmeridge Clay *sensu anglico*. Borehole three was situated at the crest of the 'Purbeck' anticline, which enabled the recovery of the whole of the Lower Kimmeridge Clay and the upper Corallian Beds (Oxfordian). A combination of the three wells has provided a complete core sequence through the entire KCF. Details of the borehole core lengths and grid references are given in Table 1.2.

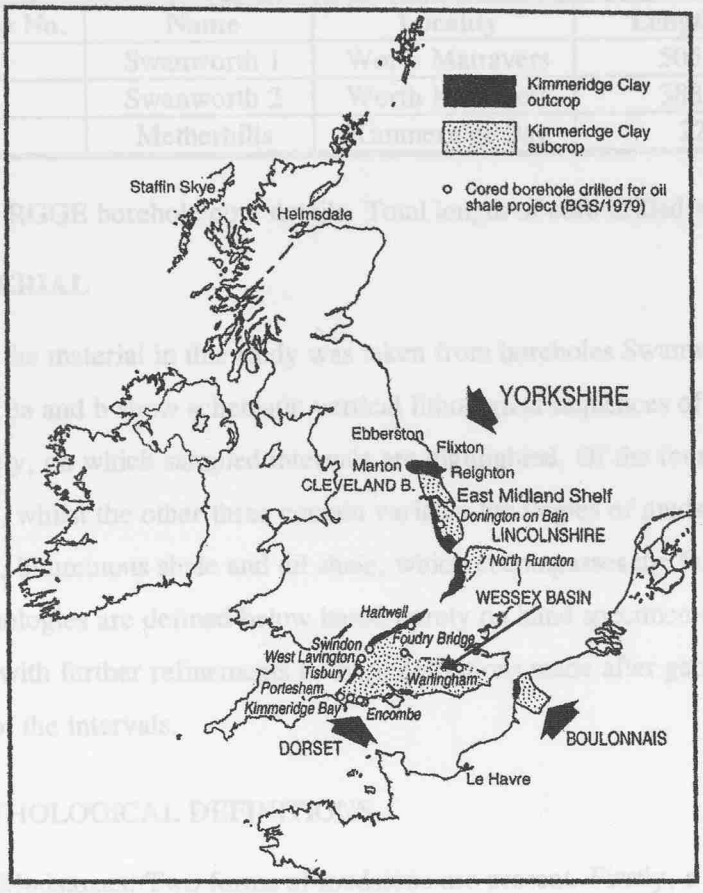

Figure 1.1 Location of the Kimmeridge Clay outcrop and subcrop for the United Kingdom and France. After Herbin *et al.*, (1995)

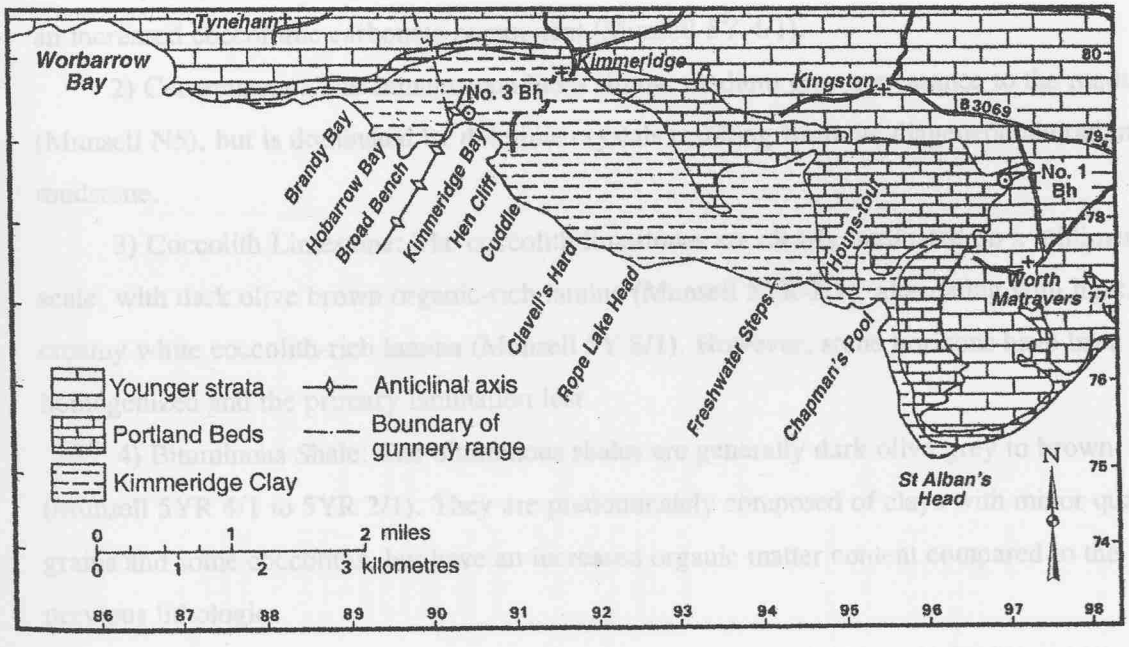

Figure 1.2 Geology of the Dorset coast showing the location of the boreholes drilled during the the RGGE project.
Modified after Cox and Gallois (1981)
Borehole 2 is not shown but is located next to borehole 1.

Borehole No.	Name	Locality	Length (m)	Grid Reference
1	Swanworth 1	Worth Matravers	505.21	SY 9675 7823
2	Swanworth 2	Worth Matravers	388.30	SY 9675 7824
3	Metherhills	Kimmeridge Bay	229	SY 9112 7911

Table 1.2 RGGE borehole core details. Total length of core drilled = 1122.51m.

1.4 MATERIAL

All the material in this study was taken from boreholes Swanworth 1 and Metherhills. Figures 1.3a and b show schematic vertical lithological sequences of the Lower and Upper KCF respectively, on which sampled intervals are highlighted. Of the four intervals, one is solely of mudstone, whilst the other three contain variable lithologies of mudstone, cementstone, coccolith limestone, bituminous shale and oil shale, which encompasses the full range of KCF lithologies. These lithologies are defined below based purely on hand specimen examination and BSEI analysis, with further refinements to these definitions made after geochemical and palynological analysis of the intervals.

1.4.1 LITHOLOGICAL DEFINITIONS

1) Mudstones: Two forms of mudstone are present. Firstly, a homogeneous, medium dark grey mudstone (Munsell N4-N5) composed of clays, with minor constituents of coccoliths, quartz and feldspar grains and organic matter. The second is an olive grey, calcareous mudstone, with an increased coccolithic carbonate component (Munsell 5Y 4/1).

2) Cementstone: The cementstone has a similar medium grey appearance to the mudstones (Munsell N5), but is dominated by dolomite crystals resulting from the diagenetic alteration of a mudstone.

3) Coccolith Limestone: The coccolith limestones are clearly laminated on a millimeter scale, with dark olive brown organic-rich lamina (Munsell 5YR 2/1), alternating with light, creamy white coccolith-rich lamina (Munsell 5Y 8/1). However, some horizons have been homogenized and the primary lamination lost.

4) Bituminous Shale: The bituminous shales are generally dark olive grey to brown (Munsell 5YR 4/1 to 5YR 2/1). They are predominately composed of clays with minor quartz grains and some coccoliths, but have an increased organic matter content compared to the previous lithologies.

5) Oil Shale: The oils shales are dark olive brown to black (Munsell 5Y 2/1 to N1), and have the greatest organic content of all the lithologies. Clays and pyrite are abundant and the coccolith-rich oil shales tend to be well laminated with some purely carbonate lamina.

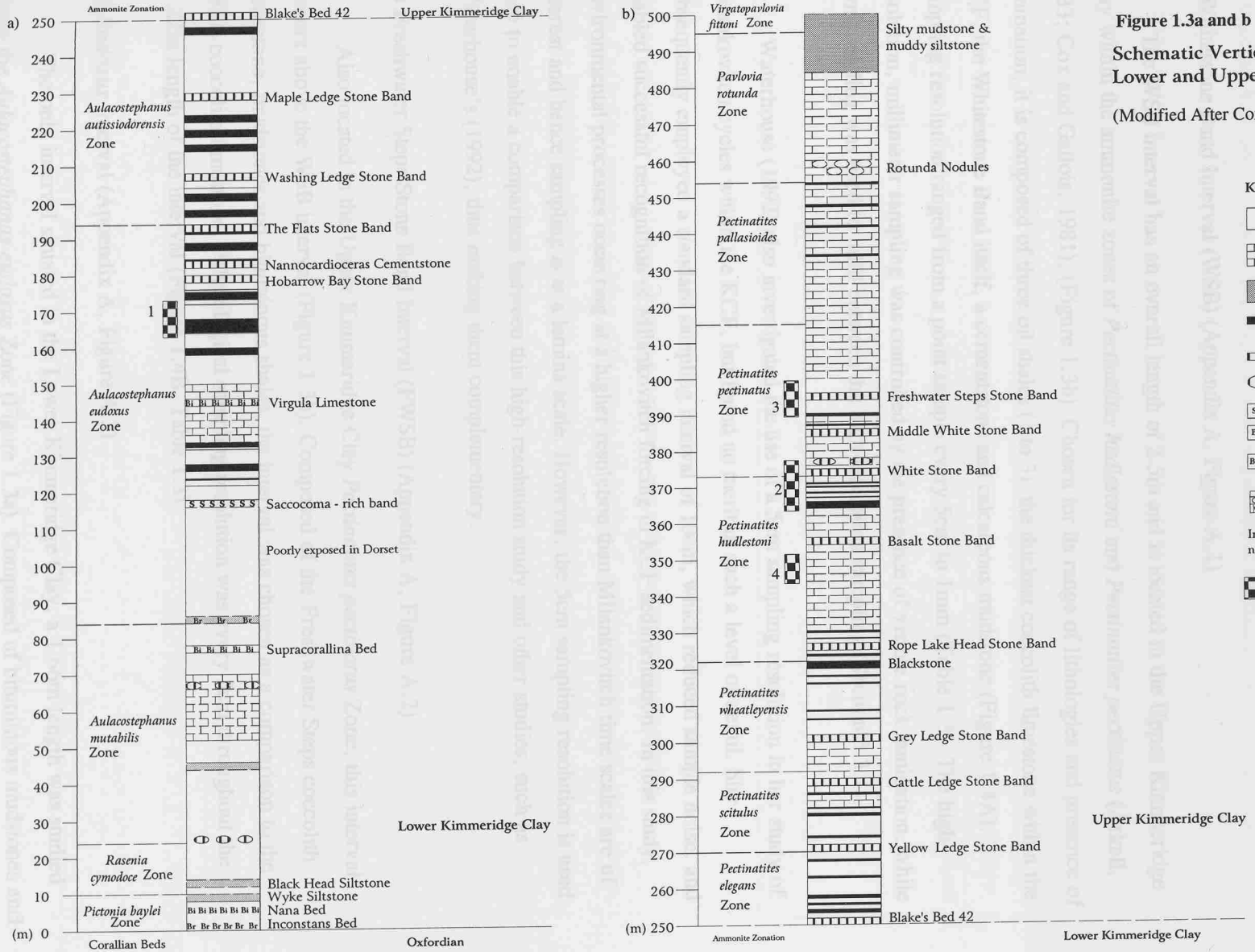

Figure 1.3a and b

Schematic Vertical Sections of the Lower and Upper Kimmeridge Clay, Dorset.

(Modified After Cox and Gallois, 1981)

1.4.2 STUDIED INTERVALS

The lithology, sampling resolution and other details of the studied intervals are described below. Figure 1.4 shows schematic logs of the four intervals, each marked with their sampling resolution. The sampling resolutions employed over the intervals are presented in more detail in Chapter 5 (Section 5.3.1) and the effects of these resolutions are discussed in Chapter 8. (Appendix A, Figures A.1 to A.4, core photographs of the intervals).

a) Whitestone Band Interval (WSB) (Appendix A, Figure A.1)

The WSB interval has an overall length of 2.5m and is located in the Upper Kimmeridge Clay within the ammonite zones of *Pectinatites hudlestoni* and *Pectinatites pectinatus* (Arkell, 1933; Cox and Gallois, 1981), (Figure 1.3b). Chosen for its range of lithologies and presence of lamination, it is composed of three oil shales (1 to 3), the thickest coccolith limestone within the KCF, the Whitestone Band itself, a cementstone and calcareous mudstone (Figure 1.4A). Sampling resolution ranged from a point sample every 5cm to 1mm (Table 1.3). The high-resolution, millimeter sampling was controlled by the presence of visible rock lamination, while 5cm sampling was used to infill between the high-resolution sampling (Section 5.3.1).

Waterhouse (1992) also investigated the use of a 5cm sampling resolution in her study of Milankovitch cycles within the KCF, but found no merit in such a level of detail. She subsequently employed a standard sampling interval of 10cm, which reduced sample noise, and enabled successful recognition of Milankovitch forcing in KCF sedimentation. In this study, environmental processes occurring at a higher resolution than Milankovitch time scales are of interest and hence sampling is at a lamina scale. However, the 5cm sampling resolution is used here to enable a comparison between this high-resolution study and other studies, such as Waterhouse's (1992), thus making them complementary.

b) Freshwater Steps Stone Band Interval (FWSB) (Appendix A, Figure A.2)

Also located in the Upper Kimmeridge Clay *Pectinatites pectinatus* Zone, this interval occurs above the WSB interval (Figure 1.3b). Composed of the Freshwater Steps coccolith limestone, mudstones and bituminous shales, the interval was chosen as a comparison to the WSB coccolith limestone. Palynological sampling resolution was every 5cm throughout the 3.22m length of the interval (Figure 1.4B, Table 1.3).

c) *Eudoxus* Interval (Appendix A, Figure A.3)

The only interval situated in the Lower Kimmeridge Clay, a 1.66m length was studied from the *Aulacostephanus eudoxus* Zone (Figure 1.3a). Composed of bituminous mudstones and

bituminous/oil shales, it represents the most extensive development of organic-rich facies within the KCF, and was chosen as a comparison to the oil shales within the WSB interval. The sampling resolution was 5cm throughout (Figure 1.4C, Table 1.3).

d) Bed 44 Interval (Appendix A, Figure A.4)

Bed 44, as numbered by Cox and Gallois (1981), is located in the Upper Kimmeridge Clay *Pectinatites hudlestoni* Zone (Figure 1.3b). This whole bed is characterized by 20m of calcareous mudstone. An interval of this bed was chosen as a form of control, in the sense that compared to the other intervals, Bed 44 does not visually display gross lithological variation. A length of 1.8m was selected and the sampling resolution was every 5cm (Figure 1.4D, Table 1.3).

Interval	**Borehole No.**	**Length (m)**	**Driller's Depth (m)**	**Lithologies**	**Sampling Resolution**
Whitestone Band	Swanworth 1	2.5	195.46 - 197.96	CL - (WSB), C, CM, BTMS, OS, M	5cm to 1mm
Freshwater Steps Band	Swanworth 1	3.22	175.87 - 179.09	CL - (FWSB) CM, BTMS, M	5cm
Eudoxus	Metherhills	1.66	375.92 - 377.58	BTMS, BOS,	5cm
Bed 44	Swanworth 1	1.8	226.77 - 228.57	CM	5cm

Table 1.3

Studied interval details, length, lithology and palynological point sampling resolution.
CL = Coccolith Limestone, CM = Calcareous Mudstone, C = Cementstone, OS = Oil Shale, BTMS = Bituminous Mudstone, BOS Bituminous/Oil Shale, M = Mudstone.

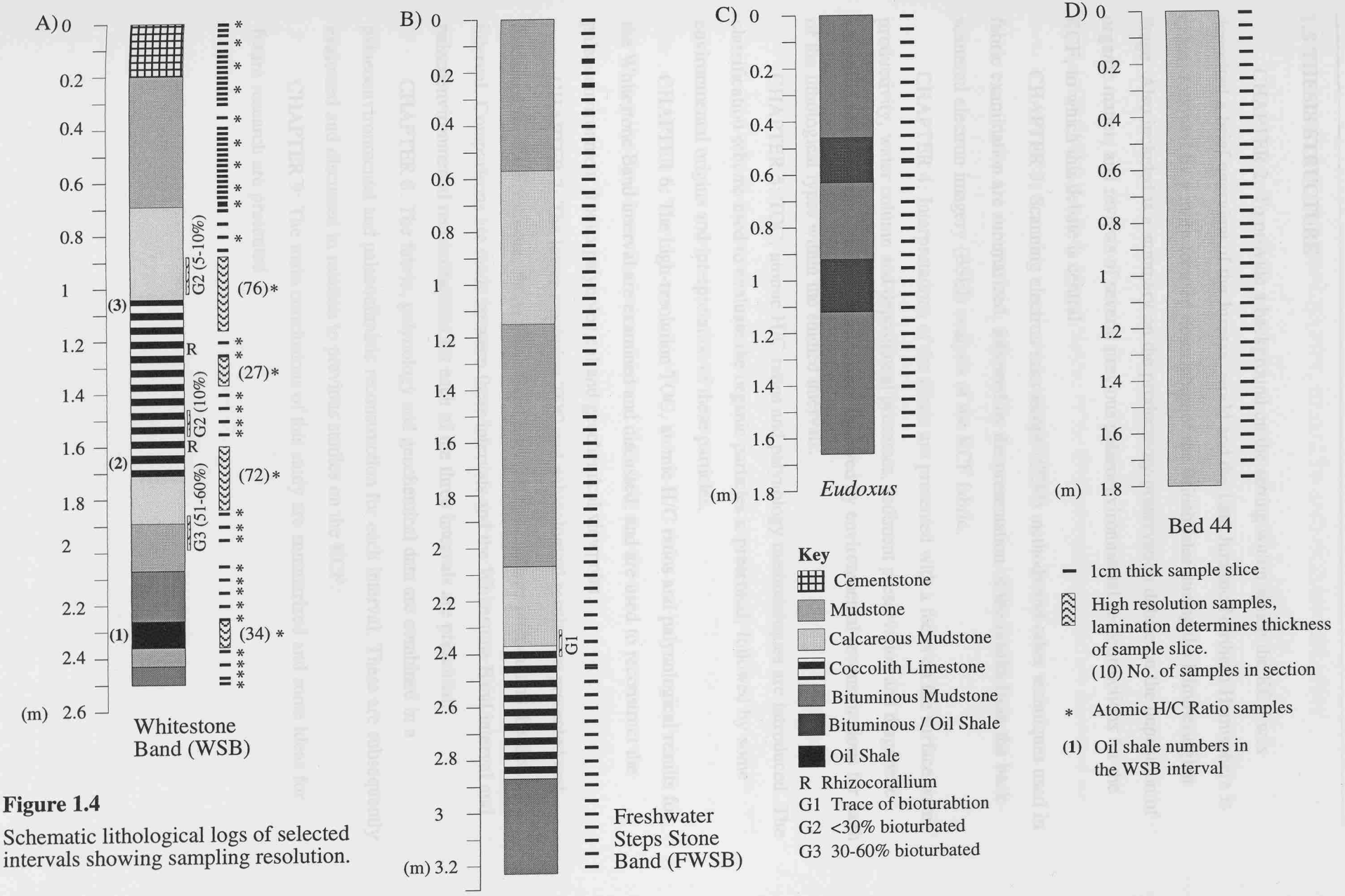

Figure 1.4

Schematic lithological logs of selected intervals showing sampling resolution.

1.5 THESIS STRUCTURE

CHAPTER 2: To provide a background on the setting within which the KCF was deposited a brief overview of the Jurassic world and the Late Jurassic Northern Hemisphere is given, followed by a more focused description of the British Isles during the Kimmeridgian Stage. Also included is a summary on the productivity/preservation debate on the deposition of organic matter, and reviews of several previous palaeoenvironmental reconstructions for the KCF, to which this debate is central.

CHAPTER 3: Scanning electron microscope (SEM) methods and other techniques used in fabric examination are summarized, followed by the presentation of the results from the back-scattered electron imagery (BSEI) analysis of the KCF fabric.

CHAPTER 4: Interpretations of the fabric are presented with a focus on the surface water productivity, water column and depositional processes, sediment preservation and diagenetic alteration of the fabric. These discussions are followed by environmental reconstructions for each of the lithological types within the studied intervals.

CHAPTER 5: TOC, atomic H/C ratios and palynology methodologies are introduced. The classification scheme used to evaluate the organic particles is presented, followed by some environmental origins and interpretation of these particles.

CHAPTER 6: The high-resolution TOC, atomic H/C ratios and palynological results for the Whitestone Band interval are examined and discussed, and are used to reconstruct the palaeoenvironment from a palynological and geochemical viewpoint.

CHAPTER 7: The lower resolution TOC and palynological results are presented and discussed for the Freshwater Steps Stone Band interval, the *Eudoxus* interval and the Bed 44 interval. Comparisons are made between these intervals and the Whitestone Band interval and palaeoenvironmental reconstructions for each of the three intervals are presented.

CHAPTER 8: The fabric, palynology and geochemical data are combined in a palaeoenvironmental and palaeoclimatic reconstruction for each interval. These are subsequently evaluated and discussed in relation to previous studies on the KCF.

CHAPTER 9: The main conclusions of this study are summarized and some ideas for future research are presented.

2.0 JURASSIC PALAEOGEOGRAPHY, CLIMATE AND OCEANOGRAPHY

An understanding of the geography, climate and oceanography during the KCF deposition is necessary if detailed palaeoenvironmental reconstructions are to be made. The following chapter sets the environmental background for this study, with descriptions of the major characteristics of the Jurassic world, together with details of the local Northwest European environment during the Kimmeridgian Stage. The productivity/preservation debate is briefly summarized before previous reconstructions of the KCF palaeoenvironment are described and some of the problems associated with them highlighted.

2.1 OVERVIEW OF THE JURASSIC WORLD

To provide a global perspective on the factors that influenced the environment during the KCF deposition, a brief overview of the continental situation and orientation, tectonic activity, climatic regimes and oceanography, are described for the Jurassic Period.

2.1.1 PALAEOGEOGRAPHY AND TECTONICS

The Jurassic Period was tectonically active, characterized by initial phases of rifting and fragmentation of the Pangean supercontinent. (Fourcade *et al.*, 1996). The Palaeo-Tethys was interposed between the two landmasses of Laurasia and Gondwana, forming an embayment of the greater Pacific Ocean, Panthalassa (Ager, 1975; Hallam, 1996).

During the Early Jurassic there was no connection between the western termination of Palaeo-Tethys and Eastern Panthalassa, with Laurasia and Gondwana still hinged together. The Proto-Atlantic during this time was only a narrow channel connecting the northern Boreal Sea to the northern tip of Western Palaeo-Tethys' large terrigenous shelf. An open seaway between the Boreal and Tethyan Seas was established in a series of marine transgressions during this time (Doré, 1991). In the Mid Jurassic a permanent marine connection across the Caribbean High to eastern Panthalassa was established, dividing Laurasia and Gondwana into two separate landmasses. The central sector of the Atlantic Ocean began to open from Mid Jurassic times onwards and Laurasia moved towards the south (Ziegler *et al.*, 1994). Major uplift in the central North Sea however, resulted in the closure of the North Sea seaway (Dorè, 1991).

The Late Jurassic saw the disappearance of the Palaeo-Tethys and the opening of Neotethys as an elongate splice from Gondwana, the Cimmerian landmass, collided with eastern Laurasia (Scotese, 1991; Hallam, 1996). Widespread rifting in the North Atlantic Seaway combined with transgression re-established the north-south marine connection between the Boreal and Tethyan marine realms. Tectonic activity was most intense during Late Jurassic times,

especially in the North Atlantic and North Sea seaways. Extensional movement characterized these events which have been related to plate re-organization in Northwest Europe (Doré, 1991) (Figure 2.1).

2.1.2 PALAEOCLIMATE

The global climate during the Mesozoic Era was more equable than at present (Axelrod, 1990; Ziegler *et al.*, 1994; Hallam, 1996). Polar latitudes experienced warm and often humid climates, which resulted in an absence of ice sheets during the Jurassic Period (Frakes, 1979; Brandt, 1986; Donn, 1987, Frakes and Francis, 1988; Frakes *et al.*, 1992; Hallam, 1984, 1994).

High latitudes show a relatively rich flora and fauna, with affinities that vary from warm temperate to subtropical and even tropical climates (Colbert, 1964; Vakhrameev, 1964, 1981, 1991 cited in Hallam, 1985 and 1994; Barnard, 1973; Hallam, 1975). This assignment of tropical temperatures to higher latitudes suggests climate equability over a wider latitudinal band than at present. However, some debate exists surrounding the temperature scale of these Jurassic Period climatic biomes, with the suggestion that they are too warm (Krassilov, 1981; Ziegler *et al.*, 1994).

The low- to mid-latitude continents were characterized by extensive desert basins (Hallam, 1975), while continental margins were dominated by salt pans and sabkhas (Frakes, 1979). Seasonal extremes of temperature on the large continental masses must have been considerable as a consequence of reduced maritime influence over these large continental areas (Hallam, 1985, 1996).

Hemispheric meridional temperature gradients were in the range of 10°C to 20°C, a substantial reduction compared with the present day 40°C range in the Northern Hemisphere (Donn, 1987). Annual growth rings of fossil Eurasian wood indicate a seasonal climatic regime for the Northern Hemisphere, influenced by seasonal oscillations in temperature and/or precipitation (Epshteyn, 1978; Frakes, 1979, Creber and Chaloner, 1984, Francis, 1983, 1984). Monsoonal winds probably had a more dominant role in the Mesozoic Era than today. As such seasonality in many regions would have been predominately controlled by precipitation rather than temperature (Hallam, 1984).

The Early Jurassic climate was humid, represented by terrigenous fluvio-lacustrine environments with coal formation, especial at higher latitudes (Hallam, 1984, 1994; Baudin, 1995; Fourcade *et al.*, 1996). Increasing climatic aridity during the Mid Jurassic is evident from expanding evaporite deposition (Frakes, 1979, Hallam, 1984), and this trend continued into the Late Jurassic. A decline in coal formation resulted from strongly arid conditions during this time,

with increased volume of evaporite deposits spreading over a higher latitudinal range (Baudin, 1995). However, continental motion has been thought to control some of the perceived climatic change during the Mid and Late Jurassic, rather than climatic palaeolatitudinal shifts (Ziegler *et al.*, 1994). Orographic effects resulting from the collision of the Cimmerian landmass have also been suggested as a cause of the Late Jurassic spread of arid conditions (Hallam, 1994).

2.1.3 GENERAL CIRCULATION MODELS FOR THE JURASSIC PERIOD

Climate reconstruction using general circulation models (GCMs) undertaken on the Jurassic Period have reproduced reasonably well the climatic characteristics evident from the geological record (Parrish and Curtis, 1982; Oschmann, 1990; Moore *et al.*, 1992; Valdes and Sellwood, 1992; Valdes 1994; Price *et al.*, 1995; Sellwood and Valdes, 1997). Employing an elevated atmospheric carbon dioxide level of 1120 ppm, four times that of the present day, Jurassic climate was predicted to have been warm with no permanent polar ice caps. However, some winter sea ice was predicted in the Boreal Sea and may have made landfall on restricted margins of this sea (Moore *et al.*, 1992).

The GCM's also show that low latitude continents were characterized by interiors whose climate was harsh and arid. Massive summer monsoonal circulation in middle latitudes resulted in increases in rainfall, which predominately fell over the oceans (Moore *et al.*, 1992, Valdes and Sellwood, 1992). Other models predicted 72% cloud cover compared to 55% of today, suggesting that elevated water vapour concentrations in the atmosphere controlled high latitude warmth (Sellwood and Valdes, 1997). Precipitation was proposed to be convective and most intense over tropical seaways and the oceans (Valdes and Sellwood, 1992; Sellwood and Valdes, 1997). Such localization of precipitation is suggested to explain why models propose greater climate humidity than geological data indicates.

2.1.4 PALAEOCEANOGRAPY

The existence of warm seaways and reduced temperature gradients towards the poles are suggested from the equability of the Mesozoic earth and the broad palaeolatitudinal spread of carbonate facies (Sellwood and Price, 1994), suggesting reduced intensity of deep oceanic circulation (Hallam, 1984). Oceanic gyres have been ascribed to Panthalassa, while an equatorial current moving westwards with the trade winds is suggested to have dominated the Palaeo-Tethys (Ager, 1975). A sluggish clockwise gyre has been postulated for the palaeo-North Atlantic (Berggren and Hollister, 1974), with an anticlockwise subpolar gyre for the Boreal Sea (Ager, 1975). Eustatic sea level rise characterized the Jurassic Period, with maximum sea level stands during the Late Jurassic (Vail and Todd, 1981; Vail *et al.*, 1984; Haq *et al.*, 1987; Hallam, 1992), resulting in reduced continental area, which combined with the suggested increased aridity during the Late Jurassic, led to reduced continental runoff (Hallam, 1984).

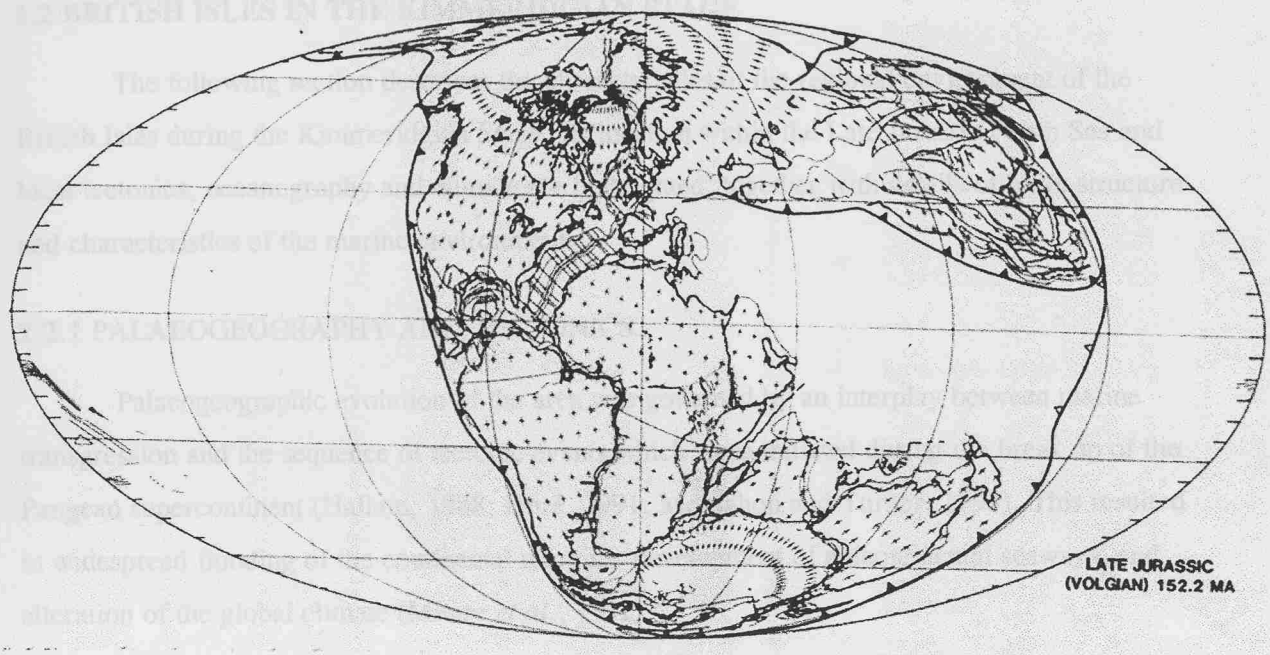

Figure 2.1
Plate tectonic reconstruction for the Late Jurassic Period.
After Scotese, (1991).

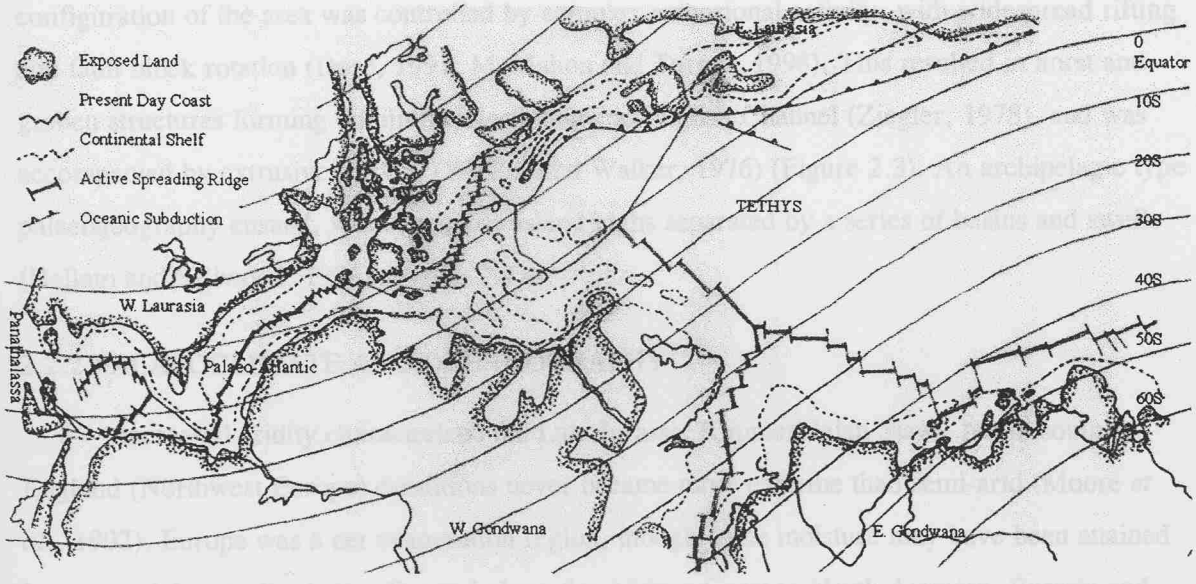

Figure 2.2
Early Kimmeridgian palaeoenvironments and palaeogeographies of the Tethys realm.
After Cecca et al., (1993)

2.2 BRITISH ISLES IN THE KIMMERIDGIAN STAGE

The following section describes the characteristics of the regional environment of the British Isles during the Kimmeridgian Stage. Its location within the Late Jurassic North Sea and local tectonics, oceanography and climate are highlighted, together with details of basin structure and characteristics of the marine environment.

2.2.1 PALAEOGEOGRAPHY AND TECTONICS

Palaeogeographic evolution of the area was governed by an interplay between marine transgression and the sequence of tectonic events which were initiated during the break up of the Pangean supercontinent (Hallam, 1988; Doré, 1991; McMahon and Turner, 1998). This resulted in widespread flooding of the continental margins, development of epicontinental seaways, and alteration of the global climate (Moore *et al.*, 1992).

The British Isles was located within the Northwest European Basin between latitudes 30 and 40°N, in an area of broad epicontinental sea on the North Atlantic Shelf (Gallois, 1976; Oschmann, 1988b). Situated at the southern end of the Atlantic Rift Domain, the tectonic configuration of the area was controlled by complex extensional activity, with widespread rifting and fault block rotation (Doré, 1991; McMahon and Turner, 1998). This resulted in horst and graben structures forming within the North Sea and English Channel (Ziegler, 1978), and was accompanied by extrusive activity (Walker and Walker, 1976) (Figure 2.3). An archipelagic type palaeogeography ensued, with numerous island highs separated by a series of basins and swells (Hallam and Sellwood, 1976) (Figure 2.4).

2.2.2 PALAEOCLIMATE AND OCEANOGRAPHY

Increased aridity characterized the Late Jurassic Kimmeridgian Stage, but in southern England (Northwest Europe) conditions never became more extreme than semi-arid (Moore *et al.*, 1992). Europe was a net evaporation region, though some moisture may have been attained by equatorial easterlies being diverted along the African Coast to North America, Eurasia and Western Europe (Parrish *et al.*, 1982). However, the existence of a relatively weak but extensive storm belt over the palaeo-Atlantic and Europe has been suggested (Valdes and Sellwood, 1992). As a consequence of this palaeoclimate and strongly transgressive regime, continental runoff is suggested to have been restricted.

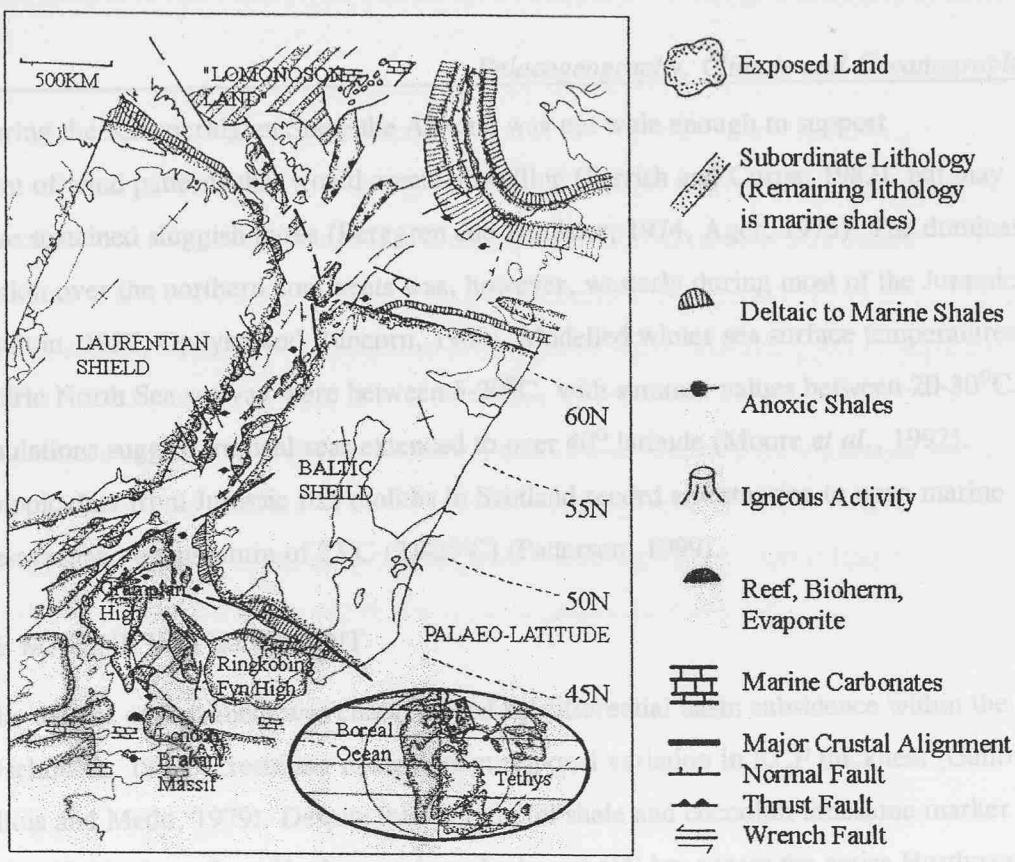

Figure 2.3
Late Jurassic sedimentary/tectonic reconstruction for Northwest Europe.
After Dore (1991)

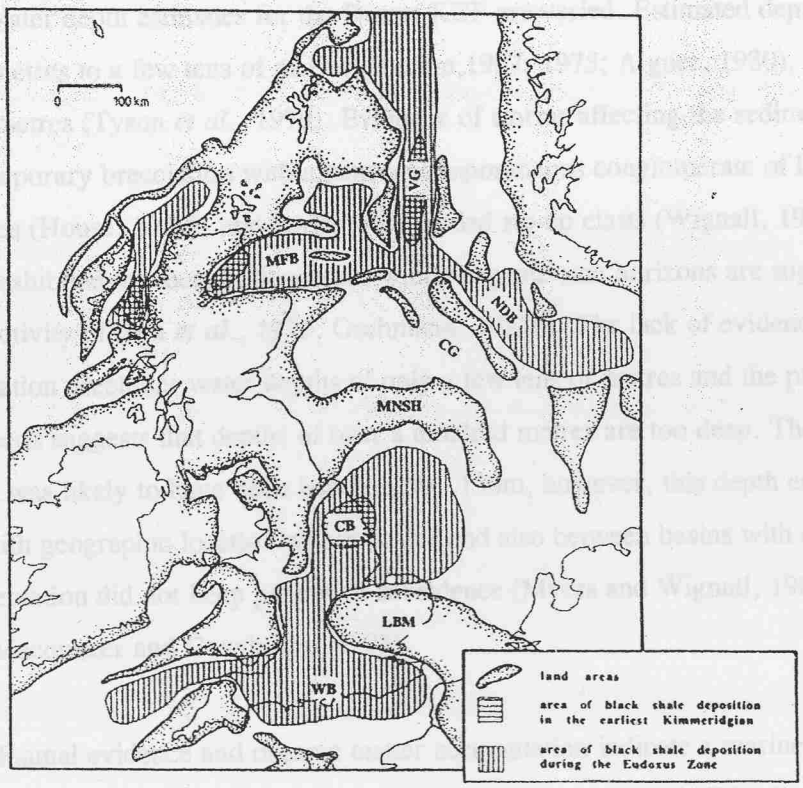

Figure 2.4
Kimmeridgian palaeogeography of northwest Europe showing the extent of black shale deposition in the earliest Kimmeridgian and at the maximum extent of black shale deposition in the Eudoxus Zone. CG - Central Graben, LBM - London-Brabant Massif, MFB - Moray Firth Basin, MNSH - Mid North Sea High, NDB - Norwegian-Danish Basin, VG - Viking Graben, WB Wessex Basin. After Wignall, (1994)

During the Kimmeridgian Stage the Atlantic was not wide enough to support development of wind patterns that would create upwelling (Parrish and Curtis, 1982), but may instead have sustained sluggish gyres (Berggren and Hollister, 1974, Ager, 1975). The dominant wind direction over the northern continents was, however, westerly during most of the Jurassic Period (Shotton, 1937; Opdyke and Runcorn, 1960). Modelled winter sea surface temperatures for the epeiric North Sea seaway were between 5-20^{o}C, with summer values between 20-30^{o}C. Model simulations suggest tropical seas extended to over 40^{o} latitude (Moore *et al.*, 1992). Recent isotopic data from Jurassic fish otoliths in Scotland record an estuarine to open marine water time-averaged temperature of 23°C (21-25°C) (Patterson, 1999).

2.2.3 THE MARINE ENVIRONMENT

The marine environment was characterized by differential basin subsidence within the rift system (Oschmann, 1988b), resulting in significant regional variation in KCF thickness (Gallois, 1976; Gallois and Medd, 1979). Despite this, certain oil shale and coccolith limestone marker beds are identifiable throughout England and can be traced 400 km across the entire Northwest European Basin (Cox and Gallois, 1981).

Water depth estimates for the Dorset KCF are varied. Estimated depths range from less than ten metres to a few tens of metres (Hallam,1967, 1975; Aigner, 1980), to depths of several hundred metres (Tyson *et al.*, 1979). Evidence of storms affecting the sediment surface is shown by contemporary brecciation with a penecontemporaneous conglomerate of lignite pieces and mud flakes (House, 1989), and horizons of graded rip up clasts (Wignall, 1989). Rare low angle contacts exhibited by coccolithic streaks within organic-rich horizons are suggestive of occasional current activity (Tyson *et al.*, 1979; Oschmann, 1988b). The lack of evidence of shallow water sedimentation precludes water depths of only a few tens of metres and the presence of storm and current beds suggests that depths of over a hundred metres are too deep. The sediment/water interface was likely to have been between 50 - 150m, however, this depth estimate would have varied with geographic location within basins and also between basins with differing subsidence if sedimentation did not keep pace with subsidence (Myers and Wignall, 1987; Oschmann, 1988b; Macquaker and Gawthorpe, 1993).

Faunal evidence and organic matter accumulation indicate a marine environment characterized by variable oxygen conditions. Facies types for the KCF, distinguished by lithology, organic matter content and the diversity and density of benthic fauna, range from silty clays to coccolith limestones and oil shales. This facies range displays increasingly stressed life conditions which suggests there was a decrease in bottom water oxygen and an increase in organic matter accumulation (Oschmann, 1988b).

The KCF organic matter is predominately marine in origin and chemical kerogen analysis shows a dominance of Type II kerogen facies (Farrimond *et al.*, 1984; Scotchman, 1991; Boussafir *et al.*, 1995; Disnar and Ramanampisoa, 1995). Rates of sedimentation across the Northwestern European Basin vary from <15 to 200m/my after compaction (Miller, 1990). This variation partly reflects normal condensed sequences on highs, but also possible sediment redistribution and slumping into grabens. A typical mean rate of 15m/my is assumed for the United Kingdom continental shelf (Miller, 1990). Other values, obtained for ammonite zones, are 4.5m/my of compacted sediment for the Upper Kimmeridge *Wheatleyensis* Zone (Macquaker and Gawthorpe, 1993), to 11 m/my in the *Hudlestoni* Zone (Cope *et al.*, 1980; Haq *et al.*, 1988). Values for the regions of the North Sea area are shown in Table 2.1.

Region	Sedimentation Rate
Northern North Sea	4-26m/my
Central North Sea	5-26m/my
Southern North Sea	19-32m/my
Wessex Basin	70m/my

Table 2.1
Mean sedimentation rates for the North Sea Region during the KCF depositional period, after Cox and Gallois (1981).

Sedimentation rates suggested for the Wessex Basin are substantially greater than for other regions within the Northwest European Basin. Further discrepancy is highlighted by comparison of total organic carbon % (TOC). Estimates of the TOC % for the KCF are variable, ranging from 1-2% to over 50%, depending on depositional location (Miller, 1990). Within the Wessex Basin, TOC % is about 7% overall (Miller, 1990), but can reach up to 35% (Oschmann, 1988b) and in excess of 50% (Myers and Wignall, 1987). Despite its contrast to other Northwest European basins, the Wessex Basin does provide a complete lithological sequence and the chance to assess the extremes of the Kimmeridgian environment.

2.3 PRODUCTIVITY / PRESERVATION MECHANISMS FOR MARINE ORGANIC MATTER

The accumulation of organic matter within the marine environment is dependent on the relative flux of various sediment components, including production of organic material, and the ease with which these are subsequently preserved on deposition and burial (Calvert, 1987). The relative importance of each of these mechanisms in the formation of organic-rich deposits is still highly debatable. A brief examination of each of these mechanisms follows with examples of

their application in KCF environmental reconstruction, while comparisons of these mechanisms to modern marine environments is discussed in Chapter 8..

2.3.1 THE PRODUCTIVITY MECHANISM

Supply of organic matter to the sediment depends on a number of factors (discussed more fully in Chapter 4), the most important of which are the rate of primary production and the depth through which particles must settle (Tyson, 1995). Enhanced productivity not only results in a high flux to the sediment but can also result in depletion of bottom water oxygen where flux rates and degradation of the organic matter exceed oxygen availability. The resultant redox conditions have a positive action on organic matter accumulation by enhancing preservation at the sediment/water interface (Tribovillard *et al.*, 1994).

2.3.2 PRODUCTIVITY CONTROLLED KCF ENVIRONMENT RECONSTRUCTIONS

The European Kimmeridgian palaeogeography of numerous island highs and subsiding basins linked by narrow straits, and a rich, land derived nutrient supply would have provided an environment favorable for enhanced primary production in the form of algal blooms (Gallois, 1976). Within the epicontinental sea, these blooms would result in increased organic matter export to the sediment surface and consequently increased oxygen depletion of the water column. Thus a temporary environment of short-lived bottom water anoxia could have been established, aiding organic matter preservation.

Such an episodically dysaerobic environment would have been characterized by sediments which were deposited under an oxygenated water column, with a redox boundary that oscillated above and below the sediment/water interface as the result of variability in the organic flux or productivity (Lallier-Vergès *et al.*, 1993). Sediment anoxia was a controlling factor in organic matter preservation but is assumed to have developed only as a consequence of high primary productivity and a shallow water column, which limited degradation of organic matter during transport to the sediment surface (Gallois, 1976; Disnar and Ramanampisoa, 1995).

2.3.3 THE PRESERVATION MECHANISM

The presence of reduced oxygen or anoxia at the sediment/water interface or within the water column results not only from biological mechanisms but also from physio-chemical mechanisms. Stratification of the water column by temperature and/or density differences restricts water circulation within the basin, preventing oxygen replenishment to the lower water column. Once all available oxygen is consumed within this lower layer, anoxia results, which through the lack of faunal consumption and oxidation of the organic matter, consequently aids the preservation of organic matter exported to the sediment surface (discussed more fully in

Chapter 4). No enhanced primary production is envisaged in this mechanism, with increased sediment organic carbon solely being attributed to the enhanced preservation of a 'normal' organic production flux (Tyson *et al.*, 1979).

2.3.4 PRESERVATION CONTROLLED KCF ENVIRONMENT RECONSTRUCTIONS

A selection of KCF reconstructions, which are based on preservational control are briefly described and problems associated with each reconstruction are summarized.

a) "Irregular Bottom Topography Model" (Hallam and Bradshaw, 1979) (Figure 2.5)

Bottom water circulation was inhibited by topographic irregularities, local depressions and areas with greater rates of subsidence, leading to isolated pockets of stagnant conditions. Stagnation within these depressions enabled enhanced accumulation of organic matter compared to areas of topographic height. Dependent on local topographic configuration, some depressions would eventually fill with sediment, allowing re-oxygenation and halting organic matter accumulation. The more rapidly subsiding depocenters however, kept pace with sedimentation and therefore did not become infilled and thus maintained bottom water anoxia, resulting in substantial thickness' of organic-rich sediment.

This simple reconstruction, suggesting localization of organic matter in isolated depressions, fails to account for the lateral extent of the oil shale and coccolith limestone marker bands across the whole Northwest European Basin (Gallois, 1976; Gallois and Medd, 1979; Cox and Gallois, 1981). These indicate that the environmental mechanisms controlling formation of these beds affected the entire area at the same time regardless of the differences in subsidence rate (Oschmann, 1988b).

b) "The North Atlantic Water Passage Model" (Oschmann, 1988b) (Figure 2.6)

During the summer months the Arctic Sea was characterized by upwelling driven by high latitude monsoonal wind circulation. The North Atlantic Shelf Sea was not wide enough to support similar upwelling (Parrish and Curtis, 1982), but the cold Arctic waters upwelled onto the northern European shelf margin. These cold waters flowed southwards in the North Atlantic Shelf Sea as a dense bottom current beneath a warmer surface water layer. As the bottom current travelled along the Viking and Central Grabens to Southern England its oxygen was consumed. Under this temperature-stratified water column, characterized by dysoxic to anoxic bottom waters, organic-rich sediments were deposited. On reaching Southern England the deep-water's temperature had increased sufficiently to be incorporated into a northward flowing counterflow of warmer, less dense surface waters. During the winter the Arctic upwelling declined and the

cold bottom current was not formed, thus water column stratification was broken down, preventing deposition of organic-rich sediments.

This reconstruction hinges on the palaeoclimate and the substantial palaeogeographic extent of the KCF. Despite this regional outlook, KCF stratigraphy shows that organic-rich sediments were restricted to two distinct regions separated by organic-poor sediments (Wignall, 1994). If a two-layer flow system was in operation, organic-rich sediment should have been evident along the entire length of the bottom current transect, but this is not the case. Also the initial upwelled Arctic waters would have been highly oxygenated and thus have travelled well beyond the most northerly limit of organic-rich sediments before becoming anoxic (Miller, 1990). Further more, the Ekman transport effect would have deflected the polar bottom current along the coastline of East Greenland and not along the North Sea grabens. KCF fauna of a northern Boreal affinity also implies the surface current flowed to the south and not the north as proposed (Miller, 1990).

c) "Warm Saline Bottom Water Model" (Miller, 1990) (Figure 2.7)

A Boreal current flowed from the polar Boreal Ocean southwards into Tethys evidenced by the Boreal nature of fauna within the KCF and a decline in radioactivity and uranium content within shales from north to south (Miller, 1990). The Coriolis force concentrated the current down the coasts of Greenland and Canada and with the constricted 'bottleneck' of the seaway from the Boreal Ocean, resulted in extremely slow rates of flow over the British Isles and North Sea. Combined with a warm climate, the slow flow rates (1km per day) led to a negative water balance for the Northwest European Basin. Here evaporation generated warm saline bottom waters (WSBW as defined by Brass *et al.*, 1982), while the southerly cold surface water flow balanced the evaporation. In basinal areas under this stratification, the water quickly became anoxic and organic-rich sediment accumulated.

To illustrate the dynamics and sensitivity of this reconstruction, oxygen isotope ratios (Irwin *et al.*, 1977) and hypothetical, but plausible, values for temperature and salinity were utilized by Miller. Surface waters of 0-26^{o}C and WSBW of 30^{o}C are suggested, an inverse temperature profile to Oschmann's model. Despite a density variation between the two water masses of only 0.00022gcm^{-3}, it would be adequate to cause basin stratification, but the stratification would also be vulnerable to break down. A cooling of the Boreal surface current by 2-4^{o}C would raise surface water density sufficiently to displace the now slightly less dense WSBW below, thus breaking the stratification.

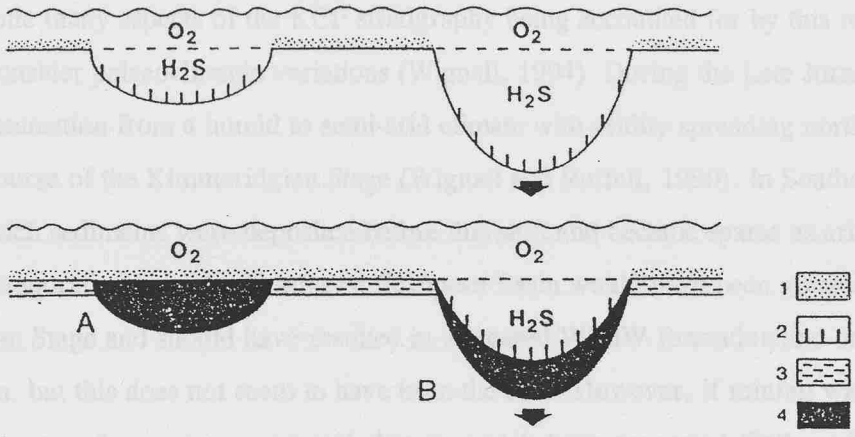

Figure 2.5
Irregular Bottom Topography Model. After Hallam and Bradshaw (1979)
Depressions, caused by topographic lows and greater subsidence rates inhibited bottom water circulation resulting in stagnant bottom conditions.
A = Local depression. B = Rapidly subsiding area. 1 = Aerobic environment.
2 = Anaerobic environment. 3 = Bioturbated shale. 4 = Bituminous shale.

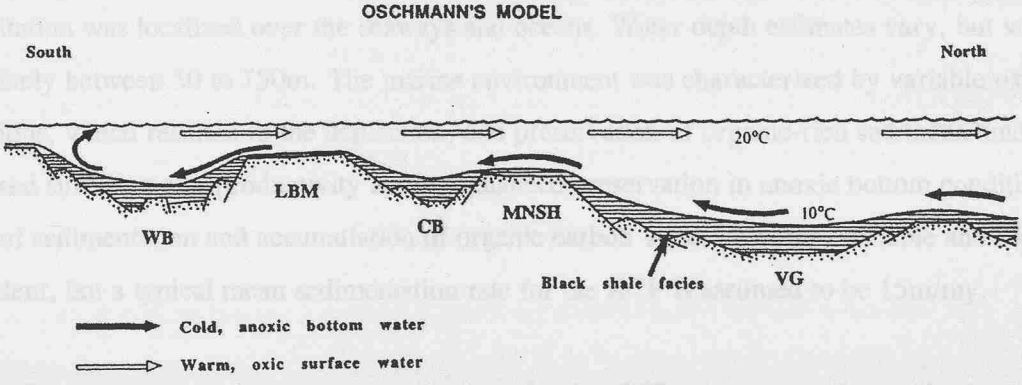

Figure 2.6
North Atlantic Passage Model. After Oschmann (1998b)
WB = Wessex Basin. LBM = London-Brabant Massif. CB = Central Basin.
MNSH = Mid North Sea High. VG = Viking Graben.

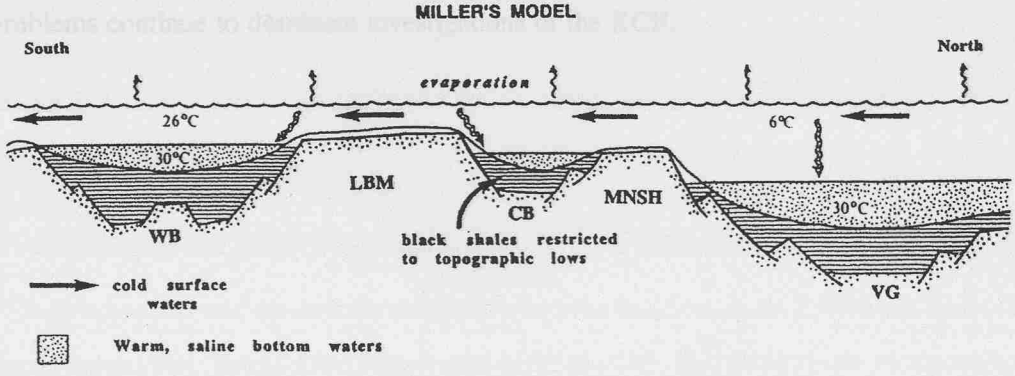

Figure 2.7
Warm Saline Bottom Water Model. After Miller (1990).

Despite many aspects of the KCF stratigraphy being accounted for by this reconstruction it does not consider palaeoclimatic variations (Wignall, 1994). During the Late Jurassic, Europe witnessed a transition from a humid to semi-arid climate with aridity spreading northwards during the course of the Kimmeridgian Stage (Wignall and Ruffell, 1990). In Southern England the organic-rich sediments were deposited before this shift and became sparse as aridity increased. Evaporation over the Northwest European Basin would have been greatest in the later Kimmeridgian Stage and should have resulted in increased WSBW formation and organic matter accumulation, but this does not seem to have been the case. However, if rainfall was predominately over the oceans, as several climate models have suggested (Sellwood and Valdes, 1997), the apparent lack of major fluvial runoff would still support a negative water balance within the sea (Miller, 1990).

2.4 SUMMARY

The deposition of the KCF took place in a series of basins in the rift system of the North Atlantic Shelf Sea. Climate is believed have been semi-arid with little continental runoff, and any precipitation was localized over the seaways and oceans. Water depth estimates vary, but were most likely between 50 to 150m. The marine environment was characterized by variable oxygen conditions, which resulted in the deposition, and preservation of organic-rich sediments under increased surface water productivity and/or enhanced preservation in anoxic bottom conditions. Rates of sedimentation and accumulation of organic carbon were, however, variable and locality dependent, but a typical mean sedimentation rate for the KCF is assumed to be 15m/my.

The palaeoenvironmental reconstructions for the KCF are varied and provide many possible explanations for its lithological sequence. However, despite these models, the environmental regime that controlled the KCF deposition is still not satisfactorily understood, both at a local and regional scale and the control of the accumulation of organic matter in the Kimmeridge environment is still divided between productivity and preservational mechanisms. These problems continue to dominate investigations of the KCF.

3.0 FABRIC ANALYSIS AND METHODOLOGY

When attempting to interpret the environment of deposition of sediments it is crucial to examine the microtextures of the lithologies and to understand the relationship between the organic matter, microfossils and the mineral matrix. The scanning electron microscope (SEM) is a powerful tool in the high-resolution, sedimentological study of rocks such as the KCF. Briefly summarised below are the SEM methods and other techniques used during this study. The results obtained from backscattered electron imagery (BSEI) analysis on the KCF fabric are presented. These results are interpreted in Chapter 4, with a discussion on the depositional environment and its processes, before environmental reconstructions are made.

3.1 PRELIMINARY METHODS

3.1.1 POLISHED THIN SECTION (PTS) PREPARATION

Vertical slices of the core were taken perpendicular to the bedding surfaces and cut into 2cm wide sections. The sections were mounted on glass slides and cut in oil to a thin plane, before being ground down to a thin section on a copper composite disc. Progressive polishing, with decreasing grades (down to 1μm) of oil based diamond polishing compound, resulted in a final polished thickness of 200μm, suitable for SEM analysis. R. Jones and J. Ford undertook this preparation. The PTS were then coated in carbon before analysis in the SEM.

3.1.2 X-RADIOGRAPHY

X-radiography has been primarily used on unconsolidated marine sediments, due to its non-destructive nature (Calvert and Veevers, 1962), to examine lamination and latent sedimentary structures within the sediments (Soutar and Crill, 1977). It is a fast, cheap and effective method and is based on the differential passage of x-radiation through a heterogeneous media onto sensitive photographic film (Hamblin, 1962; Bouma, 1969). Denser materials absorb more x-rays resulting in lower film exposure and a whiter tone, while low-density materials result in greater film exposure, giving a blacker film tone. X-radiographic prints produce the reverse of these tones. Thus denser lithogenic laminae can be distinguished from more penetrable organic carbon-rich laminae. The resolution of this method is dependent on the thickness of the sediment slab, but very thin ($<200\mu$m) lamination is rarely clearly recorded (Pike and Kemp, 1996).

X-radiography was carried out on the Whitestone Band interval. A Hewlett Packard Faxitron X-ray cabinet (model 43855) was used at 56 to 75kV for between one to ten minutes. These ranges reflect the variation in lithology within this section, with higher voltages needed to produce any form of picture through the highly dense coccolithic fabric. The resultant X-

radiographs for the majority of this section did not enhance the visual effect of lamination within the coccolith limestone or reveal latent structures in the more homogeneous mudstones. This is believed to have been a result of the fabric being dominated by coccolithic debris, and as such it lacks substantial density variations. However, one small ten centimetre section of a coccolith-rich, laminated oil shale did produce a good X-radiograph, due to the density variations between the organic carbon-rich and the coccolith lithology within this section (Figure 3.1a and b, Lower oil shale (1) Figure 1.4A).

With the limited success of this method on the Whitestone Band interval and the fractured nature of the remaining intervals, especially the Bed 44 mudstone, X-radiography was not carried out on the other intervals.

3.2 SCANNING ELECTRON MICROSCOPY (SEM) METHODS

A JEOL 6400 scanning electron microscope, which can be used in both secondary electron imagery (SEI), and backscattered electron imagery (BSEI) mode, was used for analysis of PTS samples. The JEOL 6400 is also fitted with a Princeton Gamma-Tech energy dispersive spectrometry (EDS) microanalyser and IMIX Ver.9 software which is further discussed in Section 3.2.3. Suitable operating voltages were found to be between 15kV and 20kV for PTS slides, while stubs required a lower voltage (10kV) to reduce charging effects.

Initial SEM analysis involved the production of low magnification BSEI basemaps, and BSEI photomosaics at 20X magnification of each PTS sample (Figure 3.1c). These provided preliminary base records of the sample fabric on which subsequent high-resolution analyses was carried out. During this study, the 20X BSEI photomosaics were also essential for the identification of the high-resolution palynology sample intervals. (See Appendix B for total number of PTS analyzed and listings of PTS sources for figures in this chapter).

FIGURE CAPTIONS

Figure 3.1a - Hand specimen black and white photograph of a coccolith-rich oil shale (1) below the WSB coccolith limestone. Both the lithology and microfabric are highly variable.

Figure 3.1b - X-radiographic print (actual size) of the coccolith-rich oil shale of 3.1a, WSB. Fine laminations that were not seen in hand specimens are evident with this technique.

Figure 3.1c - BSEI photomosaic (x20) of the coccolith-rich oil shale, WSB. The variability of the organic matter and carbonate, and the microfabrics can be seen in detail. Low-resolution mosaics such as this form the bases of further high-resolution analysis and provide a means of relating hand specimen to millimetre scale analysis.

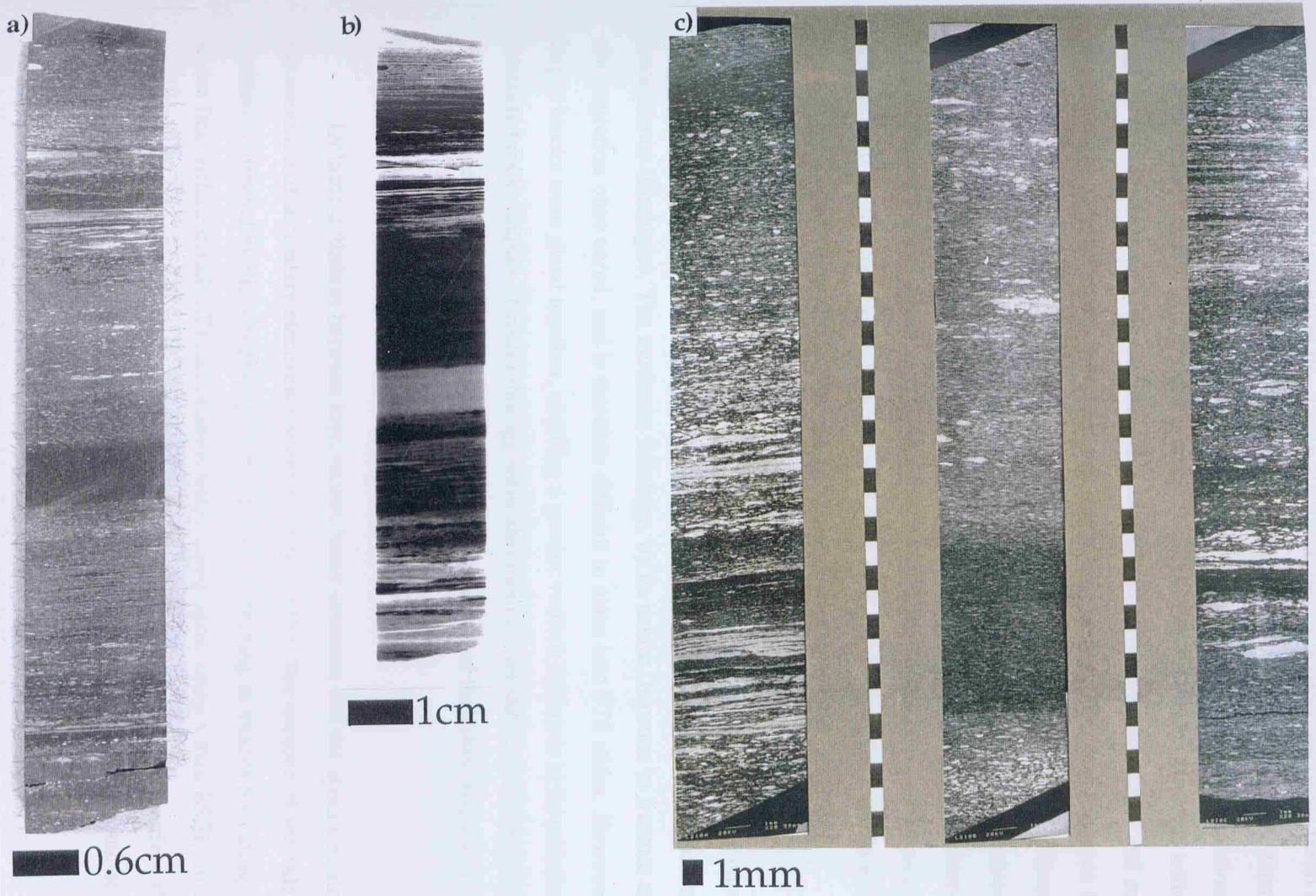

Figure 3.1

3.2.1 BACKSCATTERED ELECTRON IMAGERY (BSEI)

Backscattered electron imagery (BSEI) is used to distinguish between different elemental compositions within a material. This is shown by the grey scale contrast on the backscatter photographic image (Bishop *et al.*, 1992). Elastic collisions between energetic beam electrons and atoms within the specimen result in the emission of backscattered electrons. This is related to the backscatter coefficient, a function of the average atomic number of the specimen target, and is recorded in the brightness of the image (Goldstein *et al.*, 1992). Minerals with relatively high atomic numbers (e.g. pyrite, carbonate and quartz) have high-backscatter and subsequent bright images. Organic matter however, has low atomic numbers and thus produces low-backscatter and subsequently darker images. The backscatter image for the KCF therefore distinguishes between the high-backscatter, brighter coccolithic laminae from the low-backscatter, darker organic-rich laminae, and provides a precise and complete picture of the organo-mineral texture. Many authors have performed microstructure examination of organic-rich rocks using this technique. Previous studies of KCF fabrics include Bertrand *et al.*, (1990), Belin (1992), Macquaker and Gawthorpe (1993), and Boussafir *et al.*, (1995).

BSEI was carried out on all sections whose fabric remained consolidated enough to enable preparation of PTS slides, predominately the oil shale, coccolith limestone and cementstone lithologies. The mudstone lithology, by its nature, is prone to fracture and disintegration once cored, and is therefore difficult to make into PTS slides. However some larger blocks were glued together, enabling a greater vertical thickness to be examined. Fractured rock samples of each lithology were also mounted on stubs, coated in gold and examined under the SEM enabling topographic examination of the fabric and microfossils.

3.2.2 SECONDARY ELECTRON IMAGERY (SEI)

Inelastic collisions between high-energy beam electrons and the specimen atoms result in the emission of secondary electrons (Goldstein *et al.*, 1992). The number of secondary electrons emitted is effected by the topography of the specimen resulting in images providing information about fine surface detail. SEI can produce better topographic images than BSEI, though specimen charging in this mode can be problematical. This arises due to imperfect PTS specimen polishing owing to hardness differences, which leads to penetration and scattering from grain edges (Krinsley *et al.*, 1998).

3.2.3 ENERGY DISPERSIVE X-RAY MICROANALYSIS (EDS)

Used in conjunction with the SEM, EDS uses the production of X-ray radiation from the interaction of the electron beam with the specimen, to obtain qualitative and quantitative

chemical analysis of minerals within the PTS. The technique provides the means to undertake point analysis, line scans and elemental X-ray maps of samples. Combined with BSE images this technique provides additional chemical information to the visual PTS descriptions.

KEY TO FIGURE ANNOTATIONS FOR SECTIONS 3.3 TO 3.7

ORGANIC CARBON FORMS

OMb = Organic matter bleb

OMl = Organic matter lath

OMwr = Organic matter wavy ribbon

OMes = Organic matter elongated stringer

OMts = Organic matter thick stringer

OMel = Organic matter elongated lens

CARBONATE FORMS

CAsp = Calcisphere

Csp = Coccosphere

C = Coccolith

Cs = Coccolith stringer

Cpl = Coccolith pelletal lens

Spl = Sparry pelletal lens

OTHER FABRIC COMPONENTS

Pf = Pyrite framboid

Pe = Pyrite euhedral grain

Q = Quartz grain

F = Feldspar grain

B = Bioclast

Bs = Bioclast, shell

3.3 FABRIC ANALYSIS - LITHOLOGY

The results of the KCF SEM fabric analysis are presented in four lithological divisions; 1) mudstone, 2) cementstone, 3) oil shale and bituminous shale, and 4) coccolith limestone. These reflect the variability between the amount of organic matter, carbonate and mineral matrix constituting the fabric that is evident in the Kimmeridge lithology. Details of the types of microfabrics (Section 3.4) and other notable features (Section 3.5) follow the lithological compositional descriptions.

The majority of the fabric description is based on high-resolution SEM analysis of the Whitestone Band interval. This is followed by a comparison with the other studied intervals to highlight lithological differences (Sections 3.6 and 3.7). An interpretation and discussion of the sedimentary environment in which each lithology was believed to have been deposited is given in Chapter 4.

3.3.1 MUDSTONE

The mudstones of the KCF are organic-poor, detrital sediments with a homogeneous morphology. Calcium, silica and aluminium dominate the elemental composition, with organic carbon, sulphur and iron as more minor components (Elemental Map 3.1). The matrix is a mixture of predominantly clays and coccolithic debris (Figure 3.2a and b). Coccolith plates are found both as whole plates and as partial segments, but rarely as complete coccospheres. Preservation of the coccoliths is fair to poor, with plate details and structures perceivable in some areas (Figure 3.2c).

Dispersed within the matrix are quartz and feldspar grains, pyrite and organic matter. Quartz grains are silt sized (10-30μm diameter), sub-angular to sub-rounded and are found discretely distributed throughout the matrix. Feldspars (10-20μm diameter) are less common but are similarly distributed in the matrix. Pyrite is present as loosely clustered framboids and euhedral grains of 5-15μm in diameter (Figure 3.2a).

Organic matter within the mudstones occurs in three forms. Firstly as dispersed or diffuse organic matter which is mixed with fine clay minerals and coccoliths to form the matrix. It forms a network of organic matter in which other particles are situated, it has no visible internal structure or fixed shape, but is amorphous. This diffuse, amorphous organic matter is an integral part of all lithologies of the KCF and represents a substantial amount of the organic matter present within them.

More apparent than the amorphous, matrix organic matter, are two forms of organic matter, which display some structural shape. Found randomly distributed in the matrix, discrete oval blebs to rectangular laths (5-10μm height and 10-20μm length) are prominent organic matter forms (Figure 3.2a and c). Thin wavy organic ribbons ($<10\mu$m height, 10-40μm in length), are the second type, which frequently display some loose grouping (Figure 3.2a). These more structured organic forms are a minor component of the mudstones compared to the amorphous, matrix organic matter.

LITHOLOGICAL COMPONENT	DISTRIBUTION IN LITHOLOGY	SIZE
Clays	Matrix component	microns
Coccoliths	Matrix component	3-7 μm
Organic Matter 1) Diffuse	Matrix component	Amorphous - variable
2) Oval blebs - rectangular laths	Discrete, randomly distributed in matrix	5-10 μm height, 10-20 μm length
3) Wavy ribbons	Discrete, loosely grouped in matrix	<10 μm height, 10-40 μm in length
Quartz	Individually distributed in matrix	10-30 μm diameter
Feldspar	Individually distributed in matrix	10-20 μm diameter
Pyrite	Loosely clustered framboids and euhedral grains	5 –15 μm diameter

Table 3.1 Summary of the lithological components within KCF mudstones, their distribution and size ranges.

FIGURE CAPTIONS

Elemental Map 3.1 - EDS grey scale map (x80) of a mudstone, WSB, showing domination of the matrix by calcium with abundant quantities of aluminium, potassium and silica. Iron and sulphur are similarly distributed and together with sodium are minor elements of the mudstone lithology. Carbon is an abundant element within the matrix, but shows increased abundance in discrete lenses together with sulphur.

Figure 3.2a - BSEI photomosaic (x300) of the general WSB mudstone fabric, predominantly composed of a well-mixed matrix of clays, coccoliths and amorphous organic matter. Quartz and feldspar grains are well dispersed, while framboidal and euhedral pyrite forms display loose clustering. Structured organic matter forms are present as discrete blebs and laths, and as wavy ribbons that display loose grouping (lower left corner of the figure).

FIGURE CAPTIONS

Figure 3.2b - Detailed BSEI photograph (x1500) of the WSB mudstone matrix with abundant, well mixed clays and degraded coccoliths.

Figure 3.2c - Detailed BSEI photograph (x2000) of two discrete organic matter blebs within the clay/coccolith matrix of the WSB mudstone. Note that some coccolith plate detail is visible (indicated by the arrows).

3.3.2 CALCAREOUS MUDSTONE

The calcareous mudstone differs from the mudstone in the dominance of the coccolith component of the matrix (Elemental Map 3.2). Some fabric structure is also evident in the form of lenses (Figure 3.2d), which appear as darker patches under BSEI. These lenses average several 100μm in length and approximately 100μm in height. Detailed examination shows them to be composed purely of coccoliths and rare coccospheres (Figure 3.2e), while the remaining matrix is a mixture of clays, quartz grains and organic matter as well as coccoliths (Figure 3.2f; Elemental Map 3.2).

The organic matter present within the calcareous mudstone is found in the same forms as those of the mudstone. The wavy organic ribbons are, however, more abundant and laterally persistent (300-400μm), though the organic blebs are similar. Rare calcispheres occur in the calcareous mudstone but not in the mudstone (Figure 3.2d, more detailed examples of calcispheres can be seen in Figures 3.15b and d). Pyrite framboids are of similar size (5-10μm diameter), but are less abundant than in the mudstone, especially in coccolith-rich intervals.

The calcareous mudstone forms a transition between the mudstone and the coccolith limestone lithologies, with the abundance of coccoliths in the matrix increasing between the two. Within the clay-rich calcareous mudstones, the coccoliths have poor to fair preservation and are well mixed with clays (Figure 3.3a, b and e; Figure 3.19c). Coccolith abundances increase in the calcareous mudstones and the clays in the matrix becomes less common (Figure 3.3c). Finally in the most calcareous mudstones, coccoliths dominate the matrix and show well preserved plates and occasional scattered whole coccospheres (Figure 3.3d). The clays become very rare and are found as thin, isolated lenses (Figure 3.3f). These changes in the fabric composition are subtle and gradational during this transition from mudstone to coccolith limestone (Figure 3.3a to d).

FABRIC COMPONENT	DETAILS
Matrix	Greater dominance of coccoliths, other fabric components become rare in extremely calcareous mudstones.
Lenses	100μm in height, several 100μm in length, composed of pure coccoliths and coccospheres, lack of other fabric components.
Organic Matter - wavy ribbons	Greater lateral continuity, reaching 300-400μm in extent.
Pyrite Framboids	5-10μm diameter, less abundant.

Table 3.2 Calcareous mudstone fabric components that differ from those of the mudstone.

FIGURE CAPTIONS

Figure 3.2d - BSEI photomosaic (x100) of WSB calcareous mudstone fabric. Note the darker patches/lenses (indicated by thick arrows), and the increased lateral persistence of the wavy organic ribbons compared to those in the mudstone lithology. A partially crushed calcisphere is present in the centre right of the mosaic which, though rare in this lithology, are not found in the mudstone lithology.

Figure 3.2e - Detailed BSEI photograph (x1000) of the internal fabric inside one of the darker lenses. It is completely dominated by coccoliths with occasional coccospheres, and preservation of the coccoliths is improved when compared to coccoliths in the matrix (See Figure 3.2f). Also note the lack of clays, pyrite, quartz and feldspar grains within the lens.

Figure 3.2f -Detailed BSEI photograph (x1000) of the WSB calcareous mudstone matrix, with less well preserved coccoliths than in the lenses, and abundant clays, quartz and feldspar grains.

Elemental Map 3.2 - EDS grey scale map (x80) of a calcareous mudstone, WSB, showing an increase in calcium abundance compared to the mudstone lithology (compare to Elemental Map 3.1 (Ca)). Calcite pelletal lenses are also evident in this fabric and are associated with increases in carbon, but other elements are rare or absent in these features. The matrix also contains abundant aluminium, potassium and silica as clays . Iron and sulphur are less abundant and discrete grains are grouped into small clusters within the matrix.

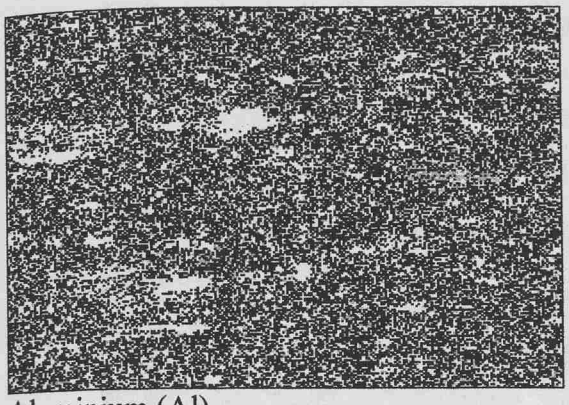

Aluminium (Al)

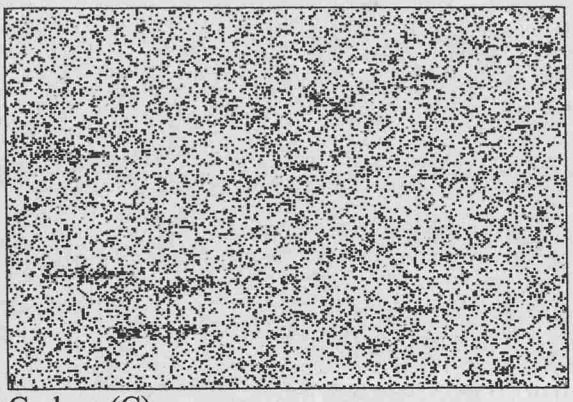

Carbon (C)

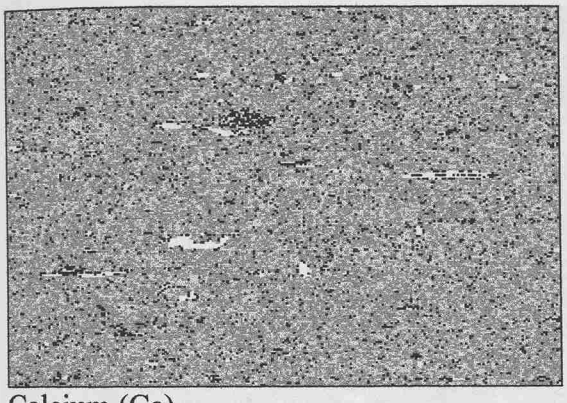

Calcium (Ca)

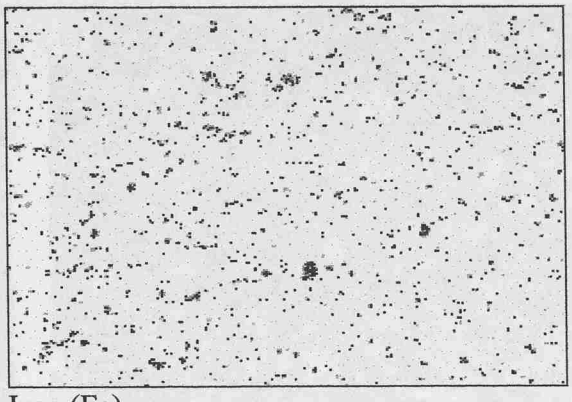

Iron (Fe)

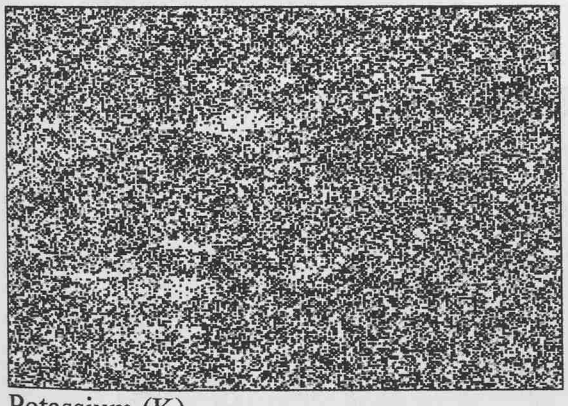

Potassium (K)

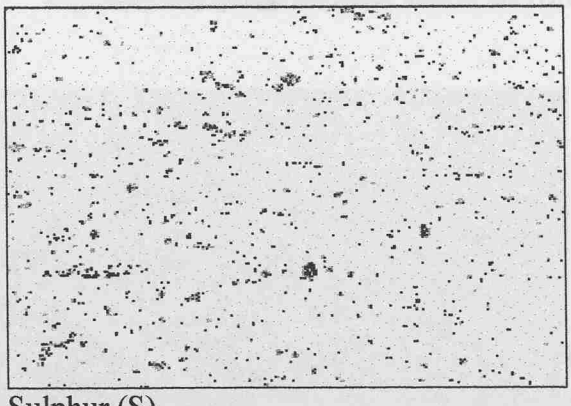

Sulphur (S)

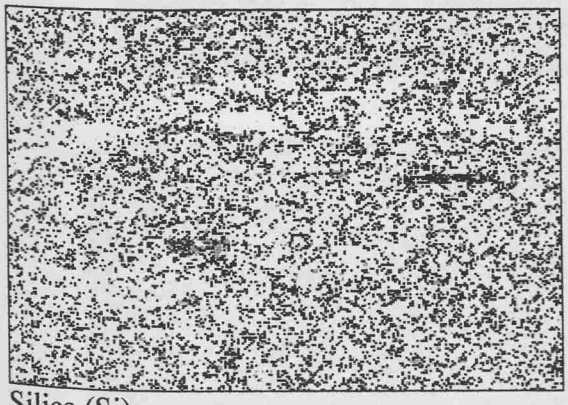

Silica (Si)

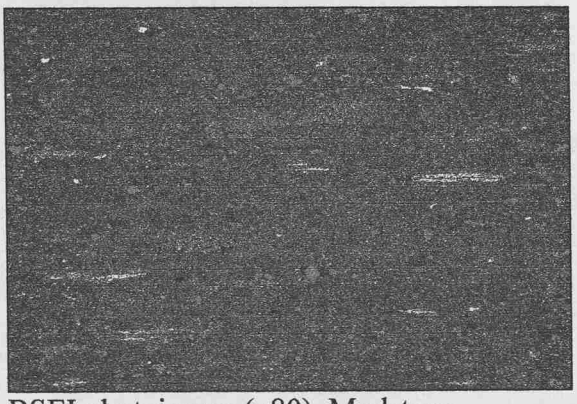

BSEI photoimage (x80), Mudstone, WSB.

Elemental Map 3.1

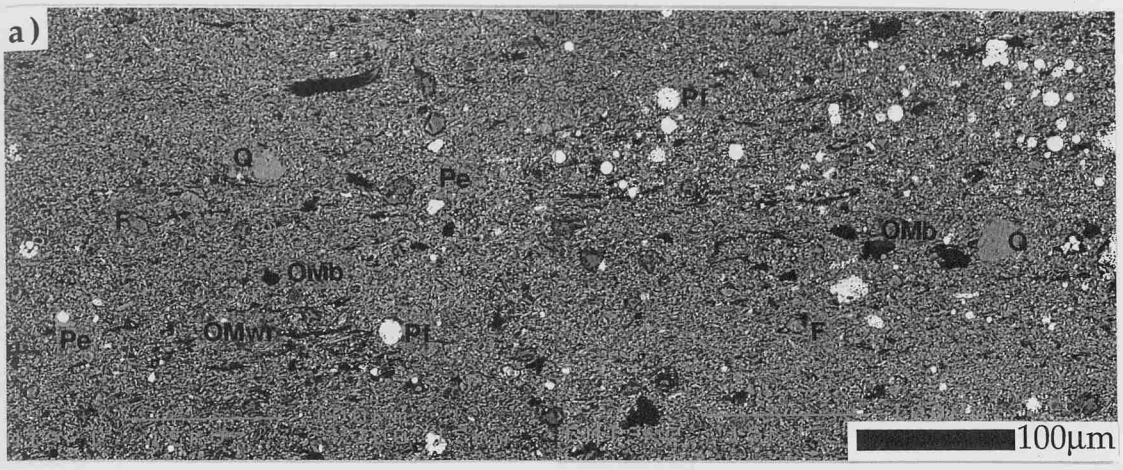
a)
Pl
Q
Pe
F
OMb
OMb
Q
Pe
OMwr
Pl
F
100µm

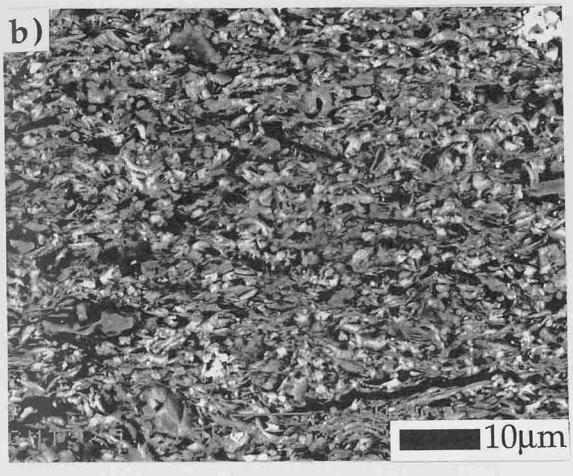
b)
10µm


c)
OMb
OMb
10µm

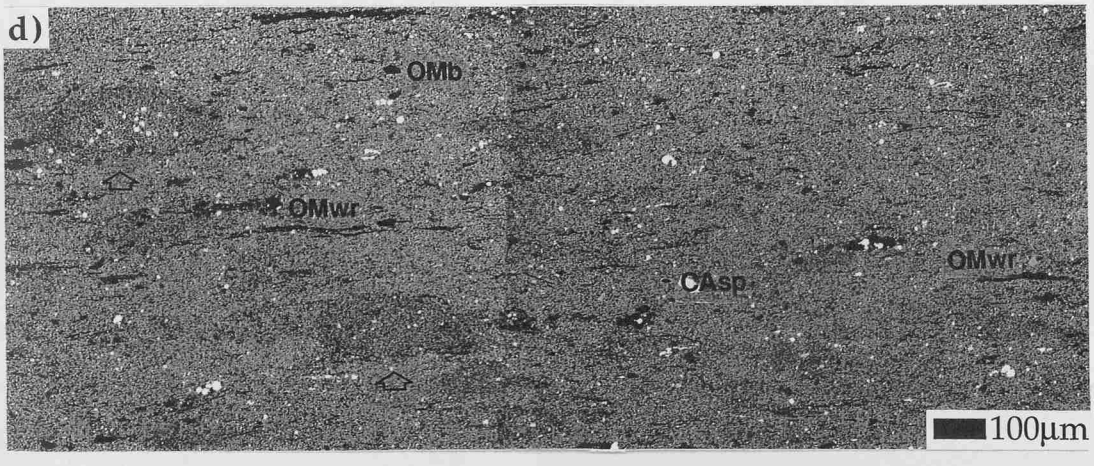
d)
OMb
OMwr
OMwr
CAsp
100µm

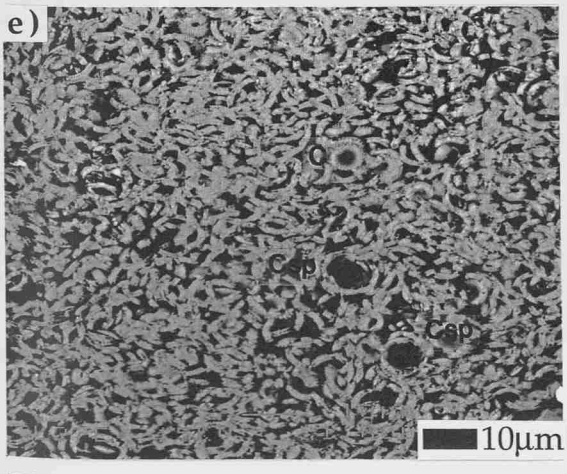
e)
Q
CAsp
CAsp
10µm

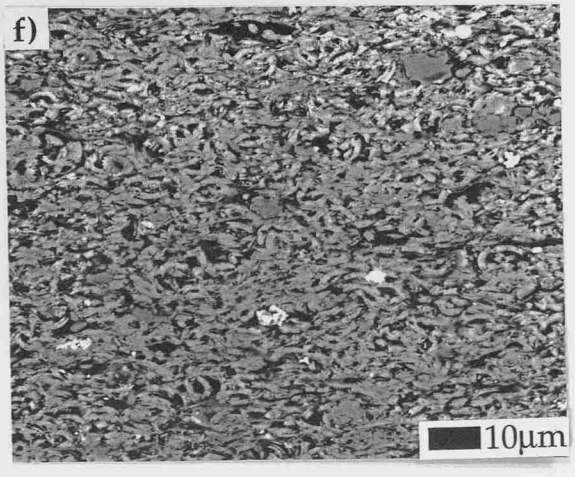
f)
10µm

Figure 3.2

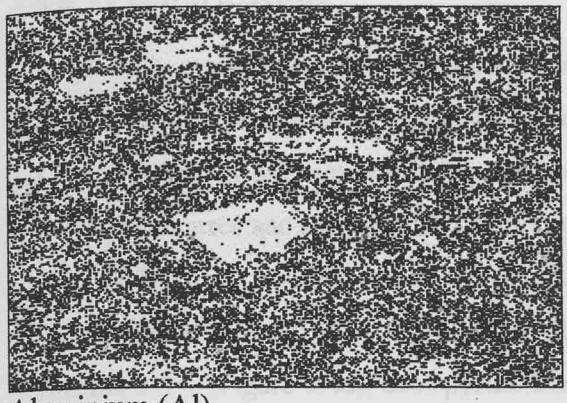

Aluminium (Al)

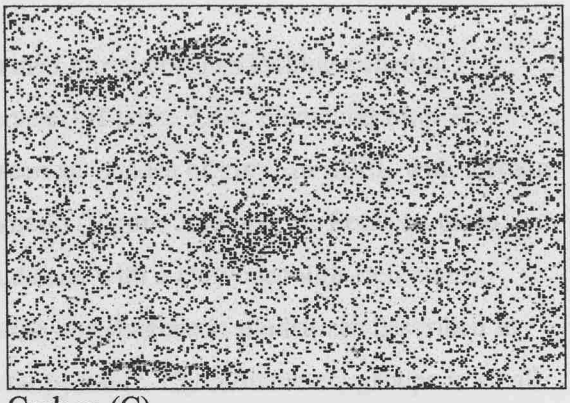

Carbon (C)

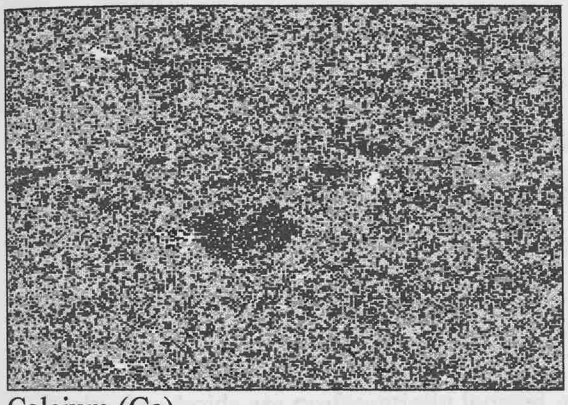

Calcium (Ca)

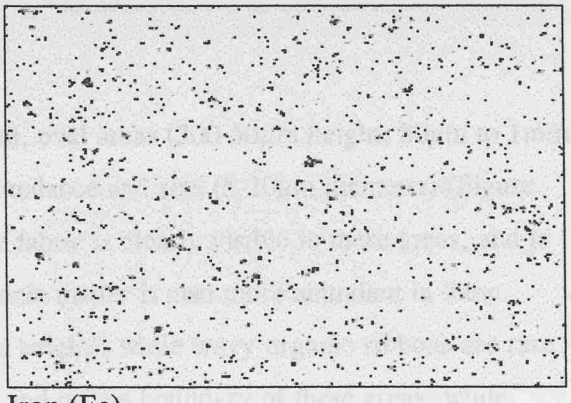

Iron (Fe)

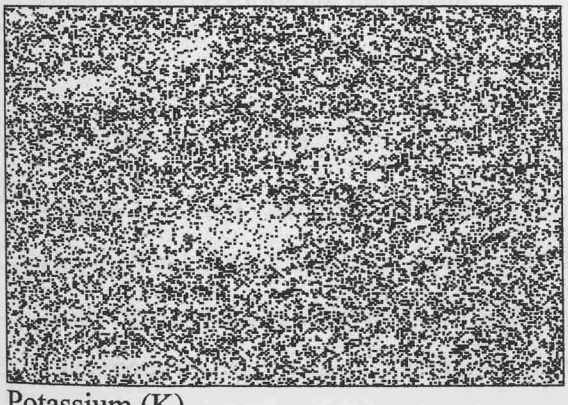

Potassium (K)

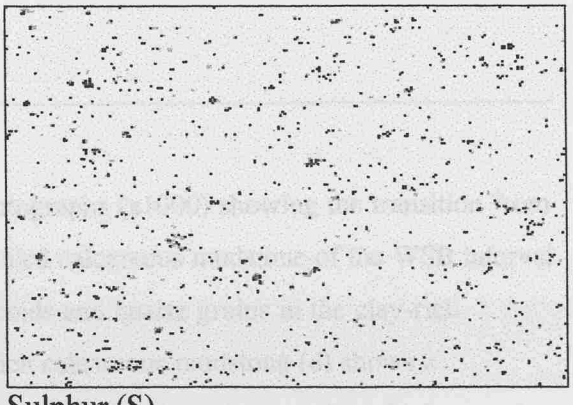

Sulphur (S)

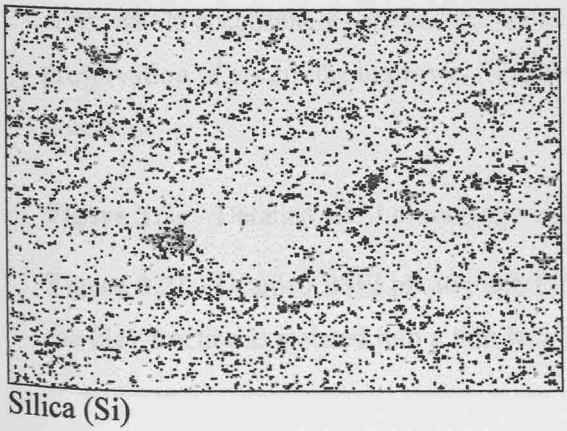

Silica (Si)

Elemental Map 3.2

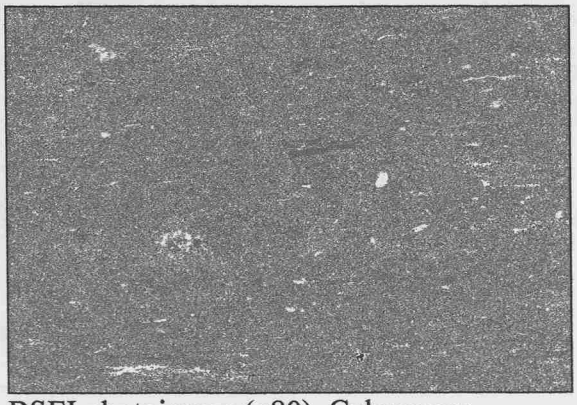

BSEI photoimage (x80), Calcareous Mudstone, WSB.

3.3.3 CEMENTSTONE

The cementstone is composed of a fine grained mosaic of interlocking euhedral / subhedral ferroan dolomitic crystals (10-50μm diameter) (Figure 3.4a; Elemental Map 3.3). Compositional differences within the crystals are seen as 'shades of grey' in BSEI, with ferroan dolomitic centres and calcitic rims (2-3μm in thickness) (Figure 3.4a and c). Between these ferroan dolomitic crystals the primary fabric is mudstone with a clay/coccolith-rich matrix. Organic matter, however, is less abundant than in the non-diagenetic mudstones described in Section 3.3.1 (Figure 3.4c), as is pyrite. Framboidal pyrite (5-15μm diameter) groups in small clusters and occurs more frequently than the euhedral pyrite grains, which occur singularly and more commonly reach 15-20μm in size.

The cementstone contains discrete flattened, oval areas (300-50μm height, 80μm to 1mm length), with reduced ferroan dolomitic crystal abundance and size (5-20μm diameter) (Figure 3.4b; Elemental Map 3.3). The primary mudstone fabric is clearly visible in these areas, and is dominated by clays and degraded coccoliths. Organic matter is also more abundant in these areas, commonly as blebs (10-30μm length, 10μm height), while wavy organic ribbons are rare. Pyrite framboids are preferentially located within and on the boundary of these areas, while euhedral pyrite forms are infrequent.

FIGURE CAPTIONS

Figure 3.3a to d - Sequence of detailed BSEI photographs (x1000) showing the transition from clay-rich calcareous mudstone to coccolith-dominated calcareous mudstone of the WSB interval. Note the presence of organic matter, pyrite framboids and quartz grains in the clay-rich calcareous mudstones (a-c). The most coccolith-rich calcareous mudstone (d) shows a dominance of coccoliths with the clay concentrated into a thin lens (indicated by thick arrow). Also, whole coccospheres are present in the most coccolith-rich calcareous mudstone, and the preservation of coccoliths improves from the clay-rich to the coccolith-rich calcareous mudstone.

Figure 3.3e - Detailed BSEI photograph (x2700) of a clay-rich calcareous mudstone, WSB.

Figure 3.3f - Detailed BSEI photograph (x2700) of a coccolith-rich calcareous mudstone, where the clay fraction is isolated into a thin lens (indicated by thick arrow).

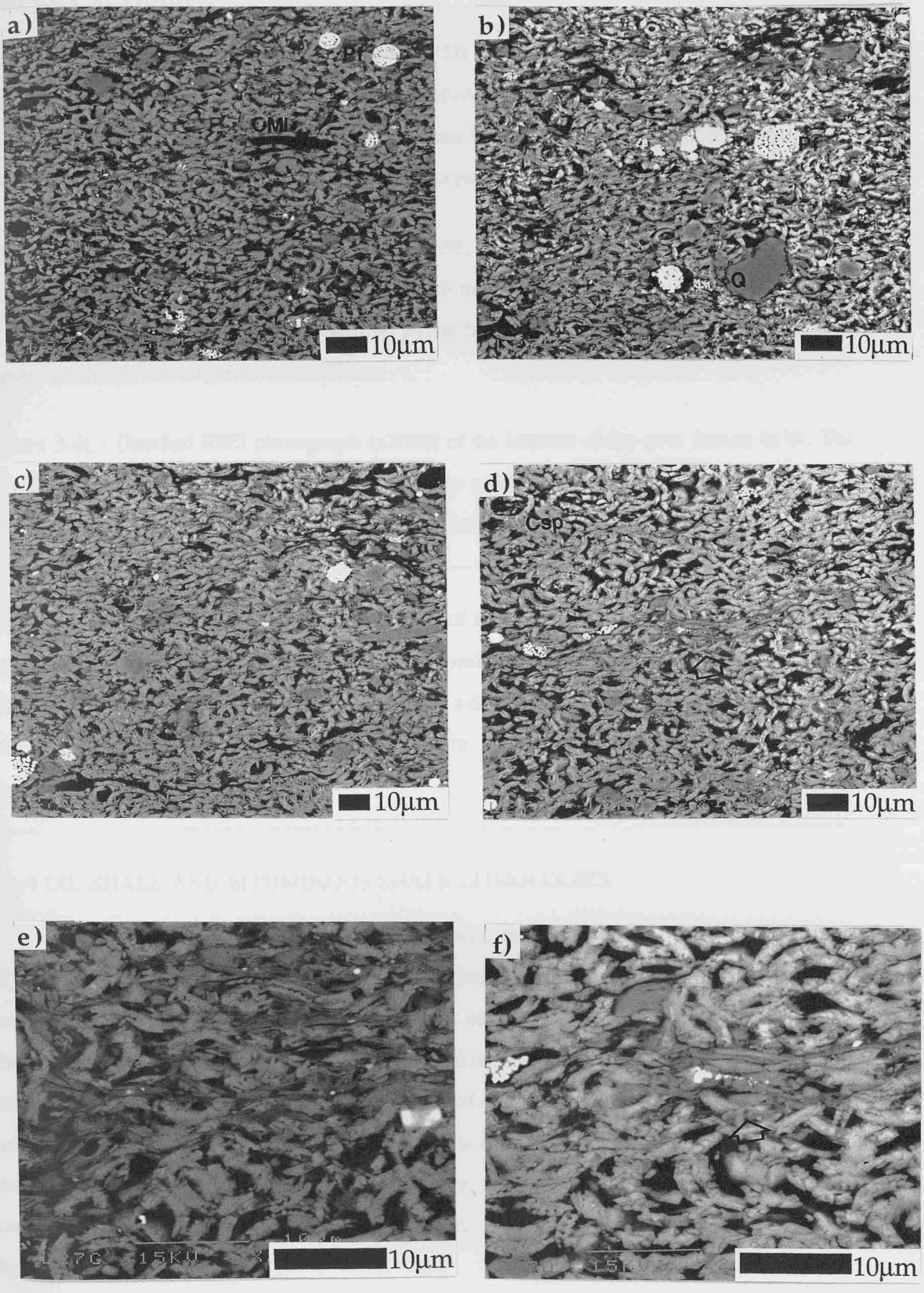

Figure 3.3

FIGURE CAPTIONS

Figure 3.4a - BSEI photomosaic (x300) of the WSB cementstone fabric showing the interlocking euhedral/subhedral ferroan dolomitic crystals. Between crystals the primary mudstone is visible. Pyrite framboids are common, while organic matter blebs are present but not abundant. Note the lighter rims around the majority of the dolomite crystals, these are calcitic.

Figure 3.4b - BSEI photograph (x120) of a discrete, flatten, oval area characterised by reduced ferroan dolomitic crystal abundance and size, with the primary mudstone fabric clearly evident in between. Note the preferential location of pyrite framboids in and around this feature and the greater abundance of organic matter blebs.

Figure 3.4c - Detailed BSEI photograph (x1000) of the interior of the oval feature in b). The clay/coccolith-rich mudstone fabric is similar to the mudstone of Figures 3.2a-c. Note the light calcitic rims on the ferroan dolomitic crystals (indicated by the arrow).

Elemental Map 3.3 - EDS grey scale map (x80) of the ferroan dolomitic cementstone, WSB, composed predominately of calcium, magnesium and iron. Aluminium, potassium and silica are also relatively abundant. In the centre of the map a discrete flattened, oval area displays a decrease in dolomite (Ca and Mg) while aluminium, silica, carbon and sulphur all increase in abundance.

3.3.4 OIL SHALE AND BITUMINOUS SHALE LITHOLOGIES

The KCF lithological composition is predominately controlled by the relative abundance of carbonate and organic matter. An oil shale or bituminous shale occurs where the organic matter component is more abundant relative to the carbonate component. Some of the KCF oil shales and bituminous shales, however, do contain carbonate laminae (Figure 3.1a to c). In such intervals some laminae are composed completely of carbonate, but over the entire interval the relative abundance of the carbonate is less than that of the organic matter. The following descriptions for the organic carbon-rich lithologies, are divided into organic matter components, carbonate components and other fabric components, with examples shown in the intervening figures.

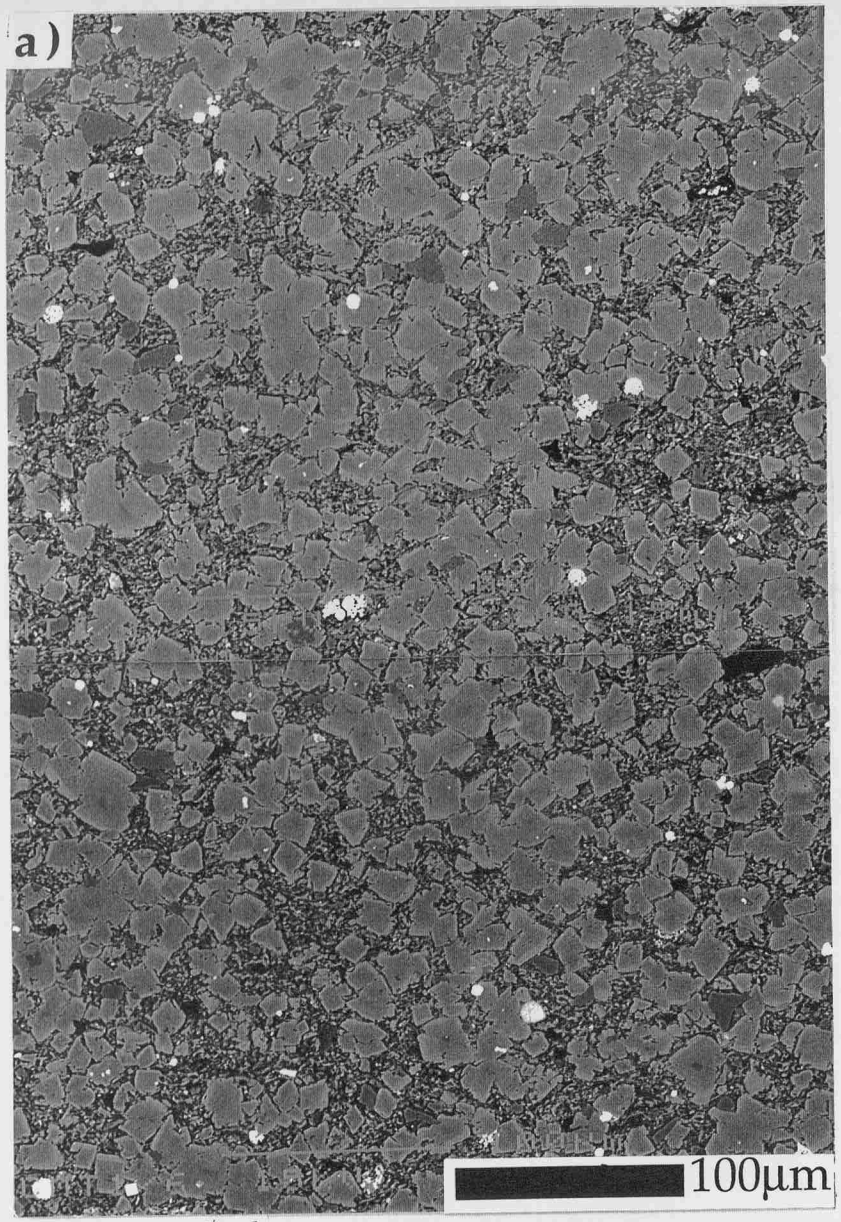

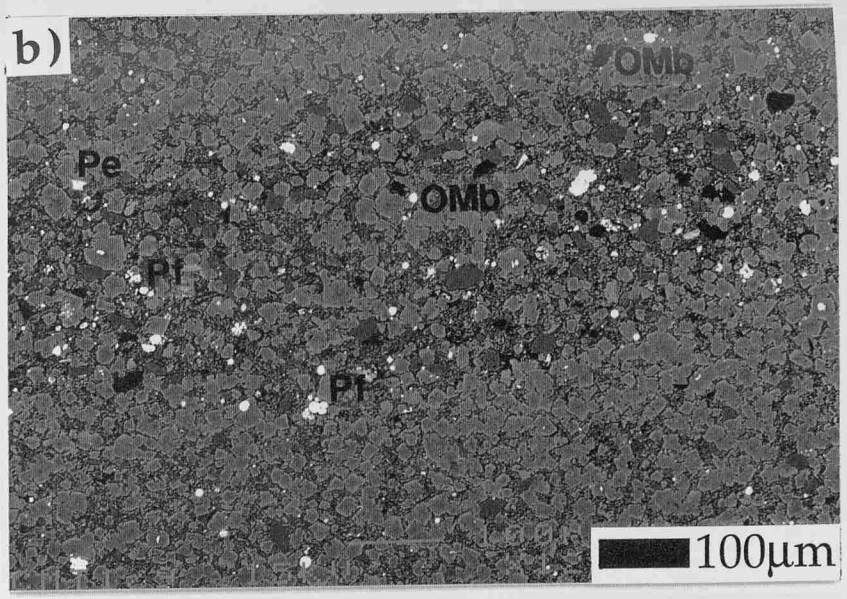

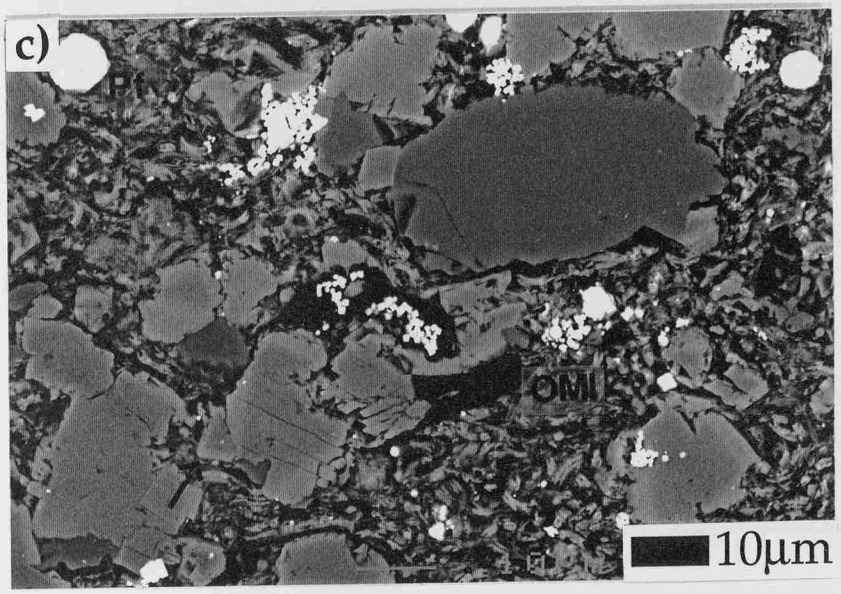

Figure 3.4

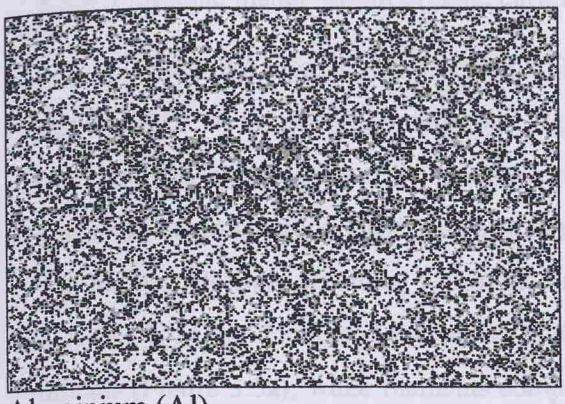

Aluminium (Al)

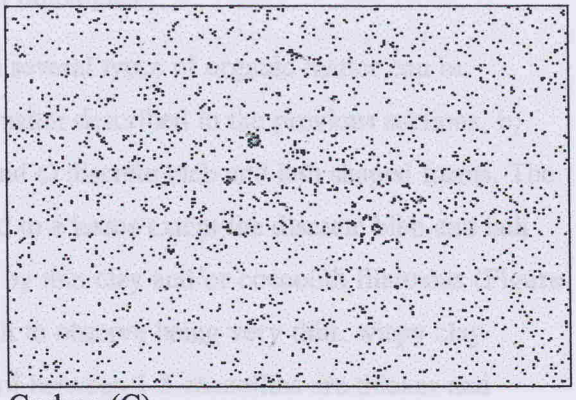

Carbon (C)

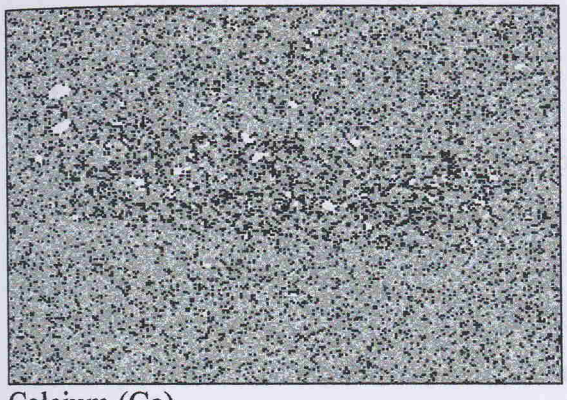

Calcium (Ca)

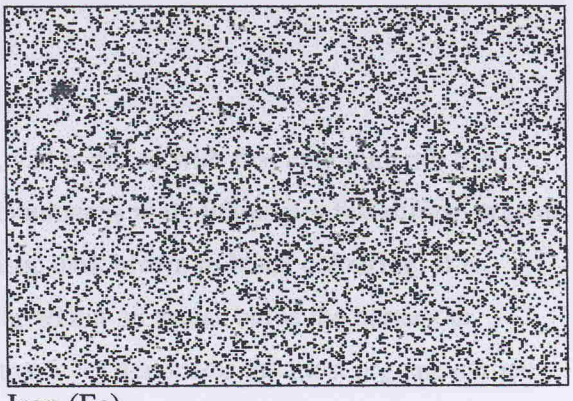

Iron (Fe)

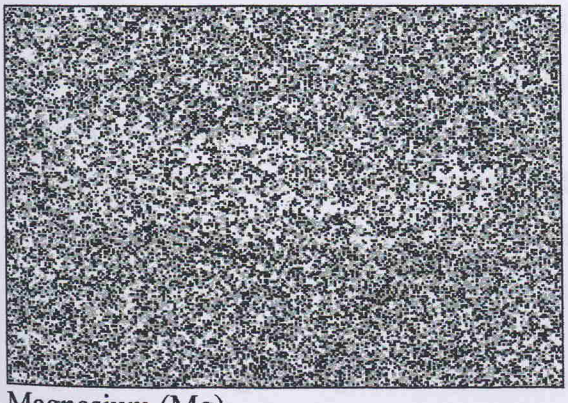

Magnesium (Mg)

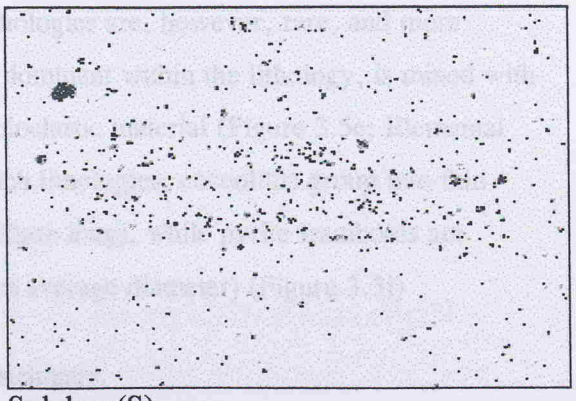

Sulphur (S)

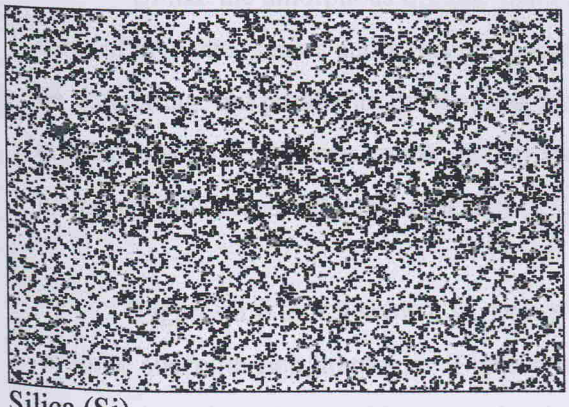

Silica (Si)

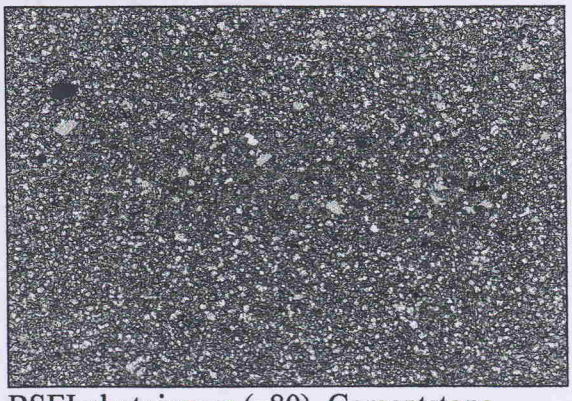

BSEI photoimage (x80), Cementstone, WSB.

Elemental Map 3.3

3.3.4.1 Organic matter within organic carbon-rich lithologies

Within the organic carbon-rich lithologies several types of organic matter can be distinguished; a) the diffuse, amorphous organic matter described in the previous sections, b) discrete elongated lenses and stringer structures and c) discrete bleb and lath shaped forms. The elongated organic carbon lenses and stringers, and to a lesser extent the discrete bleb and lath organic particles, are separated within the fabric, by thin clay and/or coccolith filaments (Figure 3.5a and b). Clay-dominated filaments are difficult to observe being very thin, wispy clay threads (Figure 3.5a), while filaments composed of between 1-5 coccoliths are thicker and therefore more prominent (Figure 3.5b).

a) Diffuse, amorphous organic matter

This type of organic matter is amorphous, and is mixed with fine clay minerals and coccoliths to form the matrix. Within the oil and bituminous shale lithologies this diffuse organic matter dominates, giving the matrix the characteristic dark brown to black colouring. It is probably the most important form of organic matter within oil shales but is the hardest to quantify. Diffuse, amorphous organic matter (Figure 3.5c) dominates the most organic carbon-rich lithologies, with small pyrite framboids ($\leq 5\mu$m average diameter), clays and coccoliths (Figure 3.5d). Such highly organic carbon-rich lithologies are, however, rare, and more commonly the amorphous organic matter, though dominant within the lithology, is mixed with abundant pyrite framboids, coccoliths, clays and bioclastic material (Figure 3.5e; Elemental Map 3.4). Within these relatively mixed carbon-rich lithologies, coccoliths group into thin elongated lenses ($< 100\mu$m thick, up to several 100μm long), while pyrite framboids are abundant, with a slightly wider size range ($\leq$5-7μm average diameter) (Figure 3.5f)

b) Discrete, elongated organic carbon lenses and stringers.

Unlike the amorphous organic matter, this type of organic matter is structured in the form of elongated lenses and stringers of highly variable length, thickness and abundance. These lie undulating, but parallel to the bedding plane and frequently drape over other lithological components such as quartz grains and carbonate pelletal structures. Stringers are more laterally continuous than lenses (Compare lenses in Figure 3.7a, to stringers in 3.9d).

Figures 3.6 to 3.9 show a variety of organic carbon-rich lithologies (Figures 3.6 - 3.7) to more coccolith-rich lithologies (Figures 3.8 - 3.9), containing different sizes and abundances of organic carbon elongated lenses and stringers. Where amorphous organic matter dominates the lithology, organic stringers and lenses are difficult to identify (Figure 3.5a and c). Slight increases in the relative abundance of carbonate/coccoliths helps to delineate the stringers and

lenses (Figure 3.6a-c). In more coccolith-dominated lithologies the organic matter stringers (Figure 3.8b-d) and elongated lenses (Figure 3.7a and 3.8a) are well defined. The relative abundance, thickness and continuity of elongated lenses and stringers increase from coccolith-rich to organic carbon-rich lithologies.

FIGURE CAPTIONS

Figure 3.5a - Detailed BSEI photograph (x1400) showing wispy, clay thread filaments, with a few loose coccoliths, dividing organic matter stringers in an organic carbon-rich lamina, WSB.

Figure 3.5b - BESI photograph (x500) of coccolith-dominated filaments, dividing organic stringers, WSB. Note the prominence of these filaments compared to the clay dominated ones.

Figure 3.5c - BSEI photograph (x120) of a highly organic carbon-rich layer (between thick arrows). Diffuse, amorphous organic matter dominates this layer, while either side an increase in other lithological components dilutes the amorphous organic matter.

Figure 3.5d - Detailed BSEI photograph of 3.5c (x300), highlighting the dominance of the diffuse, amorphous organic matter matrix and the dispersed nature of pyrite framboids, clays and coccoliths. Note that the majority of coccoliths occur singularly, but are situated in broken lines of coccoliths that are parallel to the bedding (indicated by the arrow).

Figure 3.5e - BSEI photograph (x140) of an organic carbon-rich lithology with abundant clays, coccoliths, pyrite framboids and bioclastic material, WSB.

Figure 3.5f - Detailed BSEI photograph of 3.5e (x350) showing highly abundant pyrite framboids, and coccoliths grouped in thin elongated lenses, WSB.

Elemental Map 3.4 - EDS grey scale map (x80) of a series of organic carbon-rich layers within an oil shale, WSB (See Figure 3.5c). Carbon and sulphur dominate the fabric especially in the central, highly organic layer. Either side of this layer calcium is highly abundant in pelletal lenses. Aluminium and potassium are relatively abundant in the calcium-rich layers, while iron and silica are less abundant. Within the highly organic carbon-rich layer all elements, except carbon and sulphur show reduced abundances.

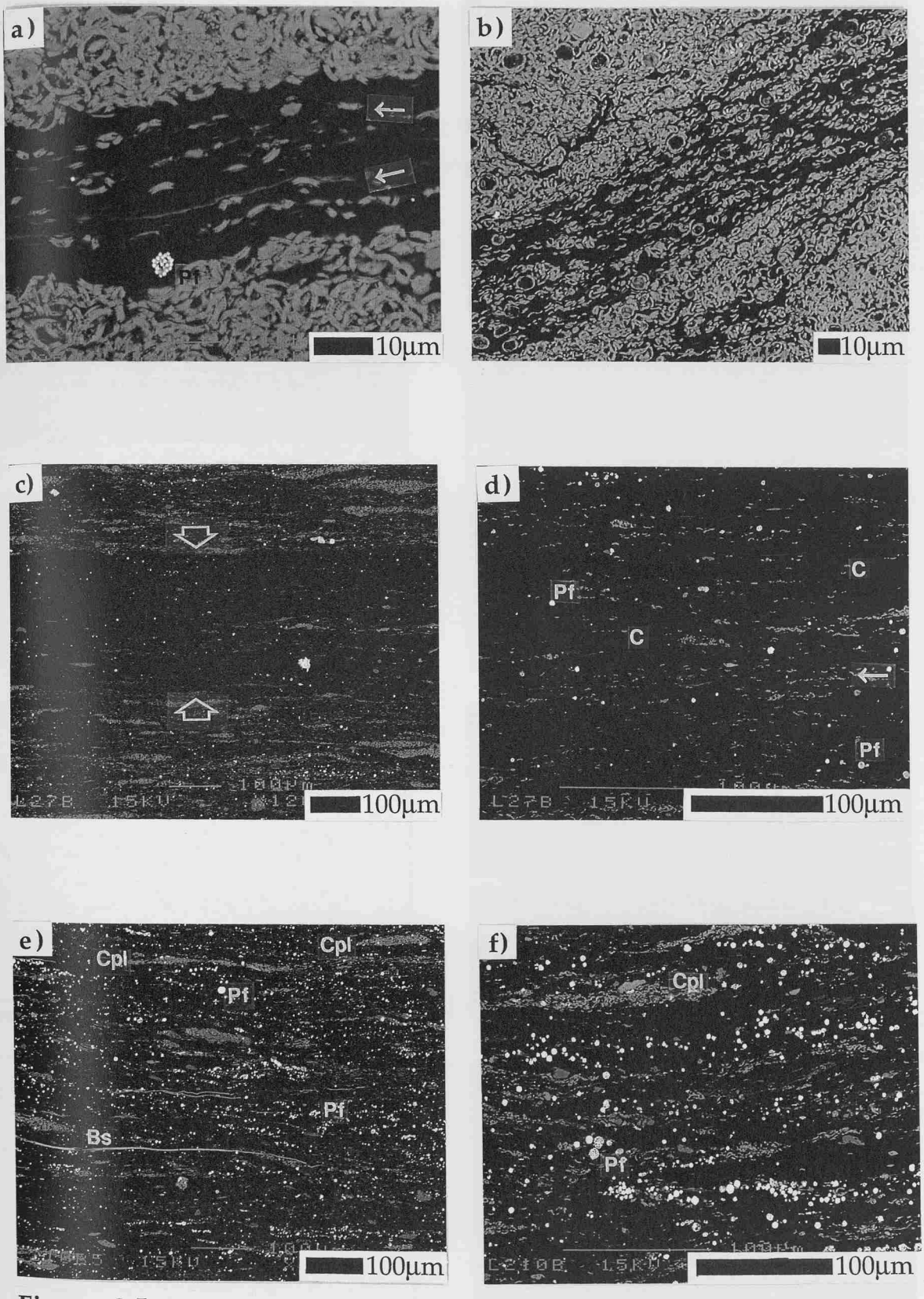
a)
Pf
10µm
b)
10µm
c)
100µm
d)
Pf
C
C
Pf
100µm
e)
Cpl
Cpl
Pf
Pf
Bs
100µm
f)
Cpl
Pf
100µm

Figure 3.5

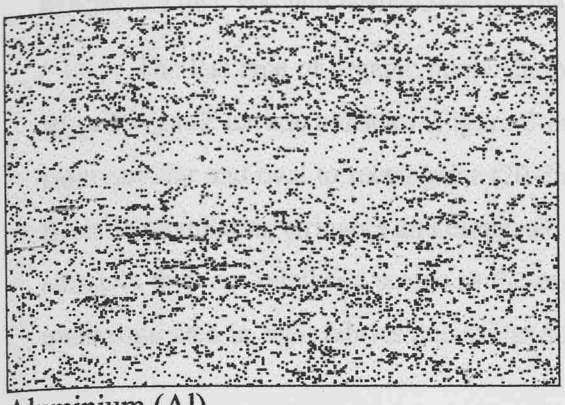

Aluminium (Al)

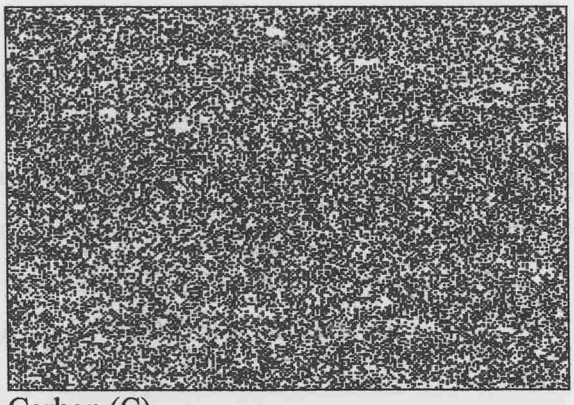

Carbon (C)

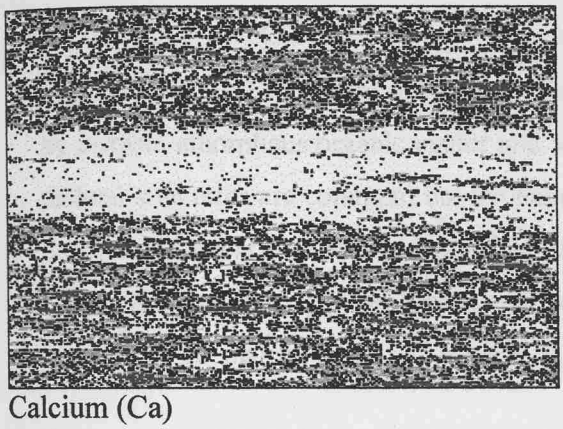

Calcium (Ca)

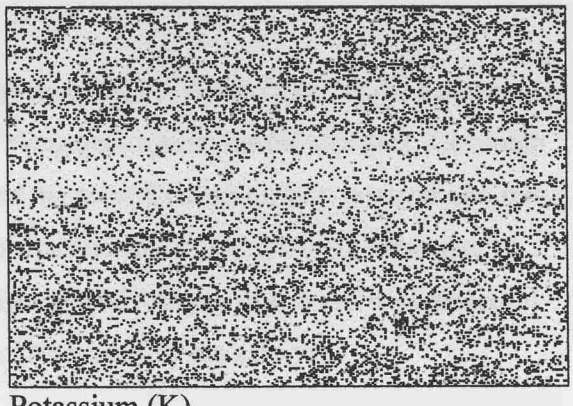

Potassium (K)

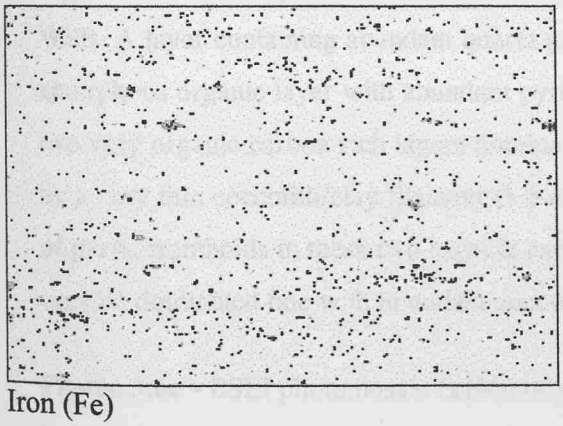

Iron (Fe)

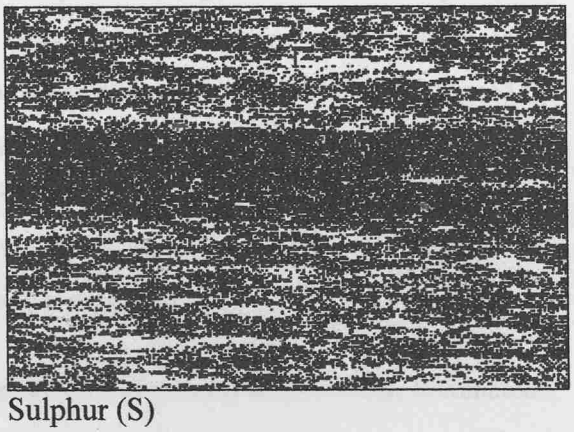

Sulphur (S)

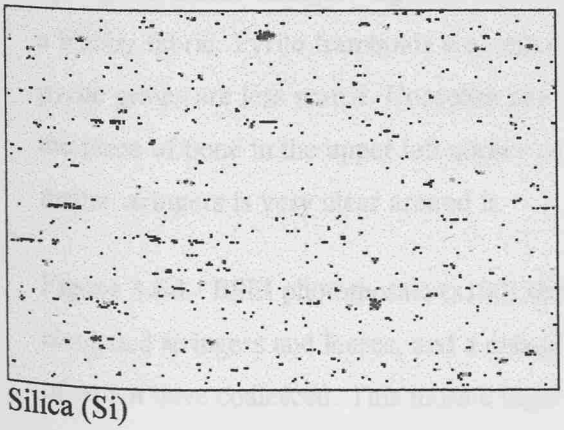

Silica (Si)

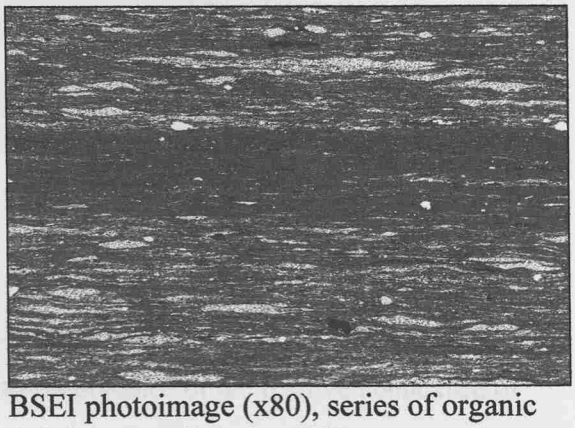

BSEI photoimage (x80), series of organic rich layers, Oil shale, WSB.

Elemental Map 3.4

c) Discrete bleb and lath shaped organic matter

The last type of organic matter in the oil and bituminous shales is discrete bleb and lath shaped organic carbon particles (Figure 3.8a and c; Figure 3.9b). These particles can range from circular and oval to rectangular (20-30μm height, 50-90μm length), and are clearly distinct from the undulating stringers and elongated lenses. Compared to the elongated lenses and stringers they are relatively scarce in the organic carbon-rich lithologies, though they may be underestimated in such fabrics due to the dominance of the other organic matter types.

FIGURE CAPTIONS

Figure 3.6a - BSEI photomosaic (x100) of an organic carbon-rich lithology, WSB, dominated by diffuse, amorphous organic matter and wavy, elongated organic matter stringers. Coccolith pelletal structures are common, but the majority of the coccoliths are loosely grouped into thin layers or stringers. Pyrite is predominately framboidal and small ($\leq$5μm average diameter), while discrete euhedral pyrite grains are scarce. Quartz and feldspar grains are well dispersed throughout the matrix, and a calcisphere is present (indicated by the arrow).

Figure 3.6b - BSEI photomosaic (x150) showing a sequence of organic carbon-rich layers, WSB. A layer containing abundant quartz grains, some with pyritic overgrowth, replaces an amorphous organic layer with abundant pyrite framboids and coccoliths. These are followed by two very organic carbon-rich layers dominated by amorphous organic matter, which are divided by a very thin coccolith/clay filament (1-5 coccoliths thick) (indicated by arrow). Note the lack of pyrite framboids in these two organic carbon-rich layers. Above, the fabric returns to an organic dominated one with abundant coccoliths and pyrite framboids.

Figure 3.6c - BSEI photomosaic (x100) of an organic carbon-rich lithology, WSB, dominated by organic matter stringers together with very abundant coccolith pelletal structures, resulting in a blebby fabric. Pyrite framboids are common, but less abundant than in 3.6a, but euhedral pyrite grains are less scarce. Coccolith pelletal structures contain abundant coccospheres. Note the piece of bone in the upper left corner of the mosaic, distortion of the coccolith and organic matter stringers is very clear around it.

Figure 3.6d - BSEI photomosaic (x190) showing an organic carbon-rich layer, WSB, with elongated stringers and lenses, and a coccolith-rich layer with abundant pelletal structures, some of which have coalesced. This mosaic highlights the importance of the relative abundance of organic matter to coccoliths, which controls the fabric lithology.

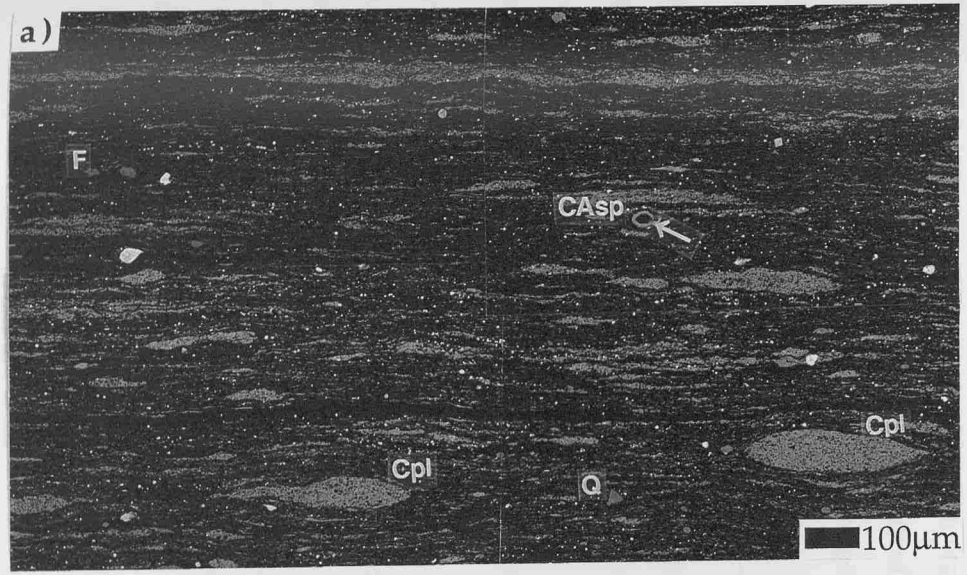
a)
F
CAsp
Cpl
Cpl
Q
100µm

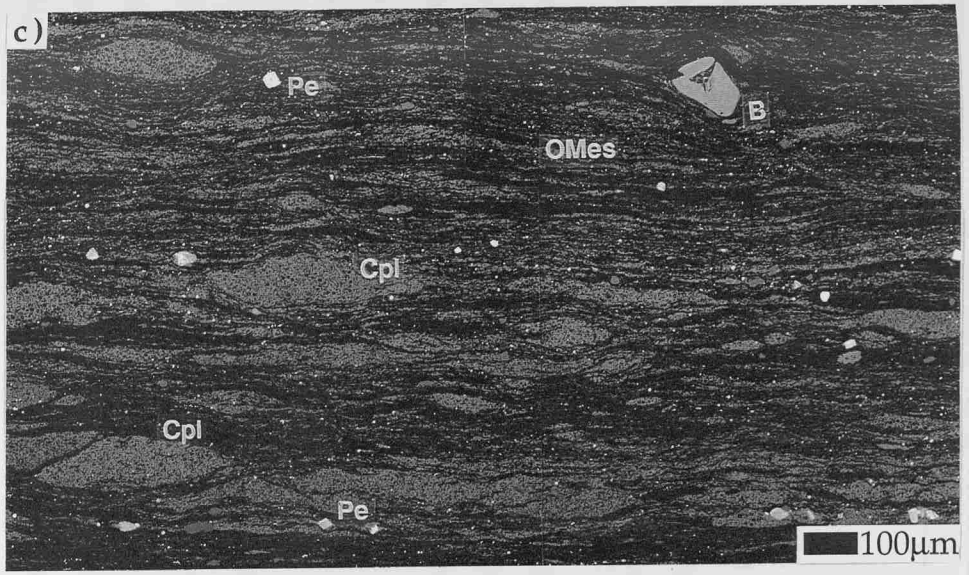
c)
Pe
B
OMes
Cpl
Cpl
Pe
100µm

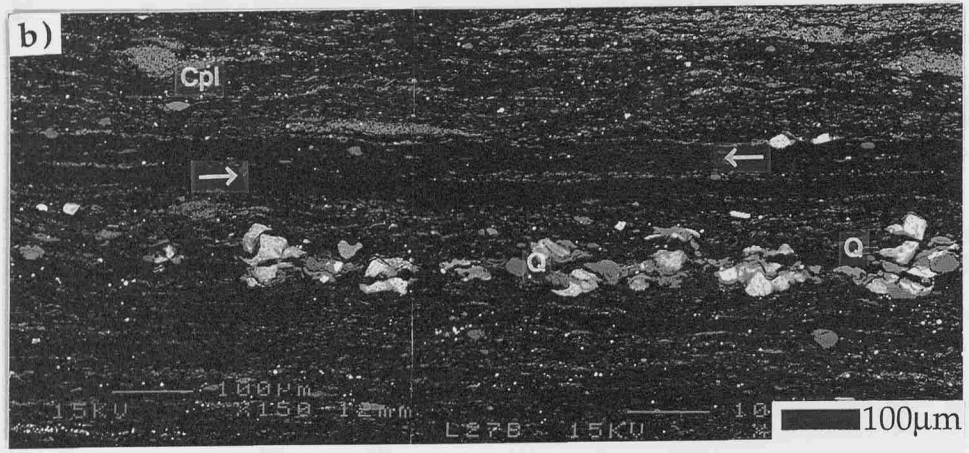
b)
Cpl
Q
Q
100µm

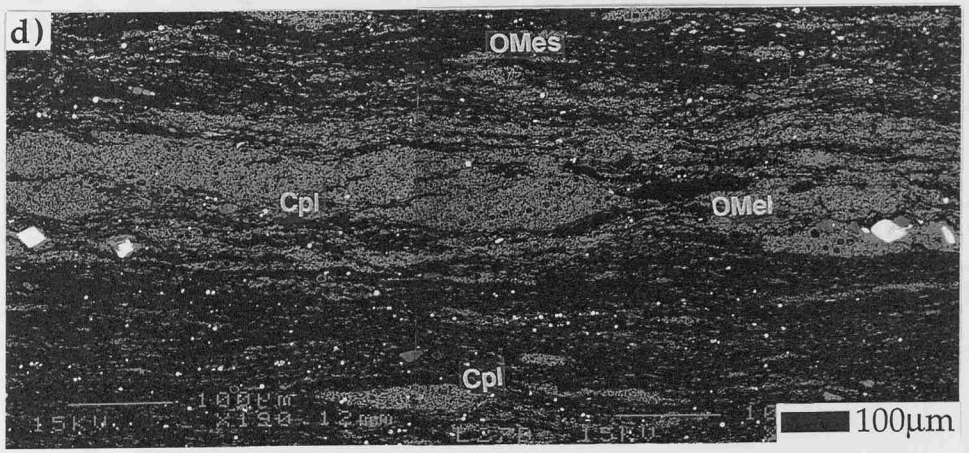
d)
OMes
Cpl
OMel
Cpl
100µm

Figure 3.6

FIGURE CAPTIONS

Figure 3.7a - BSEI photomosaic (x100) showing an organic carbon-rich lithology, WSB, composed of elongated organic matter lenses and carbonate pelletal forms, resulting in a blebby fabric. Note the pelletal structures are either composed of coccoliths or sparite crystals, and individual sparite grains and coccolith stingers are common in the fabric.

Figure 3.7b - BSEI photomosaic (x100) of an organic carbon-rich lithology, WSB, dominated by elongated stringers and sparry lensoidal groups. Note the different situation of pyrite forms, the organic matter stringers have very small framboidal pyrite, while the sparry lenses have pyritic overgrowth (indicated by the arrow). The fabric is again blebby, but some of the sparry lenses have coalesced.

Figure 3.7c - BSEI photomosaic (x100) of a laminated, but blebby, organic carbon-rich lithology, WSB. Lamina are composed of either organic matter dominated by amorphous and stringer forms or of sparry carbonate lenses and grains. The boundaries between the lamina are not sharp, but an alternation between organic carbon-rich and carbonate-rich fabric is evident (as highlighted by the black/white strip at the side, delineating these laminae). Crushed shells and ammonites are also common in this fabric (indicated by the arrow).

Figure 3.7d - BSEI photomosaic (x100) of an organic carbon-rich lithology, WSB of amorphous and elongated stringers, containing and variety of carbonate forms. The sparry lens is clearly a prominent feature, however, individual sparite grains are common as are fine coccolith wisps and stringers.

Figure 3.8a - BSEI photomosaic (x100) of a coccolith-rich, organic carbon, blebby lithology, WSB. Organic matter is present as amorphous and elongated lens forms, but some discrete organic blebs are also present. Coccoliths are the dominant type of carbonate within this fabric, grouped in pelletal structures and stringers, but sparry lenses and grains are present.

Figure 3.8b - BSEI photomosaic (x100) of a coccolith-rich organic lithology, WSB, divided by a less coccolith-rich organic layer. The organic matter is predominately elongated stringers, and the carbonate coccolithic. Apart from within the organic carbon-rich central layer, the organic matter stringers are thin and discontinuous. Pelletal carbonate structures are less common than in Figure 3.8a, while coccolith stringers are abundant resulting in a stringer, rather than a blebby fabric.

FIGURE CAPTIONS

Figure 3.8c - BSEI photomosaic (x100) of a coccolith-rich, organic lithology, WSB, composed of occasional, laterally continuous organic matter stringers, and coccolithic stringers. Pelletal structures are rare (compare to Figure 3.7a and Figure 3.8a) resulting in a stringer dominated fabric. Note the very different form of the discrete, organic matter bleb in the lower half of the photomosaic compared with the organic matter stringers (indicated by the arrow).

Figure 3.8d - BSEI photomosaic (x100) of a coccolith-rich, organic lithology, WSB, dominated by both organic and coccolith stringers. The coccolith stringers are more laterally continuous than the organic matter stringers, and flatten, elongated coccolith lenses are present but scarce.

Figure 3.9a - BSEI photomosaic (x100) of a coccolith-rich, organic carbon lithology, WSB, with elongated organic matter stringers and lenses, and coccolith pelletal structures and stringers. Organic matter lenses display marked pinching at each end, as do the coccolith pelletal structures, resulting in a symmetrical, flattened blebby fabric.

Figure 3.9b - BSEI photomosaic (x100) of a coccolith-rich lithology, WSB, containing discontinuous elongated organic matter stringers and lenses. The fabric is dominated by coccoliths in pelletal structures and in laterally persistent layers, and coccospheres are common. Pyrite is framboidal and is situated with the organic matter forms.

Figure 3.9c - BSEI photomosaic (x100) of an organic layer, within a coccolith limestone, WSB. Organic matter is in elongated stringers and lenses, and coccoliths are either in large pelletal structures or as fine stringers, some of which have coalesced forming coccolith layers. A discrete shaped organic matter bleb is present, as is a calcisphere, and quartz grains are common. Pyrite is primarily in framboidal form, but some larger euhedral grains are present.

Figure 3.9d - BSEI photograph (x100) of a coccolith-rich lithology, WSB, containing abundant organic matter stringers. This fabric occurs during transition from a coccolith limestone to an organic-rich shale. The organic matter stringers are laterally persistent, and the coccoliths are present in coalescing pelletal structures, resulting in a discontinuous blebby laminated fabric. Note the preferential situation of pyrite framboids with the organic matter stringers, the preservation of coccospheres within the coccolithic pelletal structures and the lack of other fabric components.

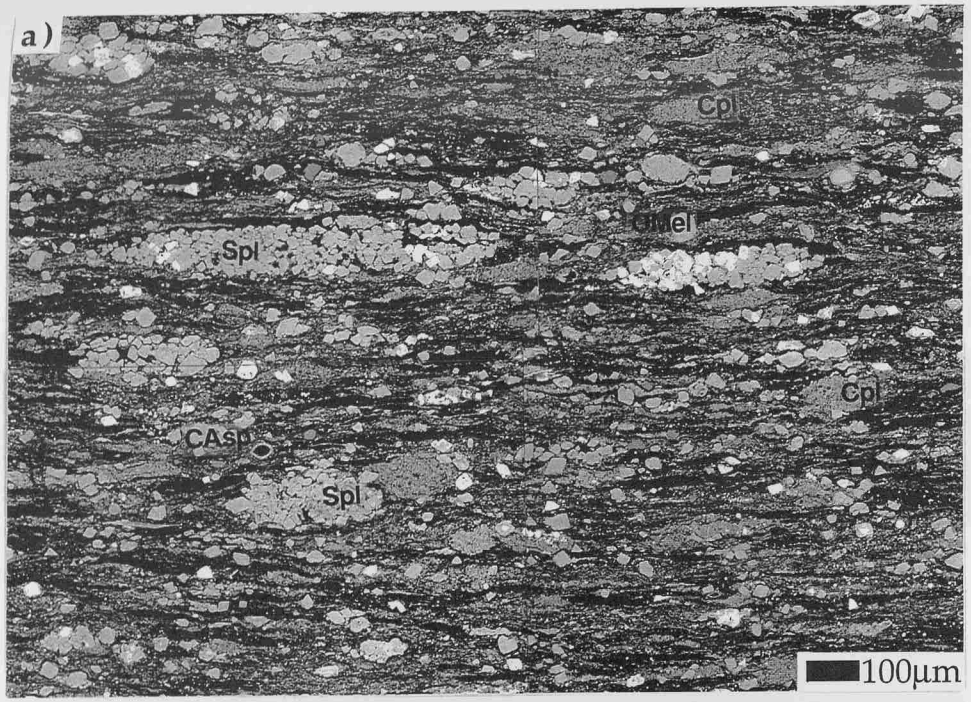
a)
Cpl
OMel
Spl
Cpl
CAsp
Spl
100µm

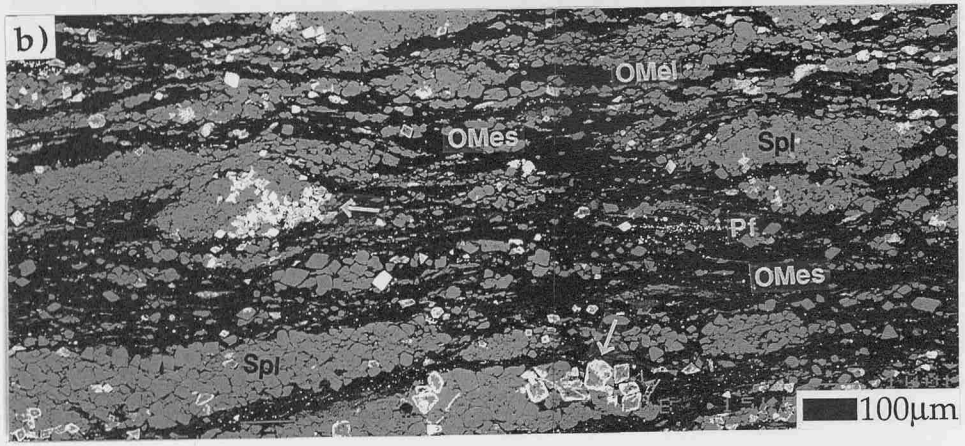
b)
OMel
OMes
Spl
Pf
OMes
Spl
100µm

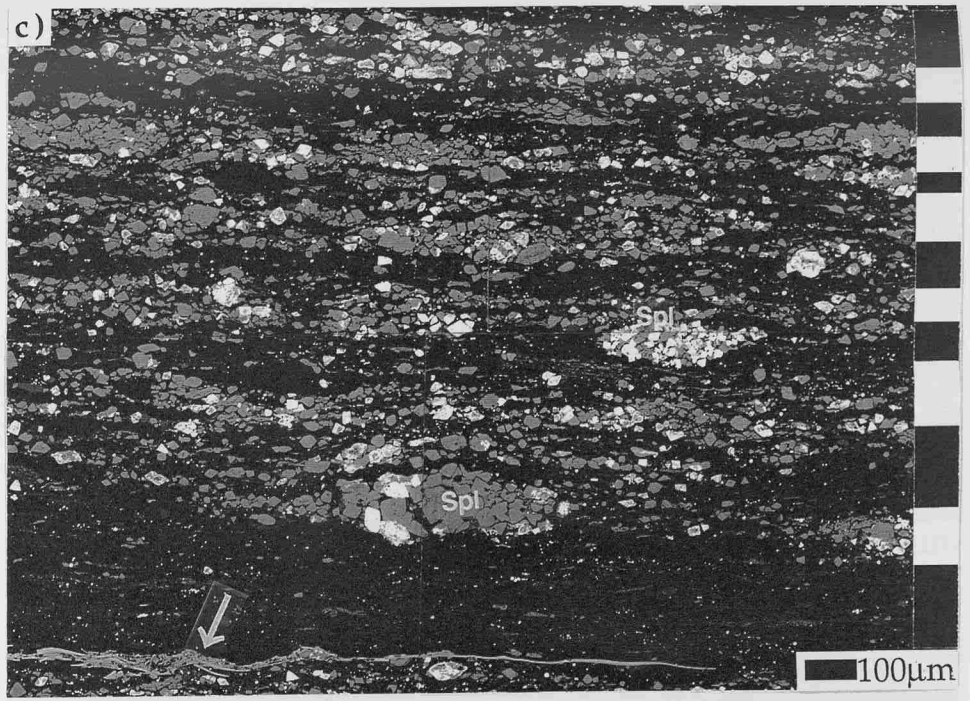
c)
Spl
Spl
100µm


d)
Spl
100µm

Figure 3.7

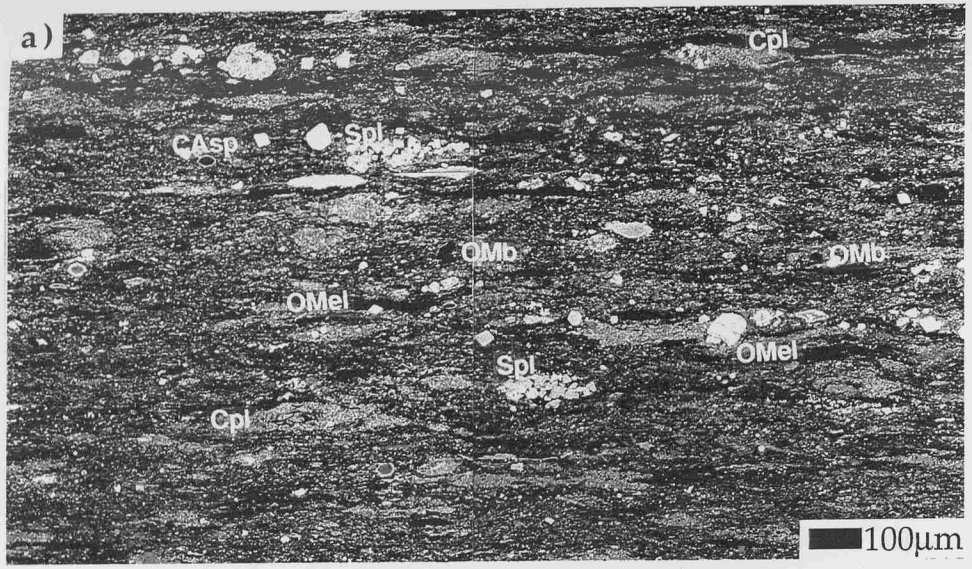
a)
Cpl
CAsp
Spl
OMb
OMb
OMel
OMel
Spl
Cpl
100µm

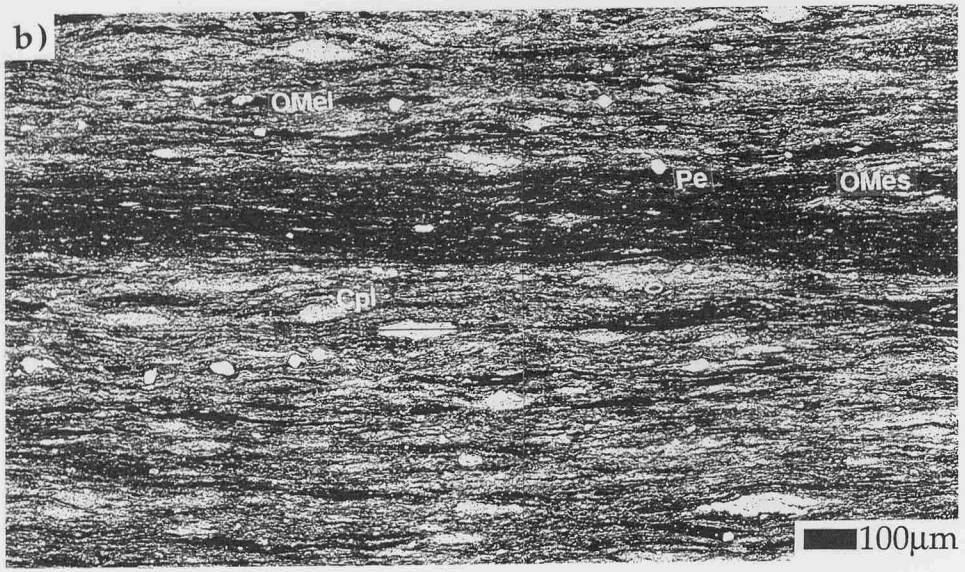
b)
OMel
Pe
OMes
Cpl
100µm

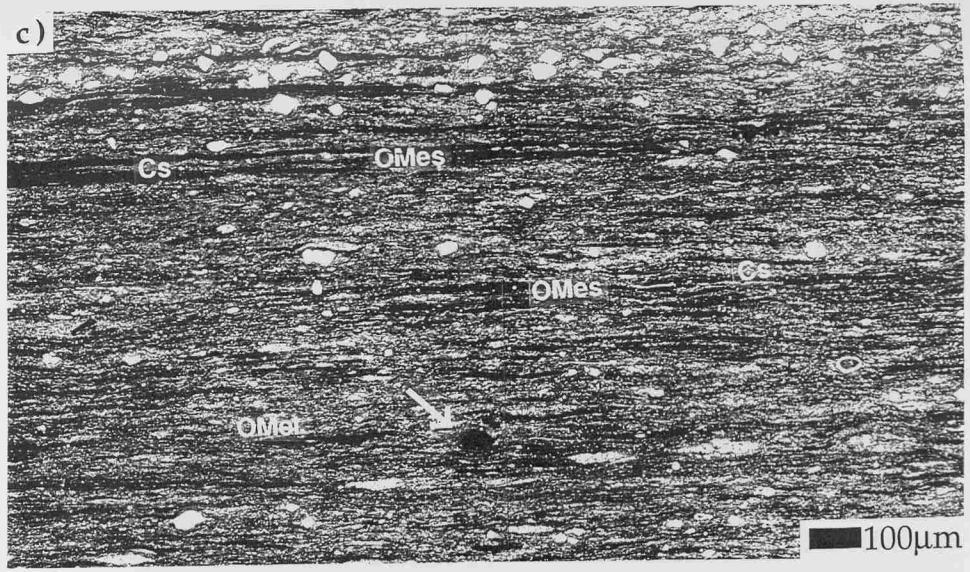
c)
Cs
OMes
OMes
Cs
OMel
100µm

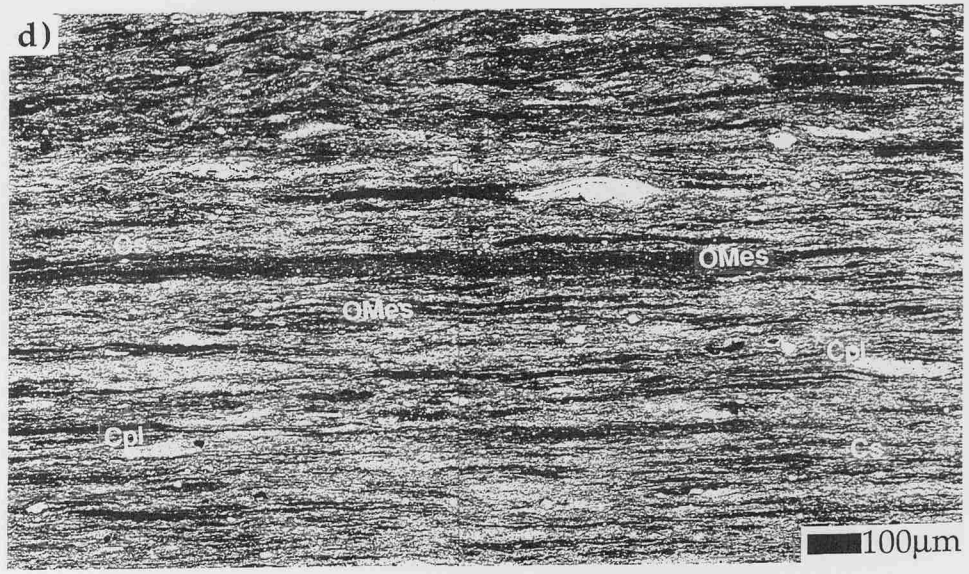
d)
Cs
OMes
OMes
Cpl
Cpl
Cs
100µm

Figure 3.8

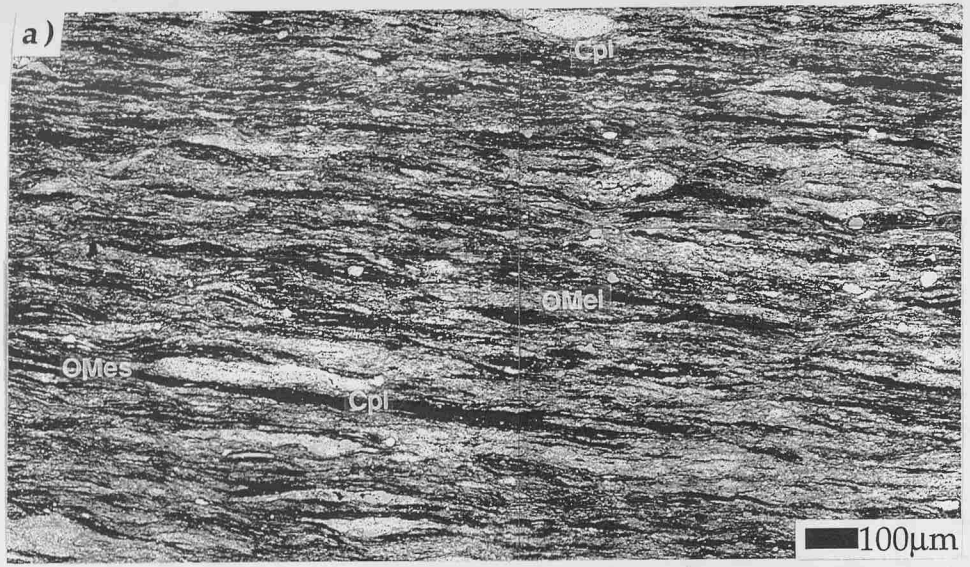
a)
Cpl
OMel
OMes
Cpl
100µm

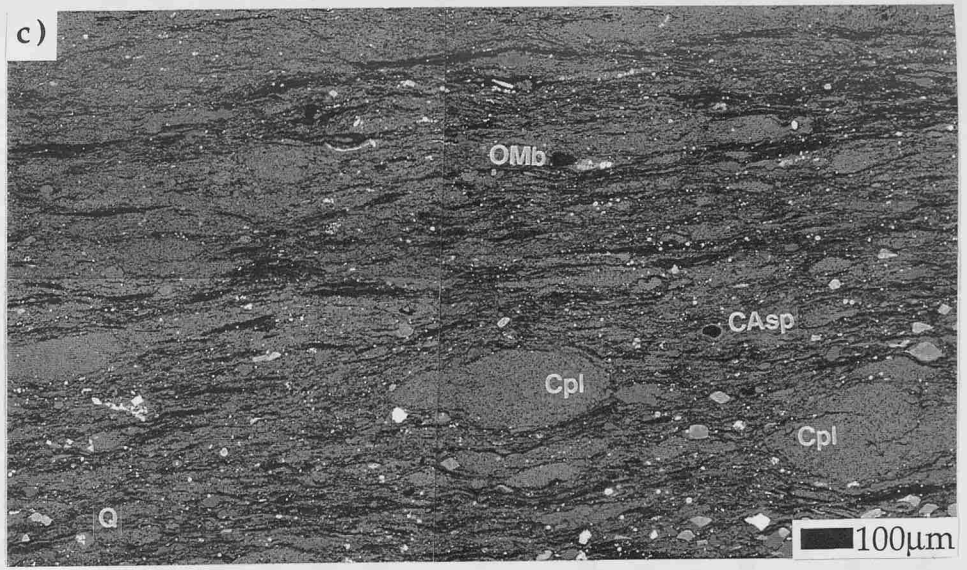
c)
OMb
CAsp
Cpl
Cpl
Q
100µm

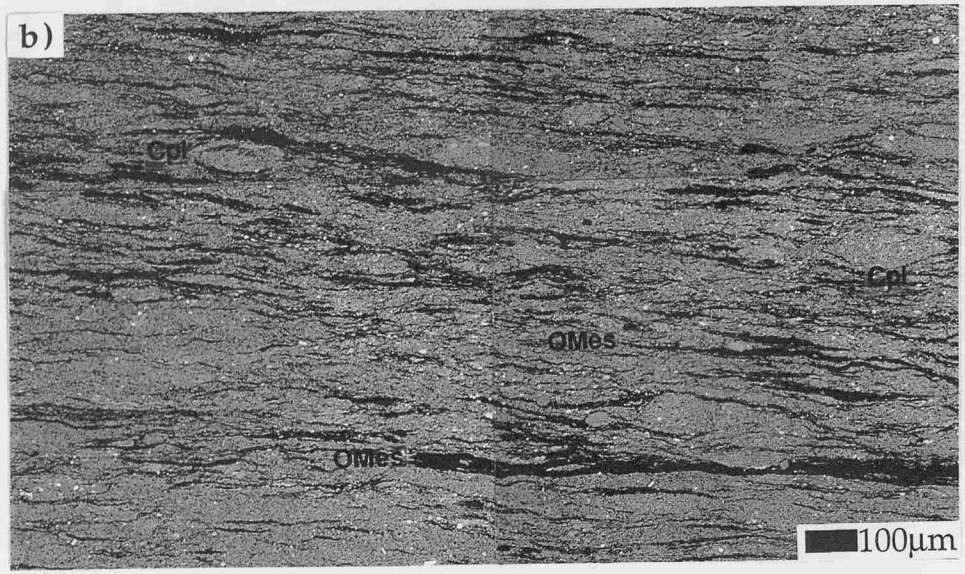
b)
Cpl
Cpl
QMes
OMes
100µm

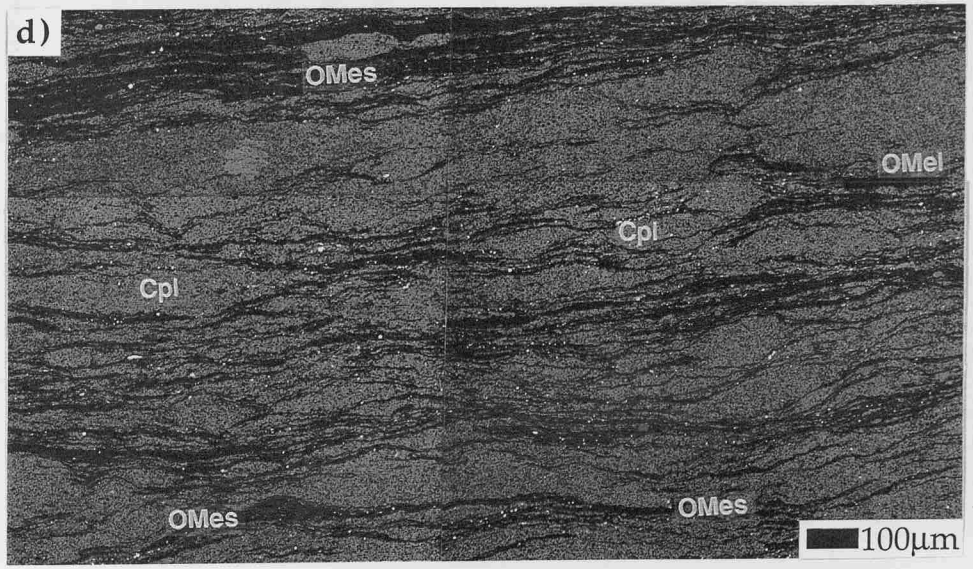
d)
OMes
OMel
Cpl
Cpl
OMes
OMes
100µm

Figure 3.9

3.3.4.2 Carbonate within organic carbon-rich lithologies

Within organic carbon-rich lithologies a substantial amount of carbonate is present. Loose coccoliths are dispersed in the matrix with amorphous organic matter, and are grouped as coccolithic stringers, and as discrete pelletal structures (Figure 3.6 and 3.11). Recrystallised carbonate in the form of sparry euhedral crystals and lensoidal groups of crystals, are also found in oil and bituminous shale lithologies (Figure 3.7 and 3.11). Both the primary coccolith debris and the diagenetic sparry crystals occur individually and as pelletal/lensoidal shapes that may coalesce into elongated ribbons and laminae.

a) Coccolith dominated carbonate forms

Coccoliths within organic carbon-rich lithologies are frequently present individually, suspended within the amorphous matrix organic matter. Though the coccoliths are commonly isolated from each other, they are orientated parallel to the bedding plane, resulting in broken lines of coccoliths (Figure 3.5d). Coccoliths of one or more, with (Figure 3.5a) and without wispy clay threads (Figure 3.5b), also comprise thin filaments or linear groups (ranging from 10-20μm to several 100μm in lateral extent), which separate organic matter bodies.

Two types of pelletal coccolith lenses are present, being either dominated by coccolith plates showing no preferred direction of orientation (Figure 3.10a and b), or contain large numbers of coccospheres (Figure 3.10c and d). Cross-sectional shapes of pelletal lenses are oval, elongated to almost ribbons (Figure 3.10a,c,e). The boundaries of the pelletal lenses are sharp making them clearly identifiable from the surrounding matrix. Where coccospheres dominate, the coccolith pelletal lenses are seen to be darker in BSEI mode due to the coccospheres' hollow centres, which increase the porosity of the lens. However, some are infilled with a single recrystallised carbonate crystal, resulting in a bright BSE image compared to hollow coccospheres (Figure 3.10d).

Another pelletal lens type is composed of calcite, the original form of which, presumably coccolithic plates, is no longer clearly visible. What remains is a hash of calcitic fragments with little of the original coccolith structure evident (Figure 3.10e and f). These lenses vary in form from almost bullet like to circular and lensoidal shapes.

b) Sparite dominated carbonate forms

Small euhedral sparite crystals (10-50μm diameter), are present individually scattered in the organic carbon-rich matrix and grouped in lensoidal forms (Figure 3.7; Figure 3.11 a and c). Unlike the cementstone, these crystals are not composed of ferroan dolomite, but are calcitic.

The lenses tend to be elongate oval to irregular lensoidal in shape, with rough angular boundaries. The sparite crystals are either clearly individually defined (Figure 3.11b), or coalesced and the individual crystals are less prominent (Figure 3.11d). Lenses commonly coalesce to become sparry laminae (Figure 3.11c and d).

Sparite crystals and coccoliths are sometimes present within the same pelletal lens (Figure 3.11e and f), resulting in irregularly lensoidal shapes with a tendency towards more circular shapes. Though lens boundaries are relatively sharp, they are also irregular due to the contrasting angular nature of the sparite to the more compact coccoliths.

Size ranges for both coccolith and sparry pelletal lenses are detailed in Table 3.3, together with details of average sizes of modern coccolith pellets produced by copepods. Coccolith-dominated lenses are generally smaller than the sparite lenses, while hash carbonate forms are the smallest. Coccolith pelletal lenses are the most common types within organic carbon-rich lithologies, however, sparry types (Figure 3.7c) dominate some layers. Though these two types usually occur separately, small areas are present where both forms occur (Figure 3.7a; Figure 3.8a). Hash pelletal lenses occur in association with coccolith lenses and have not been identified in areas dominated by sparitic forms.

Structural Type	Composition	Average Length	Average Height	Cross-section
Coccolith	Crushed coccoliths and coccospheres	170 $\pm$53.7μm	51 $\pm$21.8μm	Elongated oval to ribbons
Hash Carbonate	Non structured hash of carbonate particles	75 $\pm$53μm	15 $\pm$4.5μm	Bullet to circular and lensoidal
Sparitic	Sparite crystals	300 $\pm$147.2μm	87 $\pm$41.1μm	Elongated oval to irregular lensoidal
Coccolith / Sparitic combination	Coccoliths and sparite crystals	267 $\pm$168μm	101μm $\pm$79.2μm	Irregularly lensoidal to circular
Modern Copepod Coccolith Pellet	Crushed coccoliths and coccospheres	200 $\pm$55μm	40 $\pm$10μm	Cylindrical (Honjo and Roman, 1978)

Table 3.3 Composition and size ranges of pelletal lenses within the KCF fabric, and the average size of modern copepod coccolithic pellets.

c) Coccolith preservation

The preservation of coccoliths within organic carbon-rich lithologies is generally good, plate details are clearly seen and coccospheres are common within carbonate pelletal lenses. Some of these coccospheres show exceptional preservation, containing smaller internal coccolith

plates that were forming on time of death (Paasche, 1962, 1968). In the hash pelletal lenses, the primary form of the coccoliths has been almost totally destroyed (Figure 3.10f), while sparry lenses are a complete diagenetic alteration of the primary coccolith carbonate into sparite crystals (Figure 3.11f).

FIGURE CAPTIONS

Figure 3.10a - BSEI photograph (x120) of a pelletal coccolith lens dominated by coccolith plates.

Figure 3.10b - Detailed BSEI photograph (x1000) of 3.10a, showing the internal, disorganised arrangement of coccolith plates. Note the lack of other fabric components in this pellet and the excellent preservation of the coccolith plates.

Figure 3.10c - BSEI photograph (x200) of a pelletal coccolith lens dominated by coccospheres.

Figure 3.10d - Detailed BSEI photograph (x1400) of 3.10c, showing the internal arrangement of the coccospheres. The majority of the coccospheres have hollow centers, but some are infilled by a single euhedral calcite crystal (indicated by the arrows). Note the exceptional preservation of coccolith plates forming the coccospheres and the presence of smaller plates infilling some of the coccosphere centres. These are believed to be new plates that were forming at the time of the coccolithophorid's death.

Figure 3.10e - BSEI photograph (x600) of a pelletal lens that is composed of a hash of primary carbonate fragments, WSB.

Figure 3.10f - Detailed BSEI photograph (x1200) of 3.10e, showing the hash internal structure. It is believed that the primary carbonate form of this hash material was coccoliths.

Figure 3.11a - BSEI photograph (x100) of a pelletal lens composed of sparite crystals, WSB. Note the irregular boundary of the lens due to the euhedral crystals.

Figure 3.11b - Detailed BSEI photograph (x400) of 3.11a showing the angular, sparite crystals. Note the clear crystal boundaries and the prominent spaces between touching crystals. Also, pyrite is seen as crystal overgrowth (indicated by the arrow).

Figure 3.11c - BSEI photograph (x35) of coalesced sparry pelletal lenses, WSB.

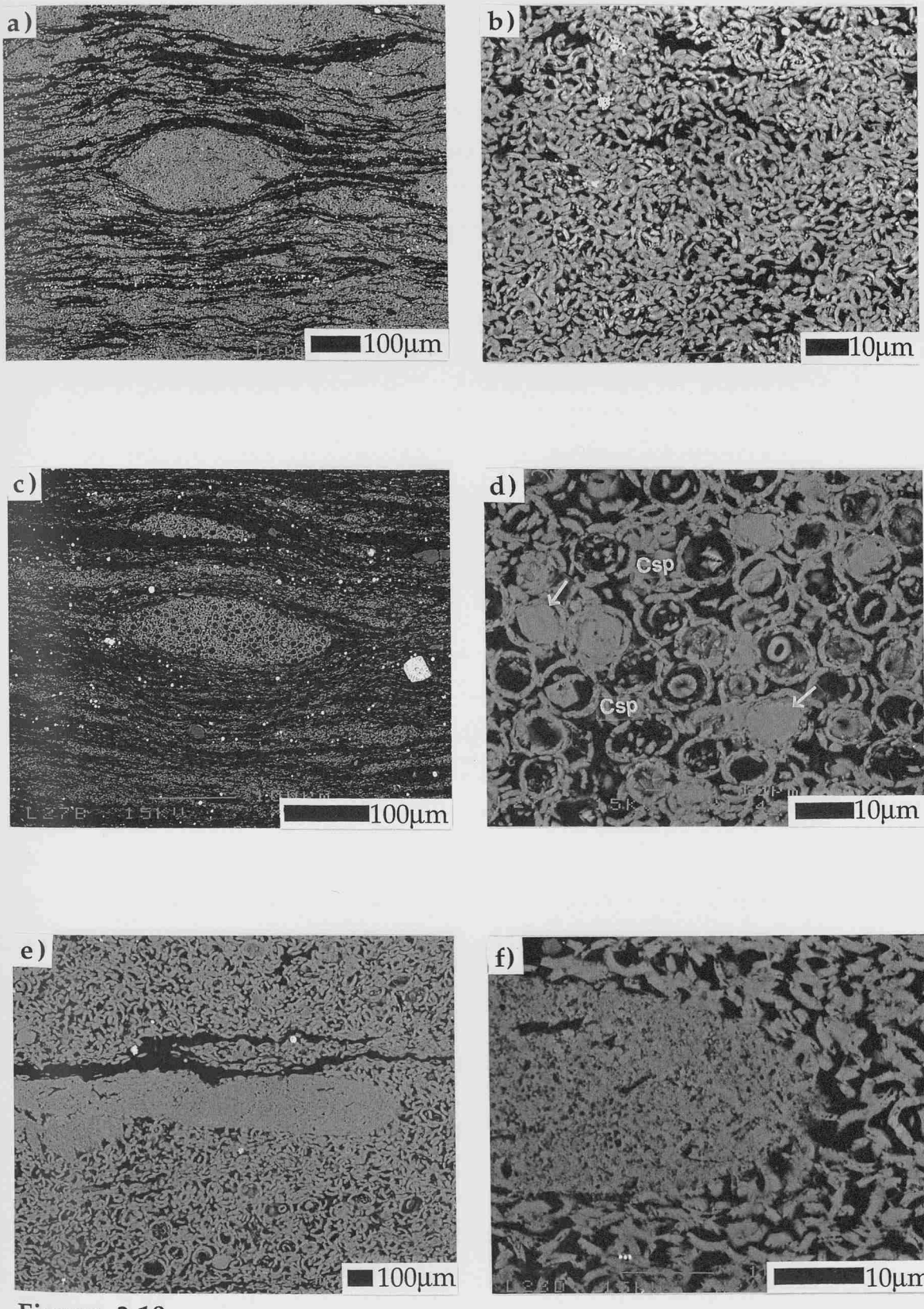

Figure 3.10

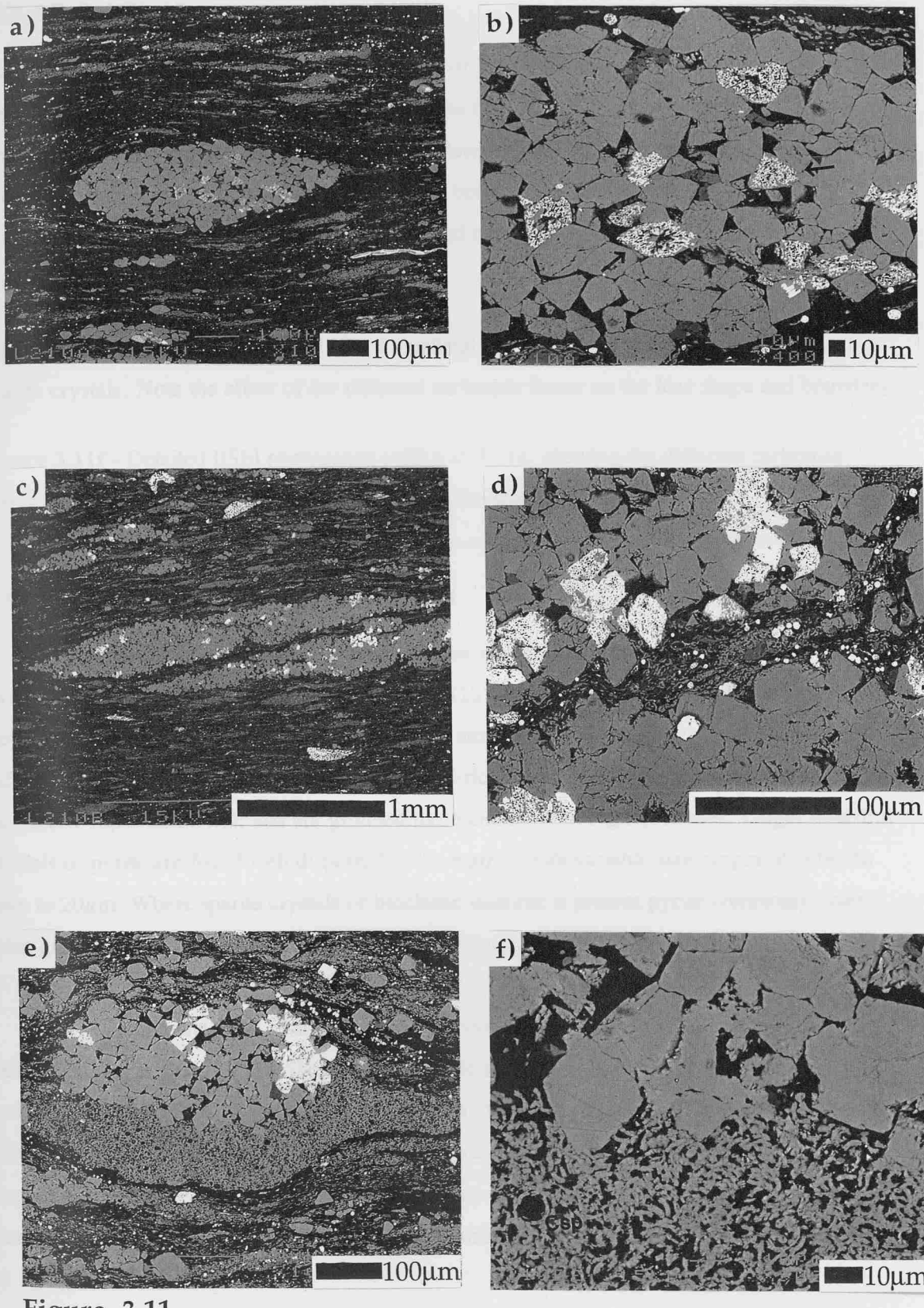

Figure 3.11

FIGURE CAPTIONS

Figure 3.11d - Detailed BSEI photograph (x350) of 3.11c, showing the boundary between two groups of coalesced sparry pelletal lenses. Note the internal coalescence of individual sparite crystals, which reduces the angular nature of the lenses. The organic carbon-rich matrix containing abundant coccolith stringers is evident between the lenses, and the difference in pyrite forms, between framboidal in the matrix and overgrowth on the sparry lens crystals, is clear.

Figure 3.11e - BSEI photograph (x160) of a pelletal lens that is composed of coccoliths and sparite crystals. Note the effect of the different carbonate forms on the lens shape and boundary.

Figure 3.11f - Detailed BSEI photograph (x900) of 3.11e, showing the different carbonate forms of coccoliths, and a few coccospheres, and the sparite crystals.

3.3.4.3 Pyrite and other minor fabric components

Pyrite is a visually abundant part of organic carbon-rich lithologies (Figure 3.12a) and is closely associated with organic matter (Figure 3.12b). Predominately framboidal in form, it is densely scattered through the fabric and sizes are small, especially in highly organic areas ($\leq 5\mu$m average diameter). Within more carbonate-rich areas, framboids are generally slightly larger (10-15μm diameter), and are grouped more closely with organic matter. Larger euhedral crystals of pyrite are found well dispersed in the matrix, with variable size ranges of between 5μm to 20μm. Where sparite crystals or bioclastic material is present pyrite commonly coats them giving an impression of even larger blocks of pyrite (Figure 3.11b and d).

Bioclastic material is a small, but obvious component of the organic carbon-rich lithologies (Figure 3.12c to f). Shells (Figure 3.12c and d) and bone fragments (Figure 3.12e and f) occur scattered throughout the matrix, or in clusters. If bioclastic fragments are large and robust enough, distortion of the microfabric is evident around these particles. Subsequently deposited material, which may have initially draped over these fragments when first deposited, has been further distorted around the fragments during sediment compaction (Figure 3.12c and e).

Quartz and feldspar grains are a minor component of organic-rich lithologies and tend to occur dispersed and isolated in the matrix. However, some clustering along discrete bedding planes does occur (Figure 3.6b). The quartz grains tend to be subrounded and between 20-50μm

across, while feldspars are smaller, 20-30μm across. Calcispheres, though not common, are also present, but isolated within the organic carbon-rich lithologies (Figure 3.6a and Figure 3.9c).

FIGURE CAPTIONS

Figure 3.12a - Detailed BSEI photograph (x1400) of pyrite framboids within an organic carbon-rich lithology, WSB.

Figure 3.12b -Detailed BSEI photograph (x900) of pyrite framboids preferentially located with organic stringers within a coccolith-rich lithology, WSB.

Figure 3.12c - BSEI photograph (x110) of a bioclastic fragment, probably part of an ammonite, WSB. Note the distortion of the fabric around the lowest tip of the feature (indicated by arrow).

Figure 3.12d - Detailed BSEI photograph (x400) of two crushed shells (indicated by arrows) within a sparry dominated, organic carbon-rich lithology (see Figure 3.7c), WSB.

Figure 3.12e - Detailed BSEI photograph (x300) of a bone segment within a coccolith stringer, organic carbon-rich lithology (see Figure 3.6c), WSB. Note the distortion of the fabric below the bone and the draping of the coccolith and organic matter stringers over the bone, this has been enhanced during lithological compression.

Figure 3.12f - Detailed BSEI photograph (x550) of a bone segment in a coccolith limestone, WSB.

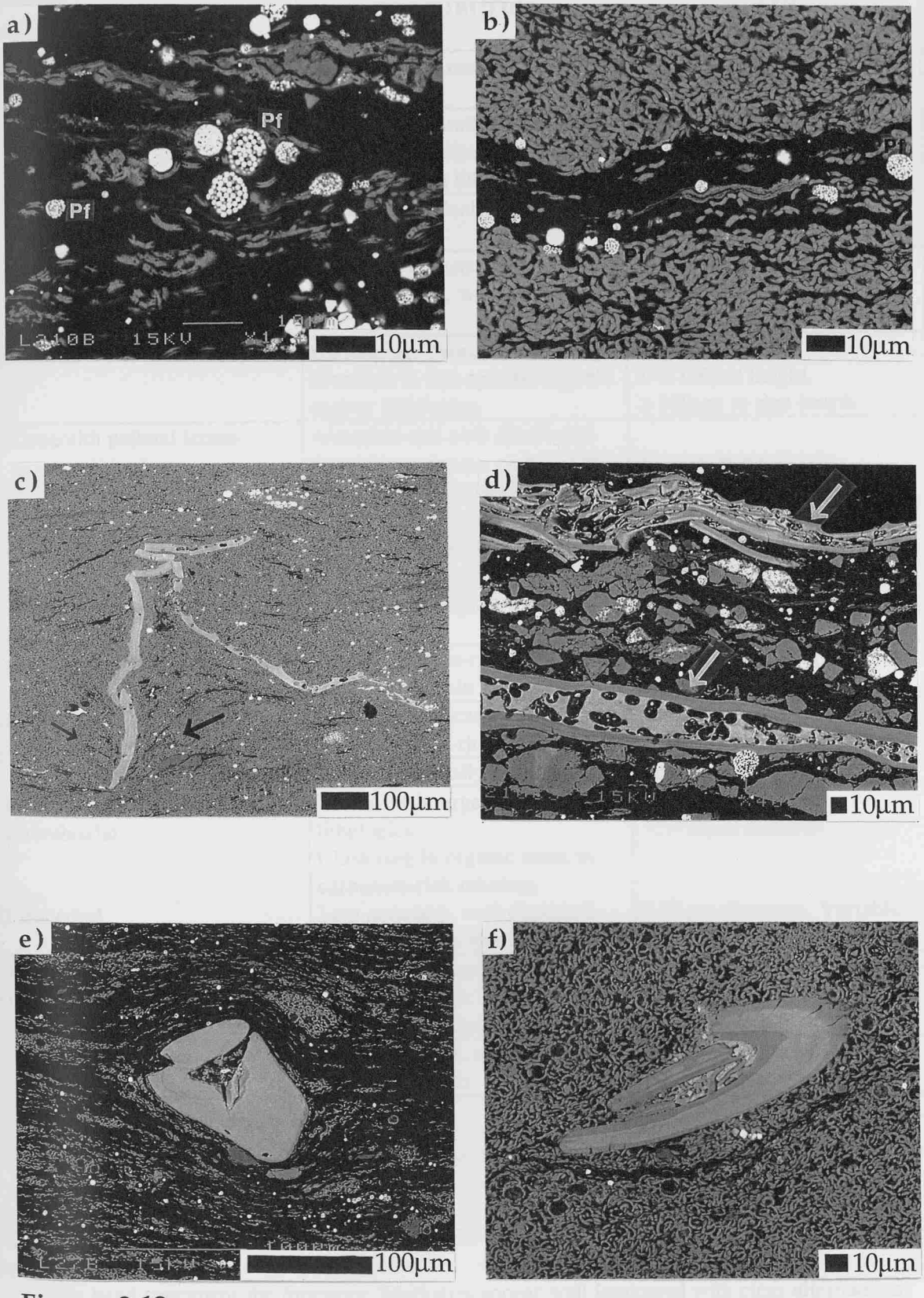

Figure 3.12

LITHOLOGICAL COMPONENT	DISTRIBUTION	SIZE
ORGANIC MATTER 1) Diffuse, amorphous	Dominates the matrix, which also contains clays.	Amorphous, variable.
2) Elongated lenses and stringers	Undulating, parallel to bedding, dominant in carbonate-rich, organic carbon lithologies.	Highly variable < 10-100μm height. 50-100μm to cm length.
3) Discrete blebs and laths	Scarce, individually dispersed.	20-30μm height. 50-90μm length.
CARBONATE - COCCOLITH 1) Individual coccoliths	1) loosely in matrix. 2) in filaments, with clays.	3-7μm diameter. < 10μm height, up to several 100μm length.
2) Coccolith stringers	Undulating, parallel to bedding, abundant in non-sparitic organic carbon lithologies.	Highly variable. 5-< 100μm height. > 100μm to mm length.
3) Coccolith pelletal lenses a) coccolith plates b) coccospheres	Abundant and well distributed throughout organic carbon-rich lithologies (not common where sparite forms occur)	50μm average height. 170μm average length.
4) Hash lenses	Rare, only present in coccolith-rich organic carbon lithologies.	15μm average height. 75μm average length.
CARBONATE - SPARITE 1) Sparite crystal grains	Individually dispersed in sparitic horizons	10-50μm diameter.
2) Sparite lensoidal groups	Only in organic-rich lithologies, limited to certain horizons.	90μm average height. 300μm average length.
MIXED CARBONATE Coccolith and sparite lenses	Grouped into scarce layers only within organic-rich lithologies.	100μm average height. 270μm average length.
Calcispheres	Rare, individually dispersed.	20-45μm diameter.
Pyrite 1)Framboidal 2) Euhedral	Dominant in organic-rich lithologies. Clustering in organic areas in carbonate-rich lithology. Less common, well dispersed. Overgrowth on sparitic crystals	< 5-15μm diameter. 5-20μm diameter. Variable.
Bioclastic material 1) Shells 2) Bone	Abundant in organic carbon-rich areas, especially where sparitic carbonate is common.	Variable, several 100μm scale.
Quartz Feldspar	Well dispersed, some clustering on discrete beds.	20-50μm diameter. 20-30μm diameter.

Table 3.4 Summary of the lithological components of the oil and bituminous shale lithologies.

3.3.5 COCCOLITH LIMESTONE LITHOLOGIES

In hand specimens the limestone lithologies appear well laminated with clear alternations between light limestone layers and dark organic carbon-rich layers (See Appendix A, Figures A1 and A2). However, the SEM provides a different perspective, showing the domination of the limestone lithology by coccoliths, while the organic carbon-rich layers are seen as very thin, discontinuous stringers (Figure 3.13a). Despite this coccolith dominance, some slight differences

are discernable in the matrix. Where coccospheres are present they produce a less dense, porous matrix, which appears darker than the surrounding matrix in BSEI mode (Figure 3.14c to f), while the remaining matrix is composed of tightly packed coccolith plates (Figure 3.14a and b).

Pelletal structures are noticeable if they contain coccospheres, however, the majority of the matrix shows little structure and is just a huge mass of coccoliths. Coccolith preservation in limestone lithologies is excellent (Figure 3.19a and b), with internal coccoliths of coccospheres frequently present (Figure 3.15a and c; Figure 3.19b). Average diameter sizes for coccoliths' range between 3-7μm (Figure 3.15e and f), with coccospheres usually between 10-12μm in diameter (Figure 3.15a,e and f). Some diagenetic alteration of the coccoliths does occur in the form of recrystallised calcite cement, which results in less well preserved coccoliths. Infilling of coccospheres with single calcite crystals is also common, destroying the internal coccosphere features.

Within the limestone, two distinctive types of matrix occur; large areas of almost pure, densely packed coccoliths, and layers where organic matter is common. Areas with more abundant organic matter can be divided further, depending on the size and continuity of the organic matter.

a) Purely coccolithic areas are either large, coalesced blebs (0.5 to 1cm across), or simply continuous layers of densely packed coccoliths (Figure 3.13a). In these areas the presence of complete coccospheres is rare, and pyrite, quartz and feldspar grains are very rare or absent (Figure 3.14a and b; Elemental Map 3.5).

b) Organic matter within carbonate-rich lithologies is seen as either short but relatively thick wavy stringers (Figure 3.13b and c) or as more continuous thin, undulating stringers (Figure 13a, d and e). The short stringers tend to range in length from 100μm to several 100μm, with thickness' reaching 20 to 50μm (Figure 3.13c). Fabric containing these short stringers has an almost mottled appearance (Figure 3.13b). The long, thin, undulating stringers have greater lateral continuity, with some reaching several centimeters in length, with thickness' less than 15-20μm (Figure 3.13d and e). Where these undulating, organic carbon stringers are present together with coccoliths that are predominantly grouped into pelletal lenses and the fabric has a blebby appearance (Figure 3.13d).

Pyrite within the coccolith limestone is not as abundant as in other lithologies and is predominantly associated with organic matter. The majority of the pyrite is present in framboidal form, ranging in size between 5 to15μm in diameter.

Calcispheres occur more frequently within the limestone lithology (Figure 3.15b and d), than in the highly calcareous mudstones and the organic carbon-rich lithologies. They are found both individually dispersed throughout the matrix, and grouped together, with up to ten individuals per group. Their diameters range between 20 and 45μm and they posses a distinct circular primary cross-section. This is constructed from two rings of carbonate material, an outer compact layer, less than 1μm thick and an inner fibrous layer, several microns thick, whereas their centres tend to be hollow. Compactional distortion of cross-sections is common and has resulted in many being completely flattened.

FIGURE CAPTIONS

Figure 3.13a - BSEI photomosaic (x50) showing a coccolith limestone lithology, WSB, composed of layers of pure coccoliths, and layers that contain thin, discontinuous organic matter stringers (indicated by thick arrows). Note the calcite veins that cut this section.

Figure 3.13b - BSEI photomosaic (x100) of coccolith limestone lithology, WSB, containing abundant short, but thick wavy organic matter stringers. Note the mottled appearance of the fabric.

Figure 3.13c - Detailed BSEI photograph (x270), showing thick, short organic matter stringers with a group of coccolith dominated, pelletal lenses.

Figure 3.13d - BSEI photomosaic (x100) of a coccolith limestone lithology, WSB, containing thin, laterally persistent, undulating organic matter stringers. This gives the fabric a blebby appearance.

Figure 3.13e - Detailed BSEI photograph (x190) of thin, undulating, laterally persistent organic matter stringers draped over coccolith dominated pelletal lenses.

Figure 3.14a - BSEI photograph (x400) of an area of pure coccolith limestone, WSB. Note the lack of any other fabric components, and the density of the coccoliths.

Figure 3.14b - Detailed BSEI photograph (x1000) of 3.14a, showing the fabric to be composed purely of unorientated coccolith plates. Note the exceptional preservation of the plate detail.

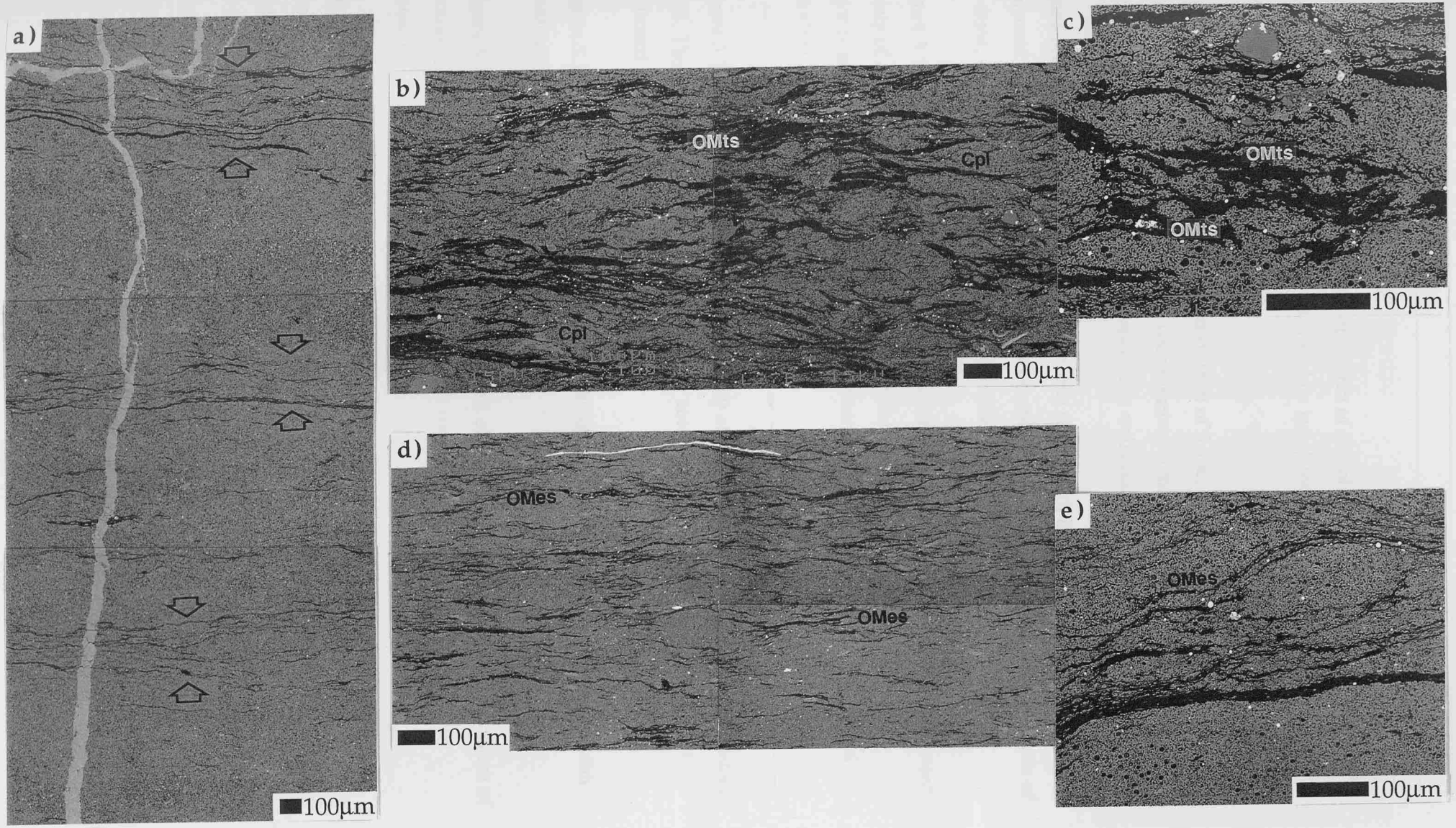
a)
100µm
b)
OMts
Cpl
Cpl
100µm
c)
OMts
OMts
100µm
d)
OMes
OMes
100µm
e)
OMes
100µm

Figure 3.13

FIGURE CAPTIONS

Figure 3.14c - BSEI photograph (x400) of an area of coccolith limestone that is composed of coccoliths and coccospheres. This fabric is slightly less dense than 3.14a, due to the voids resulting from the hollow coccospheres.

Figure 3.14d - Detailed BSEI photograph (x1000) of 3.14c, showing the fabric to be composed of both unorientated coccolith plates and coccospheres. Some of the coccospheres have been infilled by a single calcite crystal while other show well preserved internal coccolith plates.

Figure 3.14e - BSEI photograph (x400) of an area of coccolith limestone that is predominately composed of coccospheres, though coccoliths are still abundant. This fabric is the least dense of the three, due to the greater abundance of coccospheres.

Figure 3.14f - Detailed BSEI photograph (x1000) of 3.14e, showing the fabric to be composed mainly of coccospheres. A few of the coccospheres have been infilled with calcite but the majority are hollow. A substantial number of the coccospheres show no real cross-sectional distortion.

Figure 3.15a - Detailed BSEI photograph (x2300) of coccospheres within a coccolith limestone, WSB. The preservation is good and many of the coccospheres show smaller internal plates (indicated by arrows).

Figure 3.15b - Detailed BSEI photograph (x2300) of a crushed calcisphere within a coccolith limestone, WSB.

Figure 3.15c - Detailed BSEI photograph (x1500) of exceptional coccolith plate preservation of coccoliths located between two quartz grains in a coccolith limestone, WSB (indicated by arrows).

Figure 3.15d - Detailed BSEI photograph (x1000) of two calcispheres that have not been distorted. Note the two layer construction; an outer compact, thin ($< 1 \mu m$) carbonate layer and an inner fibrous layer several microns thick.

Figures 3.15e and f - Detailed BSEI photographs (x5000 and x4000 respectively) of coccospheres showing the inner detail of the coccolith plates forming the coccospheres.

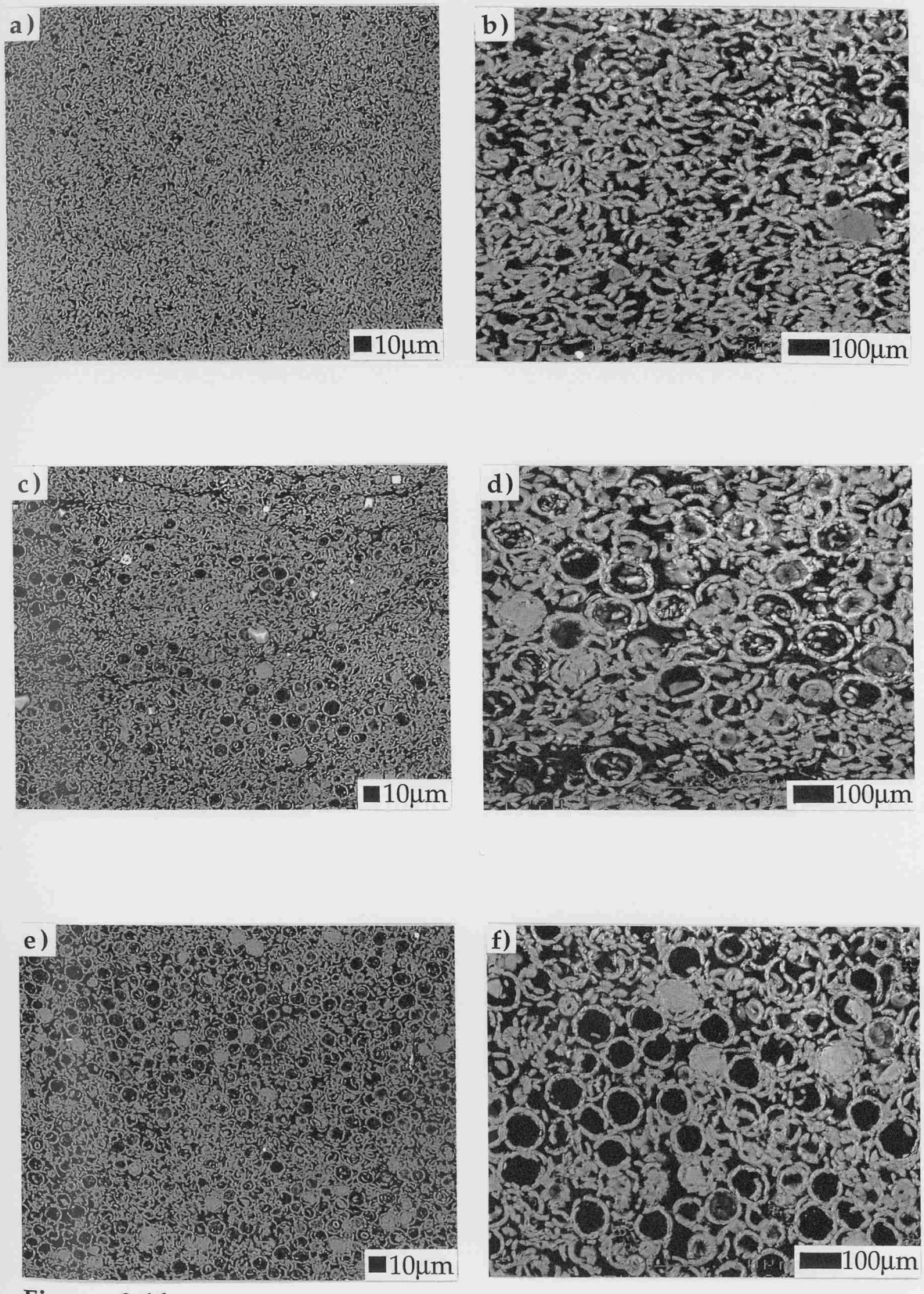

Figure 3.14

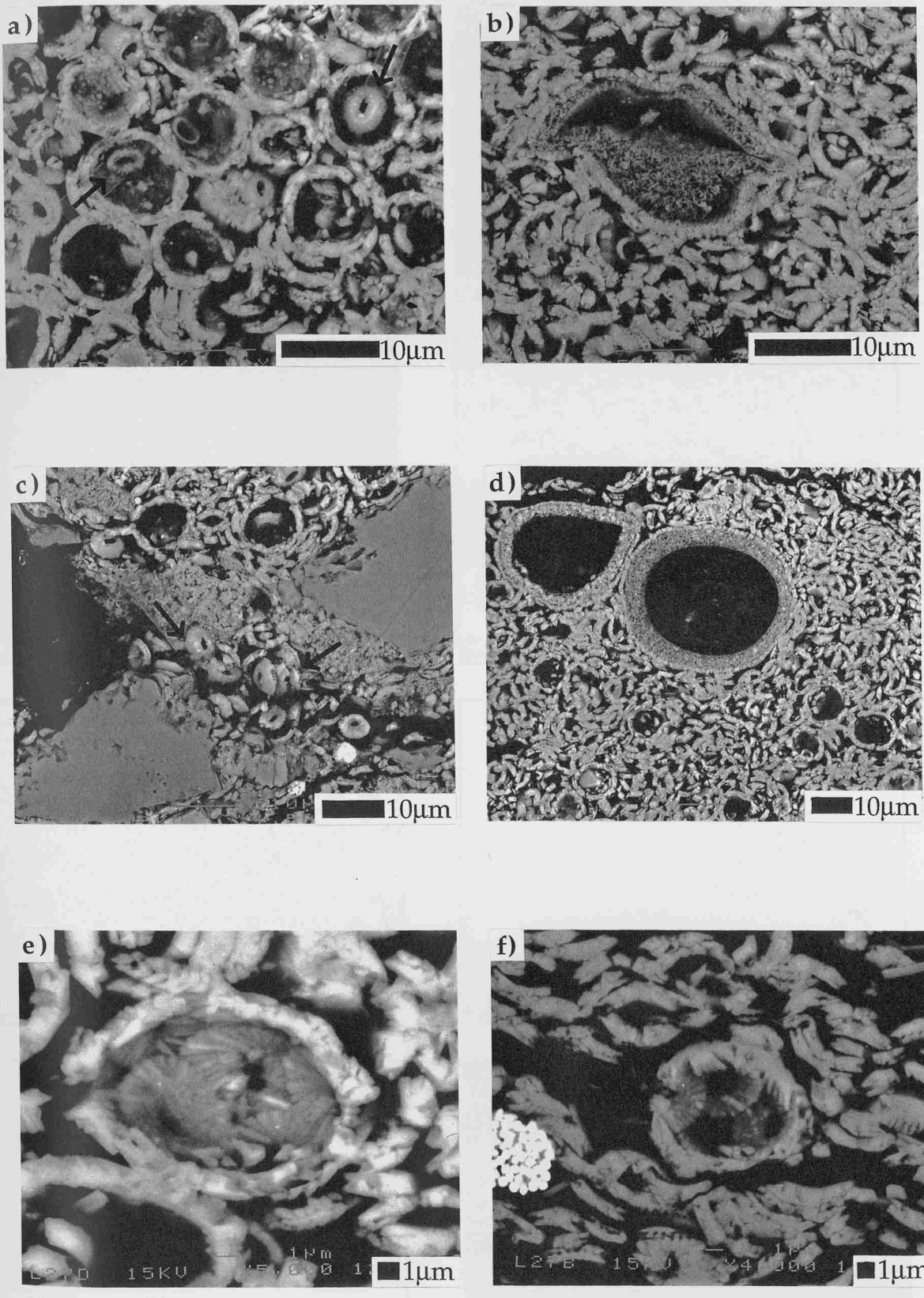

Figure 3.15

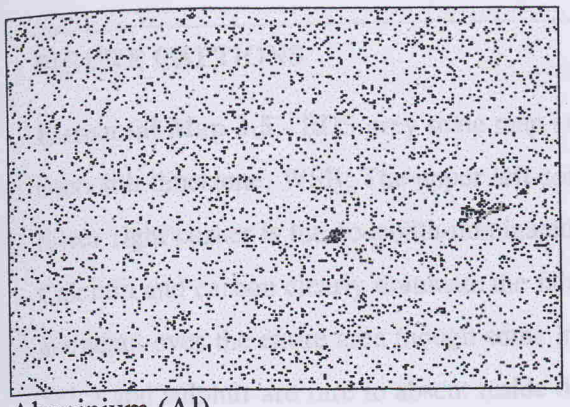

Aluminium (Al)

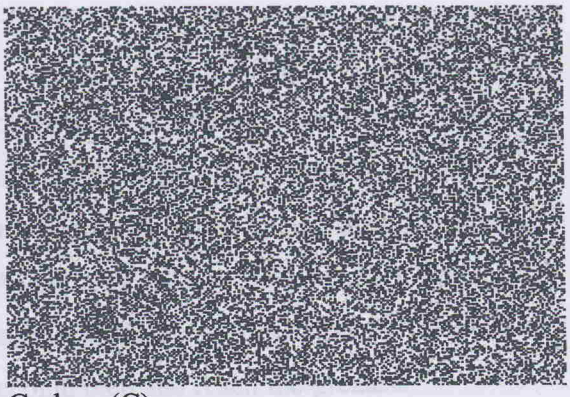

Carbon (C)

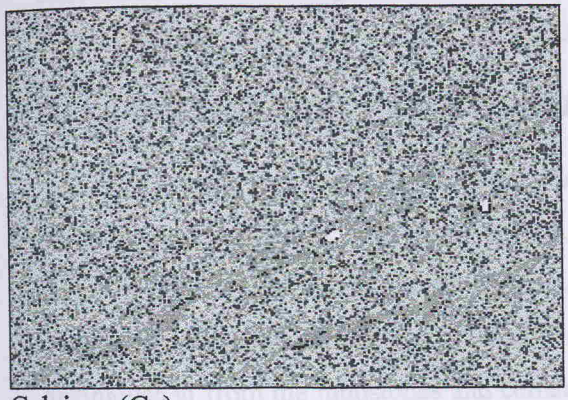

Calcium (Ca)

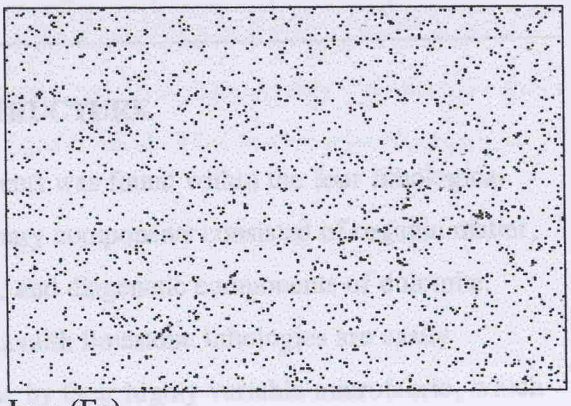

Iron (Fe)

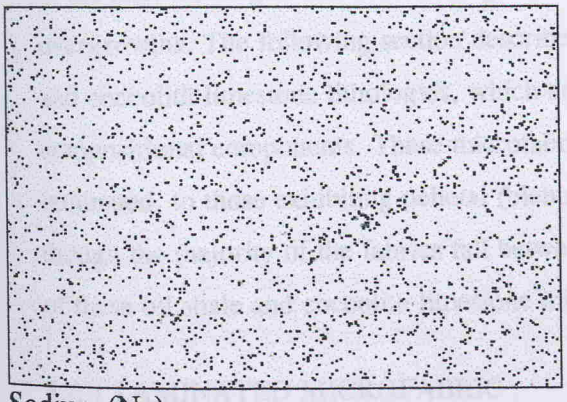

Sodium (Na)

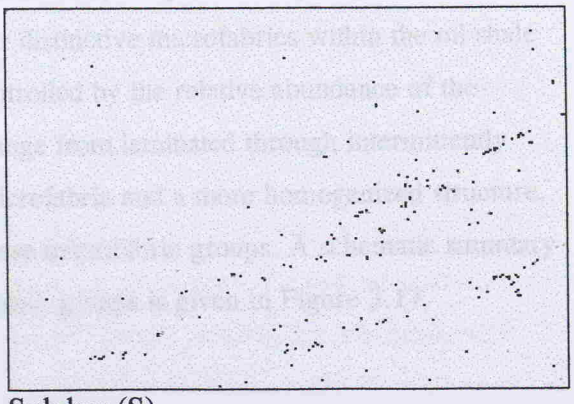

Sulphur (S)

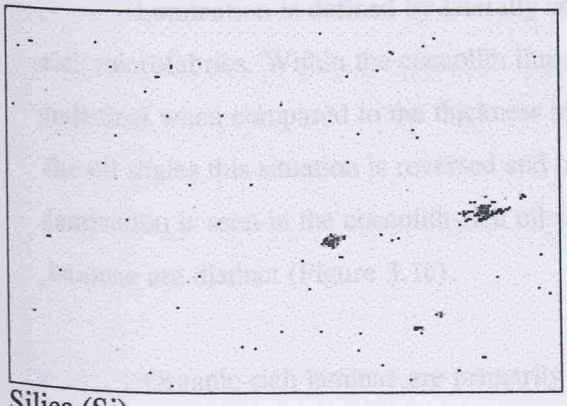

Silica (Si)

Elemental Map 3.5

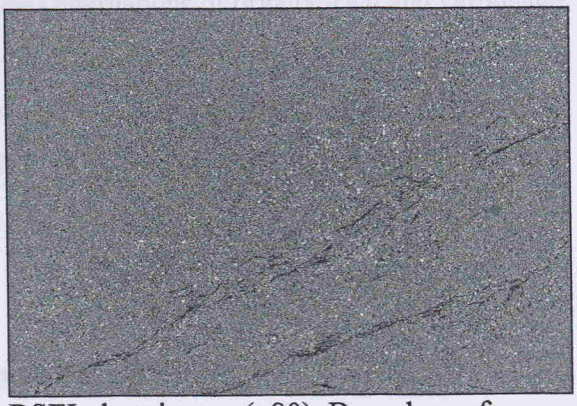

BSEI photoimage (x80), Boundary of a coccolith bleb, Coccolith limestone, WSB.

FIGURE CAPTIONS

Elemental Map 3.5 - EDS grey scale map (x80) of the edge of a pure coccolith bleb within a coccolith limestone, WSB. The upper left corner of the map is the coccolith bleb, while the lower right corner is the coccolith-dominated matrix containing some organic matter stringers. Calcium and carbon clearly dominate the fabric. Aluminium, sodium and iron are relatively abundant over the entire area though some increase in abundance is evident outside the bleb. Silica and sulphur are rare to absent inside the coccolith bleb and reach the greatest concentration with the organic matter stringers.

3.4 FABRIC ANALYSIS - MICROFABRIC STRUCTURE

A similar range of compositional components was found within the four lithological divisions previously described (Section 3.3). Primary components consisted of organic matter, coccolithic carbonate, clays, quartz and feldspars, and diagenetic components of dolomite, sparite and pyrite. However, the oil shale and coccolith limestone lithologies are easily distinguished from the mudstones and cementstone by their highly variable microfabric, which in the later lithologies has been homogenized or been completely altered by diagenetic overgrowths. The following section describes four distinctive microfabrics within the oil shale and coccolith limestone lithologies, which are controlled by the relative abundance of the compositional components. These microfabrics range from laminated through intermittently laminated, to those exhibiting pelletal (blebby) microfabric and a more homogenized structure, though the majority of the fabrics fall between these microfabric groups. A schematic summary of these oil shale and coccolith limestone microfabric groups is given in Figure 3.17.

3.4.1 LAMINATED MICROFABRIC

Lamination is defined by laterally continuous alternations of organic-rich and carbonate-rich microfabrics. Within the coccolith limestone lithology, organic-rich lamina are thin and indistinct when compared to the thickness of the carbonate lamina (Figure 3.13a), conversely in the oil shales this situation is reversed and organic matter dominates. However, the best lamination is seen in the coccolith-rich oil shales where both carbonate and organic-matter laminae are distinct (Figure 3.1c).

Organic-rich laminae are primarily composed of undulating, elongated stringers and are dominated by either diffuse, amorphous organic matter or have an abundant carbonate component of coccolith and/or sparite. Pyrite framboids are preferentially located with the organic matter and this is particularly evident in coccolith-rich, organic carbon lithologies where

organic stringers are abundant. The thickness of these stringer laminae can be less than 10μm to 100μm, with lateral continuity on a centimetre scale (Figure 3.6a, b; Figure 3.7c; Figure 3.8b).

Carbonate-rich laminae are composed of either sparite grains or coccoliths. Sparry laminae are the most distinct carbonate lamina form (Figure 3.16a to d), due to the robust, angular nature of sparry calcite euhedral crystals. Different densities and coalescence of these grains (Figure 3.16e and f) produces more, or less coherent lamina (Figure 3.16c). Laminae are laterally persistent over centimetres with thickness' from 50 to several 100μm. Lamina structure varies both in size and form, from thinner anastomosing ribbons, to thicker laminae which display pinching and subsequent thickening along their length (Figure 3.16c). The lateral persistence, distinct angular boundaries, and the robust nature of these sparry lamina make them evident in both hand specimen (Figure 3.1a-c) and under SEM /EDS examination (Elemental Map 3.6).

FIGURE CAPTIONS

Figure 3.16a - BSEI photograph (x50) showing a pair of thick (300μm) sparry lamina, WSB, divided by thin organic matter stringers.

Figure 3.16b - Detailed BSEI photograph (x130) of 3.16a, showing the coalescing euhedral sparite crystals that give the lamina a robust form. Note the preferentially situation of pyrite framboids with the organic carbon-rich lamina, while the sparite grains have pyrite overgrowths.

Figure 3.16c - BSEI photograph (x70) of alternating sparry and organic matter lamina, WSB. Note the different densities of the sparry lamina. In the upper laminae, the sparite grains are 10-50μm in diameter and have coalesced, whereas the lower sparry laminae are less dense with larger (30-100μm diameter) crystals that have not coalesced to such an extent. Also the upper sparry laminae show pinching and subsequent thickening along their length.

Figure 3.16d - BSEI photograph (x100) of a laminated sequence showing alternations between sparry lamina and organic matter lamina, WSB. Six lamina couplets of sparry and organic matter lamina are present in this photograph. Note the sparry laminae are generally two to three times thicker than the organic matter lamina.

Figure 3.16e - Detailed BSEI photograph (x600) of 3.17c, showing the coalescence of the small sparitic crystals forming the upper laminae in 3.17c.

Figure 3.16f - Detailed BSEI photograph (x600) of 3.17c, showing the larger sparitic crystals and the reduced coalescence of these crystals forming the lamina in the lower laminae of 3.17c.

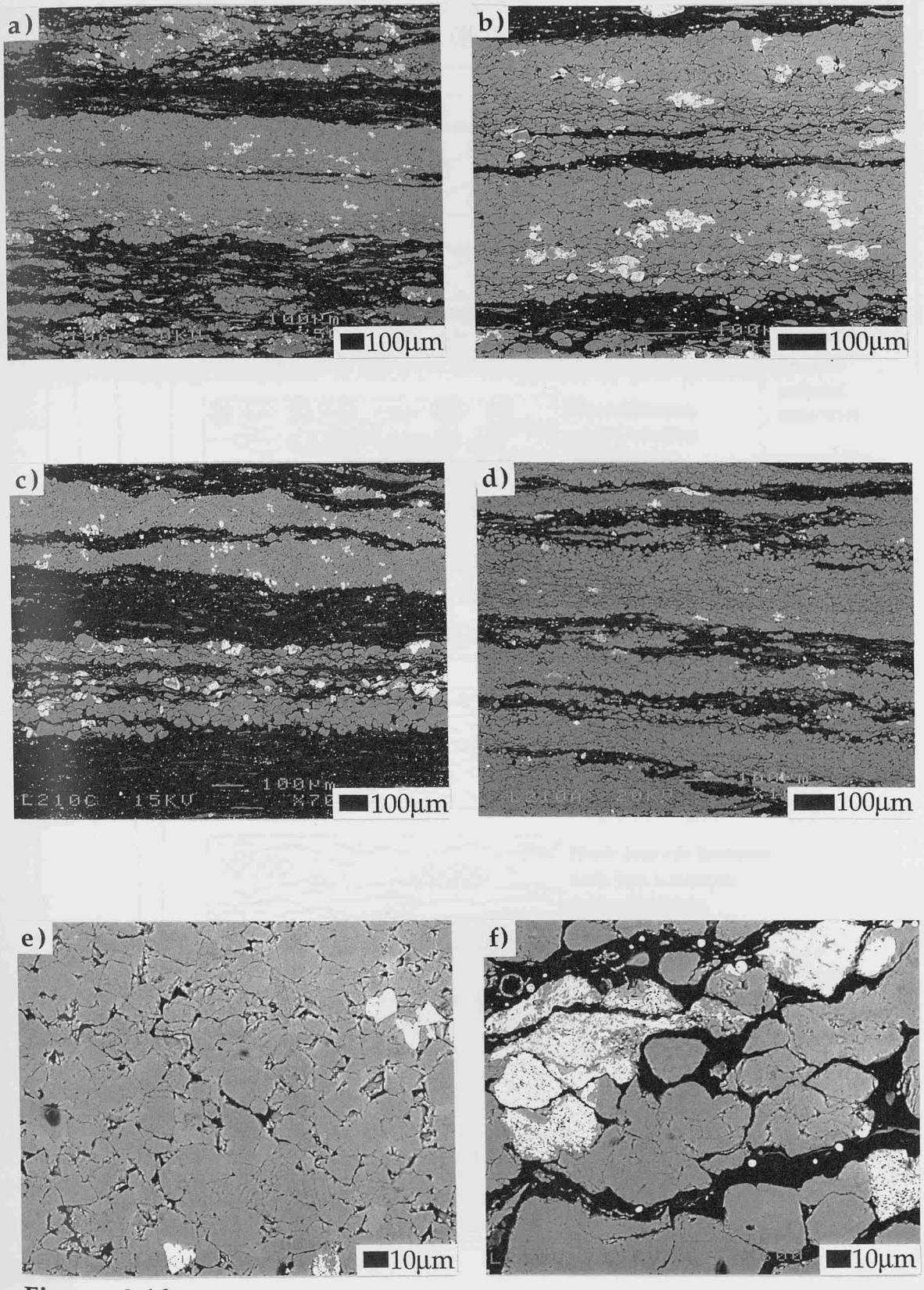

Figure 3.16

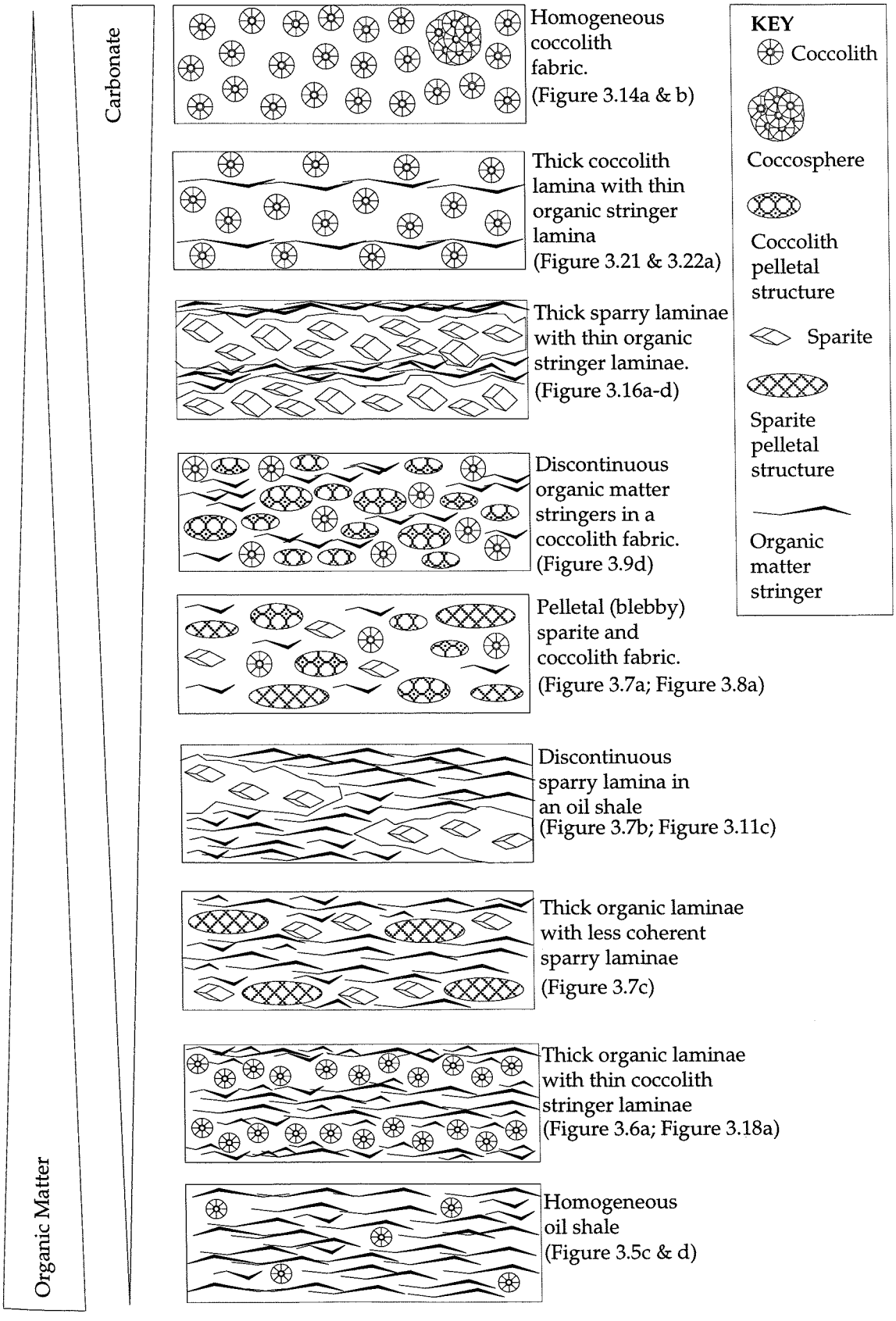

Figure 3.17

Schematic summary diagram of the KCF microfabric end members for the organic and coccolithic-rich lithologies. The relative abundance of organic matter and carbonate is indicated by the arrows to the left of the fabric cartoons. The dominant microfabric is the pelletal (blebby) fabric at the centre of the scale. Coalesence of pelletal strucutres results in discontinuous / intermittent lamination. Four types of laminated fabric are defined by the robustness of the lamina components and abundance. At either end of this scale the mircofabric is homogeneous.

FIGURE CAPTIONS

Elemental Map 3.6 - EDS grey scale map (x80) of well laminated microfabric of a carbonate-rich oil shale, WSB. The sparry laminae are clearly delineated by the calcium abundance, while sulphur and carbon highlight the organic matter laminae. Aluminium, silica and iron are predominately restricted to these organic matter laminae.

Elemental Map 3.7 - EDS grey scale map (x80) of a coccolithic pelletal (blebby) microfabric, WSB. The coccolith pelletal lenses are clearly delineated by the calcium abundance, while the organic matter stringers, which occur undulating between the lenses, are highlighted by sulphur abundance. Aluminium, silica and iron are also located with the organic matter stringers, but have low abundances.

Coccolith-dominated laminae are usually far thinner and less prominent than sparry laminae, and give the microfabric a dense, finely laminated appearance at the micron scale (Figure 3.19e). They are commonly $< 10\mu$m to 50μm thick, but can reach 100μm in thickness, with lateral continuity of several millimetres. Compared to the angular structure of the sparry laminae, coccolith lamina are commonly seen draped over other fabric components (Figure 3.6a and c; Figure 3.8c and d). Coalescence of elongated, coccolith pelletal lenses results in thicker laminae, characterised by blebby, undulating boundaries, giving a highly variable laminated microfabric (Figure 3.9b and d). The compact nature and size of coccoliths gives smooth, clear lamina boundaries.

Thicker organic/carbonate laminae (average thickness 100μm) are also present within the organic carbon-rich lithologies, but the boundaries between the lamina are less coherent than previously mentioned lamina (Figure 3.7c). Though the lamina boundaries are less distinct and lack sharpness, this lamination is evident in hand specimen, X-radiographs and more clearly under SEM examination (Figure 3.1b and c, Figure 3.7c) and is laterally persistent over several centimetres. Organic-rich lamina are composed of diffuse, amorphous and elongated stringer organic matter within minor components of individual sparitic grains, random groupings of coccoliths and pyrite framboids. Carbonate-rich lamina are predominantly composed of sparry lensoidal groups surrounded by individual and loose groups of sparitic grains. An average thickness for an organic/carbonate laminae couplet for this type of microfabric is 200μm. These thicker lamina occur in discrete vertical intervals and other lamina types are not found within a lamina sequence of this form.

Though lamination is the most noticeable of the microfabrics, laminated intervals are not dominant or highly abundant within the KCF microfabrics. Using the coccolith-rich oil shale (1) below the WSB coccolith limestone as an example (Figure 3.1), the laminated microfabrics constitute 16% of the thickness of this oil shale, compared to pelletal fabric (described in a following Section 3.4.3) which are almost 60% of the oil shale microfabric.

3.4.2 DISCONTINUOUS / INTERMITTENT LAMINATED MICROFABRIC

Carbonate and organic matter microfabric alternations also form discontinuous and intermittent lamination where the lamina is broken into laterally restricted sections. Partial coalescence of elongated organic matter lenses and stringers, or sparry/coccolith stringers and pelletal lenses, results in discontinuous lamina (Figure 3.6d; Figure 3.7b: Figure 3.9a). At low SEM magnification, microfabric composed of coccolithic and organic matter stringers is finely laminated. However, detailed, high magnification SEM examination show both the organic matter and coccolithic stringers to be laterally impersistent, resulting in discontinuous fine lamination (Figure 3.9a). The coalescence of carbonate pelletal lenses gives a intermittent lamination at both low and high magnifications due to the lenses being of greater size, especially thickness, than stringers and therefore distinct from the surrounding matrix (Figure 3.6d; Figure 3.7b). Within the lower oil shale (1) of the WSB interval this microfabric type accounts for 12% of the oil shale thickness.

3.4.3 PELLETAL (BLEBBY) MICROFABRIC

Pelletal (blebby) microfabrics are composed of trains of pelletal lenses, situated parallel to bedding within the matrix (Elemental Map 3.7). This fabric is most commonly evident in organic carbon-rich lithologies, but pelletal lenses vary widely in size and are present in both coccolith limestone and calcareous mudstone lithologies (Table 3.3; Figure 3.7a and 3.8a; Figure 3.9c). In general the pelletal lenses occur with individual and groups of loose coccoliths and sparite grains. Elongated, organic matter stringers of all sizes, and some discrete shaped organic matter blebs and laths also occur with pelletal lenses. Proportional changes in any or all of these constituents is frequent, resulting in the many subtle versions of this microfabric. Rare pelletal structures are also present in fabric that has a more homogeneous nature, be it organic-rich, or carbonate-rich. Within the lower WSB oil shale (1) pelletal fabric constituents 59% of the oil shale thickness.

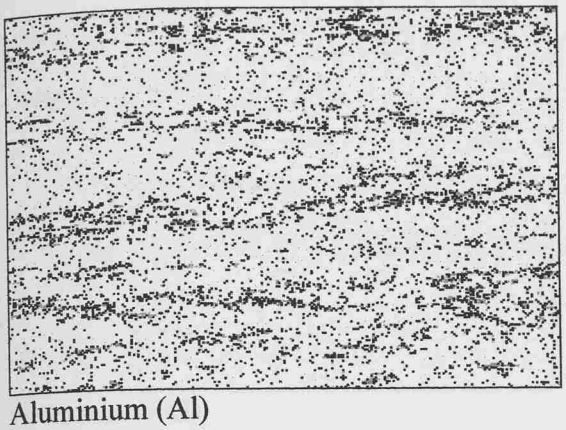

Aluminium (Al)

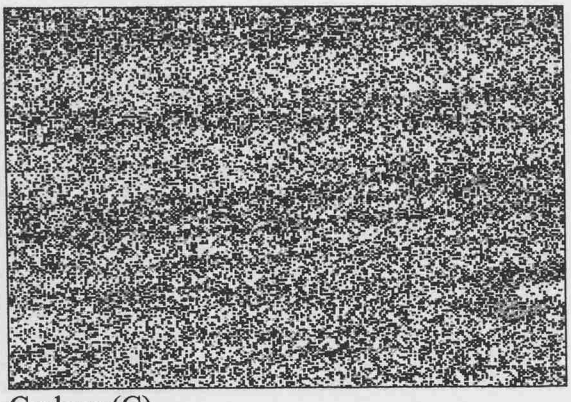

Carbon (C)

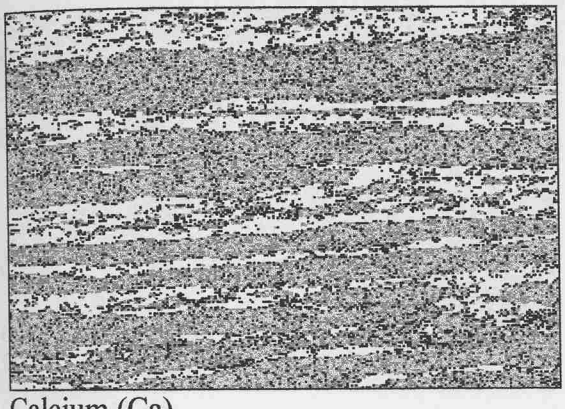

Calcium (Ca)

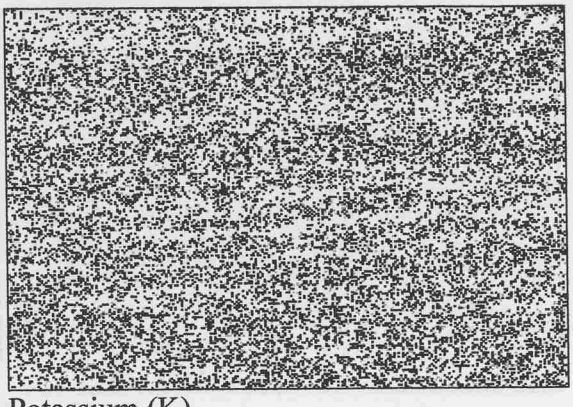

Potassium (K)

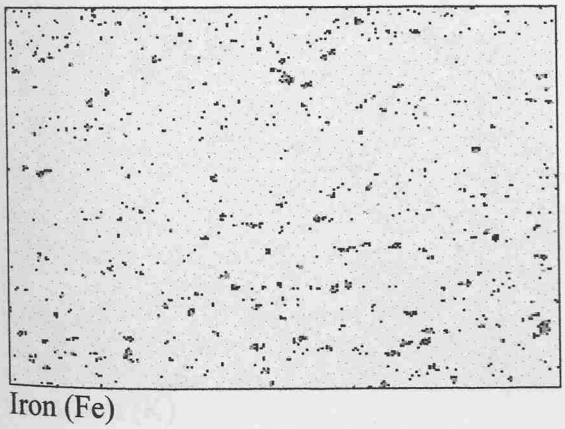

Iron (Fe)

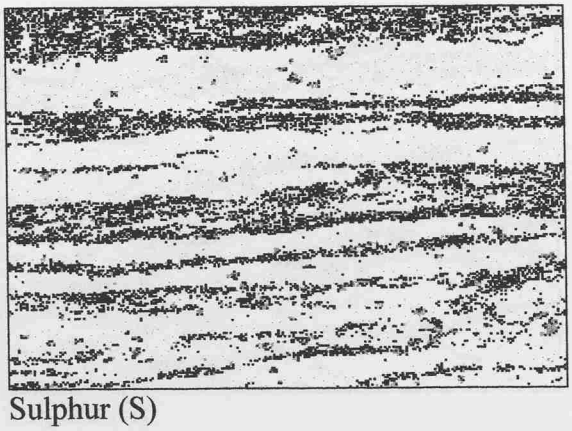

Sulphur (S)

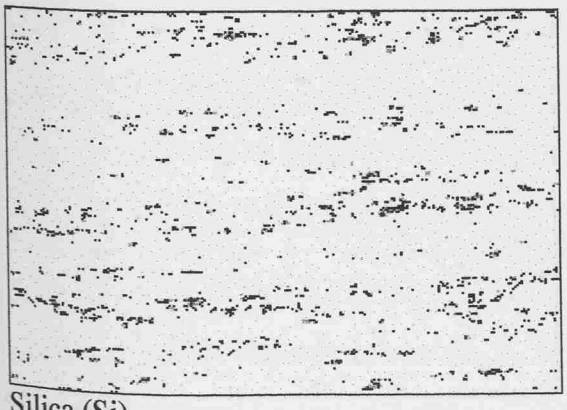

Silica (Si)

Elemental Map 3.6

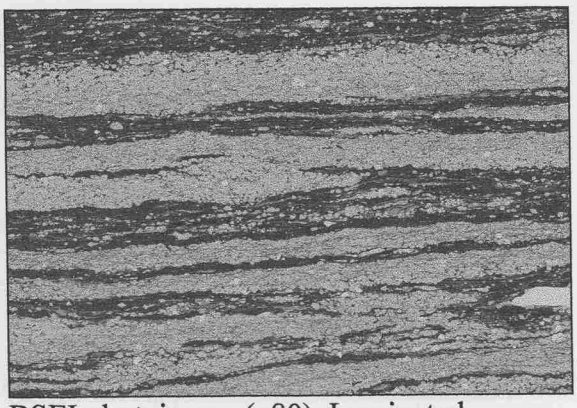

BSEI photoimage (x80), Laminated carbonate rich Oil shale microfabric, WSB

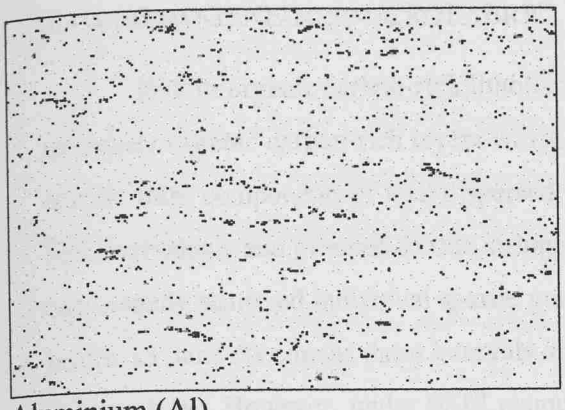

Aluminium (Al)

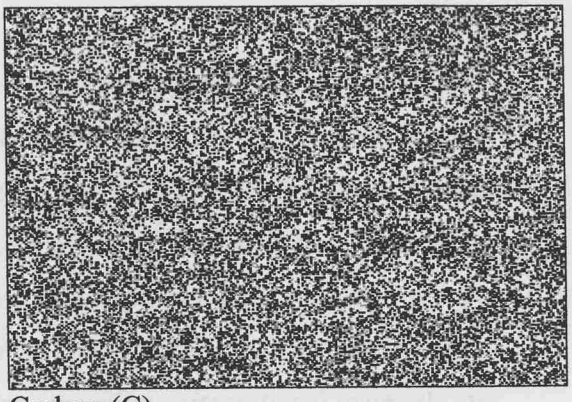

Carbon (C)

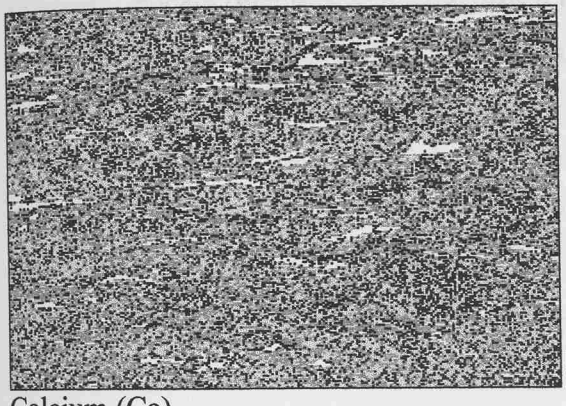

Calcium (Ca)

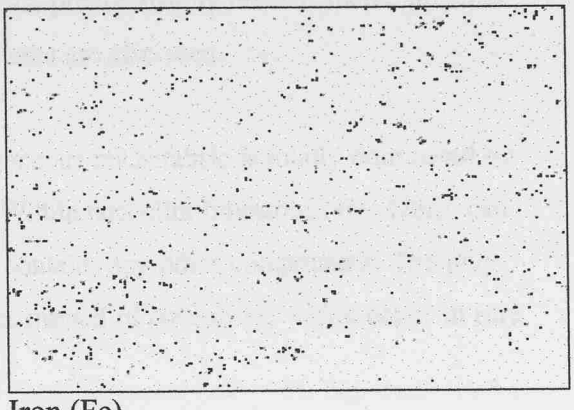

Iron (Fe)

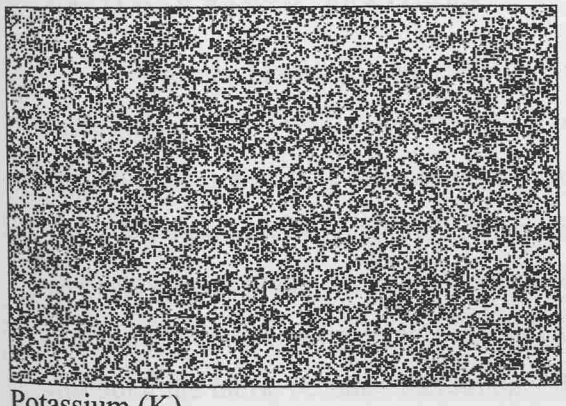

Potassium (K)

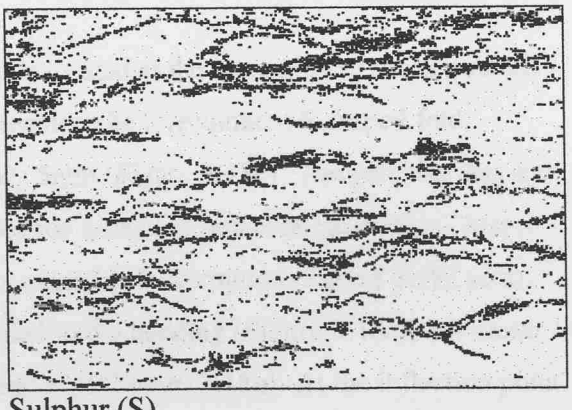

Sulphur (S)

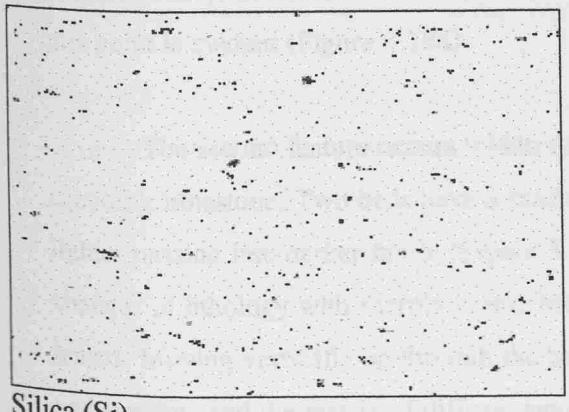

Silica (Si)

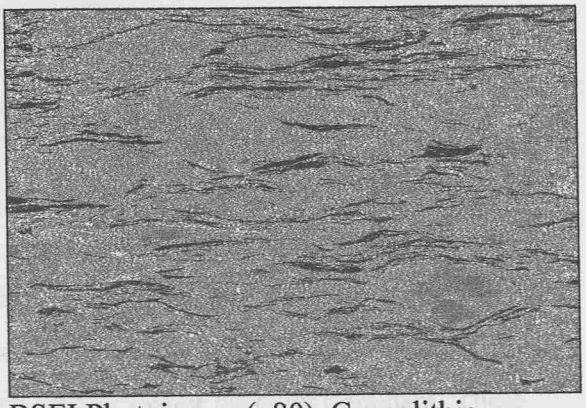

BSEI Photoimage (x80), Coccolithic, blebby microfabric, WSB.

Elemental Map 3.7

3.4.4 HOMOGENEOUS MICROFABRIC

Within organic carbon-rich lithologies homogeneous microfabrics are present as extremely organic carbon-rich layers which are dominated by diffuse, amorphous organic matter. Rare components of well dispersed pyrite framboids, clays and coccoliths, present as both individuals and grouped in thin stringers ($<200\mu m$ in length and $<20\mu m$ in height), and occasionally scattered individual sparite grains, are present within these very rich organic carbon layers. In hand specimens these intervals are seen as homogeneous, darker coloured areas (Figure 3.1a). However, under BSEI magnification, the other compositional materials are clearly evident (Figure 3.5c to f). Crushed bioclasts, predominately bivalve shells, are also common within this fabric type, and rare calcispheres are also seen.

Within carbonate-rich lithologies, homogeneous microfabric is totally dominated by densely packed coccoliths (Figure 3.14a and b). Within coccolith limestones this fabric can reach several millimetres in thickness and rarely contains any other components. The only variability evident is the presence of coccospheres instead of coccoliths, which occur in rare pelletal groupings (Figure 3.14c to f).

3.5 OTHER FABRIC FEATURES

The first feature of note is a structure that is located at the beginning of the central oil shale (2) within the WSB coccolith limestone. It seems to be a recumbent S-shaped fold, occurring over a vertical distance of approximately 5mm (Figure 3.18e). The pinching out and termination of highly organic-rich layers delineates the inflection points of the feature. Above and below these points the fabric displays various microfabric disruption (Figure 3.18a to d). Away from the inflection points the fabric is parallel to the bedding (Figure 3.18a), but closer to this point the fabric becomes increasingly tilted and bent (Figure 3.18b). At the inflection point (Figure 3.18c), overturn of the fabric can be seen and the chaotic nature of the fabric in front of this point is evident (Figure 3.18d).

The second feature occurs within the coccolith-rich oil shale (1) below the WSB coccolith limestone. Two beds have a graded nature seen as vertical variation in colour from lighter passing into darker fabric (Figure 3.18f). These beds are characterized by abrupt vertical changes in lithology with sharply planar bases, dominated by abundant, closely packed sparry lenses. Moving vertically up through the bed, the lenses become progressively more dispersed and smaller, and the matrix of diffuse, amorphous organic matter becomes dominant. These beds are located close to or within sections of fabric which are characterized by abundant carbonate laminae.

FIGURE CAPTIONS

Figure 3.18a - Detailed BSEI photograph (x370) of 3.18e, showing coccolith and organic matter stringers and lenses located away from the inflection point of the fold, which are parallel to the bedding plane. (Position of this photograph on 3.18e is marked by (A))

Figure 3.18b - Detailed BSEI photograph (x370) of 3.18e, showing the titled and bent coccolith and organic matter stringers and lenses nearer the fold inflection point. (Position of this photograph on 3.18e is marked by (B))

Figure 3.18c - BSEI photograph (x200) of 3.18e, showing the variability of fabric alignment at and around the fold inflection point. (Position of this photograph on 3.18e is marked by (C))

Figure 3.18d - Detailed BSEI photograph (x370) of 3.18e, showing the complete break down of fabric structure, with a chaotic mixture of coccoliths and organic matter, directly in front of the fold inflection point. (Position of this photograph on 3.18e is marked by (D))

Figure 3.18e - BSEI photograph (x20) of a recumbent S-shaped fold at the beginning of the central oil shale (2) in the Whitestone Band coccolith limestone (inflections indicated by arrows)

Figure 3.18f - BSEI photograph (x50) of a graded bed in the oil shale (1) located beneath the WSB coccolith limestone. Note the planar base (indicated by the thick arrows) and the abundance of sparry lenses and grains at the base of the bed. These lenses decrease in abundance and size, until the fabric is dominated by diffuse, amorphous and stringer organic matter.

Figure 3.19a - Detailed BSEI topographic photograph (x1000) showing the abundant coccolith plates of the coccolith limestone fabric, WSB. Note the lack of orientation of the coccoliths.

Figure 3.19b - Detailed BSEI topographic photograph (x500) of a complete coccosphere in amongst coccolith plates within the coccolith limestone fabric, WSB. Note the exceptional preservation of the coccolith plates and the intact coccosphere.

Figure 3.19c - Detailed BSEI topographic photograph (x2000) of less well preserved coccolith plates and clays in a calcareous mudstone, WSB.

Figure 3.19d - Detailed BSEI topographic photograph (x3000) of well preserved coccoliths in the Freshwater Steps coccolith limestone (FWSB).

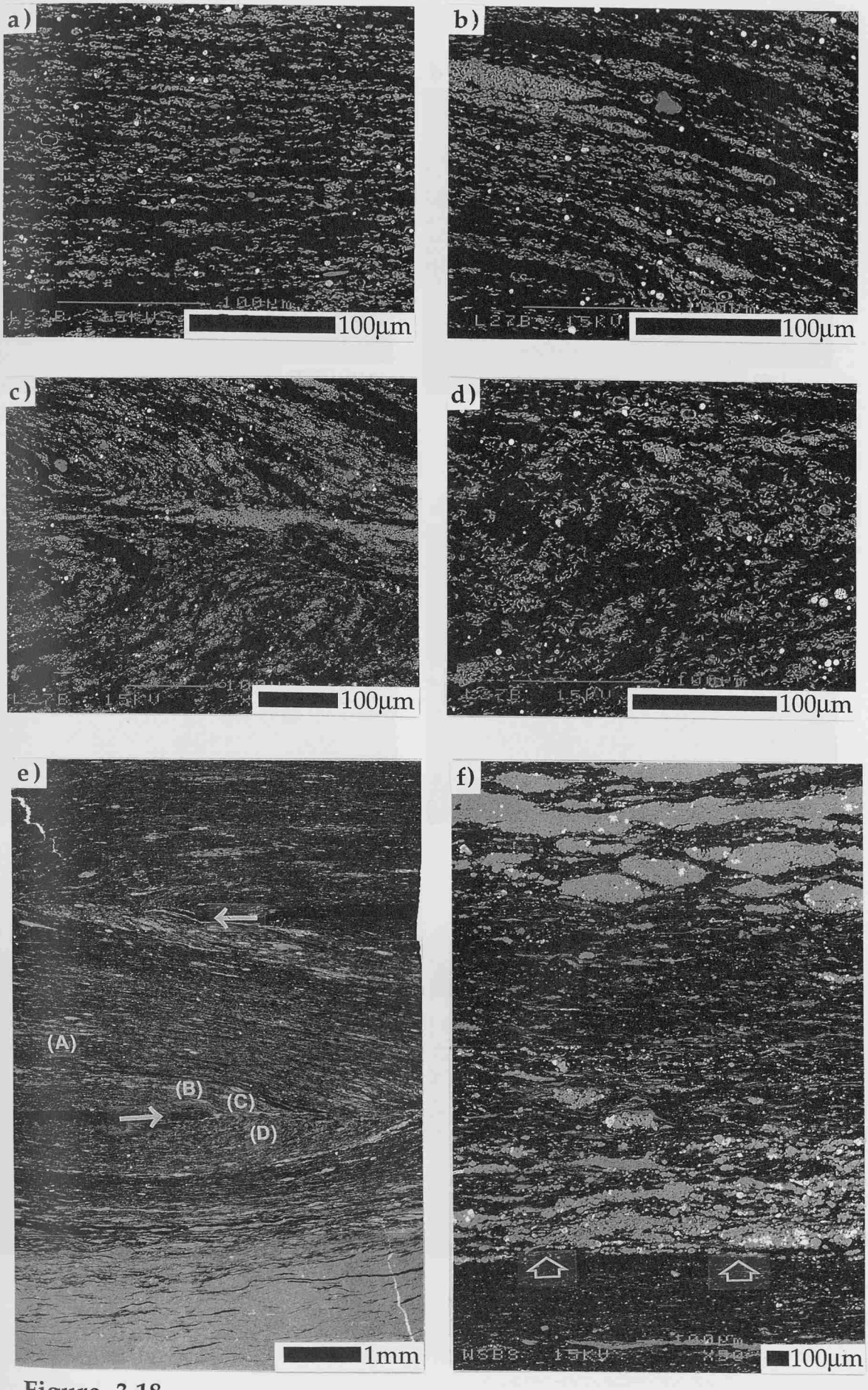

Figure 3.18

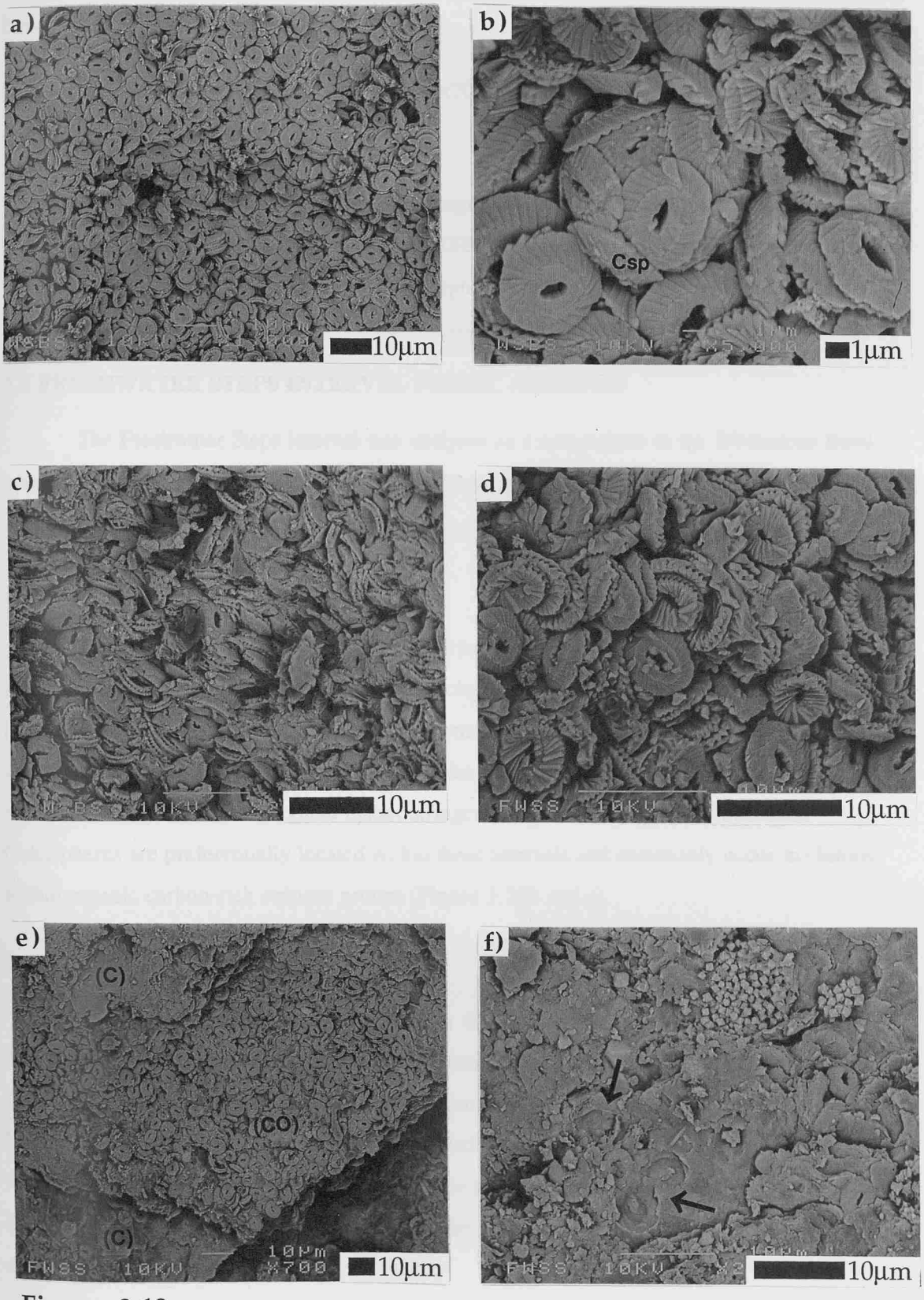

Figure 3.19

FIGURE CAPTIONS

Figure 3.19e - BSEI topographic photograph (x700) of a coccolith-rich lamina (CO) between two organic carbon-rich lamina (C), FWSB.

Figure 3.19f - Detailed BSEI topographic photograph (x2200) of coccolith imprints on an organic matter layer (indicated by arrows), FWSB. Similar imprints were seen under transmitted light where they were highly abundant on amorphous organic matter clumps (see Figure 6.7G)

3.6 FRESHWATER STEPS INTERVAL FABRIC ANALYSIS

The Freshwater Steps interval was analysed as a comparison to the Whitestone Band interval, to establish lithological differences between two of the coccolith limestones of the KCF, these are briefly presented here.

3.6.1 CALCAREOUS MUDSTONE

The calcareous mudstones of the FWSB have more abundant quartz and feldspar grains, organic matter discrete blebs and laths, and calcispheres, than the same lithology in the WSB interval (Figure 3.20a). Pyrite framboids are common and range in diameter from $<5\mu$m to 10μm. The matrix of the FWSB calcareous mudstone is dominated by clays and poorly preserved coccoliths, while organic matter stringers form restricted vertical intervals. Calcispheres are preferentially located within these intervals and commonly occur in clumps within organic carbon-rich stringer groups (Figure 3.20b and c).

3.6.2 COCCOLITH LIMESTONE

Within the coccolith limestone lithology discrete pelletal lenses, dominated by coccospheres and coccoliths, are common and can be clearly delineated from the remainder of the coccolith fabric where organic matter stringers are present (Figure 3.20b). Calcispheres are highly abundant and are again generally restricted to layers with organic matter stringers (Figure 3.20c). Similar to the WSB, coccospheres within pelletal lenses show infilling by calcite crystals (Figure 3.20d). However, the FWSB contains far fewer hollow coccospheres and preservation of internal plates is very rare.

The microfabric of the FWSB coccolith limestone differs from the WSB microfabric in the presence of thin vertical sequences of well developed coccolith-organic matter lamination, found together with a repetitive sequence of other fabric types (Figure 3.21 and 3.22a; Elemental Map 3.8).

This sequence begins with layers that contain abundant undulating organic matter stringers (< 100μm to 500μm in length, < 10μm thick). Highly abundant calcispheres are preferentially located with the organic stringers, and discrete coccolith/coccosphere pelletal lenses are common between stringers. These layers can range in thickness between 1 to 2 millimetres (Figure 3.21 (A)).

Bundles of thicker coccolith-dominated laminae follow (100-400μm thick), and are divided by thin organic carbon-rich laminae (20-50μm thick), containing continuous undulating organic stringers (Figure 3.21 (B), Figure 3.22a; Elemental Map 3.8). The coccolith lamina contain abundant coccospheres but also have substantial overgrowth patches of calcite cement, but despite this, coccolith preservation of uncemented coccoliths is excellent (Figure 3.19d). It is clearly noticeable that calcispheres are not present within the coccolith lamina but are restricted to the organic lamina. The calcite cement, which is common in the FWSB coccolith limestone, occurs as variable sized patches (in the order of several 100μm^2) in these non-pelletal coccolith rich areas, this was not observed within the WSB (Figure 3.22b and c).

The fabric then returns to organic matter stringer dominated layers (Figure 3.21 (A)), which are proceeded by massive coccolith and coccosphere dominated layers (Figure 3.21 (C)), in which other lithological components are exceptionally rare. These layers are massive in structure and range between 300μm and several millimetres, and they commonly show calcite cement patches and coccosphere infilling.

The sequence then repeats. However, it is not always repeated in the same order but generally a layer rich in organic matter stringers precedes the coccolith-organic laminations.

Within some areas, the coccolith-organic laminations of the FWSB are very disrupted and are commonly abruptly terminated (Figure 3.22d and e). Individual disruption features occur at a millimetre scale but whole polished thin sections, of 3 to 4 centimetres length, can show microfabric disturbance. Due to the more massive nature of the WSB coccolith limestone fabric, this form of disturbance was not seen under the SEM. However, macro-disturbance features (trace-fossils) were present within the WSB coccolith limestone and in the preceding calcareous mudstone (Figure 1.4).

FIGURE CAPTIONS

Figure 3.20a - BSEI photomosaic (x200) of the FWSB calcareous mudstone lithology. Quartz and feldspar grains are highly abundant and organic matter blebs and laths are common. Organic carbon stringers are grouped in restricted vertical layers and calcispheres are preferentially located within these layers. Degraded coccoliths and clays dominate the fabric matrix.

Figure 3.20b - BSEI photomosaic (x100) of undulating, elongated organic matter stringers within the FWSB coccolith limestone. The preferential location of both calcispheres and pyrite framboids with the organic matter stringers is clear. Note the presence of discrete coccosphere dominated pelletal lenses between organic matter stringers (indicated by arrow).

Figure 3.20c - Detailed BSEI photograph (x400) of 3.20b, showing calcispheres grouped next to a series of organic matter stringers, FWSB.

Figure 3.20d - Detailed BSEI photograph (x400) of 3.20b, showing a coccosphere dominated pelletal lens, FWSB. Note the calcite infilling of the majority of the coccospheres.

— —

Elemental Map 3.8 - EDS grey scale map (x80) showing well laminated microfabric of coccolith and organic matter stringers in the FWSB coccolith limestone. The thick coccolith laminae are clearly evident from the distribution of calcium, while carbon and sulphur delineate the organic matter stringer laminae. Silica, aluminium, iron and sodium are also restricted to the organic matter stringers and are rare or absent within the coccolith laminae.

— —

Figure 3.21 - BSEI photomosaic (x100) of a vertical sequence of layers that commonly occur in a repetitive order within the FWSB coccolith limestone. Layer (A) = organic matter stringer dominated, Layer (B) = coccolith-organic matter lamination, Layer (C) = massive coccolith and coccosphere dominated. Note the patches of calcite cement within the coccolith lamina of the laminated layer (B) and in the massive coccolith layer (C) (indicated by the thin arrows).

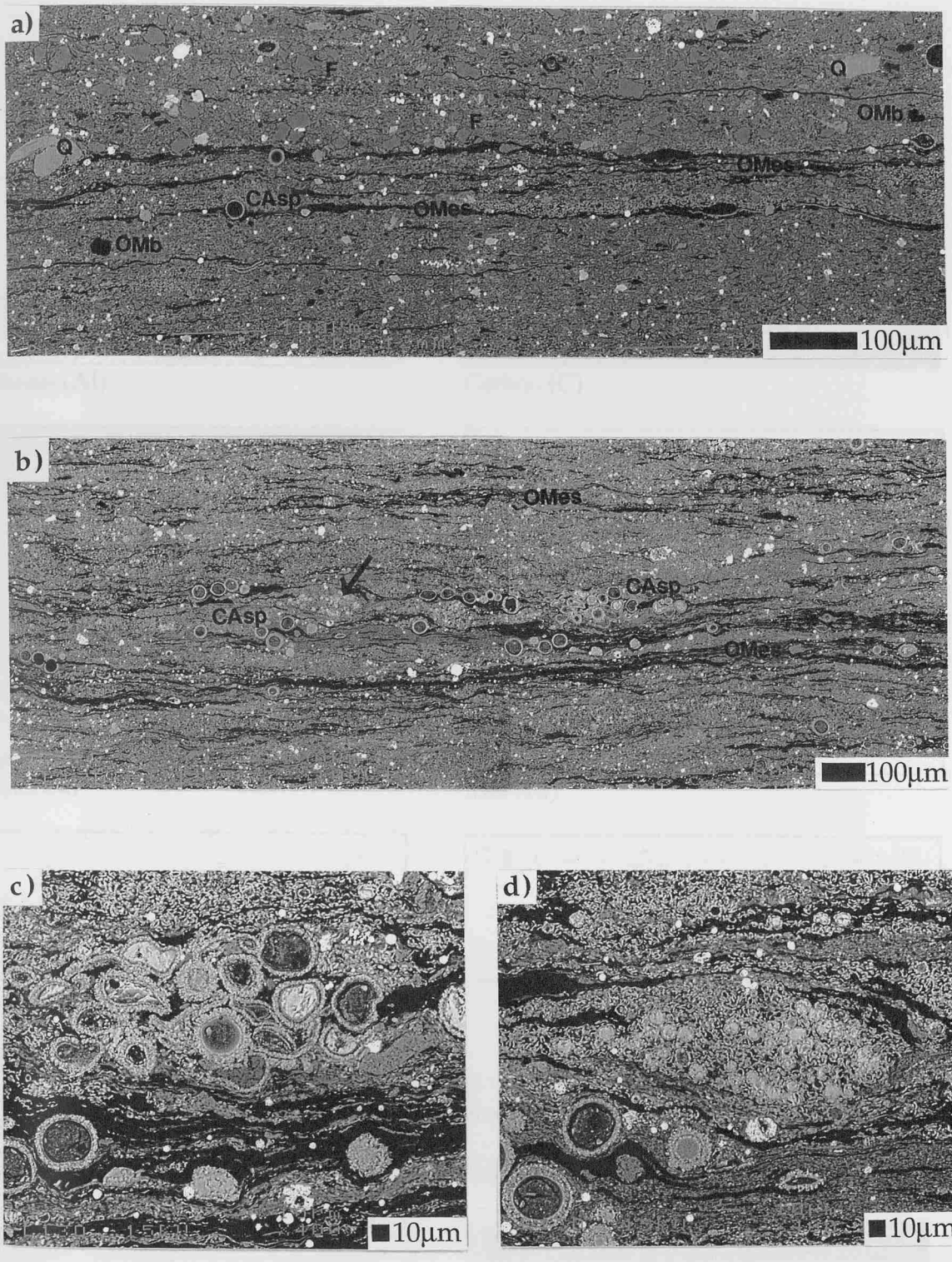
a)
F
F
Q
Q
OMb
Q
OMes
CAsp
OMes
OMb
100µm
b)
OMes
CAsp
CAsp
OMes
100µm
c)
10µm
d)
10µm

Figure 3.20

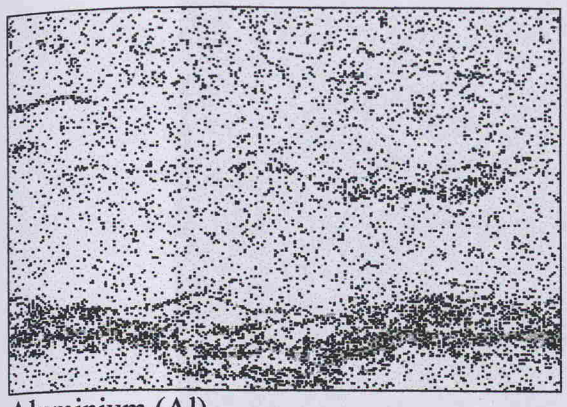

Aluminium (Al)

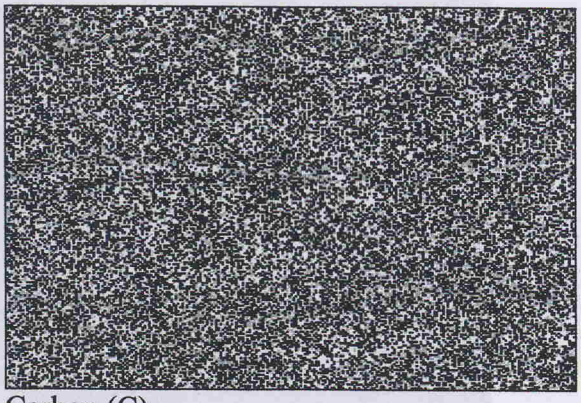

Carbon (C)

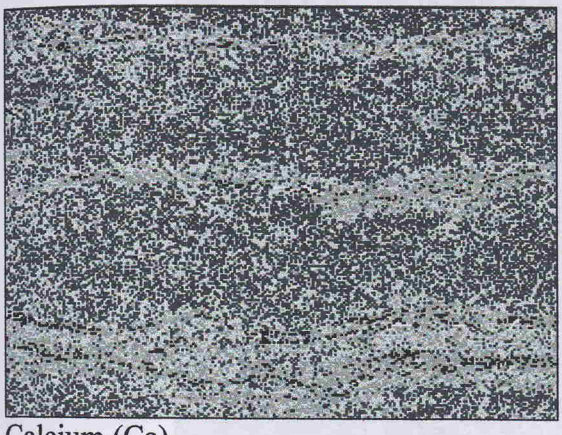

Calcium (Ca)

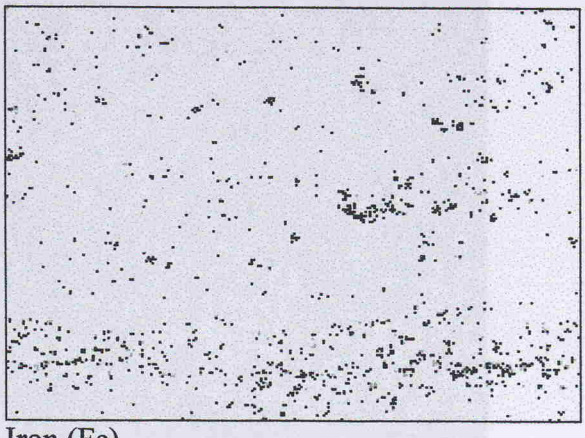

Iron (Fe)

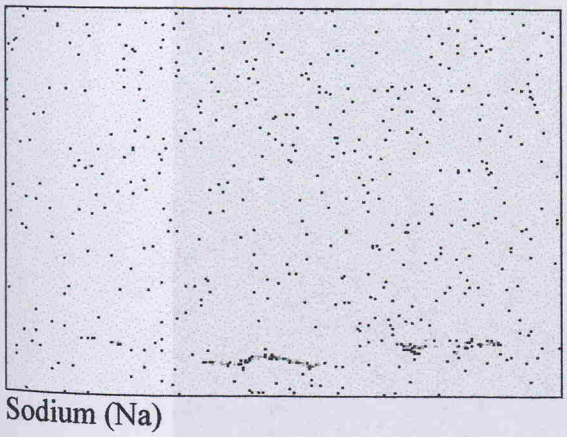

Sodium (Na)

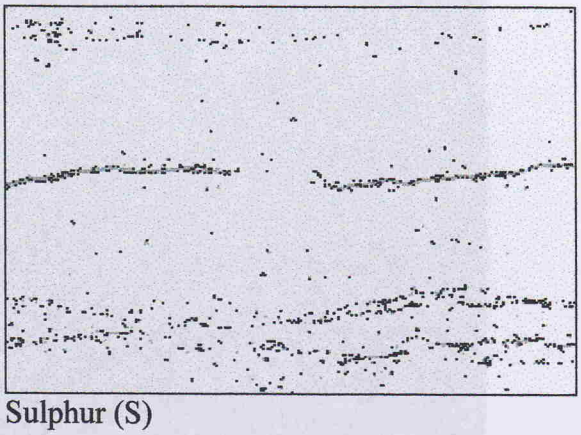

Sulphur (S)

Silica (Si)

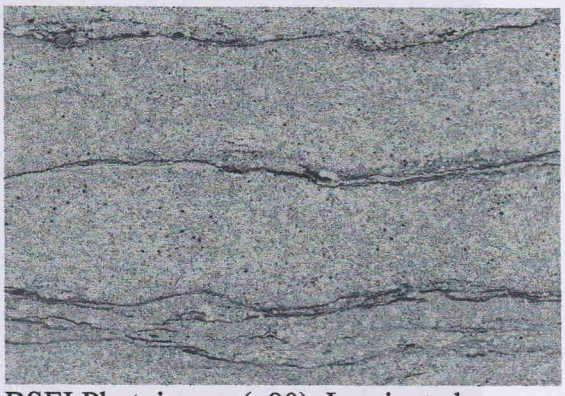

BSEI Photoimage (x80), Laminated microfabric, Coccolith limestone, FWSB

Elemental Map 3.8

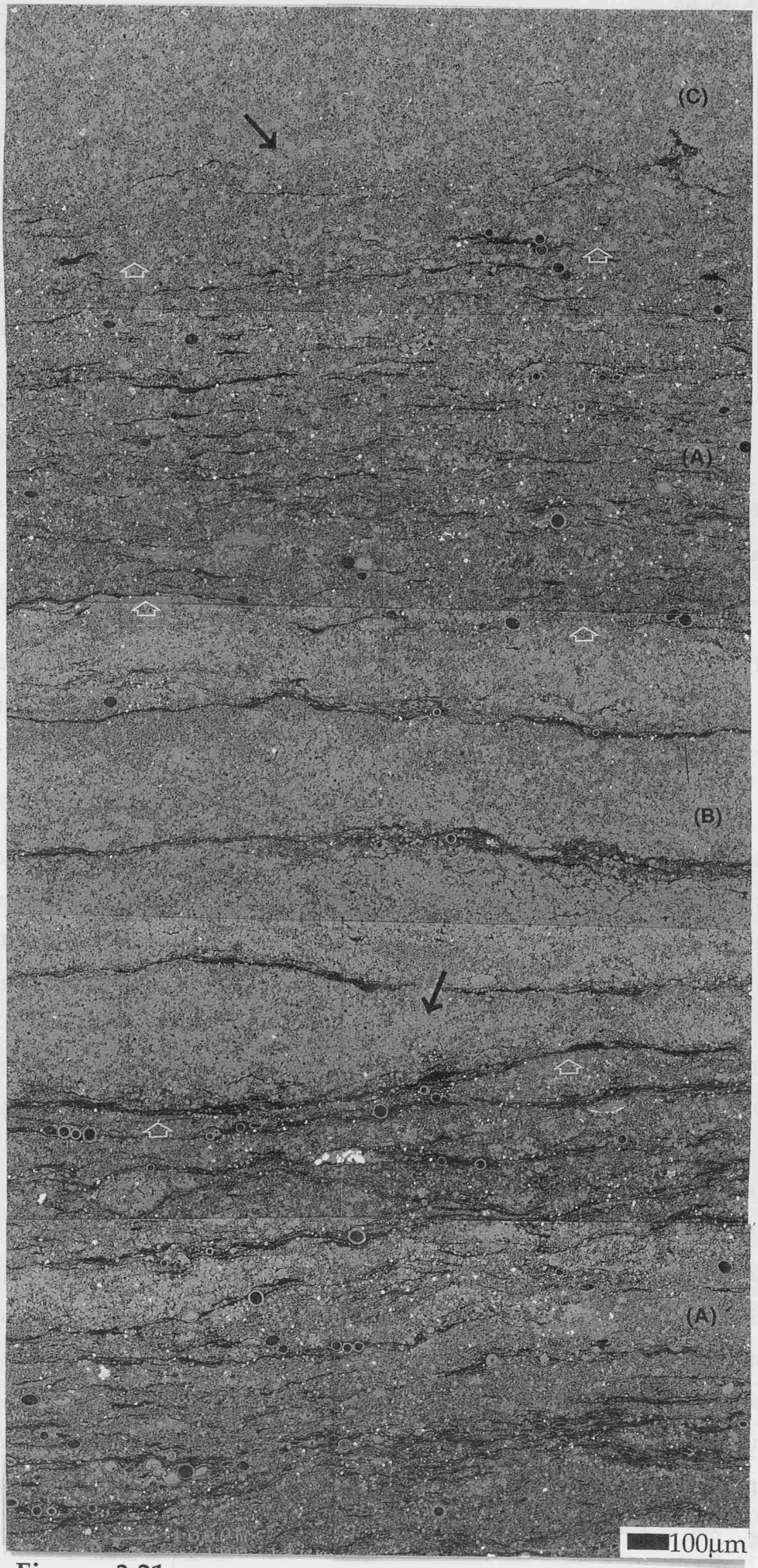

Figure 3.21

FIGURE CAPTIONS

Figure 3.22a - BSEI photomosaic (x50) of a well developed sequence of coccolith-organic stringer lamination within the FWSB. Note the calcite cement of the coccolith lamina and the calcispheres within the organic stringer lamination.

Figure 3.22b -Detailed BSEI photograph (x900) of calcite infilling coccospheres, FWSB coccolith limestone.

Figure 3.22c - Detailed BSEI photograph (x800) of patchy overgrowth of calcite cement, FWSB coccolith limestone.

Figure 3.22d - Low magnification BSEI photograph (x20) of laterally terminated coccolith-organic stringer lamination in disturbed FWSB coccolith limestone (termination line indicated by thin arrow).

Figure 3.22e - Low magnification BSEI photograph (x20) of disrupted massive coccolith layers, FWSB (disrupted section indicated by arrow).

3.7 *EUDOXUS* INTERVAL FABRIC ANALYSIS

The *Eudoxus* interval was analysed to establish intra-lithological differences between the bituminous/oil shales within the KCF. The *Eudoxus* interval represents the greatest development of oil and bituminous shales in the KCF, while oil shales within the Whitestone Band interval are discrete occurrences.

The *Eudoxus* bituminous shales contain abundant quartz and feldspar grains and discrete organic matter blebs and laths, similar to the FWSB calcareous mudstones (Figure 3.23a to c). However, the bituminous shales are dominated by diffuse amorphous organic matter and elongated organic matter lenses and stringers, which form discontinuous lamina (Figure 3.23d). Clays and degraded coccolith stringers are also abundant, and coccolith pelletal structures are common (Figure 3.23c). Pyrite framboids ($<10\mu$m diameter) are preferentially located with organic matter (Figure 3.23b) and are composed of very fine grained individual framboids ($<1\mu$m diameter) (Figure 3.24b). Calcispheres are present and are more abundant than seen in the WSB interval, but far less common than in the FWSB coccolith limestone. In more organic carbon-rich shales the fabric is blebby, dominated by abundant coccolith pelletal lenses and organic matter stringers, which are orientated parallel to the bedding (Figure 3.23d; Elemental Map 3.9). Crushed ammonite and bivalve shells are also common within these shales.

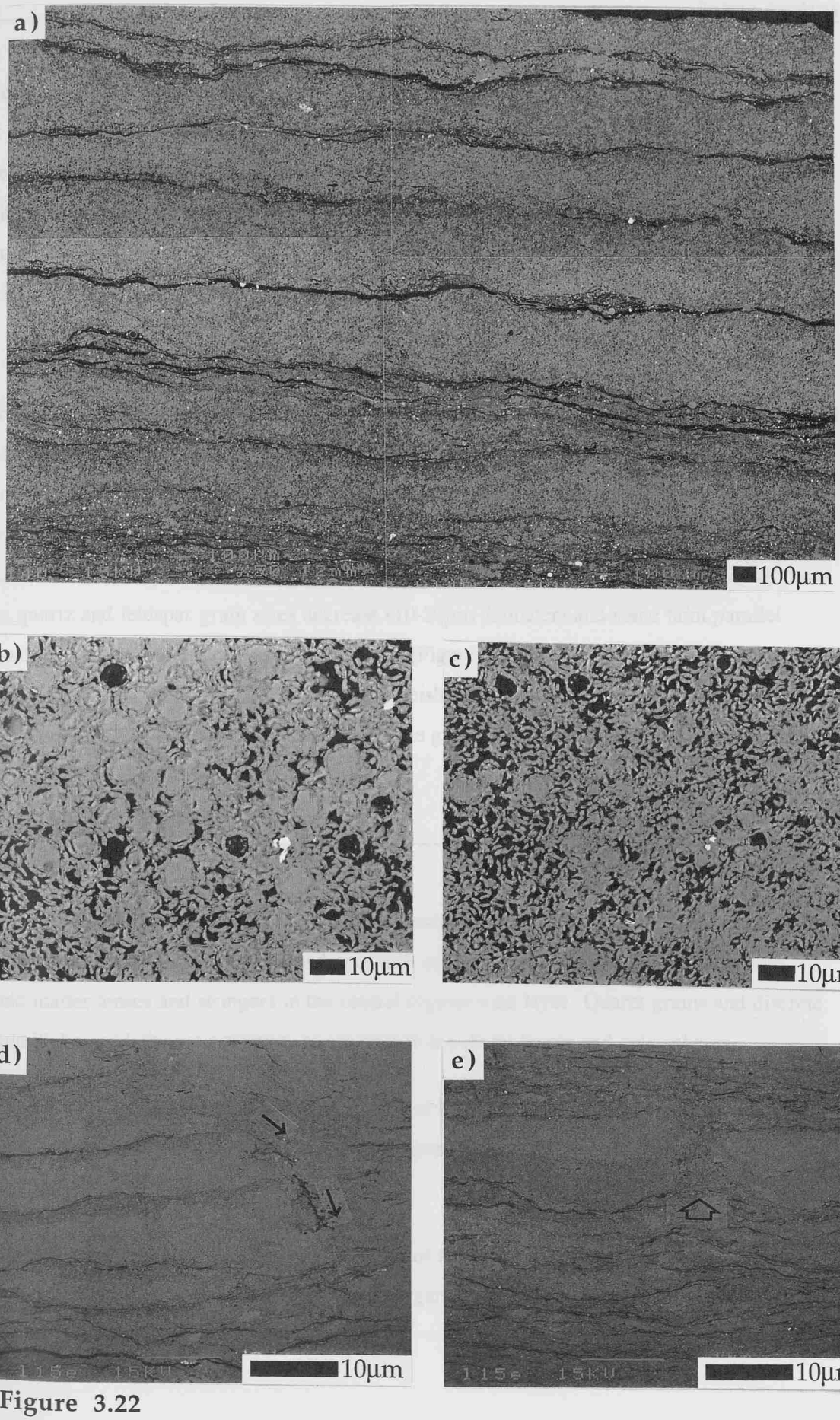

Figure 3.22

Within the *Eudoxus* shale interval, clay-coccolithic rich lithologies have abundant discrete organic matter blebs and laths (Figure 2.34b), but organic matter stringers are rare. Quartz grains are common and rare foraminifera are found (50-60μm height, 100μm length) (Figure 3.23e). Coccoliths comprising the matrix are poorly preserved. However, in common coccolith pelletal lenses, preservation is good, and coccospheres, infilled with calcite crystal, are present (Figure 3.23f). Quartz dominated pelletal lenses are also present (10-20μm diameter) but rare, as are hash pelletal lenses of carbonate (Figure 3.24a).

Rare disturbed layers have also been noted within the *Eudoxus* shale interval. The general bituminous fabric is blebby to stringer dominated, with discontinuous lamination parallel to bedding, however, in the disturbed beds, no lamination is visible and grading is evident (Figure 3.24c and d). Quartz grains (10-40μm diameter) are abundant at the base of these graded layers, organic matter is restricted to short (20-60μm length) elongated lenses and degraded coccoliths and clays are randomly orientated (Figure 3.24e). Towards the top of these layers quartz and feldspar grain sizes decrease (10-20μm diameter) and some faint parallel orientation is evident in the clay-coccolith matrix (Figure 3.24f). These graded intervals are 400-500μm in thickness, and have bases easily distinguishable from the "laminated" shale below. Pyrite framboids are also more abundant within the graded intervals than the bituminous shales below and above (Figure 3.24c and d).

FIGURE CAPTIONS

Figure 3.23a - BSEI photomosaic (x100) of a bituminous/oil shale lithology, *Eudoxus*. Note the variability in the abundance of clays and coccolith debris and the dominance of elongated organic matter lenses and stringers in the central organic-rich layer. Quartz grains and discrete organic blebs and laths are common, as are coccolith pelletal lenses and calcispheres.

Figure 3.23b - Detailed BSEI photograph (x400) of the central organic rich layer in 3.22a, showing elongated organic matter lenses and stringers, clay and coccolith stringers and quartz grains.

Figure 3.23c - Detailed BSEI photograph (x400) of the lower clay-coccolith rich layer in 3.22a, showing a coccolith pelletal lens and a discrete organic matter bleb. Also note the abundance of quartz and feldspar grains.

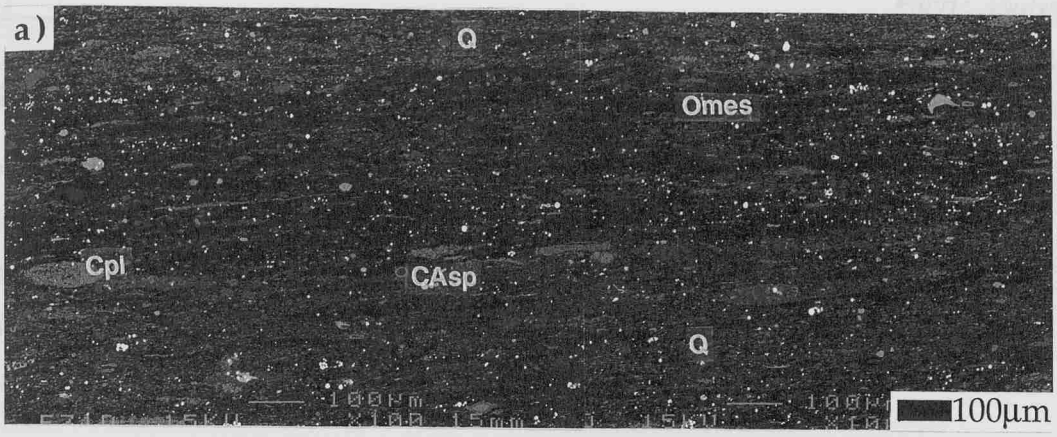
a)
Q
Omes
Cpl
CAsp
Q
100µm

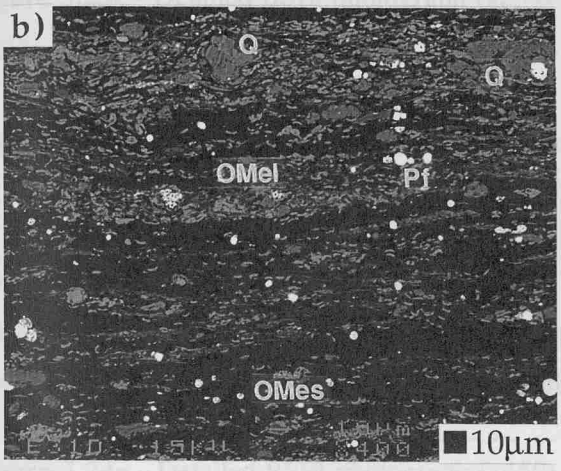
b)
Q
Q
OMel
Pf
OMes
10µm

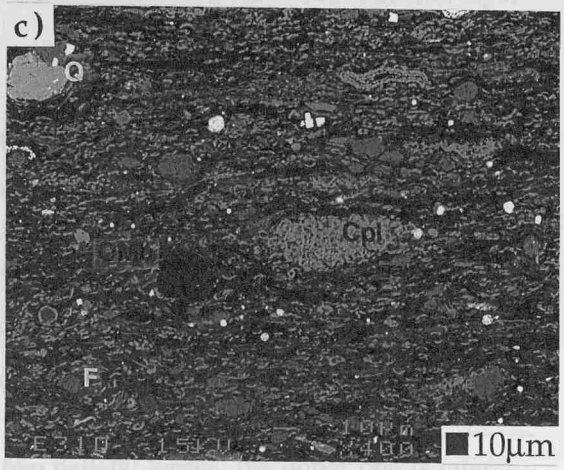
c)
Q
Cpl
F
10µm

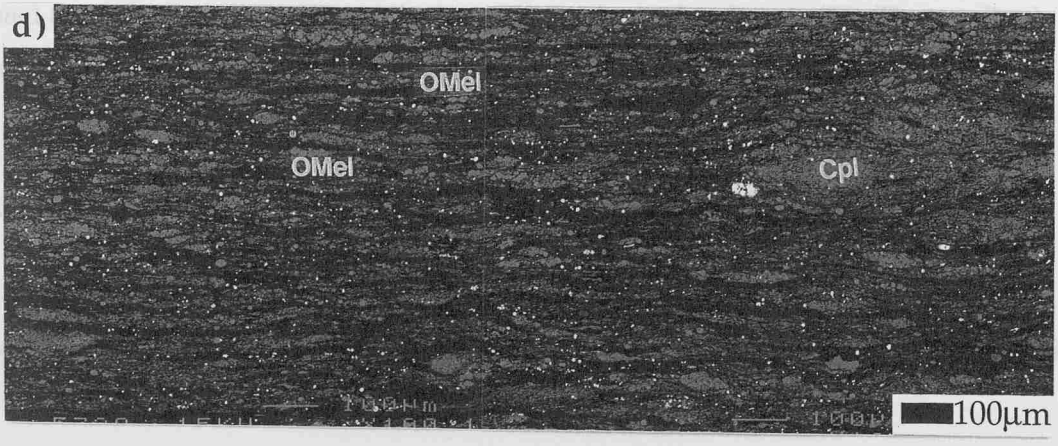
d)
OMel
OMel
Cpl
100µm

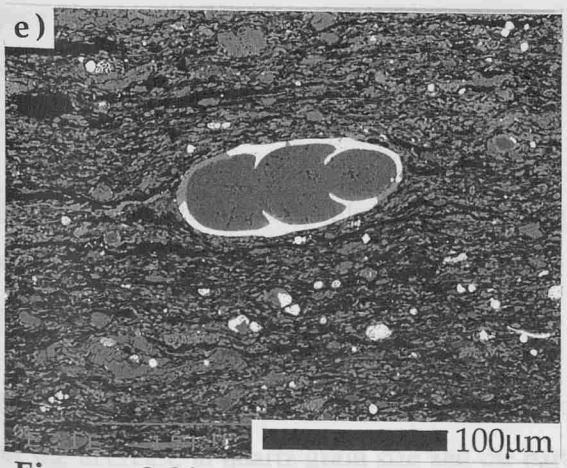
e)
100µm

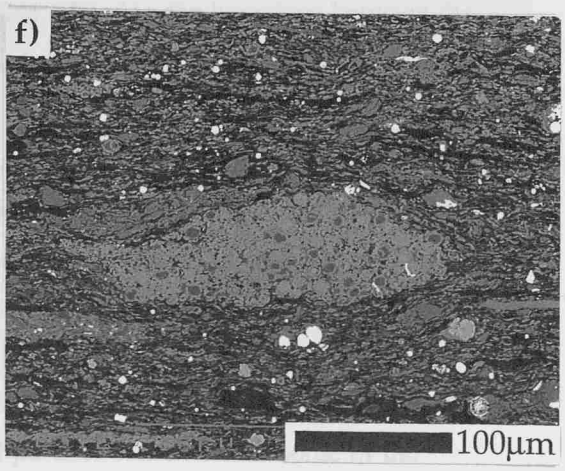
f)
100µm

Figure 3.23

FIGURE CAPTIONS

Figure 3.23d - BSEI photomosaic (x100) of a blebby bituminous shale fabric, *Eudoxus*. Coccolith pelletal lenses and stringers and organic matter stringers are highly abundant. Pyrite framboids are preferentially located with organic matter stringers. Note the brightness of the coccolith pelletal lenses resulting from calcite infilling of coccospheres, thus producing high backscatter.

Figure 3.23e - Detailed BSEI photograph (x350) of a foraminifera in a clay-coccolith rich layer within a bituminous shale, *Eudoxus*.

Figure 3.23f - Detailed BSEI photograph (x300) of a coccosphere dominated pelletal lens, with calcite infilling resulting in high backscatter, *Eudoxus*.

Elemental Map 3.9 - EDS grey scale map (x80) showing a blebby coccolith-rich bituminous shale fabric, *Eudoxus*. Calcium delineates the coccolithic pelletal lenses while aluminium, sulphur, silica, iron and carbon comprise discontinuous organic matter stringers and lenses.

Figure 3.24a - Detailed BSEI photograph (x450) of two pelletal lenses, the upper one is quartz dominated (Q) (10-20μm diameter), while the lower is a hash of carbonate (C). These pelletal types are rare within the bituminous shale lithologies, *Eudoxus*.

Figure 3.24b - Detailed BSEI photograph (x1400) showing a discrete organic matter lath and pyrite framboids composed of very fine circular grains ($<1\mu$m diameter).

Figure 3.24c - BSEI photograph (x50) of a bituminous, discontinuous laminated shale, above which a graded interval occurs, *Eudoxus*. Note the greater abundance of pyrite framboids within the graded interval than in the shale below. (Thin arrow in direction of grading).

Figure 3.24d - BSEI photograph (x200), detail of 3.23c, showing the boundary between the discontinuous, laminated bituminous shale and the graded interval. (Thin arrow in direction of grading).

Figure 3.24e - Detailed BSEI photograph (x500) of the base of the graded interval, *Eudoxus*. Note the abundance of large quartz grains and the random orientation of the fabric. (Thin arrow in direction of grading).

Figure 3.24f - Detailed BSEI photograph (x500) of the upper section of the graded interval. Note the decrease in quartz grain size and the partial parallel orientation of some of the particles. (Thin arrow in direction of grading).

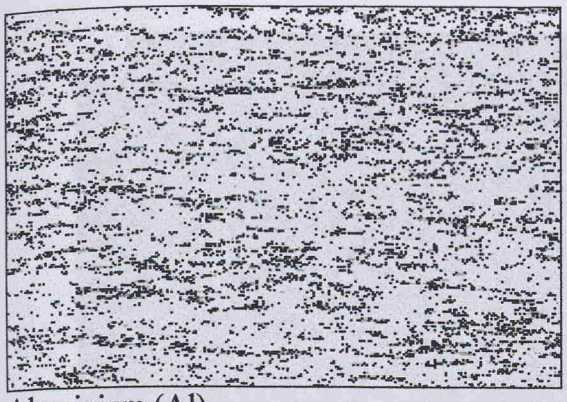

Aluminium (Al)

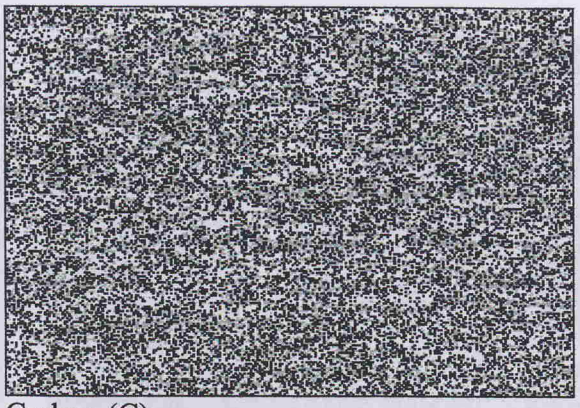

Carbon (C)

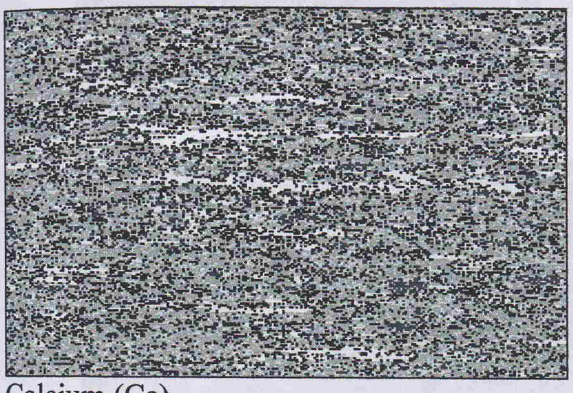

Calcium (Ca)

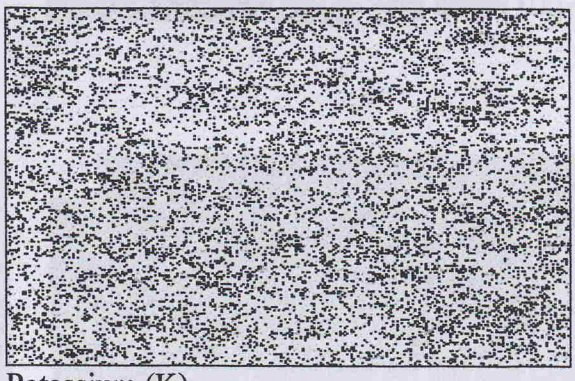

Potassium (K)

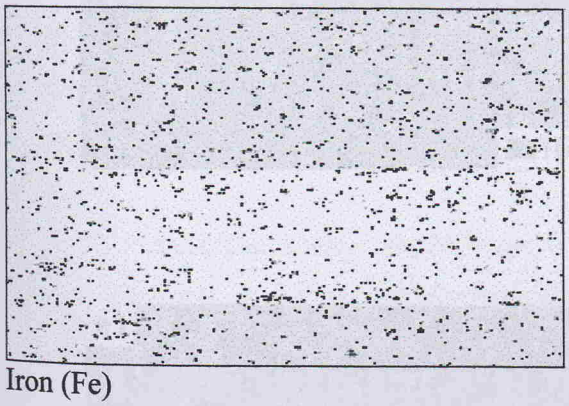

Iron (Fe)

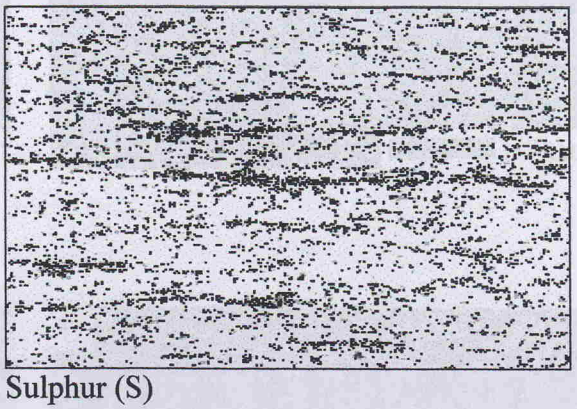

Sulphur (S)

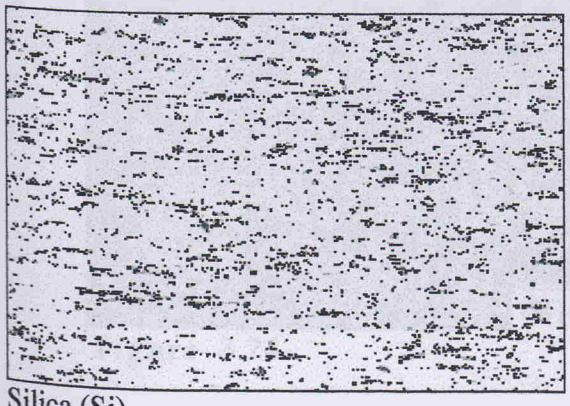

Silica (Si)

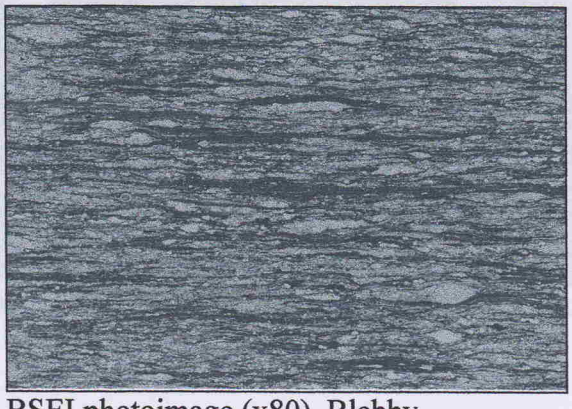

BSEI photoimage (x80), Blebby, coccolith rich bituminous shale, Eudoxus.

Elemental Map 3.9

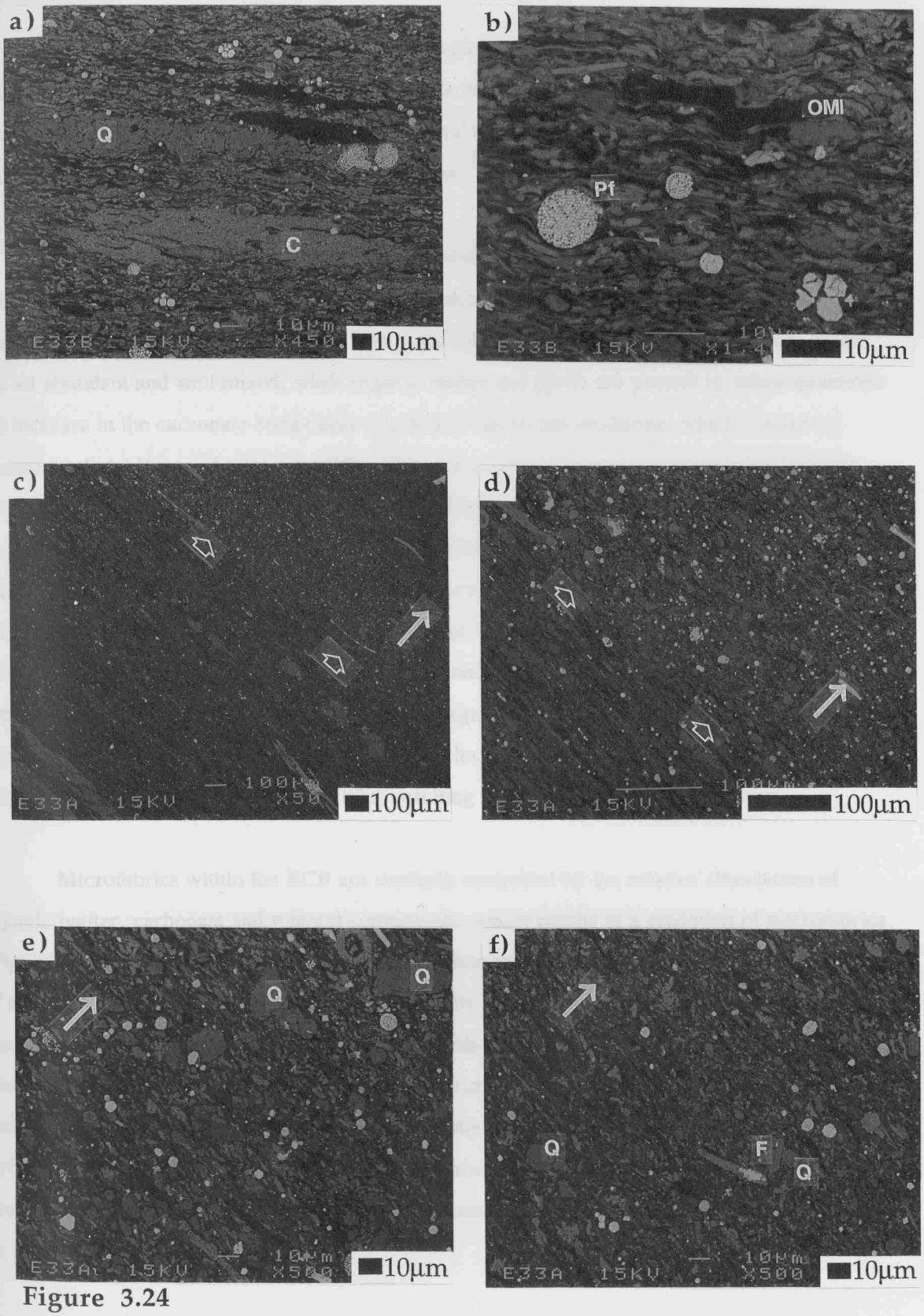
a)
Q
C
E33B 15KV X450
10µm
b)
OMI
Pf
E33B 15KV X1,4
10µm
c)
E33A 15KV X50
100µm
d)
E33A 15KV
100µm
e)
Q
Q
E33A 15KV X500
10µm
f)
Q
F
Q
E33A 15KV X500
10µm

Figure 3.24

3.8 SUMMARY

This chapter has described both the lithological and the microfabric types that are present in the KCF and has highlighted differences between similar lithologies. The relative abundance of organic matter, carbonate and mineral components of the depositional flux, primarily control KCF lithologies and microfabrics.

Mudstones and calcareous mudstones are the most common lithologies within the KCF (Figure 1.3a and b), while bituminous shales, oil shales and coccolith limestones occur as discrete bands. Within the mudstones, clays, coccoliths and quartz and feldspar mineral grains are all abundant and well mixed, while organic matter and pyrite are present in minor quantities. An increase in the carbonate component results in a calcareous mudstone, which commonly contains pelletal lenses of pure coccoliths. The calcareous mudstones are a gradation between mudstones and coccolith limestones, and as such display a range of relative abundances of the three major lithological components. Coccolith limestones occur where the carbonate component is dominant, while the organic matter and mineral components are sparse. Conversely bituminous shales result from an increase in organic matter abundance relative to the carbonate and mineral components, and like the calcareous mudstones, are a gradation between mudstones and oil shale lithologies. Oil shales occur where organic matter is dominant, but they can contain significant quantities of carbonate. In coccolith-rich oil shales the carbonate is found in discrete laminae, pelletal forms or loose coccoliths, resulting in a wide range of microfabrics.

Microfabrics within the KCF are similarly controlled by the relative abundances of organic matter, carbonate and mineral components, which results in a gradation of microfabrics (Figure 3.17). Where either organic matter or carbonate dominates, a homogeneous microfabric of either an oil shale or a coccolith limestone results. Abundant carbonate pelletal forms within a predominantly organic lithology, such as a coccolith-rich oil shale, results in pelletal microfabrics. Increases in the abundance of these carbonate pellets causes coalescence of pellets resulting in discontinuous lamination. Similar blebby fabrics also result from abundant organic stringers within a coccolith limestone which may also coalesce into discontinuous organic stringer laminae. Periods that alternate between coccolith and organic matter dominance are seen as laminated microfabrics.

Post-depositional chemical processes, such as diagenesis, also control the KCF lithology and microfabric. Dolomite cementstones are common in the KCF, the diagenetic alteration of mudstones, and result in a characteristic microfabric of a mosaic of euhedral crystals. Other

features, such as graded beds and distorted fabric resulting from post-depositional physical processes, are also present in the KCF.

Comparison of similar lithological beds, such as the Whitestone Band and the Freshwater Steps Band coccolith limestones, shows there is little difference in lithological components between such beds. However, the relative abundance of these components is not identical between the two, and small differences in the microfabric are also evident.

The KCF lithologies are therefore seen to be characterized by a wide range of microfabrics and though the major compositional elements do not change significantly, the relative abundance of these components can quite clearly be seen to act as the major control on the fabric. Thus, the processes and mechanisms, which controlled the relative abundance of organic matter, coccolith-carbonate and mineral components within the KCF marine environment, must be understood before environmental reconstruction can be made. Such processes are discussed in the following chapter with an emphasis on applying an understanding of formation processes of modern, comparable marine sediments to explain the observed KCF fabrics, and thus describe the palaeoenvironment of deposition.

4.0 FABRIC INTERPRETATION

In attempting to reconstruct the KCF depositional environment, the preserved sediment previously described needs to be interpreted so as to deduce the water column processes that occurred during sedimentation. One way of achieving this is to find recent, comparable examples, and examine and compare sediment trap data with the sediment record. Fine-grained sediments in modern marine environments develop distinctive structures in response to processes such as biological filtering, pelletization and physio-chemical flocculation. Following a downward flux, particles, flocs and pellets reach the water/sediment interface and become incorporated into the sediment. Here, processes such as diagenesis, chemical dissolution and precipitation of minerals, significantly changes the microfabric (Reynolds and Gorsline, 1992). This chapter aims to explain the observed KCF fabrics by applying an understanding of these mechanisms and processes occurring in modern, but comparable, marine environments.

The KCF lithology is predominantly controlled by the relative abundance of coccolithic carbonate, organic matter and detrital minerals, which are either autochthonous, resulting from biological production within the water column, or allochthonous, being transported into the basin. The presence of pyrite, dolomitic cementstones and calcitic infilling of coccospheres, indicates chemical alteration and diagenesis subsequent to deposition. The mechanisms and processes controlling marine production and input of terrestrial material into the marine environment are examined first, followed by discussion of diagenetic processes occurring after deposition, before environmental reconstructions are made of the KCF lithologies.

4.1 MARINE PRODUCTION AND TERRESTRIAL INPUT

Primary production (new and recycled production) is the biological fixation of carbon by phytoplankton into organic matter, with net primary production being the amount of carbon fixed by photosynthesis that exceeds the respiration demands of the plankton and goes into growth (Pinet, 2000). New, or export production is the proportion of the total photosynthesis that is dependent on nutrients that are supplied from below the euphotic zone, which is quantitatively equivalent to the organic matter that is exported from the euphotic zone without the 'production system' running down (Eppley and Peterson, 1979). Recycled production is the proportion of the total photosynthesis that depends on nutrients derived from pelagic recycling within the mixed layer.

Primary production is of great importance in the formation of organic-rich sediments for a number of reasons. Firstly, the proportion of the primary production that is new or export production determines the rate of sediment accumulation in biogenic facies, and secondly,

primary production also controls the type of plankton and thus the character of the marine organic matter available for preservation. Lastly, primary production controls the extent of the autodilution phenomena (Tyson, 1995). Autodilution is the extent to which the flux of planktonic organic matter is correlated with the flux of siliclastic or biogenic mineral matter. For example, significant changes in total organic carbon (TOC) in marine sediments can occur purely because of a change in carbonate dilution (Summerhayes and Marsan, 1983). TOC may therefore experience dilution from either biogenic or siliclastic sediments (Tyson, 1995). A significant proportion of the KCF lithology is biogenic in origin as coccolithic carbonate and organic matter, therefore primary production occupies a key position in the understanding of the KCF. But primary production is an elusive parameter which cannot be quantified with any degree of accuracy in ancient sediments, a problem which is a root cause of the 'productivity versus preservation debate' over the origin of organic-rich sediments such as the KCF (Tyson, 1995). However, in modern marine environments, quantification of primary production is more routine and can be correlated to other physio-chemical and biological processes, and thus can be used to help establish an understanding of ancient marine environments.

Terrestrial material, in the form of organic matter and detrital silts and clays, comprises the remainder of the KCF lithology. The production, preservation and transportation of these materials into the marine environment are other key processes that need to be investigated in order to fully understand the origins of the KCF.

Establishing the mechanisms and processes of production and flux of marine and terrestrial particles to the sediment surface are critical to the reconstruction of depositional environments. Transformation of organic and inorganic material from surface waters in their descent through the water column must be understood if the sediment is to be related to the surface water processes. Pelletization, flocculation and aggregation of particles, are important mechanisms in transporting particles to the sediment surface, while chemical alteration within the water column and disaggregation at the water/sediment interface determine the ultimate form of marine and terrestrial particles prior to incorporation within the sediment. Discussion of the marine and terrestrial flux follows descriptions of the carbonate, organic matter and detrital material sources for the KCF.

4.2 COCCOLITHOPHORE PRODUCTION

Coccoliths are present within all the lithologies analyzed in this study, though relative abundance of coccolithic carbonate is variable, increasing from mudstone to coccolith limestones. Even within organic-rich lithologies such as bituminous shales and oil shales, coccolithic carbonate is abundant, sometimes to the extent that pure coccolith laminae are present (Figure 3.16, Elemental Map 3.6). Such dominance suggests that these nannoplankton

may preserve some form of record of environmental change, and therefore an understanding of their dynamics is essential for any interpretation of the KCF environment (P. Bown and J. Burnett, pers. comm. 1999).

4.2.1 KCF COCCOLITHOPHORE SPECIES, AND PARAMETERS AFFECTING THEM.

Characteristics of surface waters can be gained from identification of the coccolithophore species inhabiting them. Low coccolithophore species richness was noted during the study's SEM fabric investigation (Figure 3.19a to d). This was confirmed by detailed coccolithophore species work carried out by other RGGE workers at University College London and the Natural History Museum. Their analysis showed the KCF nannofossil assemblages to be dominated by one family of coccoliths, the *Watznaueriaceae,* (P. Bown and J. Burnett, pers. comm., 1999), previously identified as *Ellipsagelosphaera* (Gallois, 1976; Gallois and Medd, 1979). It was also noted that the Wessex Basin KCF species richness is atypically low when compared to other Boreal and low-latitude coeval strata, and suggested that this was a primary surface water feature and not the result of preservational effects (J. Burnett, pers. comm. 1999).

The dominance of the *Watznaueria* spp. in the Kimmeridge Stage has been compared to the modern coccolith species *Emiliania huxleyi* (Young, 1994), which is considered a cosmopolitan species, having the broadest ecological tolerances of any living species (Brand, 1994). *E. huxleyi* is the only modern species which is regularly abundant in neritic, continental shelf seas, and has been interpreted in ecological strategy terms as r-selected, opportunist and growth-maximizing (Balch *et al.*, 1991). The abundant occurrence of *Watznaueria* spp. throughout the Mesozoic has been similarly suggested to indicate broad ecological range and an r-selected strategy (Young, 1994). Bown and Burnett (pers. comm. 1999) postulate that the *Watznaueriaceae*-dominated assemblages of the KCF reflect surface water environments that were conducive to only r-selected taxa.

Thus, embracing this assumption that *E. huxleyi* is the closest modern 'equivalent' to the Kimmeridgian *Watzernaueria* spp., some quantification can be gained on parameters which may have affected this Kimmeridgian species, by examining parameter tolerances of these modern coccolithophores. As a cosmopolitan species, *E. huxelyi* is present in both eutrophic coastal waters and oligotrophic open ocean waters, making the determination of specific figures for parameter tolerances difficult. However, in temperate regions, where water column stratification occurs for only part of the year, *E. huxleyi* becomes abundant in the spring when the water column first stratifies, and forms a major component of the spring bloom, but stays abundant until the winter, when stratification breaks down (Brand, 1994). Similarly, water column stratification of the Northwest European shelf has also been proposed during the KCF deposition

(Oschmann, 1988; Miller, 1990), and therefore it seems justifiable to compare *E. huxelyi* in such similar modern environments.

The dynamics of modern coccolithophores are affected by parameters of light intensity, turbulence, nutrient availability, temperature and salinity;

a) Light Intensity

Coccolithophore abundances are highest in well illuminated surface mixed waters. However, their overall absorption spectra are not significantly different to diatoms and dinoflagellates (Balch *et al.*, 1991). Coccoliths, however, have the ability to increase light scattering (Dring, 1990), and *E. huxleyi* growth rates are light saturated around 0.1 ly/min (Brand and Guillard, 1981).

b) Turbulence

Turbulent mixing affects coccolithophores by controlling both the distribution of nutrients within the water column, and the extent to which they can make effective use of the available light (Tyson, 1995). Turbulence greatly effects their position in the water, and removal to deeper water by mixing will limit growth. However, too much or too little mixing can reduce the level of production (Eppley and Peterson, 1979).

c) Nutrients

Nutrient limitation is known to be an important selective force on phytoplankton, and coccolithophores are known to utilize nitrate or nitrite, and organic phosphates (Brand, 1994). *E. huxleyi* has been found to have a low half-saturation constant for nitrate and ammonium uptake and can also maintain high growth rates in low iron media, indicating its adaptation to the low nutrient conditions of the open ocean (Brand *et al.*, 1983). Paasche (1968) suggested that coccolithophores utilize dissolved organic nitrate *in lieu* of inorganic nitrate, which might explain their ability to survive in stratified, low nutrient regimes. *E. huxleyi* does, however, respond to nutrient enrichment by increasing population size in both the ocean and in culture. Within coccolith blooms in the North Atlantic, coccolith cells per millilitre were found to be fixed at high phosphate levels, suggesting that calcification rates are inhibited by high phosphate concentrations (Balch *et al.*, 1991).

d) Temperature

Temperature is known to affect all biological processes, but there is no evidence that coccolithophores are affected any differently than other phytoplankton (Brand, 1994). *E. huxleyi* has one of the broadest temperature ranges of studied coccolithophores, from 1 to 31°C. Growth rates in culture of *E. huxleyi* clones isolated from the Sargasso Sea, were highest between 18 and 24°C and dropped off precipitously at 7 and 27°C (Fisher and Honjo, 1991). However,

water temperatures in regions of blooming coccolithophores have been observed to be elevated by several degrees compared to surrounding waters, but whether this was a primary feature or caused by the presence of the coccolithophores was not determined (Balch *et al.*, 1991).

e) Salinity

As with temperature, coccolithophores do not seem to respond differently to salinity compared to other phytoplankton (Brand, 1994). *E. huxleyi* is found in salinity as high as 41‰ in the Red Sea (Winter *et al.*, 1979) and as low as 18‰ in Oslo Fjord (Braarud, 1962) and 11‰ in the Black Sea (Burky, 1974). *E. huxleyi* in culture can grow in salinity ranging from 15-45 ‰, with the highest growth rates between 20 and 35‰ (Brand, 1994).

Thus, the Kimmeridgian *Watznaueria* spp., if assumed to be comparable to *E. huxleyi*, would have required relatively high light levels and relatively low levels of turbulence, and be adapted to low nutrient conditions, but bloom when nutrients were available. Able to survive in a wide range of temperatures, 17 - 25°C, a range of salinity (15 - 45‰) was also probably tolerated. The surface water environment of the KCF is thus implied to have been unstable with respect to nutrients and salinity, which were likely to have been controlled by water column stratification and terrestrial runoff.

4.2.2 COCCOLITHOPHORE BLOOMS

The suggestion that the KCF coccolith limestones are the result of high coccolithophore productivity in the form of blooms is not a new one (Gallois, 1976; Gallois and Medd, 1979; Tyson *et al.*, 1979), and comparable coccolithophore blooms are common in modern day marine environments. Large blooms (1000-10,000's km^2 in scale) of *E. huxleyi* have been documented in the Northern Atlantic (Holligan *et al.*, 1983; Balch *et al.*, 1991) and are a frequent occurrence during the summer, autumn and early winter in the Black Sea (Hay and Honjo, 1989; Hay *et al.*, 1990). Despite the large areal extent of coccolithophore blooms, they are generally confined to the top 20m of the water column, within the mixed layer, and last in the order of weeks to months, depending on conditions (Balch *et al.*, 1991).

Observations of nutrient levels indicate that nitrate and silicate are always low within the bloom area. No solid relationships between coccolithophore abundance and nutrients have been found, but phosphate was found to be the nutrient which best explained the variance in coccolith distribution (Balch *et al.*, 1991). Within areas of the highest abundance in blooms, surface chlorophyll concentration are low (0.5-0.8 μgm^{-3}), compared to ten times this concentration outside the blooms. Such low chlorophyll levels also represent low carbon-specific biomass (Balch *et al.*, 1991). Despite this low biomass, coccolithophores maintain the ability to alter the

optical properties of the surface waters by producing coccoliths. Calculations of carbon quantities in coccoliths and in blooms have shown individual coccoliths have 2pg of carbon (Paasche, 1962), which when scaled up to a bloom may reach 50,000 tons of carbon (Balch *et al.*, 1991).

In coastal waters where the environment is more variable but nutrient rich, *E. huxleyi* is adapted to have maximum growth rates (dividing 2.5 times a day), generating large blooms when environmental conditions are optimal (Brand, 1994). The same adaptations are envisaged for the Kimmeridgian *Watznaueria* spp., with optimal environmental conditions of light and nutrient saturation leading to frequent blooms, resulting in the deposition of coccolith limestones. The seasonal succession of major phytoplankton groups has been clearly related to seasonal changes in water column stability and light availability, and today diatoms are the first phytoplankton to bloom in the spring (Holligan, 1989) (Figure 4.1). It has been suggested, however, that during Late Jurassic times, the coccolithophores dominated the position in the seasonal succession occupied at the present day by diatoms (P. Bown and J .Burnett, pers. comm. 1999). Palaeontological data suggests an absence in the diatom fossil record during the Jurassic Period, before a radiation of the diatom group in the Early Cretaceous (Philippe *et al.*, 1994). No evidence of diatoms was found in the study's SEM fabric analysis, and it is possible that the coccolithophores during the Jurassic Period were adapted to take advantage of the higher nutrient conditions directly following the spring water column stratification, as diatoms do today. There has also been some suggestion that coastal coccolithophore species have part of their life cycle as a benthic stage for 'hibernating' during times of the year when growing conditions are poor (Brand, 1994). Too few species have been studied to be certain of this, but this may provide a mechanism for the presence of a healthy standing crop of coccolithophore after the winter months, so resulting in the initial spring bloom every year.

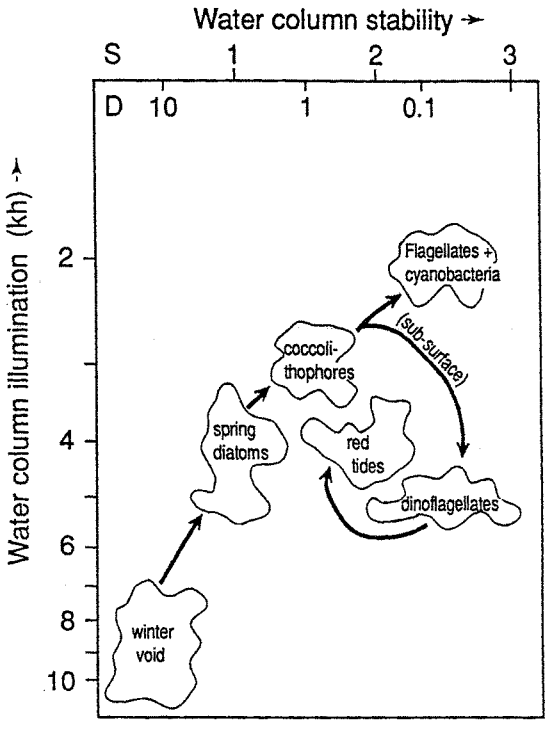

Figure 4.1 Correlation between dominant plankton type, water column stability and water column illumination in modern continental shelf waters (after Holligan, 1989). The plankton assemblage shifts from diatoms to flagellates as water column stability and illumination increases from spring to summer. The vertical stability parameter S is equivalent to $\log_{10}[h/C_d(|u|^3)]$, where; h is the height of the water column, C_d is a dimensionless bottom drag coefficient, u is the vertically averaged horizontally velocity mean M2 tidal stream, and $|u|$ its amplitude. The alternative stability parameter also shown, D, is the vertical diffusivity across the pycnocline ($cm^2\ s^{-1}$). The water column illumination parameter, kh, is the light attenuation coefficient, k, scaled by the water depth, h.

4.2.3 AUTODILUTION EFFECTS OF COCCOLITHS

The amount of planktonic carbonate produced within the marine environment has significant implications for the ultimate form of the sediment. During periods of increased coccolithophore production, the flux of other materials to the sediment will be largely diluted out due to the large and rapid flux of coccoliths. Such a high carbonate flux significantly effects the final total organic carbon (TOC), even if preservational affects within the sediment are high (Tyson, 1995), and thus, has implications on the abundance of structured palynomorphs between carbonate-rich and carbonate-poor lithologies. This effect is more fully examined in Chapter 6 (Section 6.1.2.1).

4.2.4 EFFECTS OF COCCOLITHS ON THE ECOSYSTEM

Coccolithophores not only respond to their environment but modify it as well. Honjo *et al.* (1982) estimated that, of the 80% of biologically produced carbon buried in marine sediments each year, 20 to 40% of this is formed by coccolithophores. They have been found to have an inordinate effect on light scattering in the ocean because of their coccoliths (Voss *et al.*, 1998), and there is speculation that blooms may reduce subsurface phytoplankton populations through light limitation (Dring, 1990). Chlorophyll and NH^{4+} maxima have been observed below coccolith blooms, indicating the presence of other phytoplankton such as cyanobacteria, dinoflagellates and other flagellates (Balch *et al.*, 1991). Reduction of the thickness of the euphotic layer by coccolithophores may allow more nutrient-rich water to diffuse above these Chl-maximum populations (Balch *et al.*, 1991), as NO^{3-} assimilation is light dependent (MacIsaac and Dingale, 1972). This positive feedback mechanism may be important in explaining the apparent longevity of blooms in nutrient depleted waters, which may be an important factor in the deposition of coccolith limestones.

Coccolithophores are also believed to have a biogeochemical impact on a global scale. They are known to be important producers of dimethylsulphoniopropionate (Purdie, 1996), a precursor of dimethylsuphide (DMS) (Vairavamurthy *et al.*, 1985). Charlson *et al.* (1987) pointed out that this gas oxidizes to sulfate aerosols in the atmosphere and these aerosol particles are among the most important nuclei in the atmosphere over the ocean for promoting cloud condensation. In increasing the cloud cover, the Earth's albedo also increases and therefore coccolithophores may be affecting the Earth's climate. Correlation between biological productivity, atmospheric dimethylsulphoniopropionate and dimethysulphide have been clearly demonstrated, with atmospheric species showing a strong seasonal cycle relating to surface water productivity (Ayers *et al.*, 1991; Prospero *et al.*, 1991).

Several General Circulation Models for the Kimmeridgian Stage have postulated cloud cover of 70% (compared to present day 50%), which has been proposed to explain high latitude warmth in Late Jurassic times (Sellwood and Valdes, 1997; Section 2.1.3). It is possible to envisage that coccolithophore production, not just within the Kimmeridgian North Sea basins but in Tethys and Panthalassa, may have been partly responsible for increasing cloud cover. Today coccolithophores appear to have a significant impact on their environment, being one of the major producers of calcareous sediments in the oceans and therefore influencing global biogeochemical cycles (Brand, 1994). In Late Jurassic and especially Cretaceous times, coccolithophores are likely to have played an even greater role in influencing global cycles and climate.

4.2.5 COCCOLITHOPHORE SEDIMENTATION

It is well known that sedimentation of coccolithophores is not a simple phenomenon of minute particles settling slowly through the water column (Steinmetz, 1994). The settling velocity of a single coccolith of mass 8 x 10^{-6}µg and surface area 32µm^2, is extremely slow at13.8 cm/day. Such a slow descent rate coupled with the large surface area would lead to rapid dissolution of coccolithophores in deep waters undersaturated with respect to $CaCO_3$, but coccoliths are found to be deposited in zooplankton fecal pellets (Honjo, 1975). Clearly the shallow KCF water column was not undersaturated with respect to $CaCO_3$. However, the highly abundant and predominantly well preserved coccoliths and coccospheres within pelletal structures suggests ingestion and pelletization by zooplankton was the dominant mechanism in coccolith sedimentation. This is known to be the most important sedimentation mechanism during modern coccolithophore blooms (D.Purdie, pers.comm. 2000)

a) Individual coccoliths in the water column

Individual coccoliths are most clearly observed in organic-rich KCF lithologies, where they occur singularly but often in broken lines of coccoliths parallel to the bedding (Figure 3.5a). Fecal pellets in modern marine systems have been observed to quickly transport coccoliths to depth. However, disintegration of these pellets due to both biological and physical processes results in the release of single coccoliths. The excellent preservational state of modern individually sedimented coccoliths indicates that it is highly unlikely that these individual coccoliths descended very slowly (Honjo, 1976). Thus it is envisaged that individual coccoliths within the KCF fabric are the result of dispersion from disintegrating coccolithic fecal pellets as they sank through the water column.

b) Pelletization

Grazing zooplankton commonly pass coccolithophores through their guts and excrete them in fecal pellets (Steinmetz, 1994). Fecal pellets composed of undigested carbonate and siliceous skeletal remains have been observed to be produced by copepods at rates as high as 200 pellets/individual/day (Honjo, 1976; Honjo and Roman, 1978). Size of pellets is partly a function of food concentration, but is also controlled by the zooplankton size (Dagg and Walser, 1986). Laboratory cultures of copepods when fed a purely coccolithophore diet resulted in cylindrical pellets with identical hemispheric ends, 200 ± 55µm long, 40 ±10µm wide (Honjo and Roman, 1978). These pellets are comparable to KCF pellets containing coccoliths and coccospheres (170 ±54µm long, 50 ±20µm wide), though compaction is believed to have resulted in slight differences in KCF pellet shapes (Table 3.3).

The preservation of coccoliths and intact, delicate coccospheres is very common in the KCF pellets (Figure 3.10c and d). Minimal mechanical and chemical effects have been found on coccoliths during digestion by modern copepods, and commonly coccospheres are found intact within pellets (Honjo, 1975, 1976, Honjo and Roman, 1978). Experimental data suggests that copepod guts are not acidic, and though not directly measured, the gut pH is presumed to be similar to the surrounding seawater. Aragonite crystals introduced into copepod diets were found to be unaltered by gut passage, therefore the chemical state of minerals such as calcite would not be altered by transport in copepod fecal pellets (Honjo, 1978). Thus, copepods are protective rather than destructive to skeletal particles of less than 10μm. Therefore, the similarity in size, shape, and coccolith preservation of KCF pellets to modern ones, clearly suggest a fecal origin, the result of ingestion by 'copepod' zooplankton in the Kimmeridgian surface waters.

The vertical transportation of coccoliths and coccospheres in fecal pellets is very rapid. Fecal pellet sinking rates of copepods fed on a purely coccolithophore diet in 15°C water was approximately 120 m/day (range 80 to 150m/day, Honjo, 1978; 100 to 300 m/day, Steinmetz, 1994). When placed within the KCF water column with its supposed depth of approximately 50 to 150m (Section 2.2.3), the deposition of pellets is a day, instantaneous! The strength of fecal pellets during suspension in seawater also affects the vertical flux, with the surface membrane providing a smooth covering that decreases fictional drag, thus increasing sinking rates. Fecal pellet surface membranes may also perform an important role by allowing the release of dissolved fluids after perforation by bacterial activity, while retaining solids such as carbonate and clay particles. Thus, nutrients such as phosphorus and nitrogen may be recycled to the shallower water column, enhancing nutrient regeneration where copepod grazing is high.

It has been observed both in laboratory experiments and in the natural environment that zooplankton fecal pellets are contained within a continuous organic membrane, or "pellicle", shielding the pellet interior from seawater (Honjo, 1978). It is proposed here that the presence or absence of a pellicle membrane determined the character of two of the KCF pelletal structures identified within this study (Section 3.3.4.2). Biodegradation of modern fecal pellets, results from the rapid colonization of bacteria on pellet surfaces in seawater, and microbial colonization has been observed to be greater at higher water temperatures. Pellets exposed to 20 to 25°C seawater were found to show surface membrane degradation within 3 hours. However, at lower temperatures (15 and 10°C) rates of biodegradation were significantly reduced (Honjo, 1978). As bacteria break down the surface of the membrane, the internal contents of the pellet are exposed, and eventually bacteria colonize the whole fecal pellet, destroying its integrity, and dispersing the undigested contents.

Of the three types of identified KCF pellets, those containing only coccoliths and intact coccospheres are the most comparable to modern coccolithic fecal pellets (Figure 3.10a to d, Table 3.3). Though no organic membranes were observed during SEM investigation on any of the KCF coccolith pellets, it is highly probable that on deposition these pellets had such membranes. It is suggested here that the exceptional preservation of the coccoliths and especially the coccospheres within some KCF pellets resulted from the protection afford by a pellicle membrane. Thus, a possible explanation for the contrast between the coccolith-dominated KCF pellets and the sparry pellets may be the presence or absence of a pellicle membrane. If the pellicle were to be perforated, the internal coccoliths would become exposed to biological and chemical degradation and dissolution. Subsequent calcite precipitation within the pellet on reaching the sediment would therefore result in the sparry calcite grains. Such pellets are seen in substantial numbers within the KCF fabric (Figure 3.11a and b). A partial loss of the membrane may also explain why some pellets are observed to be part coccolithic and part sparry calcite (Figure 3.11e and f). A notable feature between these two forms of pellets is the sparry pellets are generally 100-200μm longer and 50-100μm wider than the coccolithic pellets (Table 3.3). This may be solely due to the length of time available for sparry crystal formation and/or the level of expansion allowed by the partially intact membrane.

The rate at which pellicle membranes are perforated and destroyed has been found to depend on the water temperature through which the pellets are falling (Honjo, 1978). Water temperature effects both the speeds at which bacteria colonize the fecal pellets, and their subsequent destruction of the pellicle membrane. This may go part way to explain why during some depositional periods the KCF fabric is seen to be dominated by sparry pellets (Figure 3.7), while others contain predominately primary coccolith pellets (Figure 3.9). During periods of warmer waters, pellet membranes were destroyed in far greater numbers and more quickly, resulting in sparry pellets, while cooler water periods reduced bacterial growth, so reducing pellicle damage and thus allowed the sedimentation of primary coccolith pellets.

The above interpretation takes no account of sedimentation rates and the effect of burial and diagenetic processes on the preservation of pellets. For example, does a high sedimentation rate result in preservation of pellets and help prevent degradation of those pellets with intact membranes? Those pellets reaching the sediment surface with perforated pellicles may be subjected to relatively fast diagenetic process occurring very shortly after pellet deposition. The length of time these initial diagenetic processes get to act on the vulnerable pellets may also be dependent on sedimentation rate. A more detailed discussion of the diagenetic processes occurring at and within the marine sedimentary environment is given in a later section (4.9).

The third type of pellet observed in the KCF fabric is composed of hash carbonate (Figure 3.10e and f). EDX analysis of this carbonate indicates it was primarily coccolithic in origin. However, the dramatically different internal structure to the coccolithic pellets suggests that during ingestion and pelletization the coccoliths and coccospheres have become crushed and mechanically chewed into this hash. These pellets are notably smaller than the other pellet types, and are infrequently present (Table 3.3). Where the hash pellets are present, they are only found in fabric which contains primary coccolith pellets, do not show evidence of diagenetic alteration, and may therefore have possibly retained an intact pellicle during sedimentation. The source of these pellets is uncertain. However, the size, different structure and calcite preservation of these pellets suggests them to be the result of smaller zooplankton, possibly micro-zooplankton, where ingestion and gut characteristics have resulted in a loss of the primary coccolithophore form.

In summary, the KCF pelletal structures are fecal pellets of copepod-like zooplankton that fed on abundant coccolithophores blooming in the Kimmeridgian surface waters. The carbonate form in which these pellets were sedimented is proposed to be dependent on the presence, partial or complete absence of a pellicle membrane, which in turn may have been linked to water temperature and its effect on bacterial populations. Intact membranes preserved primary coccolith and coccosphere pellet interiors during cooler water periods, while perforated membranes in warmer water periods allowed chemical alteration of interior carbonate to sparry crystals. Smaller zooplankton may have produced the small pellets with hash interiors, though this is uncertain.

4.3 OTHER CARBONATE SOURCES

Calcispheres, though not highly abundant within the KCF fabric, are common within coccolith limestones, especially the Freshwater Steps Stone Band, and are an alternative form of carbonate in an otherwise coccolithic fabric (Figure 3.20c and d). The origin of these forms is some what undecided, but are most likely calcified phytoplankton, such as dinoflagellates (Janofshe, 1996). Their presence within the coccolith-rich lithologies indicates that dinoflagellate populations were in existence during coccolith blooms, and calcification of their cysts implies the water column was saturated with respect to calcite. Palynological analysis of all the intervals show that dinoflagellates dominated the marine palynomorphs despite the abundance of coccolithophores in the surface waters throughout much of the studied intervals (Chapters 6 and 7).

4.4 ORGANIC MATTER SOURCES

The organic matter present within the KCF lithologies was divided into three categories in the previous chapter (Section 3.3.4.1). The most abundant, but difficult to quantify, is the amorphous organic matter (AOM) which occurs in all lithologies but is the dominant component in oil shales (Section 3.3.4.1a). More structured organic matter forms are seen as elongated, undulating lenses and stringers (Section 3.3.4.1b), and as discrete blebs and laths (Section 3.3.4.1c). The origin of these organic materials is not as easily identified as that of the carbonate, but some inferences can be made from their form within the fabric. More detailed divisions of this material will be given and discussed in the following chapters in which the palynological examination of the KCF is presented.

4.4.1 AOM AND STRINGER/LENS ORGANIC MATTER

The amorphous organic matter (AOM) within the KCF appears structureless under the SEM (Figure 3.5c and d). Modern AOM has a variety of potential components including phytoplankton, algal and bacterially derived matter, higher plant resins and amorphous products of diagenesis of macrophyte tissues (Tyson, 1995). The production of AOM is partly dependent on marine production and terrestrial matter input in surface waters, but also on aggregation and degradation effects within the water column and the sediment. Within the water column, physio-chemical flocculation and aggregation of particles results from a variety of processes which cause collisions, such as differential settling and turbulent mixing, and leads to the production of marine snow (Turley *et al.*, 1995; Lampitt, 1996). Large amounts of organic matter are known to be sedimented from the euphotic zone following or during the decline of phytoplankton blooms, as marine snow strongly promotes the export of organic matter (Alldredge and Silver, 1988). In the modern marine environment, diatoms form major blooms, as do dinoflagellates (Purdie, 1996). However, an absence in the diatom fossil record occurs until after the Kimmeridgian Stage (Philippe *et al.*, 1994). Thus, dinoflagellates were probably the most prominent phytoplankton blooms after the coccolithophores, and together they provided much of the organic matter for export, which subsequently coagulated into AOM aggregates (marine snow).

The origin of the stringers and elongated lenses is more difficult to ascertain than the AOM, but they probably consist of similar components that have flocculated and aggregated into strands and stringers and swept down through the water column to be deposited as laterally continuous stringers. Reynolds and Gorsline (1992) have described such flocs in the Santa Monica Basin, Californian Continental Borderlands.

Another possibility for the organic matter stringers are microbial mats constituted by blue-green algae and sulphur bacteria (Tyson, 1995). These organisms do not normally fossilize as recognizable entities, as they are composed of highly metabolizable material. However, each bacterial filament is covered by a sheath which has a higher preservational potential (Arntz *et al.*, 1991). Despite this, even modern bacterial mat material is amorphous and it is unlikely that organic matter derived from such mats can be morphologically differentiated in ancient sediments (Tyson, 1995). Certainly no internal structure is evident within the KCF undulating stringers, only their strand like form within the fabric (e.g. Figure 3.9c and d) differentiates them from AOM.

It seems most likely that both the AOM and the undulating stringers and lenses of the KCF fabric are composed of the same or similar materials deriving largely from phytoplankton, algal and bacterially derived matter, though some terrestrial organic matter may also be incorporated. Aggregation processes occurring during flux and sedimentation of these organic matter types seems to have been an important factor in their ultimate form within the fabric.

4.4.2 TERRESTRIAL ORGANIC MATERIAL WITHIN THE MARINE ENVIRONMENT

The least abundant form of organic matter within the KCF fabric are discrete blebs and laths (Figure 3.8c and 3.24b). Compared to the other forms of organic matter, these blebs and laths do not show distortion of their shape, indicating a stronger structure. These particles are interpreted here as terrestrial particles, mainly pollen, spores and 'wood' fragments. Though they are structured, they are likely to be incorporated into AOM aggregates both in their descent to the sediment and after deposition. More detailed division of these terrestrial components within the KCF will be discussed in the next chapters. However, factors affecting the production, transportation to the marine environment and the subsequent flux to the sediment surface will be mentioned here.

The production of terrestrial material is highly dependent on (seasonal) precipitation, mean temperature, annual temperature cycle, nutrient levels and successional status. Quantitative figures on the temperature and precipitation during the deposition of the KCF is impossible to obtain from just SEM examination of the fabric. However, palynological examination of these particles enables some inferences to be made. Here all that can be interpreted from the presence of these particles is that the hinterlands around the Wessex Basin supported vegetation. The limited amount of these particles compared to other organic matter suggest several scenarios; the vegetation was sparse, the transport mechanisms from the hinterland into the basin carried only limited amounts of terrestrial material to the depositional site, or that marine productivity diluted the influx of terrestrial matter. From the fabric investigation any of these hypothesis is a

possibility, the detail provided by the high-resolution palynological study is needed to differentiate between these scenarios.

4.5 PROCESSES CONTROLLING VERTICAL FLUX IN MARINE SYSTEMS, AND SEDIMENTATION OF MARINE AND TERRESTRIAL ORGANIC MATTER

The regulation of vertical fluxes in the marine environment is controlled by retention versus export food chains. Retention food chains recycle organic matter and nutrients, and minimize sinking losses, while export food chains, which prevail during new production episodes, maximize them (Eppley and Peterson, 1979). Vertical flux is dependent on seasonal variability of physical and biological processes in the upper water column (Peinert *et al.*, 1989), and provides a close link between surface production and particle sedimentation (Duesser *et al.*, 1981; Asper *et al.*, 1992). Thus the vertical export of organic matter regulates (a) the residence time of phytoplankton, organic matter and nutrients in the upper ocean and (b) determines the amount, quality and temporal variation of organic matter supply to the deep ocean and sediments (Wassmann, 1998).

The sedimentation mechanisms of the KCF coccoliths and organic matter by pelletization and aggregation respectively, have already been mentioned (Sections 4.2.5 and 4.4.1), however these are not isolated processes. Modern marine systems are characterized by highly complex interactions between biological, chemical and physical processes and the water column flora and fauna. It seems unlikely that the Kimmeridgian marine system was significantly different in core processes and relationships from marine systems today. Thus, this section touches upon some of the mechanisms and processes which were probably essential elements of the KCF water column, but for which there is no definitive fabric evidence.

4.5.1 MATCH AND MISMATCH BETWEEN PHYTO- AND ZOOPLANKTON

The match and mismatch between phyto- and zooplankton is one such controlling factor and differences between the purely coccolithic fabric within the KCF and the organic-rich lithologies characterized by pelletal fabric, may be indicative of this balance. All phytoplankton blooms are an indication that there is temporary mismatch between producers and consumers (Wassmann, 1998). Ecosystems of shallow coastal areas or shelves (< 100m depth, KCF's approximate water depth, Chapter 2) are generally characterized by mismatch scenarios during the spring, where there is a considerable time lag between the phytoplankton bloom and the increase of major grazers such as copepods. Such mismatch leads to increased suspended biomass, which aggregates and is subsequently exported to the sediment. It is proposed that the purely coccolithic areas seen as coalesced blebs or continuous layers of densely packed coccoliths (Sections 3.3.5, Figure 3.13a and Elemental Map 3.5) are the resultant fabric of such

a bloom export which resulted from the phyto-zooplankton mismatch. Causes of this mismatch may have been that the zooplankton community was not able to catch up with the increase in phytoplankton growth, that microzooplankton was preferentially grazed by mesozooplankton (thus grazing pressure on coccolithophores decreased) and/or that the mesozooplankton did not successfully over-winter at shallow depths. The dominance of this fabric within the coccolith limestones implies that the KCF surface water during these periods was commonly affected by mismatch of phyto- and zooplankton. However, such mismatch does not imply that zooplankton populations were low, only that phytoplankton population increased more rapidly than the zooplankton. Thus it is highly probable that during the deposition of the more homogeneous coccolith limestone fabric both phyto- and zooplankton populations were high, relative to other lithological depositional periods.

Conversely, the presence of numerous carbonate pellets within the organic-rich KCF lithologies (Figures 3.7 to 3.9 and Section 3.4.3), which are comparable in size and shape to modern copepod pellets (Section 4.2.5 and Table 3.3), indicate a match between phyto- and zooplankton within the Kimmeridgian surface waters. In modern marine environments a match between phyto- and zooplankton intensifies recycling, the phytoplankton standing stock is kept low, aggregation of phytoplankton is limited, and the vertical export is ultimately based on detritus and fecal pellets. This match is achieved by the successful over-wintering of zooplankton, which can therefore execute a strong grazing pressure on phytoplankton in the early spring (Wassmann and Slagstad, 1993). However, similar to the mismatch scenario, a match of phyto- and zooplankton does not imply a high zooplankton population. A low phytoplankton population may only support a limited number of zooplankton therefore such fabrics may well be an indication of low populations of both phyto- and zooplankton. Such a strong correlation between organic-rich fabric and a match between phyto- and zooplankton populations also implies there is a link between permanent water column stratification and low surface water production and flux. Thus, to result in such organic-rich fabrics, enhanced organic matter preservation ought to have occurred. Processes leading to such organic matter preservation are discussed in Sections 4.7.3 and 4.8.

4.5.2 ZOOPLANKTON MEDIATED FLUX AND FOOD WEB DYNAMICS

Other factors that may well have had a pivotal role on the ultimate form of the biogenic material sedimented during the KCF, but for which there is no surviving evidence within the fabric are based on zooplankton mediated flux and food web dynamics. The fecal pellets preserved within the KCF fabric are most probably a reduced number compared to that produced, as not all would have reach the sediment. Mechanisms that mediate the vertical flux are caused by zooplankton; (a) by grazing directly on fecal pellets (coprophagy) and (b) by

manipulation of fecal pellets resulting in fragmentation (coprohexy) (Noji, 1991; Wassman, 1998). A third flux mediation mechanism also occurs from the colonization of fecal pellets by bacteria and protists that destroy the peritrophic membrane. This mechanism has already been highlighted as a possible explanation, for the differences between the coccolithic and sparry pellets found in the KCF (Section 4.2.5b).

Another factor for which no evidence is preserved in the KCF fabric, but which is known to be important in modern marine systems is the effect zooplankton communities have on the vertical flux (Banse, 1995). A modelled percentage of phytoplankton carbon, which leaves the euphotic zone during blooms, has been found to vary between 30 and 70% (Figure 4.2). This is dependent on the trophic behavior of various types of zooplankton and the structure of the zooplankton community (Figure 4.2) (Wassmann, 1998). In order to promote recycling of organic matter, herbivory by meso- and in particular microzooplankton must be efficient and compete with aggregation, while omnivory and carnivory promote the export of organic matter. Such mechanisms are clearly impossible to quantify from fabric analysis, but are included here as the presence of both phyto- and zooplankton in the KCF marine system imply that these interactions probably took place and would thus have affected the organic matter flux.

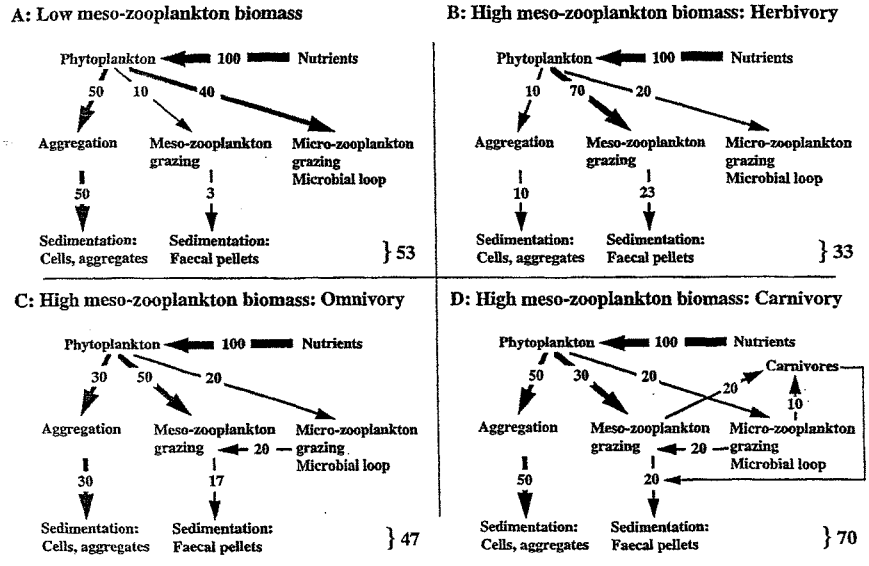

Figure 4.2 Schematic presentation of the influence of various zooplankton trophic impact on recycling and export of phytoplankton blooms. 100% of nutrients are taken up by phytoplankton. Four scenarios are given: (A) Low mesozooplankton biomass, (B) high zooplankton biomass and assuming an exclusively herbivorous feeding mode, (C) high zooplankton biomass and assuming an omnivorous feeding mode and (D) high zooplankton biomass and assuming omnivory as well as grazing pressure by carnivores.

In summary the zooplankton community structure seems to be of pivotal importance to the regulation of pelagic-benthic coupling. Therefore, comparing the primary production with the vertical carbon export without quantifying the organic matter degradation rate and food web dynamics prevents a complete picture of this coupling. Unfortunately this will always be the case when investigating the KCF marine system. However, in trying to understand this system via a water column process perspective, it would be incorrect not to highlight such complexity that probably had pivotal roles in the KCF system as they do in modern marine systems.

4.6 DETRITAL INPUT

The mineral or detrital input into the KCF marine environment would have consisted of a range of particle types and sizes, as in any marine basin with surrounding continental land. The dominance of clays and the sparse abundance of silts and large detrital particles within the KCF lithology indicate that the part of the basin investigated here was distal from the detrital source, or that the main sediment path bypassed this area. Establishing the provenance of these sediments was not undertake in this project but the main sediment source for the Wessex Basin is believed to be the London-Brabant Massif situated to the northeast of the basin (Refer to Chapter 2, Figures 2.3 and 2.4). Other possible hinterland sources may have been smaller islands to the west and southwest, such as the Cornubian Massif (McMahon and Turner, 1998).

4.6.1 TRANSPORTATION OF TERRESTRIAL MATERIAL INTO THE MARINE SYSTEM

Both terrestrial organic matter and continental detritus are transported from the land into the marine system by either aeolian or fluvial mechanisms. Fluvial transport probably results in the greatest flux of material, though aeolian transport may be crucial in movement of fine dust particles and small pollen. Fluvial transport results in point source supplies for marine basins, but can carry substantial quantities of material, conversely aeolian provides a dispersed source but the size and amount of particles transported is limited. The Kimmeridgian climate during the deposition of the KCF is believed to have been semi-arid (Moore *et al.*, 1992), similar to the present day Mediterranean climate, therefore it seems reasonable to suggest that fluvial runoff was seasonally controlled and some aeolian input was likely.

4.7 WATER COLUMN CHARACTERISTICS AND EFFECTS ON FLUX PRESERVATION

The physical and chemical characteristics of the water column are as important in the formation of an organic-rich rock such as the KCF, as the productivity and flux. The stability, depth, and redox situation of the water column are critical in the preservation of the flux and will be briefly discussed here, but though discussed in separate sections these factors are highly interrelated.

4.7.1 WATER COLUMN STABILITY AND THE SEASONAL PLANKTON CYCLE

The presence of laminated fabric, coupled with highly organic-rich facies within the KCF lithology has been taken by many workers to imply that during these episodes the water column was stratified (Tyson *et al.*, 1979; Oschmann, 1988, 1990; Wignall and Hallam, 1991). Thus, the water column would have been layered with water masses divided by a boundary zone which was characterized by a sharp temperature/salinity/density gradient. In the case of the Kimmeridgain water column, stratification is believed to have most likely been temperature controlled (*Tyson et al.*, 1979; Wignall and Hallam, 1991). The situation of the NW European archipelago with relatively isolated basins and slow flow rates (Miller, 1990), does support the fabric evidence that during these episodes the KCF water column was stratified either on a seasonal basis or more permanently in the deeper parts of the basins. However, the dominant homogenized mudstone lithology indicates that these episodes were interspersed with longer periods where the water column was less stable and was characterized by increased oxygen levels.

Water column stability in modern marine systems is known to have a crucial effect on the plankton cycles and thus on the deposition of organic-rich sediments. In seasonally stratified waters the presence or absence of stratification determines the nutrient supply in the mixed surface waters and therefore ultimately determines the primary production. Also the presence of a thermo or pycnocline within the water column acts as a barrier to the input of oxygen to the bottom water and thus oxidation of organic particles will ultimately lead to dysoxic/anoxic bottom waters and sediment, which enhance preservation of the flux material. Thus, water column stability affects both production and preservation of organic matter. From the KCF fabric alone it cannot be determined with certainty whether enhanced production resulted in stratification, or if stratification resulted purely from physical and chemical processes. However, the application of the match and mismatch of phyto- and zooplankton scenarios discussed previously (Section 4.5.1) suggests that physical and chemical mechanisms more likely resulted in the KCF water column stratification during oil shale depositional episodes and not enhanced productivity.

4.7.2 WATER COLUMN DEPTH

The shallow estimated water column (< 150m) of the Wessex Basin during the Kimmeridgian Stage is probably an important variable in the organic richness of this formation. The amount of organic carbon and carbonate that reached the seafloor is more critical than the level of primary production. Settling material is exposed to continuous degradation processes (Section 4.5) so its survival and flux to the sediment is dependent on the residence time in the

water column and thus the sinking rate and water column depth (Tyson, 1995). Some 97% of the variance in organic carbon flux has been accounted for by water depth and annual primary production (Hargrave, 1985).

Water column depth is also known to effect the abundance of bioturbating fauna, which in turn effects oxic degradation within the sediment, and increases both the preservation of organic carbon and the fabric structure. The shallow nature of the Wessex Basin water column, combined with the regional archipelago environment, where water circulation was reduced, would have resulted in stratification being a prominent feature, and thus have lead to increased flux preservation. Thus, for the KCF marine environment the surface production would have been positively correlated with the carbon flux due to the shallow nature of the water column.

4.7.3 LEVELS OF OXIDATION IN THE WATER COLUMN

Several inferences have been made to the levels of oxygen in both the water column and the sediment in the previous sections, highlighting the inter-relationships between water depth, column stability and the redox situation. The oxygenation and redox status of the water column is an important control on organic matter preservation and TOC (Pelet, 1983). Once a water column is anoxic, the metabolizable organic matter fraction undergoes less degradation during its transit to the sediment (Glenn and Arthur, 1985; Canfield, 1989). Zooplankton is excluded once the oxygenation drops to about 0.15ml l^{-1}, thus reducing pelagic consumption of organic matter (Wishner *et al.*, 1990). The effect of bioturbation is also reduced by the presence of a dysoxic-anoxic water column and is completely absent if dissolved oxygen levels remain below 0.2 ml l^{-1} (Douglas, 1981; Savrda *et al.*, 1984). All these factors therefore result in the increase of the organic content of the surficial sediment. In the Black Sea, a negligible decrease in particulate organic carbon flux was observed with depth below the chemocline (down to at least 350m), consequently the flux to the basin floor was nearly two orders of magnitude greater than for an equivalent oxic basin (Karl and Knauer, 1991).

The resultant sedimentary fabric is also affected by water column anoxia, not just with an increase in organic matter but also with a change in structure. Increased particulate organic matter flux and lack of bioturbation leads to the presence of laminated fabrics. A variety of fabric structures are evident within the KCF, from homogeneous mudstones to laminated oil shales. From the lack of any fabric structure and low abundance of AOM within the mudstones it is evident that this fabric was well bioturbated and deposited under an oxic water column regime. In contrast, the lack of trace fossils and fabric disturbance and presence of lamination and planar fabric structure within the coccolith-rich oil shales indicates deposition under an anoxic water column regime. However, the coccolith limestones do show a certain amount of

fabric homogenization suggesting that some bioturbation occurred. But bioturbation does not have to be continuous, prolonged or especially intense in order that primary lamination is destroyed (Soutar *et al.*, 1981; Savrda *et al.*, 1984). Small increase in the order of 0.05 ml l^{-1} above 0.2ml l^{-1} have been found to allow limited benthos to destroy lamination (Soutar *et al.*, 1981). Therefore the intermittent planar fabric of the coccolith limestones seems to suggest that small increases in water column oxygenation occurred periodically throughout the deposition of this lithology. Bioturbation is also often correlated with increased cementation (carbonate cements derived from bacterial degradation of metabolizeable organic matter) (Tyson, 1995), and thus may have played a part in the formation of KCF cementstones. Such diagenetic alteration is discussed in Section 4.9, where the chemical processes that occur within the sediment and their effect on the resultant fabric are examined.

4.8 PRESERVATION OF FLUX AT AND IN THE SEDIMENT

The degradation and diagenesis of the particulate flux at and within the sediment are the final stages in the formation of the preserved sediment (excluding lithification). These chemical processes are highly complex and outside the scope of this project, however they are still critical in the formation of any sediment and therefore a brief outline will be given. The processes involved in the degradation of organic matter, and the formation of pyrite and calcitic cement are especially important for understanding the preservational state of the KCF fabrics.

4.8.1 PHASES OF ORGANIC MATTER DEGRADATION

The organic matter remaining in ancient sediments (> 1Ma) is almost entirely refractory, and the relative proportions of metabolizable and refractory fractions of the flux material are affected by diagenetic conditions, especially the redox potential and oxygen availability, as well as biological production (Tyson, 1995). Neither of these organic matter forms is constant. However, nitrogen- and phosphorus-rich organic matter is selectively and more rapidly degraded, resulting in preferential degradation of planktonic organic matter (Toth and Lerman, 1977). Therefore, a substantial part of the planktonic particulate organic matter is thus very rapidly lost or degraded either in the water column, at the sediment-water interface, or within the top few millimetres of the sediment (Carney, 1989). The greatest proportion of the organic matter within the KCF lithologies is believed to be planktonic in origin (Lallier-Verges *et al.*, 1993), which is predominately seen as AOM. It is likely that a substantial proportion of this organic matter flux was degraded both within the water column and in the sediment

On reaching the sediment the KCF organic matter would have undergone several phases of degradation, which were dependent upon the available oxidants. Within 5 days of deposition some 25-40 wt% of the original carbon and 40-60 wt% of the original nitrogen in the plankton

dominated organic matter would have been lost in what is recognized as the 'leaching phase' (Newell *et al.*, 1981; Garber, 1984). This would have been followed by several 'decomposer phases' which are known to be strongly influenced by temperature and dissolved oxygen content, and are greatest under warm and oxic conditions (Rudnick and Oviatt, 1986; Harvey *et al.*, 1986; Tarutis, 1992). Degradation during the decomposer phase may be significantly stimulated by bioturbation (Andersen and Kristensen, 1992; Kristensen *et al.*, 1992). The first decomposer phase would have been oxic degradation. In the absence of bioturbation, diffusion of oxygen in shallow shelf sediments such as the KCF would have been limited to the upper 1-2mm, and even with intense bioturbation would have probably only extended down to 20-30mm (Rhoads, 1974). Aerobic degradation does not appear to be limited by oxygen supply until suboxic (≤ 0.2 ml l^{-1}) conditions are attained on at least a local level (Canfield, 1993) (See Table 4.1 for definitions of oxygen terminology). All available evidence indicates that there is no major difference in the intrinsic efficiency of aerobic and anaerobic bacterial degradation of metabolizable organic matter (Emerson and Hedges, 1988; Canfield, 1986; Lee, 1992). However, where as oxic and suboxic diagenetic processes can result in complete or extensive ($\leq$ 60%) loss of sediment TOC (Muller, 1977), anoxic post depositional alteration commonly results in no more than a 20-33% reduction of near surface TOC values (Berner, 1982; Pelet, 1983).

Thus, if the assumption were made that the KCF flux of organic matter to the sediment was constant, the differences between an organic-rich and organic-poor lithology could be put down to anoxic–oxic postdepositional alteration of organic matter. Clearly such an assumption would not be valid, but it does highlight the fact that the preserved organic matter within ancient lithologies is dependent not only on processes within the water column, but also on those within the sediment.

Oxygen (ml l^{-1})	Oxygen regimes	Biofacies	Redox/diagenetic regime
8.0 - 2.0	Oxic	Aerobic	Oxic
2.0 - 0.2	Dysoxic	Dysaerobic	Oxic
0.2 - 0	Suboxic	Quasi-dysaerobic	Suboxic
0	Anoxic	Anaerobic	Anoxic

Table 4.1 Oxygen Terminology (after Tyson and Pearson, 1991)

Following oxic degradation with the onset of suboxic dissolved oxygen concentrations below about 0.2ml l^{-1}, denitrification would have occurred. However, in modern shelf sediments it is thought that only 3% of the organic matter is oxidised by denitrifying bacteria (Jorgensen, 1983; Henrichs and Reeburgh, 1987). Once all available dissolved oxygen and nitrate were exhausted, dissolved sulphate would have been consumed by sulphate-reducing bacteria, in a zone which was probably 2 to 3 orders of magnitude thicker than the oxic zone (Jorgensen,

1983a and b). In organic-rich coastal sediments (where there is a high supply of metabolizable organic matter and thus low oxygen penetration) sulphate reduction has been found to oxidize at least as much organic matter as oxic processes (Jorgensen, 1982b; Henrichs and Reeburgh, 1987; Christensen, 1989). Sulphate reduction is thought to be responsible for about 90-95% of the total anaerobic carbon loss in marine sediments (Ivanov *et al.*, 1989). Thus both oxic and sulphate reduction within the sediment would have substantially degraded the KCF organic matter flux upon incorporation into the sediment.

The principal products of sulphate reduction are bicarbonate, hydrogen and hydrosulphide ions, and thus a consequence of this net increase in acidity is that any mineral carbonates in the sediment will tend to dissolve (Curtis, 1980). This has significant ramifications when considering the KCF, but the presence of abundant, well preserved coccolith and coccospheres in the highly organic-rich facies implies that other processes counteracted this acidity. The coccolithic carbonate flux to the sediment in the KCF in the form of zooplankton pellets may have been pivotal in this carbonate preservation. It is possible that the pellicle membrane was an affective barrier that prevented dissolution. However, when this was perforated, carbonate dissolution balanced the sediment pore water acidity and frequently carbonate was re-precipitated as sparry calcite.

4.8.2 BURIAL RATE INFLUENCES

The role of sediment accumulation rates was previously thought to be a major factor in the preservation of organic-rich sediments (Curtis, 1980). High sedimentation rates allowed for rapid burial of material to zones of lower bacterial activity (Curtis, 1987). However, such emphasis on sediment accumulation rates overlooks the fact that bacteria (which degrade the organic matter) are able to rapidly adapt to changes in the supply of substrates (Billen, 1982), and also fails to distinguish between the fates of metabolizable and refractory organic matter. The fraction that is most significantly affected by sediment accumulation rate is the metabolizable fraction (quantitatively dominant in the original organic matter), which is least likely to survive under any conditions (Tyson, 1995). Tyson (1995) also makes the point that "such models do not correspond with geological observations which indicate that many source rocks are either associated with slow sediment accumulation rates, or that their formation is insensitive to sediment accumulation rates as long as the bottom waters are dysoxic to anoxic".

A number of authors have calculated sedimentation rates for the Kimmeridge Clay, which have been predominately based on dividing the duration of ammonite zones by the number of sedimentary cycles within it (Table 4.2m, first group). However, these sedimentation rates are somewhat averaged, especially when considered on the scale of this study's analysis.

Therefore an attempt has been made to gain more detailed sedimentation rates, primarily for the oil shale and coccolith limestone lithologies, from this study's fabric analysis. The assumption has been made that a lamina couplet of one organic-rich lamina and one coccolithic lamina represent a year's worth of deposition. However, several scales of lamination are evident within these lithologies. Within the oil shale lithologies, lamination ranges from very thin organic-rich stringers and coccolithic stringers (Figure 3.6c, 3.8b to d) to far thicker carbonate laminae (Figure 3.16a to d), while within the coccolith limestone, coccolithic lamina are predominately thicker than the thin organic-rich stringer laminae (Figure 3.13a, 3.21 and 3.22a). Despite these variations in thickness it is conceivable that these laminae all represent the same depositional time period of a year and that the thickness variability is due to the relative amounts of both carbonate and organic-matter flux during different times.

The results of these sedimentation rate calculations are displayed in Table 4.2, in the last group. It can be seen that the episodes of deposition characterized by thick coccolithic/carbonate lamina of the limestone show the greatest sedimentation rates (30 to 118cm per 1000 years). It is also notable that these thicker carbonate lamina occurring within the oil shales show comparable rates to the limestone (average of 23 cm per 1000 years). However, the thin couplets within the oil shales show a dramatically reduced sedimentation rate (5cm per 1000 years) which would imply that the remaining non-laminated fabric, forming the majority of the oil shale, was deposited at even lower sedimentation rates. Thus these results are taken to suggest that the coccolith limestone lithologies were deposited at far higher sedimentation rates than the oil shale lithologies. The order of magnitude of the sedimentation rates calculated in this study are similar to those of Scotchman (1989), but are an order of magnitude greater than those calculated from the length of ammonite zones. This is believed to result from the averaging of lithological variations over a whole ammonite zone, when there are actually strong lithological differences within these zones, which are unlikely to have been deposited at the same rate.

Similar calculations have been made for the Black Sea, a modern analogue for the formation of organic-rich sediments and carbonaceous rocks (Calvert *et al.*, 1991). Comparable to the KCF in its sediment composition, the Black Sea sediment is characterized by alternating light and dark bands. The light layers are composed primarily of coccolithic carbonate from the coccolithophore *E. huxleyi* which usually blooms in the surface waters during the summer and fall. The dark layers are composed of enriched lithogenic matter and are deposited primarily in the spring (Hay *et al.*, 1988). Thus, this couplet has been assumed to be annual and termed a varve. Varve counting of Black Sea sediment cores have provided mass accumulation rates (MAR) between 150 to 170 $gm^{-2}y^{-1}$ (Hay, 1988), however, accumulation rates determined from ^{210}Pb analysis are less than half of varve counted rates, at 70 to 89 $gm^{-2}y^{-1}$ (Arthur *et al.*, 1994;

Buesseler and Benitez, 1994). This discrepancy arises partly from the difficulty in finding recognizable couplets throughout the core. The key to couplet counting is the ability to recognize and distinguish laminae couplets each and every year they are deposited. This is a somewhat unrealistic aim with the thin Black Sea lamina (50-200μm thick), which commonly interweave with one another. Large variances in laminae thickness and colouration also suggest extreme interannual variations in sediment sources and fluxes, including the possibility of either non-deposition or overshadowing of dark laminae due to large carbonate bloom (Lyons, 1991). The absence of coccolithophore bloom signals in one of every five annual cycles in sediment trap data (Hay *et al.*, 1990) argues against a strict annual interpretation for the varve couplets and an over estimation of the MAR by 25%.

Thus, taking the Black Sea sedimentation as a modern analogue to the KCF deposition it seem highly likely that the assumption of an annual assignment to a light and dark laminae couplet will result in excessively high sedimentation rates. There is also similar difficulty in distinguishing individual laminae within the KCF fabric as in the Black Sea sediments. Despite this knowledge the assumption of a yearly couplet for the KCF fabric must be used if any assessment of sedimentation rates are to be gained within the coccolith limestones and oil shale lithologies.

AUTHOR	LITHOLOGICAL ZONE/TYPE	SEDIMENTATION RATE IN CM PER 1000 YEARS
Evaluated by dividing the duration of an ammonite zone by the number of sedimentary cycles within it.		
Bertrand and Lallier-Verges, 1993	*Eudoxus* Zone	3.3cm
Cope *et al.*, 1980	*Hudlestoni* Zone	1.1cm
Macquaker and Gawthorpe, 1993	*Wheatleyensis* Zone	0.45cm
Miller, 1990	Average for the whole Kimmeridge Clay	1.5cm
Using methods and assumptions of Penn *et al.*, 1989.		
Scotchman, 1989	*Eudoxus* Zone	28.4 to 79.4cm
From this study using the assumption that a laminae couplet of one organic-rich lamina and one coccolithic lamina are a year's deposition.		
This study	Thick coccolith lamina with thin organic stringers (FWSB) (Figures 3.21 and 3.22a)	27 to 33.3cm, average 29.8cm
This study	Thick coccolith lamina with thin organic stringers (WSB) (Figure 3.13a)	118cm
This study	Coccolith-rich oil shale (1) (WSB) (Figure 3.16)	17.6 to 29.4cm, average 22.77cm
This study	Very organic-rich oil shale (Figures 3.6b and c)	4.5 to 5cm

Table 4.2 Summary of sedimentation rates calculated for the Kimmeridge Clay in cm per 1000years. The first group are based on length of ammonite zones, the second on the assumptions of Penn *et al.*, 1989; (the Kimmeridgian Stage lasted 3.8Ma, contains 10 zones and 49 stratigraphic units), and the last group from this study on a yearly lamina couplet. All these rate are compacted sediment rates.

4.9 DIAGENETIC EFFECTS WITHIN THE SEDIMENT

4.9.1 SULPHIDE, ORGANIC SULPHUR AND PYRITE FORMATION

During sulphate reduction H_2S and refractory organic sulphur compounds are produced. Incorporation of this sulphur into the sediment is mostly due to the formation of pyrite and assuming a ready supply of H_2S, depends largely on the availability of reactive iron (Berner, 1985). Pyrite within the KCF is predominately in framboidal form, though some euhedral grains are commonly present. However, large pyrite deposits are strongly localized to the vicinity of macro-organism remains (Section 3.3.4.3, Figure 3.12a and b). Only a visual assessment of the pyrite presence was undertaken in this study, as other RGGE workers at Leeds University carried out more detailed work. However, it was quite clear that some division in framboid size and the abundance of euhedral and bioclastic coatings of pyrite existed between lithologies. In

general, framboids were most abundant and consistently small (≤5-10 μm diameter) in the organic-rich lithologies. These facies also contained more abundant pyrite correlated to bioclastic and macro-organism remains. Within the coccolith limestone lithologies pyrite, as framboids, was rare and preferentially located with organic stringers and lenses. Both the mudstones and cementstone contained larger framboids (5-20 μm diameter) and euhedral forms were more common.

Pyrite framboid size distributions analyzed from a range of modern environments have been correlated to the oxygen condition of the water column and sediment (Wilkin, Barnes and Brantley, 1996; Wilkin, Arthur and Dean, 1997). Framboids formed in a euxinic water column (where the water column is H_2S bearing and oxygen free) were found to be "on average smaller and less variable in size than framboids formed diagenetically in sediments underlying oxic or dysoxic water columns". Thus, the framboid sizes within the KCF fabric imply that the bituminous and oil shale organic-rich lithologies were deposited under euxinic water columns, while the organic-poor mudstones and the cementstone were deposited under oxic water columns. The rarity of pyrite framboids in the coccolith limestones and their preferential location in organic-rich lamina, suggest that this lithology was deposited under a water column which fluctuated between oxic-dysoxic and anoxic conditions.

Within the RGGE project, Wignall and Newton (1998) investigated such a proposition for the KCF by analysing pyrite framboid size and calibrating them against a palaeoecologically determined oxygen-restricted biofacies (ORB) scheme which provided an independent assessment of bottom water oxygenation. A close correlation was found between these data sets which showed that euxinic water column conditions were characterized by tiny framboids (<5μm diameter) with a narrow size range, and an absence of benthic and nektobenthic taxa. Lower dysaerobic biofacies containing discrete, benthos bearing bedding planes, had a euxinic framboid signature but with the addition of rare larger framboids, while under upper dysaerobic biofacies, substantially larger framboids were found with a broader size distribution. Wignall and Newton (1998) also noted that the average size of KCF euxinic framboids (3μm, rarely exceeding >5.5μm diameter) was far smaller than the average 6μm diameter of framboids found in the Black Sea euxinic water column (Muramoto *et al.*, 1991). This they implied to be the result of the arresting of framboidal growth at an earlier stage in the KCF than in the Black Sea, indicating more rapid settling fluxes. They suggested that the salinity-stratification of the Black Sea is a more intense density contrast in the water column than in the Kimmeridge Clay Seas, which are regarded to have been temperature stratified (Tyson, Wilson and Downie, 1979; Wignall, 1984; Wignall and Hallam, 1991).

4.9.2 CEMENTSTONE DIAGENESIS

The cementstone analyzed within this study was found to be characterized by fabric that was similar to that of the mudstones (a homogenous mixture of predominately clays and coccoliths), masked by an interlocking mosaic of euhedral and subhedral dolomitic crystals. The relationship between these two fabrics implies that the mosaic of euhedral crystals resulted from the diagenetic alteration of a mudstone fabric. Once primary degradation processes (Section 4.8.1) have stopped due to the removal of all available oxidants, further microbiological degradation takes place with the activity of methanogenic organisms. This releases methane, bicarbonate and hydrogen ions into the system and the style of subsequent mineral transformation is dependent on the availability of ferric compounds (Curtis, 1980). Provided iron compounds are available for reduction, conditions are such as to favor precipitation of carbonates, especially those containing iron: siderite, ankerite and ferroan varieties of calcite and dolomite. In the absence of iron reduction aggressive solutions will be generated and dissolution of carbonate and other unstable minerals will occur (Curtis, 1980). From the preservation of coccoliths in the KCF fabric, even within the mudstones, clearly such an aggressive dissolution of carbonate may be ruled out and therefore conditions were suitable for the deposition of dolomitic grains resulting in a cementstone. Detailed work on the formation of carbonate-rich concretionary horizons in the KCF have proposed them to be the result of early cementation (at 10m or less depth within the sediment) at specific horizons by ferroan dolomite forming concretionary layers. These grew more or less symmetrically by accretion to both the upper and lower margins during continued burial to 500m (Irwin, 1980). It has also been proposed that a hiatus in sedimentation is a crucial factor in the formation of such cementstones, as this would allow sediment alkalinity to increase and thus promote carbonate precipitation (Bellamy, 1980; Raiswell, 1987).

A closer inspection of the euhedral dolomitic cementstone grains during this study identified a relatively lighter zone around grain edges (Figure 3.4). EDX analysis showed these rings to be calcite which were surrounding the dolomitic centers of the grains. This 'zoning' implies that during early diagenesis, two phases of growth took place. Feistner (1989) similarly noted several carbonate phases in other KCF cementstones, which he confirmed through EDX analysis to be ferroan dolomite and calcite. He stated that " the exact sequence of precipitation is difficult to determine but at least some of the calcite clearly postdates the ferroan dolomite as euhedral calcite rims to ferroan dolomite crystals". Thus, the KCF cementstone studied here is suggested to have formed due to a hiatus in, or low, sedimentation, at a shallow burial depth in the sulphate reduction zone over a relatively short time-scale and have undergone several phases of precipitation, controlled by the availability of iron within the sediment.

4.10 STORM EFFECT AND OTHER FABRIC DISTURBANCE

Several horizons within the studied sections show graded beds, with grading of particles and carbonate pellet sizes and characterized by a less carbonate and more organic-rich composition up sequence (Figure 3.18f). This grading combined with sharply planar bases suggests deposition from a rapidly decreasing flow that initially resulted in some erosion of underlying fabric. The small size of the particles involved, and especially the presence of carbonate pellets, suggests that possible re-suspension of the sediment occurred either at the point of deposition or from less distal areas. It is likely that storms were the cause of such events with the greatest intensity ones resulting in an increase in storm wave base, which affected the deeper basin, either directly or via input from near by areas. Slumping of material off basin highs may also have resulted in such features. This hypothesis is also believed to apply to the graded interval within the *Eudoxus* bituminous shale (Section 3.7, Figures 3.24c to f).

The other feature noted in the fabric was a recumbent S-shaped fold within the central oil shale of the WSB (Figures 3.18a to e). This may have possibly resulted from tectonic disturbance of the fabric at some point during fabric lithification. Stretching, tilting and bending of the laminated fabric is clearly evident and at the inflection point the fabric is total disrupted. This implies that the fabric was susceptible to alteration but it was lithified sufficiently to retain some of its original structure. During the Mid and Late Jurassic, the Northwestern European Basin was a region of tectonic activity with the opening of the palaeo Atlantic, therefore it is likely the tectonic forces did occasionally affect the deposited KCF within the Wessex Basin (Sections 2.1.1 and 2.2.1, McMahon and Turner, 1998; Newell, 2000). However, oil shales are known to show contractional fabrics that are akin to tectonic deformation (Belin, 1992), as well as being easily deformed when over pressured (J.E.A.Marshall, pers. comm. 2000).

4.11 ENVIRONMENTAL RECONSTRUCTIONS AND SUMMARIES

The previous sections of this chapter focused on explaining the characteristics of the KCF fabrics, described in Chapter 3, through comparison with modern marine environments. The following sections aim to combine these explanations to form environmental reconstructions for the KCF lithologies. These reconstructions will draw upon evidence from the general nature of the lithologies and from the more detailed examination of the microfabrics (Section 3.4). The oil shale and coccolith limestone fabrics are the most complex and thus will be reconstructed first, followed by reconstructions for the mudstone and cementstone lithologies. All the reconstructions are based on the assumption that the KCF marine environment was a complex mixture of interactions that were controlled and functioned in a similar manner to modern marine systems. The major inputs and processes envisaged for the KCF marine system are

summarized in Figure 4.3, which brings together the different elements of the system discussed in the previous sections.

4.11.1 ENVIRONMENTAL RECONSTRUCTION FOR THE OIL SHALE LITHOLOGY

The oil shale lithologies of the KCF are notable for their organic richness, which implies an increase in primary production and/or enhanced preservation of the organic matter flux. The presence of lamination, especially in the coccolith-rich oil shales (Figure 3.1) indicates a lack of bioturbation and thus anoxic sediments and bottom waters. This is further supported by the presence of abundant small pyrite framboids (Section 3.3.4.3, Figure 3.12a) which are believed to have formed within the water column (Section 4.9.1). Thus not only were the bottom waters anoxic, but the fabric evidence implies that the water column was euxinic. As such any level of organic matter flux would have undergone enhanced preservation, but the stratification may have resulted from either biological or physical mechanisms.

The palaeogeography of the Northwest European region of generally shallow (< 100m) epicontinental shelf seas characterized by basins and swells (Hallam and Sellwood, 1976), combined with a semi-arid climate (Moore *et al.*, 1992), would have resulted in restriction between basins and sluggish circulation (Miller, 1990). The temperature stratification was therefore most probably a function of both the climate and the geographic/environmental setting of the region (Tyson *et al.*, 1979). The semi-arid climate would also have restricted terrestrial runoff in amount and seasonally, with more frequent runoff events during the winter. Such restriction of terrestrial runoff combined with water column stratification would have resulted in nutrients in the surface waters being minimal over the majority of the year and thus primary production low. The oil shale are therefore suggested to have been deposited under relatively oligotrophic surface waters with a euxinic water column and sediment, with low primary production but enhanced preservation of the limited organic matter flux, which led to the deposition of organic-rich sediment. This is in agreement with geological observations where organic-rich lithologies are deposited at low sedimentation rates under anoxic bottom (Tyson, 1995; Section 4.8.2).

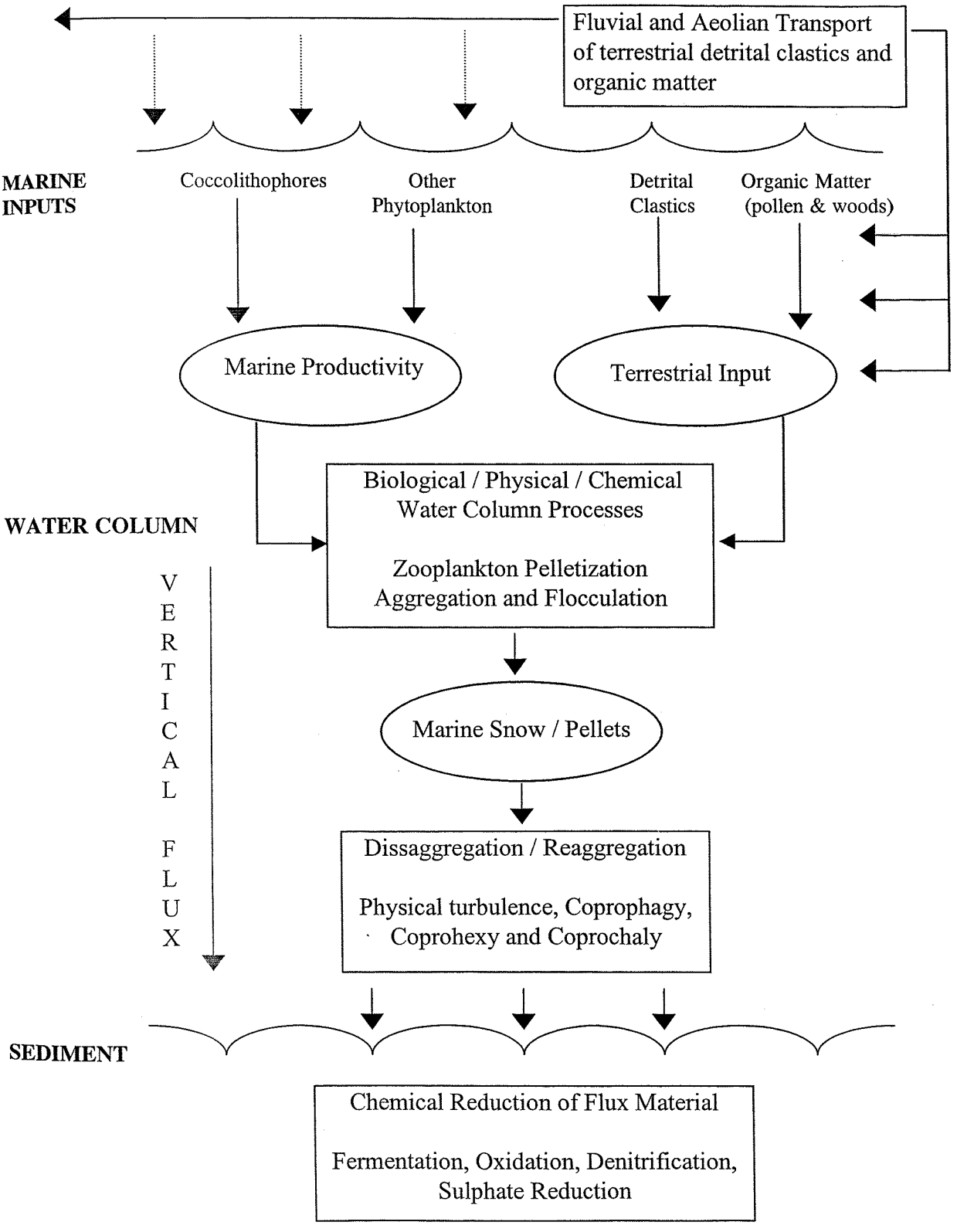

Figure 4.3

A simplified schematic summary of the processes and materials envisage for the KCF marine system. Ovals represent materials, while rectangles are processes, the arrows show the movement paths within the system, but not any quantitative relationships.

The oil shale lithologies were divided into four major fabric types (Section 3.4). End members of these types were the homogeneous fabric (Section 3.4.4, Figures 3.5c to f, 3.6a and b) and the laminated fabric of thick organic laminae with coccolith stringers (Section 3.4.1, Figure 3.6c). Between these end members, pelletal fabric (Section 3.4.3, Figure 3.8a) and discontinuous organic-rich laminated fabric (Section 3.4.2, Figures 3.6d and 3.8b to d) occur, and diagenetic alteration is seen in all fabric groups (Figure 3.7a to d, 3.16a to d). The relationships between these fabric types are displayed in Figure 4.4.

The homogeneous fabric is dominated by AOM with short, thin coccolith stringers and small pellets. The low coccolith carbonate in this fabric type suggests that coccolithophore productivity was minimal, supporting the hypothesis of relatively oligotrophic surface waters. It is probable that other phytoplankton production was low, thus the abundance of AOM is suggested to be the result of excellent preservation of a reduced organic matter flux. The low phytoplankton populations would also have led to low zooplankton populations, which is borne out by the low pellet abundances in this fabric end member (Figure 3.6a). The euxinic water column would also have restricted the vertical movement of any zooplankton and thus zooplankton flux mediation would have been minimal (Section 4.5.2). Figure 4.5A shows an idealized basin during the deposition of a homogeneous oil shale fabric during the KCF, highlighting the water column oxygen levels, phyto- and zooplankton productivity and flux of carbonate and organic matter.

The laminated fabric of the oil shales, characterized by alternations of organic matter and coccolithic carbonate, imply that for short periods coccolithophore productivity increased. These 'blooms' would have required some eutrophication of the surface waters, which may have resulted from either increased terrestrial runoff or input of nutrients from below the thermocline via mixing and overturn of the upper water column. The hypothesis of increased terrestrial runoff cannot be tested just from the fabric analysis: palynological analysis is needed (See Chapters 6 and 7). However, the mixing of the nutrient-rich water column with the oligotrophic surface waters can be examined more readily. If the thermocline were to reach just below or even up into the euphotic zone, an overturn or mixing of the upper euxinic water column would provide abundant nutrients directly to where the phytoplankton could take immediate use of them. Such mechanisms as wind mixing or storm turbulence may have resulted in this nutrient supply to the surface water, and the latter would also have resulted in increased terrestrial runoff and nutrient input.

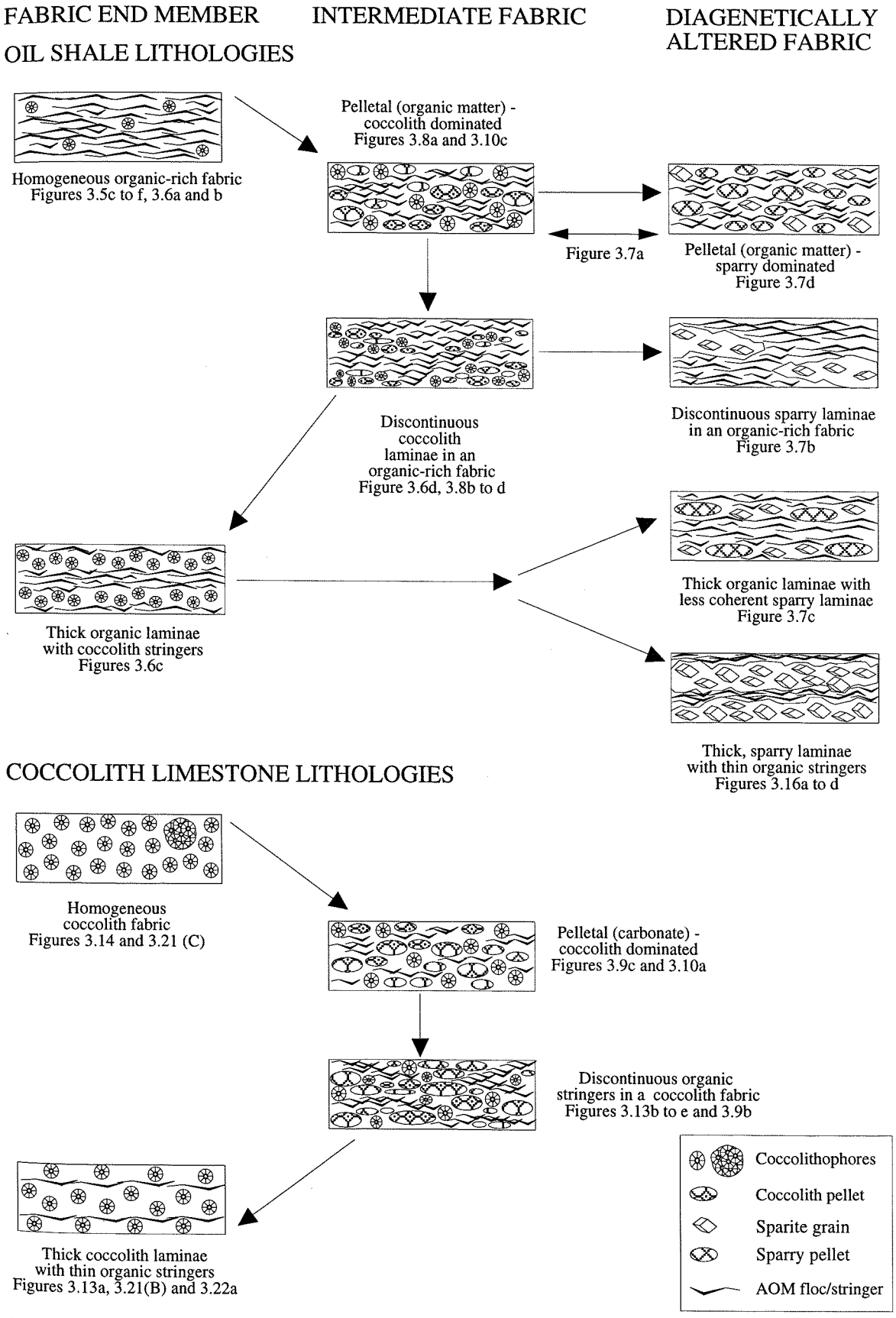

Figure 4.4
Flow diagrams of the relationships between the microfabrics within the oil shale lithologies (upper group) and the coccolith limestone lithologies (lower group). For these two lithologies there are two end members, a homogeneous fabric and a laminated fabric. Linking these end members are pelletal and discontinuous laminated fabrics. The third column contains diagenetically altered versions of the fabrics in the other two columns, though this is most clearly seen in the oil shale lithologies. Within the coccolith limestone lithologies diagenetic effects tend to be seen as small patchs of calcite cement and infilled coccosphere and are thus not depicted.

It is notable that several scales of lamination occur within the oil shales (Section 4.8.2). Those that are characterized by thin coccolith stringer laminae (Figures 3.6c, 3.8b to d), and those that show far thicker carbonate laminae (Figure 3.16a to d). It seems reasonable to suggest that the thinner coccolith stringer lamina were the result of only a small nutrient input, probably best explained by limited periods and intensities of wind mixing. The thicker laminae, however, must represent greater blooms and thus nutrient supply, possibly the result of more extensive winter storms? Graded intervals associated with such thicker carbonate laminae have been noted within the coccolith-rich oil shale of the WSB interval, which suggests that such storm disturbance did occur during oil shale depositional periods (Section 3.5, Figure3.18f, Section 4.10). It is also feasible that both these lamina scales represent similar time periods, a yearly couplet? (Section4.8.2). During the summer, greater aridity would have occurred and led to highly stable stratification of the water column. Surface waters would therefore have been oligotrophic and thus phytoplankton production was very low, but the resultant sediment would have been organic-rich due to enhanced preservation. However, during the winter, the weather would have become less stable possibly with storms, or at least increased wind and precipitation. This would have resulted in mixing of the nutrient-rich waters below the thermocline with the nutrient-poor surface waters and thus have led to phytoplankton blooms. The ability of the r-strategist coccolithophores to take advantage of the high surface water nutrients would have resulted in these blooms being dominated by the coccolithophores and may highlight some mismatch between the phyto- and zooplankton (Section 4.5.1). Thus this hypothesized system results in an organic-rich fabric containing greater amounts of carbonate compared to the homogeneous fabric (Figure 4.5B).

Within the oil shale (1) below the WSB coccolith limestone (Figure 3.1), thicker coccolithic laminae tend to be grouped together. This pattern seems to imply that though the majority of the oil shale deposition was characterized by stable climatic and environmental conditions, several groups of years were less stable with increased numbers and/or intensities of winter storms. The finer coccolith/organic matter lamination is occasionally seen over greater vertical extents and thus over a far greater number of 'years' than the thicker laminae, implying that larger storms were not the norm, but periods of increased windiness were more common.

The pelletal and discontinuous laminated organic-rich fabrics form a bridge between the two fabric end members (Figure 4.4). Pelletal fabric is more closely related to the homogeneous fabric, but both phyto- and zooplankton populations were probably greater and the nutrient limitation in the surface waters not so severe. However, both the organic matter and carbonate flux to the sediment were probably still relatively low. Conversely the discontinuous laminated fabric indicate that coccolithophores periodically bloomed, but not to the extent of those forming

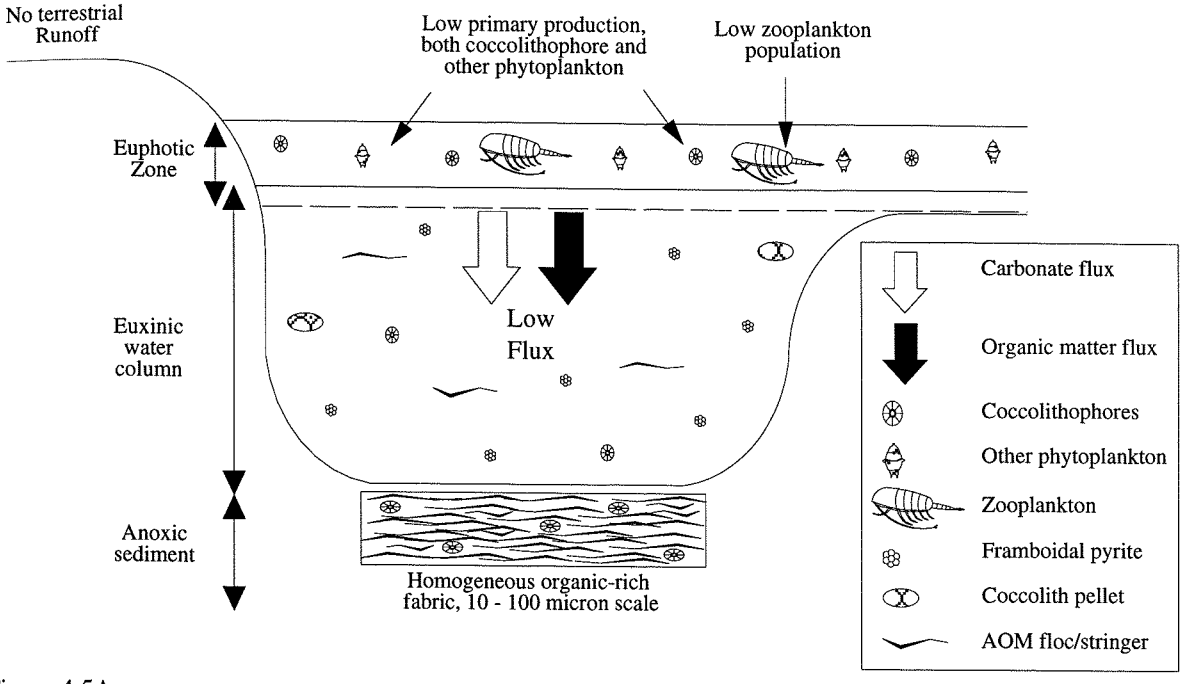

Figure 4.5A
A schematic diagram of the KCF marine environment during the deposition of the homogeneous organic-rich fabric within the oil shale lithology. The water column depth is <100m. The stratification is highly stable, and euxinic waters possibly reached up into the euphotic zone. A semi-arid to arid climate dominates with no terrestrial runoff, and thus togther with the stratification, results in oligotrophic surface waters. Productivity for both phyto- and zooplankton is therefore low and thus the organic matter and carbonate flux is low, but flux preservation is excellent leading to an organic-rich sediment.

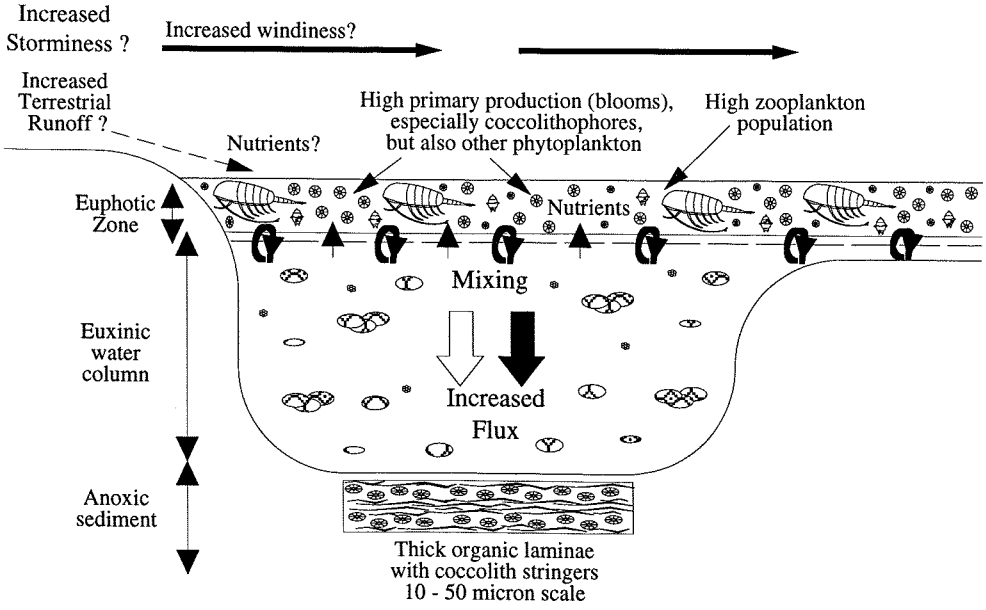

Figure 4.5B
A schematic diagram of the KCF marine environment during the deposition of the organic-rich and coccolith stringer laminated fabric within the oil shale lithology. No change in water column depth. The climate is still semi-arid but is characterized by periods of increased storminess, and/or increased windiness and/or precipitation? The upper level of the euxinic stratification is broken down by wind mixing and/or storm turbulence to below the chemocline, but stable stratified euxinic waters occur below this level of mixing. Thus, a brief period of eutrophication of the surface waters occurs resulting in the blooming of the phytoplankton, especially the coccolithophores. There is also a subsequent increase in zooplankton. The overall carbonate and organic matter flux therefore increases and the euxinic water column still provides enhanced preservation, leading to the deposition of a finely laminated organic matter and coccolithic fabric.

the continuous laminated fabric, implying that mixing or overturn of the euxinic waters was not as great. The coccolithophore blooms were probably more 'patchy', but overall the flux of organic matter and carbonate was greater than for the pelletal fabric, but less than for the laminated fabric.

4.11.2 ENVIRONMENTAL RECONSTRUCTION FOR THE COCCOLITH LIMESTONE LITHOLOGY

The KCF coccolith limestone lithologies are clearly the result of extreme primary production of coccolithophores, which implies that surface waters were eutrophic and environmental conditions perfect for this phytoplankton during these periods. The monospecific nature of these blooms, dominated by *Watzernaueria* spp., reinforces the strongly favorable environmental conditions for these growth maximizing and opportunistic, r-strategist phytoplankton (Section 4.2.1), possibly to the detriment and suppression of other phytoplankton (Section 4.2.4). In order to maintain surface water eutrophication, strong water column nutrient recycling and/or high terrestrial runoff would be needed, thus increased storm frequency would provide a mechanism for both these processes. However, no direct evidence for these processes can be ascertained from the fabric.

Similar to the oil shales, the coccolith limestone fabric can be divided into two end members (Section 3.3.5, Figure 4.4), a homogeneous fabric (Figure 3.14) and a laminated fabric (Figure 3.13a). However, unlike the oil shale, this fabric variability is believed to be the result of the presence or absence of benthic fauna. The homogeneous fabric is suggested to have resulted from bioturbation and thus indicates more oxic bottom water conditions, while the laminated fabric indicates no bioturbation and suboxic to anoxic bottom waters. Thus bottom water oxygen levels are believed to have been variable during the coccolith limestone deposition, despite the high primary productivity, and it is likely that the majority of the water column was oxic to dysoxic. This hypothesis is also reinforced by the lack of very small pyrite framboids (as seen in the oil shales) implying that the water column was significantly more oxygenated than during oil shale deposition. However, the fabric is frequently laminated, indicating suboxic/anoxic bottom waters were not uncommon. Thus, the climate and the marine environment of Northwest Europe were believed to have been relatively more unstable during the deposition of the coccolith limestone lithologies than during the oil shale deposition.

The homogeneous fabric occurs over significant vertical intervals within the coccolith limestones (Figure 3.21(C)). Evidence of macrofauna trace fossils in hand specimen over some of these intervals, and the massive nature of this fabric compared to the coccolith-dominated lamina in the laminated intervals (Figure 3.21(B)), suggests it to be the result of bioturbation.

Thus bottom waters must have been relatively oxic, though with the high primary production, dsyoxia may have been more common. Coccolithophore production was very high during these periods, probably as large, frequent blooms. Though no pelletal evidence has been preserved within the fabric, it is highly likely that zooplankton populations were also high, though some mismatch to the phytoplankton is envisaged. To sustain this high production the surface waters must have been highly eutrophic, probably maintained via high terrestrial runoff and strong water column nutrient recycling. These mechanisms are believed to have resulted from an increase in climate humidity and precipitation, possibly manifested as increased storm frequencies and intensities. The relatively oxic nature of the water column combined with a significant mediation of the organic matter flux by the abundant zooplankton led to the reduced preservation of the organic matter. Also the large amount of coccolithic carbonate would have significantly diluted other flux materials, resulting in a predominately carbonate deposition. Figure 4.6A shows a summary of these ideas on an idealized KCF marine basin.

The laminated fabric composed of alternations of thick coccolith lamina with thin organic matter stringer lamina, indicate that though coccolithophore production was still high, their production was interspersed by periods where organic matter was more dominant. The laminated nature of the fabric indicates that the bottom waters during these periods were suboxic/anoxic with no benthic fauna. Thus, coccolithophore production is suggested to have declined and water column stability to have increased during these episodes and it is also possible that the decline in coccolithophore resulted in increases in the previously suppressed dinoflagellate population. It is suggested that the climate became less humid and precipitation less frequent and lower in intensity during the deposition of this laminated fabric. It is also possibly that each coccolith and organic matter laminae are a 'varve' couplet and thus represent a year of deposition. These hypotheses are summarized in Figure 4.6B.

4.11.3 ENVIRONMENTAL RECONSTRUCTION FOR THE MUDSTONE LITHOLOGY

A homogeneous mixture of clays and coccoliths with minor components of large detrital grains, organic matter and pyrite (Section 3.3.1, Elemental Map 3.1) dominate the mudstone lithologies of the KCF. This homogeneous fabric (Figures 3.2a to c) indicates that the sediment was highly bioturbated and supported a rich benthic fauna, thus indicating that both the bottom water and the water/sediment interface were oxic. The larger pyrite framboids and the presence of euhedral pyrite grains implies formation within the sediment and not in a euxinic water column as was the case of the very small pyrite framboids of the oil shales (Section 4.9.1, Wilkin, Barnes and Brantley, 1996). This therefore reinforces the suggestion of an oxic water

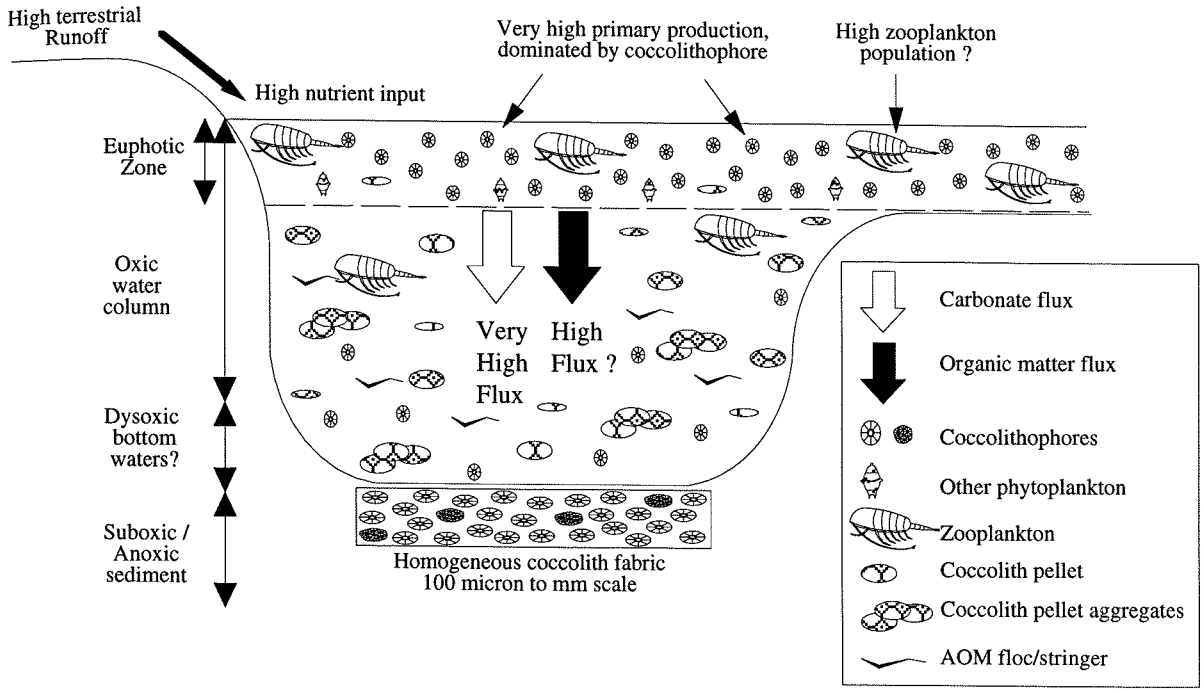

Figure 4.6A

A schematic diagram of the KCF marine environment during the deposition of the coccolith homogeneous fabric within the coccolith limestone lithology. The water column depth is <100m. The water column is predominately oxic, though the bottom waters were likely to have been dysoxic to suboxic. However, brief periods of benthic colonization and bioturbation occurred. Precipitation was high and the climate may possibly have been more humid, which lead to increased terrestrial runoff, and thus eutrophication of the surface waters and frequent large coccolithophore blooms. The zooplankton population was probably also relatively high and combined with the oxic water column reduced the preservation of the organic matter flux. However, the carbonate was preserved leading to a homogeneous coccolithic carbonate fabric.

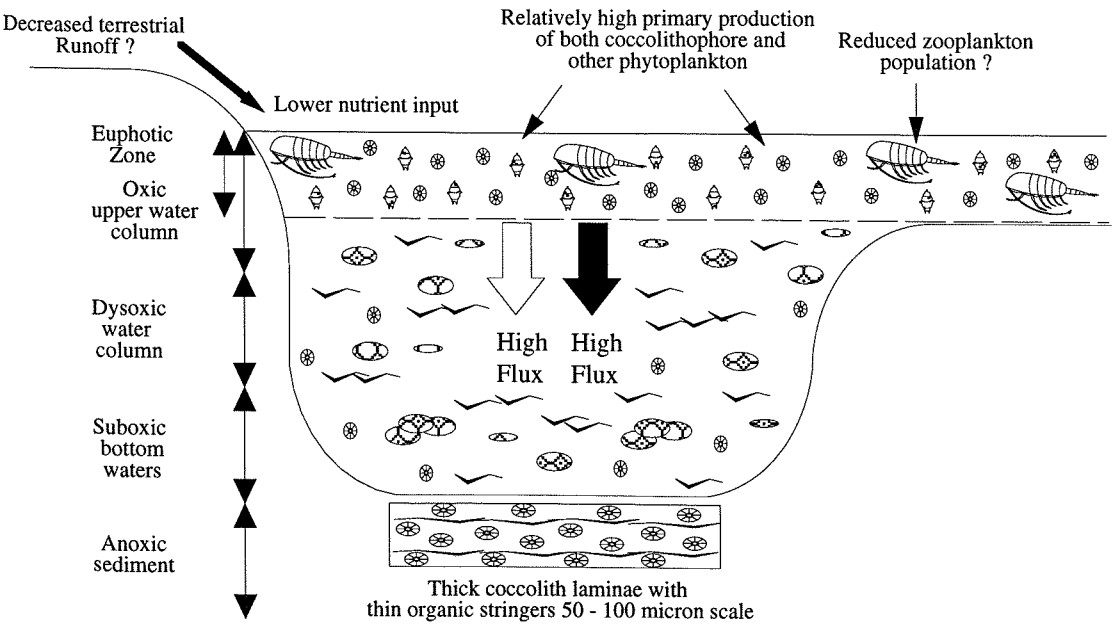

Figure 4.6B

A schematic diagram of the KCF marine environment during the deposition of the laminated coccolith and organic matter stringer fabric within the coccolith limestone lithology. Again the water column is <100m deep. The climate is less humid, precipitation is reduced, and terrestrial runoff is therefore less. Thus surface water eutrophication is reduced, leading to less frequent coccolithophore blooms, but possibly other phytoplankton bloomed.Water column stability has also increased with a greater proportion of the water column becoming dysoxic, in turn leading to suboxic bottom waters and restricting benthic fauna so that there is no bioturbation. Zooplankton population is slightly reduced and their vertical movement more restricted , thus consumption of organic matter is reduced. Combined with less oxic waters this results in increased preservation of the organic matter and led to the deposition of laminated coccolithic and organic matter fabric.

column during the deposition of the mudstones, which would have resulted in a lack of preservation of the organic mater flux.

The dominance of the clays in the mudstone matrix and the relatively sparse abundance of larger clastic grains indicates that deposition took place at some distal location from the clastic source, or that the main sediment path bypassed this area (Section 4.6). Coccoliths also comprise a substantial proportion of the matrix, implying that coccolithophore production was relatively high, but not on the scale of blooms during the deposition of the coccolith limestones. Though all fabric evidence has been destroyed by bioturbation, it is likely that the zooplankton population was also relatively high, which helped to mediate the organic matter flux within the water column. This substantial level of both phyto- and zooplankton production would have required a reasonable level of nutrients, which may have been maintained by water column nutrient recycling and relatively low terrestrial runoff. The water column overturn and oxygenation must have been continuous processes during these periods, suggesting that the climate was less arid than during oil shale deposition, and that lower amounts, but more frequent precipitation occurred than envisaged during coccolith limestone deposition. These characteristics for the KCF marine environment during the deposition of the mudstone lithologies are summarized in Figure 4.7A.

Within the studied intervals, the mudstones are also commonly more calcareous (Section 3.3.2, Figures 3.2c to f), forming transitional lithologies between the mudstone and coccolith limestone lithologies. The increase in coccolithic carbonate within the matrix (Figure 3.3) clearly indicates that coccolithophore production increased. Thus, surface water nutrient levels must also have increased, possibly via an increase in terrestrial runoff? The increase in primary production and thus carbonate and organic matter flux may also have resulted in a decrease of water column oxygenation levels, especially the bottom waters. The organic matter within the calcareous mudstones is more abundant than in the mudstones, which would suggest slightly greater preservation of the organic matter flux probably by dysoxic, and perhaps for short periods, suboxic bottom waters. This is further supported by the presence of pelletal structures in the fabric, which are similar in character to the planktonic pellets seen in more organic-rich lithologies (Figure 3.10). Thus, a reduction in bioturbation due to a decrease in bottom water oxygen levels aided the preservation of these pellets. The calcareous mudstones are therefore believed to differ from the mudstones by an increase in coccolithophore production brought about by slight increases in terrestrial runoff and therefore precipitation and a subsequent increase in organic matter due to increased preservation caused by increased primary production.

4.11.4 ENVIRONMENTAL RECONSTRUCTION FOR THE CEMENTSTONE LITHOLOGY

The cementstone lithology resulted from the diagenetic alteration of a mudstone, as is evidenced by the sequence of homogeneous clay/coccolith-rich fabric masked by an interlocking mosaic of euhedral ferroan dolomitic crystals (Figure 3.4, Section 4.9.2). Thus, the primary mudstone lithology is envisaged to have formed under the same environmental and climatic conditions as the other KCF mudstones (Section 4.11.3, Figure 4.7A). However, these conditions subsequently altered, resulting in the growth of dolomite crystals, which eventually formed a mosaic and almost completely destroyed the primary mudstone fabric. It was also noted that zoning of the dolomite crystals was common within the cementstone lithology (Section 4.9.2), which is indicative of several phases of growth (Feistner, 1989).

The formation of such carbonate-rich concretionary horizons in the KCF has been quite extensively studied, and it has been proposed that they result from early diagenetic processes occurring at 10m or less depth within the sediment (Bellamy, 1980; Irwin, 1980). These mudstone cements represent the end products of microbiological degradation of organic matter in the sulphate reduction and methanogenic zones which results in changes to the sediment pore water chemistry (Curtis, 1980). In order for sediment pore water alkalinity to build up sufficiently to promote carbonate precipitation, a lull in sedimentation is required (Bellamy, 1980; Raiswell, 1987). Thus, sedimentation rates are an important regulation on early diagenetic reactions, controlling the amount of organic matter in the sediment and the extent of oxygen and sulphate diffusion from overlying seawater (Scotchman, 1989). The restriction of cementstones to specific horizons attests to the development of such sedimentation hiatuses (Raiswell, 1987).

Thus the cementstone lithology is suggested to have formed at shallow burial depth during a period of either very low sedimentation or a hiatus, and have undergone several phases of precipitation (Bellamy, 1980; Feistner, 1989). A hiatus in sedimentation implies that primary production and terrestrial runoff were minimal, thus surface waters were probably oligotrophic and the climate was semi-arid to arid during these depositional periods (Figure 4.7B). Though not developed to the same extent, the euhedral carbonate lamina, pellets and grains evident in the oil shale lithologies also support the hypothesis that diagenetic alteration of the KCF fabrics occurred during periods of low sedimentation and an arid climate.

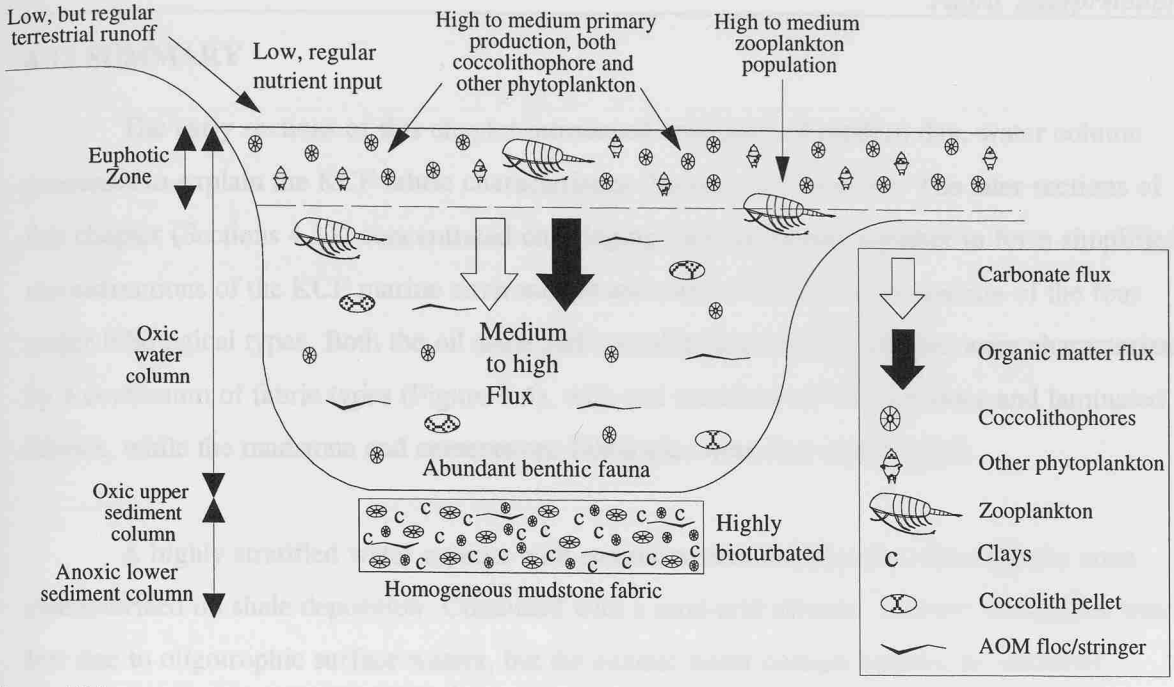

Figure 4.7A

A schematic diagram of the KCF marine environment during the deposition of the mudstone lithology. The water column depth is <100m. The whole of the water column is oxic and the upper sediment column is also oxic, though deeper in the sediment anoxic conditions prevail. Thus, benthic fauna was rich and the sediment highly bioturbated. High to medium levels of primary production of both coccolithophores and phytoplankton occurred, together with relatively high zooplankton populations. The climate was probably less arid than during oil shale deposition, and was characterized by low but more frequent precipitation than during coccolith limestone deposition. Thus a low but regular supply of nutrients was available to support a relatively high primary production. The flux of both carbonate and organic matter was therefore relatively high, however high organic matter flux mediation in the water column, combined with high levels of bioutrbation and thus oxygen in the surface sediments resulted in low preservation of the organic matter. Overturn and mixing of the water column was also important.

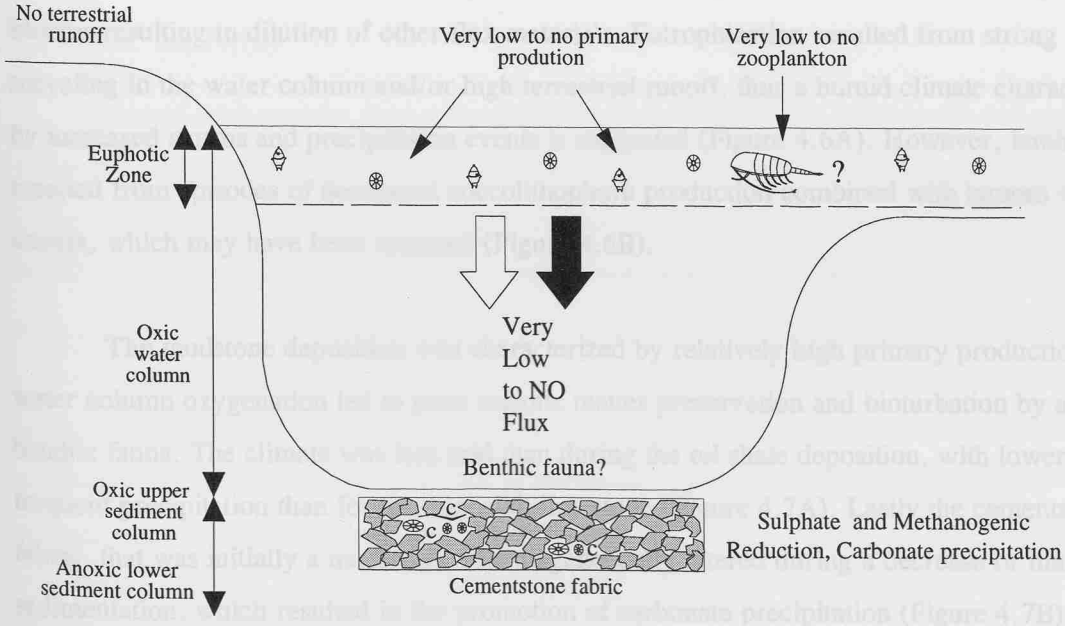

Figure 4.7B

A schematic diagram of the KCF marine environment during the deposition of the cementstone lithology. The water column depth is <100m. The primary form of the this lithology was a mudstone, thus the marine environment would have had the same characteristics as dipicted above (Figure 4.7A). However these conditions changed and resulted in the diagenetic alteration of the mudstone fabric to a cementstone. The most critical factor in this change was a reduction of sedimentation rate with both primary production and terrestrial runoff drastically reduced so that a hiatus occurred. This allowed alkalinity to build up in the sediment and promoted carbonate precipitation as euhedral crystal mosaics which masked the primary mudstone fabric. Such a hiatus in sedimentation was probably caused by an increase in aridity.

4.12 SUMMARY

The early sections of this chapter introduced analogues of modern day, water column processes to explain the KCF fabric characteristics (Sections 4.1 to 4.10). The later sections of this chapter (Sections 4.11) concentrated on bringing these processes together to form simplified reconstructions of the KCF marine environment and climate during the deposition of the four major lithological types. Both the oil shale and coccolith limestone lithologies were characterized by a continuum of fabric types (Figure 4.4), with end members of homogeneous and laminated fabrics, while the mudstone and cementstone lithologies were less complicated.

A highly stratified water column with euxinic waters reaching into the euphotic zone characterized oil shale deposition. Combined with a semi-arid climate, primary production was low due to oligotrophic surface waters, but the euxinic water column resulted in enhanced preservation of the organic matter (Figure 4.5A). Increased storminess/windiness punctuated these stable conditions, resulting in overturn of the upper euxinic water column, surface water eutrophication and coccolithophore blooms. Thus carbonate lamina were deposited within the oil shales (Figure 4.5B).

The coccolith limestone deposition was characterized by highly eutrophic surface waters and highly variable water column oxygen levels, with exceptional levels of coccolithophore blooms resulting in dilution of other flux materials. Eutrophication resulted from strong nutrient recycling in the water column and/or high terrestrial runoff, thus a humid climate characterized by increased storms and precipitation events is suggested (Figure 4.6A). However, lamination resulted from episodes of decreased coccolithophore production combined with bottom water anoxia, which may have been seasonal (Figure 4.6B).

The mudstone deposition was characterized by relatively high primary production but water column oxygenation led to poor organic matter preservation and bioturbation by a rich benthic fauna. The climate was less arid than during the oil shale deposition, with lower, more frequent precipitation than for the coccolith limestone (Figure 4.7A). Lastly the cementstone fabric, that was initially a mudstone, was diagenetically altered during a decrease or hiatus in sedimentation, which resulted in the promotion of carbonate precipitation (Figure 4.7B).

These environmental reconstructions are therefore preliminary attempts at placing the KCF lithologies into an environmental and climatic context based purely on fabric evidence. The following chapters (6 and 7) concentrate on geochemical and palynological evidence with the aim of refining the fabric based interpretations and reconstructions.

5.0 ELEMENTAL ANALYSIS AND PALYNOLOGY METHODS

Though SEM analysis of the KCF fabric allows substantial information on the fabric structure and composition, the chemical and particulate characteristics of the organic component are not discernible. Elemental analysis and palynology enables this organic component to be both quantified and the individual particulate components of the organic matter to be characterized. TOC, atomic H/C ratios and palynological methods are described in the following sections, together with the palynology classification scheme and particle palaeoenvironmental interpretations used in the study.

5.1 TOTAL ORGANIC CARBON (TOC)

The carbon and nitrogen content of the KCF was measured using a Carlo Erba EA1108 Elemental Analyzer. Within the Analyzer, samples are flash combusted, converting the C, H and N into oxides. The resultant gases (CO_2 and NO_x) pass through a reduction column into a chromatographic column in a carrier gas (helium), where they are separated and then measured with a hot wire detector. The Analyzer has an accuracy of better than 0.3% absolute value (0.5-3mg sample) and a reproducibility of better than 0.2% absolute value (0.5-3mg sample) for C, H and N. TOC was calculated for the four studied intervals (a total of 400 samples, refer to Figure 1.4 for sampled points and resolution), providing profiles of organic carbon variation within each interval.

5.1.1 TOC METHOD

Cleaned rock samples were ground into fine powder using an agate pestle and mortar, and divided into two parts. One part was treated with Analar grade HCl to remove any inorganic carbon in the form of carbonate, and then decanted and washed with milliQ water. Both the acidified and non-acidified parts of the sample were oven dried ($<60^0$C) before being placed in tin capsules, weighed and processed through the Elemental Analyzer. The machine was calibrated with two comparable standards over the lengthy analysis period; sulphanilamide (standard 41.88% carbon) and acetanilide (standard 71.09% carbon). After every five samples a standard was run, if it was within 0.3% of the theoretical value the samples needed no correction. If the samples were up to 0.6% from the theoretical value they were corrected by averaging them with the current standard value. If the standard produced errors greater than 0.6% from the theoretical value for 3 consecutive analyses, the machine was recalibrated.

The Elemental Analyzer only measures the percentage of carbon in each sample. In order to calculate TOC, corrections need to be made to remove the influence of carbon in the form of

carbonate (especially calcite) contained within the samples. This is done using the following equation (1):

$$TOC\ \% = 100 \times \frac{((8.33C_T)/100-1)}{8.33 - (100/C_A)} \qquad (1)$$

Where C_T = total carbon of the sample, C_A = carbon content of the acidified sample and 8.33 = the molecular weight of calcite / atomic weight of carbon.

It follows that the percentage calcite of the samples can be calculated using equation (2):

$$Calcite\ \% = 100 \times (1-(TOC/\ C_A)) \qquad (2)$$

The TOC results were either plotted as vertical profiles for each interval, or averaged to give spot TOC values for each lithology. Due to the abundance of calcite in the form of coccoliths, and its dilution effect on TOC, especially within the coccolith limestone and calcareous mudstone lithologies, TOC was also calculated as $CaCO_3$Free TOC using the following equation (3):

$$CaCO_3\text{Free TOC}\ \% = 100 \times (TOC/\ (100 - \text{calcite}\ \%)) \qquad (3)$$

5.2 ATOMIC H/C RATIOS

Atomic hydrogen and carbon was also measured on the Elemental Analyzer with the water trap removed. Wet samples that had previously been demineralized with HCl and HF acids were placed in tin capsules and oven dried before processing in the Analyzer. A weightless method of calibration (peak ratios) was used where by a series of pure compounds, with known H and C ratios, were used to calibrate the peak area response of H and C to their atomic H/C ratio. The known standards used were acetanilide, benzoic acid, 2nitrobenzoic acid and sulphanilimide. Due to time constraints only selected samples from the Whitestone Band were analyzed for H and C (refer to * on Figure 1.4), with the analysis carried out by Mr Shir Akbari.

5.3 PALYNOLOGY AND PALYNOFACIES ANALYSIS

Palynology is the systematic study of organic matter within sedimentary rocks, of which marine shales such as the KCF contain a wide range of types. The term "palynofacies" was originally applied to the general aspect of palynological preparations from sedimentary rocks (Combaz, 1964), and has two main applications; source rock evaluation and palaeoenvironmental interpretation, the latter on which this study is based. The classification of organic particles into

distinct palynofacies has always been rather subjective and there is no universally accepted scheme. Most schemes are only applicable on specific stratigraphic units. However, steps are being taken to produce a widely acceptable organic matter classification based on a multi level descriptive system (Waterhouse, 1992). At present this classification only covers the differentiation of structured and structureless organic matter under transmitted light, and therefore individual schemes are generally employed. The classification scheme used in this study is described in Section 5.3.4.

5.3.1 SAMPLING

The sample resolution for both palynology and TOC for each of the studied intervals was discussed in Section 1.5.2, with sample locations displayed in Figure 1.4. Two levels of sampling were employed, a high-resolution, lamina scale and a lower resolution point sample every 5cm. The lamina level of sampling was ultimately determined by the fabric characteristics. Detailed hand specimen logging and low magnification SEM base maps were combined to determine high-resolution changes in fabric composition and structure, which thus identified the sample divisions. This process resulted in large numbers of samples over relatively short vertical sections (an average of 2 to 4 samples per cm), and samples varied in thickness between 1mm to 0.5cm. Once sample boundaries were clearly defined, a rock slab (<2cm thick) which had been taken vertically through an interval, was securely placed on a Testbourne Model 850 wire saw. Using a 10x magnifying lens fixed above the diamond wire blade, the rock slab was carefully positioned so that the diamond wire would make a cut parallel to the fabric lamination at each sample division. Samples were sliced off the rock slab one directly after the other, as due to the wire's thickness (0.254mm) some of each sample was unavoidably lost in the cutting. In addition, some very thin lamina were not possible to cut out. The lower resolution samples were also cut on the same diamond wire saw, but these sample division were purely based on distance over the interval. Point sample divisions were every 5cm, with the each sample a composite $1cm^3$ block of rock.

The resultant weights of the material available for processing was therefore adequate at several grams for the $1cm^3$ block samples, while the lamina slices were considerable less, between 0.1 to 1 gram. The limited amount of material from the lamina slices is inherent in the thin nature of the laminated sediment, as well as the limited size of the rock slab that can be accommodated on the saw. No attempt was made to increase the amount of material, by cutting the same slices from two slabs of rock, as identical lamina slices would be impossible to obtain due to both cutting errors and fabric variability along the lamina. Additionally, cutting the thin slices was very time-consuming, with organic-rich lithologies taking the order of an hour to cut one slice, though softer coccolith lithologies were faster. Despite the smaller amount of sample at

the high-resolution scale, the organic richness of the KCF lithologies enables sufficient amounts of organic matter to be obtained for examination and analysis.

5.3.2 PALYNOLOGICAL METHODS

A summary of the palynological processing techniques is given in Table 5.1. A total of 400 rock samples, (combined $1cm^3$ blocks and thin lamina slices), were cleaned and dried before being crushed into 0.5-2mm diameter granules. Samples of between 0.1g to 2g were processed using standard palynological processing techniques (e.g. Traverse, 1988) to produce palynological residues. These involved two demineralization treatments, firstly with HCl, followed by washing to neutral, then with HF at 60% concentration, followed by a second wash to neutral. An exotic spike, in the form of *Lycopodium* tablets was then added, followed by sieving at 10μm and a 30 second treatment in boiling HCl to remove neo-formed fluorides. No oxidation was carried out during processing as all particles in the samples were of interest and oxidation may selectively remove some particles (Waterhouse, 1992, 1995).

However, AOM was so abundant in these KCF samples that it obscured most of the other organic particles on the slides. Only structured particulate organic matter was deemed of interest and therefore AOM, being structureless and difficult to quantify, was not included in particle counts. The AOM was selectively removed using a 600W Jencons high-intensity ultrasonic probe, followed by sieving. Short ultrasonic treatments have been found to disaggregate AOM alone, whilst other particles remain intact (Tyson, 1984). Times for the ultrasonic dissemination of the AOM ranged from 5 seconds in the mudstones, to 40 seconds in the very organic-rich shales. The presence of well preserved details of sculpturing and delicate structures on some particles (e.g. chorate dinocysts), even after more extensive treatment, suggest that this treatment is AOM selective. The effects of the ultrasonic treatment on KCF structured particles were thoroughly tested by Waterhouse (1992), who found that treatment under two minutes did not effect the number of structured particles present or preferentially break down certain particle groups with respect to others. The final organic residue was well mixed prior to pipetting the analysis portion onto glass cover slips, which were then left to dry naturally. Once dried, the cover slips were mounted on rectangular glass microscope slides using Elvacite 2044.

	PROCESS	PURPOSE
1)	All samples washed and dried	To remove surface contamination.
2)	Crush samples to 0.5 x 0.5cm pieces	To increase surface area for acid digestion.
3)	Weigh to nearest 0.1g	To enable absolute abundance data calculations.
4)	HCl (28% conc.)	To remove carbonates and Ca which will produce insoluble neo-formed fluorides.
5)	Decant and wash 3 to 4 times	To dilute to neutral.
6)	HF (60% conc.)	To remove silicates.
7)	Decant and wash 2 times	Reduce acidity
8)	Spike with *Lycopodium* tablets	To enable absolute abundance data calculations.
9)	Decant and wash up to 5 times, or until neutral	To dilute to neutral.
10)	Sieve at 10μm	Remove fine fraction $<10\mu$m
11)	Boil in HCl (28% conc.)	To remove any neo-formed fluorides.
12)	Sieve at 10μm	
13)	Examine under microscope	To establish need to ultrasonic
14)	Ultrasonic (if necessary)	To remove AOM
15)	Sieve at 10μm	Remove newly broken down AOM.
16)	Mount in Elvacite 2044	

Table 5.1 Palynofacies processing technique

5.3.3 LYCOPODIUM SPIKING

An 'exotic spore' spike of the genus *Lycopodium* was added to all samples during processing. This technique enables absolute abundance of particles per gram of rock to be calculated (Stockmarr, 1971). If only relative abundance is used it cannot be determined whether the abundance of a particle type is really varying with time, or is merely responding to a variation in another type of particle. Thus, the ability to obtain absolute particle numbers of any category per gram of original rock enables comparison between samples. The *Lycopodium* spores are readily identifiable within the sample by their morphology and colour, and were counted simultaneously to, but separately from, the palynofacies particle count (Figure 5.3R). The determination of the absolute abundance per gram of each particle category is achieved using several simple ratios. The calculation is based on the assumption that the number of *Lycopodium* counted is in the same proportion to the total number of *Lycopodium* added, as the weight of the sample portion counted is to the weight of the total sample prepared. Thus:

$$\frac{\textit{Lycopodium}\text{ counted}}{\textit{Lycopodium}\text{ added}} = \frac{\text{Kerogen counted}}{\text{Weight of total sample (g)}} \qquad (1)$$

Re-arrangement of (1) enables the kerogen counted to be found:

$$\text{Kerogen counted (g)} = \frac{\textit{Lycopodium}\text{ counted}}{\textit{Lycopodium}\text{ added}} \times \text{Total sample weight (g)} \qquad (2)$$

Any portion of kerogen counted can now be found, and therefore the absolute number of particles in any category can be calculated using Equation 3:

$$\text{Particle abundance /g} = \frac{\text{particle count}}{\text{Kerogen counted (g)}} \quad (3)$$

Lycopodium spores were used as tablets (available from the Laboratory of Quaternary Biology, Tornavagen 13, S-223 63 Lund, Sweden), each containing a known number of *Lycopodium* spores (Batch 124961 = 12542 spores per tablet, Batch 710961 = 18470 spores per tablet). These are held together by sodium bicarbonate and water-soluble organics, which are washed away by water and HCl during subsequent processing. This method provides an accurate and uncomplicated way of introducing exotic spores into samples (Stockmarr, 1971). To avoid bias between different batches of samples, the tablets were always introduced after the second rinse subsequent to HF digestion. This choice of timing has a number of reasons. Firstly, the organic matter is not completely released from the mineral matrix until after HF digestion. To avoid bias in the absolute abundance, the introduced and indigenous microscopic particles must ideally behave in a similar manner. This will not be achieved until all the organic matter has been released from the mineral matrix. Care is needed when decanting samples prior to tablet addition so as not to lose any sample, as this may bias the results by causing sample particle abundance to be under represented compared to *Lycopodium* spores. Secondly, the addition of tablets after the HF has been partially diluted is safer for the operator.

The number of *Lycopodium* tablets added to samples to enable accurate quantitative particle counts varied according to the concentration of organic matter within the rock. The greatest number of tablets was needed for organic-rich samples, and the least for mudstone samples. However, the most organic-rich samples were lamina resolution and therefore generally needed a maximum of 1 tablet per 0.1g, while the mudstones generally required between 2-5 tablets for 2g of rock.

5.3.4 COUNTING

Counts were undertaken on the strew mounts of the samples in transmitted white light using an Olympus BHT 112 microscope (no. 234347). Within each field of view all particles were counted and then the view moved on to another completely new view. Special care was taken to ensure that each field of view did not overlap the previous one. Thus, each particle was equally weighted using this counting technique, which was carried out for both lamina and 5cm point samples, so preventing any errors between the two different sampling scales as a result of the counting technique.

A minimum of 500 particles was usually counted per sample. This figure excludes *Lycopodium* spores, which were counted simultaneously but separately to the particle count, with the aim of counting at least 100 *Lycopodium* spores per sample. However, it was not always possible to count the desired numbers of particles, even with several strew mounts being counted. This was the case for those lamina samples that were characterized by especially organic-rich lithologies. Within these samples, the majority of the organic component was composed of AOM, which was not counted in this study, and structured particles were very rare. In this situation a minimum of 300 particles were counted, though in a few cases the total figure was considerably less. These counting regimes result in standard error margins of 12% for the 300 counts and 11.4% for the 500 counts (Stockmarr, 1971) (Box 5.1, Figure 5.1). These standard errors were the smallest errors that could be obtained with this counting regime, which is realistic with respect to the time and effort expended for the gains in error reduction (Figure 5.1).

All counts were converted to absolute abundance per gram of rock, but it should be noted that this does not necessarily equate to abundance per unit weight of rock per unit time. Relative particle abundance as percentages of the total number of particles within each sample were not used but are illustrated as ratios between selected pairs of particle types. Ratios are not affected by data closure effects, which are inherent in percentage data. In some cases the specific ratio was greater than 1.0, therefore to prevent the exaggeration of the apparent importance of the x component at the expense of y, the $\log_{10}$ of the ratio data was taken (Tyson, 1995). For the same degree of relative dominance, this results in an equal offset to either the left or right of the central 0:0 (1:1) value, and thus a more symmetrical diagram that is more easily interpreted. Categories were also calculated as a percentage of one of the three major groups, called group percentages. Thus, trends within each major particle group, rather than in the total counted particles could also be examined.

Figure 5.1
Estimated Error on Calculated Number of Palynomorphs in Sample Using Lycopodium Tablets (After Stockmarr, 1971)

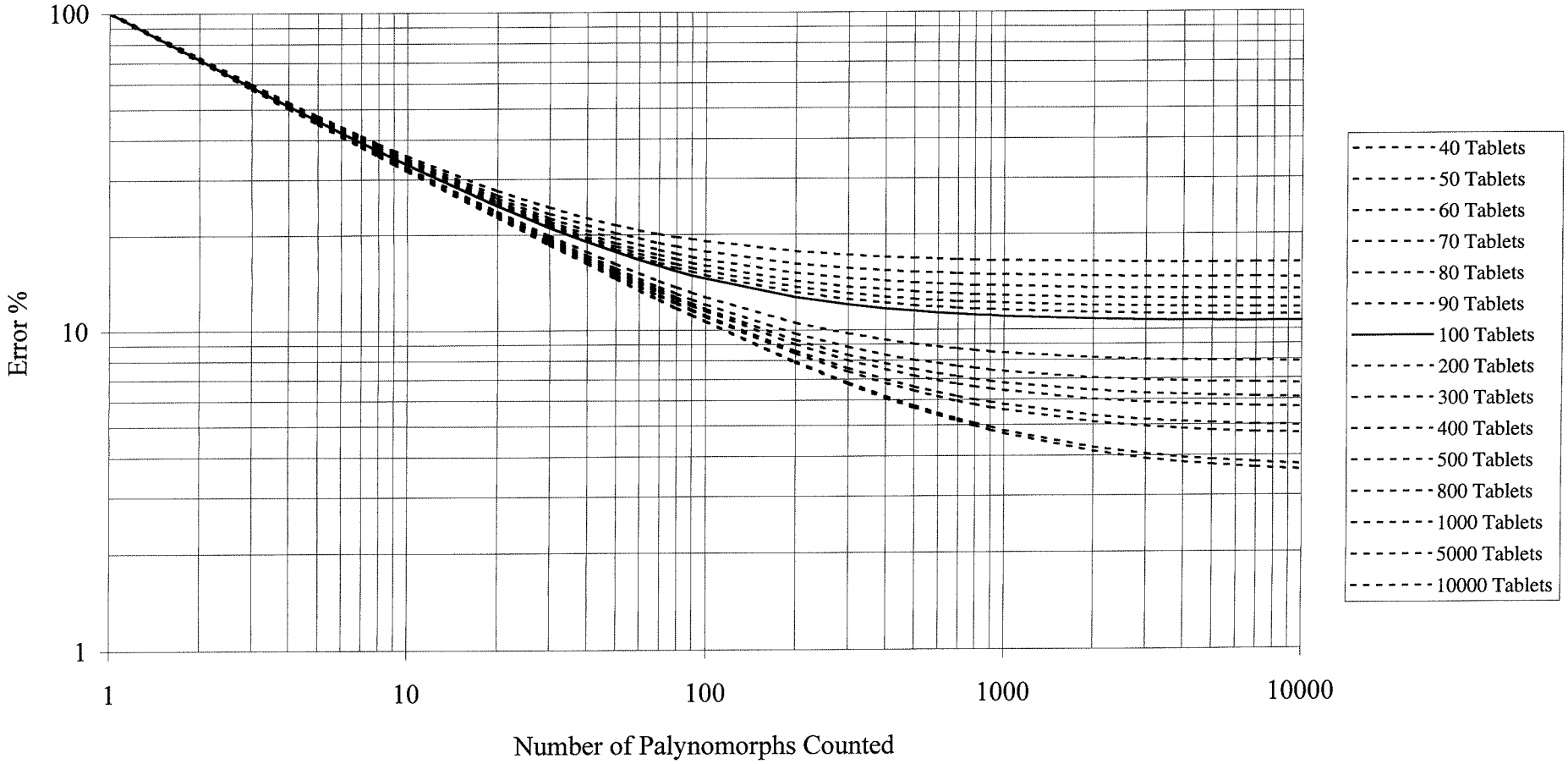

BOX 5.1
PALYNOLOGY COUNT ESTIMATED ERROR CALCULATIONS
(After Stockmarr, 1971)

$$\text{Total Error} = \frac{\sigma_1 x2}{3}\ \% = \pm 100 \sqrt{\frac{(\sigma_1)^2}{(r_1)} + \frac{(\sigma_2)^2}{(r_2)} + \frac{(\sigma_3)^2}{(r_3)}}$$

Where;
σ_1 = standard error on r_1 (number of spores in 5 *Lycopodium* tablets)

For *Lycopodium* tablets from Batch No. 124961 from Lund University.
Average number of spores in 5 tablets, X = 62712 (r_1),
and therefore $\sigma_1 = s = \pm 2081$, a 3.3% error

σ_2 = standard error on r_2 (number of pollen grains (particles) counted in the sample)
$\sigma_2 = \pm\sqrt{r_2}$

σ_3 = standard error on r_3 (number of *Lycopodium* spores counted in the sample)
$\sigma_3 = \pm\sqrt{r_3}$

5.3.5. PALYNOFACIES CLASSIFICATION SCHEME

A particle classification scheme was chosen from an initial examination of samples and a review of Waterhouse's (1992) particle classification scheme. Counted particles are grouped under three major groups of marine palynomorphs, terrestrial palynomorphs and terrestrial structured debris, each of which contains several categories of palynomorph and debris types (Table 5.2). Waterhouse's scheme was devised to enable as much palaeoenvironmental and palaeoclimatic information as possible to be gained from the palynofacies analysis. This study has a similar aim of palaeoenvironmental reconstruction and since both studies are based on the KCF it seemed appropriate to have comparable classification schemes. The scheme is essentially a morphological classification, and though particle provenance is also incorporated, a systematic taxonomy was not carried out due to time constraints.

The palynomorphs are primarily divided into three broad systematic groups of marine and terrestrial palynomorphs and structured terrestrial debris. Each group was then divided into individual particle types within these broad environments. Marine palynomorphs were subdivided into three dinocyst morphotypes; chorate, proxi-chorate and proximate, foraminiferal test linings, acritarchs, prasinophytes and simple sacs. Terrestrial particles were divided into palynomorphs of pollen and spores and structured debris into phytoclasts and cuticle. Pollen were divided into non-saccate pollen, dominated by simple inaperturate forms, saccate pollen as bisaccate forms, and *Classopollis,* which was the most commonly recognizable pollen species. Spores were not further divided due to their low abundance throughout. Phytoclast particles were a variety of different shapes, sizes and colours, and were therefore categorized by colour into opaque/dark

types and brown/stripy/light types, and by shape into lath and equidimensional forms. There was no definite division between equidimensional and lath shapes since there was generally a continuum, though laths were defined as length 2x width. The same operator undertook counts throughout and the decisions made were constant, therefore this should not cause any problems. An unknown category was also included for structured particles that were too degraded to be assigned to a specific category, but which were clearly not amorphous.

This classification scheme was devised with palaeoenvironmental interpretation as the goal of the palynological investigation of the KCF, and particles can provide specific environmental information. The origin of these particles and their interpretation are presented in the following section.

MARINE PALYNOMORPHS (TMP)

Total Dinocysts (TD) :- Chorate cysts (C)
Proxi-chorate cysts (PxC)
Proximate (P)

Foraminiferal test linings (FTL)
Acritarchs (Acrit)
Prasinophytes (Pras)
Simple Sacs (SS)

TERRESTRIAL PALYNOMORPHS (TTP)

Total Pollen (TP) :- Non-saccate pollen (dominated by inaperturate pollen) (Opol)
Saccate pollen = Bisaccate (B)
Total *Classopollis* (TC) :- Fresh *Classopollis* (FC)
Degraded *Classopollis* (DC)

Spores (Spor)

STRUCTURED TERRESTRIAL DEBRIS (TSD)

Total Phytoclast Laths (length 2x width) (TPL) :- Opaque/dark (BDL)
Brown/stripy/light (BSLL)

Total Equidimensional Phytoclast (length < 2x width) (TEP):-Opaque/dark (BDEq)
Brown/stripy/light (BSLEq)

Unknown (Ukn) - unidentifiable / degraded structured particles

Table 5.2

Palynofacies classification scheme used in this study. Particles are divided into three main groups based on provenance, with further subdivision into individual particle categories by morphology. AOM is not included in the classification as only structured particles were of interest, but unknown, highly degraded structured particles were counted. Letters in brackets are abbreviations used for each category.

5.3.6 PARTICLE ORIGINS AND INTERPRETATIONS

5.3.6.1 Marine Palynomorphs (TMP)

1) Dinocysts

Only about 10% of all living dinoflagellate species are known to form cysts (Evitt, 1985), and less than 70% of these may produce cysts that are preserved as fossils (Dale, 1976). The uncertain correlation between the thecate and cyst stages of modern dinoflagellates further complicates the picture; only a third of modern cyst types have been correlated to their motile stages (Evitt, 1985). Subsequently understanding fossil cysts is difficult and only a small percentage of the ancient dinoflagellate population will be represented. However, some environmental information can be gain from fossil dinocysts assemblages.

"Dinoflagellates are thought of essentially as exploiters of calm, stratified conditions" and are adapted to environments with strong vertical gradients (Taylor, 1987). However, the production of cysts and their diversity are greatest in unstable seasonal environments, especially continental shelves (Dodge and Harland, 1991). Though the fundamental reason for cyst production is a sexual phase in the life cycle, cysting is often environmentally controlled (Evitt, 1985). Thus, increases in dinocysts within the KCF fossil record may either be primarily related to an actual increase in the total dinoflagellate population or to the existing population responding to undesirable environmental conditions by cysting. However, increased preservation of cysts from the existing dinoflagellate population by anoxic conditions either in the water column or the sediment, is another possibility for an increase in fossilized dinocysts.

The dinocyst morphotypes are believed to reflect hydrodynamic behaviour. Proximate and chorate cysts are defined by process length as a percentage of the shortest diameter of the central body (<10% and <30% respectively), with intermediate types classified as proxi-chorate (Figure 5.2 F and I) (Sarjeant, 1982). High proportions of thick-walled cysts (proximate) are considered indicative of unstable, nearshore environments (Figure 5.2 A to E), while an abundance of thin-walled delicate cysts with elaborate processes (chorate) are believed to characterize offshore, open marine environments (Figure 5.2 G and J) (Sarjeant *et al.*, 1987; Tyson, 1985, 1989). Tyson (1995) notes that there is little doubt that at the very least differential sorting of morphotypes occurs, but whether this is purely a passive hydrodynamic process, or a reflection of functional morphology on the part of the cyst forming dinoflagellate is unknown.

ii) Acritarchs

The term 'acritarch' was introduced by Evitt (1963b) (meaning 'of uncertain origin') as an informal holding category for all non-sporomorph and non-dinoflagellate palynomorphs (Figure 5.2 L). Based on their occurrence, it is universally accepted that they are marine phytoplankton

(Tappan, 1980). Most studies have demonstrated that the relative abundance of acritarchs are characteristic of shallow water marginal marine conditions (Erkmen and Sarjeant, 1980; Downie, 1984). The relative distribution of dinocysts and acritarchs has therefore been used in an attempt to delineate brackish-saline influences (Hancock and Fisher, 1981). For nearshore Mesozoic acritarchs, relative abundance is seen to decline rapidly once dinocysts are recorded (Dimeter and Smelror, 1990).

Though considered as a separate particle category, simple sacs are also believed to be marine palynomorphs of uncertain origin. Within the studied KCF intervals, simple sacs are commonly present, though generally in low abundance, but their use for environmental interpretation is somewhat limited. They can only be taken to indicate increased or decreased cysting of some unknown species of plankton, possibly in response to less or more favourable environmental conditions.

iii) Prasinophytes

The abundance of prasinophyte algae has been shown to be strongly correlated with the occurrence of marine organic-rich, finely laminated sediments deposited under dysoxic to anoxic conditions (Tyson, 1995). However, horizons with high prasinophyte abundance can be very thin and very localized within black shale formations (Leckie *et al.*, 1990; Piasecki *et al*, 1990). Prasinophytes have been referred to as disaster species which are most abundant in the absence of other phytoplankton (Tappan, 1980), and blooms occur preferentially in cool marine water with significantly lowered salinity (Prauss and Reigel, 1989). In general, prasinophyte abundance in many organic-rich shales is at least partly a relative effect of reduced *in situ* dinocyst or acritarch production in permanently stratified basins (Tyson, 1984; Prauss and Reigel, 1989). The ratio of prasinophytes to dinocysts or acritarchs has therefore been used as an index of hydrographic stability.

Within the studied KCF intervals, prasinophyte abundances are found to be low and occurrences rare, even in the organic-rich lithologies. The abundant coccoliths within all the lithologies studied may explain this lack of prasinophytes, as the surface waters would probably have been too saline for the prasinophytes. A modern example of this effect has been noted in the Black Sea, the type euxinic basin, which would be assumed to contain a significant abundance of prasinophytes solely on the basis of the organic-richness of the sediment. This is certainly the case in Unit 2, a laminated, organic-rich sapropel which was deposited under low salinity waters ($<11‰$), but in Unit 1, a coccolith carbonate-rich laminated sequence deposited under increasingly saline conditions, prasinophytes are rare (Wall and Dale, 1974; Pilskaln and Pike, in press 2000). Thus, it is suggested that the KCF surface waters were too saline, as indicated by

the presence of abundant coccoliths, for the prasinophytes despite the anoxic bottom waters implied by the deposition of the organic-rich KCF lithologies.

iv) Foraminiferal Test Linings

The tectin linings of foraminifera are often conspicuous elements of marine palynomorph assemblages (Tyson, 1995) and are as least as resistant as sporopollenin palynomorphs (Traverse, 1988) (Figure 5.2 H and K). Similar to dinoflagellates, not all foraminifera produce linings. However, fossilizable linings appear to be produced mainly by benthic foraminifera (Tyson, 1995). The presence of foraminiferal test linings thus appears to be a reliable indicator of marine conditions (Stancliffe, 1989). The abundance of foraminifera generally increases with TOC and is fairly independent of oxygen concentrations up until the point that true anoxia is established (Alve, 1991). At the suboxic to anoxic transition the abundance of foraminiferal linings may therefore go from very high to zero (provided there is no redeposition). High populations under suboxic conditions appear to result from the lack of macrobenthos for which such conditions would be anaerobic, i.e. high abundances are attributed to decreased benthic grazing and abundant food supply (Douglas, 1981). The consistent presence of foraminiferal linings with AOM dominated palynological assemblages has been found to be common in ancient marine sediments which are thought to represent dysoxic-anoxic shelf to suboxic-anoxic basin environments (Batten, 1982; Al-Ameri *et al.*, 1999).

A simple descriptive classification scheme for foraminiferal linings was proposed by Stancliffe (1989) based on linings of Oxfordian age, where biserial, planispiral and trochospiral forms were the most commonly recorded. Today small benthic foraminifera living beneath high productivity waters mainly belong to the rotaliine superfamily Buliminacea, which have high trochospiral to biserial tests. These species have been termed 'quasi-anaerobic' as they can tolerate oxygen concentrations as low as 0.1 ml/L^{-1} (Phleger and Soutar, 1973; Brasier, 1995). Foraminifera during KCF times were also benthic and have been found to be predominantly trochospiral in form, suggesting an adaptation to low oxygen bottom water conditions (C.D. Jenkyns, pers.comm. 1999).

FIGURE CAPTION

Figure 5.2 :- Dinocyst, acritarch and foraminiferal test lining (FTL) transmitted light photographs. A) *Trichodinium* sp. Eisenack and Cookson, 1960; B) and D) *Cribroperidinium* sp. Downie, 1957; C) *Geiselodinium* sp.? Drugg 1978; E) *Glossodinium dimorpum* Ioannides, Stavrinos and Downie, 1976; F) *Cyclonephelium* sp.? Deflandre and Cookson, 1955; G) *Systematophora areolata*, Klement, 1960; H) and K) Trocospiral, Type one FTL, Stancliffe, 1989; I) *Hystrichodinium* sp. and J) *Systematophora* sp. Ioannides, Stavrinos and Downie, 1976; L) Spheroidal acritarch.

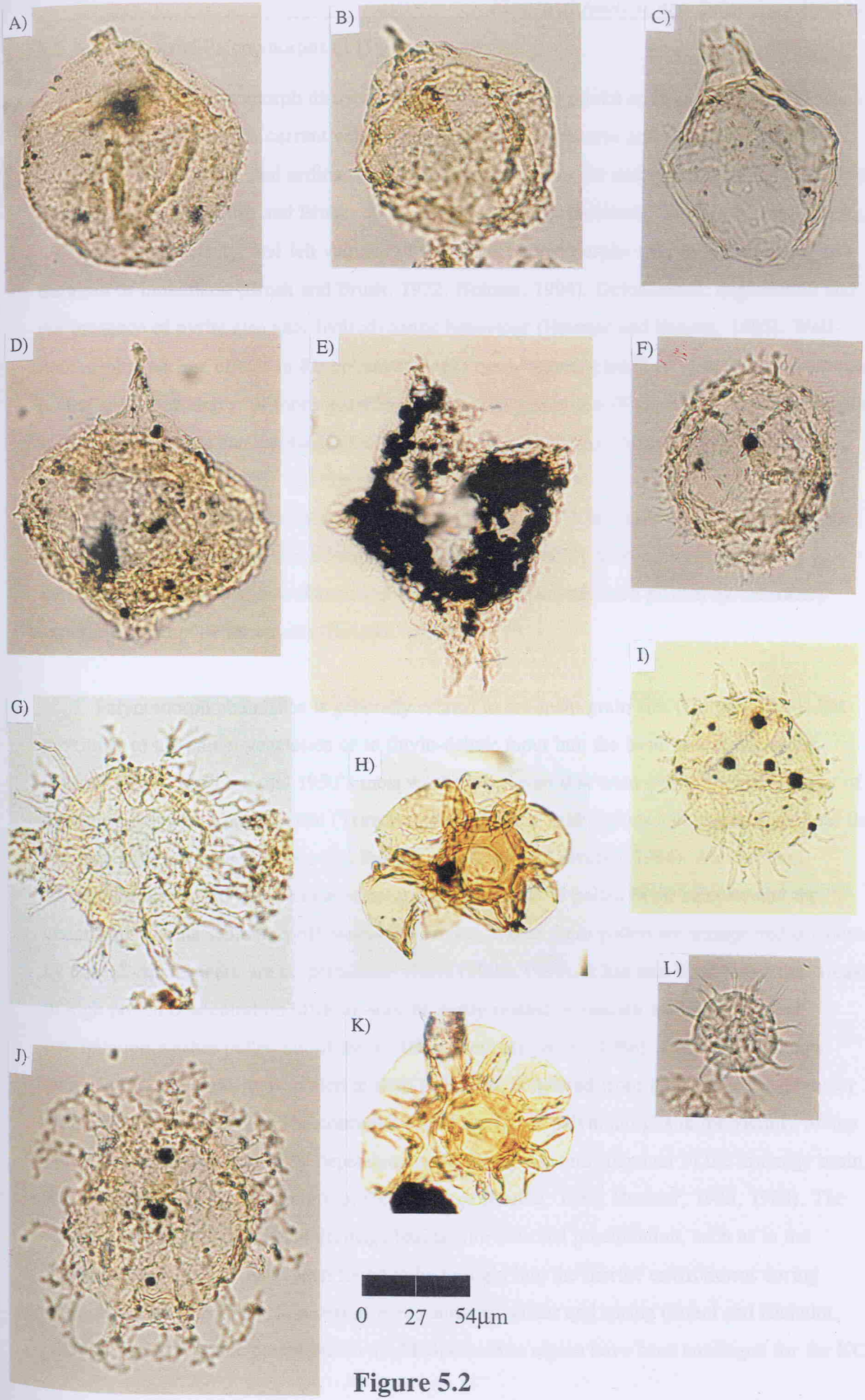

Figure 5.2

5.3.6.2 Terrestrial Palynomorphs (TTP)

Terrestrial palynomorph distribution in the marine and fluvial environments is influenced primarily by water depth, current velocity and turbulence (Traverse and Ginsburg, 1966; Reynolds, *et al.*, 1990), and sedimentation of these palynomorphs usually takes place within finer grained sediments (Brush and Brush, 1972, Traverse, 1994). However, unlike mineral particles, the size, shape, density, and fall velocity of terrestrial palynomorphs also varies according to duration of immersion (Brush and Brush, 1972, Holmes, 1994). Deformation, degradation and the presence of pyrite also alter hydrodynamic behaviour (Heusser and Balsam, 1985). Well-documented sorting effects in Recent assemblages occur between small, thin-walled, non-saccate pollen and other larger, or more dense, non-saccate sporomorphs (Traverse, 1988). Stratification of the water column can emphasize the spatial sorting of grains of different hydrodynamic equivalence (Tyson, 1995), with the vertical flux of small pollen (20μm diameter) restricted by the pycnocline and thus they become relatively concentrated in the sediments further from the littoral source. Larger and more dense pollen sink more quickly thorough the pycnocline and thus settle close to the source (Brush and Brush, 1972). This has been proven by laboratory experiments on pollen transport (Holmes, 1994).

Palynomorph abundance is generally related to sediment grain size (Holmes, 1994) but proximity to the parent vegetation or to fluvio-deltaic input into the basin is also important (Tyson, 1995). Until the mid 1950's most workers believed that wind was the primary agent of terrestrial palynomorph dispersal (Traverse, 1988), and in arid regions and coastal shelf seas this can indeed be the case (Heusser and Balsam, 1977, 1985; Traverse, 1994). An excellent correlation was found between the concentration of bisaccate pollen in air samples and the underlying marine sediments off north-west Africa, where these pollen are transported offshore by dust storms as there are no permanent rivers (Melia,1984). It has also been found that areas of high pollen concentration offshore may be partly related to rainbelt association where precipitation washes pollen out of the air (Hooghiemstra, *et al.*, 1986). However, it is now believed that the majority of pollen in shelf sediments is derived from fluvial sources (Heusser 1983, 1988; Clark, 1986). The concentration of terrestrial palynomorphs in the vicinity of any particular river is also strongly dependent on the flora, size and character of the drainage basin, and the magnitude and variability of the discharge (Mudie, 1982; Heusser, 1983, 1988). The majority of pollen in semi-arid drainage basins with seasonal precipitation, such as in the Mediterranean region, have been found to be brought into the marine environment during irregular large floods which occurred in the autumn, winter and spring (Streel and Richelot, 1994). Similar climatic conditions to the Mediterranean region have been envisaged for the KCF

(Chapter 2) and thus it is highly probable that rainfall was seasonal and the majority of terrestrial palynomorphs were transported into the marine environment during peak discharge events.

The palynological record is generally strongly biased towards wind dispersed pollen because of the much larger numbers in which these grains are produced (a biological adaptation to the low probability of successful pollination, r-strategy) (Traverse, 1994). However, up to 95% of all pollen may be deposited initially within 1 km of the parent plant (Traverse, 1988). Although maximum aeolian transport distances may sometimes be much higher than observed in fluvial transport, it is generally estimated that 90% of pollen grains are finally deposited within 50-100 km of their source. This bias (relative dilution effect) means that samples taken too near to the parent plants yield assemblages unrepresentative of the regional flora, but also with more extensive transport there is an increasing selection for more buoyant (especially saccate) morphotypes that also distorts regional pollen assemblages, termed the 'Neves effect' (Traverse, 1988). However, when miospore assemblages are more dependent on water transportation, Streel and Richelot (1994) proposed pollen is transported in two distinct groups. Firstly, fluvial transportation of miospores primarily derived from nearby coastal and alluvial plains (the 'Hopping effect'), and secondly transportation of miospores mainly derived from 'remote' upland areas (the 'Muir' effect). For example, Chaloner and Muir (1968) recognized that the sediments of wet deltaic environments would tend to have relatively autochthonous and spore-dominated assemblages. However, marine shales are undiluted by *in situ* spore production and therefore have assemblages with a higher percentage of allochthonous (saccate) pollen derived from the floras of more 'upland' or drier (interfluve) habitats. It has also been noted that seasonal changes in the concentration of pollen in particulate matter in coastal waters does not seem to coincide with seasonal changes in pollen production and emission onshore (Heusser, 1988). In general, the composition of marine pollen assemblages on the continental margin reflect the regional coastal vegetation (Heusser, 1988). Thus, the pollen within this study is likely to reflect the regional flora, rather than local assemblages, and be biased towards more buoyant morphotypes.

The type of pollen available for transportation to the marine environment also has a significant effect on the resultant depositional pattern. Within the KCF the dominant pollen species (inaperturate, *Classopollis* and bisaccate) are all believed to be coniferalean. Modern conifer species are known to produce larger numbers of saccate pollen, and both aeolian and fluvial transportation has been shown to be involved in delivering such pollen to the marine environment, with these types of grains characterized by relatively efficient dispersal in both media (Heusser, 1988). The majority of the KCF pollen is non-saccate but these small spherical forms also travel well and do not sink quickly. The environmental aspects of the different pollen types found in this study of the KCF are described in the following sections.

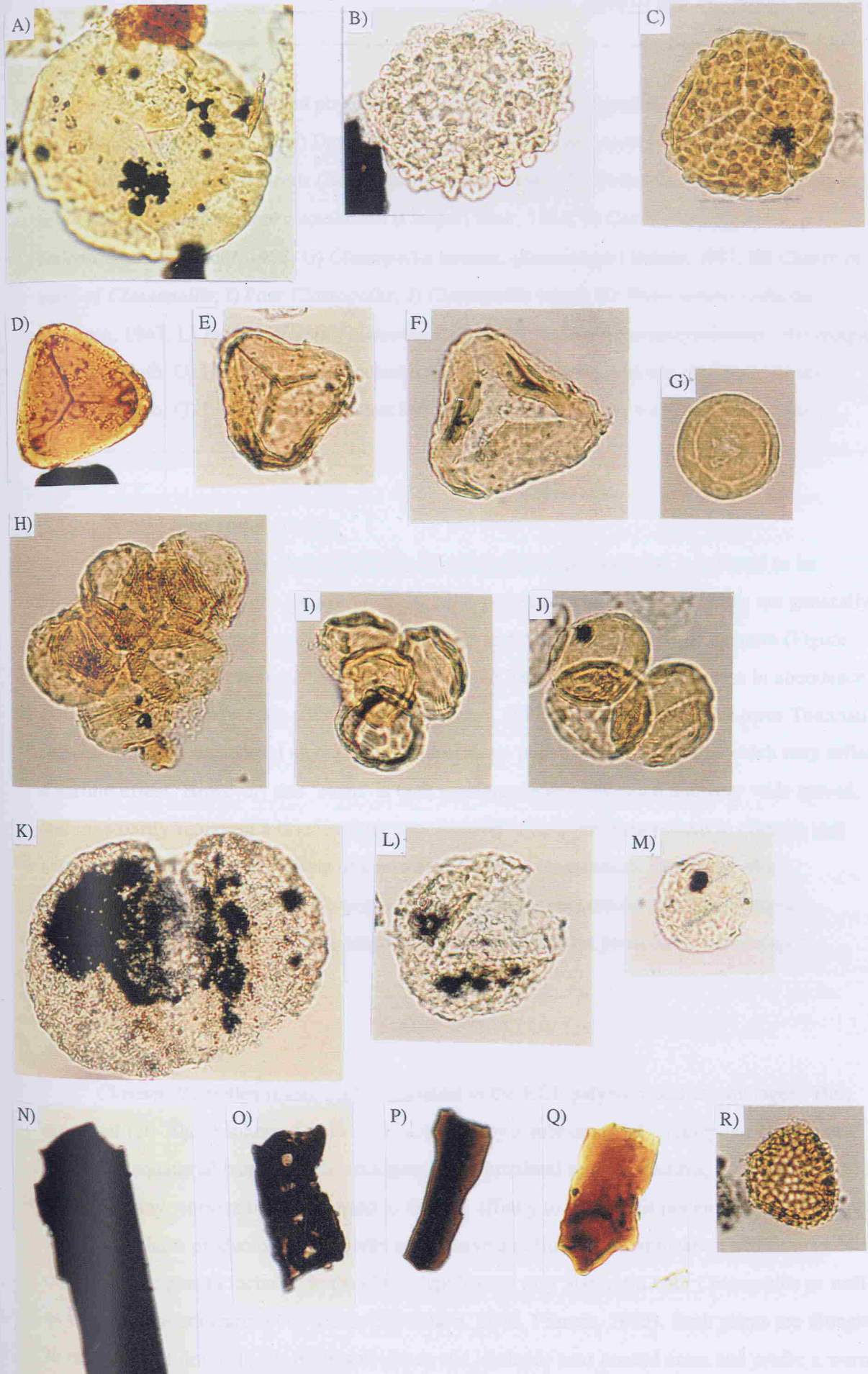

Figure 5.3

FIGURE CAPTION

Figure 5.3 :- Spores, pollen and phytoclast transmitted light photographs.
A) *Callialasporites* sp. (Balme) Dev, 1961; B) *Cerebropollenites macroverrucosus*, Nilsson, 1958; C) *Uvaesporites argentaeformis* (Bolchovitina) Schulz, 1967; D) *Deltoidspora australis* (Couper) Muir, 1964; E) *Deltoidospora equiexinus* (Couper) Muir, 1964; F) *Concavissimisporites* sp. Delcourt and Sprumont, 1955; G) *Classopollis torosus*, (Reissinager) Balme, 1957; H) Cluster or mass of *Classopollis*; I) Four *Classopollis*; J) *Classopollis* tetrad; K) *Podocarpites reductus*, Cookson, 1947; L) *Perinopollenites elatoides*, Couper, 1958; M) *Inaperturopollenites*; N) Opaque phytoclats lath; O) Black/brown phytoclast lath showing bordered pore pits; P) Brown/stripy phytoclast lath; Q) Light/stripy phytoclast lath; R) *Lycopodium* spore, used for exotic spike.

i) Thin-Walled Inaperturate Pollen

This pollen is highly abundant within the studied KCF sections and is believed to be produced by similar conifer species as *Classopollis* pollen (discussed below). They are generally 10-30μm in diameter and have been seen in tetrads and clumps over up to 10 or more (Figure 5.3 L and M). Similar thin-walled inaperturate pollen have been found to increase in abundance distally in European Jurassic sediments (Frederiksen, 1980). In some European Lower Toarcian sediment there is an unusual abundance of inaperturate pollen (Dybkaer, 1991) which may reflect a sorting effect. However, this 'event' is both stratigraphically restricted and very wide spread, and may partly represent a brief evolutionary development in the flora related to climatic and other palaeoenvironmental effects of the early Toarcian transgression. Due to the close resemblance of these pollen to *Classopollis* pollen, similar adaptations and environmental characteristic are envisage for inaperturate pollen, as are similar production and transport mechanisms.

ii) *Classopollis* Pollen

Classopollis pollen is also highly abundant in the KCF palynological assemblages. They are small (20-30μm) spherical pollen characterized by a subequatorial circumpolar canal and thickened equatorial band, a distal crytopore and a proximal scar (Srivastava, 1976) (Figure 5.3 G to J). Many workers have attempted to find the affinity to which this pollen is related and most agree that plants producing *Classopollis* pollen have an affinity with araucarian and/or gnetalean conifers. The genera included in the Cheirolepidiaceae may also yield both *Classopollis* as well as inaperturate araucariaceous pollen (Srivastava, 1976, Francis, 1983). Such plants are thought to occupy well-drained soils of upland slopes and lowlands near coastal areas and prefer a warm climate (Pocock and Jansonius, 1961). Vakhrameev (1964) believed that *Classopollis* bearing

plants were drought resistant, low growing thermophilous trees and shrubs resembling modern juniper bushes and that these plants were the dominant vegetation in the Late Jurassic during which time they formed unmixed thickets. The wide occurrence of *Classopollis* during the Mesozoic may indicate that the plants producing it had a wide range of tolerance from a dry to a wet climate in coastal and upland areas. However, Krassilov (1981) points out though plants producing *Classopollis* pollen are conventionally placed among the conifers, they are distinct from normal conifers not only in their pollen grains, but also their ovuliferous organs which exhibit some angiospermous characteristics.

Classopollis pollen (about 30μm), and small ($< 50\mu$m) thin-walled inaperturate pollen were found to increase with decreasing sediment grain size in fluvio-deltaic Wealden (140.7-124.5 Ma) sediments (Hughes and Moody-Stuart, 1967). Mesozoic sediments of the central Atlantic Ocean usually exhibit an abundance of *Classopollis* pollen (Tyson, 1984). The relative abundance of *Classopollis* in Callovian (161.3-157.1 Ma) DSDP palynomorph assemblages are largely independent of facies and seem to indicate long-term floral and climatic trends (Tyson, 1984). The distribution of cheirolepidacean conifers and thus their pollen, *Classopollis*, is clearly influenced by climatic factors. *Classopollis,* as relative abundance values of the sporomorph population, apparently indicate temperate conditions (1-10%), warm subtropical conditions (20-50%) and semi-arid to arid climatic conditions (60-90%) (Vakhrameev, 1981). This pollen species is generally more abundant during warm geological intervals, such as the early Toarcian (187-183 Ma) and Late Jurassic (Srivastava, 1976). Tetrads and pollen masses are common in ancient prodelta facies, but those of small buoyant pollen, such as *Classopollis*, may also have occurred in low energy shelf or oceanic sediments which were deposited many kilometres from land (Tyson, 1984) (Figure 5.3 H to J). Modern examples of such pollen composites are found to be an abundant group in aerosol samples taken off the northwest African coast (Melia, 1984). Thus, the abundance of such pollen as *Classopollis* compared to other pollen types in marine sediments is a function of both the abundant production of this pollen and differential transportation effects.

iii) Bisaccate Pollen

The general abundance and widespread distribution of modern bisaccate pine pollen reflects the fact that they are produced in vast numbers and have a comparatively resistant, sporopollenin wall (Havinga, 1964) (Figure 5.3 K). However, high relative abundances of bisaccate grains also relates to their buoyancy, and experiments have shown that 90% of bisaccates remain afloat for several weeks when both sacs are full of air, while those that sink have one or both sacs full of water (Traverse, 1988). Though bisaccate pollen is generally buoyant, once they become waterlogged they settle rapidly (Brush and Brush, 1972; Holmes,

1994). Two different scenarios have been proposed for bisaccate entry into the fluvial and/or marine environment:-

1) Bisaccates are carried in the higher atmosphere by winds but are brought back to the Earth's surface by rain. They are therefore sufficiently wet to enable quick incorporation into the suspended load of the stream, where they settle.

2) Due to local topography and wind conditions bisaccates are deposited on the stream surface without being rained out and therefore remain afloat for a considerable time before being incorporated into the water column.

Within marine sediment, major bisaccate concentrations have been found to be confined to localized deeper water areas with more fine-grained, silty sediment, suggesting that this 'facies control' largely obscures any direct relationship with the parent flora (Traverse and Ginsburgh, 1966). Many Recent continental margin sediments show a consistent relative offshore increase in bisaccate pollen compared to other sporomorphs (Heusser and Balsam, 1977; Mudie, 1982). However, these far transported pollen are present in only small absolute amounts (Huesser, 1983, 1988). Within the KCF palynomorph assemblages, bisaccate pollen has the lowest abundance of all the pollen types, which is most probably due to the dilutionary effect of the highly abundant small spherical pollen, and differential grain sorting effects. Width and length measurements were taken of the KCF bisaccate pollen during counts to investigate possible proximal/distal trends during the studied intervals (Figure 5.4). Generally more than ten bisaccate grains were counted; however, in some samples bisaccates were rare. For each sample, average width and lengths were determined.

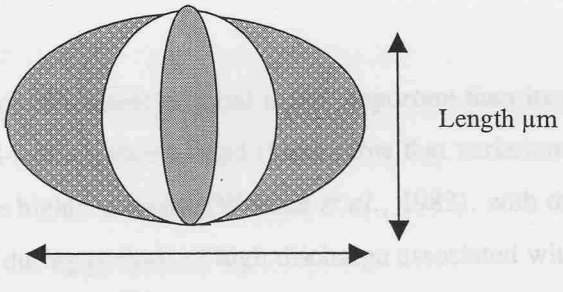

Figure 5.4
Schematic diagram of bisaccate pollen grain showing the width and length dimensions measured in this study.

iv) Spores

Spores generally tend to be abundant only in nearshore settings near the mouths of major rivers (Mudie, 1982) (Figure 5.3 A to F). Such trends are partly a reflection of the preferred humid habitat of most pteridophyte plants, but seem largely due to more limited spore transport. In general, spore abundance within the KCF is low, though a variety of species are present but

were not identified in detail during this study. The abundance of all spores is closely correlated with humid habitats and if facies-independent trends can be identified they are also a potential palaeoclimatic indicator (Groot *et al.*, 1967). Spores have been found to be consistently present as small percentages in marine sediments, while most thin-walled pollen showed highest percentages in fine-grained sediments (Muir, 1964). The effect of grain size on the composition of UK Wealden (140.7-124.5 Ma) sporomorph assemblages found that those $>50\mu m$ showed the highest percentages in fine sands, and those $<30\mu m$ were relatively more abundant in medium silts or finer lithologies (Hughes and Moody-Stuart, 1967; Batten, 1974). Most studies of marine facies show that proximal sediments are comparatively enriched in spores relative to saccate pollen (e.g. Tyson, 1989).

5.3.6.3 Terrestrial Structured Debris (TSD)

Terrestrial structured debris or phytoclasts are also a significant component of the KCF palynology assemblages. The classifications into opaque/dark (Figure 5.3 N and O), and brown/stripy/light laths and equidimensional types (Figure 5.3P and Q) in this study are believed to represent different sources and transportation mechanisms. Within the KCF phytoclast assemblage the most conspicuous lignified structures are fragments of 'xylem elements', comprising tracheids which are easily recognized by their boardered pore 'pits' (Figure 5.3 O). Tracheid cells form 90-95% of the wood tissue in coniferous softwoods (Butterfield and Meylan, 1980). Commonly brown phytoclasts are characterized by a stripy appearance where by darker-parallel bands are seen either side of thinner (and thus lighter) central parts bearing the boardered pits, which is caused by triple junctions in the wood where the walls of adjacent tracheids meet and are thickened.

The transportability of phytoclast material is less important than its availability (Naiman, 1982). Most studies of mid-latitude streams and rivers show that variations in particulate organic matter (POM) transport are highly seasonal (Wallace *et al.*, 1982), with the bulk of terrestrial material being transported during periods of high discharge associated with storms (Hedges *et al.*, 1988). Periods of high river discharge result in erosion, entrainment, and transport of soil organic matter from the adjacent flood plains (Ittekot *et al.*, 1986) and lead to terrestrial carbon being carried further out to sea than is normal, and in greater amounts (Silverberg *et al.*, 1985). The material entrained by the rising water of floods is often degraded and highly refractory. In high-order streams this material has probably been degraded by subaerial exposure adjacent to the channel, while in lower order ('river') channels it may largely reflect recycling of older organic matter. All organic particles $<500\mu m$ in diameter are easily transported, and any organic particles $<50\mu m$ can apparently be taken into suspension in large amounts (Mann, 1972). The size and relative concentrations of the transported particle types and the rate and style

of sedimentation are probably at least equal in significance to density-based hydrodynamic sorting.

The colour of phytoclasts provides significant information on the processes that these particles have undergone between their source and deposition. The preservation of phytoclasts is enhanced by the highly stable, resistant and hydrophobic nature of lignin, which makes up about 25-30wt% of the wood of arborescent plants. Lignin is richer in softwood conifers (gymnosperms) (Correia, 1971; Harmon *et al.*, 1986), and appears to be chemically more resistant to degradation than hardwood (angiosperm) lignin (Cooke and Rayner, 1984). Oxidation and carbonization degrade phytoclast material and result in the gradational change of phytoclast colour from light brown to dark and opaque particles

Oxidative degradation is highest where wood is at least periodically exposed to the atmosphere in alternating wet-dry cycles (Rayner and Boddy, 1988). Thus strong seasonality with pronounced dry periods and major water table fluctuations result in the greatest degradation rates (Campbell, 1991). When woody material is exposed to atmospheric oxygen, desiccation, oxidation and fungal mouldering take place resulting in dark to opaque granular phytoclast which are irregularly shaped, of degraded appearance, and do not show good structural preservation. In arid or strongly seasonal onshore climates a greater production of such opaque material occurs (Reyre, 1973). Thus, the semi-arid, seasonal climate proposed for the Kimmeridgian of Northwest Europe (Moore *et al.*, 1992) would lead to the expectation of substantial abundance of opaque and degraded phytoclasts.

The formation of such material via subaqueous oxidation, and not atmospheric oxidation, must be far less effective and slower than atmospheric attack (as water contains ≥26 times less oxygen than air), and therefore require very much longer exposure (Tyson, 1995). However, some marine aquatic fungi have been found tolerant to low oxygen, although are still oxygen-limited. Wooden blocks placed in the core of the oxygen minimum zone off California (dissolved oxygen 0.3 ml l^{-1}) were uncolonized after 13 months, but were rapidly colonized in areas where oxygen values were ≥1.3 ml l^{-1} (Kohlmeyer and Kohlmeyer, 1979). However, bacterial degradation of wood, which is generally unimportant (Rayner and Boddy, 1988), may be of greater significance under water-saturated, oxygen-stressed conditions (Eaton and Hale, 1993). Therefore, degradation of phytoclasts within the KCF sediment is also likely to have occurred, and together with aerial oxidation would be expected to result in opaque phytoclasts dominating the structured debris which was found to be the case in all of the studied intervals (Chapters 6 and 7).

The process of natural pyrolysis of terrestrial macrophyte material, the action of high temperatures under conditions of oxygen starvation, also results in dark and opaque phytoclasts, termed charcoal (Cope, 1980, 1981; Chaloner, 1989). Conifer softwoods are thought to produce about four times as much charcoal as hardwoods, apparently related to their higher lignin content (Goldberg, 1985). They are also known to burn much more easily than hardwoods, at least in the Northern Hemisphere (Patterson *et al.*, 1987). Today the main global sources of sediment charcoal are wild fires in the forests and grasslands of the middle latitudes (Chaloner, 1989). Such fires tend to alter the properties of the soil surface, and, along with the destruction of plant cover, may promote greater runoff (and associated charcoal transport) during subsequent periods of rainfall (Graf, 1988). During fires, charcoal fragments are lofted up to 5 km into the atmosphere by thermal plumes (Clark, 1988). Some 90% of these particles are $<1\mu$m in diameter, too small to contain cellular structure. Within this study such fragments would have been lost during sieving. However, larger (10-50μm diameter) opaque (internite) and dark phytoclast were retained in the palynological residues.

Although wind can easily transport charcoal particles up to 150μm or more in diameter, the smaller particle sizes are always dominant, and the majority of 'pollen slide charcoal' is usually in the range 5-20μm (Clark, 1988). However, pollen slide charcoal is a size that is difficult to lift, but once entrained stays in suspension. Source areas for this size of charcoal is sub-continental to global and are biased toward non-local charcoal. As such, it can be used to interpret the importance of charcoal on a broad, spatial and temporal scale. The opposite is true for larger (50-10,000μm diameter) particles, which show local catchment fire regimes.

After a fire, larger charcoal particles are moved more readily than pollen-slide sized charcoal, due to cohesive forces that build up between smaller particles. The porous structure of charcoal results in a low effective density, making the particles buoyant and capable of flotation in water (Patterson *et al.*, 1987). Small charcoal particles however, become water logged 'quickly' and therefore sink first (Davies, 1967). Analysis of charcoal distribution in modern marine sediments suggests that most 'never travels beyond coastal sediments, which probably are the primary reservoir for charcoal' (Griffin and Goldberg, 1975). Most of the charcoal of distal areas is probably aeolian in origin, but are usually no more than several microns in diameter (Smith *et al.*, 1973). It is likely that such aeolian charcoal was lost during processing of the KCF lithology, but it is possible that some of the larger opaque pytoclasts may be charcoal, though this has not be proven.

Tyson (1989) documented a general distal increase in the ratio of opaque 'black wood' material to well preserved 'brown wood' material in Upper Jurassic (157.1-145.6 Ma) shale

facies from the UK. The size of opaque particles generally diminishes offshore (Gorin and Monteil, 1990; Barnard *et al.*, 1981). Such size and ratio trends reflect fractionation during transport, resulting in a relative offshore (distal) increase in more fine-grained and refractory opaque material (but an inevitable absolute decrease as phytoclast TOC declines offshore). A number of studies report higher relative opaque-inertinite phytoclast percentages in ancient nearshore marine facies (Barnard and Cooper, 1981; Fisher and Miles, 1983; Williams, 1992).

Although charcoal is biologically refractory, it is brittle, extremely sensitive to mechanical stress and disintegrates along shrinkage cracks to produce fine, angular, splintery fragments. Elongate, angular, prismatic particles with length:width ratios >3.0 are most typical (Cope, 1980; Goldberg, 1985). Trends have been observed between lath and equant phytoclast shapes. Parry *et al.* (1981) found that opaque material exhibited a tendency to decrease in size and change from equant to lath-shaped with increasing distance from the Brent delta front (Middle Jurassic North Sea; 178-161.3 Ma). Whitaker (1984) extended such observations into an energy-dependent model to explain the morphological variability of opaque phytoclasts in marginal marine and shallow water sands (Late Jurassic North Sea; 157-145.6 Ma). In transgressive, high-energy settings associated with reworking of coastal sediments, large equidimensional opaque particles were absent (due to diminished supply or having been fragmented during reworking?), with the lath:equidimensional ratio increasing offshore. Gorin and Steffen (1991) also observe that the proportion of elongate (blade-shaped) opaque particles increases in the more distal facies of Early Cretaceous Berriasian (145.6-140.7 Ma) carbonate sediments in the Voncontian Basin (South-East France). However, they also note that the sorting and rounding of the equidimensional opaque particles increases offshore as their particle size diminishes.

Rounding of equidimensional particles may occur in either high-energy proximal facies (intensity of reworking) or in distal facies (duration of reworking during transport?) (Tyson, 1995). Several workers found that reworked and recycled opaque phytoclasts may be more equidimensional and more rounded (Creaney, 1980; Habib, 1983; Piasecki and Stemmerik, 1991). However, Van Waveren (1989a) observed in modern Indonesian sediments that small equidimensional opaque particles are most abundant in deltaic facies, while elongate particles become dominant further offshore. Lath:equant sorting trends are both size-and volume dependent, as many lath-shaped fragments are thin and thus lighter particles derived from tracheoid walls rather than whole tracheids. Assemblages dominated by rounded woody debris or opaque material are generally thought to represent extensive degradation due to wet and dry cycles (Campbell, 1991; Gastaldo *et al.*, 1989). Thus, phytoclast laths within the KCF palynomorph assemblages are taken to imply a further offshore, distal depositional environment, while equant forms represent more proximal environments.

5.3.7 SUMMARY

A substantial amount of palaeoenvironmental information can be gained from palynological particle abundances, though it is clear that particle presence may result from a variety of processes and not just from primary production. The assignment of ancient palynomorphs and debris to specific species with detailed environmental and climatic inferences is highly problematic and it is more realistic that several sources and processes result in the fossil assemblages. Therefore, palaeoenvironmental interpretation generally provides qualitative results rather than quantitative, with several hypothesis explaining individual particle presence. The KCF palynological data are no exception and some broad characteristics of these data together with expectations have already been mentioned in this chapter. Environmental hypothesis for each particle used in the study are summarized in Tables 5.3 and 5.4, which are partly based on similar tables by Waterhouse (1995) and provide the basis for environmental reconstructions in the next two chapters.

Table 5.3. *Origin of the palynofacies particles and their interpretation for absolute and relative abundances, used for this study. Only those parameters which were used to make interpretations are included here for clarity.*

PARTICLE	BIOLOGICAL AFFINITIES	PARAMETER/OBSERVATION	INTERPRETATION
All particles		High absolute abundance.	Good preservation of organic matter due to low energy, low oxygen conditions. Low dilution by detrital minerals and biogenic carbonate. Or high marine productivity and/or terrestrial influx to the marine environment.
TOC	All organic content of rock, including AOM.	High relative abundance.	Low marine energy, low oxygen, high productivity of organic walled plankton, low productivity of inorganic walled plankton, low sedimentation accumulation rate, high input of terrestrial organic matter, fine grained sediment texture (Tyson, 1987; Tribovillard *et al* ., 1994).
CaCO3	Calcareous microfloral and faunal exoskeletons, dominated by coccolithophores, direct precipitation from seawater.	High relative abundnces.	Breakdown of stratification (Scotchman, 1991), increased production of carbonate walled plankton (Herbin *et al* ., 1991; Tribovillard *et al* ., 1994), little dilution by organic-walled plankton or terrestrial input.
Clay, quartz etc.	Terrestrially derived mineral matter.	High relative abundance.	High terrestrial output (with high organic terrestrial particles), low plankton productiviy.
Total Dinocysts	Resistant cyst walls of unicellular dinoflagellate algae.	Increased abundance of dinoflagellates.	Increased distance from shore, increased productivity due to increased light or nutrient supply affected by vertical mixing or horizontal supply (Pedersen & Calvert, 1990), decrease hydrographic stability (Tyson, 1987). Increase cysting of normal dinoflagellate populations due to unstable seasonal environments (Dodge and Harland, 1991).
Chorate Dinocysts	Dinoflagellate algae with cyst process length <30% of diameter	Increase in abundance.	Shift to more open marine conditions (Sarjeant *et al* ., 1987; Tyson, 1985, 1989)
Proximate Dinocysts	Dinoflagellate algae with cyst process length <10% of diameter	Increase in abundance.	Shift to more unstable, near shore environment (Sarjeant *et al* ., 1987; Tyson, 1985, 1989).
Foraminiferal Test Linings.	Tectin' linings of benthic foraminifera.	Increased absolute abundance.	Suboxic conditions (0.1ml/l-1) (Phleger and Soutar, 1973; Brasier, 1995), Lack of macrobenthos (Douglas, 1981), AOM dominated assemblages.
Total Terrestrial Palynomorphs	Pollen and Spores.	Increase abundance of terrestrial palynomorphs.	Represents regional, coastal flora (Heusser, 1988; Traverse, 1988). Increased flux to the marine environment via:- 1) Fluvial source - increased precipitation / storms leading to increased runoff 2) Aeolian source - increased off shore wind, possibly increased aridity. Increased precipitation and thus pollen rain out.
Inaperturate and *Classopollis* Pollen	Coniferalean pollen, 20-30 microns diameter, spherical pollen.	Increased abundance.	Biased wind dispersal (Traverse, 1988). Distal, low energy environment (Frederiksen, 1980; Tyson, 1984). Warm climate of transgressive seas (Pocock & Jansonius, 1961). Dry to wet climate in coastal and upland areas (Vakhrameev, 1984).
Fresh Classopollis	No signs of degradation.	High absolute abundance	Short transit period, increased energy of transporting medium. Close to pollen source, dominate lowland near coastal areas (Srivastava, 1976).
Degraded Classopollis	Highly degraded forms	High absolute abundance	Longer time in transit, decreased energy of transporting medium. Distant pollen source, well drained upland slope source (Srivastava, 1976).

Table 5.3 *Continued, Origin and interpretation of palynology particles.*

PARTICLE	BIOLOGICAL AFFINITIES	PARAMETER/OBSERVATION	INTERPRETATION
Bisaccate Pollen	Saccate coniferalean pollen.	High absolute abunbdance.	Distal, deep water environment, no direct realtionship to parent flora (Traverse & Ginsburgh, 1966). Enhanced aeolian transport, rained out and settle out quickly (Melia, 1984). Fluvial transportation to distal environment due to buoyancy (Traverse, 1988).
Spores	Spores of pteridophyte plants.	High absolute abundance.	Humid habitats, proximal sediments, nearshore settings close to river mouths (Groot *et al* ., 1967)
Terrestrial Structured Debris	Broken down parts of terrestrial plants.	High absolute abundance.	Proximity to terrestrial source of particles, high source avaliability (Naiman, 1982). Increased terrestrial output and run-off, wetter climate, storm frequency increased (Hedges *et al* ., 1988).
Brown/stripy and light wood	Unoxidized or little oxidized wood.	High absolute abundance.	Indicator of proximity, or increased terrestrial output to distal area.
Black equdimensional wood	Oxidation of brown wood or or carbonization to charcoal.	High absolute abundance.	Long time intransit, or in storage, a distal source. Exposed to alternating wet and dry cycles, strongly seasonal onshore climate (Reyre, 1973).
Black / Dark wood laths	Highly oxidized brown wood, very resistant	High absolute abundance.	Decreased energy of transporting medium (rivers or marine currents) (Cope, 1981). More distal environment. Good preservation of organic matter due to low energy, low oxygen conditions. Low dilution by mineral matter (detrital or biogenic).
	or carbonization to charcoal from forest fires.	High absolute abudance.	Increased wind-blown charcoal (Cope, 1981) - hotter, arid climate. More distal environment of deposition (Parry *et al* ., 1981)
Degraded palynomorphs	Unidentifiable as distinct types.	High abundance.	Variable oxygen conditions, variable to high energy conditions.

Table 5.4. Interpretation of ratios of palynofacies particles used in this study.

RATIO	LOG RATIO Negative / positive	INTERPRETATION
Marine playnomorphs : terrestrial debris	negative	High terrestrial output/run-off - dilution of marine particles by terrestrial, low marine productivity.
Chorate : proximate Dinocysts	positive	Increasingly stable, more 'open-marine' conditions (Sarjeant *et al* ., 1987)
Terrestrial debris : terrestrial palynomorphs	positive	High energy transport medium (run-off or marine currents). Reduced aeolian pollen input?
Degraded : fresh *Classopollis*	positive	Moderatley low oxygen, moderatley low energy ? Increased storage of pollen on land.
Bisaccate : spores	positive	More distal facies / decreased marine current activity (increased offshore wind or decreased run-off) (Traverse, 1988).
Lath : equdimensional wood	positive	Low energy marine currents (and/or run-off). Distal depositional environment (Tyson, 1989).
Black/dark : brown/stripy phytoclasts	positive	Distal environment, long transport distance, high period of terrestrial storage and thus oxidation. And/or increased charcoal input, regional coastal hinterland fire prone, more arid climate?.

6.0 WHITESTONE BAND GEOCHEMISTRY AND PALYNOLOGY RESULTS

In the previous chapters the results of the SEM fabric analysis were discussed (Chapter 4) and an environmental reconstruction made for each major KCF lithological type (Section 4.11). However, it was not possible, purely from the fabric information, to establish the role of terrestrial input into the KCF marine environment, which is suggested to have been a critical factor in these reconstructions. Neither was any idea gained on the phytoplankton structure of the surface waters, except for qualitative changes in the coccolithophore population. In order to understand more fully the interaction between the terrestrial and marine environments, and clarify some ideas from the fabric-based reconstructions, the organic component of the intervals was analyzed using the geochemical and palynological techniques discussed in Chapter 5.

Similar to the fabric analysis, the Whitestone Band (WSB) interval was studied in the most detail (Section 1.4.2) and thus a whole chapter is given over to this interval's geochemical and palynological results. The results of the other three intervals are presented and discussed more briefly in Chapter 7. The TOC, atomic H/C ratios and palynofacies results for the Whitestone Band interval are therefore presented and discussed in the following sections (6.1 to 6.3 respectively). Combination of these results provides evidence for changes in the marine and terrestrial environment over the WSB interval, which can be linked to climatic effects (Section 6.4).

6.1 TOTAL ORGANIC CARBON (TOC)

The TOC % weight over the WSB interval was obtained by flash combustion of powdered whole rock and de-carbonated rock samples using an Elemental Analyzer (Section 5.1, Equation (1)). Together with the acidified sample results, this TOC % can be used to calculate the carbonate content of each sample (Section 5.1.1, Equation (2)). With both TOC and carbonate measured as percentages, 100% - (TOC + carbonate) results in a remainder which was not removed by either combustion or by acidification. This remainder is composed of clays and other clastic minerals, and commonly within the KCF samples, pyrite. Thus these three components provide information not only on the organic matter within the samples, but quantitative figures on the autochthonous carbonate production and allochthonous terrestrial clastic input into the KCF marine environment.

6.1.1. TOC, CARBONATE AND REMAINDER % WEIGHT

The three sample components of TOC, carbonate and the remainder % weight are displayed in Figure 6.1 as vertical profiles over the WSB interval, and summarized in Table 6.1. The TOC profile (Figure 6.1A) clearly shows the three oil shales (1-3) within this interval,

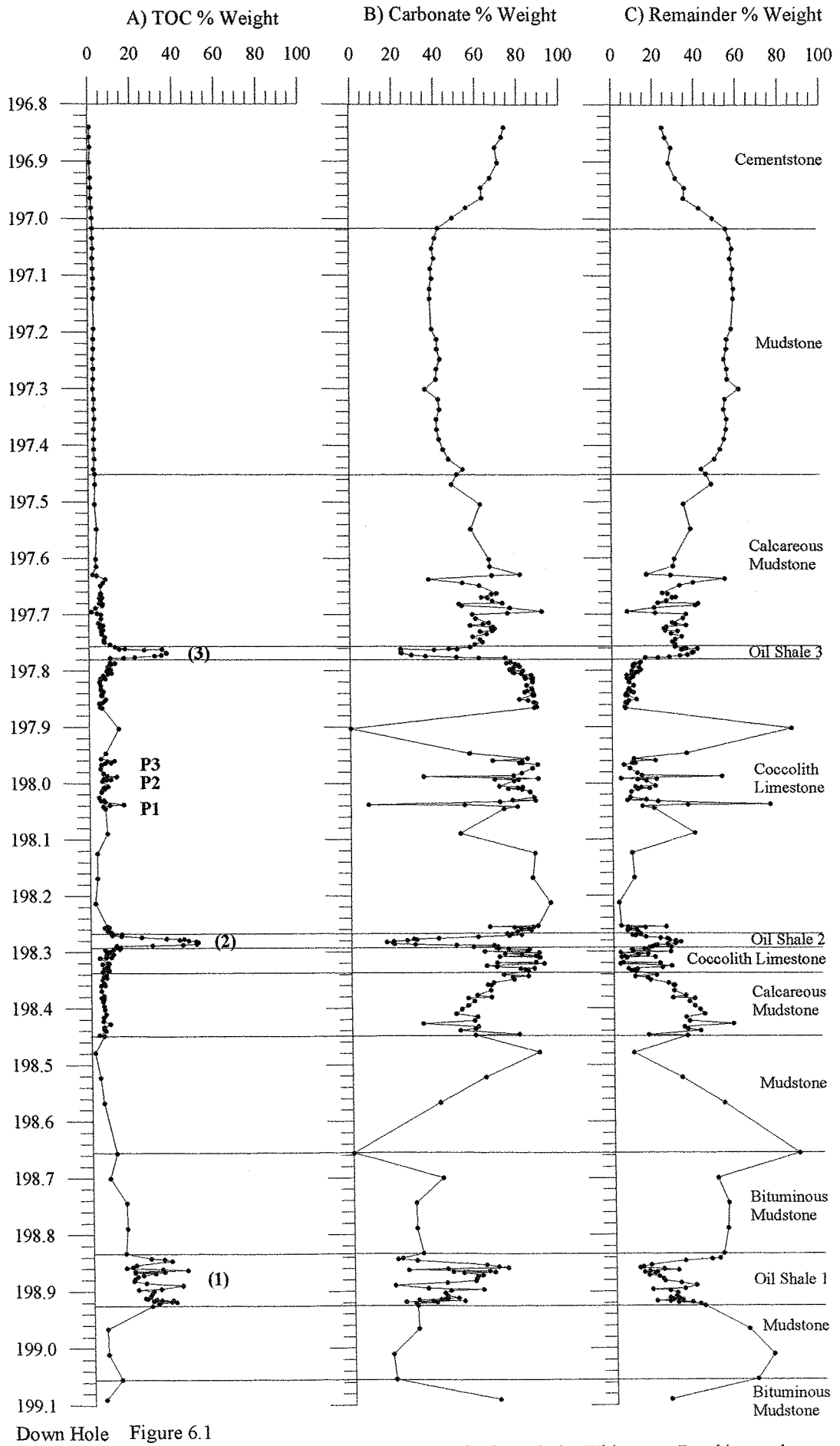

Down Hole Depth (m)

Figure 6.1
TOC, carbonate and remainder as % weight through the Whitestone Band interval.

reaching a maximum of 51% in oil shale 2. All three oil shales are the result of either high primary production or enhanced organic matter preservation or both, but oil shale (1) has a more variable signal than the other two oil shales, composed of organic matter and abundant carbonate. The majority of the interval however, displays far lower values, averaging 3-4% TOC, but three small peaks (P1 to P3) within the coccolith limestone indicate that brief episodes of increased organic matter flux and/or preservation punctuated the predominately coccolithic carbonate sedimentation. Conversely, the carbonate profile (Figure 6.1B) displays high values (average of 62%, Table 6.1). Over the coccolith limestone the profile is broadly convex, reaching a maximum of 95%. However, episodes of low carbonate do interrupt this profile and can be correlated to times of high TOC. The variability in the TOC over oil shale (1) is due to brief episodes of relatively high carbonate, seen as carbonate laminae in the fabric analysis (Figure 3.1). The mudstones are generally characterized by the lowest carbonate values, but there is a clear increase over the cementstone resulting from the presence of diagenetic carbonate in this lithology. Lastly the remainder profile (Figure 6.1C) is almost the opposite of the carbonate profile, which is inherent in the percentage calculation of this component. Thus a concave profile of lower values occurs over the coccolith limestone, while higher values characterize the rest of the interval. Interestingly, there is a positive correlation between remainder and TOC during the oil shales that was not expected if it is assumed that oil shale deposition took place under low sedimentation rates and a semi-arid to arid climate (Section 4.11.1, Figure 4.5A). However, the remainder is composed of clastic material and pyrite formed by the oxidation of organic matter during sulphate reduction; thus this positive correlation between TOC and remainder is supervious. This and the effect of the abundant carbonate on the profiles are discussed in the following section.

Bulk Geochemical Sample Component	Minimum % Weight	Maximum % Weight	Average % Weight
TOC	0.8	51	11.4
Carbonate	8.2	95.1	62
Remainder	2.7	75.7	26.6
$CaCO_3$Free TOC	3.1	69.8	31.5
Estimated TPOM	1.5	91	20.4
Estimated Clastics	0 (-9.7)	70.7	17.7

Table 6.1

Minimum, maximum and average TOC, carbonate and remainder % weights over the WSB interval. Also shown are $CaCO_3$Free TOC percentages, TPOM (total organic matter and pyrite organic matter) and clastic material percentages, which are discussed in the following sections.

6.1.2 CARBONATE DILUTION AND THE EFFECT OF PYRITE FORMATION

Several problems exist with the profiles in Figure 6.1. Firstly the TOC profile is adversely affected by dilution from the coccolith carbonate (Section 4.2.3), and secondly the remainder profile is unreliable for interpreting the terrestrial clastic input into the marine system due to the remainder not only being composed of clastic materials but also pyrite.

6.1.2.1 Carbonate Dilution

Carbonate dilution in modern pelagic sediments by the input of planktonic carbonate (usually in the form of coccoliths) has been found to significantly change TOC, with the greatest difference between TOC and carbonate-free TOC occurring in conjunction with the greatest carbonate (Summerhayes and Marsan, 1983). Thus the high abundance of carbonate within the WSB interval will have had a strong dilutionary effect on TOC, especially in the calcareous mudstones and the coccolith limestone. However, this dilution can be corrected for by using a simple equation (Equation (3), Section 5.1.1), resulting in a carbonate-free TOC % (Figure 6.2, Table 6.1). As predicted the greatest change to the TOC profile occurs over the calcareous mudstones and coccolith limestone, where it is evident that during the limestone deposition the quantity of sediment organic matter was similar or greater than that during the oil shale deposition. However, the extreme levels of coccolithophore production during these periods resulted in substantial dilution of this organic component. Within the mudstone lithologies the difference between TOC and $CaCO_3$Free TOC is reduced indicating less dilution and thus reduced coccolithophore production during these periods.

6.1.2.2 Pyrite Formation and the Remainder Profile

The remainder % weight of the each sample is composed of both clastic material and pyrite, but the formation of pyrite is an autochthonous process in the marine environment while the clastics are the result of allochthonous terrestrial input. Pyrite formation also relies on the oxidation and degradation of organic matter during sulphate reduction (Section 4.9.1), and thus the pyrite could be considered as a proportion of the TOC and not the remainder. This may explain the positive correlations seen between the TOC and remainder profile over the oil shales (Figure 6.1A and C). Assuming this is the case it would be advantageous to ascertain the amount of pyrite in each sample. Unfortunately the methods used to obtain the bulk geochemical sample components in this study were not set up to distinguish the proportion of pyrite within samples, therefore, only an empirical method can be used to make an assessment of pyrite levels.

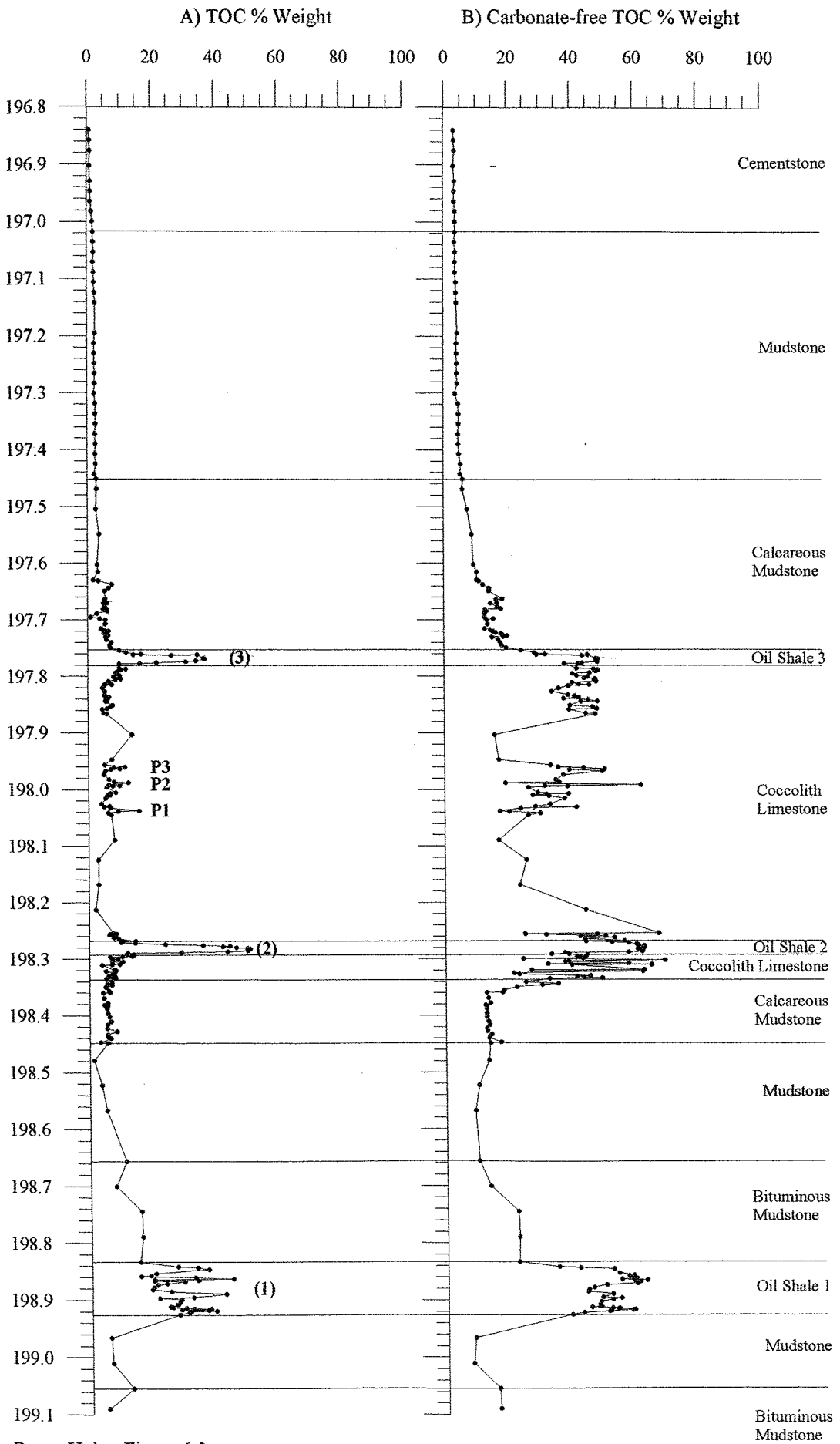

Down Hole Depth (m)

Figure 6.2
TOC and carbonate-free TOC % weight through the Whitestone Band interval.

When TOC % was plotted against carbonate % weight and samples were grouped in lithological types as differentiated in Figure 6.1, two points were notable (Figure 6.3). Firstly all lithologies display moderate to strong negative correlations with correlation coefficients ranging between -0.5 to -0.9. In modern marine sediments such an overall negative correlation between TOC and carbonate, results from a combination of autodilution effects and differential preservation (Lyons and Berner, 1992). Secondly, there is a clear upper boundary to the samples which is delineated by oil shale and coccolith limestone samples. Assuming these samples are composed solely of carbonate and TOC, and that pyrite is always present, but clastic material is not, the gradient of the line should equal minus one. However, the sample line gradient is less than minus one. Thus, the portion between this sample line and the theoretical 50/50 line represents other elements of hydrogen, oxygen, and nitrogen, which together with carbon form organic matter, and a proportion of organic matter, that was used during sulphate reduction in the formation of pyrite. Therefore the 50/50 line represents the total organic matter in the samples together with that used in pyrite formation (TPOM line).

From the graph (Figure 6.3) it is possible to estimate the percentage of carbon needed to project the sample line onto the TPOM line, which was found to be TOC/0.56, for the WSB samples. Thus, these new projected total and 'pyrite' organic matter (TPOM) figures can be used to estimate the clastic material percentage of the remainder % weight, using the equation (100 – carbonate – (TOC/0.56)). The results of these calculations are shown in Figure 6.4 and Table 6.1. The TOC profile (Figure 6.4A) is now the estimated TPOM profile, which displays an overall increase in percentages, with a maximum of 91% in oil shale (2). There are also subtle changes to the remainder profile, which is now the estimated clastic material profile (Figure 6.4C). The most prominent change is seen in the oil shales, which no longer display positive correlations to the TOC, but negative ones, this is in agreement the fabric evidence from this study (Section 4.11.1). During the oil shales and over parts of the coccolith limestone the estimated clastic % is minimal possibly indicating low terrestrial flux and sedimentation over these periods. However, in the other lithologies, especially the mudstones, the estimated clastic material % is greater.

This graphical estimation of the percentage of clastic material within the sample is not without error and it can be seen that over the oil shales and a few limestone samples that the percentages become negative. This is believed to be partly the result of inaccuracies in the sample line placement, but also the formation of pyrite requires iron. This reaches the marine system with clays and thus is also an integral part of the clastic %. Iron limitation from lack of reactive iron during sulphate reduction may also have an effect (Leventhal, 1993).

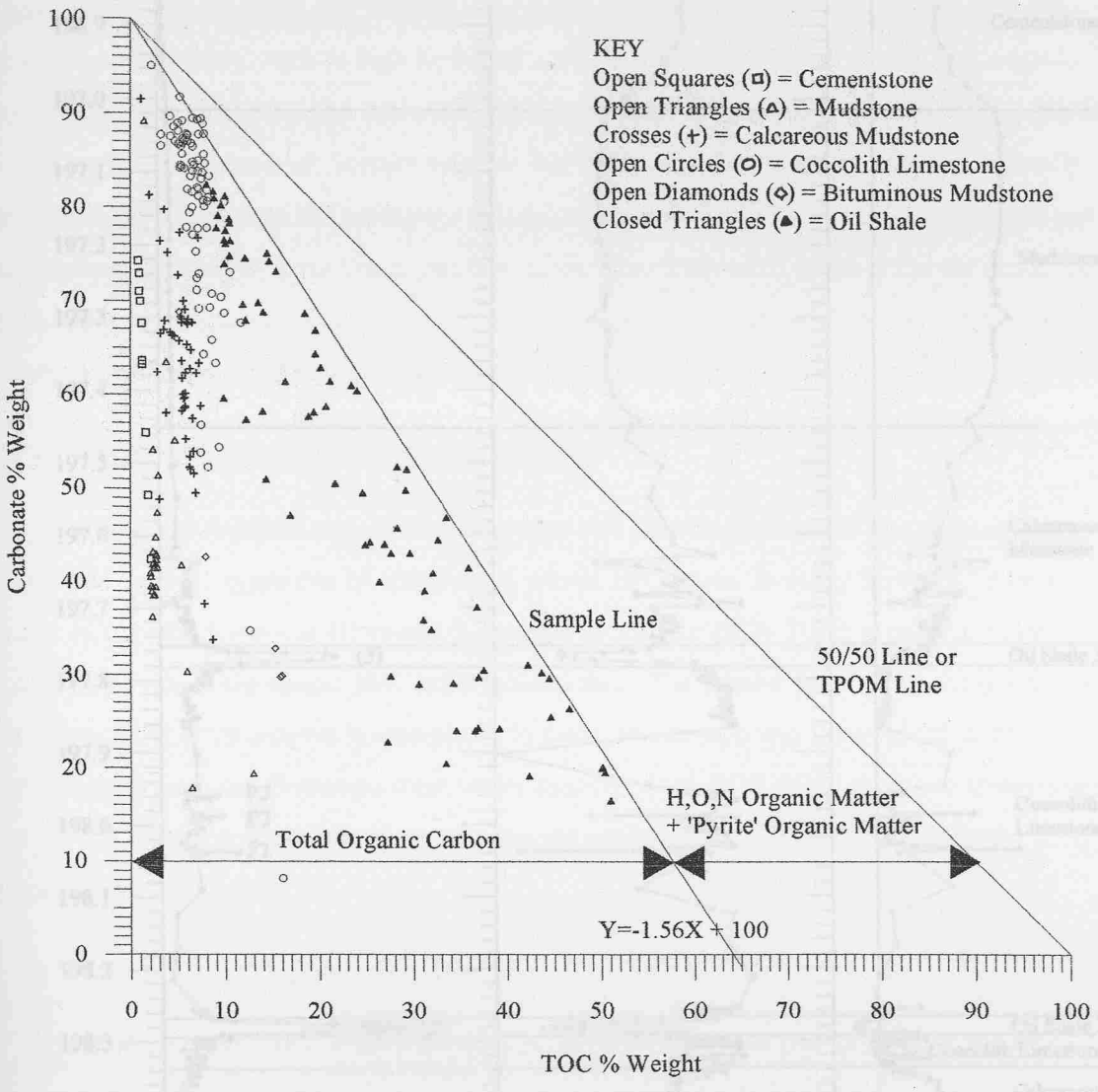

Figure 6.3
TOC % weight plotted against carbonate % weight with samples grouped into lithological types. Notice the negative correlation for all lithologies and the clearly defined linear upper boundary depicted by the oil shale and coccolith limestone samples. The difference between this sample line and the TPOM line is the other elements (H, O, N) comprising the organic matter and the organic matter which was used in the fomation of pyrite. This difference equals 0.56, thus TOC/0.56 gives the TPOM of the samples. This can then be used to estimated the percentage of clastic material within the remainder % weight using the equation (100 - carbonate (TOC/0.56)), thus allowing an assessment of the terrestrial clastic flux. Tyson (1995) used a multiplication factor to convert TOC to % weight organic matter, for Type I kerogen this factor was TOC x 1.25, and x 1.34 for Type II kerogen. Percentage weight of organic matter calculated using Tyson's factors are greater than the empirically calculated values in this study. Tyson's factors take into account the organic matter source, water column and sedimentation degradation and not just purely the loss of organic matter via oxidation during sulphate reduction and pyrite formation as done here. Thus this study's calculation is an initial approximation.

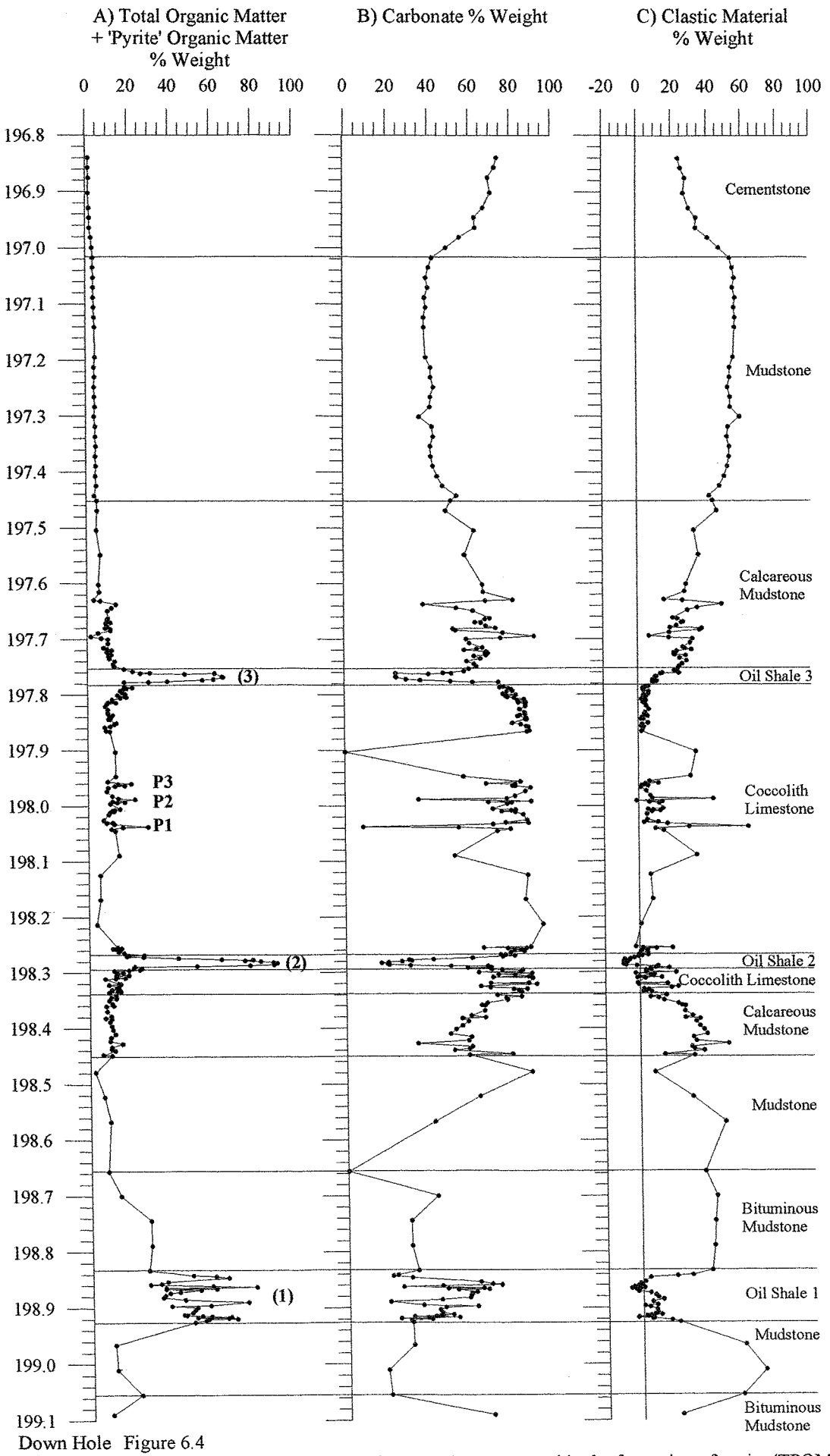

Down Hole Depth (m)

Figure 6.4 Estimated total organic matter plus organic matter used in the formation of pyrite (TPOM), carbonate and estimated clastic material (remainder - pyrite) as % weight through the Whitestone Band interval.

6.1.3 SUMMARY

The bulk geochemical components of TOC, carbonate and remainder over the WSB interval have quantitatively confirmed the oil shales, coccolith limestone and the other lithologies, which comprise this interval. The detail of the sampling also highlights variation within these lithologies such as high carbonate occurrences within the oil shales, and organic-rich events during the coccolith limestone deposition. The effect of carbonate dilution, especially over the coccolith limestone, is quite marked, and TOC over this lithology reaches the levels seen in the oil shales once the carbonate has been removed. The presence of the oil shales and the detailed sampling of these lithologies has enabled the removal of pyrite from the remainder % and thus an estimation of the amount of clastic material over the WSB interval, allowing insight into the terrestrial flux into the KCF marine system.

6.2 ATOMIC HYDROGEN / CARBON RATIOS

The preservational state of organic matter and the classification of immature organic matter into kerogen types can be found using atomic H/C ratios. In many studies a proxy to atomic H/C ratios known as HI values (Hydrogen Index, mg HC/g TOC) is quoted. However, in this study values are atomic H/C ratios unless stated. The greater proportion of organic matter within the KCF WSB interval is amorphous in form, and as such was not counted in the palynological analysis. However, some understanding of the KCF AOM character is necessary and the H/C ratios provide details on the type and preservation of the AOM at different TOC percentages.

6.2.1 ATOMIC H/C AND TOC PLOTS

Plots of atomic H/C ratios against TOC over the WSB interval show there is a good relationship between the two (Figure 6.5A). Ratio values initially increase from below 1 at TOC <5%, and level off to a plateau between 1.4-1.8 at between 5 to 10% TOC. These ratios are similar to those obtained by Van Kaam-Peters *et al*, (1998) for the KCF, and equal to an HI range of 500 to 850mg HC/g TOC, which is typical of type II to type I kerogen. The levelling off of the atomic H/C ratio reflects the attainment of optimal preservational conditions (via qualitative effects on preservation and quantitative effects due to increased AOM percentages) (Tyson, 1995). This pattern is still seen in sediments where there is virtually no terrestrial input (Lallier-Verges *et al.*, 1993), indicating that it does reflect AOM preservation as well as changes in the percentage of AOM. The levelling-off of the KCF WSB atomic H/C ratios at approximately 1.5 at low TOC levels is a known characteristic of marine carbonate source rocks. This is believed to result from the much greater marine to terrestrial kerogen ratios, the

greater frequency of Type I kerogen in these facies and their low hydrocarbon retention characteristics (Tyson, 1995).

The levelling off of the H/C ratios represent the attainment of sufficiently anoxic conditions so as to prevent further degradation of the refractory organic matter and any further fluctuation in TOC values are thought to be due to other (non-preservational) factors, for example sediment dilution and granulometry. The WSB interval samples do show such fluctuations and the data were re-plotted in lithological types to ascertain which lithologies were varying (Figure 6.5B). The cementstone and mudstones comprise the rising limb of the graph, while calcareous mudstones make up the majority of the values that begin to level off at 1.4-1.6 atomic H/C ratio. The coccolith limestone, bituminous shale and oil shale lithologies all form the plateau section of the plot. It is interesting to note that though the coccolith limestone samples show relatively low TOC, they reach atomic H/C ratios of the same level as the oil shales, indicating similar sources of organic matter, namely planktonic (Tyson, 1995). The coccolith limestone and especially the oil shale samples show wide ranges of both atomic H/C ratios and TOC, which may reflect variation in sediment rates, water column oxygen levels, and possibly variability between coccolith and other phytoplankton production?

The maximum atomic H/C ratio is determined by the nature of the original source of the organic matter, and commonly the proportion of terrestrial material generally declines as TOC increases, often due to dilution by preserved 'AOM' (Tyson, 1995). It was noted, both in the fabric analysis and the TOC/carbonate relationships, that oil shale (1) was different to oil shales (2) and (3). This difference was investigated with the atomic H/C ratios to see if the organic material of the three oil shales varied, though preservational conditions were assumed to be optimal for all the shales (Figure 6.5C). It was found that the majority of the oil shales' sample ratios fell in a band between 1.3 to 1.6, with TOC ranging from 7 to 51%, but oil shale (1) was more commonly characterized by higher TOC. A faint division in atomic H/C ratios between the three oil shales was also present. Below 1.3 atomic H/C ratio the majority of the values are from oil shales (2) and (3), with oil shale (2) displaying the highest TOC, while above 1.6, oil shale (1) is more dominant. Thus, there is a weak difference between the oil shales. However, transmitted light analyses of samples from these three oil shales do not show significant differences in the proportion of terrestrial material within them. Therefore, this small difference seen in atomic H/C ratios is most likely to be due to variation in diagenetic factors during the formation and preservation of the AOM.

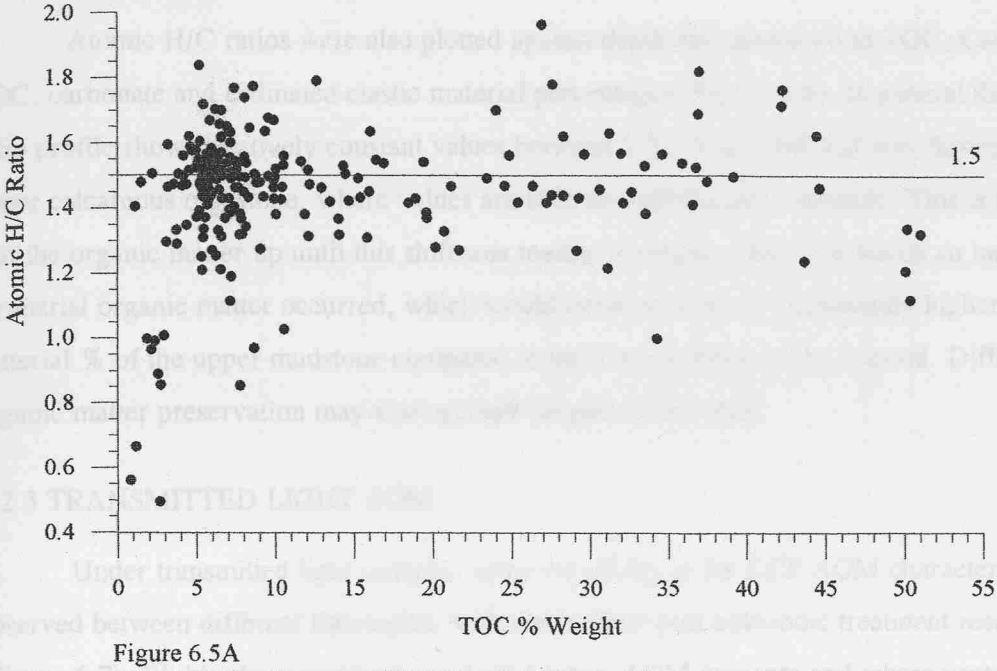

Figure 6.5A
Atomic H/C ratio against TOC % weight for the Whitestone Band interval.

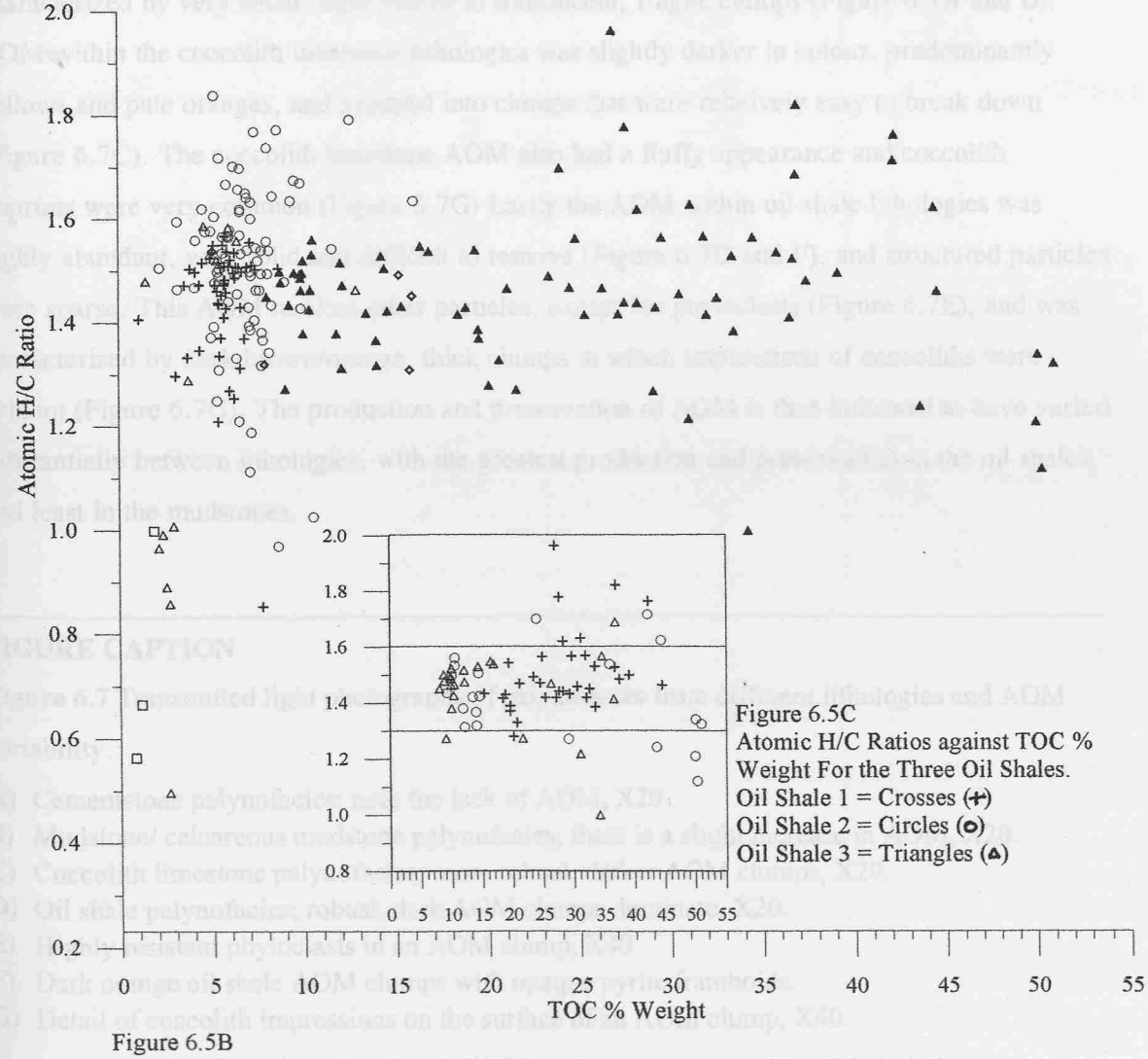

Figure 6.5C
Atomic H/C Ratios against TOC % Weight For the Three Oil Shales.
Oil Shale 1 = Crosses (+)
Oil Shale 2 = Circles (o)
Oil Shale 3 = Triangles (▲)

Figure 6.5B
Atomic H/C Ratio against TOC % Weight with samples grouped into lithological types, Whitestone Band Interval. Open squares (□) = Cementstone, Open triangles (△) = Mudstone Crosses (+) = Calcareous Mudstone, Open circles (o) = Coccolith Limestone, Open diamonds (◇) = Bituminous Mudstone, Closed triangles (▲) = Oil Shales.

6.2.2 DEPTH PLOTS OF ATOMIC H/C RATIOS

Atomic H/C ratios were also plotted against depth and compared to TOC, $CaCO_3$Free TOC, carbonate and estimated clastic material percentages (Figure 6.6). In general the vertical ratio profile shows relatively constant values between 1.3-1.6 up until mid way through the upper calcareous mudstone, where values are seen to decline quite markedly. This is suggestive that the organic matter up until this shift was marine in origin, while afterwards an increase in terrestrial organic matter occurred, which would coincide with the consistently higher clastic material % of the upper mudstone compared to the lower portion of the interval. Differences in organic matter preservation may also account for part of this shift.

6.2.3 TRANSMITTED LIGHT AOM

Under transmitted light analysis, some variability in the KCF AOM character was also observed between different lithologies, with the residual post ultrasonic treatment residues (Figure 6.7). Within the cementstone and mudstones, AOM was rare and where present was characterized by very small, light yellow to translucent, fragile clumps (Figure 6.7A and B). AOM within the coccolith limestone lithologies was slightly darker in colour, predominantly yellows and pale oranges, and grouped into clumps that were relatively easy to break down (Figure 6.7C). The coccolith limestone AOM also had a fluffy appearance and coccolith imprints were very common (Figure 6.7G) Lastly the AOM within oil shale lithologies was highly abundant, very solid and difficult to remove (Figure 6.7D and F), and structured particles were sparse. This AOM masked other particles, except for phytoclasts (Figure 6.7E), and was characterized by dark brown/orange, thick clumps in which impressions of coccoliths were evident (Figure 6.7G). The production and preservation of AOM is thus indicated to have varied substantially between lithologies, with the greatest production and preservation in the oil shales, and least in the mudstones.

FIGURE CAPTION

Figure 6.7 Transmitted light photographs of palynofacies from different lithologies and AOM variability.

A) Cementstone palynofacies; note the lack of AOM, X20.
B) Mudstone/ calcareous mudstone palynofacies; there is a slight increase in AOM, X20.
C) Coccolith limestone palynofacies; more robust, darker AOM clumps, X20.
D) Oil shale palynofacies; robust, dark AOM clumps dominate, X20.
E) Highly resistant phytoclasts in an AOM clump, X40
F) Dark orange oil shale AOM clumps with opaque pyrite framboids.
G) Detail of coccolith impressions on the surface of an AOM clump, X40.

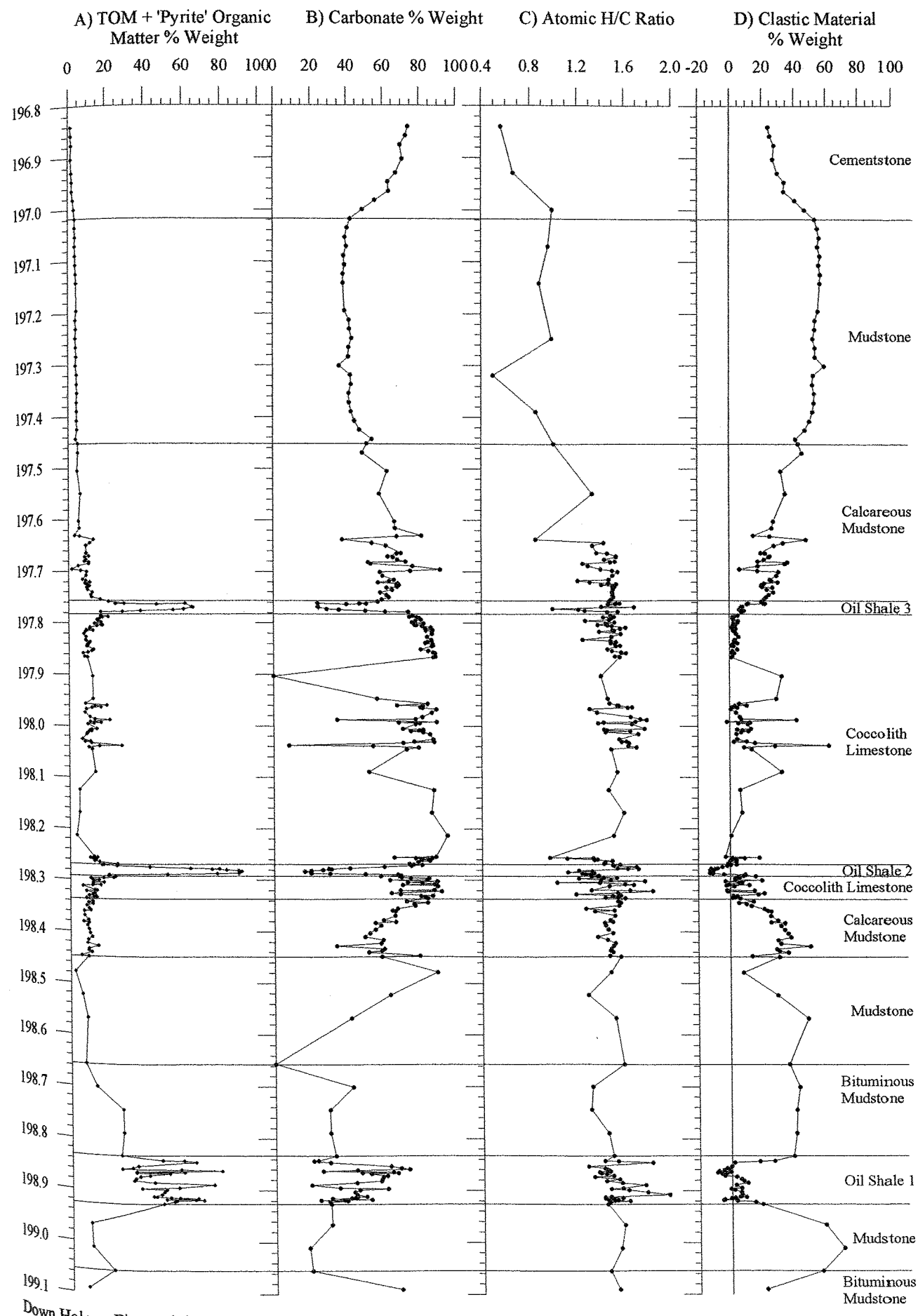

Figure 6.6
Estimated TPOM (total organic matter plus 'pyrite' organic matter), carbonate and estimated clastic material % weight and atomic H/C ratios over the Whitestone Band Interval.

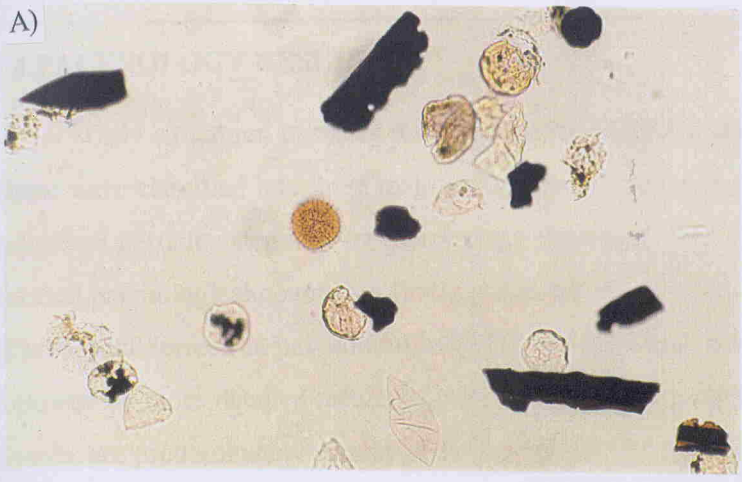

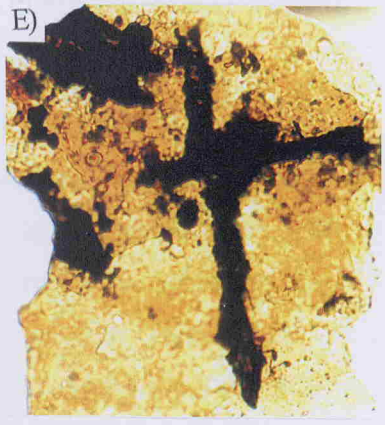

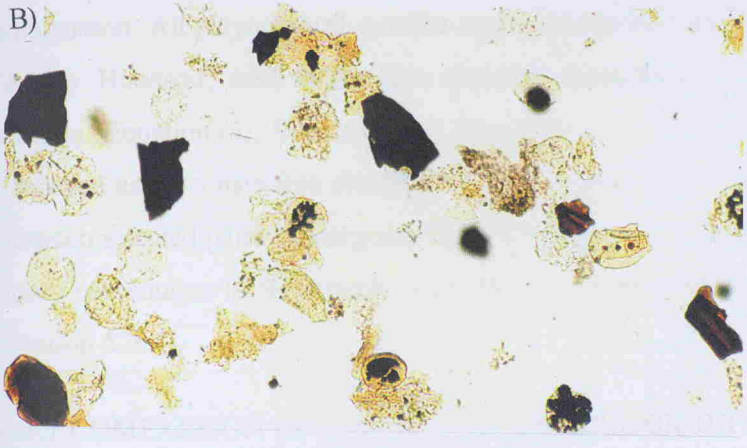

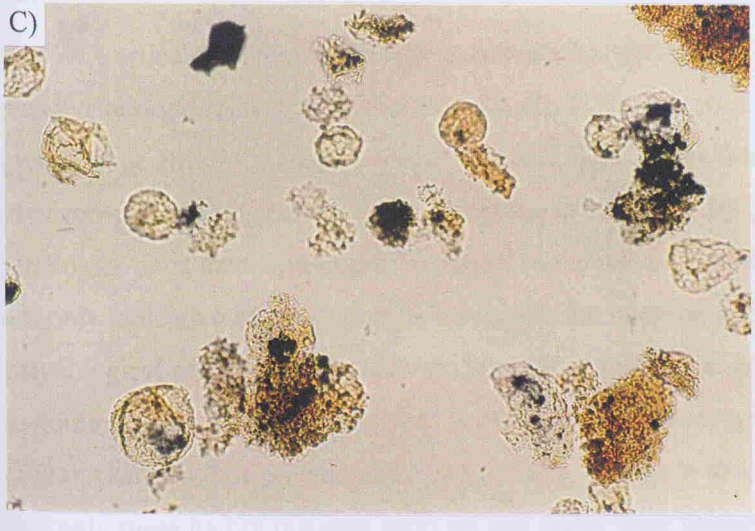

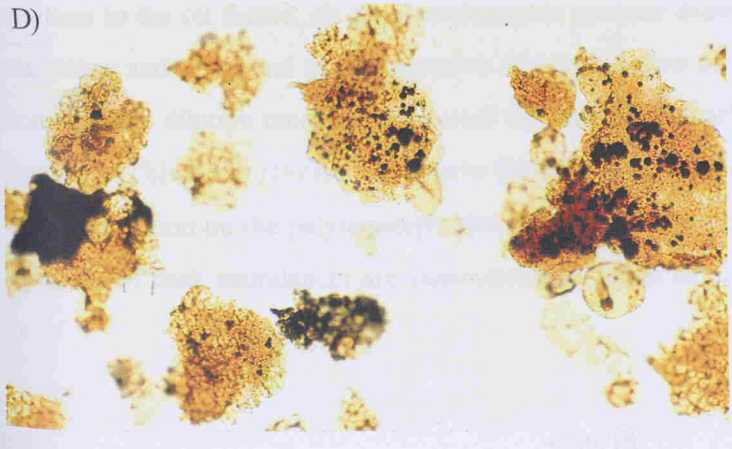

FIGURE 6.7

6.3 PALYNOLOGY RESULTS

Only structured particles were counted during the palynological analysis of the intervals. These were classified into three main groups based on provenance and further subdivided into individual particle categories by morphology (Section 5.3.5, Table 5.2). The results of the WSB interval palynological counts are firstly presented as group totals of total marine palynomorphs (TMP), total terrestrial palynomorphs (TTP) and total structured debris (TSD). These are followed by more detailed results of individual categories within these total groups (Table 5.2). Results are predominately displayed as vertical profiles over the WSB interval, together with estimated total plus 'pyrite' organic matter (TPOM) and estimated clastic material % weight for comparison. All palynomorph profiles represent absolute particle abundance per gram of rock (AA/g). However, these values have also been recalculated to remove the effects of carbonate dilution (Equation (3), Section 5.1.1), as was done for the TOC (Section 6.1.2.1), and are thus displayed as carbonate-free absolute abundances per gram of rock ($CaCO_3$Free AA/g). Ratios between selected pairs of categories are used to illustrate relative (%) particle abundances, while group percentages (G%) provide information on trends within each main palynomorph group (Section 5.3.4).

6.3.1 COMPARISON OF THE MAJOR PARTICLE GROUPS (TMP, TTP AND TSD)

6.3.1.1 Absolute Abundance Vertical Profiles

Vertical profiles of the three major particle groups, together with total organic matter plus pyrite organic matter (TPOM) and clastic % weight, are displayed in Figure 6.8. All three groups quite strikingly display almost identical signals over the interval. The oil shales show very reduced abundances, which is surprising considering the greater level of compaction these lithologies must have undergone compared to the rest of the interval. However, these profiles are only indicative of structured particles over the interval, not the AOM, which from both palynological sample preparation (Section 6.2.3) and atomic H/C data (Section 6.2.1) is known to dominate these very organic-rich lithologies. Of the three groups only the structured debris (TSD), composed of predominately phytoclasts, is seen in abundance in the oil shales, indicating that only these highly resistant particles and AOM were preserved during oil shale deposition. In contrast to the oil shales, all group abundances increase dramatically in the lower calcareous mudstone and at the end of the coccolith limestone below oil shale (3). This is interesting, as considerable dilution must have occurred due to the high carbonate sedimentation rate over these episodes. This is the reverse situation to the oil shales and the effect of both sedimentation rate and compaction on the palynomorph abundance will be discussed in the following section. These episodes of peak abundances are characterized by high amplitude and high frequency signals.

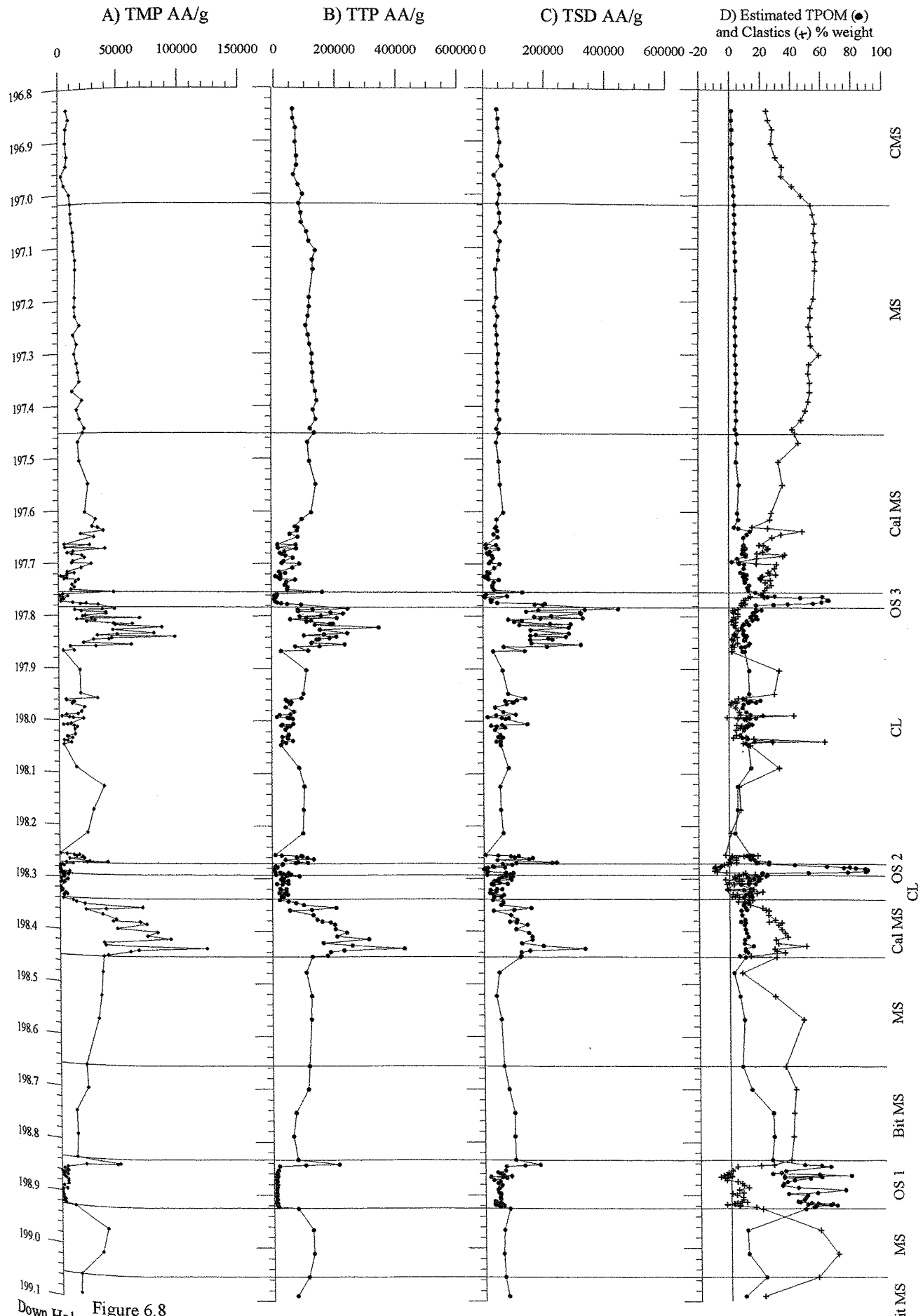

Figure 6.8
Vertical profiles of the three major particle groups (TMP, TTP, TSD) as absolute abundance per gram of rock (AA/g) and estimated TPOM (total organic matter plus 'pyrite' organic matter) and clastic material as % weight over the Whitestone Band Interval. (Lithology notation:- CMS = Cementstone, MS = Mudstone, CalMS = Calcareous Mudstone, BitMS = Bituminous Mudstone, CL = Coccolith Limestone, OS = Oil Shale)

However, the remaining coccolith limestone and the upper calcareous mudstone after oil shale (3) display low abundances in comparison. The other lithologies display consistent abundances, which are commonly slightly greater than the abundances in the central coccolith limestone.

6.3.1.2 Sedimentation Rates and Compaction

The effect of sedimentation rates and compaction levels on the abundance of palynomorphs in different lithologies is a critical one, but is also very difficult to quantify. Taking the oil shales and the coccolith limestone as opposite lithological examples, the relative effects of these mechanisms can be ascertained (Table 6.2). The assumption is made that the palynomorph abundance is fixed during the deposition of both lithologies, and that compaction is greatest for the oil shales, while sedimentation rates are greatest for the coccolith limestone (Section 4.8.2, Table 4.2). It can be seen from Table 6.2 that if a constant number of palynomorphs were deposited with these lithologies, concentration would occur in the oil shales, while abundances would be diluted in the coccolith limestone. But the data from the WSB interval do not follow this pattern, with the lowest abundances over the oil shales and more variable and greater abundances in the coccolith limestone. It would therefore seem that these patterns are probably a real effect and the structured organic particles were more abundant in the coccolith limestone than the oil shale.

Lithology	**Sedimentation Rate And Effect**		**Compaction And Effect**		**Influence on Palynomorph Abundance**
Oil Shale	LOW	Concentrate	HIGH	Concentrate	CONCENTRATE
Coccolith Limestone	HIGH	Dilute	LOW	Dilute	DILUTE

Table 6.2

The effects of both sedimentation rate and compaction on a fixed palynomorph abundance in the oil shale and coccolith limestone lithologies.

6.3.1.3 Carbonate Dilution

As expected from the $CaCO_3$Free TOC, the $CaCO_3$Free absolute abundance profiles for the main groups show the greatest difference from the absolute abundance profiles over the calcareous mudstones and coccolith limestone (Figure 6.9). In general, the overall profiles change little in pattern, but an increase in abundance for all groups occurs at the beginning of the upper calcareous mudstone that was not evident in the absolute abundance profiles (Figure 6.8). This shows similar high amplitude and frequency fluctuation as at the end of the coccolith limestone, but these episodes are clearly divided by very reduced abundances in oil shale (3).

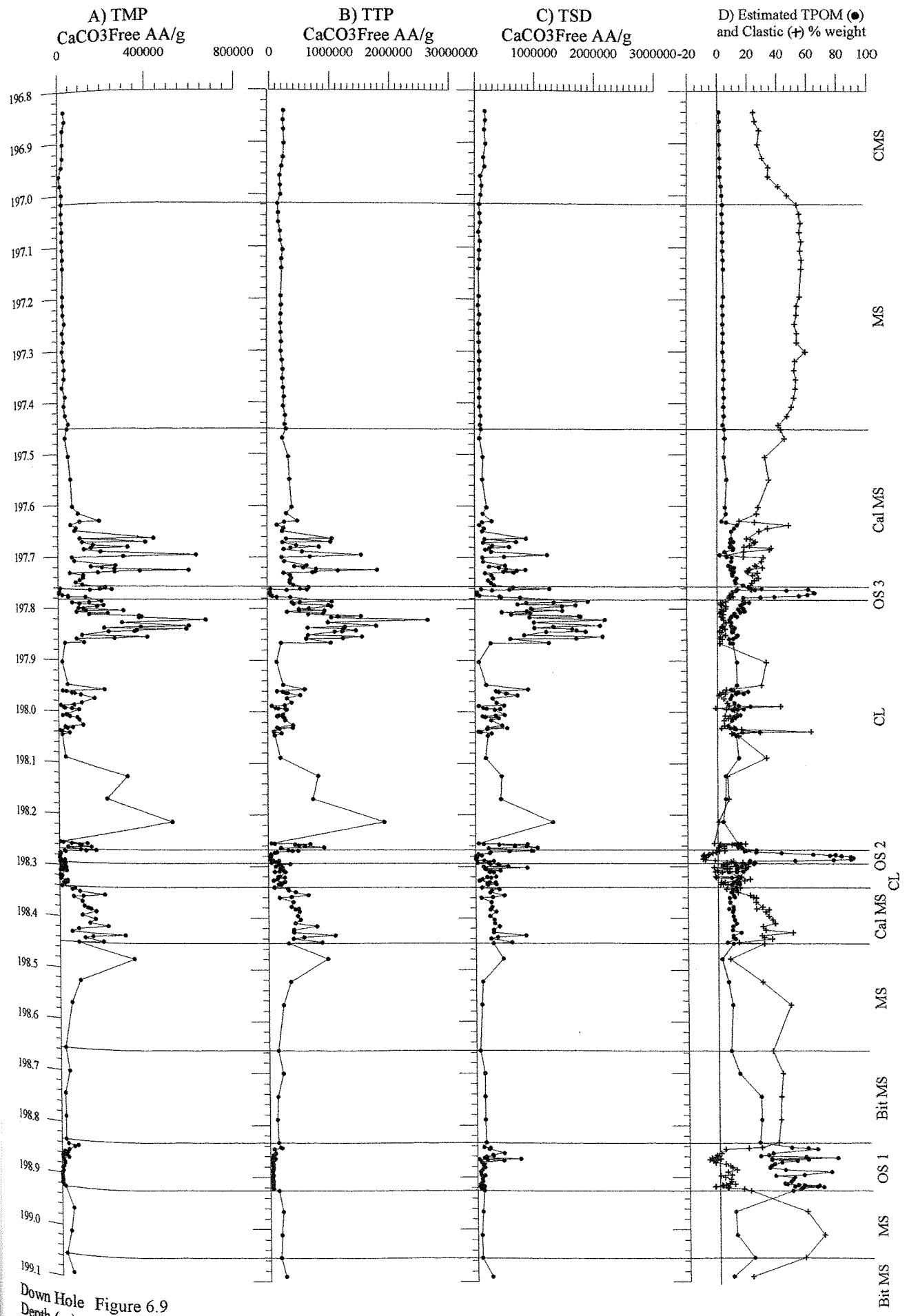

Figure 6.9
Vertical profiles of the three major particle groups (TMP, TTP, TSD) as carbonate-free absolute abundance per gram of rock (CaCO3Free AA/g) and estimated TPOM (total organic matter plus 'pyrite' organic matter) and clastics as % weight over the Whitestone Band Interval. For lithology notation see Figure 6.8 caption.

All the oil shales still display very low $CaCO_3$Free abundances, except for the TSD profile over the upper half of oil shale (1), which shows several small increases most likely due to the effect of thicker and more frequent carbonate laminae over this area (Figure 3.1, 3.16a to d).

6.3.1.4 Quantitative Comparisons of the Major Particle Groups

Though the overall vertical profiles of the three major groups display almost identical patterns, there are quantitative differences between the groups (Table 6.3). The total marine palynomorphs (TMP) group has the lowest abundances of all the groups, while the structured debris the highest. This is clearly shown by the average percentage of each total group in the total particle count, where TMP = 10%, TTP = 38% and TSD = 52%. Thus, terrestrial particles dominate the counted structured particles of the WSB interval. However, it must be remembered that the majority of the organic matter in this interval is AOM, and planktonic in origin (Section 6.2.1). In order to assess the correlation of the three main groups with each other, reduced major axis line (RMA) regression was used and resulted in positive correlations between all groups. RMA regression of TMP against TTP produced $r = 0.94$, and $r^2 = 0.88$ (Figure 6.10A), indicating a strong correlation between these two groups. However, the correlation between TMP and TSD ($r = 0.77$, $r^2 = 0.6$) is not so strong (Figure 6.10B). Correlation between TTP and TSD is slightly stronger than against TMP, with $r = 0.85$, $r^2 = 0.72$ (Figure 6.10C). Thus, these correlations suggest that there was a close link between the marine palynomorphs and the terrestrial material.

TOTAL CATEGORY Av % of total particle count	MINIMUM		MAXIMUM		AVERAGE	
	AA/g	$CaCO_3$Free AA/g	AA/g	$CaCO_3$Free AA/g	AA/g	$CaCO_3$Free AA/g
TMP 10% (max. 25%)	0	0	124,000	674,000	19,000	98,500
TTP 38% (max. 67%)	0	0	196,000	2644,000	40,000	342,000
TSD 52% (max. 100%)	1,000	7,000	447,000	2183,000	80,000	384,000

Table 6.3

Minimum, maximum and average absolute abundance (AA/g) and carbonate-free absolute abundance ($CaCO_3$Free AA/g) for the three main particle groups over the WSB interval. Average and maximum percentages for each group of the total particle count are also included.

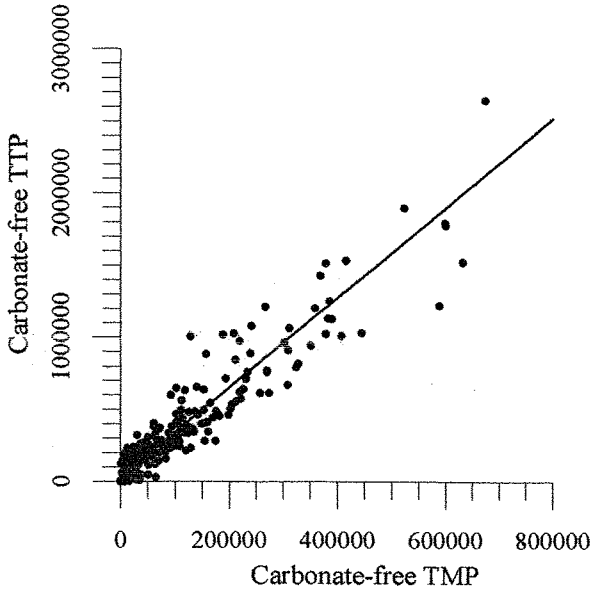

Figure 6.10A)
Reduced major axis line regression
for TMP against TTP, WSB interval.
The isogonic growth line is shown,
with details given below.

y = 37114 + 3.1x
r = 0.94, r-squared = 0.88, n = 265
95% confidence interval for the slope (b)
b = 3.1± 0.13,
95% cofidence interval for the intercept (a)
a = 37114 ± 25845.

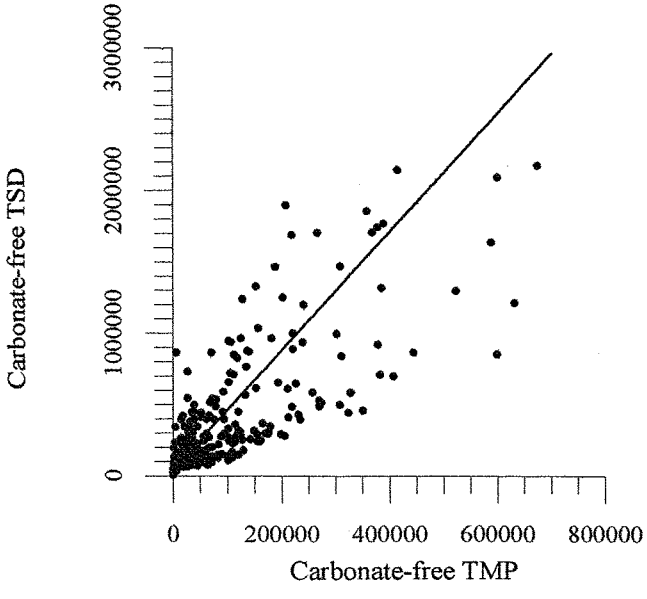

Figure 6.10B)
Reduced major axis line regression
for TMP against TSD, WSB interval.
The isogonic growth line is shown,
with details given below.

y = 42262 + 3.47x
r = 0.77, r-squared = 0.6, n = 265
95% confidence interval for the slope (b)
b = 3.47 ± 0.26,
95% cofidence interval for the intercept (a)
a = 42262 ± 53591

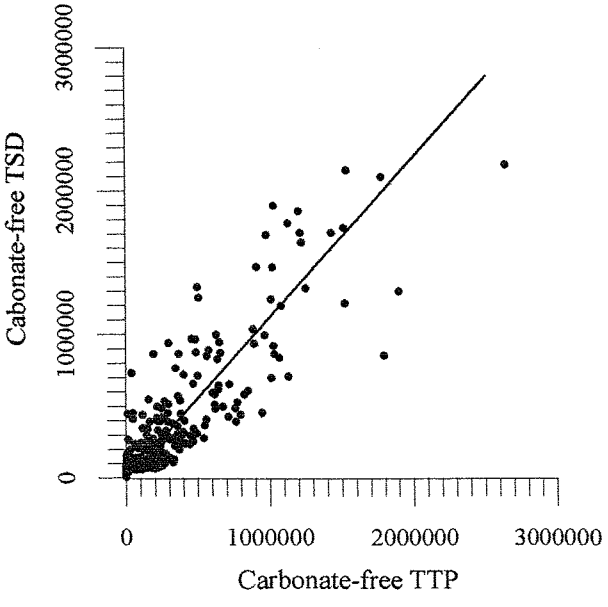

Figure 6.10C)
Reduced major axis line regression
for TTP against TSD, WSB interval.
The isogonic growth line is shown,
with details given below.

y = 615 + 1.12X
r = 0.85, r-squared = 0.72, n = 265
95% confidence interval for the slope (b)
b = 1.12 ± 0.07,
95% confidence interval for the intercept (a),
a = 615 ± 48867

6.3.1.5 Summary

The palynomorph and structured particles within the WSB interval were found to be dominated by terrestrial types. However, all major groups display almost identical profiles and strong positive RMA correlations over this interval. All particle groups are characterized by very reduced abundances in the oil shales possibly resulting from the domination of AOM in these lithologies. Conversely, the calcareous mudstones and coccolith limestone display episodes of high abundances characterized by high amplitude and frequency fluctuations. These patterns were found to be in contradiction to those predicted by sedimentation rate and compaction processes in these lithologies, suggesting that these signals are likely to reflect true variability. The location of the high abundance episodes before the limestone and at the end of the limestone suggests they may have exerted some influence on both the initiation and cessation of the coccolith limestone.

The fact that all the major groups display the same peak abundance episodes indicates that the palynomorph flux was unsorted and the high-frequency fluctuations, which are very characteristic of these episodes, imply this flux occurred as short, sharp pulses of particle deposition. At first glance these characteristics seem to indicate two episodes of high terrestrial flux into the marine system, probably related to increased periods of fluvial discharge and therefore precipitation. However, the estimated clastic material profile shows variable to low percentages over these episodes, especially at the end of the limestone. Therefore another mechanism is needed to explain these episodes of high frequency and amplitude pulses of terrestrial organic material but only a small but variable clastic input, probably dominated by clays. The palaeogeography of the region characterized by small, low-relief islands combined with a predominately arid climate would suggest that any rivers would be short and probably flow for only a small part of the year. As such this would have facilitated storage of the terrestrial flux (both organic matter and clastics) on the shelf. However, during storms these shelf areas would have experienced frequent sediment disturbance and re-suspension. It is possible that the terrestrial palynomorphs, structured organic matter debris and clays were moved further offshore during stormy periods and did not settle out of the water column until reaching the distal basin, where as the larger sized clastic material was retained in more proximal areas. Thus, the close correlation between the two major terrestrial groups can be accounted for, while the close correlation to TMP can be explained by increased dinoflagellate encystment due to the stressful environmental conditions during these storm episodes.

Nutrients would also have been brought into the distal basin surface waters during storm periods, and were taken advantage of by the r-stratigist coccolithophores, resulting in

coccolithophore blooms. This may explain the position of the first high abundance episode, but not the second, which for all groups is characterized by greater abundance pulses, and thus storm intensity. Therefore it is suggested that though nutrients were not limiting, the increased disturbance caused by the frequent severe storms at the end of the limestone, was detrimental to the coccolithophore population which went into decline, thus terminating the coccolith limestone deposition. Despite the lack of extreme coccolithophore populations, their numbers clearly increase again in the calcareous mudstone after oil shale (3), before gradually declining in abundance in the succeeding mudstone.

Thus from these total group profiles the coccolith limestone deposition is suggested to have been related to episodes of increased storminess. These in turn were probably the result of a climatic change possibly a shift in the position of the Palaeo-Atlantic storm track belt (Valdes and Sellwood, 1992) and/or an intensification of this storm belt. These hypotheses are further investigated in the following sections by analysis of individual particle categories within the three major groups, and discussed in relation to modern day storm deposits in Chapter 8.

6.3.2 MARINE PALYNOMORPHS

The total marine palynomorph group (TMP) was found to be the least abundant of the total groups. However, it provides an insight into the phytoplankton structure of the surface waters excluding the coccolithophores. The TMP group was divided into seven particle categories (See Table 5.2, Section 5.3.5), but not all these categories were found to play a significant role in the TMP variability. Acritarchs, prasinophyte and proxi-chorate dinocysts were not sufficiently abundant in raw counts to enable reliable interpretation and are therefore not discussed. Simple sacs, though more abundant are difficult to use in environmental reconstruction due to their unknown affinity. However, chorate and proximate dinocysts and foraminiferal test linings were consistently more abundant in raw counts and therefore environmental interpretations are possible. As for the total groups, particles are measured as absolute abundance (AA/g) per gram of rock, and carbonate-free absolute abundance ($CaCO_3$Free AA/g), while TMP group percentage (G%) for each particle category and ratios between categories are also calculated.

6.3.2.1 Absolute Abundance Vertical Profiles

Vertical profiles of chorate, proximate and total dinocysts and foraminiferal test linings (FTL) absolute abundance over the WSB interval in general display the same pattern as the group totals (Figure 6.11). However, though both dinocyst morphotypes display substantial increase in the lower calcareous mudstone, only the proximate dinocysts show peak abundance at the end of the coccolith limestone before oil shale (3) (Figure 6.11A and B). Chorate

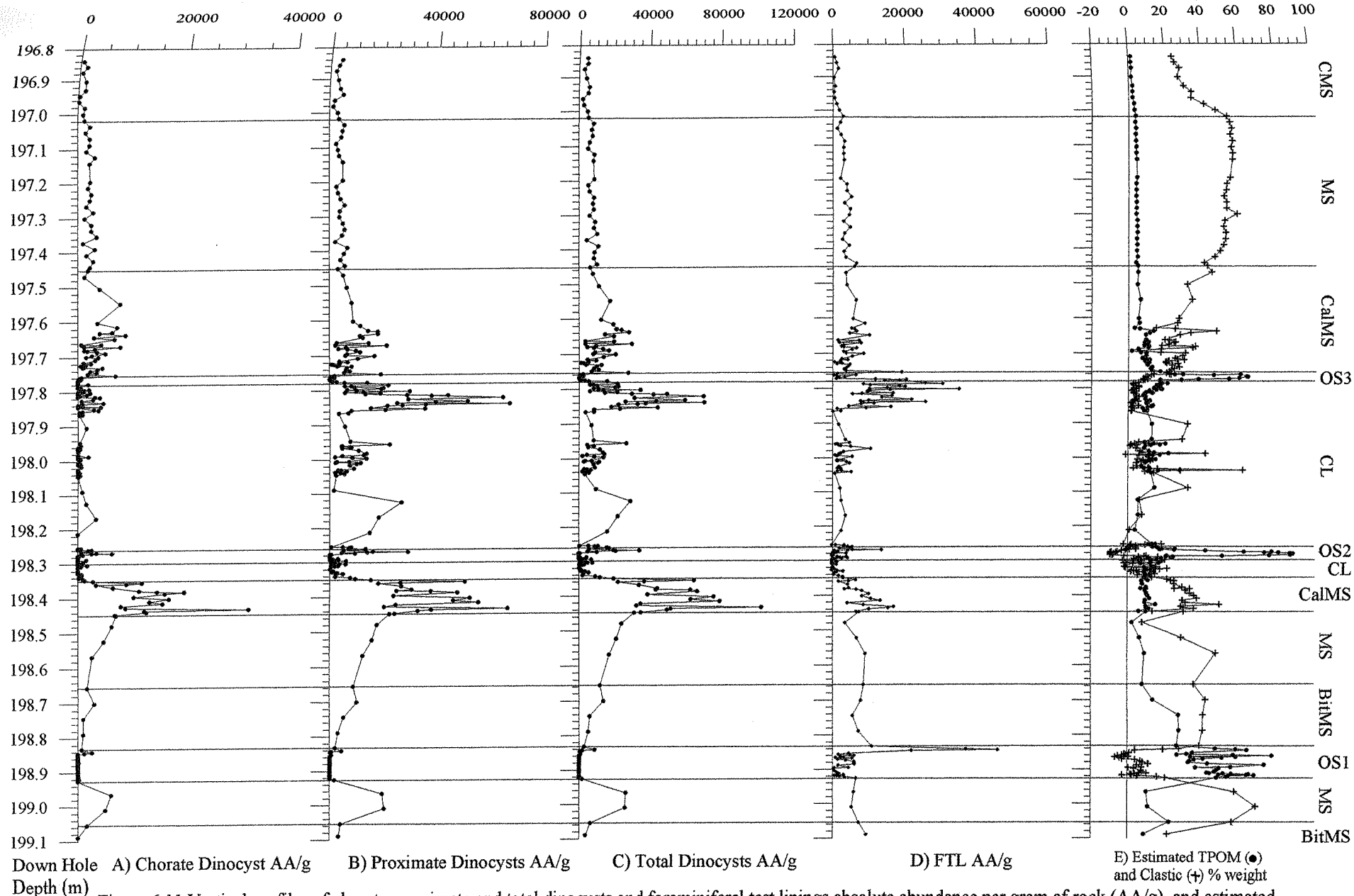

Figure 6.11 Vertical profiles of chorate, proximate and total dinocysts and foraminiferal test linings absolute abundance per gram of rock (AA/g), and estimated TPOM (total organic matter + 'pyrite' organic matter) and clastics % weight over the Whitestone Band Interval. For lithology notation see Figure 6.8 caption.

dinocysts show very low abundances over the majority of the limestone, but increase slightly towards the end of the upper calcareous mudstone (Figure 6.11A). For all the oil shales, dinocyst abundance is very low.

Dinocyst abundance is not easily correlated to surface water dinoflagellate populations (Section 5.3.6.1, i)). An increase in dinocysts may results from an increase in the overall dinoflagellate population, an increase of cysting in a stable population or an increase in preservation of cysts from either of the previous two scenarios. The variability of cyst abundance within the different WSB lithologies possibly excludes the preservation scenario, though this might be an important factor during oil shale deposition. Therefore, the peak abundance episodes indicate either an increase in the overall dinoflagellate population or increased encystment of a stable population. Thus environmental conditions were either optimal or highly stressful during these episodes. Considering the storm hypothesis and the domination of coccolithophores in the surface waters during the limestone deposition, it seems more likely that these episodes were stressful for the dinoflagellates and thus increased encystment occurred.

The morphological variability of cyst abundance at the end of the limestone may also relate to stressful conditions. Chorate cysts are believed to represent open marine, more stable conditions, while proximate cysts are indicators of more proximal, unstable environments (Section 5.3.6.1 i)). It is possible that the marine environmental instability was substantial at the end of limestone deposition, thus chorate dinoflagellates were almost completely excluded, while proximate dinoflagellates were abundant but under significant stress resulting in an increase in cysting. This would also help explain why chorate cysts increase above the limestone in the upper calcareous mudstone, presumably stability increased enabling an increase in the population of chorate dinoflagellates.

The very low abundance of all dinocysts morphotypes during the oil shales may either indicate that the dinocysts were not preserved or that very few cysts were produced. It has been mentioned that the oil shales are dominated by AOM (Section 6.2.3) and it is conceivable that any cysts would have been incorporated into AOM flocs. It is also equally likely that the very stable, low nutrient surface waters envisage for the oil shale depositional period (Section 4.11.1, Figure 4.5A) resulted in conditions which did not promote or require large scale encystment. Either or both of these hypotheses are possible but it cannot be determined with certainty which, if either, was more dominant. Despite low encystment it is probable that the majority of the AOM in the oil shales was from dinoflagellate and other similar phytoplankton, as coccolithophore populations were very low and no terrestrial flux occurred due to climate aridity during these depositional periods.

The FTL profile also displays peak abundances in the lower calcareous mudstone and upper coccolith limestone, and again this second episode is characterized by greater abundances. However, a large, but short-lived increase is seen at the very end of oil shale (1), and similar but smaller peaks are evident at the end of the other two oil shales. The foraminifera represented by the FTL are benthic and as such they are *in situ*, and therefore provide a reliable indication of the oxygen levels in the bottom waters (Stancliffe, 1989; Tyson, 1995). Though FTL test morphology and size were not quantitatively noted within this study, FTL were primarily trochospiral in form (Figure 5.2H and K). Jenkins (pers. comm., 1999) also found an abundance of trochospiral forms in his detailed study of foraminifera in the KCF Blackstone Band. Such trochospiral dominated assemblages are termed quasi-anaerobic and indicate highly reduced bottom water and sediment surface oxygen conditions (Brasier, 1995). The greatest abundance of such foraminifera are found at the transition between suboxic to anoxic conditions and high abundances are attributed to decreased benthic grazing and abundant food supply (Section 5.3.6.1 iv); Douglas, 1981). This is believed to be the situation at the end of the oil shales and perhaps their abundance in the second peak episode also presents an interplay between bottom water oxygen levels and benthic populations. However, it is possible that some of the FTL in these peak abundance episodes were re-deposited from the proximal shelf during re-suspension events. The variation in abundances between the first and second group of peak FTL abundances could be taken to support a greater level of re-suspension and thus storminess at the end of the limestone. Also the FTL abundance peak at the end of the oil shales may reflect storm overturn of the stable water column and thus cessation of oil shale deposition.

6.3.2.2 Carbonate Dilution

Carbonate-free absolute abundance of dinocysts and FTL vertical profiles over the WSB interval are shown in Figure 6.12. As for the total groups, the greatest increase in abundance is seen over the calcareous mudstones and the coccolith limestone, but other differences to the $CaCO_3$Free absolute abundance profiles are evident. Firstly the scale of the first peak abundance episode in the lower calcareous mudstone is somewhat reduced in relation to the second when compared to the same two peaks in the absolute abundance profiles. However, the most notable change is the large increase in abundance in the lower half of the upper calcareous mudstone after oil shale (3), which was not evident in the absolute abundance profiles (Figure 6.11). This is most prominent in the chorate dinocyst profile where peak cyst abundance reaches almost three times the level at the end of the limestone. All the oil shales display low $CaCO_3$Free abundances except for increases in FTL at the end of the shales.

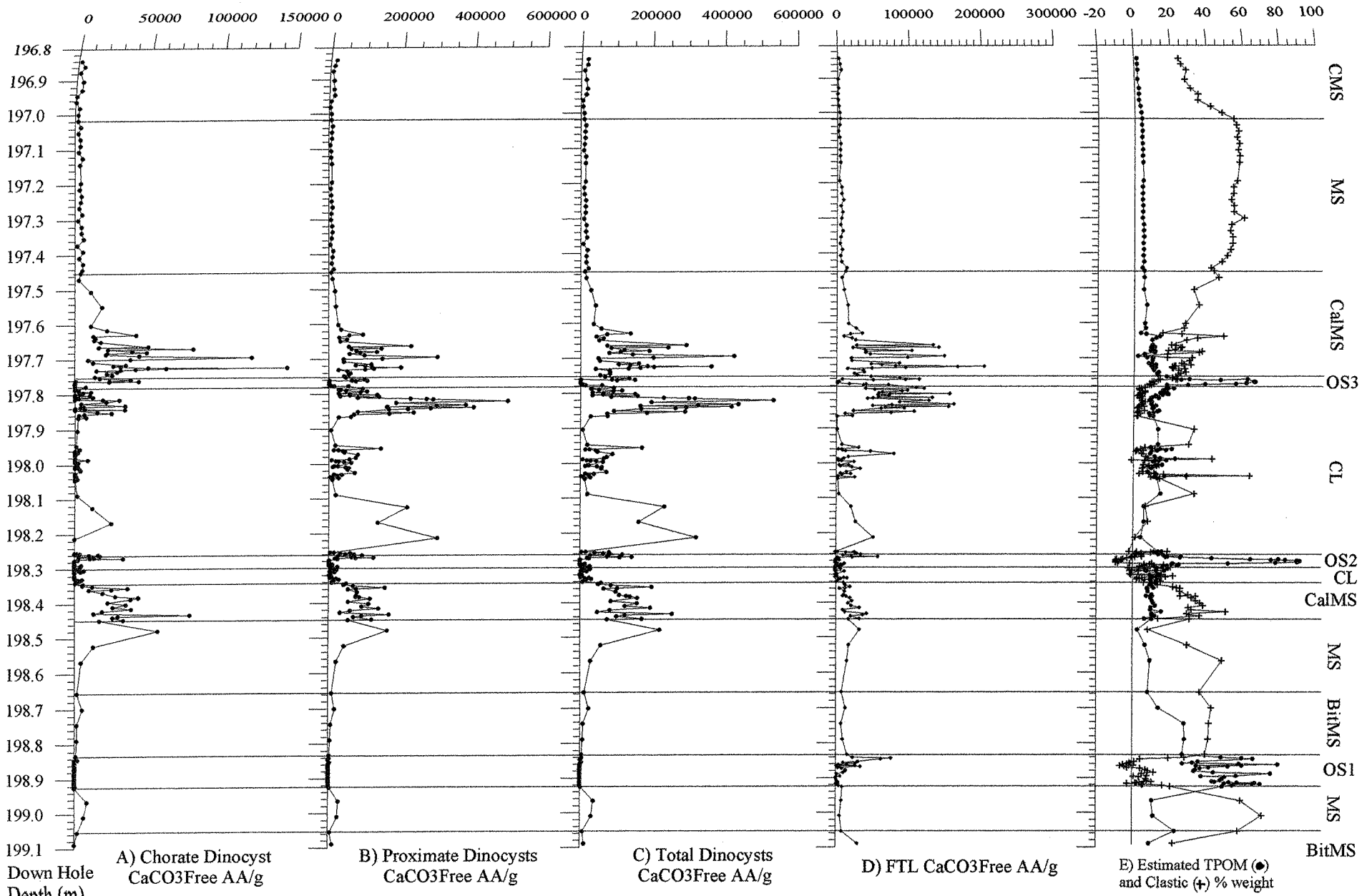

Figure 6.12 Vertical profiles of chorate, proximate and total dinocysts and foraminiferal test linings carbonate-free absolute abundance per gram of rock (CaCO3Free AA/g), and estimated TPOM (total organic matter + 'pyrite' organic matter) and clastics % weight over the Whitestone Band Interval. For lithology notation see Figure 6.8 caption.

6.3.2.3 Quantitative Comparisons of TMP Categories and Ratios.

Quantitatively the proximate dinocysts are the most abundant TMP particle type within the WSB interval, reaching an average of 40% of the TMP group and frequently attaining a maximum of 100% (Table 6.4). However, FTL are also abundant and like the proximate dinocysts occasionally reach a maximum of 100% within the TMP group, and an average of 37%. Chorate dinocysts are notably less abundant than either the proximate cysts or FTL, reaching a maximum of only 31% of the TMP group, and an average of 8%. Table 6.4 also shows the other categories, which have not been discussed and the lack of significant numbers of particles in these categories is quite clear. However, simple sacs are as abundant, if not slightly more abundant, than the chorate dinocysts but their unknown affinity, beyond a marine phytoplankton cyst, diminishes the usefulness of this category.

TMP PARTICLE CATEGORY	MINIMUM			MAXIMUM			AVERAGE		
		$CaCO_3$Free			$CaCO_3$Free			$CaCO_3$Free	
	AA/g	AA/g	G%	AA/g	AA/g	G%	AA/g	AA/g	G%
Chorate Dinocyst	0	0	0	31,000	145,000	31	2,000	10,000	8
Proxi-chorate Dinocyst	0	0	0	8,000	41,500	25	800	3,500	3
Proximate Dinocyst	0	0	0	67,000	492,000	100	9,000	51,000	40
Total Dinocyst	0	0	0	102,000	535,000	100	12,000	64,000	52
Foraminifera Test Lining	0	0	0	46,000	204,000	100	5,000	27,000	37
Simple Sac	0	0	0	10,500	150,000	67	1,000	6,000	9
Prasinophytes	0	0	0	1,000	6,000	10	24	95	0.2
Acritarchs	0	0	0	3,000	13,000	19	171	600	1

Table 6.4 Minimum, maximum and average absolute abundance (AA/g), carbonate-free absolute abundance ($CaCO_3$Free AA/g) and group percentage (G%) for the individual particle categories in the TMP group over the WSB interval.

Within the TMP group the relative (%) abundance of the chorate and proximate dinocysts and FTL particle categories were assessed using $\log_{10}$ ratios between pairs of categories (Figure 6.13). The first ratio of chorate against proximate dinocysts shows the overall dominance of the proximate cysts, especially over the coccolith limestone, though these morphotypes are similar in importance in the upper mudstone and cementstone (Figure 6.13A). This pattern is also strongly evident in the ratio of chorate against total dinocysts (Figure 6.13B). However, values are less negative in the oil shales, either implying an increase in chorate cysts or a decrease in other morphotypes. This may indicate a slight relative increase in the chorate dinoflagellate population in the highly stable marine environment during the oil shale deposition. Against FTL, chorate cysts are seen to lack dominance over the majority of the coccolith limestone and in the oil shales, but these two particle types are generally similar in the upper

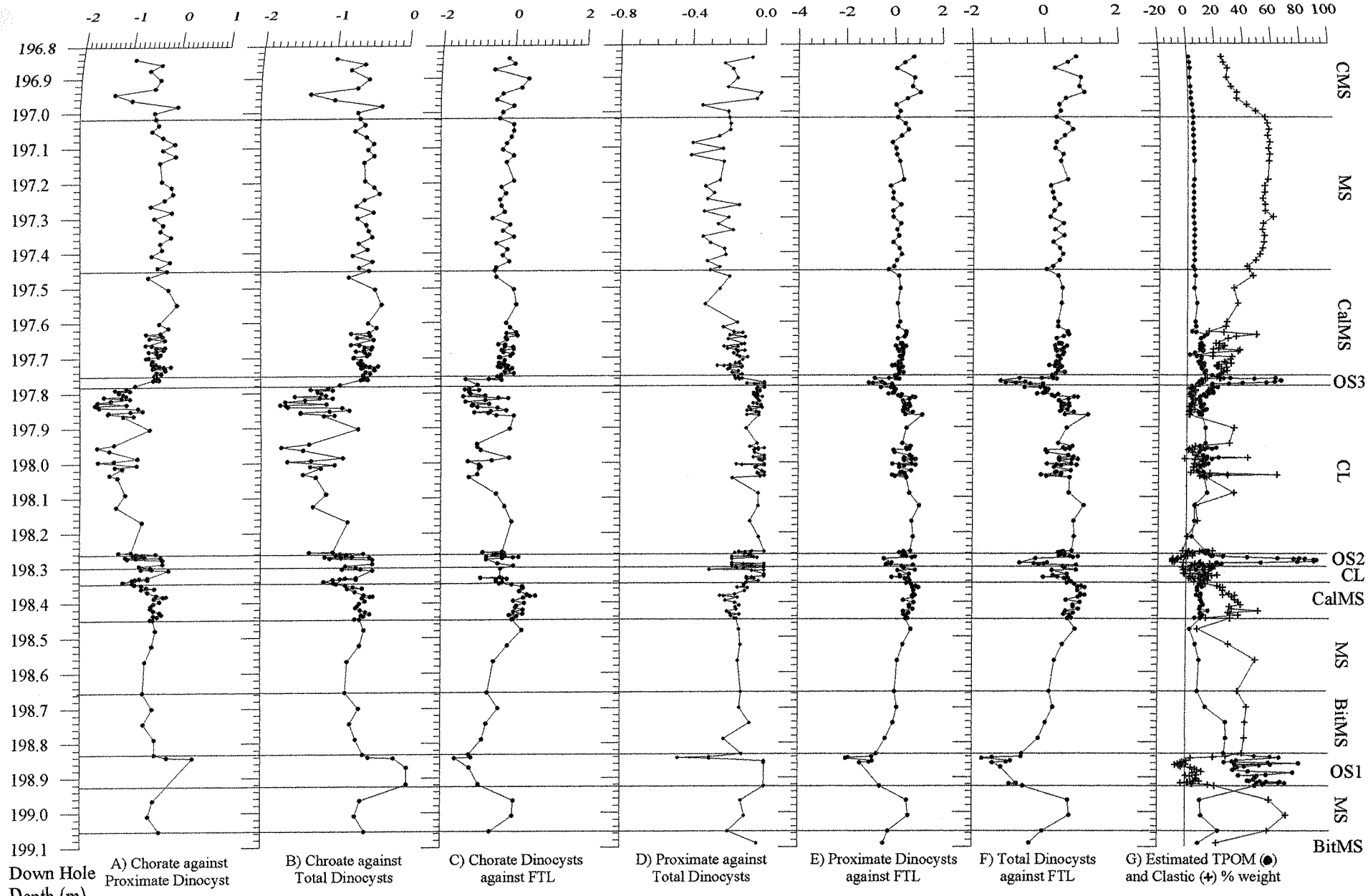

Figure 6.13 Selected ratios of individual categories within the TMP group as vertical profiles and estimatedTPOM (total organic matter + 'pyrite' organic matter) and clastics % weight over the Whitestone Band Interval. For lithology notation see Figure 6.8 caption.

portion of the interval (Figure 6.13C). The ratio of proximate cysts to total dinocysts also clearly highlights the dominance of this morphotype during the coccolith limestone, but a reduction in importance over the remainder of the interval, especially after oil shale (3) (Figure 6.13D). Against FTL, proximate cysts are more dominant except for the oil shales where FTL are clearly important especially towards the end of these lithologies (Figure 6.13E). This pattern is also shown by the ratio of total dinocysts to FTL (Figure 6.13F).

6.3.2.4 Summary

Despite being the least abundant of all the major groups, the TMP group allows an insight into both the phytoplankton structure of the KCF surface waters during the WSB interval and the bottom water oxygen levels. The phytoplankton (excluding coccolithophores), are seen to be dominated by dinoflagellates, with those species producing proximate cysts generally being the most abundant. These proximate cysts dominate the coccolith limestone indicating unstable marine conditions over this time, while other dinoflagellates producing chorate cysts are more prominent in other lithologies suggesting more stable conditions during these periods. FTL are also abundant over the interval, especially at the end of the oil shales, where they are taken to indicate a change in bottom water conditions from anoxic to suboxic, or re-deposition during a storm re-suspension event, which resulted in water column overturn and cessation of oil shale deposition.

All these categories essentially display the same abundance profiles over the WSB interval with low abundance in the oil shales and two episodes of increased abundance in the lower calcareous mudstone and at the end of the coccolith limestone. The lack of dinocysts in the oil shales is believed to be due to a low dinoflagellate population and stable conditions, which did not promote encystment and the low FTL due to anoxic bottom waters throughout the majority of these periods. Conversely the two episodes of peak abundances for all the categories are suggested to be the result of storminess which produced stressful conditions for the phytoplankton thus increasing cysting, and the re-deposition of FTL from the shelf. Removal of carbonate results in a clear differentiation in size between these two 'storm' episodes, with the largest being at the end of the limestone, and thus probably the most detrimental to the phytoplankton. Abundances are also seen to increase in the lower half of the upper calcareous mudstone with carbonate removal suggesting continuing storm activity, which perhaps helped to prevent coccolithophore populations re-establishing their former bloom abundances. Thus both the dinocysts and FTL data over the WSB interval seem to support the idea of storm driven event instability, which was possibly a factor in controlling the coccolith limestone deposition.

6.3.3 TERRESTRIAL PALYNOMORPHS

The terrestrial palynomorph group (TTP) was found to be the second most abundant group of particles within the WSB interval. This group is divided into pollen and spores, and the pollen was further categorized into three more specific types, inaperturate, *Classopollis* and bisaccate pollen (Table 5.2, Section 5.3.5). Similar to the TMP group two categories were not particularly abundant in raw counts, these being bisaccate pollen and spores. However, despite the reduced confidence in these categories, these particles will be briefly mentioned to provide a contrast to the other pollen types.

6.3.3.1 Absolute Abundance and $CaCO_3$Free Absolute Abundance Vertical Profiles

Vertical profiles of inaperturate, total *Classopollis* and bisaccate pollen and spores absolute abundance over the WSB interval again display low abundance during the oil shales and two peak abundance episodes in the lower calcareous mudstone and at the end of the limestone (Figure 6.14). However, the bisaccate and spore profiles also show an increase after oil shale (3) to the upper calcareous mudstone/mudstone boundary before values decline over the cementstone (Figure 6.14C and D). Interestingly there are also short-lived peaks evident for all categories at the very end of the oil shales. This was seen in the FTL profile and taken to indicate a change from anoxic to suboxic bottom water conditions. However, this same feature in the TTP profiles suggests that there was also a pulse of terrestrial material from the shelf into the basin at these times; therefore some of the FTL may have been re-deposited. It is also conceivable that the short but probably intense storm periods that resulted in these terrestrial pulses could have caused the overturn of the stratified basin and thus caused the cessation of oil shale deposition.

The strong similarity between the pollen and spore category profiles, especially the peak abundance episodes, reinforces the hypothesis that this material was brought into the distal marine environment in unsorted pulses. The increase after oil shale (3) for the bisaccate and spores, which is correlated to an increase in clastics, suggests a less distal depositional environment, as spores are generally found to be more abundant in more proximal sediments (Tyson, 1989, Section 5.3.6.2 iv)). However, bisaccate grains are usually assumed to increase distally (Mudie, 1982, Section 5.3.6.2 iii)), but they can be strongly affected by differential sorting effects. Both the inaperturate and total *Classopollis* pollen show very similar profiles, which is to be expected considering the probable common source of these pollen types and their similar size and thus sorting characteristics (Section 5.3.6.2 i) and ii)).

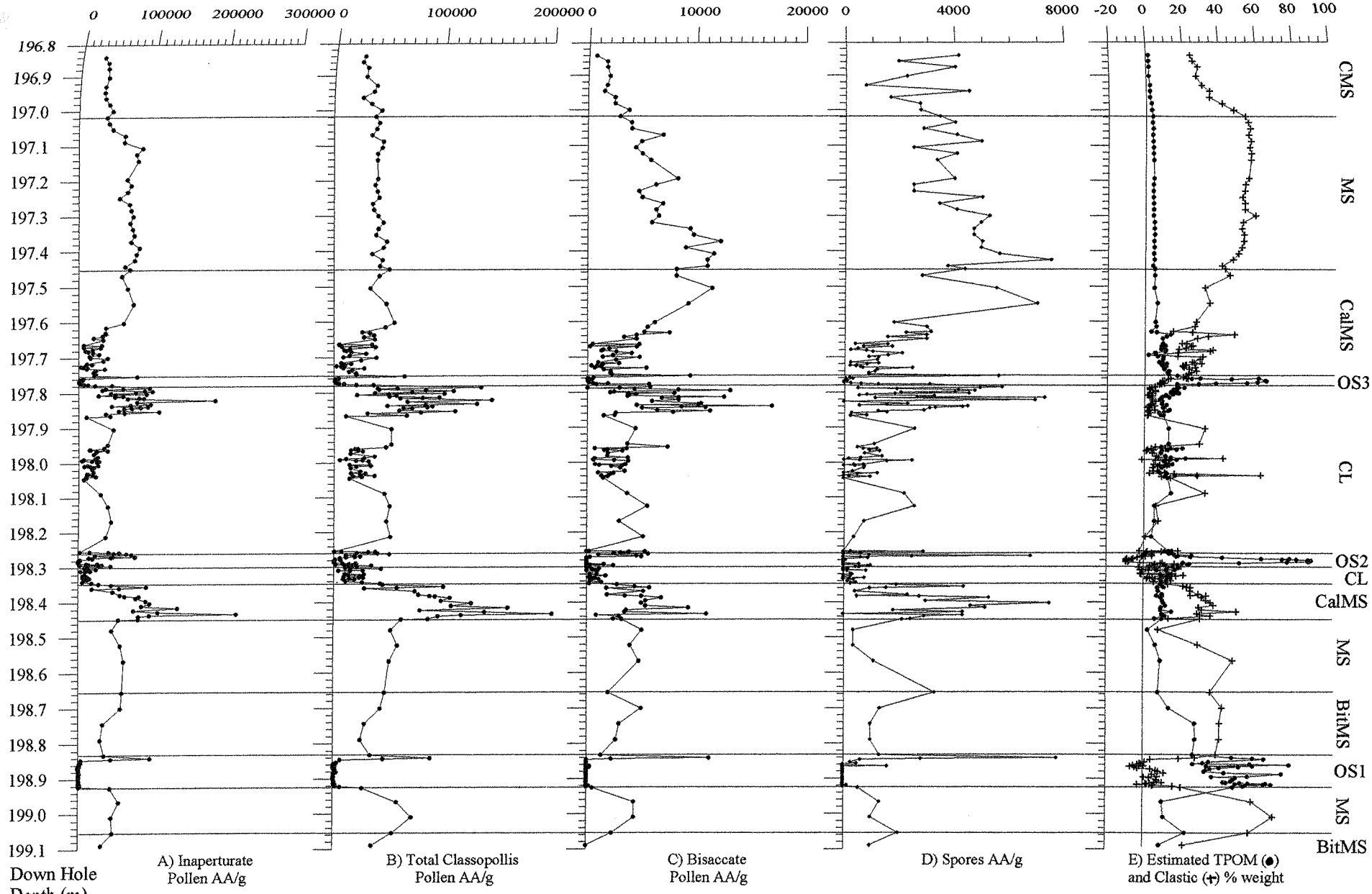

Figure 6.14 Vertical profiles of inaperturate, total Classopollis and bisaccate pollen and spore absolute abundance per gram of rock (AA/g), and estimated TPOM (total organic matter + 'pyrite' organic matter) and clastics % weight over the Whitestone Band Interval. For lithology notation see Figure 6.8 caption.

When these categories are plotted as carbonate-free absolute abundances a similar situation to the TMP profiles is seen (Figure 6.15). The first peak abundance episode is diminished in scale with respect to the second peak episode at the end of the coccolith limestone, and there is a third episode of peak abundances after oil shale (3). This reinforces the hypothesis that episode one was smaller than episode two and thus less stressful to the phytoplankton, and also that high-intensity storm conditions still occurred after oil shale (3), which may have prevented the re-establishment of the coccolithophore blooms.

6.3.3.2 Quantitative Comparisons of TTP Categories and Ratios

Inaperturate pollen, closely followed by total *Classopollis* pollen, dominates the TTP signal (Table 6.5). Both of these pollen types commonly reach a maximum of 100% of the TTP group and on average inaperturate pollen are 48% of this group, while *Classopollis* reach 46%. In comparison, bisaccate pollen is much reduced, only reaching a maximum of 17% of the total TTP group and an average of 4%. Similar figures are evident for the spores, though they do attain a slightly greater maximum of 33%, but a smaller average of 3%. The inaperturate and *Classopollis* pollen are probably dominant for two reasons. Firstly these pollen are believed to have been produced by plants of coniferalean affinity which generate high numbers of pollen for wind dispersal. Secondly the small size and buoyancy of these spherical pollen grains enables considerable transportation by both fluvial and aeolian mechanisms before deposition (Tyson, 1984; Section 5.3.6.2 ii)). Hence these two pollen categories dominate the more distal basin terrestrial palynomorph signal and also dilute other pollen species. Despite this bias it can be said that the regional vegetation of the Wessex Basin hinterland was probably dominated by conifers which produced both inaperturate and *Classopollis* pollen, though certain species produced bisaccate pollen, and in suitable sites, spore producing plants were also present.

TERRESTRIAL PALYNOMORPHS	MINIMUM $CaCO_3$Free			MAXIMUM $CaCO_3$Free			AVERAGE $CaCO_3$Free		
	AA/g	AA/g	G%	AA/g	AA/g	G%	AA/g	AA/g	G%
Inaperturate Pollen	0	0	0	215,000	1424,000	100	35,000	163,000	48
Fresh *Classopollis*	0	0	0	171,000	931,000	100	28,000	131,000	33
Degraded *Classopollis*	0	0	0	29,000	172,000	100	6,000	25,000	13
Total *Classopollis*	0	0	0	199,000	1102,000	100	33,000	156,000	46
Bisaccate Pollen	0	0	0	17,000	109,000	17	3,000	15,000	4
Total Pollen	0	0	0	425,000	2590,000	100	71,000	332,000	97
Spores	0	0	0	8,000	75,000	33	2,000	7,000	3

Table 6.5

Minimum, maximum and average absolute abundance (AA/g), carbonate-free absolute abundance ($CaCO_3$Free AA/g) and group percentage (G%) for the individual particle categories in the TTP group over the WSB interval.

Classopollis-bearing plants are commonly taken to infer arid conditions (Section 5.3.6.2 ii). Also the percentage of *Classopollis* pollen of the total pollen has been used to estimate climatic regimes of sediments, such that 1-10% *Classopollis* pollen of the TTP group is an indication of temperate conditions, 20-50% warm to subtropical conditions and 60-90% semi-arid to arid conditions (Vakhrameev, 1981). Table 6.6 shows the average and maximum group percentages of *Classopollis* pollen for the different lithologies within the WSB interval. All the average percentages suggest a warm subtropical climatic regime was dominant throughout the interval, but maximum figures are more suggestive of semi-arid to arid conditions. This is especially the case during the oil shale and coccolith limestone lithologies. However, it must be remembered that the pollen within the coccolith limestone is assumed to have been deposited in this lithology as the result of re-suspension of material from the shelf and therefore may not be representative of the climate during the limestone deposition.

LITHOLOGY	TOTAL *CLASSOPOLLIS* AVERAGE G%	TOTAL *CLASSOPOLLIS* MAXIMUM G%
Mudstone	41	59
Cementstone	43	51
Oil Shale	44	100
Bituminous Mudstone	45	52
Calcareous Mudstone	46	60
Coccolith Limestone	52	97

Table 6.6

Average and maximum TTP group percentages for total *Classopollis* pollen.

The size of bisaccate pollen is also used to assess environmental conditions as an indicator of proximal/distal trends in marine sediments, where it is assumed that smaller pollen are carried further offshore than larger pollen grains. Bisaccate width and length measurements were therefore taken during particle counts (Section 5.3.6.2 ii), Figure 5.4) to ascertain if the WSB interval showed any proximal/distal trends. Figure 6.16 shows the results of these measurements. There is no obvious change in either the width or length profiles over the WSB interval (Figure 6.16A and B), but by taking the square root of the area of the bisaccate pollen, a slight increase in size over the calcareous mudstone and coccolith limestone lithologies is evident. This would agree with the hypothesis that terrestrial palynomorphs were being re-

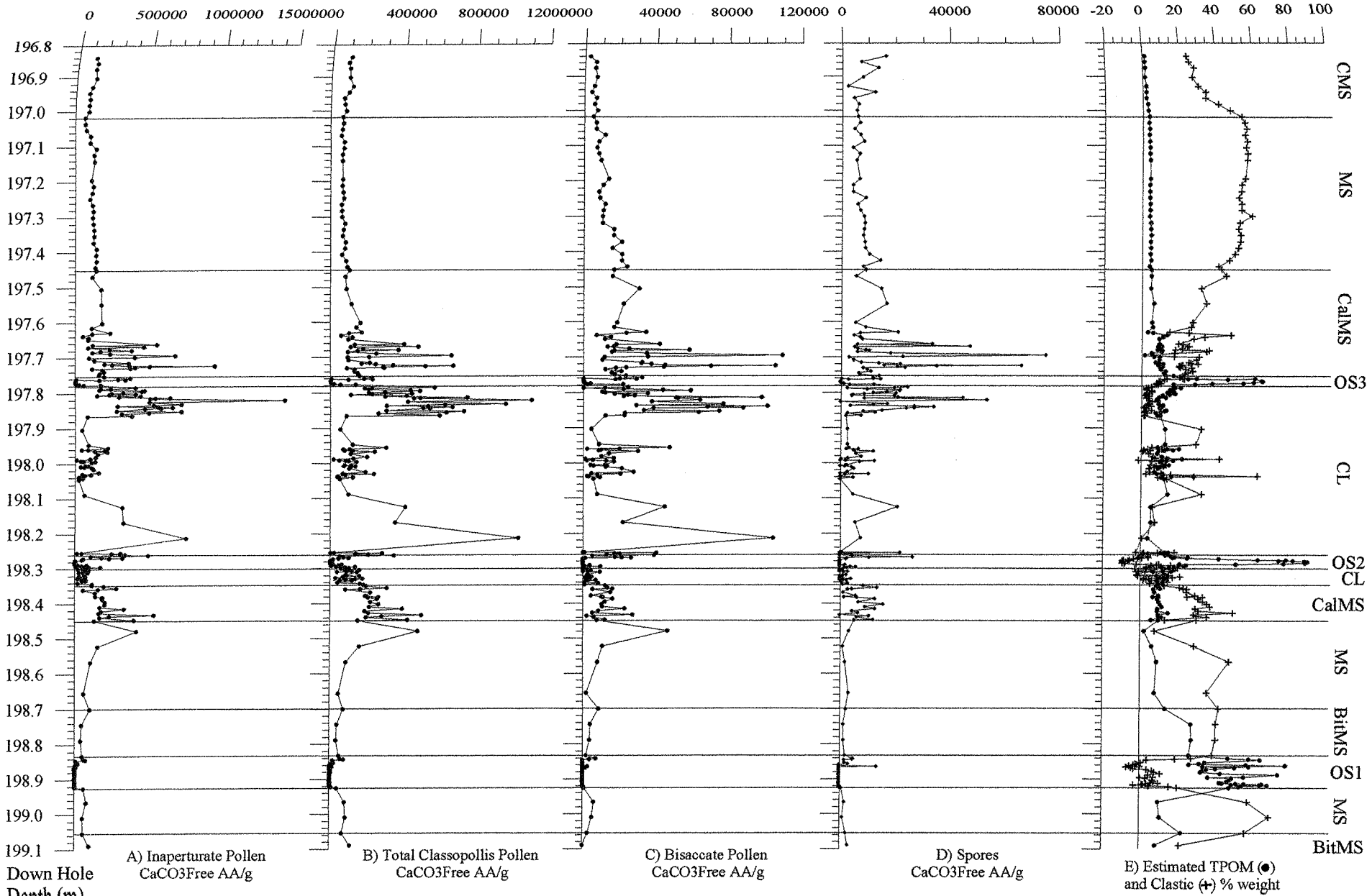

Figure 6.15 Vertical profiles of inaperturate, Classopollis and bisaccate pollen and spores carbonate-free absolute abundance per gram of rock (CaCO3Free AA/g), and estimated TPOM (total organic matter + 'pyrite' organic matter) and clastics % weight over the Whitestone Band Interval. For lithology notation see Figure 6.8 caption.

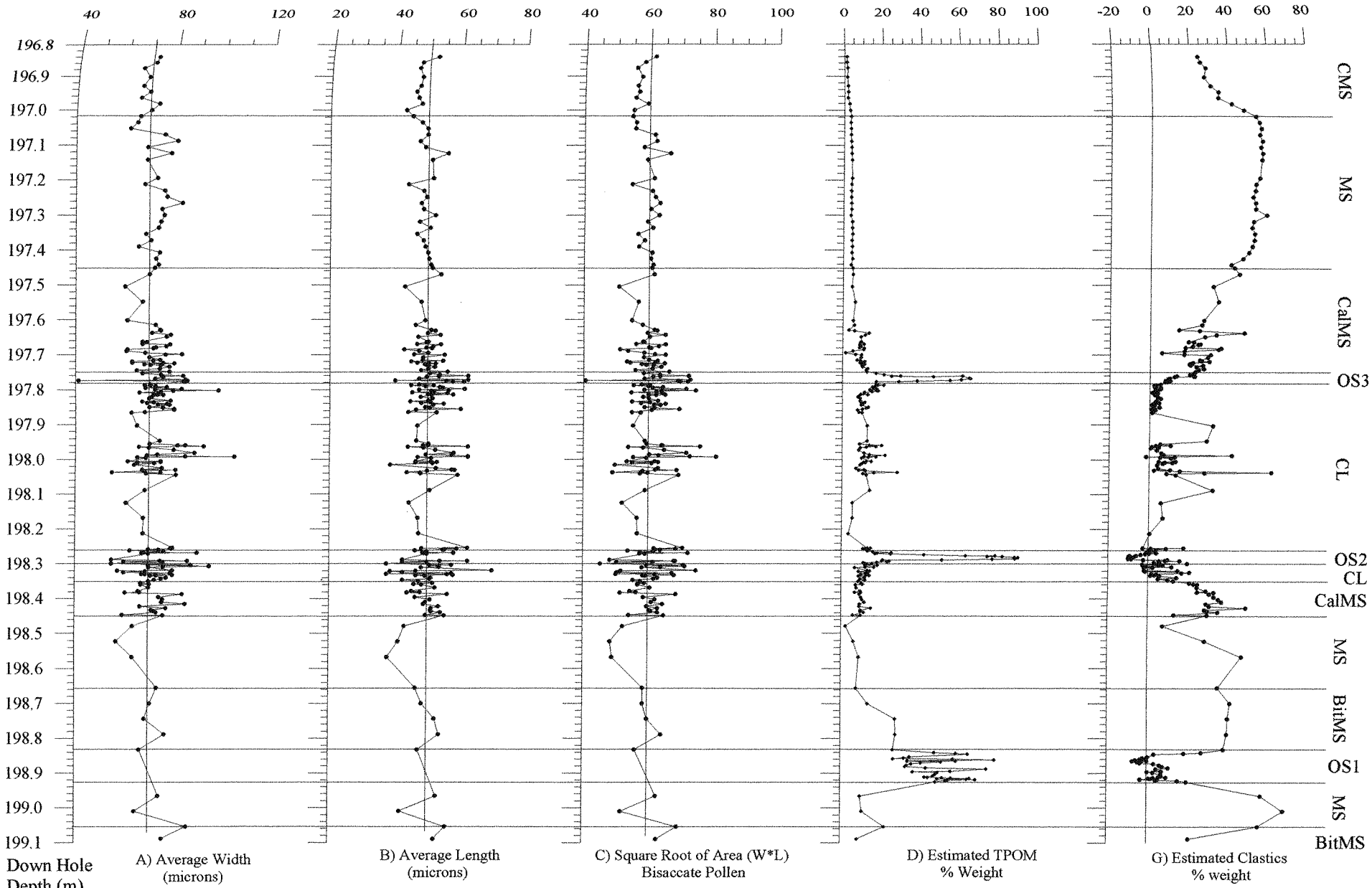

Figure 6.16 Measurements of bisaccate pollen to determin proximal/distal relationships and estimated TPOM (total organic matter + 'pyrite' organic matter) and clastics % weight over the Whitestone Band Interval. For lithology notation see Figure 6.8 caption.

deposited from the shelf into the distal basin at the same time as the larger pollen grains, which under less extreme conditions would be deposited in a proximal setting, are mixed with other palynomorphs and deposited in the distal basin.

Ratios between TTP categories, and against total dinocyst were also calculated to evaluate the relationship between particle types (Figure 6.17). The dominance of the terrestrial palynomorphs over the whole WSB interval is highlighted by the ratio of total dinocysts against total pollen, with highly negative values throughout (Figure 6.17A). Within the TTP group, the inaperturate pollen and *Classopollis* pollen are the most dominant and the ratio of these two categories shows that they are generally of similar importance, though some variability is evident in oil shales (1) and (2) and the lower coccolith limestone (Figure 6.17B). *Classopollis* pollen counts were divided into fresh and degraded forms to determine if there was any variation in the state of degradation of this pollen in different lithologies. The ratio of fresh to degraded *Classopollis* clearly indicates that the fresh forms were dominant, apart from within the oil shales, where values become negative. This increase in importance of degraded forms implies increased degradation possibly as a result of reworking or increased residence time at the sediment/water interface during these depositional periods. Lastly the ratio of bisaccate pollen to spores shows that bisaccate pollen are commonly more dominant over the interval but the profile is relatively variable possibly indicating fluctuations in production and differential sorting of these particles, as well as effects of the low counts for these categories.

6.3.3.3 Summary

The terrestrial palynomorphs within the WSB interval are dominated by small spherical pollen of inaperturate and *Classopollis*, while bisaccate pollen and spores are poorly represented. This may indicate the composition of the regional flora, but the pollen record is likely to be bias towards the small spherical types due to their production in large numbers and ability to be transported over large distances to the distal marine environment. However, despite these abundance differences, a generally similar profile is seen for all the categories over this interval with lower abundance in the oil shales, and peak abundance episodes in the lower calcareous mudstone and at the end of the coccolith limestone. Carbonate-free abundance profiles also imply that a third episode of peak abundances occurred after oil shale (3). Thus these profiles suggest that the terrestrial palynomorphs entered the distal marine environment in unsorted pulses thus supporting the hypothesis that they resulted from storm re-suspension events. The very low abundances of all the terrestrial palynomorphs in the oil shales also support the lack of terrestrial input envisaged during these depositional periods (Section 4.11.1, Figure 4.5A).

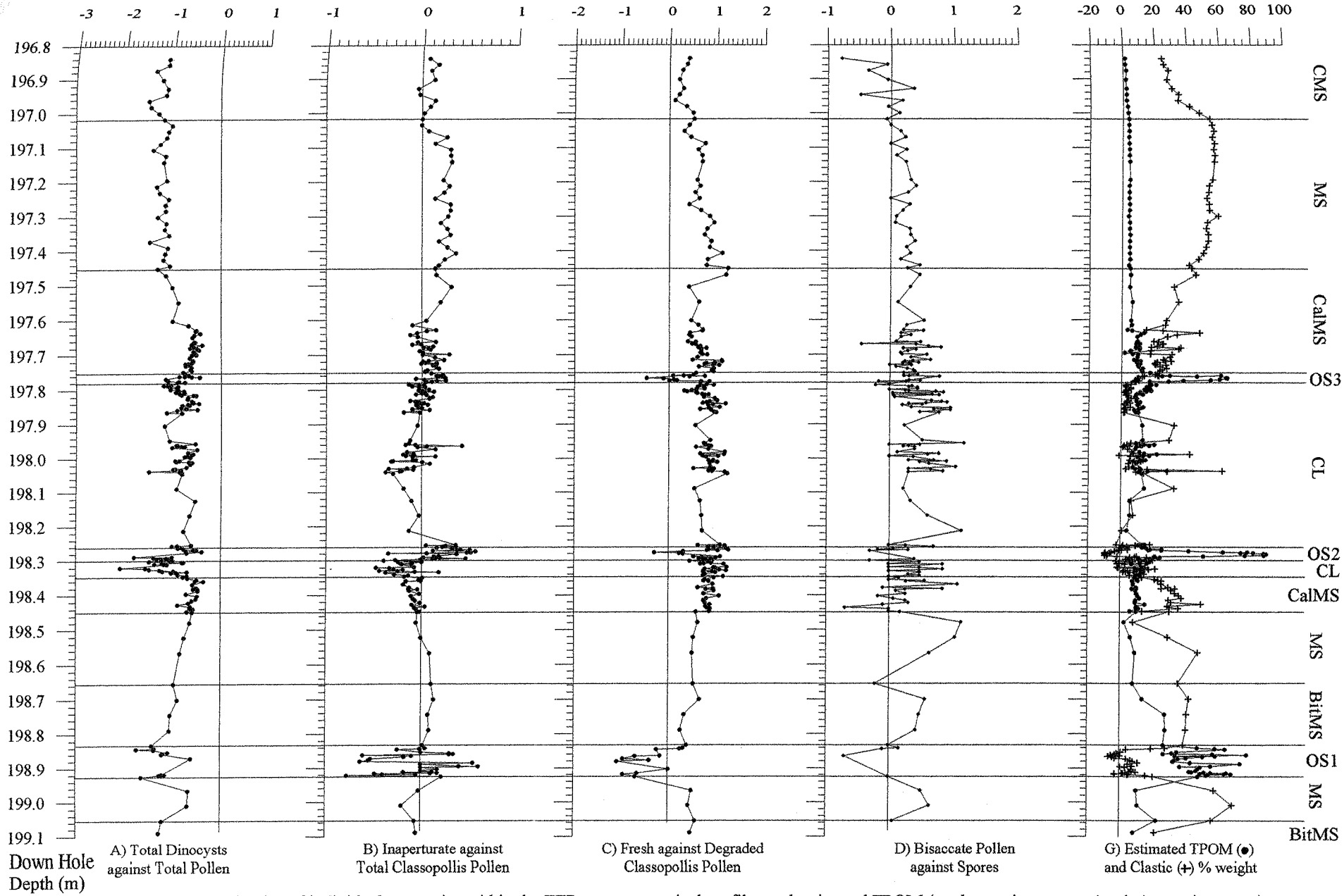

Figure 6.17 Selected ratios of individual categories within the TTP group as vertical profiles and estimated TPOM (total organic matter + 'pyrite' organic matter) and clastics % weight over the Whitestone Band Interval.For lithology notation see Figure 6.8 caption.

6.3.4 TERRESTRIAL STRUCTURED DEBRIS

The terrestrial structured debris group (TSD) was the most abundant group within the WSB interval. This group is divided into phytoclasts and cuticle, though cuticle was not significantly abundant in raw counts to enable reliable interpretation and is therefore not discussed. The phytoclast category was further divided into lath and equidimensional phytoclasts, which were both split into two colour categories of black and dark types and brown/stripy and light particles. An unknown category was also counted which was composed of unidentifiable or degraded structured particles. Though this category includes particles from all the major groups it will be mentioned here.

6.3.4.1 Absolute Abundance and $CaCO_3$Free Absolute Abundance Vertical Profiles

The vertical absolute abundance profiles for total phytoclast laths and total equidimensional phytoclasts are displayed in Figure 6.18 (A and D) and it is clear that both these phytoclast shapes show almost identical profiles. Again, as in all the other groups, abundances are lower in the oil shales and two episodes of peak abundances occur in the lower calcareous mudstone and at the end of the coccolith limestone. Also notable are short-lived peaks at the end of the oil shales, which support similar pulses seen in the TTP profiles. The storm periods indicated by these short, sharp pulses probably resulted in the termination of the oil shale by breaking down the stratification. Within the oil shales, abundances are reduced but not to the level seen for the other groups, due to the highly resistant nature of these particles and their ability to be seen through the AOM dominating these lithologies. Profiles of black/dark laths and brown/stripy/light laths also show identical profiles, again reinforcing the idea of a completely unsorted flux of terrestrial material into the distal basin. The unknown category also shows a generally similar profile with the largest abundance correlated with the peak abundance episodes of the other categories. This is as expected, especially as the terrestrial material is deposited as pulses of unsorted particles. It is highly probable that the number of degraded particles in these pulses is also high.

Carbonate-free absolute abundance profiles for the TSD group categories (Figure 6.19) show similar results to the other group categories. The peak abundance episode in the lower calcareous mudstone is less obvious, while the second peak at the end of the limestone dominates and a third peak abundance episode is present in the lower half of the upper calcareous mudstone after oil shale (3).

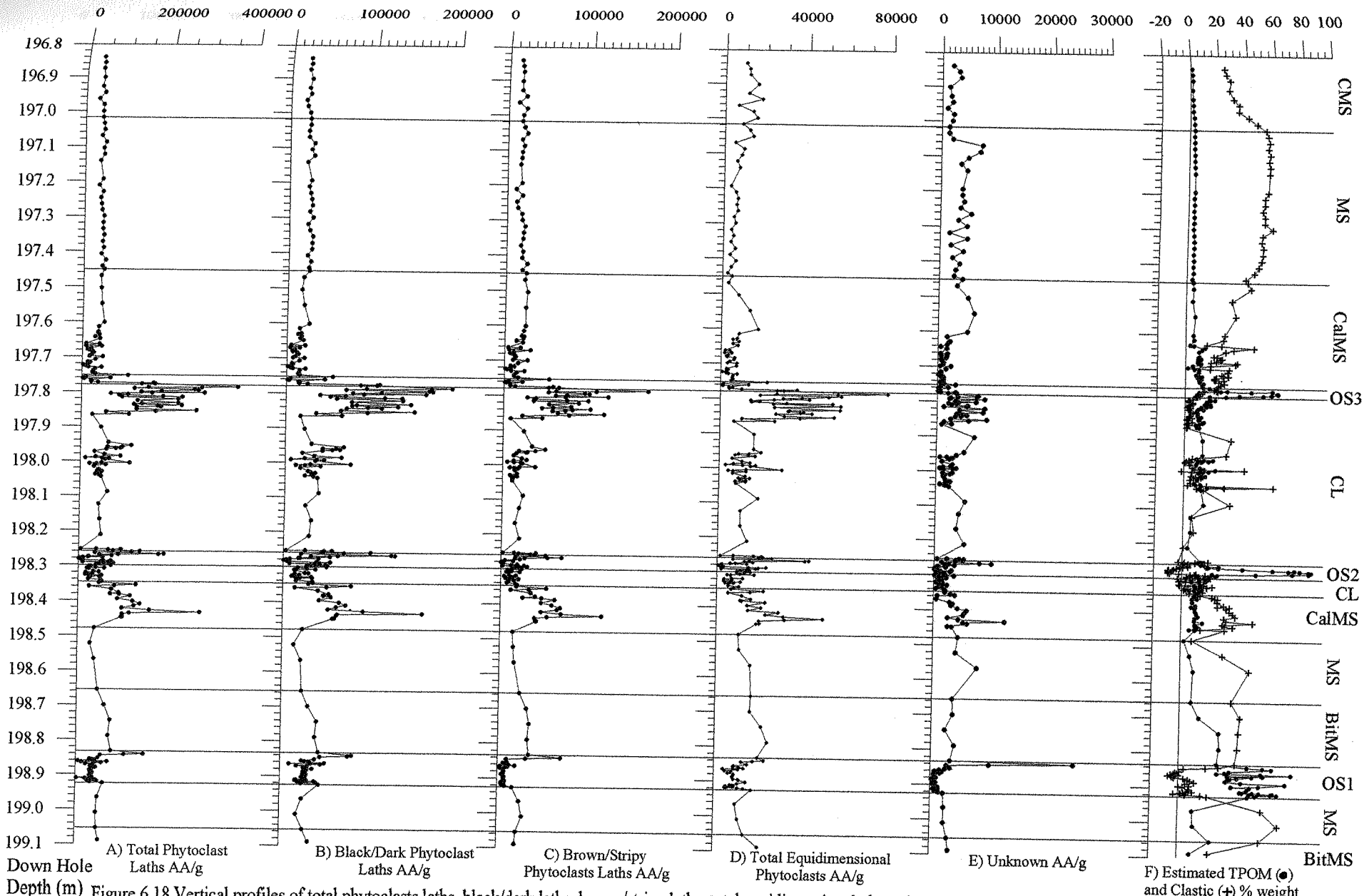

Figure 6.18 Vertical profiles of total phytoclasts laths, black/dark laths, brown/stripy laths, total equidimensional phytoclasts and unknown particles absolute abundance per gram of rock (AA/g), and estimated TPOM (total organic matter + 'pyrite' organic matter) and clastics % weight over the Whitestone Band Interval. For lithology notation see Figure 6.8 caption.

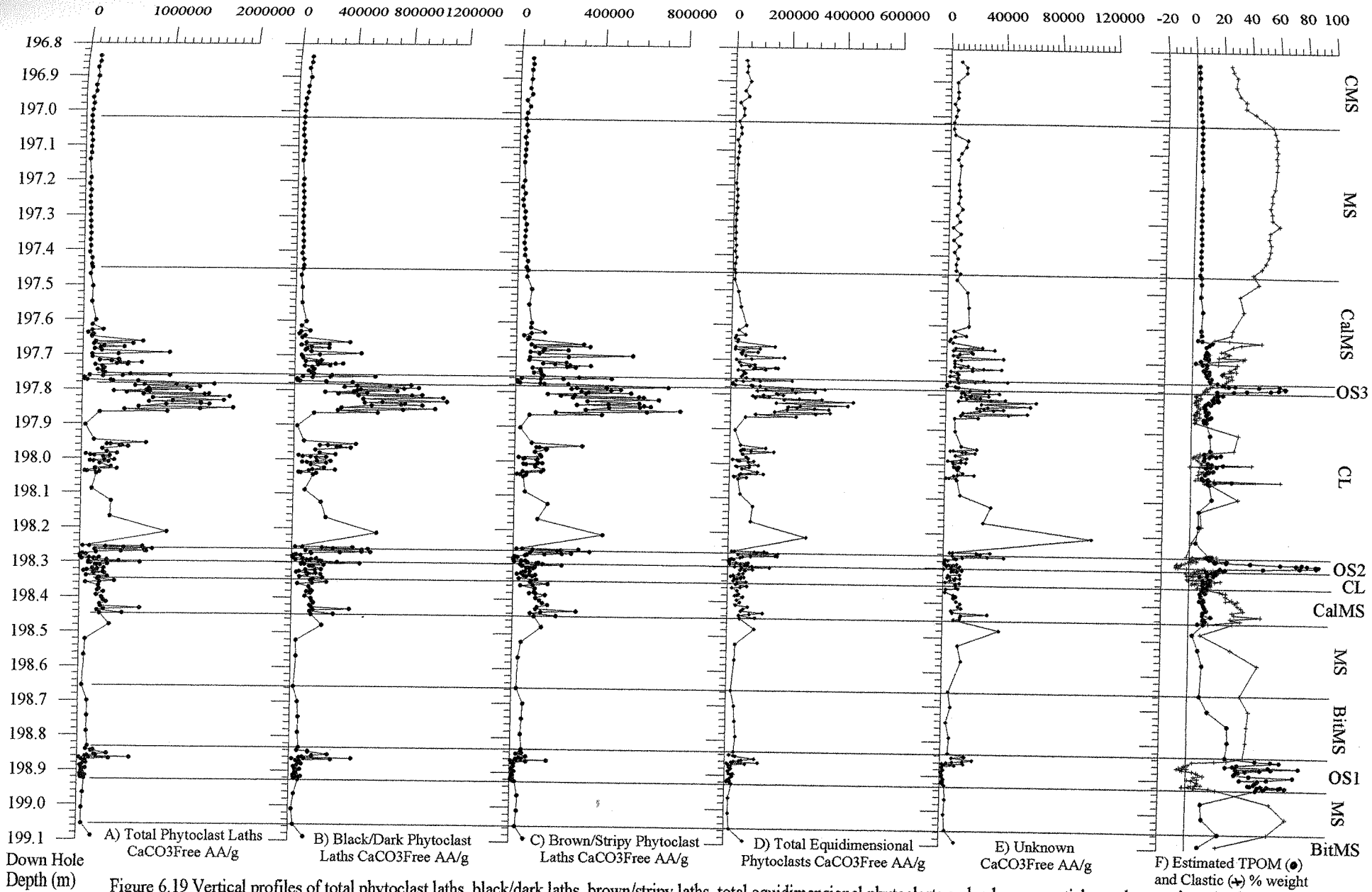

Figure 6.19 Vertical profiles of total phytoclast laths, black/dark laths, brown/stripy laths, total equidimensional phytoclasts and unknown particles carbonate-free absolute abundance per gram of rock (CaCO3Free AA/g), and estimated TPOM (total organic matter + 'pyrite' organic matter) and clastics % weight over the Whitestone Band Interval. For lithology notation see Figure 6.8 caption.

6.3.4.2 Quantitative Comparison of TSD Categories and Ratios

Lath phytoclasts are the most dominant of the TSD group over the WSB interval reaching an average of 82% and a maximum of 94% of the TSD group (Table 6.7). This abundance indicates that the environment of deposition was distal as phytoclast particles become increasingly lath-shaped distally (Parry *et al.*, 1981; Tyson, 1989). Conversely, equant phytoclasts are considerably less abundant, reaching an average of only 18%, and a maximum of 33%. The distality of the depositional environment is also suggested by the lack of cuticle. For both lath and equant phytoclasts the black/dark coloured types are the most abundant (Table 6.7). This implies that the majority of the phytoclasts have undergone significant oxidation during transport to and in the marine environment. It is also possible that some of the opaque laths are the result of carbonization, but charcoal was not possible to differentiate in transmitted light counts. However, it is likely that fires were relatively common on the hinterland and charcoal fragments were frequently transported into the marine environment together with oxidized phytoclasts

TERRESTRIAL STRUCTURED DEBRIS	MINIMUM			MAXIMUM			AVERAGE		
		$CaCO_3$Free			$CaCO_3$Free			$CaCO_3$Free	
	AA/g	AA/g	G%	AA/g	AA/g	G%	AA/g	AA/g	G%
Black/Dark Laths	500	4,000	30	196,000	1088,000	72	40,000	189,000	50
Brown/Stripy Laths	200	1,000	12	172,000	788,000	60	26,000	129,000	32
Total Phytoclast Laths	700	5,000	67	368,000	1792,000	94	66,000	318,000	82
Black/Dark Equants	170	1,000	3	43,000	332,000	27	9,000	43,000	12
Brown/Stripy Equants	0	0	0	37,000	159,000	17	5,000	23,000	6
Total Equants	300	2,000	5	79,000	439,000	33	14,000	66,000	18
Cuticle	0	0	0	704	4,000	7	14	100	0.05

Table 6.7

Minimum, maximum and average absolute abundance (AA/g), carbonate-free absolute abundance ($CaCO_3$Free AA/g) and group percentage (G%) for the individual particle categories in the TSD group over the WSB interval.

The ratio of total dinocysts to total phytoclasts laths shows the dominance of the phytoclasts over the whole interval and especially over the oil shales (Figure 6.20A). Though total pollen is more dominant than the total lath phytoclasts, the laths again are clearly dominant in the oil shales (Figure 6.20B). Over the entire interval, total phytoclast laths are found to be more important than the total equidimensional phytoclasts, as seen from the ratio of these two categories (Figure 6.20C). Black/dark laths are also seen to dominate over much of the interval,

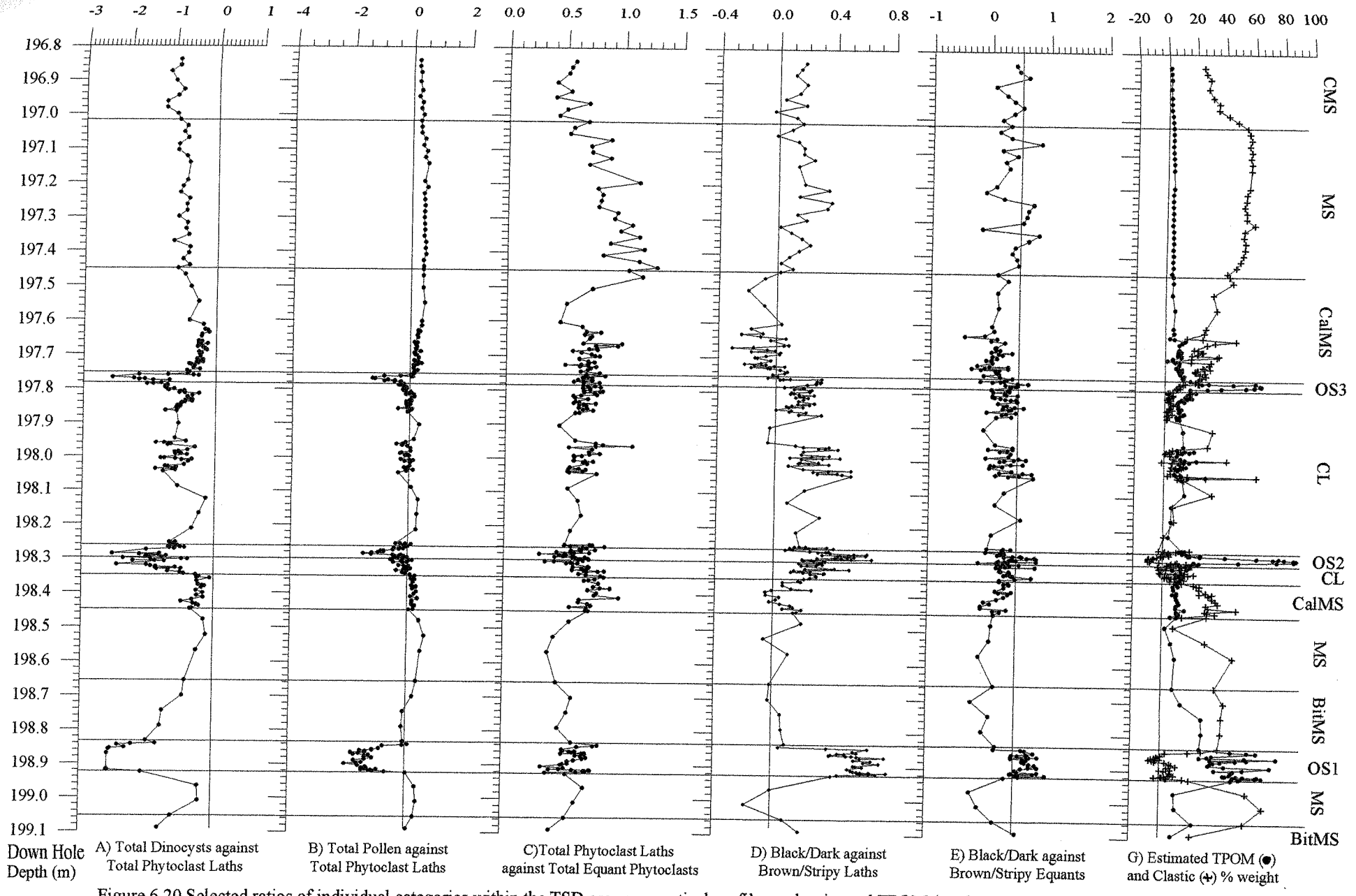

Figure 6.20 Selected ratios of individual categories within the TSD group as vertical profiles and estimated TPOM (total organic matter + 'pyrite' organic matter) and clastics % weight over the Whitestone Band Interval. For lithology notation see Figure 6.8 caption.

especially in the oil shales; however, after oil shale (3) values become negative, indicating an increase in the importance of the brown/stripy (unoxidized) phytoclast laths before values again become positive in the upper mudstone (Figure 6.20D). Lastly the ratio of black/dark to brown/stripy equants shows that the black types are generally more dominant, but both types are relatively similar (Figure 6.20E).

6.3.4.3 Summary

The dominance of the lath phytoclasts and lack of cuticle over the WSB interval suggest that the environment of deposition was distal. All TSD categories display almost identical profiles, especially during the peak abundance episodes, implying that the terrestrial structured debris, like the terrestrial palynomorphs, entered the marine environment unsorted. The amplitude and frequency of the peaks characterizing these episodes also support the hypothesis of high abundance pulses of unsorted particles from the shelf resulting from increased storm frequency and /or intensity. Smaller storm periods are also implied by the short-lived peaks at the end of all the oil shales and have been suggested to have resulted in the cessation of the oil shale deposition due to the breakdown of the water column stratification. The low abundances for all the TSD categories in the oil shales again supports a low sedimentation rate for this lithology, but these abundances are generally greater than the other major groups over these intervals. This is due to the highly resistant nature of the phytoclasts and that they can be seen to be counted despite abundant AOM. The dominance of black/dark phytoclasts also implies that the majority of the these particles had undergone significant oxidation, though it is possible that some may be charcoal, thus indicating that fires occurred on the hinterland, though this point is uncertain from this data. Thus, overall the TSD particles also support the idea of storm driven re-suspension events into the more distal marine environment, which possibly was a factor in the duration of the coccolith limestone deposition.

6.4 ENVIRONMENTAL RECONSTRUCTION AND SUMMARY

The different lithologies comprising the WSB interval were quantitatively defined by the TOC, carbonate and remainder % weight, and the detailed nature of sampling over certain sections resulted in highlighting the fine-resolution variability in both the coccolith limestone and the coccolith-rich oil shale (1). It was found that the high levels of coccolith carbonate had a significant dilutionary effect on the profile, especially over the calcareous mudstones and coccolith limestone. Thus, measures were taken to remove this carbonate so that carbonate-free TOC% and palynological particle abundances could be assessed. With the carbonate removed it was clear that the organic matter deposited during the coccolith limestone was of a similarly large amount as that present in the oil shales. This is not surprising, considering the level of primary production occurring during this interval. The presence of oil shales and their detailed sampling enabled an estimation of the clastic material in the remainder component of the samples and also the organic matter was corrected for the production of pyrite. This was significant as it enabled an estimate to be made of the flux of clastic material into the marine environment.

Atomic H/C ratios classified the kerogen within the WSB interval as type I to type II kerogen. Samples were seen to level off at 1.5 atomic H/C ratio and thus have attained optimal preservation conditions at low TOC percentages of between 5 and 10%. The lithologies of cementstone and mudstones did not reach this level of preservation, while coccolith limestone samples showed H/C ratios of the same level as the oil shales but at far lower TOC%. This was believed to represent the dominance of planktonic organic matter in both these lithologies. A slight difference was also ascertained between the three oil shales from the H/C data, which was interpreted as variability in the diagenetic processes resulting in AOM formation and preservation.

The most striking characteristic of the palynological analysis of this interval was the clear correlation between all the categories, from marine to terrestrial organic particles, suggesting a close interaction between the marine and terrestrial environments. In summary, the general palynological profile over this interval is composed of very low abundances during the oil shales and very high abundances in the calcareous mudstones and at the end of the coccolith limestone. The remaining lithologies generally display low to medium abundances, though the remainder of the coccolith limestone shows lower abundances. Thus, these profiles all suggest that both the terrestrial input and the marine phytoplankton populations were very low during the oil shale deposition, supporting the idea that sedimentation rates were low and the climate arid during these periods. Conversely, the situation of the peak abundances of unsorted particles

directly before the start of the limestone and at the end of the limestone is suggested to be related. The peak abundance episodes are believed to be the result of re-suspension of terrestrial material and clays from the shelf sediments by storms, which subsequently carried the material offshore and deposit it in the distal marine basin. Such events would have provided nutrients to the distal surface waters where the opportunistic coccolithophore populations could take advantage of them resulting in blooms. However, the intensity and frequency of these storm events are suggested to have been critical in the production of blooms and thus the deposition of the coccolith limestone. The first peak episode before the limestone is seen to be of a smaller scale than those at the end of the limestone and after oil shale (3). It is thus hypothesized that these latter episodes resulted in conditions that even the coccolithophores found stressful and thus bloom level production was prevented. Peaks in abundance of terrestrial organic material and FTL also suggest that storm events resulted in the cessation of the oil shale deposition, through overturn of the water column.

The results for the WSB interval geochemical and palynological analyses are summarized in Figure 6.21, together with notes on the environmental and climatic interpretations occurring over the interval.

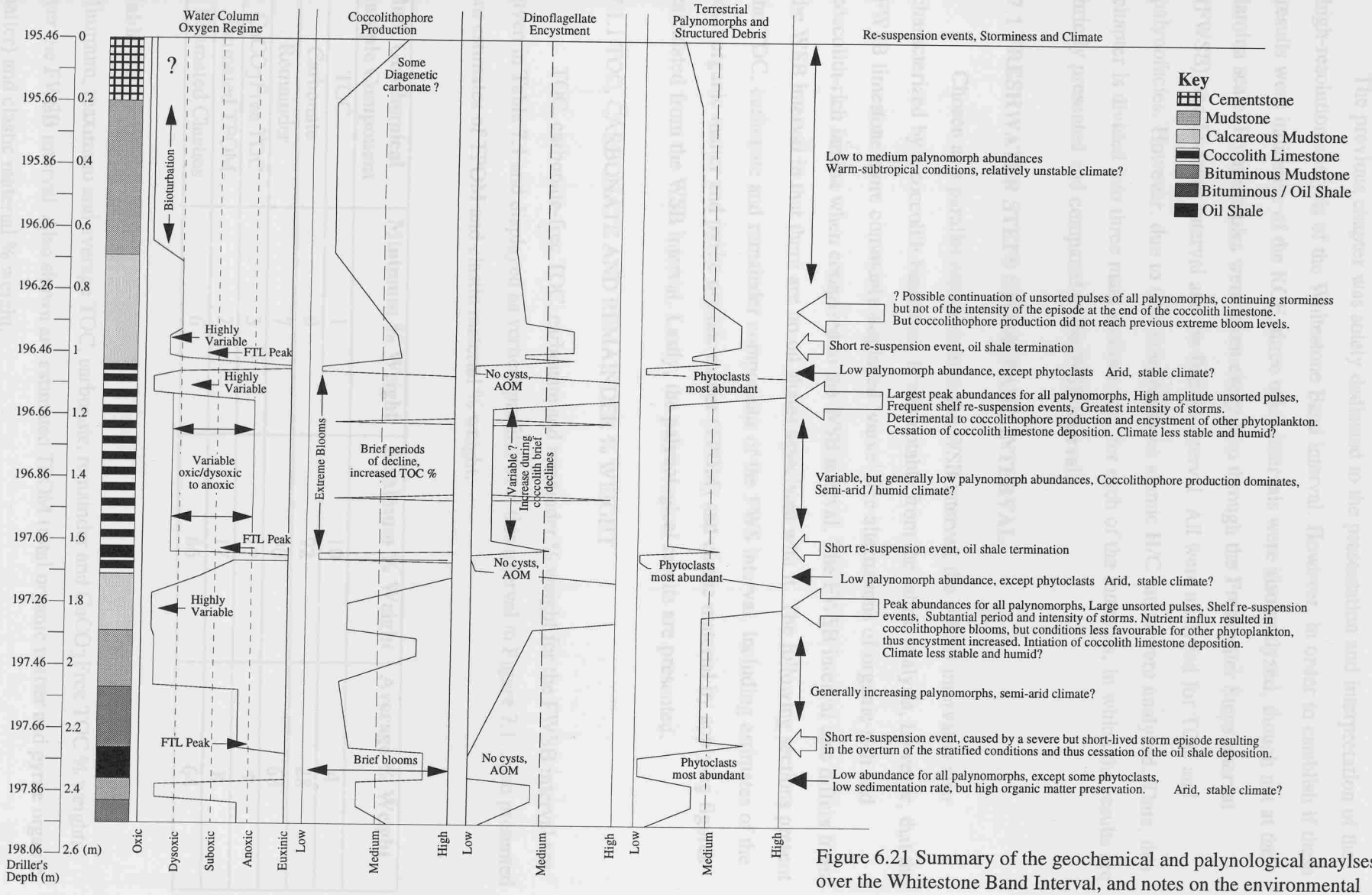

Figure 6.21 Summary of the geochemical and palynological anaylses over the Whitestone Band Interval, and notes on the environmental and climatic implication of these results.

7.0 GEOCHEMISTRY AND PALYNOLOGY RESULTS FOR OTHER KCF BANDS

The previous chapter was solely dedicated to the presentation and interpretation of the high-resolution analysis of the Whitestone Band interval. However, in order to establish if these results were indicative of the KCF, three other intervals were also analyzed, though not at the lamina scale. Point samples were taken every 5cm through the Freshwater Steps interval (FWSB), the *Eudoxus* interval and the Bed 44 interval. All were analyzed for TOC and palynofacies. However, due to time constraints no atomic H/C ratios were analyzed. Thus, this chapter is divided into three main sections, one for each of the intervals, in which the results are briefly presented and compared to the WSB interval.

7.1 FRESHWATER STEPS STONE BAND INTERVAL

Chosen as a parallel comparison to the WSB interval, the FWSB interval is also characterized by a coccolith limestone. It was notable from the fabric analysis, however, that the FWSB limestone more commonly displayed 'varve' like alternations of organic-rich and coccolith-rich lamina when compared to the WSB interval. The FWSB interval also differs from the WSB interval in that there are no oil shales associated with it. The following sections present the TOC, carbonate and remainder components of the FWS interval, including estimates of the total organic matter and pyrite organic matter (TPOM) and clastic material by applying figures calculated from the WSB interval. Lastly, the palynological results are presented.

7.1.1 TOC, CARBONATE AND REMAINDER % WEIGHT

TOC, carbonate-free TOC, carbonate and remainder % weight for the FWSB interval are given in Table 7.1 and displayed as vertical profiles over this interval in Figure 7.1. Also presented are estimates of TPOM and clastic material % weight.

Bulk Geochemical Sample Component	Minimum % Weight	Maximum % Weight	Average % Weight
TOC	1	10	4
Carbonate	0	92	28
Remainder	7	90	68
$CaCO_3$Free TOC	3	17	7
Estimated TPOM	2	17	8
Estimated Clastics	6	86	64

Table 7.1

Minimum, maximum and average TOC, carbonate, remainder and $CaCO_3$Free TOC % weights over the FWSB interval. Also shown are estimated TPOM (total organic matter and pyrite organic matter) and clastic material % weight.

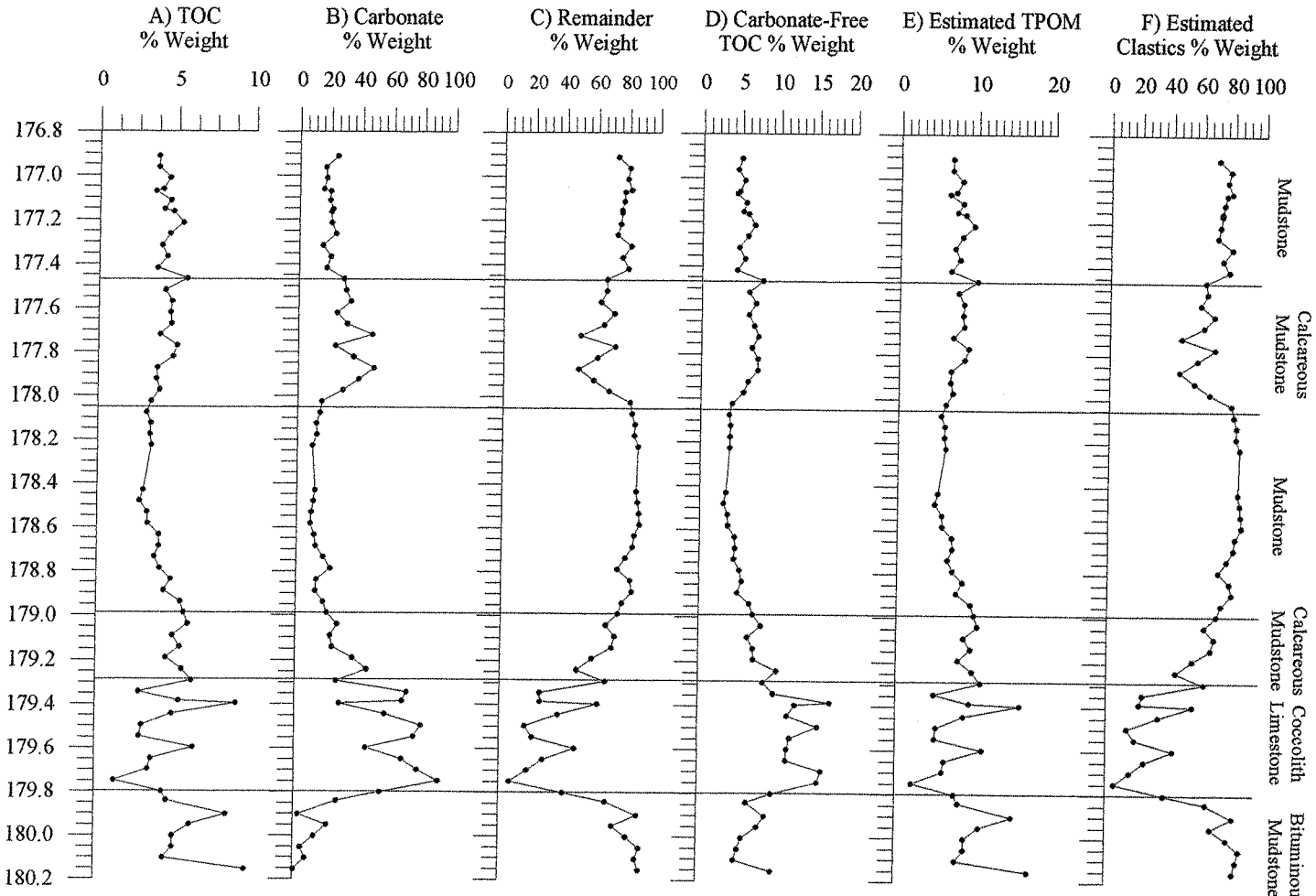

Figure 7.1
TOC (A), Carbonate (B), Remainder (C), Carbonate-free TOC (D), estimated TPOM (total organic matter plus pyrite organic matter) (E) and estimated clastic material (F) as % weight per gram of rock, Freshwater Steps Stone Band Interval.

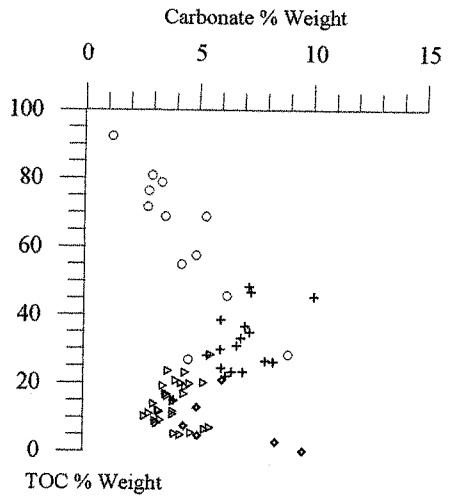

Figure 7.2
Plot of TOC % weight plotted against carbonate % weight with samples grouped into lithological types.

KEY
Open Triangles (Δ) = Mudstone
Crosses (+) = Calcareous Mudstone
Open Circles (O) = Coccolith Limestone
Open Diamonds (◊) = Bituminious Mudstone

The lack of oil shales is immediately obvious (Figure 7.1A), with the TOC % range much reduced compared to the WSB interval (Table 6.1). However, the coccolith limestone and calcareous mudstones are clearly evident from the carbonate profile (Figure 7.1B). The coccolithic carbonate also exerts a strong dilutionary effect on these two lithologies, as was the case for the WSB interval, and $CaCO_3$Free TOC % are seen to be greater and remain high over the limestone (Figure 7.1D). For the mudstones and bituminous mudstones this autodilution effect is minimal with average differences between TOC and $CaCO_3$Free TOC of only 0.5-1%. The estimated TPOM % profile (Figure 7.1E) displays increased values compared to the TOC % weight (Figure 7.1A) (Table 7.1). The remainder (Figure 7.1C) and the estimated clastics % profile (Figure 7.1F) display profiles which are almost the opposite to the carbonate (Figure 7.1C), but the clastics % is greater than the remainder % (Table 7.1). TOC plotted against carbonate % weight for FWSB samples grouped into lithological types (Figure 7.2), generally display poor correlation when compared to a similar plot for the WSB samples (Figure 6.3). However, the coccolith limestone samples display a relatively strong negative correlation.

7.1.2 FWSB INTERVAL PALYNOLOGY RESULTS

As for the WSB interval, the three main particle groups (TMP, TTP and TSD) are presented first, followed by details of each group's sub-categories. Both absolute and carbonate-free absolute abundances per gram of rock are displayed as vertical profiles and all category figures are tabulated. Log_{10} ratios were also calculated, but only specific ratios are mentioned.

7.1.2.1 Comparison of the Three Main Particle Groups for the FWSB Interval

Quantitative figures for the three main particle groups are presented in Table 7.2, where it can be seen that the terrestrial palynomorph group (TTP) is the most abundant of the three, though the terrestrial structured debris (TSD) abundance is of the same order of magnitude. This is the reverse situation to the WSB interval, which was dominated by the TSD group. However, as for the WSB interval, the FWSB interval TMP group is substantially lower in abundance than the other two groups, though again the greater abundance of the organic matter is in amorphous form and marine in origin. Reduced major axis line (RMA) regression produced positive correlations between TMP and TTP, and TMP and TSD of $r = 0.77$, and $r^2 = 0.59$ (Figure 7.3A and B), which was similar to the WSB interval. This suggests that processes affecting the transportation and/or input of terrestrial palynomorphs into the marine environment also affected the marine system. Correlation between TTP and TSD was strongly positive ($r = 0.9$, $r^2 = 0.8$) (Figure 7.3C), indicating that both these terrestrial groups entered the marine environment via the same mechanism. Certainly a storm driven shelf re-suspension of unsorted organic material and clays, transported into the distal basin, as suggested for periods in the WSB interval, would also partly explain these strong correlations between the main FWSB particle groups.

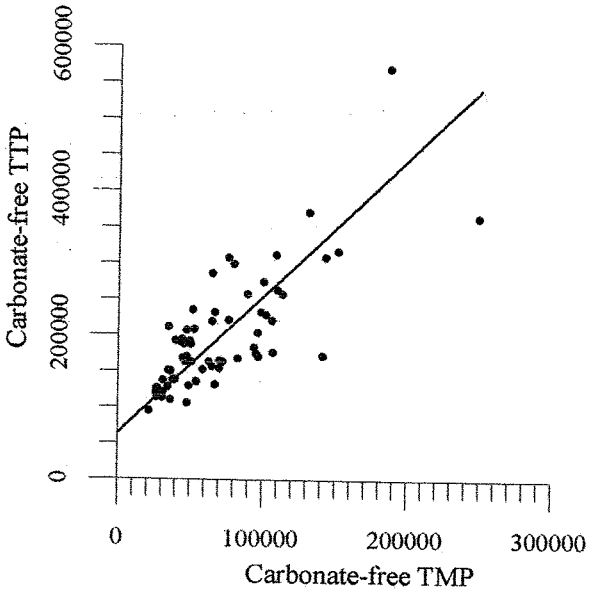

Figure 7.3A)
Reduced major axis line regression
for TMP against TTP, FWSB interval.
The isogonic growth line is shown,
with details given below.

$y = 63708 + 1.91x$
$r = 0.77$, r-squared = 0.59, $n = 65$
95% confidence interval for the slope (b)
$b = 1.91 \pm 0.3$,
95% cofidence interval for the intercept (a)
$a = 63708 \pm 24{,}000$.

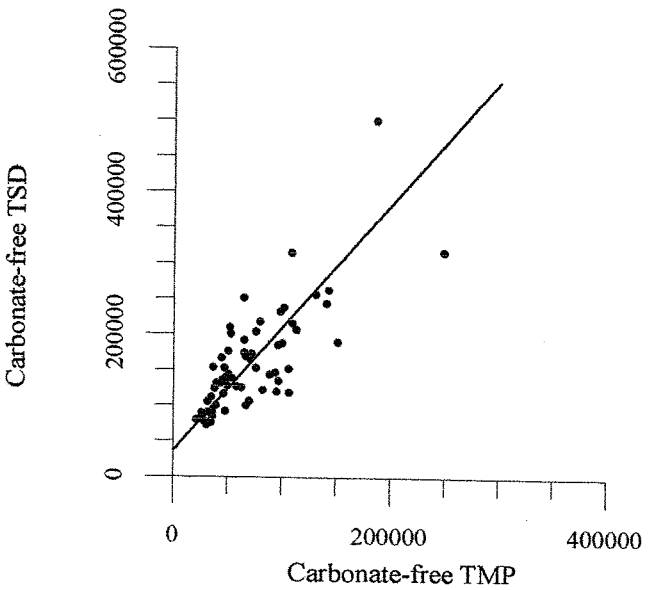

Figure 7.3B)
Reduced major axis line regression
for TMP against TSD, FWSB interval.
The isogonic growth line is shown,
with details given below.

$y = 36390 + 1.73x$
$r = 0.77$, r-squared = 0.59, $n = 65$
95% confidence interval for the slope (b)
$b = 1.73 \pm 0.27$,
95% cofidence interval for the intercept (a)
$a = 36390 \pm 22{,}000$

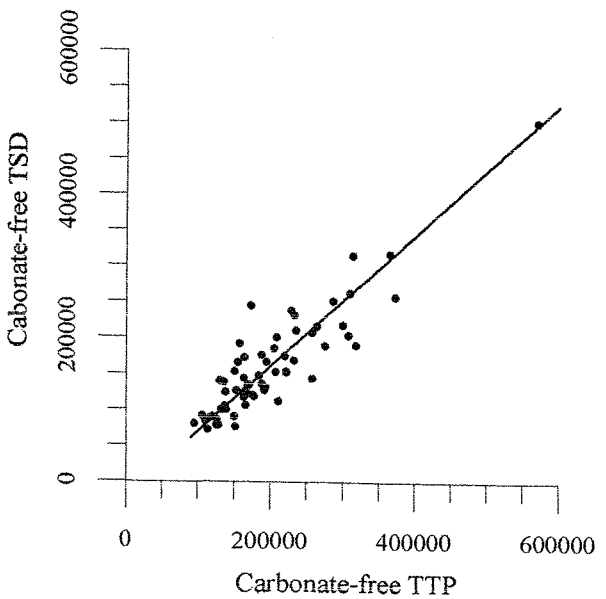

Figure 7.3C)
Reduced major axis line regression
for TTP against TSD, FWSB interval.
The isogonic growth line is shown,
with details given below.

$y = 0.91X - 21375$
$r = 0.897$, r-squared = 0.8, $n = 65$
95% confidence interval for the slope (b)
$b = 0.91 \pm 0.1$,
95% confidence interval for the intercept (a),
$a = -21375 \pm 21{,}000$

TOTAL CATEGORY Av. % all total particles	MINIMUM AA/g	MINIMUM $CaCO_3$Free AA/g	MAXIMUM AA/g	MAXIMUM $CaCO_3$Free AA/g	AVERAGE AA/g	AVERAGE $CaCO_3$Free AA/g
TMP 16% (max.26%)	18,000	21,000	105,000	249,000	44,000	71,000
TTP 47% (max.58%)	28,000	95,000	252,000	571,000	135,000	198,000
TSD 37% (max.46%)	24,000	73,000	249,000	502,000	106,000	158,000

Table 7.2

Minimum, maximum and average absolute abundance (AA/g) and $CaCO_3$Free absolute abundance ($CaCO_3$Free AA/g) per gram of rock for the three main particle groups over the FWSB interval. Average and maximum percentages for each group of the total particle count are also included.

The vertical profiles of the three main particle groups also display very similar patterns (Figure 7.4), as was found to be the case for the WSB interval main groups. The carbonate autodilution effect is evident over the coccolith limestone and calcareous mudstone lithologies. However, once this effect is removed, these lithologies display the greatest abundances in all groups. It is also notable that for all three groups, the beginning and end of the limestone is characterized by two major peaks, the largest of which (Peak 1) occurs at the end for the two terrestrial groups, but at the beginning for the marine group. The carbonate % weight also shows these peaks in the limestone and thus these organic particle increases may reflect greater carbonate dilution during these episodes. However, the opposite magnitude of carbonate and terrestrial organic material peaks in the limestone, combined with a similar pattern evident from the WSB absolute abundance data, suggest these features are real increases in the organic material via input of terrestrial material from outside the distal basin. Over the rest of the interval, abundances are relatively low and change little, though small increases are evident in all groups in the upper calcareous mudstone. It would therefore seem that both the FWSB and the WSB interval limestones were characterized by unsorted pulses of organic material being deposited into the distal basin at or near the beginning of the limestone, and with the greatest abundance at the end. Thus, as for the WSB interval, it is suggested that the FWSB limestone formation is also controlled by mechanisms which resulted in these peak pulse events, such as increased humidity, instability and storminess, which caused shelf sediment re-suspension and influx of organic material, clays and nutrients. The variation in peak size is also suggested to control the initiation and cessation of the limestone, with the most intense storm episodes at the end of the limestone, which ultimately caused a decline in coccolithophore production.

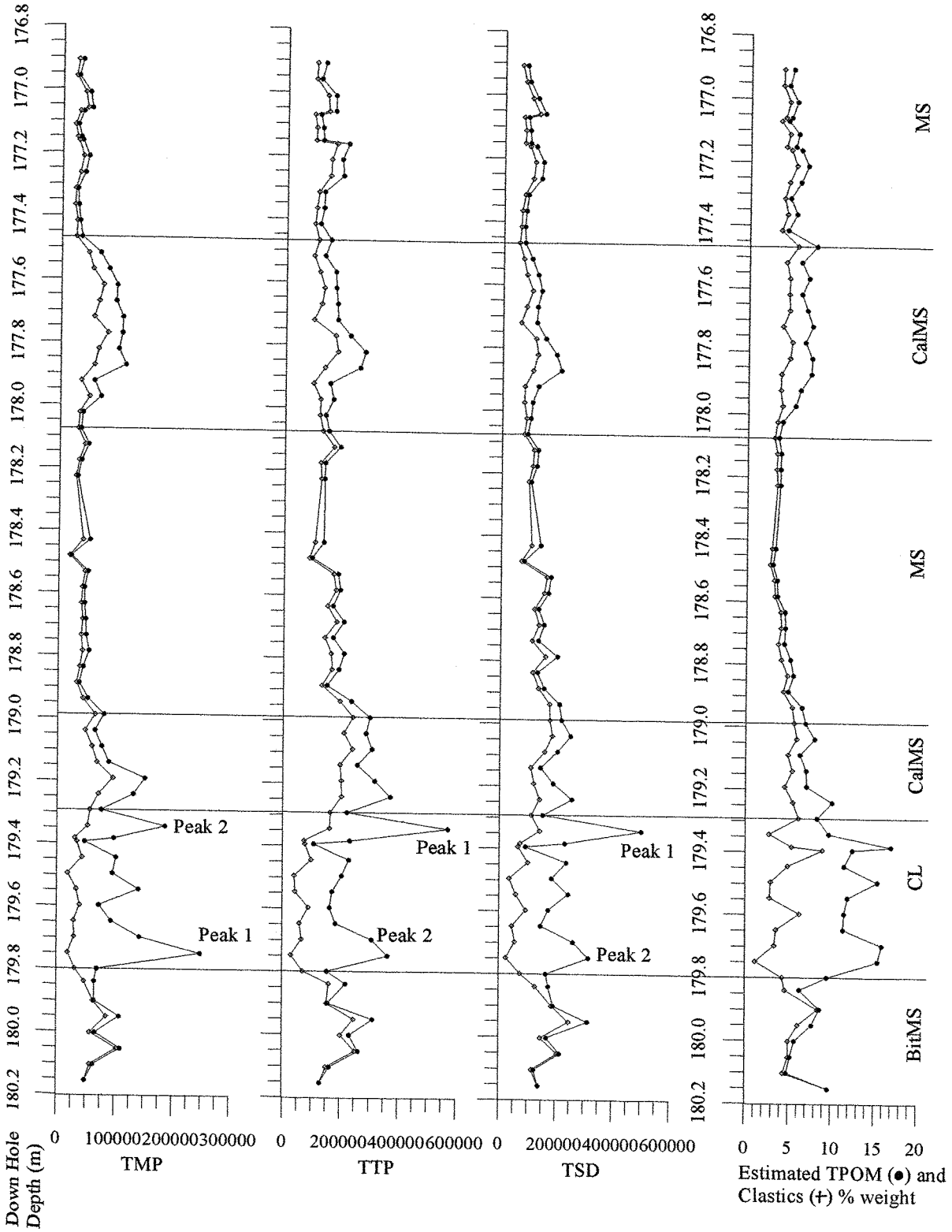

Figure 7.4
Vertical profiles of the absolute abundance (open diamond (◊)) and carbonate-free absolute abundance (closed circles (●)) per gram of rock for the three total palynology groups, togther with estimated TPOM (total organic matter and pyrite organic matter) and clastics % weight for the FWSB interval. Peak 1 is the greatest abundance peak in the coccolith limestone, while Peak 2 is the second greatest. Note the reversal in position of these two peaks between the marine and terrestrial particle groups.

KEY: MS = Mudstone, CalMS = Calcareous Mudstone, CL = Coccolith Limestone, BitMS = Bituminous Mudstone.

7.1.2.2 Comparison of the Marine Palynology Group (TMP), FWSB Interval

Table 7.3 shows details of absolute and $CaCO_3$Free absolute abundance figures and group percentages for all the individual particle categories of the TMP group. The proxi-chorate dinocysts, prasinophytes and acritarchs were not sufficiently abundant in raw counts to enable reliable interpretation and will therefore not be discussed. Dinocysts, especially proximate morphotypes are the most abundant, followed by simple sacs and foraminiferal test linings (FTL). This was also generally the case of the WSB interval, but WSB palynomorph abundances were greater overall.

TMP PARTICLE CATEGORY	MINIMUM			MAXIMUM			AVERAGE		
	AA/g	$CaCO_3$Free AA/g	G%	AA/g	$CaCO_3$Free AA/g	G%	AA/g	$CaCO_3$Free AA/g	G%
Chorate Dinocyst	0	0	0	25,000	43,000	81	4,000	7,000	10
Proxi-chorate Dinocyst	0	0	0	4,000	6,000	8	1000	2,000	3
Proximate Dinocyst	0	0	0	68,000	170,000	82	28,000	45,000	62
Total Dinocysts	11,000	14,000	53	77,000	210,000	89	33,000	54,000	76
Foraminifera Test Linings	1000	1,300	3	12,000	15,000	24	4,000	6,000	9
Simple Sacs	1000	1,400	3	37,000	58,000	38	6,000	9,000	13
Prasinophytes	0	0	0	4,000	6,000	5	400	600	1
Acritarchs	0	0	0	3,000	4,000	7	600	800	1

Table 7.3 Minimum, maximum and average absolute abundance (AA/g), carbonate-free absolute abundance ($CaCO_3$Free AA/g) and group percentage (G%) for all individual particle categories within the TMP group over the FWSB interval.

Vertical profiles of absolute and carbonate-free absolute abundance over the FWSB interval for total dinocysts, proximate and chorate dinocyst morphotypes, FTL and simple sacs are displayed in Figure 7.5. In general the dinocysts show very similar profiles with the greatest abundance over the calcareous mudstones and coccolith limestone when carbonate dilution is removed. The FTL profile, which though affected by data noise, also shows similar peak abundances, while the simple sac profile is slightly different with only peak abundance at the end of the limestone. The close similarity in peak abundance for the dinocysts and FTL, combined with a peak in simple sacs, which represent other phytoplankton cysts, suggests that the same processes affected all categories, with the most severe disturbance at the end of the limestone. Thus, they support the hypothesis of storm disturbance during these intervals which would have resulted in stressful conditions for the phytoplankton and thus increased levels of encystment, while FTL were possibly partly re-deposited from the shelf.

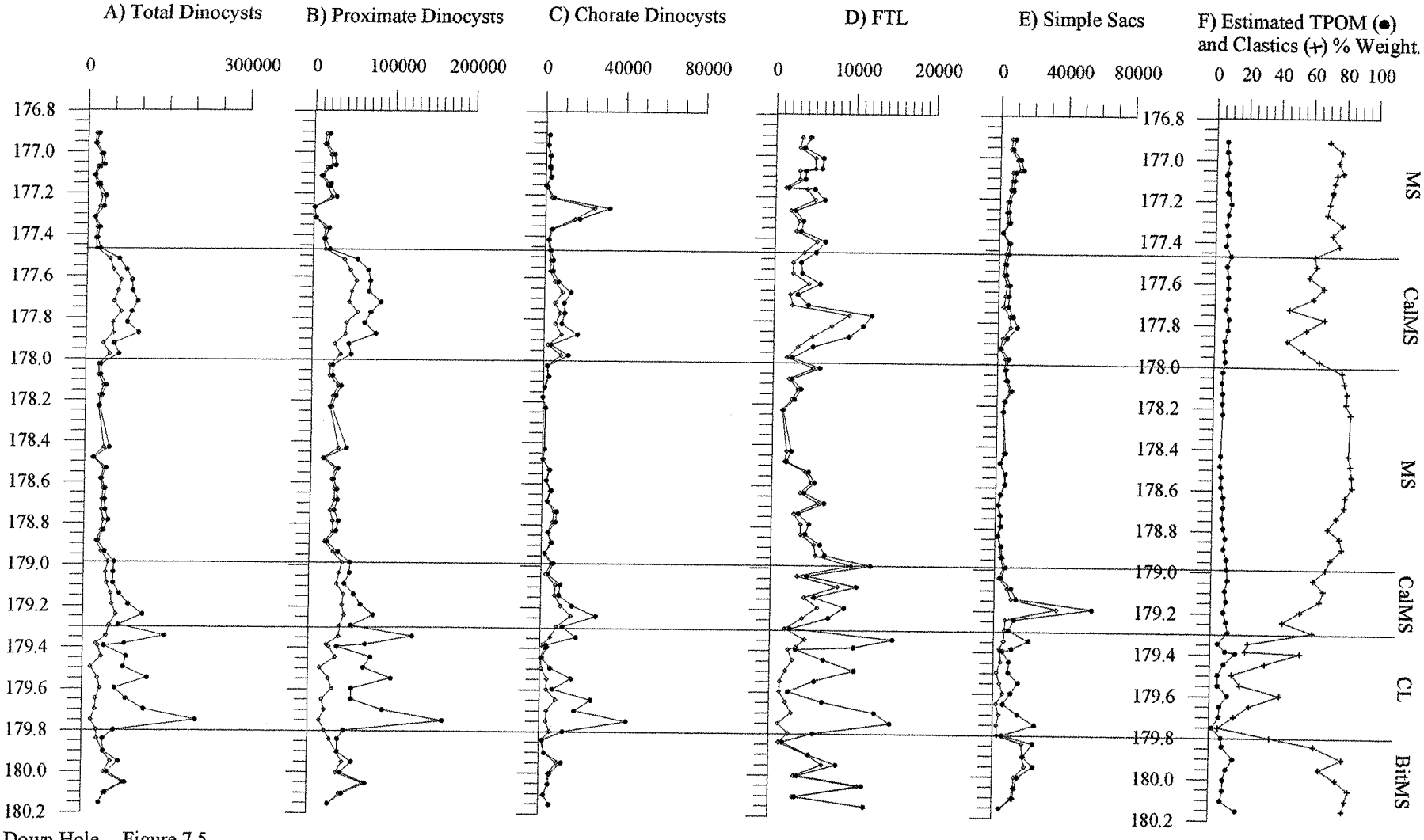

Down Hole Depth (m)

Figure 7.5
Vertical profiles of absolute abundance (open diamonds (◇)) and carbonate-free absolute abundance (closed circles (●)) per gram of rock for marine palynomorphs, dinoflagellates (A to C), foraminiferal test linings (D) and simple sacs (E) and estimated TPOM (total organic matter and pyrite organic matter) and clastics % weight (F) over Freshwater Steps Stone Band Interval.
For lithological notation see Figure 7.4 caption.

7.1.2.3 Comparison of the Terrestrial Palynomorph Group (TTP), FWSB Interval.

Inaperturate pollen is the most abundant of the terrestrial palynomorphs followed by *Classopollis* pollen, while bisaccate pollen and spores are more minor components (Table 7.4). Fresh forms dominate the total *Classopollis* pollen, while the degraded *Classopollis* are only slightly more abundant than either the bisaccate pollen or the spores. Together, on average, degraded *Classopollis*, bisaccates and spores comprise $<15\%$ of the TTP group. Thus, the FWSB interval is dominated by small spherical pollen, which was also found to be the case for the WSB interval, though again WSB abundances were greater (Table 6.5)

TTP PARTICLE CATEGORY	MINIMUM			MAXIMUM			AVERAGE		
		$CaCO_3$Free			$CaCO_3$Free			$CaCO_3$Free	
	AA/g	AA/g	G%	AA/g	AA/g	G%	AA/g	AA/g	G%
Inaperturate Pollen	21,000	60,000	41	250,000	317,000	68	80,000	110,000	56
Fresh *Classopollis*	13,000	22,000	19	100,000	166,000	45	38,000	58,000	29
Degraded *Classopollis*	1,600	4,000	2	17,000	46,000	12	8,000	12,500	6
Total *Classopollis*	14,000	27,000	22	115,000	212,000	51	47,000	71,000	35
Bisaccate Pollen	300	2,000	1	14,000	22,000	7	6,000	8,000	4
Total Pollen	27,000	90,000	91	243,000	550,000	99	130,000	190,000	96
Spores	500	2,000	1	15,000	20,000	9	6,000	9,000	4

Table 7.4 Minimum, maximum and average absolute abundance (AA/g), carbonate-free absolute abundance ($CaCO_3$Free AA/g) and individual particle categories group percentage (G%) within the TTP group over the FWSB interval.

Vertical profiles of total pollen, inaperturate, total *Classopollis*, and bisaccate pollen and spores over the FWSB interval are displayed in Figure 7.6. Like the marine palynomorphs, these terrestrial categories show similar profiles with the greatest carbonate-free abundances over the calcareous mudstones and the coccolith limestone. Some variability is evident in the bisaccate pollen and spore profiles, which tend to display continually high abundance from the end of limestone to the end of the first calcareous mudstone, whereas the spherical pollen goes into decline after the major peak at the end of the limestone. Thus, the terrestrial palynomorphs also support the hypothesis of pulses of unsorted material entering the distal basin during periods of intense storms via re-suspension from the shelf, with the most intense storm episode occurring at the end of the limestone. The dominance of the spherical pollen may reflect the regional floral population but is also likely to indicate a primary bias in the production as well as preferential transportation to the distal environment.

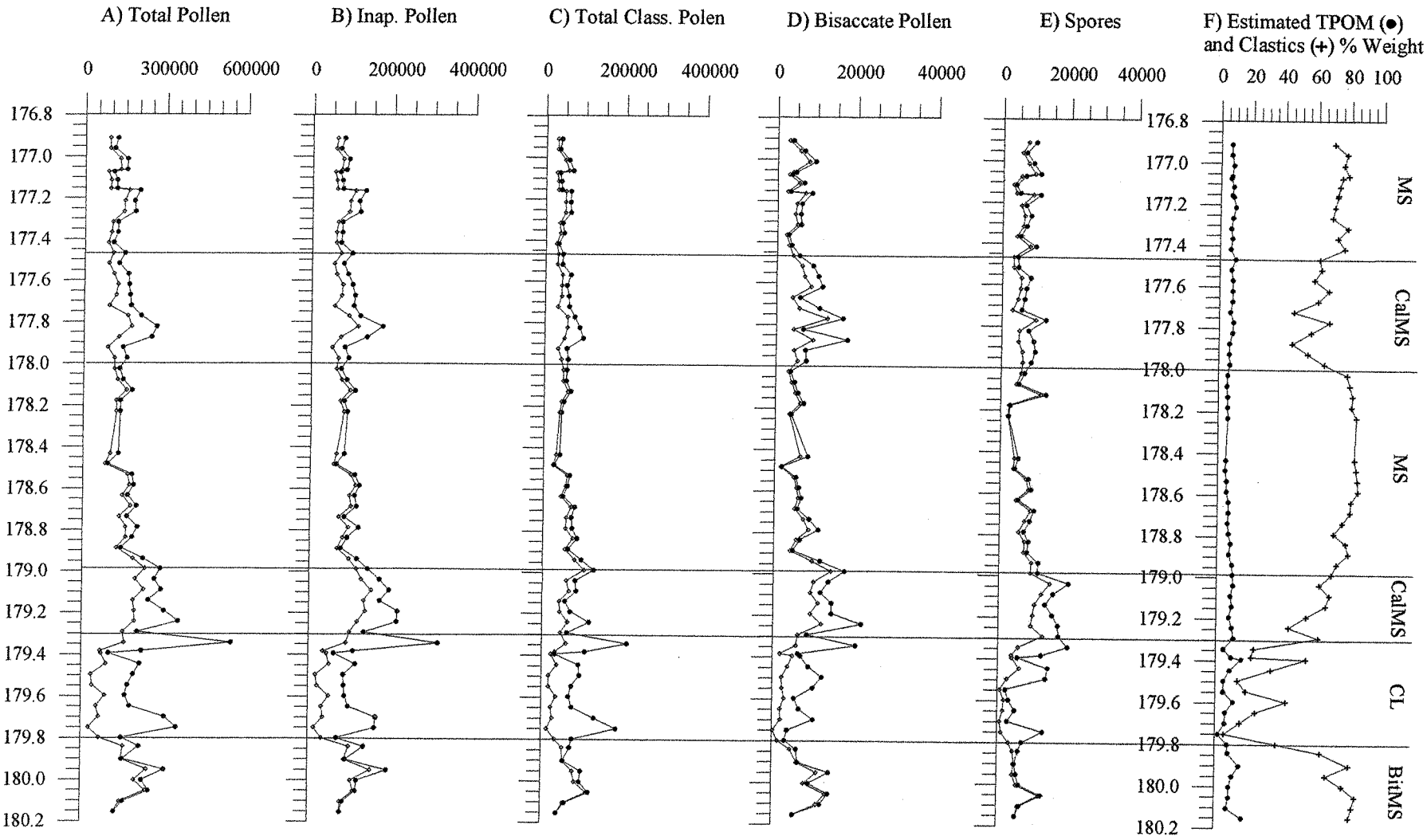

Down Hole Depth (m)

Figure 7.6
Vertical profiles of absolute abundance (open diamonds (◇)) and carbonate-free absolute abundance (closed circles (●)) per gram of rock for terrestrial palynomorphs, total pollen (A), inaperturate pollen (B), total Classopollis pollen (C), bisaccate pollen (D) and spores (E), and estimated TPOM (Total organic matter and pyrite organic matter) and clastics % weight (F) over Freshwater Steps Stone Band Interval. For lithological notation see Figure 7.4 caption.

7.1.2.4 Comparison of the Terrestrial Structured Debris Group (TSD), FWSB Interval

Laths are the dominant forms of the phytoclasts in the FWSB interval, with black/dark types being the most abundant (Table 7.5). Equant phytoclasts are consistently present but remain a less dominant component throughout the interval. However, black/dark types are again the most abundant. Cuticle is very rarely present and comprises $< 1\%$ of the TSD group percentage and thus will not be discussed further. These relationships were also found for the WSB interval, however, the abundance of these particles is notably greater than in the FWSB interval.

TSD PARTICLE CATEGORY	MINIMUM			MAXIMUM			AVERAGE		
		$CaCO_3$Free			$CaCO_3$Free			$CaCO_3$Free	
	AA/g	AA/g	G%	AA/g	AA/g	G%	AA/g	AA/g	G%
Black/dark Laths	15,000	29,000	39	124,000	251,000	60	53,000	81,000	50
Brown/stripy Laths	5,500	19,000	16	87,000	164,000	41	31,000	46,000	29
Total Phytoclast Laths	20,000	56,000	68	211,000	415,000	88	84,000	127,000	80
Black/dark Equants	3000	10,000	8	32,000	49,000	27	15,000	22,000	15
Brown/stripy Equants	1000	2,000	2	16,000	38,000	11	6,000	9,000	6
Total Phytoclast Equants	4000	16,000	12	40,000	87,000	32	21,000	31,000	20
Cuticle	0	0	0	500	1000	0.5	20	40	0.1

Table 7.5 Minimum, maximum and average absolute abundance (AA/g), carbonate-free absolute abundance ($CaCO_3$Free AA/g) and individual particle categories group percentage (G%) within the TSD group over the FWSB interval.

The vertical profiles of total phytoclast laths and total equant phytoclasts, black/dark and brown/stripy laths and equants over the FWSB interval are displayed in Figure 7.7. All categories display the greatest abundances over the calcareous mudstones and the limestone, with peak abundance at the beginning and end of this lithology. All phytoclast categories, thus indicate that several large pulses of unsorted structured terrestrial material entered the basin during the coccolith limestone deposition, supporting the suggestion of storm re-suspension events from the shelf, bringing both organic material and nutrients into the distal basin.

7.1.2.5 Ratios, FWSB Interval

The dominance of the proximate dinocyst morphotype is evident from the ratio of chorate to proximate dinocysts, especially at the end of the limestone, implying greater instability of the marine environment (Figure 7.8A). The greater abundance of pollen compared to dinocysts over the FWSB interval is shown by the total dinocyst : total pollen ratio (Figure 7.8B), though dinocysts show some increase in importance in the coccolith-rich lithologies. In

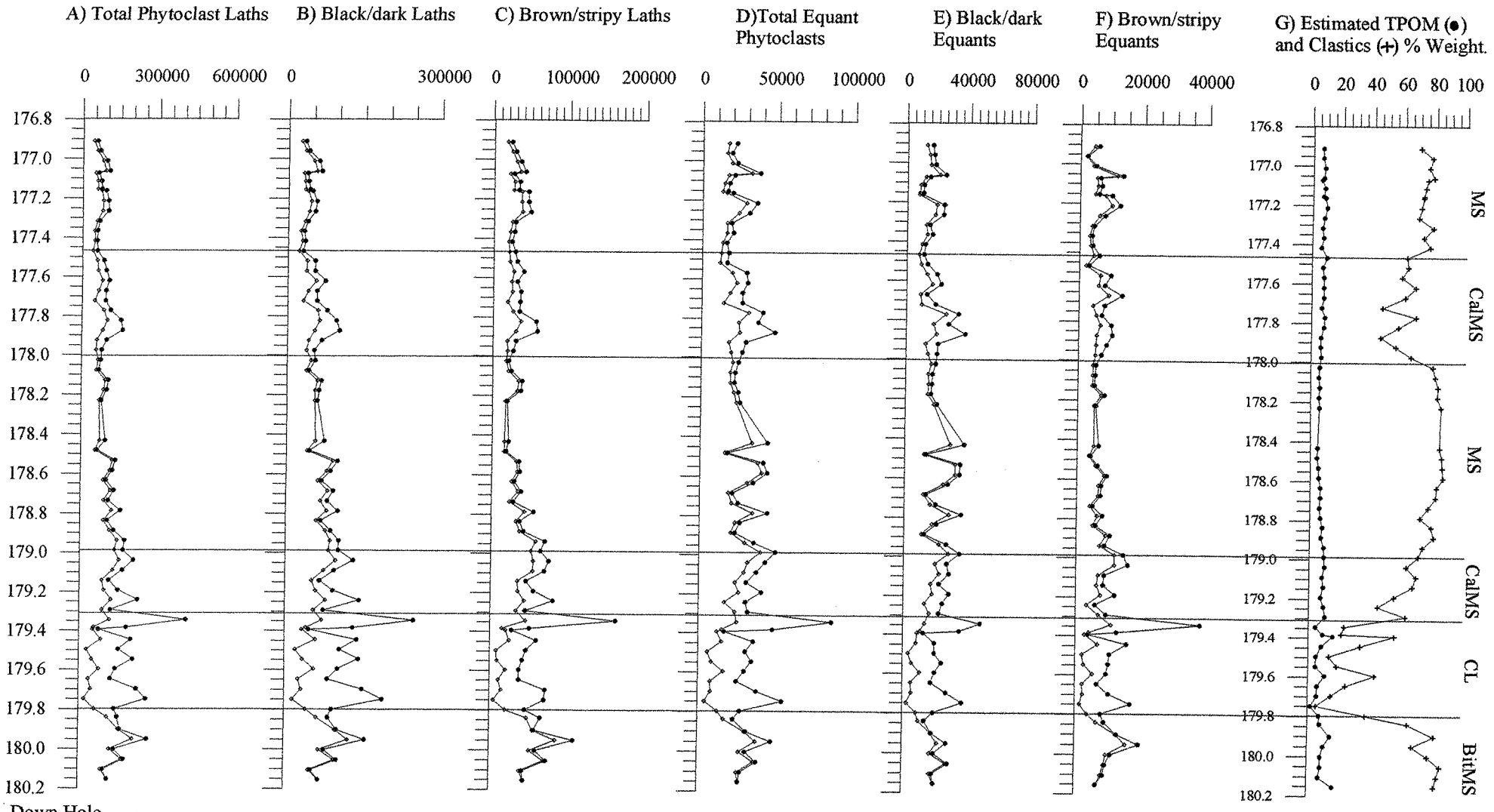

Figure 7.7
Vertical profiles of absolute abundance (open diamonds (◇)) and carbonate-free absolute abundance (closed circles (●)) per gram of rock for terrestrial structured debris, total phytoclast laths (A), black/dark laths (B), brown/stripy laths (C), black/dark equants (D) and brown/stripy equants (E), and estimated TPOM (Total organic matter and pyrite organic matter) and clastics % weight (F) over Freshwater Steps Stone Band Interval. For lithological notation see Figure 7.4 caption.

general, over the interval, inaperturate pollen dominates, but the ratio of inaperturate : *Classopollis* pollen indicates that *Classopollis* are very slightly more important at the beginning of the limestone (Figure 7.8C). The ratio of fresh *Classopollis* to degraded *Classopollis* shows the dominance of the fresh types; however, the ratio does not vary significantly over the interval, implying a consistent relative input of both types (Figure 7.8D). Black/dark laths against brown/stripy laths show a positive ratio indicating the dominance of the black/dark type. But at the start and end of the limestone and in the calcareous mudstones, brown/stripy laths have relatively greater impact, an indication of less well oxidized particles being brought into the distal basin (Figure 7.8E). Though the signal is more variable, a similar pattern is seen for the ratio of black/dark equants to brown/stripy equants.

7.1.3 SUMMARY(Figure 7.9)

The low overall TOC % weight and lack of laminated oil shale lithologies within the FWSB interval, implies that the marine environment and climate did not reach highly stable, arid conditions and that the water column oxygen levels were probably highly variable during this interval. Both high calcite and $CaCO_3$Free TOC % weight over the limestone imply increased surface water production and /or non-carbonate phytoplankton encystment over this period, indicating both increases in nutrients and environment instability. The three main particle groups of TMP, TTP and TSD all show very similar profiles, with peak abundances over the coccolith-rich lithologies, especially at the beginning and end of the limestone. As implied for the WSB interval, the peak FWSB abundances are also suggested to result from storm re-suspension events bringing unsorted pulses of organic material, clays and nutrients from the shelf into the basin, which subsequently resulted in coccolithophore blooms. The size of the pulses is also suggested to be a link to the initiation and cessation of carbonate deposition. The smallest pulse episode occurred at the start of the limestone, which though stressful to the majority of phytoplankton, was tolerated by the r-strategist coccolithophore who took advantage of the increase in nutrients, such as nitrates, phosphates and iron, and bloomed. At the end of the limestone, the storm episodes are indicated to have been more intense, with greater amounts of organic material brought in off the shelf. It is hypothesized that though the coccolithophore population initially increased, the level of disturbance eventually resulted in the decline of the coccolithophore and thus the termination of the limestone deposition.

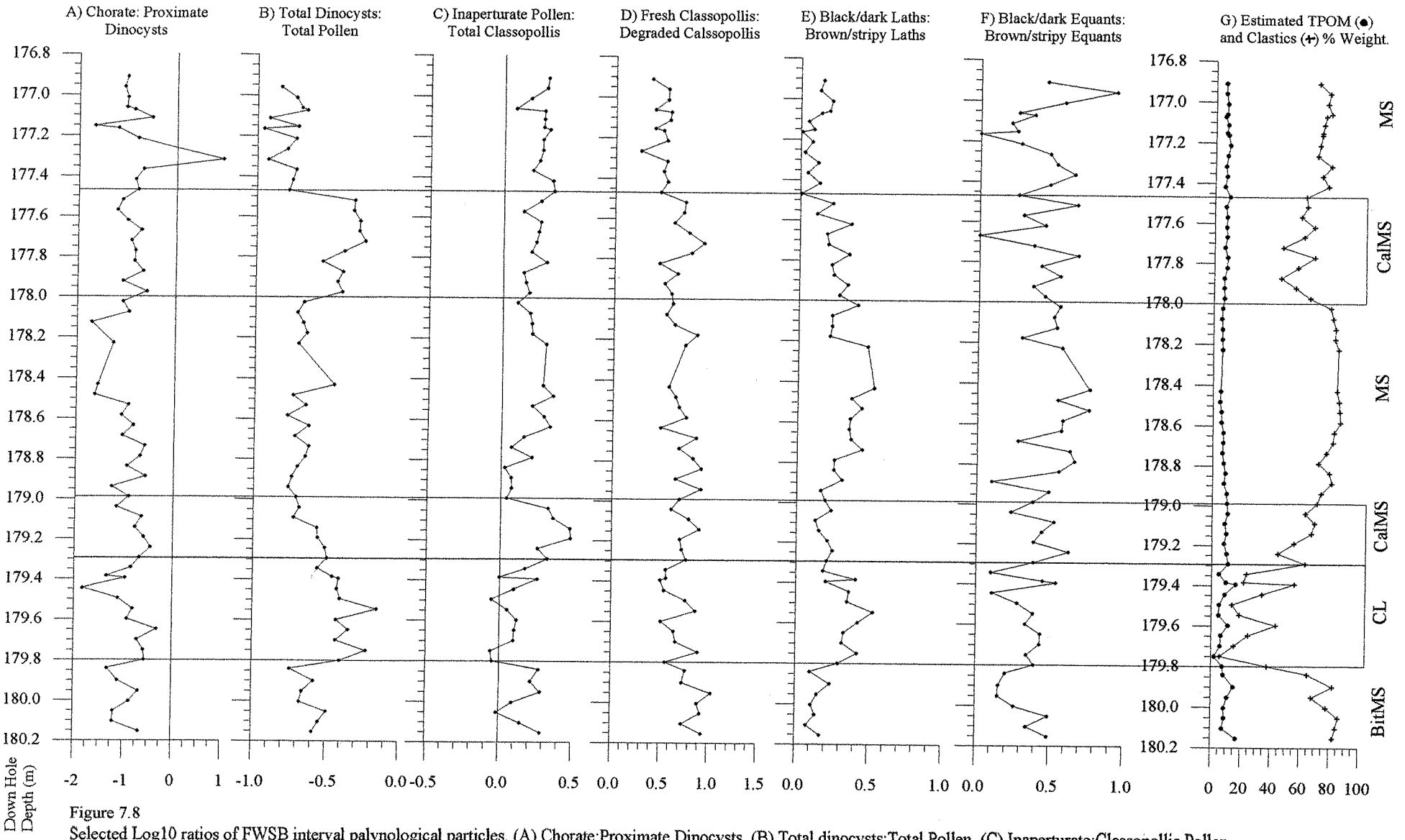

Figure 7.8

Selected Log10 ratios of FWSB interval palynological particles. (A) Chorate:Proximate Dinocysts, (B) Total dinocysts:Total Pollen, (C) Inaperturate:Classopollis Pollen, (D) Fresh:Degraded Classopollis, (E) Black/dark:Brown/stripy Laths, (F) Black/dark:Brown/stripy Equants, (G), and estimated TPOM (Total organic matter and pyrite organic matter) and clastics % Weight (G). For lithological notation see Figure 7.4 caption.

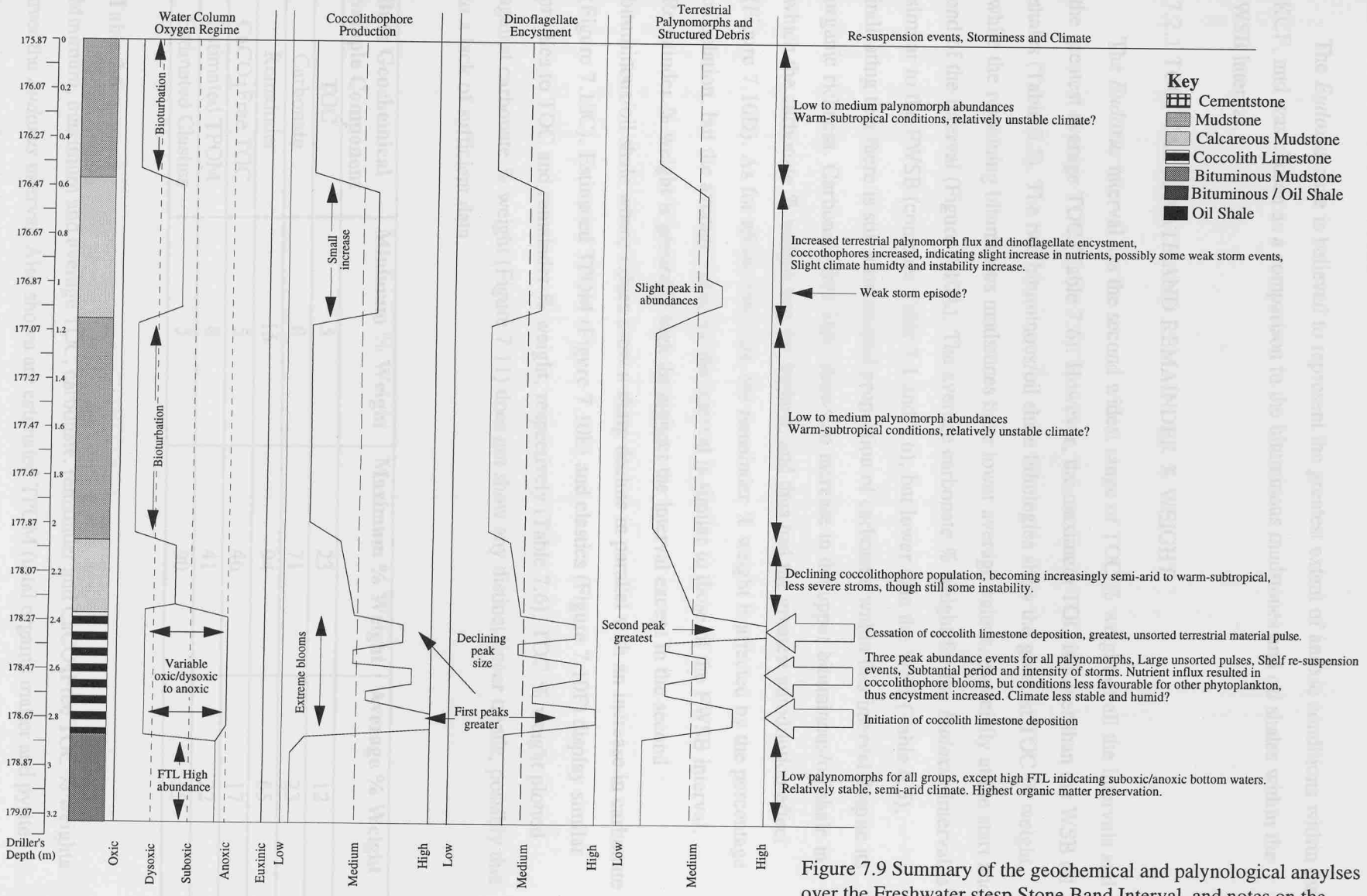

Figure 7.9 Summary of the geochemical and palynological anaylses over the Freshwater stesp Stone Band Interval, and notes on the environmental and climatic implication of these results.

7.2 *EUDOXUS* INTERVAL

The *Eudoxus* zone is believed to represent the greatest extent of anoxic conditions within the KCF, and was chosen as a comparison to the bituminous mudstones and oil shales within the WSB interval.

7.2.1 TOC, CARBONATE AND REMAINDER % WEIGHT

The *Eudoxus* interval has the second widest range of TOC % weight of all the intervals and the greatest average TOC (Table 7.6). However, the maximum TOC is lower than the WSB oil shales (Table 6.5). The two bituminous/oil shale lithologies show the greatest TOC % weight, while the remaining bituminous mudstones have lower average values, especially at the start and end of the interval (Figure 7.10A). The average carbonate % weight for the *Eudoxus* interval is similar to the FWSB (compare Table 7.1 and 7.6), but lower than the WSB (Table 6.5), indicating that there is still a substantial proportion of carbonate within this interval despite its organic richness. Carbonate-free TOC shows an increase in the upper bituminous/oil shale in which the carbonate % weight was the highest, and thus had the greatest autodilution effect (Figure 7.10D). As for all the intervals, the remainder % weight is affected by the percentage calculation, but the average value for the interval is similar to those of the FWSB interval. Remainder % weight is generally high throughout the interval except in the second bituminous/oil shale where values show a sharp decline in parallel with an increase in carbonate (Figure 7.10C). Estimated TPOM (Figure 7.10E) and clastics (Figure 7.10F) display similar profiles to TOC and remainder % weight, respectively (Table 7.6). TOC % weight plotted against carbonate % weight (Figure 7.11) does not show any distinct linear trends, possibly due to a lack of sufficient data.

Bulk Geochemical Sample Component	**Minimum % Weight**	**Maximum % Weight**	**Average % Weight**
TOC	5	23	12
Carbonate	0	71	23
Remainder	15	94	65
$CaCO_3$Free TOC	5	46	17
Estimated TPOM	8	41	22
Estimated Clastics	5	90	55

Table 7.6

Minimum, maximum and average TOC, carbonate, remainder and $CaCO_3$Free TOC % weights over the *Eudoxus* interval. Also shown are estimated TPOM (total organic matter and pyrite organic matter) and clastic material % weight.

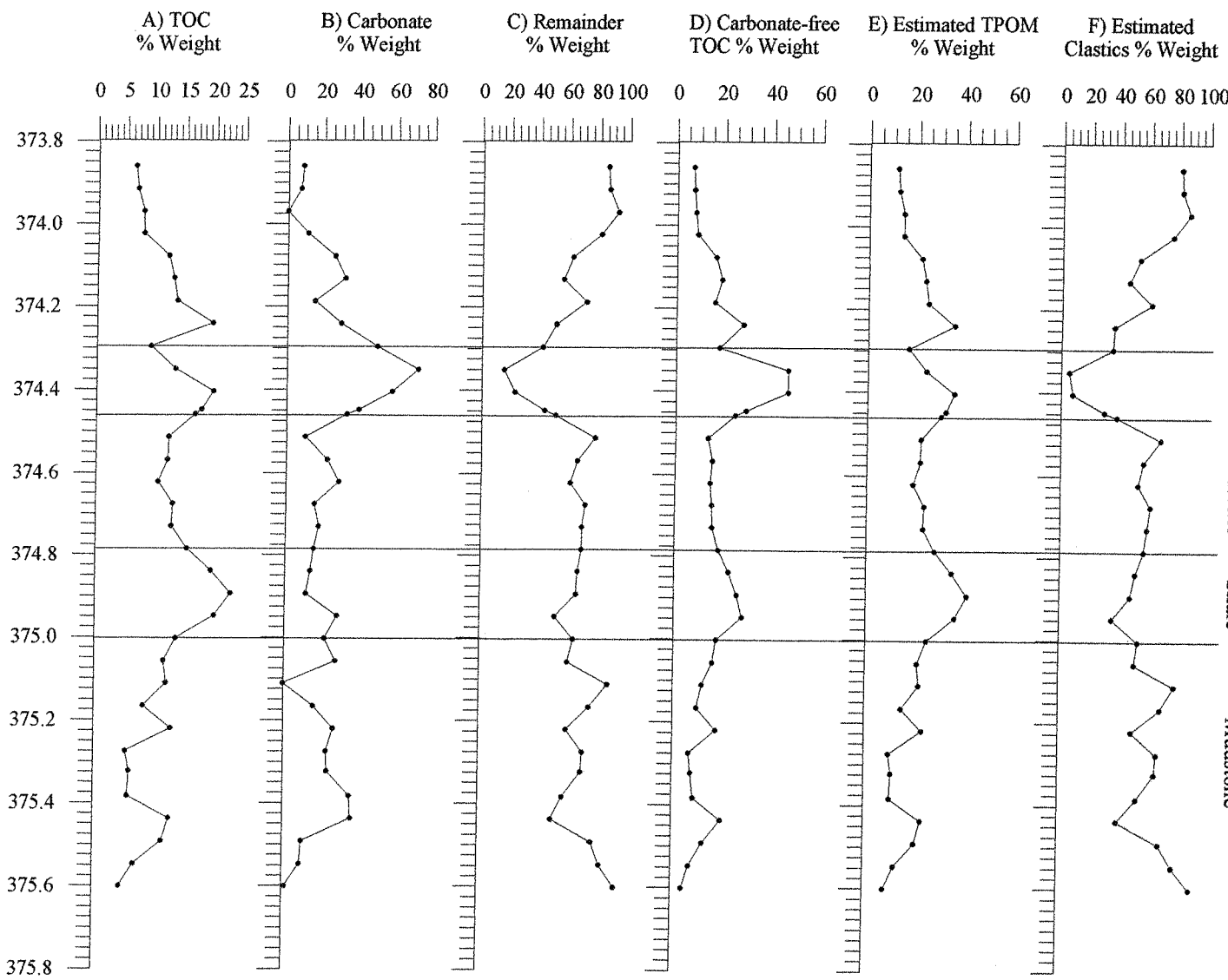

Figure 7.10
TOC (A), carbonate (B), remainder (C), carbonate-free TOC (D), estimated TPOM (total organic matter and pyrite organic matter) (E) and estimated clastics (F) as % weight of rock, Eudoxus Interval.

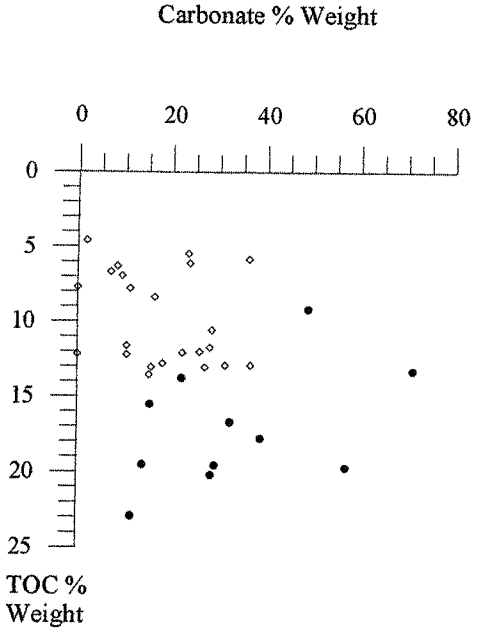

Figure 7.11
Plot of TOC % weight plotted against Carbonate % weight with samples grouped into lithological types.

KEY
Open Diamonds (◇) = Bituminous Mudstone,
Closed Circles (●) = Bituminous/Oil Shale

7.2.2 *EUDOXUS* PALYNOLOGY RESULTS

7.2.2.1 Comparison of the *Eudoxus* Interval Three Main Particle Groups

Quantitative figures for the three main particle groups are presented in Table 7.7, where the terrestrial structured debris (TSD) is the most abundant group, though terrestrial palynomorphs (TTP) abundance is of the same magnitude. As for all the studied intervals the total marine palynomorphs (TMP) are the least abundant, but again AOM was dominant in this interval. Abundances for all the *Eudoxus* total groups are generally slightly greater than those in the FWSB interval, but are still substantially lower than in the WSB interval. Reduced major axis line regressions were calculated between TMP and both TTP and TSD, with a relatively strong correlation between TMP and TTP ($r = 0.82$, $r^2 = 0.68$) (Figure 7.12A), but far weaker against TSD ($r = 0.61$, $r^2 = 0.38$) (Figure 7.12B). TTP against TSD also shows a relatively strong correlation to TTP ($r = 0.8$, $r^2 = 0.63$) (Figure 7.12C). Though these correlations are weaker than those obtained for the 'coccolith limestone' intervals, in general both the marine and terrestrial environments were affected in a similar manner in the *Eudoxus* interval. However, the weakest correlation between TMP and TSD implies different mechanisms affected the deposition of these organic particles in the marine environment and the phytoplankton populations.

TOTAL CATEGORY Av. % of total particle count	MINIMUM		MAXIMUM		AVERAGE	
	AA/g	$CaCO_3$Free AA/g	AA/g	$CaCO_3$Free AA/g	AA/g	$CaCO_3$Free AA/g
TMP 6% (max.18%)	300	750	83,000	84,000	26,000	33,000
TTP 37% (max.53%)	2000	5000	400,000	450,000	180,000	220,000
TSD 56% (max.89%)	23,000	53,000	450,000	640,000	210,000	270,000

Table 7.7 Minimum, maximum and average absolute abundance (AA/g) and carbonate-free absolute abundance ($CaCO_3$Free AA/g)per gram of rock for the total particle groups, *Eudoxus* interval. Average and maximum total particle percentages for each group are also displayed.

Vertical profiles of the three main particle groups over the Eudoxus interval are displayed in Figure 7.13. As for the other intervals there is a general similarity in all three profiles, with the lowest abundances characterizing the two-bituminous/oil shale lithologies, while the bituminous mudstones display slightly higher but more variable abundances. These profiles suggest that the lowest sedimentation rates occurred during the bituminous/oil shales, which compares to the oil shale palynofacies abundances in the WSB oil shales. Thus the implication is that, like the WSB oil shales, the *Eudoxus* bituminous/oil shales were deposited under a stratified water column and an arid climate with little or no runoff.

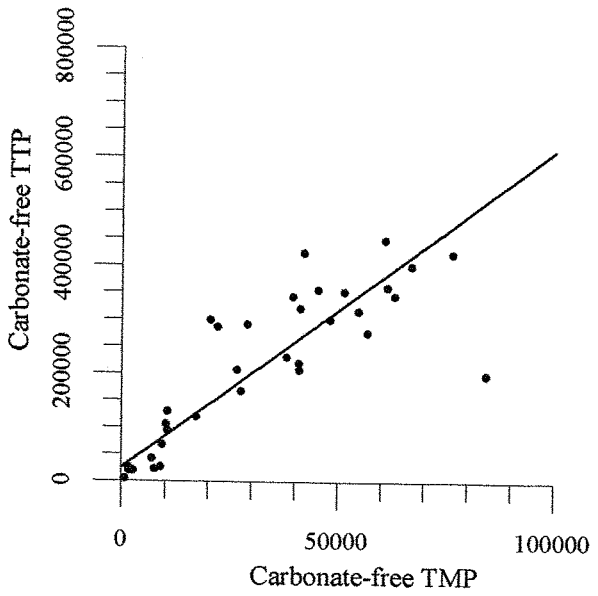

Figure 7.12A)
Reduced major axis line regression
for TMP against TTP, Eudoxus interval.
The isogonic growth line is shown,
with detials given below.

y = 25516 + 5.87x
r = 0.82, r-squared = 0.68, n = 34
95% confidence interval for the slope (b)
b = 5.87 ± 1.12,
95% cofidence interval for the intercept (a)
a = 25516 ± 46,000.

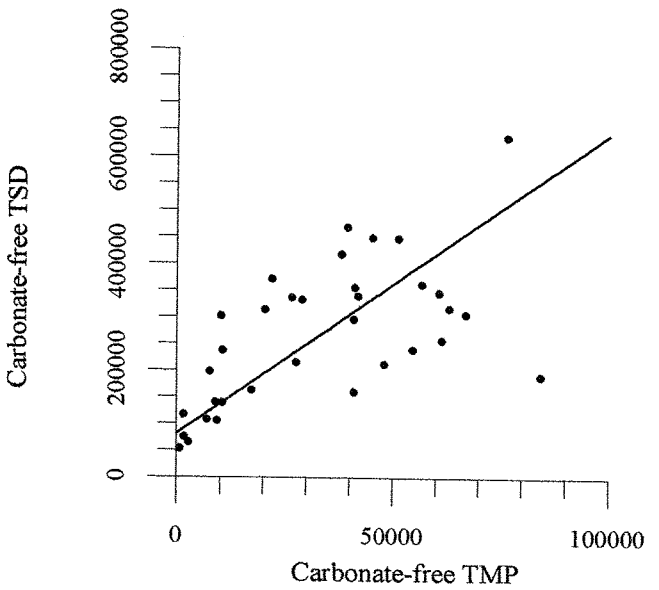

Figure 7.12B)
Reduced major axis line regression
for TMP against TSD, Eudoxus interval.
The isogonic growth line is shown,
with detials given below.

y = 80913 + 5.62x
r = 0.61, r-squared = 0.38, n = 34
95% confidence interval for the slope (b)
b = 5.62 ± 1.49,
95% cofidence interval for the intercept (a)
a = 80913 ± 67,000

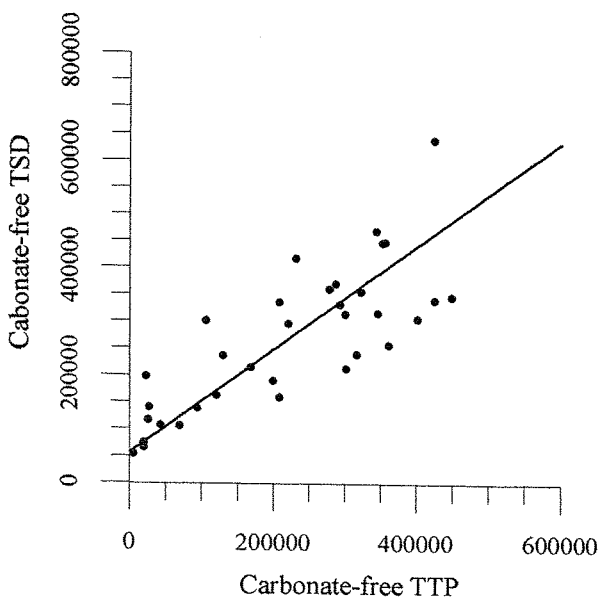

Figure 7.12C)
Reduced major axis line regression
for TTP against TSD, Eudoxus interval.
The isogonic growth line is shown,
with detials given below.

y - 56491 + 0.96x
r = 0.8, r-squared = 0.63, n = 34
95% confidence interval for the slope (b)
b = 0.96 ± 0.19,
95% confidence interval for the intercept (a),
a = 56491 ± 51,000

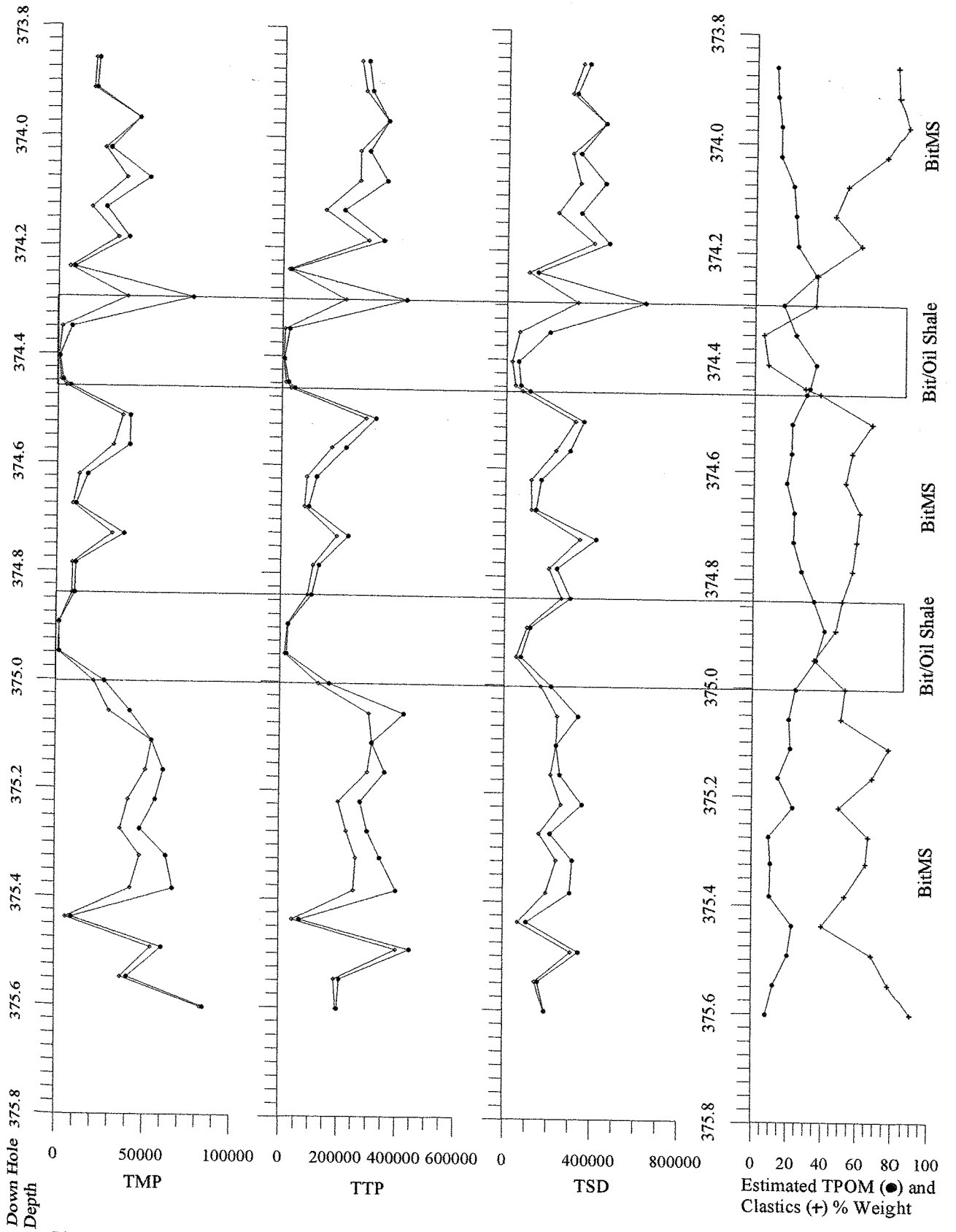

Figure 7.13
Vertical profiles of the absolute abundance (open diamonds (◇)) and carbonate-free absolute abundance (closed circles (●)) per gram of rock for the three total palynology groups, together with estimated TPOM (total organic matter and pyrite organic matter) and clastics % weight for the Eudoxus Interval.

KEY: BitMS = Bituminous Mudstone, Bit/Oil Shale = Bituminous/Oil Shale.

7.2.2.2 Comparison of the Marine Palynology Group (TMP), *Eudoxus* Interval

Table 7.8 shows details of absolute and $CaCO_3$Free absolute abundance figures and group percentages for all the individual particle categories of the TMP group. Dinocysts are again the most abundant of the marine palynomorphs, closely followed by foraminiferal test linings, while acritarchs and simple sacs are less abundant but reach similar abundances to chorate and proxi-chorate dinocysts. Prasinophytes were the least abundant, comprising $< 1\%$ of the TMP group and are therefore not sufficiently abundant compared to the other marine palynomorphs and will not be discussed further. FTL are more abundant in the *Eudoxus* interval (compare Table 7.3 to Table 7.8), indicating that bottom water conditions were more commonly dysoxic, which enable benthic foraminifera to flourish due to lack of predation and abundant food supply.

TMP PARTICLE CATEGORY	MINIMUM			MAXIMUM			AVERAGE		
		$CaCO_3$Free			$CaCO_3$Free			$CaCO_3$Free	
	AA/g	AA/g	G%	AA/g	AA/g	G%	AA/g	AA/g	G%
Chorate Dinocyst	0	0	0	26,000	26,000	31	5,000	3,000	6
Proxi-chorate Dinocyst	0	0	0	6,000	6,000	12	1000	1000	2
Proximate Dinocyst	0	0	0	33,000	39,000	74	9,000	13,000	33
Total Dinocysts	0	0	0	63,000	64,000	81	13,000	17,000	41
Foraminifera Test Linings	300	800	4	28,000	31,000	99	6,000	10,000	38
Simple Sacs	0	0	0	7,000	12,000	43	2,000	4,000	12
Prasinophytes	0	0	0	1000	8,000	33	300	2,000	8
Acritarchs	0	0	0	9,000	1000	2	3,000	100	0.2

Table 7.8 Minimum, maximum and average absolute abundance (AA/g), carbonate-free absolute abundance ($CaCO_3$Free AA/g) and group percentage (G%) for all individual particle categories within the TMP group over the *Eudoxus* interval.

Vertical profiles of total dinocysts, proximate and chorate dinocyst morphotypes, FTL, acritarchs and simple sacs over the *Eudoxus* interval are displayed in Figure 7.14. For all categories the lowest abundances are evident in the bituminous/oil shale, while more variable, higher abundances occur over the rest of the interval. Again, this compares to the very low organic particle abundances in the WSB oil shale lithologies and indicates anoxic bottom waters and preservation of organic matter as AOM during these lithologies. Dinocysts show the greatest abundances at the start of the interval and decline towards the first bituminous/oil shale, but the chorate dinocysts remain low for the remainder of the interval, while proximate types are variably more abundant. The decline of acritarchs in the bituminous/oil shales further implies high salinities, and thus possible a relatively more arid climate during these episodes.

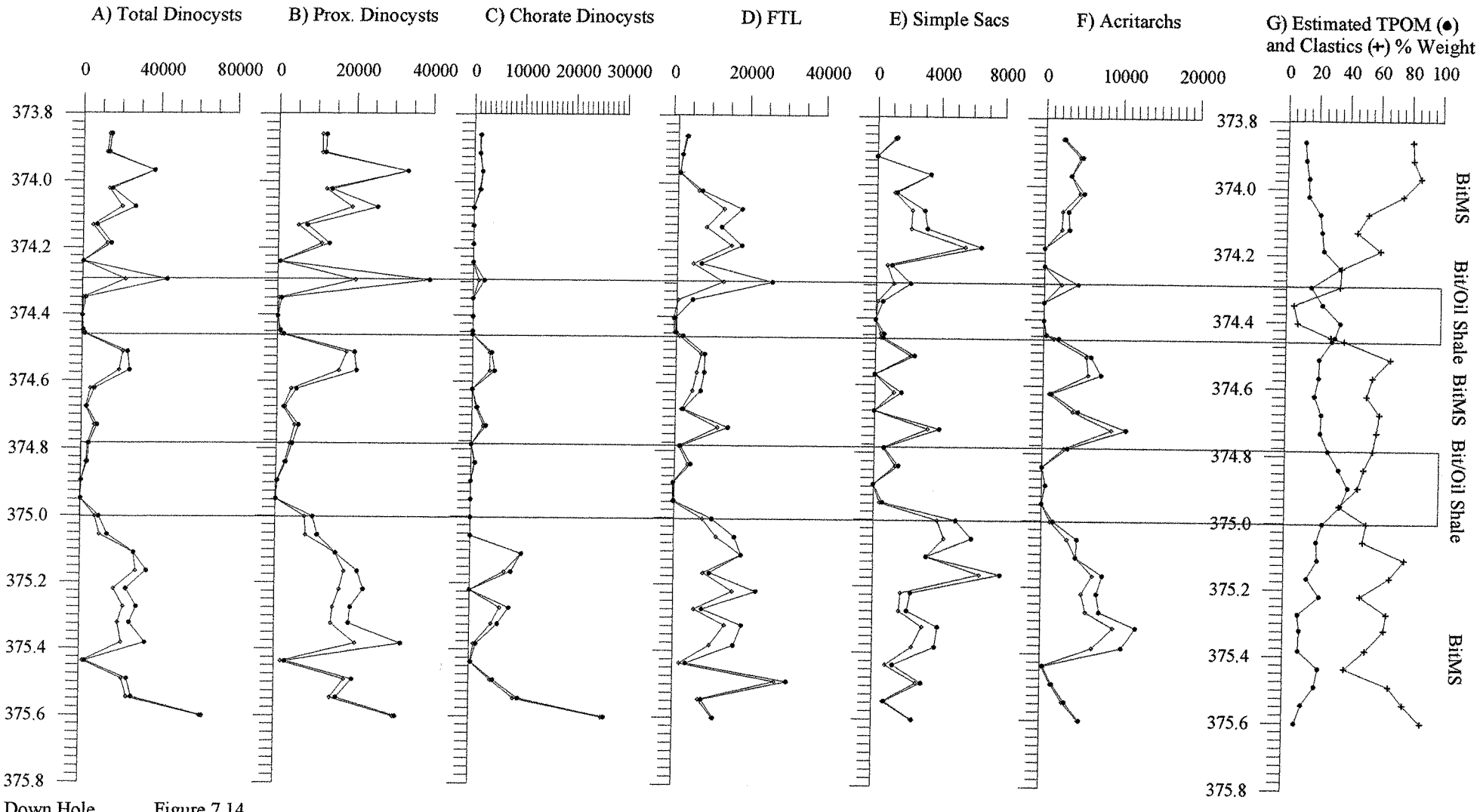

Figure 7.14
Vertical profiles of absolute abundance (open diamonds (◇)) and carbonate-free absolute abundance (closed circles (●)) per gram of rock for marine palynomorphs, dinoflagellates (A to C), foraminiferal test linings (D) and simple sacs (E), acritarchs (F) and estimated TPOM (total organic matter plus pyrite organic matter) and clastics % weight (G) over Eudoxus Interval. For lithological notation see Figure 7.13 caption.

7.2.2.3 Comparison of the Terrestrial Palynomorph Group (TTP), *Eudoxus* Interval

As for the FWSB interval, inaperturate pollen are again seen to be the most abundant pollen type in the *Eudoxus* interval, but *Classopollis* pollen are far less abundant than previously seen (Table 7.9). Both bisaccate pollen and spores are the least abundant, each reaching a maximum of 10% of the TTP group, though together these are on average <10%, but are similar in abundance to those of the FWSB interval.

TTP PARTICLE CATEGORY	MINIMUM			MAXIMUM			AVERAGE		
		$CaCO_3$Free			$CaCO_3$Free			$CaCO_3$Free	
	AA/g	AA/g	G%	AA/g	AA/g	G%	AA/g	AA/g	G%
Inaperturate Pollen	1000	3,000	45	362,000	405,000	90	140,000	173,000	75
Fresh *Classopollis*	300	1000	3	85,000	95,000	47	19,000	23,000	14
Degraded *Classopollis*	400	700	0.4	19,000	28,000	18	5,000	6,000	4
Total *Classopollis*	900	2,000	5	104,000	116,000	50	24,000	29,000	18
Bisaccate Pollen	0	0	0	22,000	31,000	10	7,000	9,000	3
Total Pollen	2000	5,000	90	389,000	434,000	100	171,000	212,000	96
Spores	0	0	0	22,000	22,000	10	7,000	8,000	4

Table 7.9 Minimum, maximum and average absolute abundance (AA/g), carbonate-free absolute abundance ($CaCO_3$Free AA/g) and individual particle categories group percentage (G%) within the TTP group over the *Eudoxus* interval.

The vertical profiles of total pollen, inaperturate, *Classopollis* and bisaccate pollen and spores over the *Eudoxus* interval are displayed in Figure 7.15. The total pollen profile is similar to the total dinocysts, with the lowest abundances characterizing the bituminous/oil shale lithologies and more variable abundances over the rest of the interval (Figure 7.15A). However, the inaperturate pollen show the highest abundances in the lower and upper bituminous mudstones, while the central portion of the interval is characterized by far lower abundances, especially in the bituminous/oil shales (Figure 7.15B). Conversely, the *Classopollis* pollen is the reverse with relatively low abundances characterizing the majority of the interval, but two prominent peaks in the central bituminous mudstone (Figure 7.15C). Bisaccate pollen, though far lower in abundance, displays a similar profile to the inaperturate pollen (Figure 7.15D). The pollen flux therefore seems to have been divided between inaperturate and bisaccate pollen in the lower and upper sections of the interval, while the central portion was dominated by *Classopollis* pollen. This pattern may be indicative of changes in the regional flora possibly resulting from drier conditions during the central part of the interval. Though far lower in abundance, in general, spores display a similar profile to the inaperturate and bisaccate pollen with the greatest abundance at the start and end of the interval (Figure 7.15E).

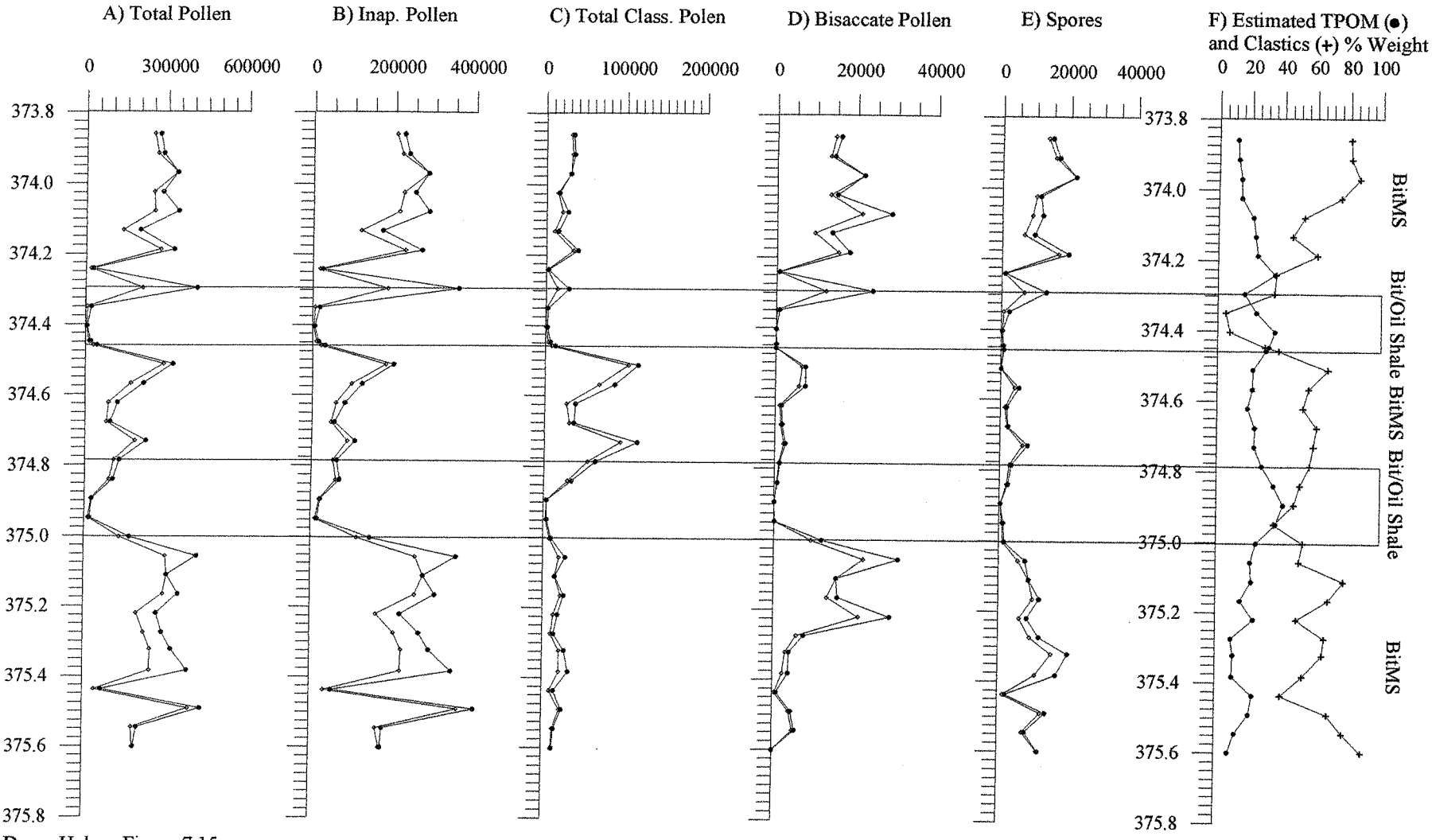

Down Hole Depth (m)

Figure 7.15
Vertical profiles of absolute abundance (open diamonds (◇)) and carbonate-free absolute abundance (closed circles (●)) per gram of rock for terrestrial palynomorphs, total pollen (A), inaperturate pollen (B), total Classopollis pollen (C), bisaccate pollen (D) and spores (E), and estimated TPOM (total organic matter plus pyrite organic matter) and clastics % weight (F) over Eudoxus Interval. For lithological notation see Figure 7.13 caption.

7.2.2.4 Comparison of the Terrestrial Structured Debris Group (TSD), *Eudoxus* Interval

The structured debris within the *Eudoxus* interval is dominated by phytoclasts while cuticle fragments are rare (Table 7.10), which was also found to be the case with FWSB and WSB intervals. Total abundances of *Eudoxus* phytoclasts are generally slightly greater than in the FWSB interval, but are far lower than in the WSB interval. Again laths are the dominant phytoclast shape, with black/dark types being the most abundant. However, equant forms are present throughout, reaching a maximum of 20% of the TSD group, but similarly the brown/stripy types were the least abundant.

TSD PARTICLE CATEGORY	MINIMUM $CaCO_3$Free			MAXIMUM $CaCO_3$Free			AVERAGE $CaCO_3$Free		
	AA/g	AA/g	G%	AA/g	AA/g	G%	AA/g	AA/g	G%
Black/dark Laths	14,000	33,000	38	199,000	306,000	63	101,000	130,000	50
Brown/stripy Laths	6,000	13,000	25	172,000	206,000	46	77,000	98,000	35
Total Phytoclast Laths	20,000	46,000	79	371,000	566,000	91	179,000	228,000	85
Black/dark Equants	2,000	5,000	6	50,000	50,000	12	19,000	24,000	9
Brown/stripy Equants	1000	2,000	2	31,000	36,000	11	12,000	15,000	6
Total Phytoclast Equants	3,000	7,000	9	77,000	84,000	21	31,000	39,000	15
Cuticle	0	0	0	900	900	<1	30	35	<1

Table 7.10 Minimum, maximum and average absolute abundance (AA/g), carbonate-free absolute abundance ($CaCO_3$Free AA/g) and individual particle categories group percentage (G%) within the TSD group over the *Eudoxus* interval.

All the phytoclast categories display very similar vertical profiles, though clearly different abundances, over the *Eudoxus* interval (Figures 7.16A to F). The greatest abundances occur in the lower and upper bituminous mudstones characterized by relatively high amplitude fluctuations, while the bituminous/oil shales contain the lowest abundances. Thus the structured debris particles show a very similar profile to the total pollen. The almost identical profiles for all the phytoclast types imply that these particles were brought into the basin as unsorted fluxes via the same mechanism, possibly low intensity storm re-suspension events. The greater proportion of lath particles implies that deposition was relatively more distal, and the abundance of black/dark forms suggests substantial oxidation either during transport and/or after deposition. Though brown/stripy forms are the least abundant, they are present throughout both as laths and equant particles, thus some of the terrestrial debris did not undergo substantial oxidation, thus supporting rapid transport from the proximal shelf into the deeper basin. During periods of bituminous/oil shale deposition the low phytoclast abundances imply low flux into the basin and thus an increase in climate aridity and stability.

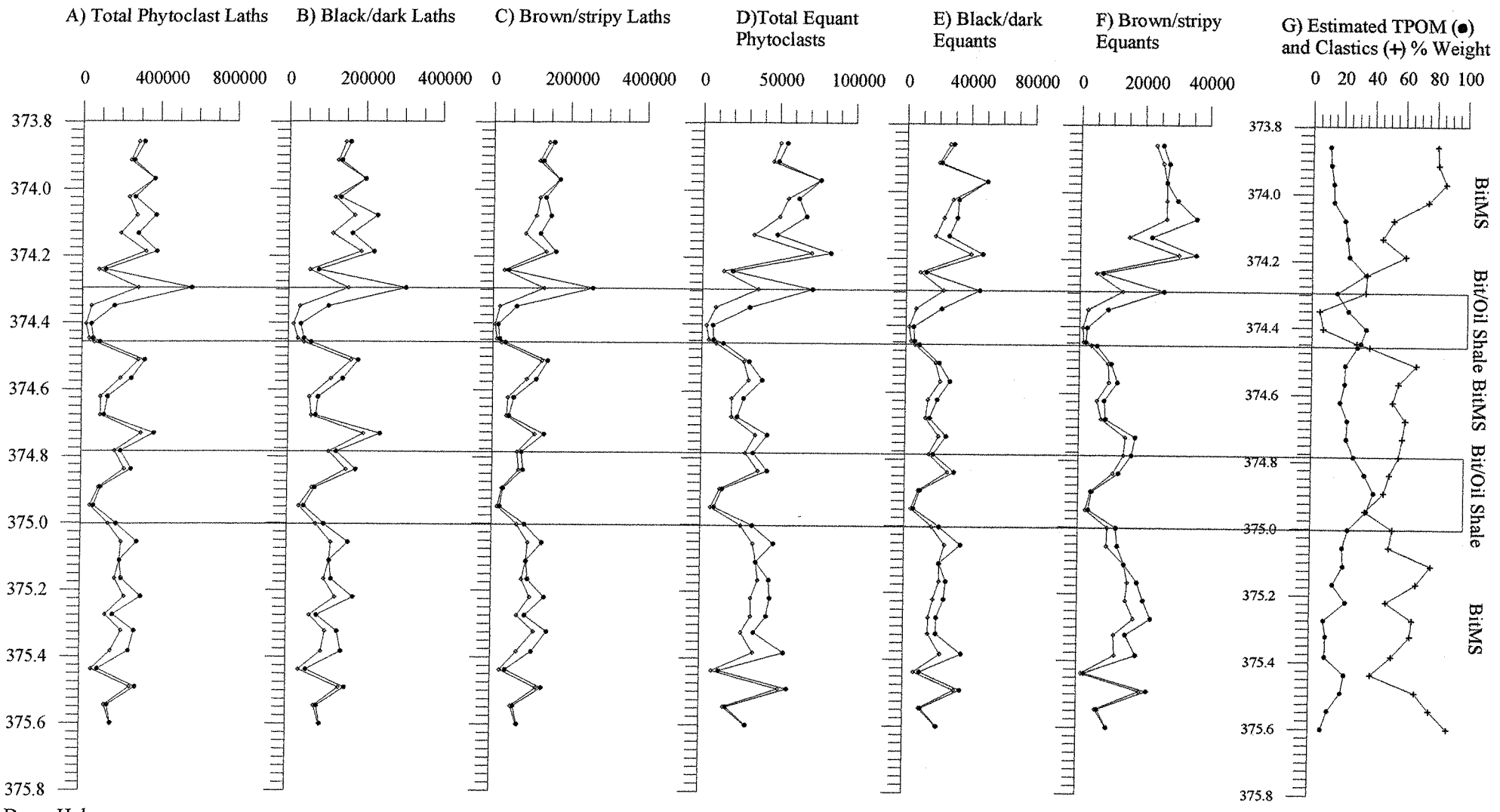

Figure 7.16
Vertical profiles of absolute abundance (open diamonds (◇)) and carbonate-free absolute abundance (closed circles (●)) per gram of rock for terrestrial structured debris, total phytoclast laths (A), black/dark laths (B), brown/stripy laths (C), black/dark equants (D) and brown/stripy equants (E), and estimated TPOM (total organic matter plus pyrite organic matter) and clastics % weight (F) over Eudoxus Interval. For lithological notation see Figure 7.13 caption.

7.2.2.5 Ratios, *Eudoxus* Interval

The ratio of chorate and proximate dinocysts clearly highlights the dominance of the proximate dinocysts, though a greater similarity in dominance is seen over the bituminous/oil shales and the central bituminous mudstone (Figure 7.17A). Total dinocysts, however, are seen to be far less abundant than the total pollen as indicated by the negative ratio of these two categories (Figure 7.17B), though dinocysts are slightly more abundant at the start of the interval. The different influx of inaperturate and *Classopollis* pollen over the interval is also quite clear from the ratio of these two pollen types (Figure 7.17C), with less positive ratios during the central portion of this interval indicating the greater importance of the *Classopollis* pollen. The ratio of fresh *Classopollis* to degraded *Classopollis* is predominately positive over the whole interval which indicates the dominance of the fresh forms. However, in the second bituminous/oil shale the degraded forms are slightly more dominant (Figure 7.17D). The ratio of black/dark to brown/stripy laths shows predominately positive values, especially over the central section of the interval, indicating the dominance of the black/dark laths and a more distal environment (Figure 7.17E). Black/dark equant phytoclasts are also seen to be more dominant over the central portion of the interval than at either end as seen by the predominately positive ratio of black/dark to brown/stripy equant phytoclasts.

7.2.3 SUMMARY (Figure 7.18)

As expected, the *Eudoxus* interval was organic-rich, though peak TOC % values are less than those of the WSB oil shales. However, despite this organic richness, carbonate values are still relatively high, implying that coccolithophores were an important part of the KCF phytoplankton in all lithologies. The greater abundance of FTL in this interval suggests that bottom water conditions were suboxic for the deposition of the bituminous mudstones, while lack of FTL in the bituminous/oil shales implies anoxic bottom waters. Thus organic matter preservation was generally good throughout this interval. The similar profiles for total palynomorphs and phytoclasts suggest similar mechanisms controlled deposition of these particles in the marine environment, possibly relating to weak storm activity causing some re-suspension of proximal sediments. However, the split in pollen type abundances and the pattern of spore abundance over the intervals implies that very subtle shifts in climate from wetter to drier and back to wetter conditions may have occurred. However, the overall climate was probably semi-arid and relatively stable, though weak storm episodes may have been common.

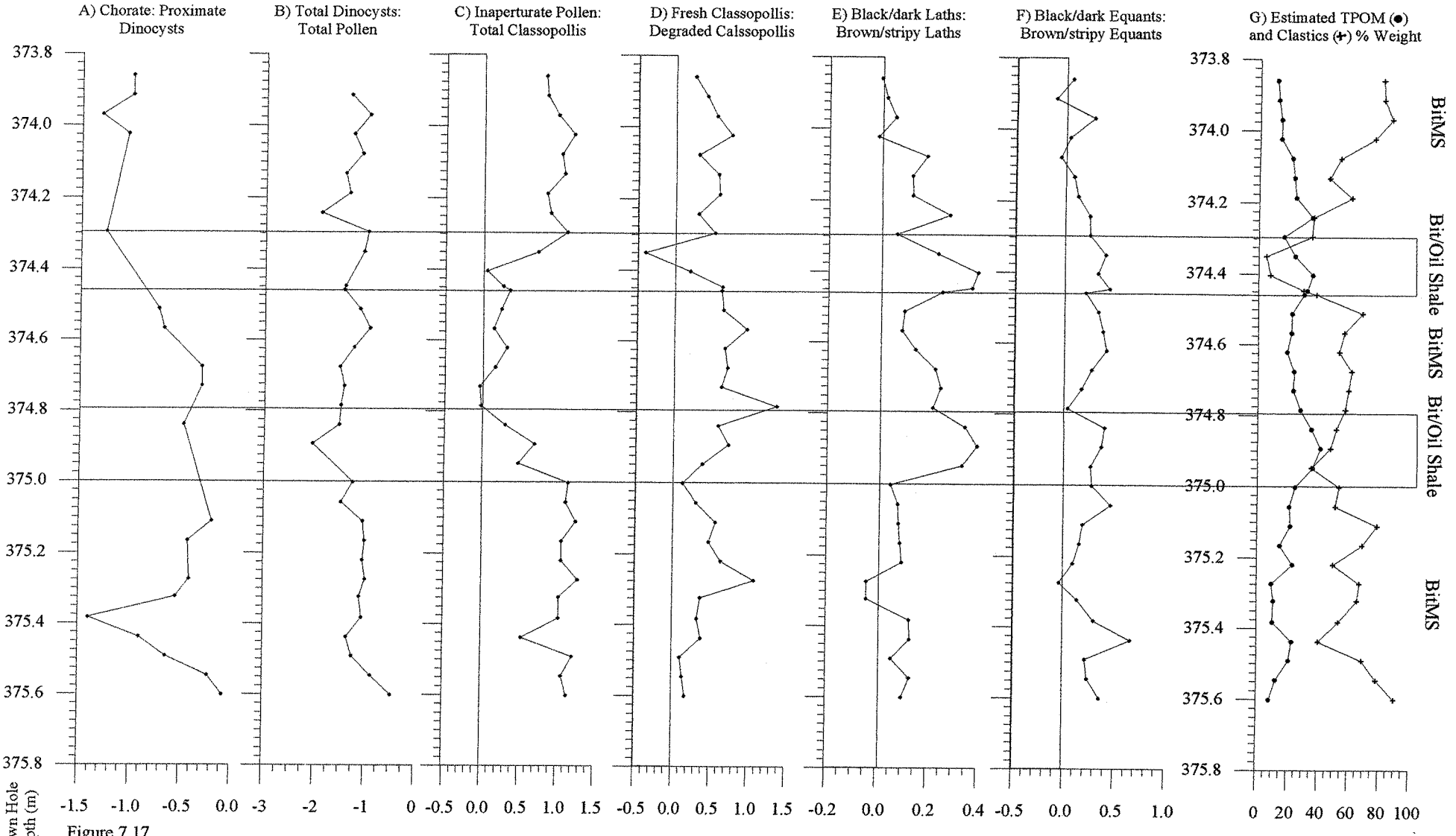

Figure 7.17

Selected Log10 ratios of Eudoxus interval palynological particles. (A) Chorate:Proximate Dinocysts, (B) Total dinocysts:Total Pollen, (C) Inaperturate:Classopollis Pollen, (D) Fresh:Degraded Classopollis, (E) Black/dark:Brown/stripy Laths, (F) Black/dark:Brown/stripy Equants, (G) Estimated TPOM (total organic matter plus pyrite organic matter) and Clastics % Weight. For lithological notation see Figure 7.13 caption.

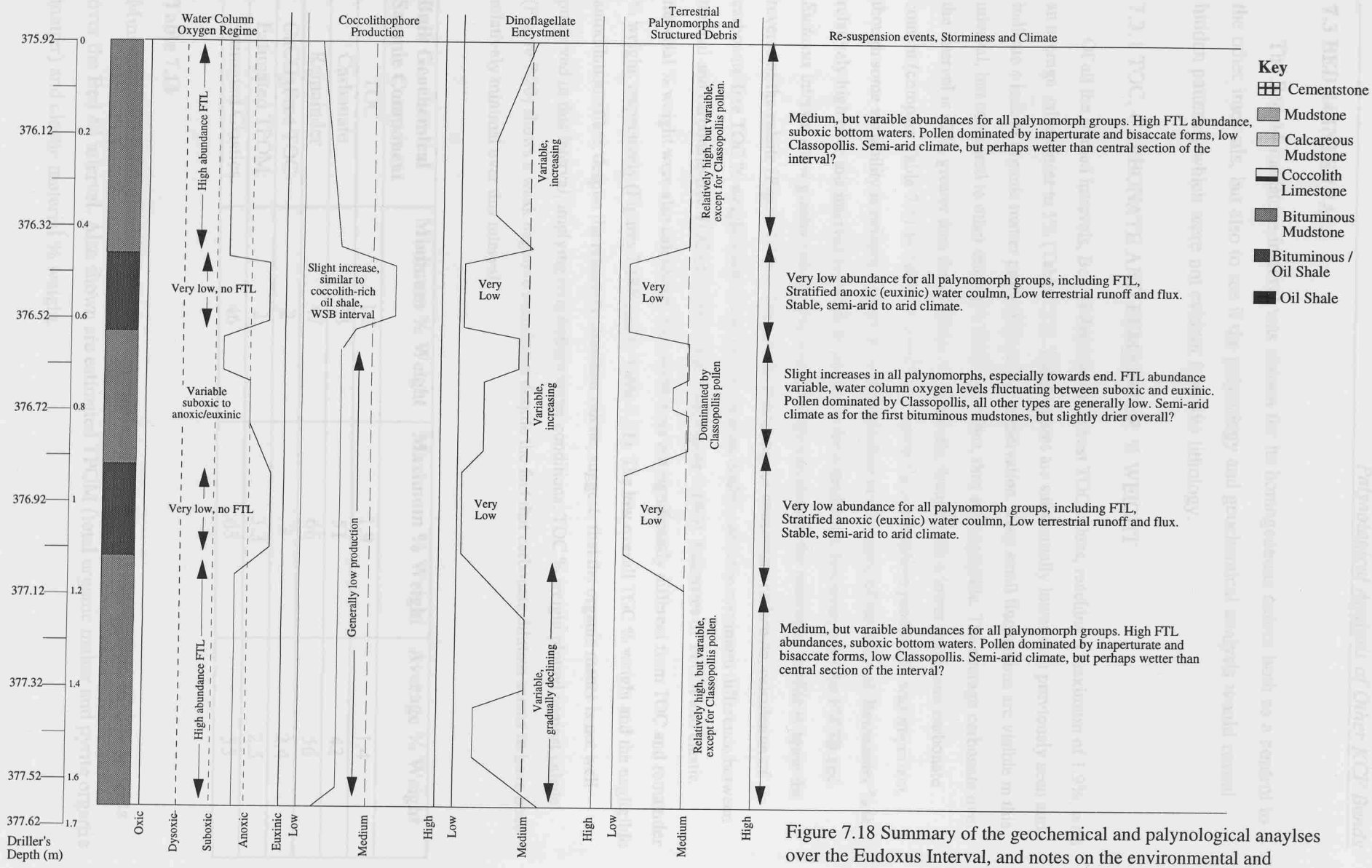

Figure 7.18 Summary of the geochemical and palynological anaylses over the Eudoxus Interval, and notes on the environmental and climatic implication of these results.

7.3 BED 44 INTERVAL

The Bed 44 mudstone interval was chosen for its homogeneous nature both as a control to the other intervals, but also to see if the palynology and geochemical analysis would reveal hidden patterns, which were not evident from the lithology.

7.3.1 TOC, CARBONATE AND REMAINDER % WEIGHT

Of all the studied intervals, Bed 44 displays the lowest TOC values, reaching a maximum of 1.9%, with an average value closer to 1% (Table 7.11). These figures are substantially lower than previously seen and indicate a lack of organic matter production and/or preservation. Very small fluctuations are visible in this interval, but compared to other interval's TOC % profiles, they are negligible. The average carbonate over the interval is 42%, greater than the previous two intervals, though with a lower maximum carbonate content (compare Table 7.11 to Tables 7.1 and 7.6). Again coccolithophore production was important, though some variability is evident, especially a sharp decline in the centre of the interval. Remainder % is relatively high over this interval as would be expected for a mudstone; however, both the FWSB and *Eudoxus* interval show greater values. Due to percentage calculation, the remainder profile is again the reverse of the calcite (Figure 7.19C). Despite the abundance of coccolithic carbonate, calculation of carbonate-free TOC % weight showed values did not even double, with the maximum difference between normal and carbonate-free TOC of 1.5% (Table 7.12; Figure 7.19D). Estimates of TPOM and clastic material % weight were also calculated, but results were not significantly different from TOC and remainder % weight, respectively (Figures 7.19E and F; Table 7.11). The low overall TOC % weight and the negligible autodilution effect, despite the relatively abundant calcite, suggests that the organic matter is not well preserved in this interval, implying oxic bottom water conditions. TOC % weight plotted against calcite (Figure 7.20) shows a weak negative correlation despite the fact that carbonate dilution seems to have been relatively minimal over this interval.

Bulk Geochemical Sample Component	Minimum % Weight	Maximum % Weight	Average % Weight
TOC	1.2	1.9	1.4
Carbonate	33	51	42
Remainder	47	66	56
$CaCO_3$Free TOC	2	3	2.4
Estimated TPOM	2	3.3	2.5
Estimated Clastics	46	65	55

Table 7.11

Minimum, maximum and average TOC, carbonate, remainder and $CaCO_3$Free TOC % weights over the Bed 44 interval. Also shown are estimated TPOM (total organic matter and pyrite organic matter) and clastic material % weight.

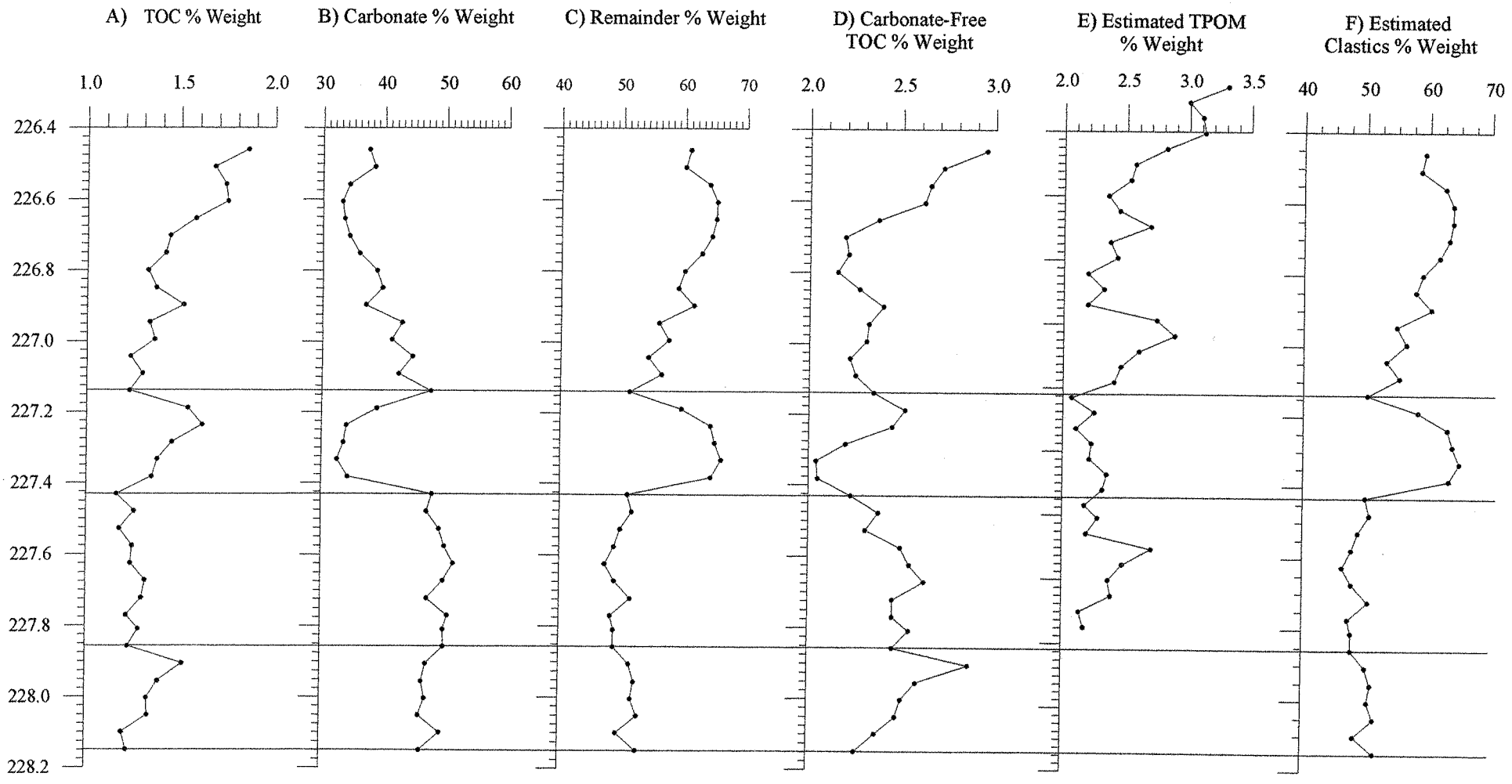

Figure 7.19
TOC (A), carbonate (B), remainder (C), carbonate-free TOC (D), estimated TPOM (total organic matter plus pyrite organic matter) (E) and clastics (F) as % weight of rock, Bed 44 Interval.

7.3.2 BED 44 INTERVAL PALYNOLOGY RESULTS

7.3.2.1 Comparison of the Three Main Particle Groups, Bed 44 Interval.

Similar to the FWSB interval, the terrestrial palynomorphs (TTP) dominate in Bed 44, but terrestrial structured debris (TSD) is approximately half of TTP, though again marine palynomorphs (TMP) show the smallest abundances (Table 7.12). Overall Bed 44 abundances for all the total groups are far lower than for the other intervals. Reduced major axis line regression of these Bed 44 groups resulted in quite different relationships than observed for the other intervals. Very poor correlations were obtained for TMP against TTP where $r = 0.77$, $r^2 = 0.49$ (Figure 7.22A), for TMP against TSD where $r = 0.27$, $r^2 = 0.08$ (Figure 7.22B), and TTP against TSD where $r = 0.37$, $r^2 = 0.14$ (Figure 7.22C). These suggest that either the marine and terrestrial particles were not affected by the same mechanisms, or that changes have occurred after deposition. Taking into account the oxic water column and sediment bioturbation, it is more probably that differential preservation occurred after deposition.

TOTAL CATEGORY Av. % of total particle count	MINIMUM		MAXIMUM		AVERAGE	
	AA/g	$CaCO_3$Free AA/g	AA/g	$CaCO_3$Free AA/g	AA/g	$CaCO_3$Free AA/g
TMP 8% (max.14%)	4,000	8,000	14,500	29,500	9,000	16,000
TTP 57% (max.64%)	64,000	101,000	112,000	207,000	89,000	156,000
TSD 38% (max.49%)	35,000	57,000	65,000	128,000	52,000	92,000

Table 7.12 Minimum, maximum and average absolute abundance (AA/g) and carbonate-free absolute abundance ($CaCO_3$Free AA/g) per gram of rock for the total particle groups, Bed 44 interval. Average and maximum total particle percentages are also displayed for these three groups.

Vertical profiles of the three main groups do not show any clear fluctuations, though abundances are very slightly greater in the lower half of the interval (Figure 7.21). The profiles also highlight the relative consistency of the carbonate autodilution effect over this interval. The indication is therefore, that compared to the other intervals, there is little change in the absolute abundances for all the main particle groups, which may imply relatively constant marine production and terrestrial input during the Bed 44 interval. Conversely, it may also be a function of the preservational state of the water column and sediment, with intense bioturbation destroying or have at least smoothing any flux variability.

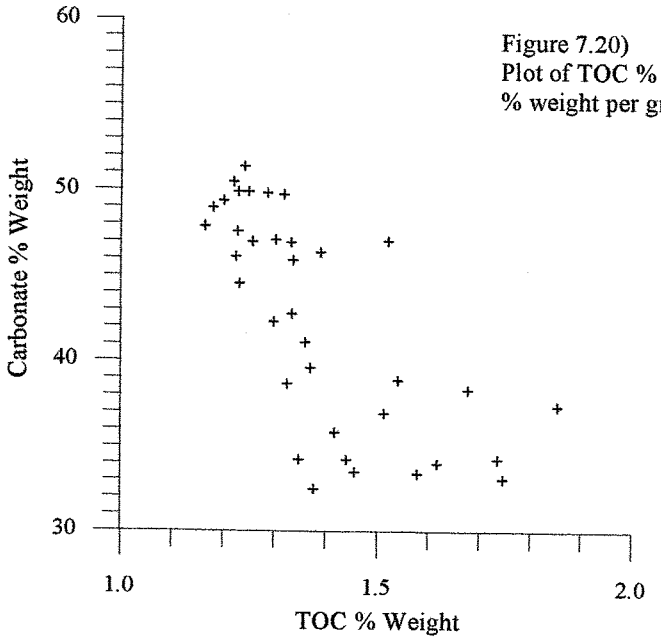

Figure 7.20)
Plot of TOC % weight against carbonate
% weight per gram of rock for the Bed 44 Interval.

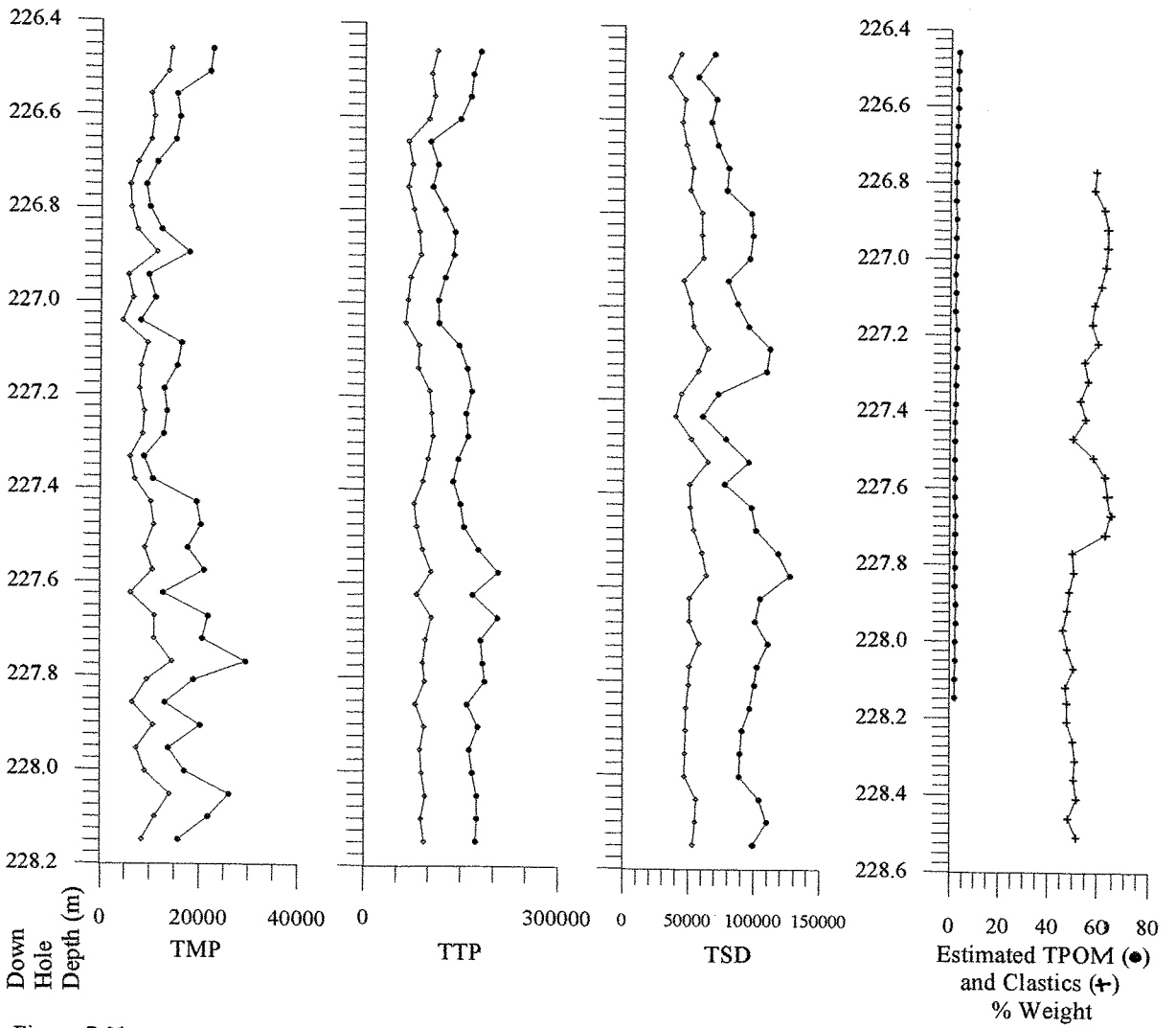

Figure 7.21
Vertical profiles of absolute abundance (open diamonds (◇)) and carbonate-free absolute abundance (closed circles (●)) per gram of rock for the three total palynology groups, together with estimated TPOM (total organic matter plus pyrite organic matter) and clastics (+) % weight for the Bed 44 interval.

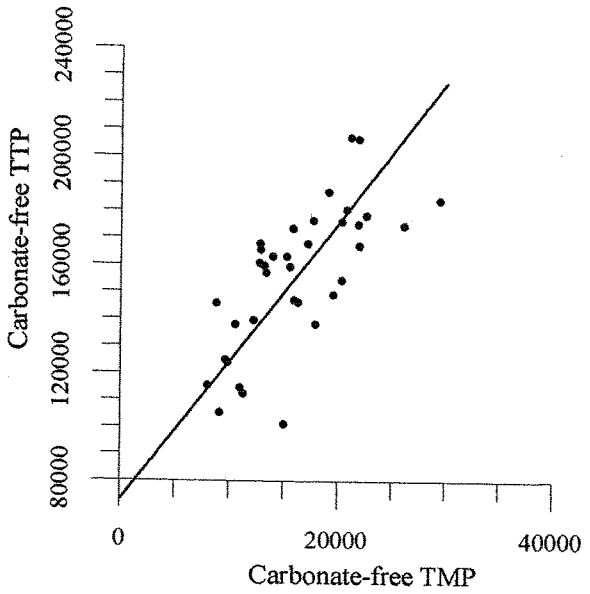

Figure 7.22A)
Reduced major axis line regression
for TMP against TTP, Bed 44 interval.
The isogonic growth line is shown,
with detials given below.

$y = 72806 + 5.14x$
$r = 0.7$, r-squared = 0.49, $n = 36$
95% confidence interval for the slope (b)
$b = 5.14 \pm 0.89$,
95% cofidence interval for the intercept (a)
$a = 72806 \pm 15{,}000$.

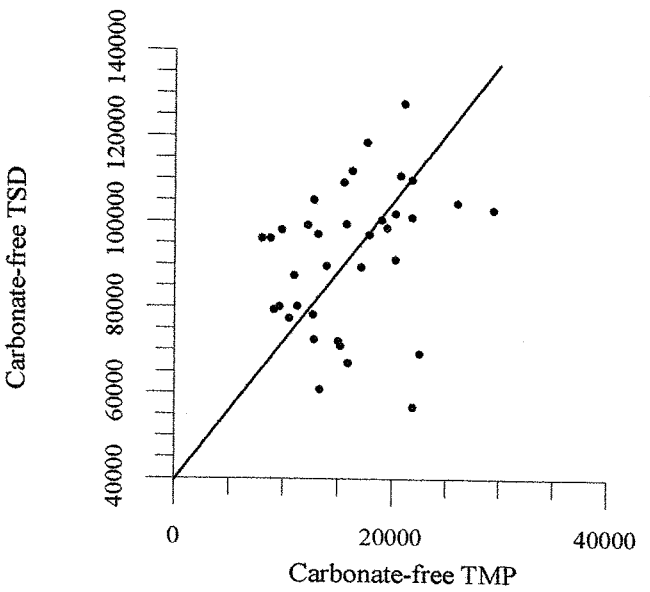

Figure 7.22B)
Reduced major axis line regression
for TMP against TSD, Bed 44 interval.
The isogonic growth line is shown,
with detials given below.

$y = 39612 + 3.24x$
$r = 0.27$, r-squared = 0.08, $n = 36$
95% confidence interval for the slope (b)
$b = 3.24 \pm 0.76$,
95% cofidence interval for the intercept (a)
$a = 39612 \pm 13{,}000$

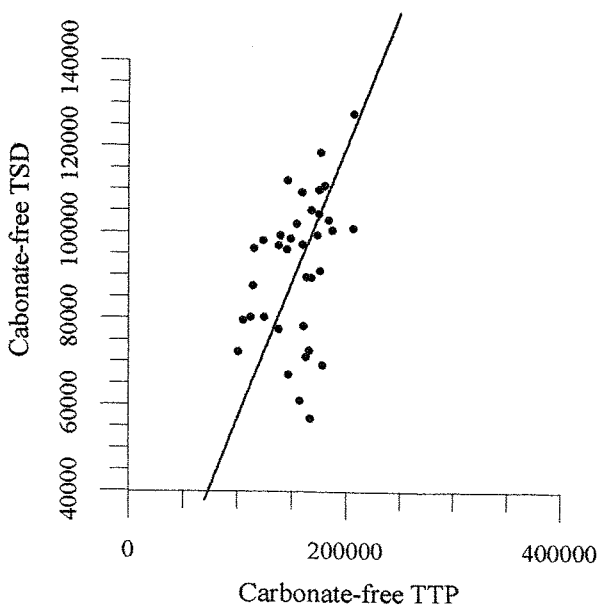

Figure 7.22C)
Reduced major axis line regression
for TTP against TSD, Bed 44 interval.
The isogonic growth line is shown,
with detials given below.

$y = 0.63x - 6326$
$r = 0.37$, r-squared = 0.14, $n = 36$
95% confidence interval for the slope (b)
$b = 0.63 \pm 0.14$,
95% confidence interval for the intercept (a),
$a = -6326 \pm 22{,}000$

7.3.3.2 Comparison of the Marine Palynomorph Group, (TMP), Bed 44 Interval.

As seen for the other intervals, dinocysts are also the most abundant of the marine palynomorphs within the Bed 44 interval, though foraminiferal test linings are very similar in abundance (Table 7.13). Proximate cysts make up the majority of the dinocysts present, while both chorate and proxi-chorate cysts are far less abundant. However, on average both simple sacs and acritarchs are similar in abundance to the proximate cysts, which was not the case for the other intervals, and prasinophytes were not seen within this interval.

TMP PARTICLE CATEGORY	MINIMUM			MAXIMUM			AVERAGE		
		$CaCO_3$Free			$CaCO_3$Free			$CaCO_3$Free	
	AA/g	AA/g	G%	AA/g	AA/g	G%	AA/g	AA/g	G%
Chorate Dinocyst	0	0	0	1,500	2,500	11	300	400	3
Proxi-chorate Dinocyst	0	0	0	3,000	4,500	21	500	800	5
Proximate Dinocyst	500	800	7	4,000	7,000	38	2,000	3,500	22
Total Dinocysts	900	1,600	8	8,000	13,500	61	3,000	5,000	29
Foraminifera Test Linings	1000	2000	17	5,000	10,000	57	3,000	5,000	34
Simple Sacs	600	900	7	3,000	6,000	37	2,000	3,000	19
Prasinophytes	0	0	0	0	0	0	0	0	0
Acritarchs	200	500	2	4,000	7,500	30	1,500	3,000	17

Table 7.13 Minimum, maximum and average absolute abundance (AA/g), carbonate-free absolute abundance ($CaCO_3$Free AA/g) and group percentage (G%) for all individual particle categories within the TMP group over the Bed 44 interval.

The vertical profiles for total dinocysts, proximate and chorate dinocysts, FTL, simple sacs and acritarchs over the Bed 44 interval are displayed in Figure 7.23. All profiles display relatively noisy signals, but on average are generally consistent over the whole interval. The dominance of the proximate cysts implies a relatively unstable marine environment, but in general the dinoflagellate population is indicated to have remained relatively constant, except for the end of this interval when an increase occurs. FTL are seen to be present throughout the interval, but at slightly lower abundances than in the FWSB interval, and at far lower than in the *Eudoxus* interval, possibly indicating food competition and predation from other benthos under an oxic water column. Simple sacs show a similar profile to the total dinocysts, possibly again indicating an unstable marine environment. Acritarchs, however, are slightly more common at the beginning of the interval, possibly suggesting slightly less saline surface waters than at the end of the interval when dinocysts abundances are seen to increase.

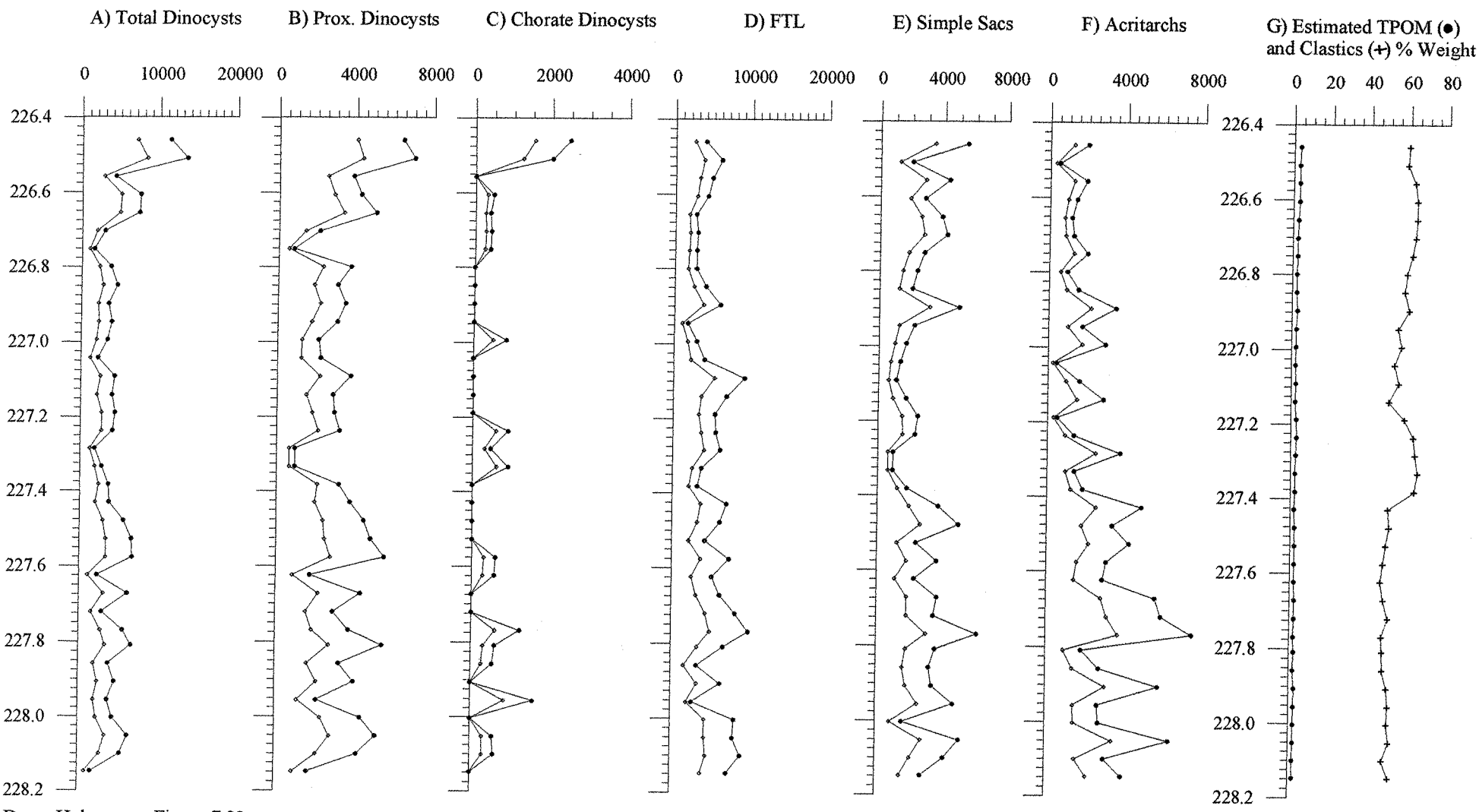

Figure 7.23
Vertical profiles of absolute abundance (open diamonds (◇)) and carbonate-free absolute abundance (closed circles (●)) per gram of rock for marine palynomorphs, dinoflagellates (A to C), foraminiferal test linings (D) and simple sacs (E), acritarchs (F) and estimated TPOM (total organic matter plus pyrite organic matter) and clastics % weight (G) over Bed 44 Interval.

7.3.2.3 Comparison of the Terrestrial Palynomorph Group (TTP), Bed 44 Interval

The terrestrial palynomorph group of the Bed 44 interval is again dominated by pollen, which are predominately small, spherical types. Inaperturate pollen is slightly more abundant than total *Classopollis* pollen, while bisaccate pollen is a very minor component (Table 7.14). *Classopollis* pollen is dominated by fresh forms as found for the other intervals, though the abundance of degraded forms is not much less than the fresh forms, suggesting degradation of pollen after deposition. Spores are found throughout the interval and are more abundant than the bisaccate pollen. However, together on average these two categories only comprise <5% of the TTP group (Table 7.15).

TTP PARTICLE CATEGORY	MINIMUM			MAXIMUM			AVERAGE		
		$CaCO_3$Free			$CaCO_3$Free			$CaCO_3$Free	
	AA/g	AA/g	G%	AA/g	AA/g	G%	AA/g	AA/g	G%
Inaperturate Pollen	31,000	53,000	47	67,000	109,000	64	48,000	85,000	54
Fresh *Classopollis*	13,000	22,000	16	42,000	68,000	38	22,000	38,000	24
Degraded *Classopollis*	9,000	15,000	9	25,000	46,000	25	15,000	27,000	17
Total *Classopollis*	25,000	40,000	32	53,000	91,000	49	37,000	65,000	42
Bisaccate Pollen	0	0	0	2,500	5,000	3	1000	2,000	1
Total Pollen	63,000	98,000	94	107,000	201,000	99	86,000	152,000	97
Spores	600	900	<1	6,000	12,000	6	2,000	4,000	3

Table 7.14 Minimum, maximum and average absolute abundance (AA/g), carbonate-free absolute abundance ($CaCO_3$Free AA/g) and individual particle categories group percentage (G%) within the TTP group over the Bed 44 interval.

The vertical profiles of the total pollen, inaperturate, *Classopollis* and bisaccate pollen and spores over the Bed 44 interval are displayed in Figure 7.24. Both total pollen and inaperturate pollen profiles are fairly constant, though abundances are slightly greater in the lower half of the interval (Figure 7.24A and B). Total *Classopollis* pollen has a slightly more variable profile, but displays the same major pattern (Figure 7.24C). Both the bisaccate pollen and spores also display the same general profile, though at substantially lower abundances (Figures 7.24D and E). Thus again small, spherical pollen dominate probably indicating both the regional flora and differential transportation sorting effects.

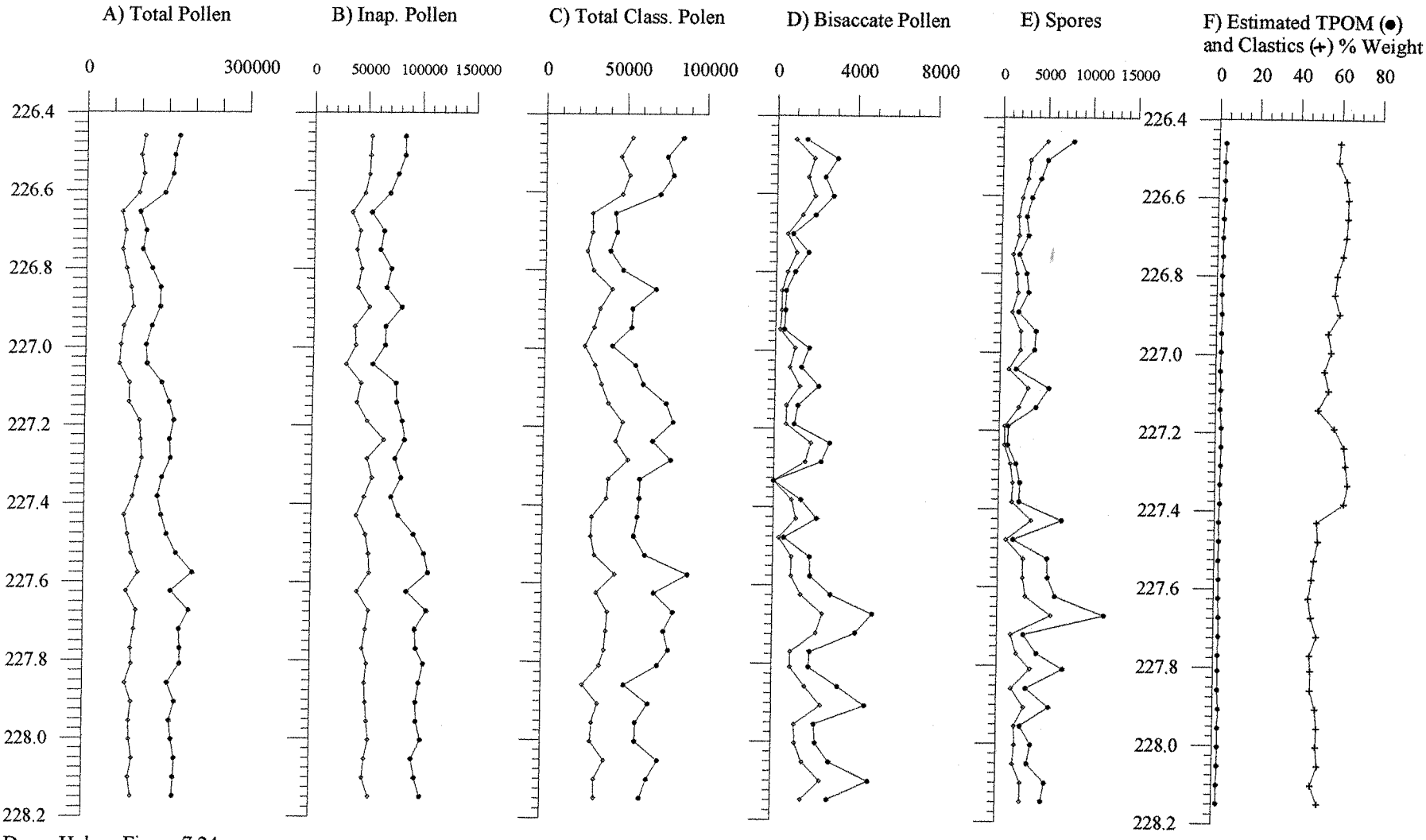

Figure 7.24
Vertical profiles of absolute abundance (open diamonds (◇)) and carbonate-free absolute abundance (closed circles(●)) per gram of rock for terrestrial palynomorphs, total pollen (A), inaperturate pollen (B), total Classopollis pollen (C), bisaccate pollen (D) and spores (E), and estimated TPOM (total organic matter plus pyrite organic matter) and clastics % weight (F) over Bed 44 Interval.

7.3.2.4 Comparison of the Terrestrial Structured Debris Group (TSD), Bed 44 Interval

For all the other intervals the most dominant form of phytoclasts were laths and the Bed 44 interval is no exception, including the greater numbers of black/dark forms compared to brown/stripy forms for both laths and equant phytoclasts. However, the overall abundance of phytoclasts within this interval is far less than seen in the other intervals, but similarly cuticle is not abundant (Table 7.15).

TSD PARTICLE CATEGORY	MINIMUM			MAXIMUM			AVERAGE		
	AA/g	$CaCO_3$Free AA/g	G%	AA/g	$CaCO_3$Free AA/g	G%	AA/g	$CaCO_3$Free AA/g	G%
Black/dark Laths	14,000	22,000	33	28,000	55,000	50	21,000	36,000	40
Brown/stripy Laths	18,000	12,000	17	8,000	35,000	33	14,000	24,000	26
Total Phytoclast Laths	24,000	37,000	52	44,000	89,000	75	34,000	61,000	66
Black/dark Equants	6,000	9,000	15	16,000	27,000	32	11,000	20,000	22
Brown/stripy Equants	2,500	4,000	5	10,000	20,000	17	6,000	11,000	12
Total Phytoclast Equants	11,000	18,000	25	24,000	46,000	48	18,000	31,000	31
Cuticle	0	0	0	300	600	<1	20	30	<1

Table 7.15 Minimum, maximum and average absolute abundance (AA/g), carbonate-free absolute abundance ($CaCO_3$Free AA/g) and individual particle categories group percentage (G%) within the TSD group over the Bed 44 interval.

The vertical profiles of the phytoclasts over the Bed 44 interval show relatively similar patterns as the pollen profiles. The lath phytoclasts display generally higher constant values at the start of the interval (Figures 7.25A to C), but a notable decline is seen in the centre, which can be correlated to a decline in carbonate (Figure 7.19B). This may be an indication of a small decline in terrestrial flux into the basin, thus causing a decline in phytoclasts, as well as a decrease in nutrients, which affected the coccolithophore production. The equant phytoclasts display a less variable signal than the laths and values are seen to be relatively constant throughout the interval (Figure 7.25D to F). For both the laths and equant particles black/dark types are almost twice as abundant as the brown/stripy types, indicating a distal basin and significant oxidation of particles both in transport to and once within the basin sediment.

7.3.2.5 Ratios, Bed 44 Interval

The ratio of chorate to proximate dinocysts shows the dominance of the proximate morphotype over this interval (Figure 7.26A). However, total dinocysts are far less dominant than total pollen, with a highly negative ratio between these two categories (Figure 7.26B).

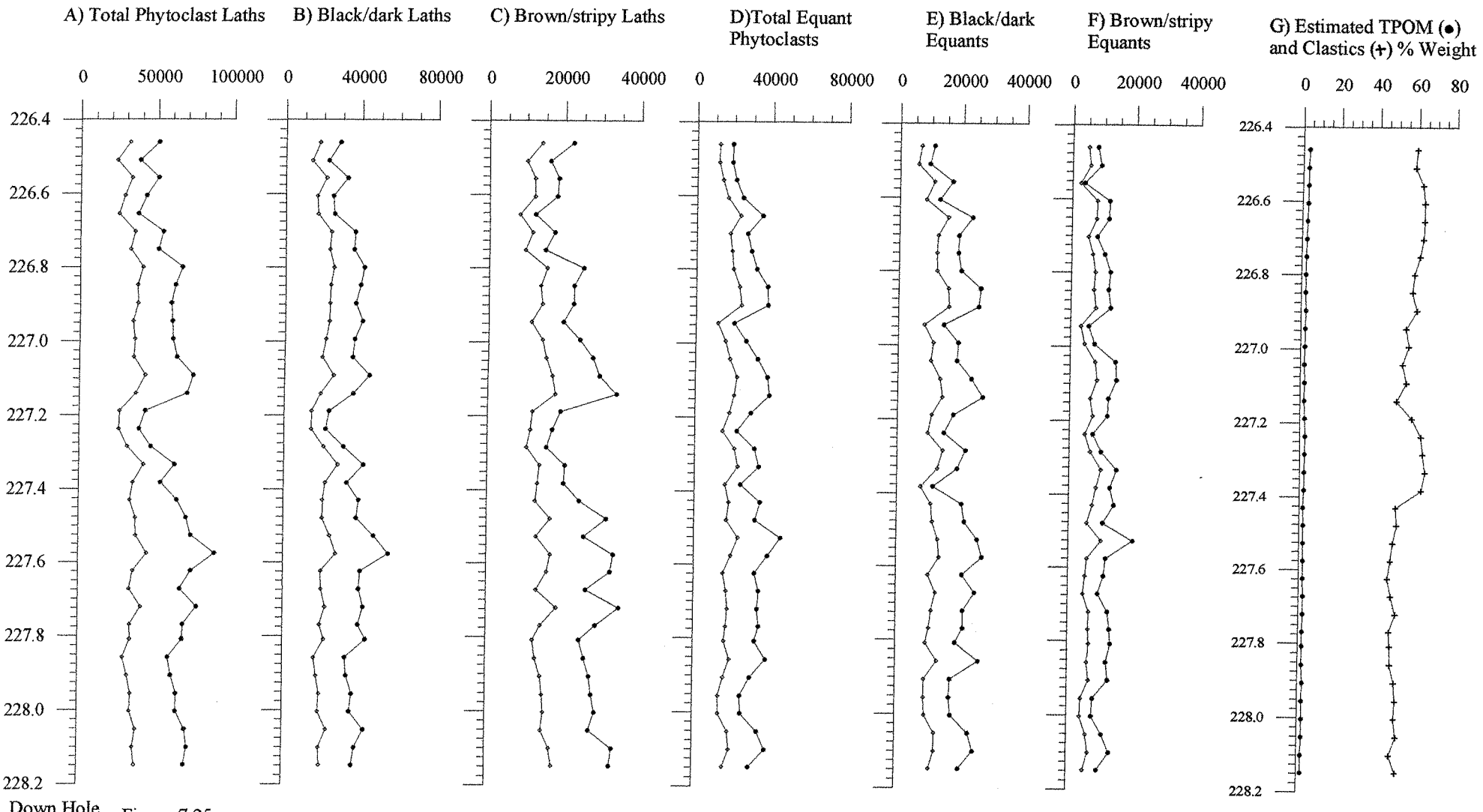

Figure 7.25
Vertical profiles of absolute abundance (open diamonds (◊)) and carbonate-free absolute abundance (closed circles (●)) per gram of rock for terrestrial structured debris, total phytoclast laths (A), black/dark laths (B), brown/stripy laths (C), black/dark equants (D) and brown/stripy equants (E), and estimated TPOM (total organic matter plus pyrite organic matter) and clastics % weight (F) over Bed 44 Interval.

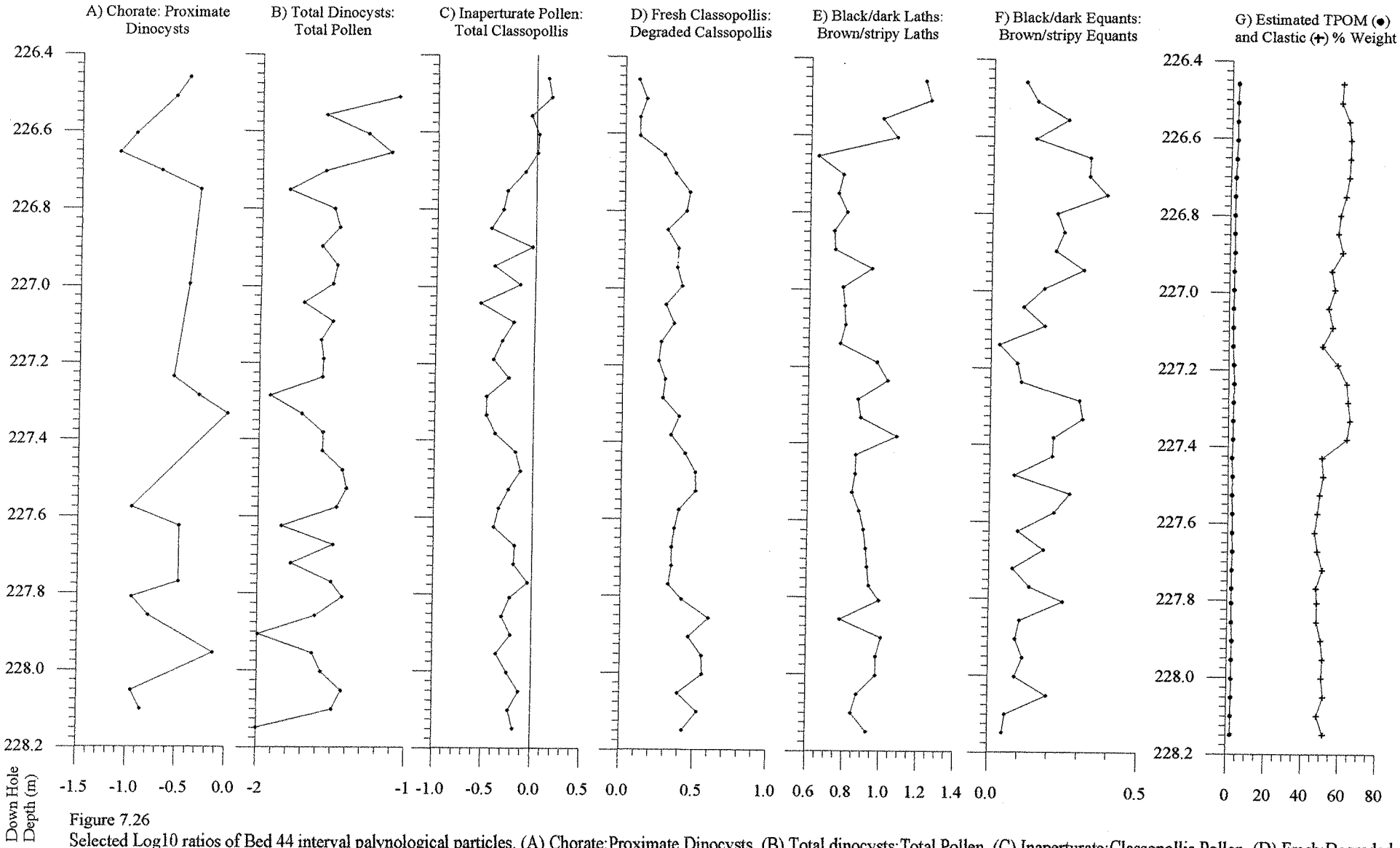

Figure 7.26
Selected Log10 ratios of Bed 44 interval palynological particles. (A) Chorate:Proximate Dinocysts, (B) Total dinocysts:Total Pollen, (C) Inaperturate:Classopollis Pollen, (D) Fresh:Degraded Classopollis, (E) Black/dark:Brown/stripy Laths, (F) Black/dark:Brown/stripy Equants, (G) estimated TPOM (total organic matter plus pyrite organic matter) and clastics % Weight.

Though the abundance of both inaperturate pollen and total *Classopollis* pollen are very similar, the ratio of these two small, spherical pollens clearly indicates that actually *Classopollis* were slightly more important over the majority of the interval until the end when values become positive (Figure 7.26C). This relationship is also seen from the ratio of fresh to degraded *Classopollis*, which is highly positive for the majority of the interval, but becomes less positive at the end of the interval indicating an increase in importance of the degraded forms (Figure 7.26D). Thus, these two ratios suggest that *Classopollis* pollen was more important over the majority of the interval but at the end inaperturate pollen increased, while *Classopollis* declined and was represented by degraded forms. Black/dark forms dominate both phytoclast laths and equants over the interval indicating significant degradation of particles both during transport to and once within the distal basin sediment (Figures 7.26E and F).

7.3.3 SUMMARY (Figure 7.27)

The homogenous nature of the Bed 44 interval is evidenced by the lack of variability in both the TOC and the palynological particles, implying an oxic water column and rich benthic fauna and thus bioturbation, during the depositional period. It is also notable that the majority of the organic matter in this interval was structured and AOM particles were rare compared to the other intervals. The low abundance of FTL also supports an oxic water column, as FTL populations would have been constrained due to competition for food and predation by the other benthic fauna. Carbonate was seen to be a substantial component in this interval, with some variability especially near the centre of the interval, which possibly relates to a small decline in terrestrial flux and nutrients into the basin. As in the other intervals, dinocysts were the dominant phytoplankton after the coccolithophores and the abundance of the proximate morphotypes indicates some instability in the marine environment. Again small, spherical pollen dominate throughout the interval indicating both the regional flora and differential production and transportation of these pollen types. The dominance of the black/dark lath phytoclasts compared to the other phytoclast forms indicates a distal depositional environment with substantial oxidation of particles during transportation and once deposited. As for the WSB mudstones, a warm subtropical to semi-arid climate is suggested to have been dominant, though any evidence of variability has been destroyed and homogenized by the sediment bioturbation.

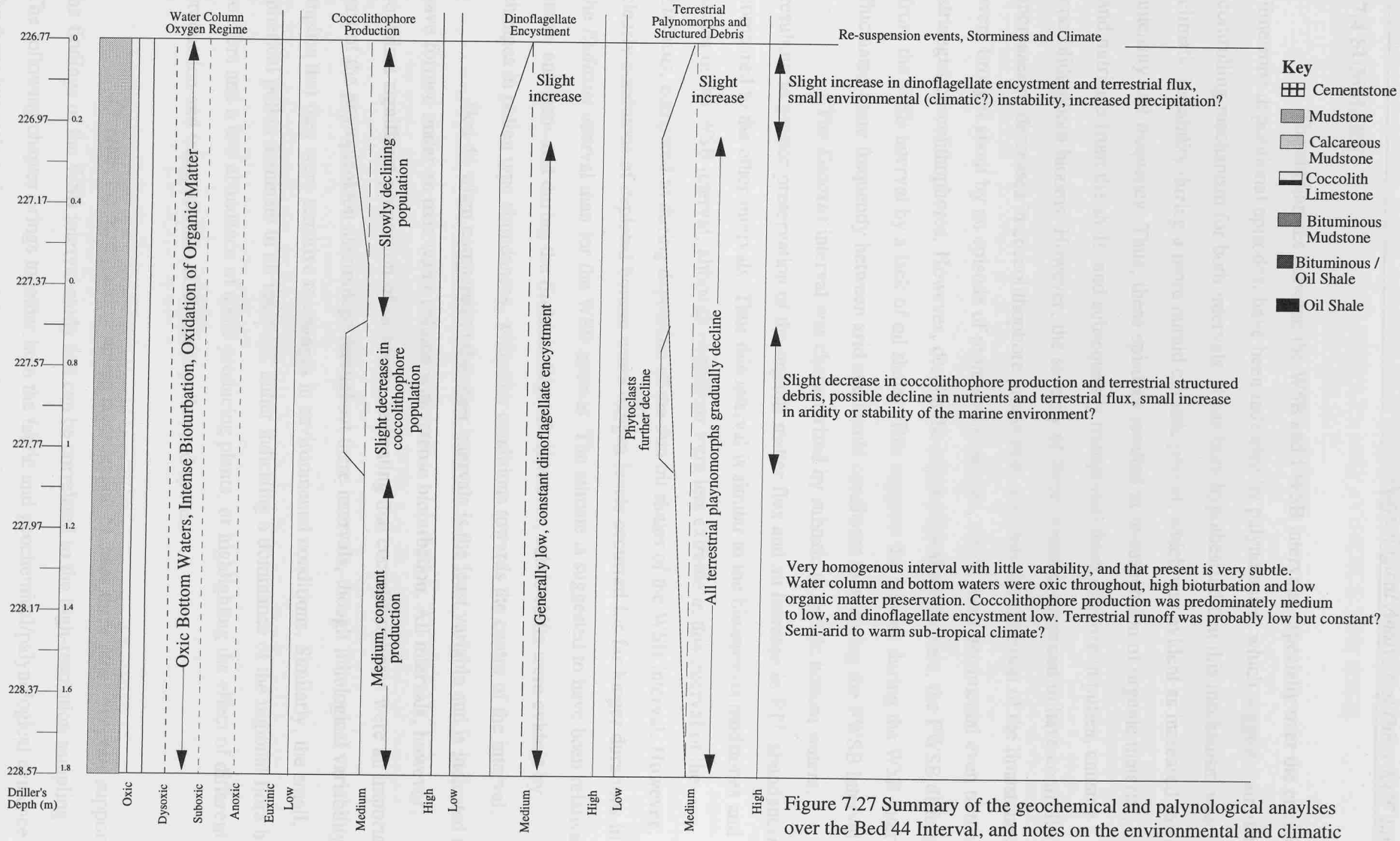

Figure 7.27 Summary of the geochemical and palynological anaylses over the Bed 44 Interval, and notes on the environmental and climatic implication of these results.

7.4 SUMMARY

The similarities between the WSB and FWSB intervals, especially over the coccolith limestone depositional episodes, have been indicated by palynofacies, which suggest a similar controlling mechanism for both intervals. It has been hypothesized that this mechanism was climatic instability during a more humid climatic period, which was evident as increased storm intensity and frequency. Thus, these episodes resulted in re-suspension of organic material, clays and nutrients from the shelf, and subsequently transported them offshore in pulses, causing coccolithophore blooms. However, the severity of these storms is proposed to have controlled increases or decreases in coccolithophore production, and thus the cessation of the limestones were brought about by an episode of more severe storms, which were detrimental even to the r-strategist coccolithophores. However, despite the palynological similarities, the FWSB differs from the WSB interval by a lack of oil shales. This suggests the climate during the WSB interval fluctuated more frequently between arid and humid conditions than during the FWSB interval.

The *Eudoxus* interval was characterized by suboxic to anoxic bottom waters, resulting in greater preservation of the organic matter flux and an increase in FTL abundances compared to the other intervals. Thus this interval is similar to the bituminous mudstones and oil shales of the WSB interval, although conditions were less extreme in this interval of the *Eudoxus*, compared to during deposition of the thin oil shales of the WSB interval. However, clearly conditions of depleted bottom water oxygen levels occurred for far longer durations in the *Eudoxus* interval than for the WSB interval. The climate is suggested to have been relatively stable and semi-arid during the *Eudoxus* interval. However, subtle shifts were evident by changes in pollen type abundances, with drier conditions towards the centre of the interval.

Bed 44 when compared to the other intervals is the least variable and is indicated to have formed under an oxic water column with intense bioturbation. All intervals, however, contain a significant proportion of carbonate, indicating that coccolithophores were an important part of the phytoplankton assemblage throughout these intervals, though lithological variability implies that they were sensitive to changes in environmental conditions. Similarly, the small, spherical pollen dominate in all intervals, either indicating a dominance of the regional flora by conifers and a low abundance of spore producing plants, or highlighting the effect of differential production and transportation of different pollen and spores.

Overall, the 5cm point sampling investigation of these three other intervals support the findings of the WSB interval study and can be correlated to the high-resolution sampling. The following chapter brings together both the fabric and geochemical/palynological evidence for these intervals and summary interpretations are presented and discussed.

8.0 INTERPRETATION OF ALL RESULTS AND EVIDENCE FOR HIGH RESOLUTION ENVIRONMENTAL CHANGE.

The objectives of this study were two fold. Firstly to determine the KCF sediment fabric composition and structure, in order to relate these to both surface and benthic processes, and secondly to identify changes in organic matter at a high resolution and relate them to the sediment fabric. The first objective was dealt with in Chapters 3 and 4, with detailed descriptions of the fabric and discussion on the complex system of water column and benthic processes operating during the KCF deposition. Reconstruction and interpretations of the environment, based on this fabric evidence, were produced for the four main lithological types of the studied intervals. However, information on the interaction between the terrestrial and marine environments via runoff and terrestrial flux could not be ascertained purely from the fabric evidence. Thus, high-resolution geochemical and palynological analyses of the organic matter within these lithologies were undertaken (Chapters 6 and 7), providing quantitative compositional information and evidence of terrestrial flux variability over the studied intervals. In this chapter the second objective is achieved with both the fabric and the geochemical/palynological analyses results being brought together, enabling clarification of the environmental reconstructions. The final aim of the study was to establish high-resolution environmental reconstructions and assess climatic change over the KCF intervals. This chapter is therefore divided in three, assimilation and interpretation of all analysis results for each lithology within the intervals, discussion of these interpretations with respect to previous studies and lastly summaries of the environmental and climatic variability over each of the intervals. This final section also includes a brief comment on the effects of sampling resolution.

8.1 INTERPRETATION OF ALL ANALYSES RESULTS

The major points of evidence from both the fabric and the geochemical/palynological analyses are summarized in Table 8.1, with brief interpretations for each point. The table is divided into four parts, representing the major lithologies of oil shale, coccolith limestone, mudstone and cementstone, as for the reconstructions in Chapter 4 (Section 4.11). However, two further lithologies of calcareous and bituminous mudstone are also included, which are seen as transitional lithologies between the mudstone and the coccolith limestone and the oil shale respectively. The following sections are brief summaries of the main environment and climatic characteristics of the KCF depositional system for each lithology, with a schematic representation given in Figure 8.1.

Table 8.1 Summary of fabric, geochemical and playnological analyses results of this study and environmental interpretation.
Part A - Oil Shale Lithology.

LITHOLOGY	FABRIC EVIDENCE	FABRIC INTERPRETATION	GEOCHEMICAL/PALYNOLOGICAL EVIDENCE	GEOCHEMICAL/PALYNOLOGICAL INTERPRETATION
Oil Shale	Dominated by low backscatter organic-rich fabric	Abundant organic matter (OM) either high production or enhanced preservation.	Peak TOC % weight, maximum >50%	High organic mater prduction and/or preservation
	AOM and elongated stringer/lense OM dominate the oil shale fabric.	Flocculated and aggregated planktonic marine biomass.	Distinctive linear relationship between TOC % and carbonate % weight, enabled calculation of total (TOM) and 'pyrite' organic matter, max. 90%	Proportion of organic matter used during sulphate reduction to form pyrite. Removal from remainder % weight results in % of clastic terrestrial input.
	Lamination	Lack of bioturbation, low benthic fauna. Indicates anoxic sediment and bottom water. Stratified basin and OM preservation.	Low clastic % weight	Low clastic flux. Reduced terrestrial input, low precipitation. Arid climate, low terrestrial nutrient input, oligotrophic waters.
	Highly abundant, very small (<5µm diameter) pyrite framboids.	Formation within a euxinic water column. Strong stratification and enhanced OM preservation.	Low coccolith carbonate % weight Except for coccolith lamina	Low coccolithophore production, oligotrophic surface waters. Coccolithophore blooms, brief episodes of eutrophication.
	Relatively sparse, well dispered clastic material e.g. quartz and feldspar grains, clays more abundant.	Very low terrestrial clastic input, distal basin.	High H/C ratio	Phytoplankton origin for OM,Type I and II kerogen. Maximum level of preservation reached, anoxic bottom waters.
			Dark ogrange to brown AOM	Greatest development of anoxic/euxinic conditions.
	Individual cocoliths and coccolith pellets, well dispersed in organic-rich matrix	Coccolith flux as pellets, match between phyto- and zooplankton. Overal low coccolithophore productivity, oligotrophic surface waters.	Low dinocysts	Stable, stratified marine environment. Lack of encystment or low phytoplankton population due to oligotrophic conditions.
	Coccolithic carbonate lamina	Coccolithophore bloom periods, surface water eutrophication. Water column nutrient recycling from wind or storm mixing, euxinic waters reached up into the photic zone Or terrestrial flux, increased precipitation.	Low FTL Sharp increase of FTL at end of oil shale.	Anoxic bottom waters, well stratified basin. Bottom waters become suboxic to dysoxic. Or redeposition from the shelf via a re-suspension event. Either are indicative of oil shale termination.
			Low TTP (both pollen and spores) Small increase in TTP at the end of oil shale.	Very low/no terrrestrial flux, arid climate High intensity, short-lived storm episode, re-suspension event. Water column overturn causing oil shale termination.
	Graded intervals associated with abundant carbonate lamination within the organic-rich fabric	Current / strom disturbance to sediment and water column. Stratification overturn, nutrients released to surface waters causing blooms.	Low/medium TSD Small increase in TSD at end of oil shale.	Very low/no terrestrial flux, arid climate. Preferential preservation of phytoclasts. High intensity, short-lived resuspension event. Water column overturn causing oil shale termination.

Table 8.1 Continued:- Summary of fabric, geochemical and playnological analyses results of this study and environmental interpretation.
Part B - Coccolith Limestone Lithology.

LITHOLOGY	FABRIC EVIDENCE	FABRIC INTERPRETATION	GEOCHEMICAL/PALYNOLOGICAL EVIDENCE	GEOCHEMICAL/PALYNOLOGICAL INTERPRETATION
Coccolith Limestone	Dominated by coccoliths.	High coccolithohpore primary production. Extreme blooms, no nutrient limitation, eutrophic surface waters. High water column nutrient recycling, and/or high terrestrial flux, increased storms and precipitation. Increased humidity and thus climate instability.	Dominated by carbonate % weight, up to 95%	High coccolithophore production, eutrophic surface waters.
			Short episodes of low carbonate associated with high TOC % weight	Decreased coccolithophore production, decreased dilution, reduction in nutrients. Increased production of other previously supressed phytoplankton. Decreased bottom water oxygen levels and increased OM preservation.
	Monospecific species:- *Watznaueriaceae*	r-stratergy species (*Emiliani huxleyi* as an analogue). Surface water conditions conducive to r-stragery species, commonly unstable.		
			Predominately low clastic % weight throughout.	Low terrestrial flux, low runoff, or transgressive regime trapping sediment in the proximal marine environment.
	Purely homogeneous coccolithic fabric, massive structure.	Episodes of bioturbation and benthic colonisation, Oxic/dysoxic bottom waters, no stable stratification. Mismatch between phyto- (coccolithophore) and zooplankton, thus sedimentation as coccolith pellets and flocs/aggregates.	AOM pale ogrange to yellow, fluffy, but relatively abundant.	Frequent development of anoxic conditions.
			High H/C ratio, but low TOC % weight (5-10%)	Domination by phytoplankton organic biomass thus type I and II kerogen, but TOC % diluted by coccoliths.
	Organic matter stringer lamina.	Decrease in coccolithopore bloom production. Increased production by other phytoplankton. Episodes of suboxic/anoxic bottom waters, thus no bioturbation and enhanced OM preservation. Increased climate stability, increased aridity. Lower surface water nutrients.	Predominately low/medium but variable dinocysts.	Variable marine environment conditions, suppression by the dominant coccolithophore extreme production.
			Dinocysts dominated by proximate morphotypes.	Unstable marine conditions common, stressful to dinoflagellates.
			High frequency and amplitude peak dinocyst abundance at the end of the limestone.	Episodes of extremely stressful conditions causing enhanced encystment, perhaps also an increase in population.
	Alternation of homogeneous and laminated fabric.	Variable water column oxygen levels. Climatic variability as more or less humid conditions leading to fluctuations in water column stratification and surface water nutrient levels.	FTL very high abundance at end of limestone.	Re-deposition from shelf, possible increased basin population.
			Medium/low TTP abundance, except at the end of the limestone, peak abundances.	Generally medium/low terrestrial flux, thus runoff. Or material prevented from reaching distal basin due to trangressive regime. Episodes of unsorted pulses of terrestrial material, re-suspension from the proximal shelf by frequent, high intensity storms.
	Overall low organic matter	Variable bottom water oxygen conditions and OM preservation. Extreme dilution by coccoliths.		
			Medium/low TSD abundance, except at the end of the limestone, peak abundances.	Generally medium/low terrestrial flux, thus runoff. Or material prevented from reaching distal basin due to trangressive regime. Episodes of unsorted pulses of terrestrial material, re-suspension from the proximal shelf by frequent, high intensity storms.

Table 8.1 Continued:- Summary of fabric, geochemical and playnological analyses results of this study and environmental interpretation.
Part C - Mudstone, Calcareous Mudstone and Bituminous Mudstone Lithologies.

LITHOLOGY	FABRIC EVIDENCE	FABRIC INTERPRETATION	GEOCHEMICAL/PALYNOLOGICAL EVIDENCE	GEOCHEMICAL/PALYNOLOGICAL INTERPRETATION
Mudstone	Homogeneous fabric	Intense bioturbation and rich benthic fauna. Oxic bottom waters and the upper sediment column.	Low TOC % weight (4-5% average)	Low organic matter, poor preservation or low production.
	Pyrite as large framboids (5-15µm diameter) and euhedral grains.	Formed within the sediment, oxic water column.	Low to variable carbonate % weight (average 40%)	Lower coccolithophore production than for limestone, less nutrient availability.
	Low organic matter.	Low preservation of OM due to oxic water column and bioturbation.	High clastic % weight (60-80%)	Continual, high clastic input, continual terrestrial runoff and flux
	Dominated by clays, but sparse larger clastic grains.	Distal location from sediment source, or bypassed by main sediment path. But continual clatics flux, low but continual runoff, frequent, low precipitation, less arid climate.	Low H/C ratios, lack of AOM	Oxic water and upper sediment column , poor OM preservation. Increased terrestrial organic matter.
	Substabtial abundance of coccoliths in matrix.	Coccolithophore production was relatively high, but not at limestone bloom levels. Zooplankton population also relatively high. Nutrients relatively abundant, water column mixing and overturn, and terrestrial flux.	Constant and low TMP abundance	Low dinoflagelate and FTL populations, lack of cysting, lack of preservation.
			Medium to low and variable TTP abundance.	Relatively constant flux of terrestrial palynomorphs, thus runoff, consistent but low precipitation. Some aeolian input.
			Medium to low TSD abundance.	Consistent but low terrestrial flux of phytoclasts, thus runoff and precipitation.
Calcareous Mudstone	Increased coccolithic carbonate in matrix compared to the mudstone.	Increased coccolithophore production, increased nutrient availability, increased terrestrial runoff and flux, increased precipitation.	Increased TOC and carbonate % weight	Increased OM and coccolithophore production and increased preservation, dysoxic to suboxic bottom waters.
	Greater organic matter than the mudstone fabric.	Dysoxic to suboxic bottom waters due to increasingly elevated productivity in surface waters, thus increased OM preservation.	Medium to high clastic % weight.	Some terrestrial runoff and flux, but not as great as the mudstone.
			Relatively high H/C ratio, some AOM.	Increased phytoplankton production and OM preservtaion.
	Coccolith pellets, some fabric structure.	Decreased bioturbation due to decreasing oxygen levels in the bottom water, some fabric structure preserved.	For TMP, TTP and TSD peak abundance episodes, high frequency and amplitude unsorted pulses.	Episodes of unsorted pulses of terrestrial material, re-suspension events from the proximal shelf by high intensity and frequent storms. Phytoplankton stressed, increased encystment.
Bituminous Mudstone	Increased organic matter in matrix than mudstone.	Increased preservation of organic matter, suboxic bottom waters. Possible increase in phytoplankton (not coccolithophores) compared to mudstone.	Relatively high TOC, low carbonate and clastic % weight.	Increased OM production and preservation, decreased coccolithophore production, low terrestrial flux and runoff.
	Planar fabric structure parallel to bedding, faint lamination.	Lack of bioturbation, suboxic bottom waters, stratified water column, increasing climate stability (aridity)	High H/C ratio and abundant brown AOM.	High phytoplankton OM and enhanced preservation, suboxic to anoxic bottom conditions, stratified basin.
			Low/medium TMP abundance.	Increasingly stable environment, low encystment.
	Increased abundance of small (<10µm diameter) pyrite framboids.	Possible some formation within lower water column, suboxic to anoxic conditions.	Low/medium TTP and TSD abundance	Low but continuous terrestrial flux and runoff, low precipitation, semi-arid climate.

Table 8.1 Continued:- Summary of fabric, geochemical and playnological analyses results of this study and environmental interpretation.
Part D - Cementstone and Diagenetic Lithologies.

LITHOLOGY	FABRIC EVIDENCE	FABRIC INTERPRETATION	GEOCHEMICAL/PALYNOLOGICAL EVIDENCE	GEOCHEMICAL/PALYNOLOGICAL INTERPRETATION
Cementstone	Interlocking mosaic of euhedral dolomitic crystals masking a mudstone fabric.	Diagenetic alteration of a mudstone, lull or hiatus in sedimentation. Arid climate but lack of water column stratification.	Lowest TOC % weight of all lithologies (average <4%)	Reduction of organic matter in the sulphate reduction zone during diagenetic alteration of the mudstone fabric.
	Zoning of diagenetic crystals.	Several phases of growth, controlled by iron avaliability in the sediment.	High carbonate % weight (up to 80%).	Indicative of the dolomitic and calcite composition of the diagenetic crystals.
			Reduced clastic % weight (down to 40%)	Decrease in clastic sedimentation, low runoff, arid climate.
			Low H/C ratios and lack of AOM.	As for the Mudstone. Oxic water and upper sediment column poor OM preservation.
			Low abundances for all palynomorph groups (TMP, TTP and TSD)	Low phytoplankton populations due to oligotrophic surface waters caused by lack of nutrients. Low terrestrial flux, low runoff, very low sedimentation rates, arid climate.
All other lithology diagenetic alterations	Euhedral carbonate lamina, pellets and grains in the oil shales. Carbonate cements and single grain infilling of coccospheres in the coccolith limestone.	Similar to the cementstone, formation during periods of low sedimentation, but over short timescales and localised areas controlled by the availability of iron.		

8.1.1 OIL SHALE ENVIRONMENTAL AND CLIMATIC INTERPRETATION

A permanently stratified water column and an arid climate were the dominant features of the environment and climate during the oil shale deposition. Stratification was likely the result of a combination of the climate and the palaeogeography of the region, which restricted circulation between basins and caused basin isolation and stagnation. Terrestrial runoff was very low and probably seasonal, if at all, thus the clastic and terrestrial organic matter flux was minimal, with an accompanying lack of nutrient input into the surface waters. This, together with the stratification, which prevented nutrient recycling within the water column, led to oligotrophic surface waters and thus very low primary production. Over the majority of these depositional episodes, both carbonate and organic matter flux were low, but stratification enhanced the preservation of the organic matter flux, resulting in the deposition of an organic-rich lithology.

A substantial proportion of the water column was euxinic during these episodes, possibly reaching up to and even into the lower photic zone. During occasional periods of increased windiness or brief storms, mixing to below the thermo/chemocline resulted in nutrient release to the surface waters and subsequent coccolithophore blooms, which were deposited as carbonate laminae in an otherwise organic-rich lithology. Thus, during the majority of the depositional period, sedimentation rates were very low, but infrequent periods of substantially increased carbonate flux occurred. The termination of the oil shales was initiated by a brief, but intense storm event, as evidenced by an increase in all terrestrial particle abundances, which caused water column overturn and break down of the stratification.

8.1.2 COCCOLITH LIMESTONE ENVIRONMENTAL AND CLIMATIC INTERPRETATION

A less stable marine environment and a more humid climate characterized the coccolith limestone deposition. Increased precipitation and thus terrestrial runoff provided nutrients to the marine environment, though the transgressive nature of the system resulted in both clastic and terrestrial organic material being trapped on the shelf and prevented from reaching the distal basin. Thus, combined with relatively strong nutrient recycling in the water column, surface water eutrophication occurred and led to extreme coccolithophore productivity, while other phytoplankton were suppressed. Despite the high coccolithophore production, increased basin circulation resulted in a relatively oxic to dysoxic water column, with some benthic colonization, though the sediment would have been very soft and soupy. However, episodes characterized by slight increases in aridity led to decreases in nutrients and subsequently coccolithophore production, and the formation of suboxic to anoxic bottom waters, resulting in the deposition of organic-rich laminae. This may have been an annual cycle characterized by a

Mediterranean style climate. However, such an annual cycle has not be proven and deposition may have occurred on a longer timescale of several years to tens of years, with a predominately humid climate that was briefly punctuated by arid spells. Thus both the water column oxygen levels and the climate were variable during the limestone deposition.

The termination of the limestone was characterized by episodes of high frequency and very high intensity storms, which resulted in the re-suspension of sediment on the shelf and depositional pulses of unsorted terrestrial organic matter and clays into the distal basin. These episodes were highly stressful for the phytoplankton and led to increased levels of encystment. Together these events resulted in a significant duration of environmental instability. Though nutrients were not limiting and the coccolithophore were opportunistic and growth maximizing and thus adapted to unstable conditions, this disruption led to a decline in the coccolithophore blooms, and ultimately coccolith limestone deposition ceased.

8.1.3 MUDSTONES AND CEMENTSTONE ENVIRONMENTAL AND CLIMATIC INTERPRETATIONS

Oxic water column and bottom waters, with intense bioturbation by a rich benthic fauna, dominated the mudstone deposition. Both coccolithophore and dinoflagellate production were moderate and terrestrial runoff and flux were relatively high. Thus, compared to the limestone, a less seasonal, warm subtropical? climate characterized by continuous, but low intensity precipitation, is suggested for the mudstone deposition.

Calcareous mudstone deposition was dominated by an increase in coccolithophore productivity and thus surface water nutrient levels. Terrestrial runoff was relatively high, probably greater than for the mudstone, and the climate became increasingly unstable and humid. Commonly episodes of moderate to high intensity storms occurred, resulting in the re-suspension of terrestrial organic matter from the shelf and abundant pulses of unsorted organic material into the distal basin. Phytoplankton encystment also increased under these stressful conditions. However, these episodes were less intense than those at the end of the limestone deposition. The r-strategist coccolithophores were therefore able to take advantage of the increase in nutrient levels despite the instability, and their populations increased, thus resulting in the deposition of an increasingly coccolith-rich lithology.

Conversely, the bituminous mudstone deposition was characterized by a decline in coccolithophore production and an increase in water column stratification, with the climate becoming increasingly stable and arid. The terrestrial runoff and nutrient supply were therefore reduced, thus restricting coccolithophore production and the bottom waters became increasingly

suboxic to anoxic, restricting benthos and decreasing bioturbation. Just as the calcareous mudstone was a precursor to the coccolith limestone deposition, so the bituminous mudstones are a transitional lithology between the mudstone and the oil shales.

Lastly, the cementstone lithology is dominated by the diagenetic alteration of a mudstone, possibly under conditions of reduced sedimentation rates, linked to climate aridity? Formation took place at a shallow depth in the sulphate reduction zone, commonly in several phases, and was controlled by the availability of iron within the sediment.

The key elements of these six lithological environmental and climatic interpretations are summarized in Figure 8.1.

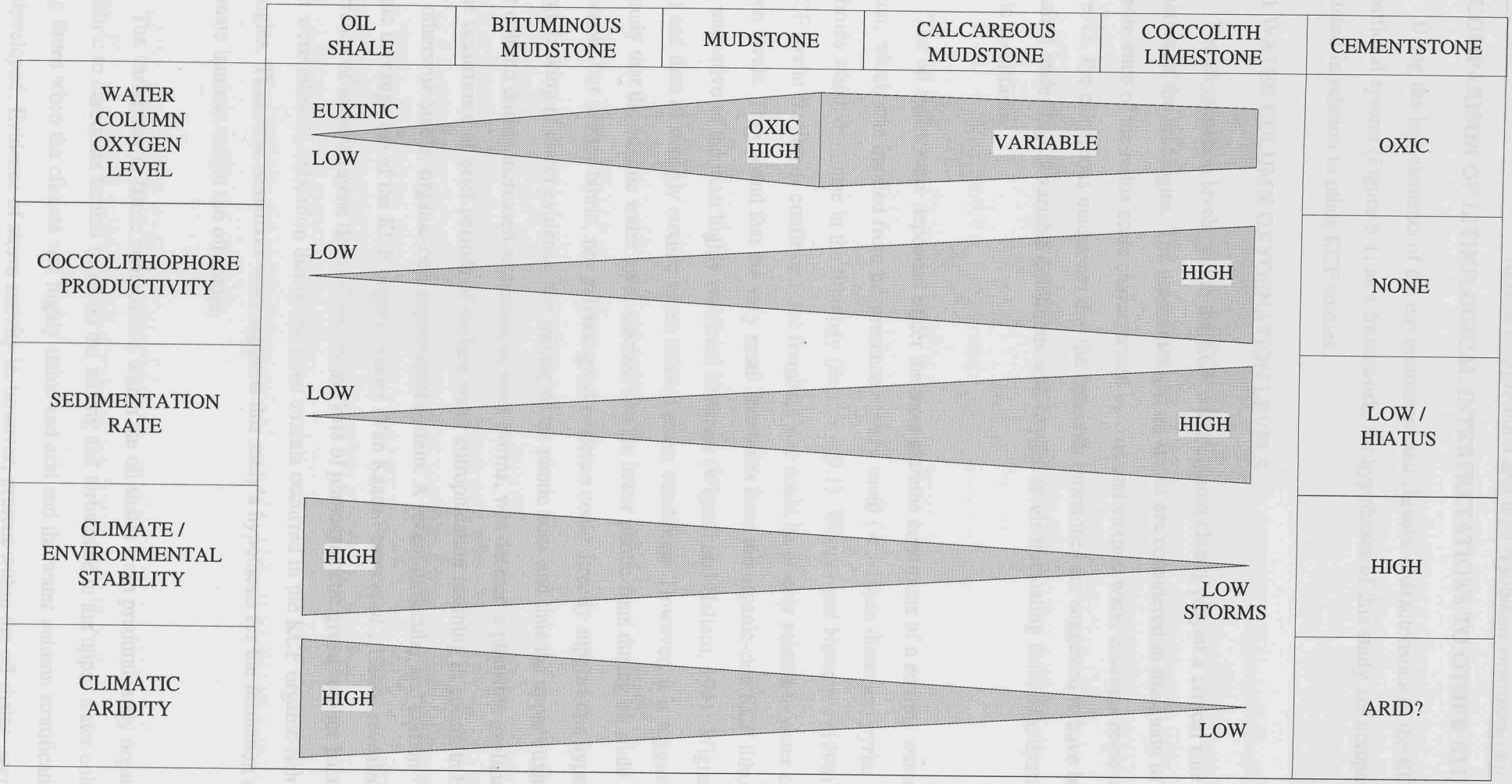

Figure 8.1
Schematic summary of the key elements of the marine environment and climate for the six lithologies within the studied intervals. Five of these lithologies can be related to each other via a scale from high to low for each key element; however, due to the diagenetic formation of the cementstone it can not be included in the scales and is thus separate.

8.2 COMPARISON OF LITHOLOGICAL INTERPRETATIONS TO OTHER STUDIES

Using the key elements of the environmental and climatic characteristics of the KCF depositional system (Figure 8.1) as a framework, the hypotheses of this study are compared and discussed in relation to other KCF studies.

8.2.1 WATER COLUMN OXYGENATION LEVELS

The oxygenation levels within the KCF water column clearly played a critical role in the formation of the lithologies. The mudstones and oil shales are considered in this study to be at opposite ends of the redox scale characterized by oxic and euxinic water columns respectively. However, the calcareous mudstones and the coccolith limestones are suggested to have been deposited under highly variable conditions with oxygen levels fluctuating from oxic/dysoxic to anoxic conditions.

The oil shales were deposited under the most extreme conditions of a euxinic water column, which was implied from the presence of very small ($<$5-10μm diameter) pyrite framboids which dominate in the lithology (Section 4.9.1). Wignall and Newton's (1998) study of KCF pyrite framboids confirmed that framboid size could be closely related to water column oxygen levels. They found that the very small framboids from the organic-rich KCF lithologies were indicative of the most highly restricted biofacies (Wignall and Hallam, 1991; Wignall, 1994) and thus of strongly euxinic water column redox conditions. However, it is suggested in this study that the euxinic water level reached into the lower photic zone during oil shale deposition, but neither fabric, nor palynological evidence could directly support this hypothesis. Though lacking in direct evidence, the mixing of the photic zone and thus the upper euxinic water column during increased windiness or brief storms, was deemed a plausible explanation for the occurrence of brief periods of surface water eutrophication resulting in coccolith blooms in an otherwise stable, organic-rich depositional system. A recent molecular and carbon isotopic investigation of the KCF organic matter (Van Kaam-Peters *et al.*, 1998), revealed the occurrence of isorenieratene derivatives, biomarkers of photosynthetic green sulphur bacteria, which were taken as indication that photic zone euxinia occurred in the KCF organic-rich lithologies. Thus, this biomarker work supports this study's hypothesis for the formation of the carbonate laminae within the oil shales.

The variability in fabric composition within the oil shales from predominately organic-rich fabric to carbonate lamina relies on the mixing and turbulence in the upper water column during times when the climate was highly stable and arid and the water column stratification well developed. Evidence of storm activity is, however, present within the oil shales, seen as

graded intervals which occur near or within sections of the fabric characterized by thick carbonate laminae (Figure 3.1, 3.18f, Section 4.10). Wignall (1989), is his paper on tempests and earthquakes during the deposition of the KCF, also highlighted similar graded horizons and other depositional features indicative of storms occurring during oil shale deposition.

The majority of studies are in agreement that the oil shale deposition occurred under either anoxic or euxinic water column conditions; however, there is greater disagreement over the water column redox character during the deposition of the coccolith limestone lithology. Taking into account the variable fabric structure of laminated and homogenous intervals (Figure 3.21) and the presence of trace fossils within certain levels of the limestone (Irwin, 1979), as well as the exceptional coccolithophore productivity during these periods, variable oxygen levels are suggested for the limestone deposition. Oxygen levels probably covered a range from oxic/dysoxic to anoxic and it is possible that the bottom waters were more frequently anoxic than dysoxic. However, photic zone euxinia is not envisaged. The presence of highly abundant, unsorted pulses of structured organic material, especially at the end of the limestones (Figure 6.8 and 6.9, Section 6.3.1; Figure 7.4, Section 7.1.2.1), suggest that the marine environment and climate were far less stable during these depositional periods. This is certainly the case when compared to the oil shale deposition, which was characterized by very minimal abundances of terrestrial organic material. It has been suggested that the high abundance and frequency peaks of structured organic material in the limestones are the result of shelf re-suspension events during intense storm periods; thus a permanently stable, stratified water column seems to be somewhat unlikely.

Irwin and Curtis (1977) and Irwin (1979) also believed that the presence of distinct burrows at certain horizons and ripple lamination within the Whitestone Band limestone was conclusive evidence that the major development of the coccolith limestone occurred in aerated bottom waters. They argued that transpositional structures within the limestone were indicative of unstable substrates and this would account for the lack of abundant benthos rather than indicating anoxic bottom waters. In agreement with other workers (e.g. Tyson *et al.*, 1979), they postulated that the oil shales marked the maximum stand of the redox interface, but argued that both the vertical movement of this interface and dilution by terrigenous material could account for differences in the organic-richness of lithologies in the KCF. Further, they proposed that the coccolith limestones accumulated when circulation increased, which resulted in an increase of nutrients in the surface waters and thus favoured the propagation of coccoliths.

However, the biomarker evidence of photosynthetic green sulphur bacteria found in the oil shale lithologies was also found in coccolith limestone samples, thus suggesting that photic zone euxinia was also a (periodic?) feature of the water column during the limestone deposition (Van Kaam-Peters *et al.*, 1998). This is in agreement with the depositional models proposed by Tyson (1985, 1996) and Oschmann (1988, 1990), in which both the coccolith limestone and organic-rich shales were deposited in frequently oxygen-depleted depositional environments. It seems difficult to reconcile this evidence with the presence of the unsorted pulses of structured terrestrial material, which suggest significant environmental instability during these periods of deposition. Perhaps, however, the environmental variability, which is suggested to have characterized the limestone deposition, may have included periods of photic zone euxinia as well as times of less oxygen-restricted deposition. The high terrestrial material abundances do not occur over the entire interval but are grouped at certain horizons. Together with the fabric structure varying between homogeneous and laminated, a depositional environment with highly variable water column oxygen levels, ranging from oxic/dysoxic to photic zone euxinia, is envisaged. Thus the environmental interpretation for the coccolith-rich lithologies made in this study is in agreement with both sides of the dispute, but perhaps brief periods of more strongly stratified conditions with a greater proportion of the water column depleted in oxygen, should be included in the proposed reconstruction. However, Van Kaam-Peters *et al.*, (1998) also included cementstone, mudstone and calcareous mudstone lithologies in his study, and found that these lithologies also contained significant levels of green sulphur bacteria biomarkers. The over whelming fabric evidence and reduced TOC % of these other lithologies, suggesting deposition under an oxic water, thus imply that such biomarker evidence may not be so conclusive in the prediction of photic zone euxinia.

Thus, water column oxygen levels are seen to be an important element in controlling the organic richness of the KCF sediments. However, variability in preservational conditions cannot be solely accountable for the loss or survival of organic in marine sediments (Tyson, 1995). Factors such as organic matter production and sedimentation rates, which are discussed next, are also important.

8.2.2 PRODUCTIVITY AND SEDIMENTATION RATES

Both productivity levels and sedimentation rates have been suggested to have varied between the lithologies, with the oil shales characterized by low primary production and sedimentation rates, while the coccolith limestones are the opposite. The mudstones are proposed to have had moderate production and sedimentation rates, while the bituminous mudstones were characterized by slightly reduced rates, and the calcareous mudstones by slightly greater rates than the mudstone.

The oil shales within this study were consistently characterized by very low abundances of structured marine and terrestrial palynomorphs and dominated by AOM. This characteristic had also been previously observed by Tyson *et al* (1979), Farrimond *et al* (1984) and Ebukanson and Kinghorn (1985), and taken to indicate very low terrestrial input and sedimentation rates during the deposition of the oil shales. The stability of these depositional periods, especially the surface water conditions, was highlighted by little to no variation found in the dinoflagellate assemblages of these lithologies (Ioannides *et al.*, 1976). Though the overall productivity was low, dinoflagellate production was probably more dominant than other phytoplankton, including coccolithophore, over the majority of oil shale deposition. Modern studies on organic carbon flux suggest that the dinoflagellate contribution is an average of 0.14pg $C\mu m^{-3}$ (Tillman and Hesse, 1998), and daily, summer dinoflagellate production in the North Atlantic was found to range between 500 and 800 $mgCm^{-2}day^{-1}$(212 $gCm^{-2}a^{-1}$) (Joint *et al.*, 1993). This is a significant amount when compared to the mean primary production of open continental shelf waters of between 100-230 $gCm^{-2}a^{-1}$ (Hargrave, 1985). If a similar production, or even a much reduced production, occurred during the deposition of the KCF oil shales, this organic matter would not have been diluted by terrestrial material, or high coccolithophore production, and thus, together with a euxinic water column severely restricting zooplankton flux mediation, would have resulted in a substantial proportion of the organic matter being preserved.

Conversely the coccolith limestones were dominated by extreme coccolithophore productivity and though clastic material was commonly trapped on the shelf, sedimentation rates were high, but dominated by autochthonous biogenic materials. During modern coccolith blooms of *Emiliania huxleyi,* the coccolith calcite flux has been found in the range of 30 to $270mgm^{-2}day^{-1}$ (Brown and Yoder, 1994b; Knappertsbusch and Brummer, 1995). Considering blooms last the order of three weeks and can reach 250,000 km^2 (Balch *et al.*, 1991; Fernandez *et al.*, 1993) a single bloom can produce a coccolith calcite flux of 1.4 $x10^{12}$ g, or 1400,000 tonnes. Balch *et al.* (1991, 1993) calculated the amount of organic carbon produced a day in a bloom of 50,000km^2 and 20 m deep, assuming 2pg of organic carbon per coccolith (Paasche, 1962), to be 50,000 tonnes. Scaling this up to a bloom of five times the size and lasting for three weeks, as was calculated for the coccolith calcite, this gives a total organic carbon production of 525,000 tonnes. From these figures it is clear that despite a high organic carbon production, the coccolith calcite would result in extreme dilution, as seen in the KCF coccolith limestones. From these two examples, it is evident that the type and quantity of marine production was also a crucial factor in determing the overall character of the KCF lithologies.

Certain periods during the coccolith limestone deposition where characterized by high abundances of unsorted terrestrial organic material and clays. Thus an increase in terrestrial flux bought terrestrial material into the distal basin. Conversely, brief episodes of reduced coccolithophore production occurred in conjunction with an increase in bottom water anoxia, resulting in the deposition of organic-rich laminae in an otherwise coccolith-dominated depositional system. Such alternations of coccolith-rich and organic-rich laminae were explained by Gallois and Medd (1979) to be alternations of coccolithophore and dinoflagellate blooms. However, due to the domination of AOM in the oil shale lithologies, such an increase in the dinoflagellate population was not ascertained in this study. They also postulated that the deposition of the coccolith carbonate occurred as fecal debris of coccolith ingesting organisms. This study supports this suggestion with a strong comparison between the KCF coccolith fecal pellets and modern day copepod pellets (Table 3.1, Section 4.2.5)).

The dominance of the coccolithophore production and the low coccolith species richness of the KCF limestone deposition has led to the suggestion that the *Watznaueria* coccolithophore were r-strategists and thus highly adaptable to a range of nutrient conditions from highly oligotrophic to highly eutrophic (Bown and Burnett pers. comm. 1999). Using the cosmopolitan modern day coccolithophore species *Emiliania huxleyi* as the nearest analogue to the *Watznaueria* spp., these coccolithophore were probably adapted to tolerate a wide range of conditions and bloom when conditions were ideal with respect to nutrients, turbulence and light. Clearly conditions must have been perfect during the interval of coccolith limestone deposition. However, the presence of the unsorted palynomorph pulses during these periods also suggests that the coccolithophores must have been able to survive and flourish in unstable conditions. Despite this adaptation, the termination of both the investigated limestones are characterized by the greatest amplitude storm re-suspended pulses, which must have been of sufficient intensity to be detrimental to the coccolithophores, and their production inevitably declined. No previous studies have highlighted these unsorted palynomorph pulses in association with coccolith limestones, which is believed to be the result of the high-resolution sampling interval employed in this study, and will be further discussed in the last section of this chapter.

The unsorted palynomorph pulses in this study are taken to be the result of storm activity which was concentrated at the beginning and end of the limestone deposition and are thus suggested to be linked to the initiation and termination of the coccolith limestone deposition. Modern analogues for storm-dominated mudrock sequences, similar to the KCF, are incomplete, because the opportunity to study the effects of large storms on muddy shelves are rare (Gagan *et al.*, 1990). As a result, little is known about the behaviour of suspended

sediment during storms or about the consequent sedimentary products. The few studies of modern cyclone, hurricane and winter storm sedimentary sequences (e.g. Wells *et al.*, 1985; Swift and Nummeda, 1987; Snedden *et al.*, 1988; Gagan *et al.*, 1990) have found that considerable quantities (several centimetres sediment thickness) of shelf sediment is eroded and re-deposited during these storm episodes. Transport of sediment has been found to be shoreward as a result of surface water flow, along shelf due to water column interior flow directed along the shelf and lastly offshore as a result of near bottom currents. These bottom currents interact with wave-orbital motion to produce a combined flow with sufficient magnitude to transport sand and silt from shoreline sources (Snedden *et al.*, 1988). Storm surge which results in significant seaward directed relaxation flow also results in sediment transport offshore (Gagan *et al.*, 1990). After storms the mud sized fraction of marine sediments are characterized by increased TOC values due to the tendency of organic carbon material being concentrated in this size fraction (Gagan *et al.*, 1990).

Though these modern studies, from the Australian and American coasts, are not directly applicable to the KCF palaeogeography, but they are the best modern examples of storm deposit analysis. Unfortunately, these studies concentrate on the inner and mid-shelf sediment characteristics and not the outershelf and deeper basin sedimentary reflections of these geostrophic storms, where this KCF study is located. Also, the type and situation of the organic particles within storm deposits has not be investigated in modern deposits and thus the palynofacies result of this study cannot be compared. Thus it would be advantageous to the study of ancient storm deposits if future research of modern storm deposits also included more detailed analysis of the organic matter within the sediment. Therefore, it can only be concluded that modern storms eroded and transport shelf sediments offshore, and thus, offshore sediment transport also occurred during ancient storm periods.

The sedimentation rates for the laminated lithologies within the studied intervals, that is the coccolith-rich oil shales and the coccolith limestones, were previously calculated to be an average of 4.5cm per 1000 years for the oil shales, an average of 30cm per 1000 years for the Freshwater Steps coccolith limestone and a 118cm per 1000 years for the thickest lamination in the Whitestone Band (Table 4.2, Section 4.8.2). These calculations were based on the assumption that each lamina couplet was a year's worth of deposition, which is a subject of debate (Wignall, 1989). Tyson *et al* (1979) noted that true millimetre-thick varve-like laminae were rarely developed over a few centimetres vertical thickness in the limestones. He compared these laminations to modern day Black Sea sediments, where seasonal variations in coccolithic and organic-clay flux form annual varves (Dickman and Artuz, 1978), but concluded that the limestone lamination was indicative of more aperiodic fluctuations. Wignall (1989) was in

agreement with this conclusion, which he suggested helped avoid the problem of exceptionally high rates of sedimentation for the coccolith limestones, which would need to be of the order of 1m per 1000 years if the couplets were assumed to be annual varves. However, this study did find such sedimentation rates occurred in the WSB coccolith limestone, though the FWSB limestone sedimentation rate was calculated to be less than a third of the WSB rate. These rates may well be too high, especially when considering the Black Sea comparison, but until a figure can be placed on the timescales of such lamina deposition, laminae sedimentation rates can only be calculated with the assumption of a yearly varve.

Francis (1984) found a close similarity between growth ring parameters of the Purbeck tree rings and those from modern Mediterranean-type trees, which she suggested indicated that the strong 'seasonal' semi-arid climate of the Late Jurassic was annual. It seems possible, therefore, that the assumption of yearly varve lamina couplets in the KCF coccolith limestones and coccolith-rich oil shales may be valid. Using these rates, the frequency of the unsorted terrestrial pulses may be very crudely estimated. Using the FWSB, 30cm per 1000 year sedimentation rate, the storm pulse events are indicated to have occurred between every 250 to 400 years. However, these high frequency peaks were only clearly differentiated in the WSB limestone, thus it is possible that had high resolution analysis been carried out on the FWSB limestone, somewhat different time periods may have been calculated. When the WSB, 118cm per 1000 year sedimentation rate is applied, values decline and the storm events are indicated to have occurred every 60 to 100 years. It is notable that today the 50 to 100 year storms are those that are the most significantly felt in the environment (T. Atkinson, pers. comm., 1996).

If the modern Mediterranean climate is thus taken to be an analogue for the KCF climate, the Mediterranean sapropels and KCF oil shales should posses similar characteristics. Both enhanced marine productivity and improved preservation of organic matter have been found to be central to sapropel formation (Bouloubassi *et al*, 1999). In comparison, no enhanced productivity is envisaged in the formation of the KCF oil shales. The major fraction of sapropel organic matter is derived from marine algal sources and has undergone variable oxidation but is dominated by AOM, which is also the case for the KCF oil shales. Accumulation of increased amounts of land-derived material has also been found at times of sapropel formation, supporting the common held hypothesis of significant periodic freshwater discharges (Bouloubassi *et al*, 1999). Such accumulations were not found within KCF oil shales, but were a significant characteristic of the coccolith limestones. Sapropels are also believed to have formed during times of wetter and warmer climates (Emeis *et al.*, 1996), the direct opposite of the conditions postulated for KCF oil shale deposition, but similar to the hypothesised climate during coccolith limestone deposition. From these brief comparisons it seems that the formation

of the Mediterranean sapropels cannot be directly applied to the KCF oil shales. The Black Sea sediment, with its alternating coccolith and organic matter-dominated laminae seems a more realistic comparison. This being the case a yearly varve deposition is a somewhat misleading assumption for the KCF laminae couplets, but is the only certain timescale that can be applied until further work has been done to ascertain high-resolution periodicities of the KCF laminae.

8.2.3 CLIMATE AND CLIMATIC/ENVIRONMENTAL STABILITY

Throughout the intervals, the climate is believed to have been warm, but aridity and stability of the climate are suggested to have varied between lithologies. The oil shale and possibly the cementstone are hypothesized as being characterized by the greatest climatic aridity and stability, while the calcareous mudstones and the coccolith limestone are suggested to have been the most humid and unstable. On a larger scale, Wignall and Ruffell (1990) found that a sudden change in climate from a humid style to a semi-arid style of deposition marked the accumulation of the Upper Kimmeridge Clay in southern England. Changes in sedimentation rates, softground fauna replaced by firmground fauna and diagenetic dolostones formed in the methanogenic zone replaced by sulphate reduction zone carbonate nodules, all indicate a change to a semi-arid climate. They further found a decline in kaolinite abundance over this period, with a clear decrease in the kaolinite/illite ratio towards the middle of the *hudlestoni* ammonite zone, which they took to infer a shift towards aridity and the 'drying out' of the hinterland.

Despite the overall indications of the dominance of semi-arid climate in the Upper Kimmeridge Clay, the kaolinite level did not remain low as expected, instead it fluctuated quite significantly. Wignall and Ruffell (1990) could not explain these variations, though they seem to broadly coincide with the coccolith limestones of the lower *pectinatus* ammonite zone, that is the Whitestone Band, the Middle White and the Freshwater Steps Stone Band. Clay data produced at Reading University, within the RGGE project (Chambers, 2000), over the Whitestone Band interval also clearly showed an increase in the kaolinite % of the clays over this limestone and the calcareous mudstones, suggesting an increase in humidity during these depositional periods. Kaolinite values increased from an average of 14% of clays below the lower calcareous mudstone to 39% within it, and up to 53% in the coccolith limestone. Values declined slightly in the upper calcareous mudstone before further decreasing to less than 20% of clays in the upper portion of the WSB interval. Unfortunately no detailed data were obtained for the Freshwater Steps interval and thus it cannot be said with certainty that this increase in humidity was a feature of all the coccolith limestones. However, if the kaolinite peaks are characteristic of the limestones it suggests that quite frequent humid intervals punctuated the semi-arid climate of the Upper Kimmeridge Clay.

Macquaker and Gawthorpe (1993) believed that much of the kaolinite within the KCF was authigenic and thus not indicative of climate humidity. However, a similar increase in the kaolinite % of clays, occurs in the Middle Purbeck beds of southern England, characterized by an increase in kaolinite of 40% (Sladen and Batten, 1980; Deconick, 1986; Allen, 1998). It was argued that transport, deposition and diagenesis did not significantly alter the clay minerals, predominantly due to short distances of transport (<300km) and shallow burial depths, and thus the 'kaolinite' event represented a climatic effect (Sladen and Batten, 1980). The Purbeck beds are believed to represent a semi-arid to arid, strongly seasonal Mediterranean-style climate indicated by the abundance of *Classopollis* producing conifers and hypersaline lagoonal facies (Francis, 1983, 1984). The 'kaolinite' event therefore suggests that a decrease in aridity and an increase in precipitation occurred during this predominately arid climatic regime. The kaolinite increases found in the KCF during the coccolith limestones by Wignall and Ruffell (1990) and Chambers (2000), similarly indicate a decrease in aridity and climate stability, and increased precipitation during the predominantly semi-arid climate of the Upper Kimmeridge Clay.

Within this study the high-frequency and amplitude pulses of unsorted palynomorphs which characterized the calcareous mudstones and the limestones were taken to indicate climatic instability with frequent storms and precipitation events. Despite the trangressive regime of the Late Kimmeridgian Stage (Haq *et al.*, 1988; Hallam, 1988) and the low relief and small size of the hinterland islands, which together conspired to reduce runoff and trap material on the shelf, these storms resulted in re-suspending the less dense organic material and clays, moving them offshore. This also resulted in increased nutrient levels in the surface waters, causing coccolith blooms and limestone deposition. Thus the climate is implied to have been a controlling factor in the deposition of the coccolith-rich lithologies and to have been characterized by more frequent and high-intensity storms.

General Circulation Models (GCM) for the Kimmeridgian Stage (Valdes and Sellwood, 1992; Valdes, 1994; Sellwood and Valdes, 1997), show that a seasonally arid climate dominated southern Europe, but that winter storminess was also a strong feature. The models predicted a relatively weak but extensive storm belt over the palaeo-Atlantic Ocean and Europe during the Kimmeridgian Stage, which is directly comparable to the Atlantic storm track of the present. The peak heat transported by the Kimmeridgian storm belt is suggested to have only been a third of the present day, though the heat transported into Europe by the mid-latitude depressions was comparable to current values. Large-scale rain associated with these mid-latitude depressions showed a maximum over the palaeo-Atlantic region from December through to February. Substantial increases in the strength of the wintertime low occurred over the palaeo-Atlantic when orography was introduced into the model, implying significant storm

belts during the winter months. Clearly the palaeo-Atlantic region was environmentally sensitive and an increase in climate humidity may have increased the heat and moisture transport over the region and thus increased the intensity of the storms, ultimately leading to coccolith-rich lithology deposition.

8.3 INTERVAL SUMMARIES OF ENVIRONMENTAL AND CLIMATIC VARIABILITY

This section brings together the environmental and climatic characteristics interpreted for each of the lithologies, over each of the four studied intervals. Vertical profiles of the key elements of water column oxygen levels, coccolithophore and dinoflagellate productivity, sedimentation rates, environmental stability and climate are presented alongside lithological logs of each interval, thus illustrating the overall environmental and climatic variability over the intervals.

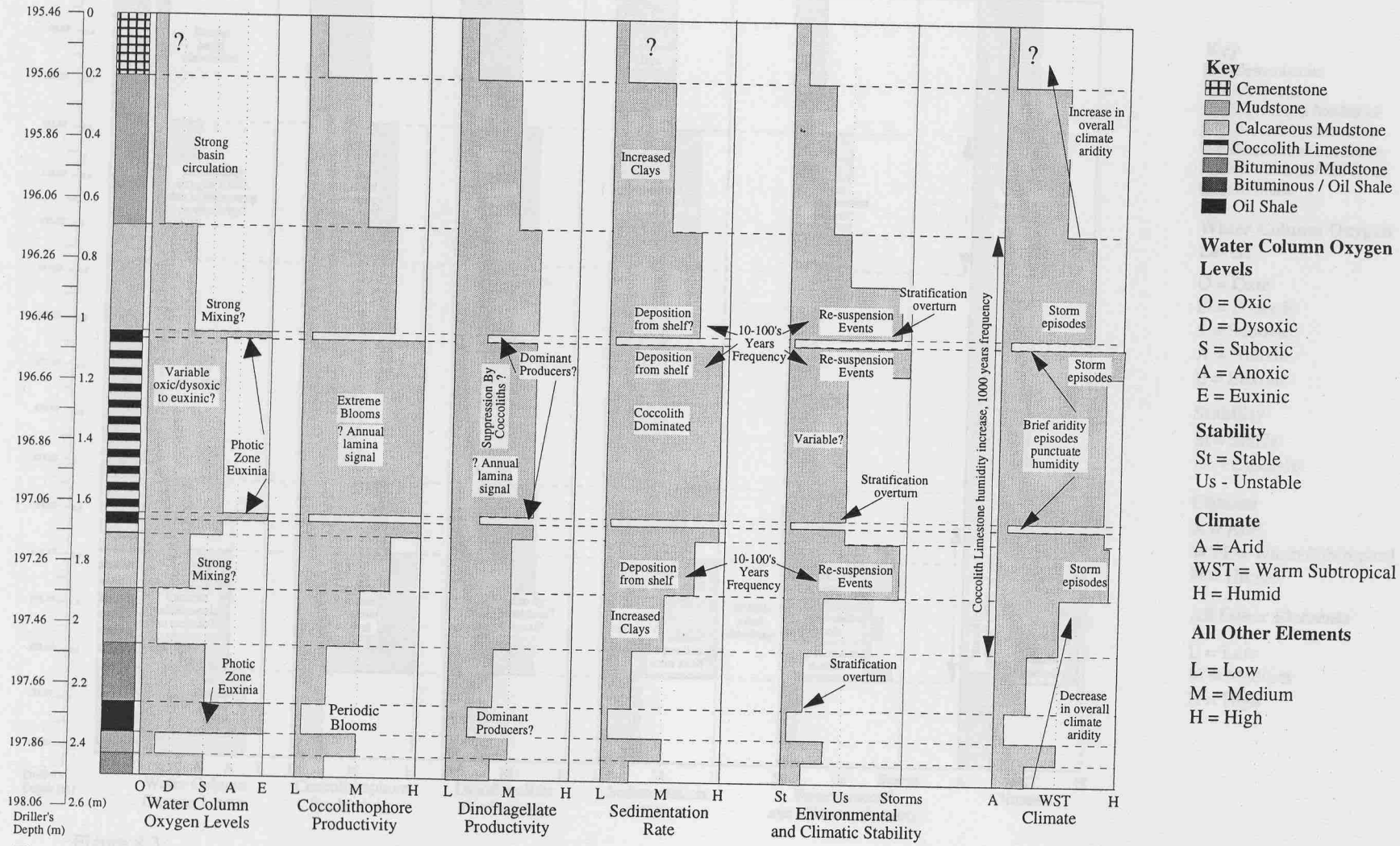

Key

- Cementstone
- Mudstone
- Calcareous Mudstone
- Coccolith Limestone
- Bituminous Mudstone
- Bituminous / Oil Shale
- Oil Shale

Water Column Oxygen Levels

O = Oxic
D = Dysoxic
S = Suboxic
A = Anoxic
E = Euxinic

Stability

St = Stable
Us - Unstable

Climate

A = Arid
WST = Warm Subtropical
H = Humid

All Other Elements

L = Low
M = Medium
H = High

Figure 8.2

Schematic summary logs of environmental and climatic elements of the KCF depositional system during the Whitestone Band Interval. Several scales of environmental and climatic change occur within the interval, from 'yearly' (seasonal?) lamina in the limestone, periodic (possibly yearly) blooms of coccolithophore within the lower oil shale, 10's to 100's years frequency strom events relating to the limestone initation and cessation, to humidity / aridity cycles of the order of several 1000 years.

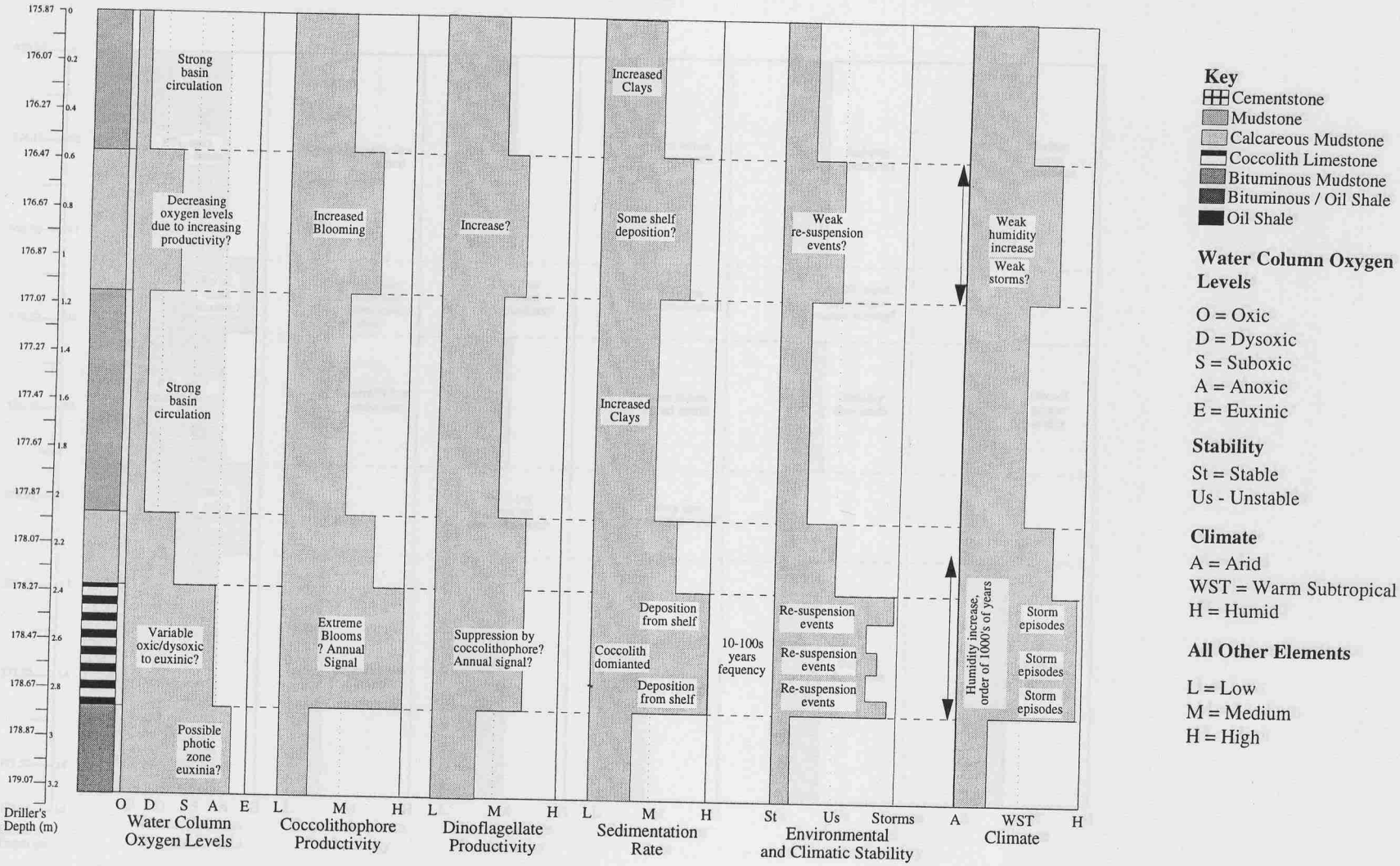

Key

- Cementstone
- Mudstone
- Calcareous Mudstone
- Coccolith Limestone
- Bituminous Mudstone
- Bituminous / Oil Shale
- Oil Shale

Water Column Oxygen Levels

O = Oxic
D = Dysoxic
S = Suboxic
A = Anoxic
E = Euxinic

Stability

St = Stable
Us - Unstable

Climate

A = Arid
WST = Warm Subtropical
H = Humid

All Other Elements

L = Low
M = Medium
H = High

Figure 8.3
Schematic summary logs of environmental and climatic elements of the KCF depositional system during the Freshwater Steps Stone Band Interval. As for the WSB interval, several scales of change occurred during the FWSB interval. Yearly (seasonal) lamina couplets within the limestone, 10 to 100's year frequency storm events relating to limestone formation and 1000's of years humidity / aridity cycle.

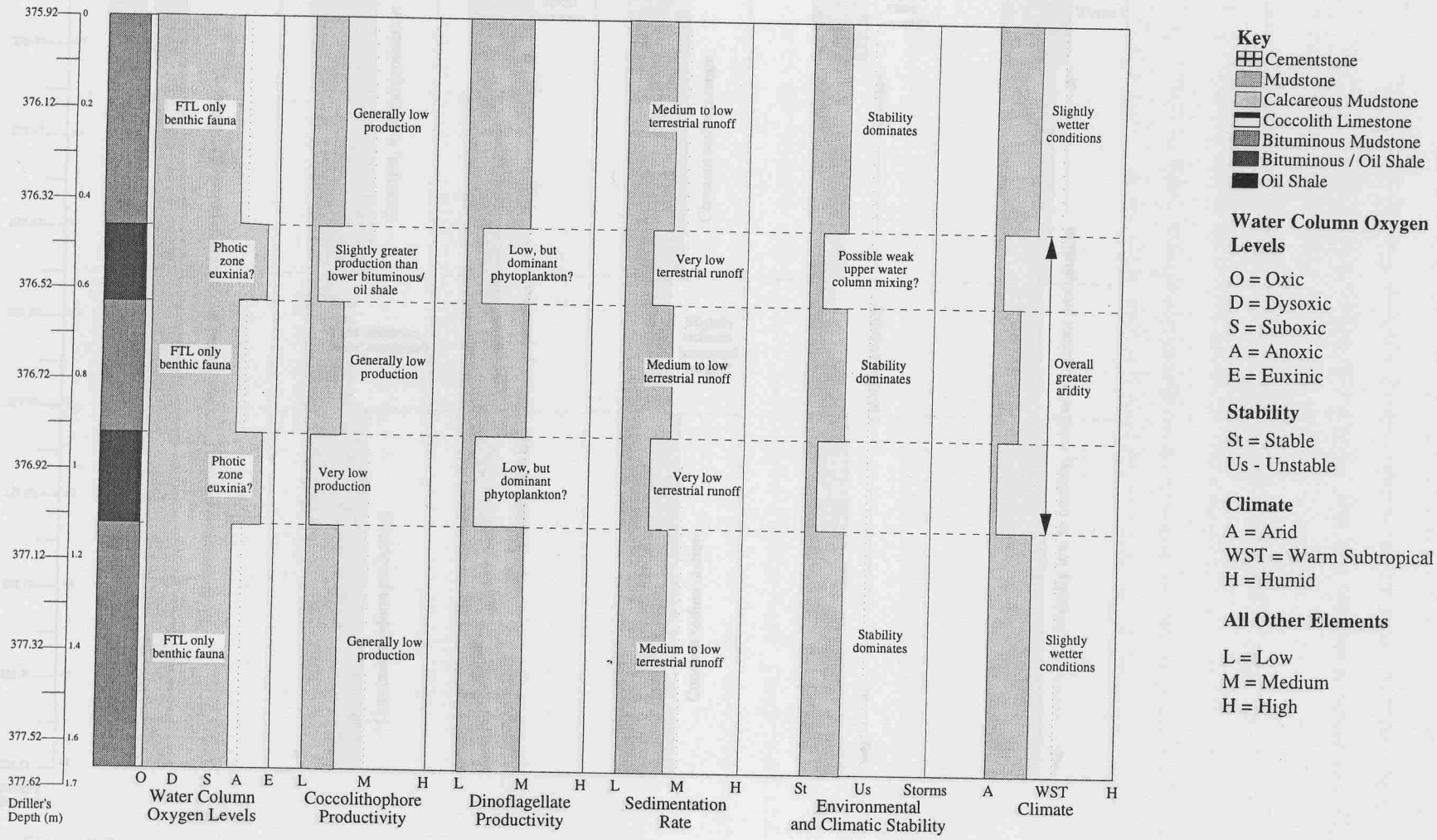

Figure 8.4

Schematic summary logs of environmental and climatic elements of the KCF depositional system during the Eudoxus Interval. In comparison to the coccolith limestone intervals (WSB and FWSB), the Eudoxus is characterized by less variability, though subtle shifts are present. Environmental and climate change are evident, but not on a yearly (lamina) scale. However aperiodic weak storm periods during the bituminou/oil shales possibly occurred and subtle shifts in climatic aridity are suggested to be present on a bed level, thus possibly controlled by Milankovitch forcing.

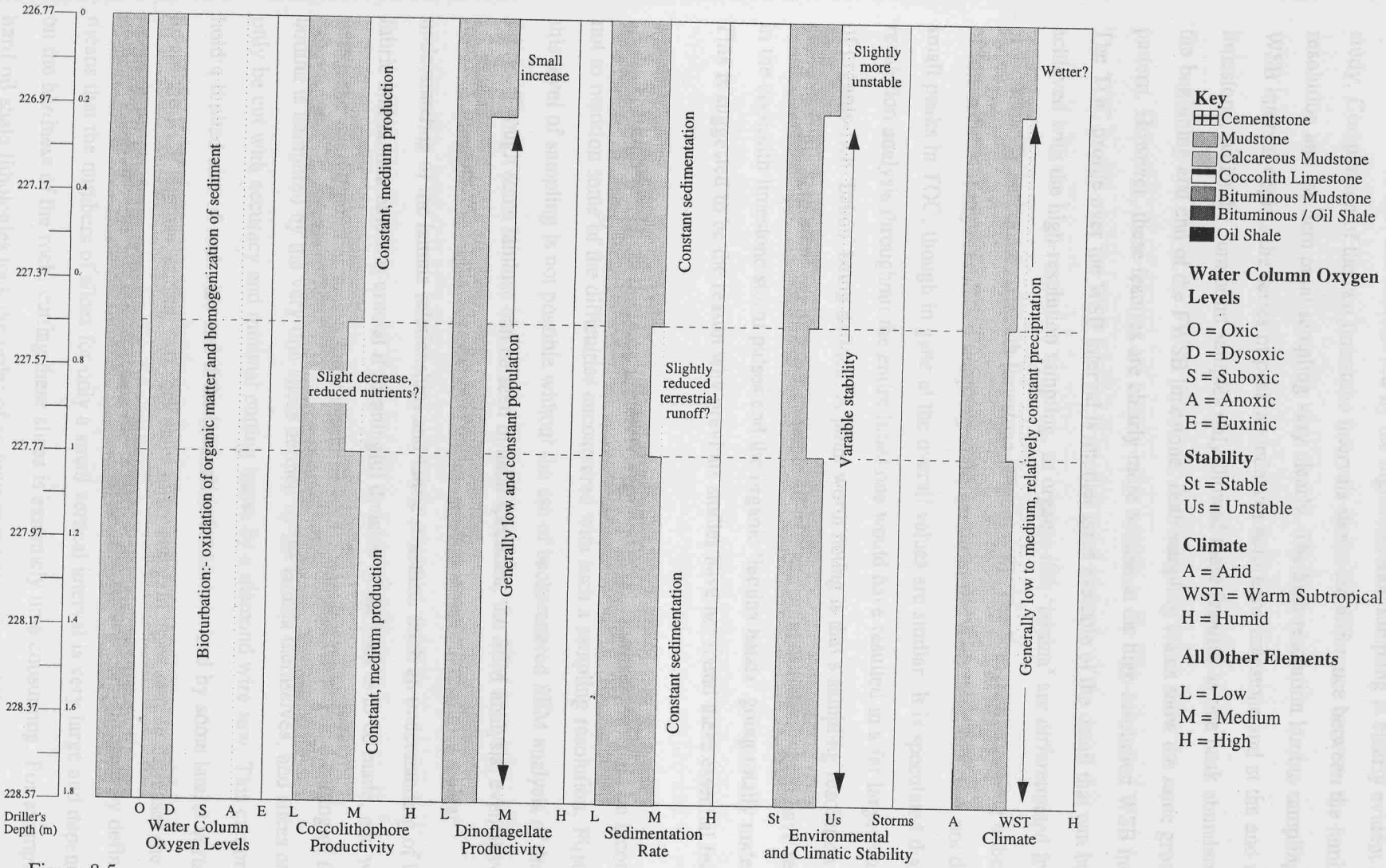

Figure 8.5

Schematic summary logs of environmental and climatic elements of the KCF depositional system during the Bed 44 Interval. Of the four intervals, Bed 44 is characterized by the least variability, with evidence of only very minor chnages through the interval, which compared to the other interval's varability are not significant.

8.3.1 SAMPLING RESOLUTION AND ITS EFFECTS

The detail that can be achieved by the high-resolution sampling is clearly evident in this study. Comparison of the two limestone intervals shows the difference between the lamina scale resolution and the 5cm point sampling very clearly. The high-resolution lamina sampling of the WSB interval depicts the series of peak abundances before the limestone and at the end of the limestone, while the 5cm point samples only showed these features as one peak abundance at the beginning and end of the FWSB limestone. Both sampling scales show the same gross pattern. However, these features are clearly more notable in the high-resolution WSB interval. The TOC profile over the WSB interval is another good example of the detail that can be achieved with the high-resolution sampling, as organic-rich 'lamina' are differentiated from the predominantly carbonate coccolith limestone (Figure 6.8). The 5cm point sampling either side of this section of high-resolution sampling in the centre of the WSB limestone does not depict small peaks in TOC, though in general the overall values are similar. It is speculated that high-resolution analysis throughout the entire limestone would have resulted in a far larger number of organic-rich 'bands' being defined. A point worth noting is that a sampling resolution any lower than the 5cm point samples, for example 10 to 20cm point samples, would have resulted in the coccolith limestone storm pulses and the organic 'lamina bands' going totally undetected. This is suggested to be the reason why previous studies have not found these essential features.

The high-resolution sampling is clearly very powerful. However, it would be incomplete not to mention some of the difficulties encountered with such a sampling resolution. Firstly, this level of sampling is not possible without the use of backscattered SEM analysis of the fabric. Though some laminae can be seen in hand specimen, the SEM analysis, even at very low 20X magnifications, clarifies the boundaries between laminae and allows a clear understanding of the lamina relationships and fabric structure. Such an understanding of the fabric and lamina nature is crucial if meaningful division of the rock is to be made, and without which the overall point of such a study would be void. Secondly, the physical cutting of the lamina is hampered by the very thin slices defined by the lamina themselves, and slices can only be cut with accuracy and minimal cutting losses by a diamond wire saw. This can only hold a limited size of rock slab and if the lamination is characterized by some lateral variability, as are the KCF laminae, cutting two rock slabs to try and gain more sample increases the likelihood that the slices do not represent the same lamina. Also the lamina scale by definition means that the numbers of slices for only a small vertical interval is very large and depending on the hardness of the rock, cutting these slices is extremely time consuming. For example, the hard oil shale lithologies took the order of an hour to cut one slice, while the softer coccolith limestone samples were faster, but could still take fifteen minutes per sample.

The palynological processing of the lamina samples also had problems and again the high numbers of samples was time consuming for the limited vertical extent of the lithology that was examined. But more importantly, unless the organic-richness of the lithology is high, as for the KCF, the small sample weights present a problem. The KCF's organic richness is high enough that processing 0.1 to 0.3g of sample (the weight of a lamina slice), still produces enough organic material to allow significant palynological counts. However, less organic-rich lithologies may struggle to gain sufficient organic matter to count. Also, the physical size of the samples compared to the standard processing beakers were too small and it was more likely that losses of particles would occur during processing. The best processing vessels were found to be 2cm diameter, flat based, high sided tubes placed in a rack, which also enabled a far large numbers of samples to be processed at any one time.

Despite these problems the lamina scale of sampling provides the most detail and thus accuracy in the environmental and climatic interpretation of such rocks as the KCF and is therefore deemed essential for any high-resolution examination of laminated lithologies.

8.4 SUMMARY

Each lithology is shown to be characterized by key environmental and climatic elements within the KCF depositional system. Water column oxygenation levels, sedimentation rates, productivity levels, environmental stability and climatic fluctuations are all critical in controlling the formation of the KCF lithologies. The organic-rich and coccolithic-rich lithologies are the most complex, with several changes in conditions within each lithology. The mudstones are less complex, though the calcareous and bituminous mudstones clearly represent transitional lithologies between the mudstones and the coccolith limestones and the oil shales, respectively. Diagenetic effects also occurred in the KCF, both as distinct lithological bands and within other lithologies. Overall the processes and mechanisms controlling the KCF deposition are highly complex, but also very subtle changes in any of the key elements, affects the lithological deposition. Thus the KCF depositional, environmental and climatic systems were closely interlinked and highly sensitive.

Comparison of the hypotheses presented here, with previous studies, finds some agreement, but also significant differences. Some of these differences can be explained, but it is clear that different methods of analyses emphasize different elements of the system. The reconstructions and interpretations presented in this study are the result of fabric analyses and bulk geochemical and palynological analyses, other geochemical and biological investigations have highlighted elements which were not discernible from just the analyses carried out here and which significantly alter the system models. Also, these intervals represent only a very

minor proportion of the whole KCF, and lamination is only preserved in rare beds. Thus, direct application of these results and interpretations to the whole KCF must be done cautiously.

The environmental and climatic variability over the four studied intervals shows that high- resolution environmental change was a part of the KCF system, but that variability was on a number of scales, all of which are under Milankovitch orbital forcing frequencies. Variability ranges from the yearly? 'varve couplet' alternation between organic-rich and coccolith-rich fabric, to 60-100 year and perhaps 200-400 year storm events, to larger scale events on the order of the lithological bands, for example humidity increases during limestone deposition which represent several 1000 year periods.

Finally the high-resolution sampling used in this study has enabled these high-frequency environmental changes to be assessed. Lower resolution studies have not been able to differentiate these high levels of variability and it is evident that lamina scale sampling is required if environmental and climatic variability below Milankovitch timescales is to be assessed. However, this level of sampling is not without it problems, the most significant of which is the very limited vertical extent of lithology that can be examined.

9.0 CONCLUSIONS AND FUTURE RESEARCH

9.1 CONCLUSIONS

Six major lithological divisions, of oil shales, coccolith limestones, mudstones, calcareous and bituminous mudstones and cementstones characterize the Upper Jurassic, Kimmeridge Clay Formation. These are dominated by three major components of organic matter, coccolithic carbonate and detrital clays and silts, the flux of which primarily controls both the lithology and microfabrics. Oil shales are dominated by organic matter, however, coccolithic carbonate can reach high levels as carbonate lamina. Conversely, the coccolith limestones are dominated by coccolithic carbonate, but organic matter is also evident as thin laminae. Detrital clays are common in the mudstones, though coccoliths are also present, while the calcareous mudstones contain greater quantities of coccoliths, and the bituminous mudstone greater quantities of organic matter. The cementstone represents post-sedimentation diagenetic alteration of a mudstone fabric, and diagenetic fabric changes are also evident within the other lithologies. Fabric structures range from laminated; through discontinuous laminated, pelletal to homogenous, both within the oil shale and coccolith limestone lithologies and from oil shales through to mudstone lithologies.

Modern day water column, benthic and sedimentary processes can be applied to ancient lithologies such as the KCF to explain the fabric compositional and structural characteristics. The KCF marine environment was shown to be highly complex and contain many elements that could be directly related to modern marine systems. Other characteristic processes that occur in modern marine environments such as zooplankton meditation of the carbonate and organic matter flux could not be directly implied from the fabric evidence but by virtue of the presence of fecal zooplankton pellets, such processes were inferred to have taken place. Sedimentation rates were calculated for the laminated oil shale and coccolith limestone lithologies with the assumption that lamination was annual and ranged from 4.5cm per 1000 years to 30-118cm per 1000 years respectively.

Geochemical analyses of TOC and atomic H/C ratios showed the studied intervals to be characterized by variable TOC% from less than 3% in the cementstone to over 50% in the oil shales. Coccolithic carbonate dilution was most extreme over the calcareous mudstones and coccolith limestones, though coccoliths were found to be present in varying quantities in all lithologies. Kerogen was predominantly Type I and II and the coccolith limestone and oil shale samples showed the greatest H/C ratios, though variable TOC%. The high-resolution sampling of the Whitestone Band interval, especially the oil shales, highlighted a strong linear relationship between TOC % and carbonate %, which was used to ascertain the proportion of

total organic matter and pyrite organic matter within samples and further used to estimate the percentage of clastic material within the interval. This empirical calculation for the WSB was then applied to the other intervals, which lacked a similarly strong TOC % and carbonate % relationship, due to both a lack of oil shales and to the lower resolution sampling.

Palynological analysis highlighted a close correlation between the marine and terrestrial environments, and significant variability between lithologies. Oil shales were consistently characterized by very low abundances for all structured particles, while the calcareous mudstones and coccolith limestones showed high-frequency and amplitude pulses of unsorted structured organic material. These were related to storms, which caused re-suspension of organic material and clays on the basin shelf and subsequently transported these materials as unsorted pulses into the distal basin. The periodicity of these storms was calculated to be every 60 to 100 years, or possibly 200 to 400 years, assuming a yearly timescale for the coccolith/organic lamina couplets within the coccolith limestones.

Environmental and climatic reconstructions were made for both the six major lithologies and over the four studied intervals. High-resolution environmental change was found to be present within these intervals of the KCF, on a variety of scales, but all at higher frequencies than Milankovitch orbital forcing scales. This variability ranged from the yearly 'varve couplet' alternations of organic-rich and coccolith-rich fabric, to 60-100 year and perhaps 200-400 year storm events, to larger scale events of the order of several 1000 years, such as humidity increases during limestone deposition. Thus, high-resolution analyses of the Kimmeridge Clay Formation enabled the detection of these high-frequency environmental and climatic changes.

9.2 FUTURE RESEARCH

This study has identified high-resolution environmental change in the Kimmeridge Clay Formation at higher frequencies than Milankovitch forcing timescales and has demonstrated how high-resolution sampling and a combination of analyses techniques enables environmental and climatic reconstructions of individual lithologies and intervals of variable lithologies. Following this several areas of potential future research may be identified:

1) Re-sample the Whitestone Band coccolith limestone at high-resolution lamina scale throughout the interval's length to assess the palynological and geochemical signatures throughout, thus clarifying the environmental and climatic stability over the entire limestone.

2) Extend the high-resolution lamina scale sampling to other laminated intervals within the KCF, for example other coccolith limestones such as the Freshwater Steps Stone Band and the

Middle Whitestone Band, to establish whether similar high-frequency and intensity storm events occurred. Also examine other coccolith-rich oil shales.

3) Apply timeseries analyses to each of the limestones and the coccolith-rich oil shales for which complete high-resolution lamina scale sampling has been carried out and thus assess any significant periodicities and relate them to forcing mechanisms below the Milankovitch scale.

4) High-resolution quantitative AOM analysis would complement the structured palynofacies analyses and provided a complete assessment of the organic component of the KCF lithology, of which the AOM is the dominant fraction.

5) High-resolution quantitative clay analysis would also compliment the organic matter analyses and enable assessment of terrestrial fluxes into the marine environment, and clarify whether kaolinite increases are a characteristic of limestone lithologies within the KCF.

6) Speciation of dinoflagellates, pollen and spores would provide more detailed environmental and climatic boundaries to the bulk abundance data.

7) Perform similar high-resolution BSEI, geochemical and palynological analyses on other ancient laminated oil shale and coccolith limestones, possibly establishing common high-resolution environmental and climatic variability characteristics with the KCF.

APPENDIX A

CORE PHOTOGRAPHS OF THE STUDIED INTERVALS

Core photographs are place from left to right across the pages. Within each core box the core sequence begins on the left hand side of the box at the top of the page, moves down the left hand side of the box until the core end, and then returns to the top of the core in the right hand side of the box. The length of the boxes are approximately 1.5m, and hold up to 3m of core.

Figure A.1 - Whitestone Band Interval Core Photograph

Figure A.2 - Freshwater Steps Stone Band Interval Core Photograph

Figure A.3 - Eudoxus Interval Core Photograph

Figure A.4 - Bed 44 Interval Core Photograph

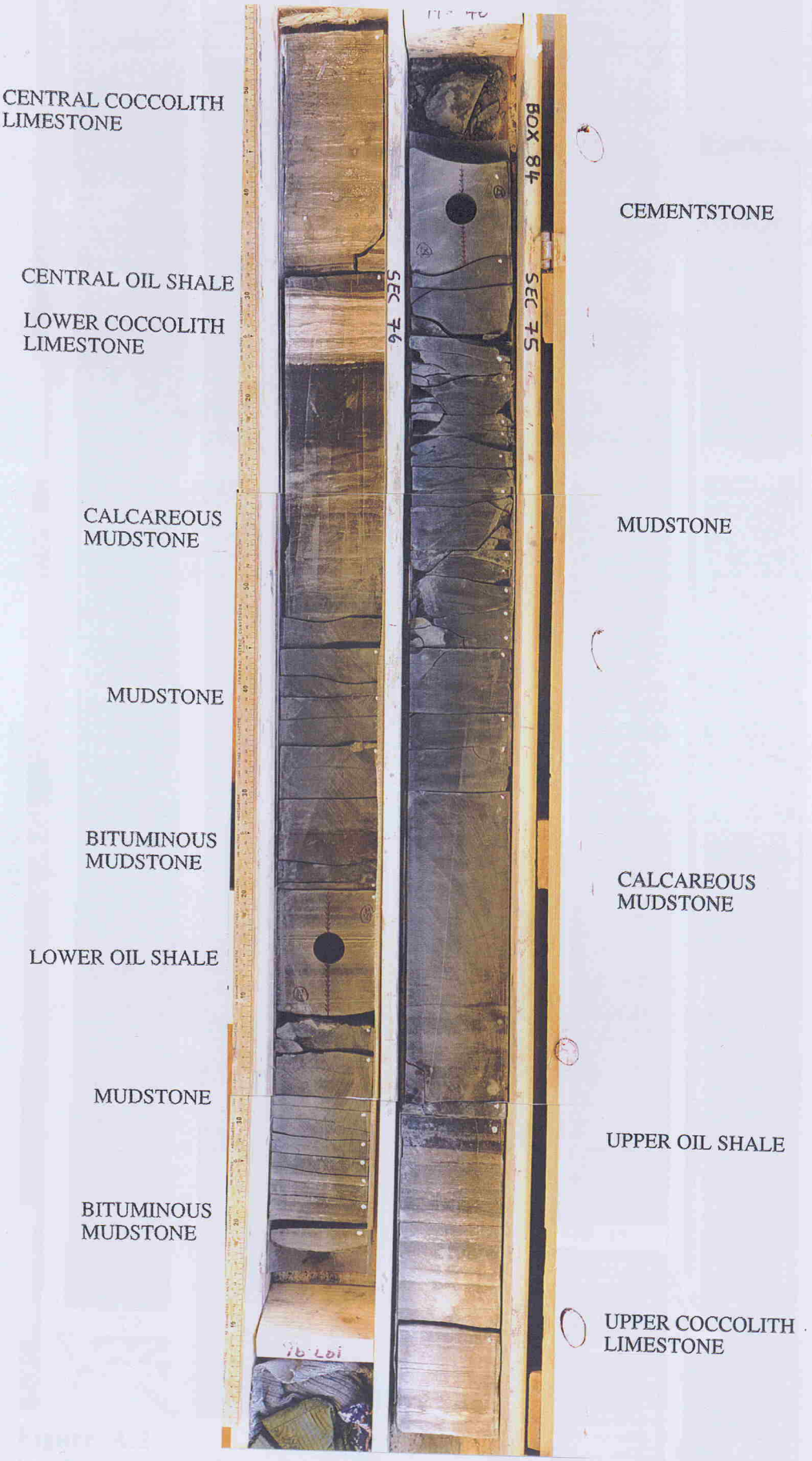

Figure A.1 Whitestone Band Interval Core Photograph

Figure A.2
Freshwater Steps Stone Band Interval
Core Photograph

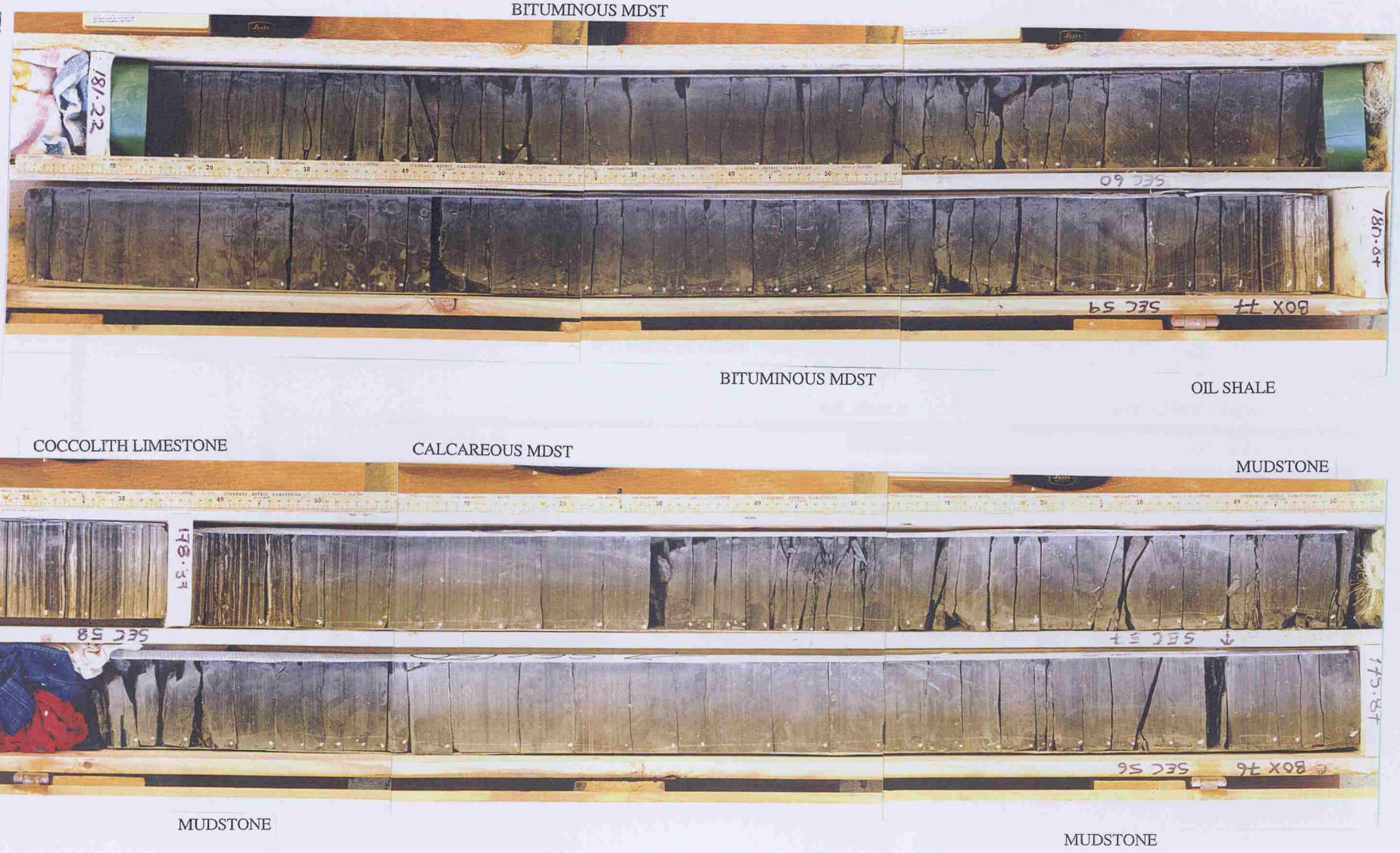

Figure A.3
Eudoxus Interval Core Photograph

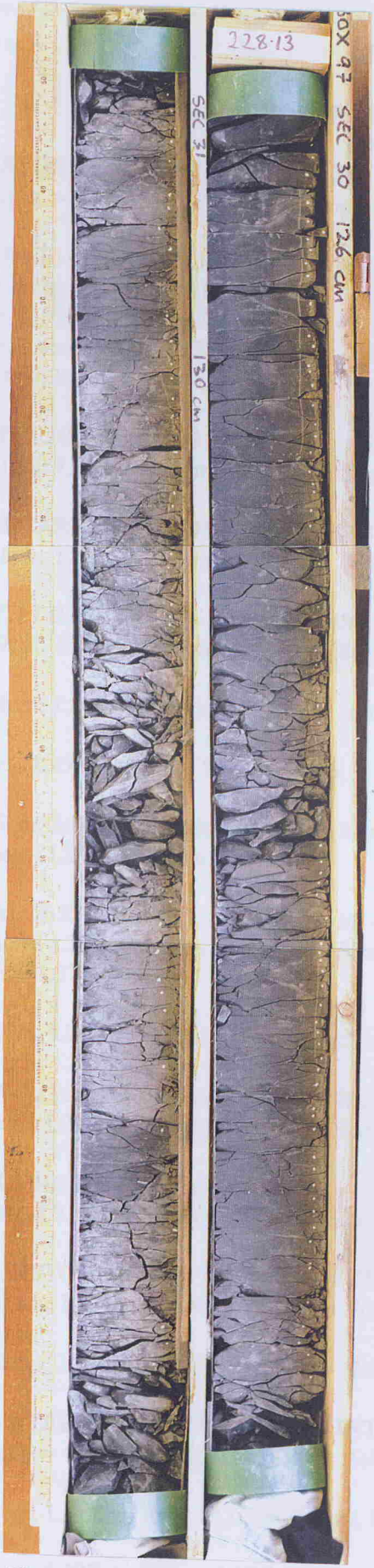

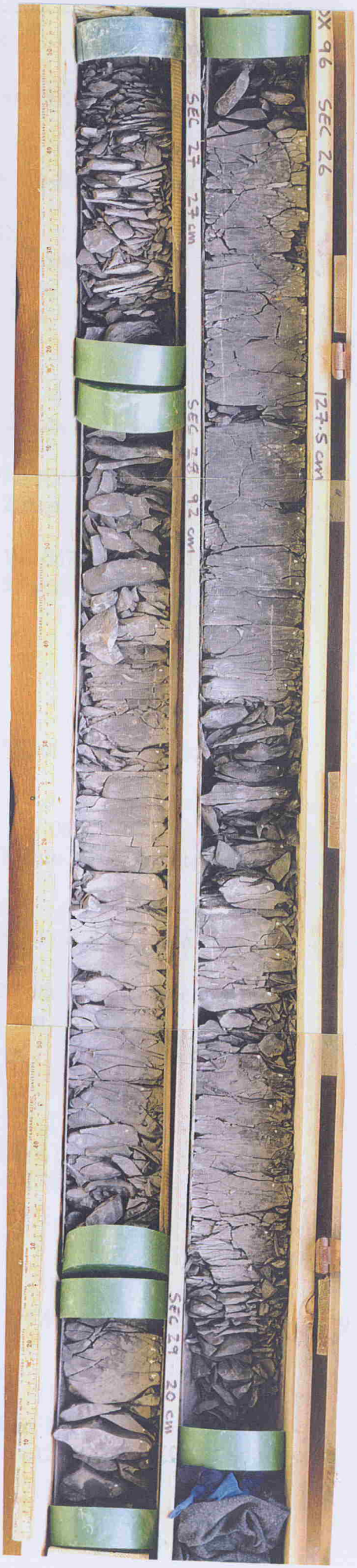

Figure A.4
Bed 44 Interval Core Photograph

APPENDIX B

SEM POLISHED THIN SECTION SAMPLE LISTINGS

1) WHITESTONE BAND INTERVAL (L2)

Driller's Depth = 195.46 to 197.96m. Down Hole Depth = 196.84 to 199.09m. Total PTS = 69.

CEMENSTONE:- 195.46 to 196.185m (Driller's Depth (DD))
L2CMT1 = 3.3cm; L2CMT2 = 3cm; L2CMT3 = 3.2cm;
L2CMT4 = 3.7cm; L2CMT5 = 3.5cm; L2CMT6 = 2cm;
L2CMT7 = 1.4cm; L2CMT8 = 2.4cm; L2CMT9 = 4cm
L2CMT10 = 4.2cm.

MUDSTONE:- 196.185 to 196.342m (DD)
L21A = 3.1cm; L21B = 3.5cm; L21C = 2.5cm; L21D = 2.4cm; L21E = 3.6cm

UPPER CALCAREOUS MUDSTONE:- 196.342 to 196.507m (DD)
L22A = 2.1cm; L22B = 3.2cm; L22C = 3.7cm; L22D = 2.9cm; L22E = 3.1cm.

COCCOLITH LIMESTONE + OIL SHALES:- 196.507 to 197.067m (DD)
L23A = 2.9cm; L23B = 2.8cm; L23C = 2.8cm; L23D = 3.3cm.

L24A = 3.4cm; L24B = 3.3cm; L24C = 3.3cm.

L25A = 3cm; L25B = 3.6cm; L25C = 4cm.

L26A = 2.5cm; L26B = 3.3cm; L26C = 3.2cm; L26D = 3.2cm; L26E = 3cm;
L26F = 2.6cm; L26G = 3.9cm.

LOWER CALCAREOUS MUDSTONE and MUDSTONE:- 197.067 to 197.7m (DD)
L27A = 2.4cm; L27B = 2.8cm; L27C = 3.2cm; L27D = 3.4cm; L27E = 3.2cm;
L27F = 3.7cm L27G = 4cm.

L28A = 3.1cm; L28B = 3cm; L28C = 3.1cm; L28D = 1.8cm; L28E = 3.6cm.

L29A = 1.9cm; L29B = 3.1cm; L29C = 1.7cm; L29D = 2.9cm; L29E = 3.6cm;
L29F = 2.8cm; L29G = 2.4cm; L29H = 2.3cm; L29I = 2.9cm

LOWER OIL SHALE:- 197.7 to 197.8
L210A = 3cm; L210B = 3.1cm; L210C = 3.4cm.

LOWER MUDSTONE and BITUMINOUS MUDSTONE:- 197.8 to 197.96
L211A = 3.1cm; L211B = 1.4cm; L211C = 2cm; L211D = 2.9cm; L211E = 1.5cm.

L212A = 3.2cm; L212B = 3.7cm; L212C = 2.2cm.

2) FRESHWATER STEPS STONE BAND INTERVAL (L1)

Driller's Depth = 175.87 to 181.27m. Down Hole Depth = 176.91 to 180.15m. Total PTS = 39

L11A = 2.2cm; L11B = 1cm; L11C = 2.6cm; L11D = 2cm.

L12A = 2.2cm; L12B = 2.7cm; L12C = 4cm; L12D = 2.3cm; L12E = 3.4cm;
L12F = 4cm; L12G = 2cm; L12H = 1.2cm; L12I = 2.3cm; L12J = 2.2cm; L12K = 2.2cm;
L12L = 1.2cm.

L13A = 4cm; L13B = 2.6cm; L13C = 4cm; L13D = 3cm; L13E = 2.1cm; L13F = 2.1cm; L13G = 2.5cm; L13H = 3cm.

L14A = 2.3cm; L14B = 2.6cm; L14C = 3.6cm; L14D = 2cm; L14E = 3cm; L14F = 2cm; L14G = 3.2cm; L14H = 2.7cm.

L15A = 1.5cm; L15B = 3.1cm; L15C = 3.1cm; L15D = 3.1cm; L15E = 3.3cm; L15F = 3.9cm; L15G = 3.9cm.

3) EUDOXUS INTERVAL (E)
Driller's Depth = 375.92 to 377.58. Down Hole Depth = 373.86 to 375.60m. Total PTS = 26

E31A = 2.1cm; E31B = 1.1cm; E31C = 3.2cm; E31D = 2.1cm; E31E = 2.7cm; E31F = 1.6cm; E31G = 3.3cm; E31H = 2.8cm.

E32A = 2.5cm; E32B = 1.4cm; E32C = 1.7cm; E32CA = 2.5cm; E32CB = 1.7cm; E32D = 2.7cm; E32E = 3cm; E32F = 2.6cm.

E33A = 3.8cm; E33B = 3.6cm; E33C = 3.6cm; E33D = 2.1; E33E = 2.1cm.

E34A = 3.8cm; E34B = 2.5; E34C = 3cm; E34D = 2.4cm; E34E = 4cm.

No PTS made of Bed 44 Interval due to its fractured nature. Stubs for topographic analysis under the SEM were made of each interval. Driller's Depth for Bed 44 = 226.77 to 228.51m, Down Hole Depth = 226.46 to 228.15m.

PTS SAMPLES - FIGURE SOURCES

Figure 3.1a = Hand specimen block of the lower oil shale, below the Whitestone Band coccolith limestone, (PTS - L210A, L210B, L210C)
Figure 3.1b - X-radiograph of the lower oil shale block, WSB (PTS as above)
Figure 3.1c - L210A, L210B, L210C
Figure 3.2a - L22A; **b** - L22A; **c** - L22A; **d** - L22D; **e** - L27E; **f** - L27E
Figure 3.3a - L27G; **b** - L27D; **c** - L27E; **d** - L27G; **e** - L27D; **f** - L27D
Figure 3.4a - L2CMT1; **b** - L2CMT1; **c** -L2CMT1
Figure 3.5a - L25A; **b** - L25A; **c** - L27B; **d** - L27B; **e** - L210B; **f** - L210B
Figure 3.6a - L27B; **b** - L27B; **c** - L27B; **d** - L27B
Figure 3.7a - L210B; **b** - L210B; **c** - L210C; **d** - L210C
Figure 3.8a - L210B; **b** - L23A; **c** - L23A; **d** - L23A
Figure 3.9a - L23A; **b** - L23A; **c** - L22E; **d** - L27A
Figure 3.10a - L27A; **b** - L27A; **c** - L27B; **d** - L27C; **e** - L23B; **f** - L23B
Figure 3.11a - L210A; **b** - L210A; **c** - L210B; **d** - L210B; **e** - L210A; **f** - L210A
Figure 3.12a - L210B; **b** - L25B; **c** - L27F; **d** - L210C; **e** - L27B; **f** - L27C
Figure 3.13a - L25B; **b** - L27B; **c** - L27B; **d** - L23D; **e** - L25A
Figure 3.14a - L27B; **b** - L27D; **c** - L27B; **d** - L27D; **e** - L27C; **f** - L25C
Figure 3.15a - L25C; **b** - L25C; **c** - L25C; **d** - L27A; **e** - L27D; **f** - L27B
Figure 3.16a - L210A; **b** - L210A; **c** - L210C; **d** - L210A; **e** - L210C; **f** - L210C
Figure 3.18a - L27B; **b** - L27B; **c** - L27B; **d** - L27B; **e** - L27B; **f** - L210A
Figure 3.19a - **c** Stub = WSB; **d** - **f** Stub FWSB
Figure 3.20a - L11D; **b** - L13D; **c** - L13D; **d** - L13D
Figure 3.21a - L14C
Figure 3.22a - L14D; **b** - L13H; **c** - L14C; **d** - L15E; **e** - L15E
Figure 3.23a - E31D; **b** - E31D; **c** - E31D; **d** - E32D; **e** - E31E; **f** - E31E
Figure 3.24a - E33B; **b** - E33B; **c** - E33A; **d** - E33A; **e** - E33A; **f** - E33A

APPENDIX C

PALYNOLOGY SAMPLES AND DATA

All palynological data produced in this study is stored in the data disk at the back of this thesis. The following files and information is held on this disk, all are saved as Excel Worksheets (.xls). Some examples of these files are given.

1) Sample Codes:- Whitestone Band = L2,
Freshwater Steps Stone Band = L1,
Eudoxus Interval = E,
Bed 44 Interval = HU.

Samples were taken down core, .ie. with the driller's depth down hole.

Whitestone Band = high resolution, two sampling scales
i) Lamina, sample codes = L2(No. No.)(Letter) eg L234A.
ii) 5cm point samples = L2(No. No.) eg L256.
Freshwater Steps Stone Band, *Eudoxus* and Bed 44 Interval = all 5cm point samples
Eg. Eudoxus = E (No. No.), E12.

2) Disk Folder Names and Contents

Folder 1) : WSB = Whitestone Band Interval.
WSBA.xls = Raw palynofacies counts.
WSBB.xls = Absolute abundance per g (AA/g) for all particle categories.
WSBC.xls = Carbonate-free absolute abundance ($CaCO_3$Free AA/g).
WSBD.xls = Group percentages (G%) for all particle categories, and bisaccate width and length data.
WSBE.xls = TOC %, carbonate %, remainder % and atomic H/C ratio data.

Folder 2) : FWSB = Freshwater Steps Stone Band Interval.
FWSBA.xls = Raw palynofacies counts.
FWSBB.xls = Absolute abundance per g (AA/g) and Group percentages (G%).
FWSBC.xls = Carbonate-free absolute abundance ($CaCO_3$Free AA/g).
FWSBD.xls = TOC %, carbonate %, remainder % data.

Folder 3) : EDX = *Eudoxus* Interval.
EDXA.xls = Raw palynofacies counts.
EDXB.xls = Absolute abundance per g (AA/g) and Group percentages (G%).
EDXC.xls = Carbonate-free absolute abundance ($CaCO_3$Free AA/g).
EDXD.xls = TOC %, carbonate %, remainder % data.

Folder 4) : BD44 = Bed 44 Interval.
BD44A.xls = Raw palynofacies counts.
BD44B.xls = Absolute abundance per g (AA/g) and Group percentages (G%).
BD44C.xls = Carbonate-free absolute abundance ($CaCO_3$Free AA/g).
BD44D.xls = TOC %, carbonate %, remainder % data.

RAW DATA COUNTS - BED 44, HUDLESTON

Sample No.	Driller's Depth (m)	Down Hole Depth (m)	Total Particles	Chor.	Px/Chor.	Prox.	Tot. Dinos.	Acrit.	Smp. Sac	FTL	Pras.	TMP	Pollen (other)	Class F	Class D	Class. Tot.	Bisac.	Tet. Pollen	Spores	TTP	DBL	DBEQ	BSLL	BSLEQ	TWL	TEW	Cut	TSD	TTD	Unknown	Lycopo.
HU2	226.77	226.46	572	6	5	13	23	4	11	8	0	46	171	138	35	173	3	347	16	363	58	22	45	16	103	38	0	141	504	22	102
HU4	226.82	226.51	504	4	9	14	27	1	4	12	0	44	168	120	31	151	6	325	10	335	45	19	32	18	77	37	0	114	449	11	102
HU6	226.87	226.56	535	0	1	8	9	4	9	10	0	32	163	129	36	165	5	333	9	342	68	35	38	8	106	43	0	149	491	12	100
HU8	226.92	226.61	508	1	6	9	16	3	6	9	0	34	150	119	32	151	6	307	7	314	53	27	38	25	91	52	0	143	457	17	100
HU10	226.97	226.65	500	1	5	13	19	3	10	7	0	39	138	74	38	112	5	255	7	262	66	60	31	30	97	90	0	187	449	12	122
HU12	227.02	226.70	504	1	1	5	7	3	10	7	0	27	155	70	35	105	2	262	7	269	87	45	41	19	128	64	0	192	461	16	114
HU14	227.07	226.75	504	1	1	2	4	5	7	7	0	23	155	56	45	101	4	260	5	265	90	47	37	26	127	73	0	200	465	16	123
HU16	227.12	226.80	508	0	0	8	8	2	5	6	0	21	153	58	45	103	2	258	6	264	88	42	53	26	141	68	0	209	473	14	109
HU18	227.17	226.85	504	0	3	6	9	3	4	8	0	24	132	67	68	135	1	268	6	274	77	51	44	23	121	74	0	195	469	11	102
HU20	227.22	226.90	523	0	0	7	7	7	10	12	0	36	164	70	39	109	1	274	4	278	74	51	45	25	119	76	0	195	473	14	100
HU22	227.27	226.95	506	0	2	7	9	4	5	4	0	22	152	66	57	123	1	276	9	285	92	33	45	13	137	46	0	183	468	16	125
HU24	227.32	226.99	511	2	1	5	8	7	4	7	0	26	158	63	37	100	4	262	9	271	66	45	57	18	143	63	1	207	478	7	126
HU26	227.37	227.04	505	0	0	5	5	1	3	9	0	18	124	64	64	128	3	255	4	259	80	42	62	32	142	74	0	216	475	12	127
HU28	227.42	227.09	514	0	1	7	8	3	2	17	0	30	142	64	49	113	4	259	10	269	82	43	54	27	136	70	0	206	475	9	100
HU30	227.47	227.14	508	0	2	5	7	5	3	12	0	27	136	75	57	132	2	270	7	277	63	47	59	21	122	68	0	190	467	14	104
HU32	227.52	227.19	517	0	3	6	9	1	5	11	0	26	169	96	67	163	2	334	2	336	48	36	39	24	87	60	0	147	483	8	104
HU34	227.57	227.24	511	2	0	7	9	3	5	12	0	29	186	95	82	147	6	339	2	341	47	32	37	16	84	48	0	132	473	9	103
HU36	227.62	227.28	540	1	1	2	4	8	2	13	0	27	164	87	81	168	5	337	4	341	66	46	33	21	99	67	0	166	507	6	100
HU38	227.67	227.33	549	2	2	2	6	3	2	8	0	19	179	73	57	130	0	309	5	314	90	41	44	32	134	73	0	207	521	9	100
HU40	227.72	227.38	504	0	1	7	8	4	4	7	0	23	162	75	56	131	3	296	5	301	72	25	44	28	116	53	0	169	470	11	104
HU42	227.77	227.43	509	0	0	7	7	9	7	13	0	36	149	55	54	109	4	262	13	275	73	35	45	26	118	64	0	182	457	16	111
HU44	227.82	227.48	504	0	2	8	10	6	9	11	0	36	169	53	48	101	1	271	3	274	68	38	56	19	124	57	0	181	455	13	105
HU46	227.87	227.53	519	0	3	8	11	7	4	7	0	29	173	54	51	105	3	281	9	290	78	42	42	33	120	75	0	195	485	5	101
HU48	227.92	227.58	588	1	1	9	11	5	6	12	0	34	176	71	75	146	3	325	9	334	89	44	54	19	143	68	0	206	540	14	101
HU50	227.97	227.62	501	1	0	3	4	5	4	9	0	22	153	66	54	120	5	278	11	289	70	36	56	19	126	55	0	181	470	9	111
HU52	228.02	227.67	539	0	3	7	10	9	6	10	0	35	173	78	53	131	8	312	19	331	64	40	42	15	106	56	1	162	493	11	100
HU54	228.07	227.72	534	0	0	5	5	10	6	14	0	35	164	74	54	128	7	299	5	304	71	36	59	21	130	57	0	187	491	8	100
HU56	228.12	227.77	512	2	1	6	9	12	10	16	0	47	157	74	52	126	3	286	7	293	63	34	46	21	109	55	0	164	457	8	101
HU58	228.16	227.81	509	1	1	9	11	3	6	11	0	31	172	66	52	118	3	293	12	305	71	31	40	22	111	53	0	164	469	9	102
HU60	228.21	227.86	501	1	0	6	7	5	6	6	0	24	185	46	48	94	6	285	6	291	60	48	47	22	107	70	0	177	468	9	114
HU62	228.26	227.91	504	0	1	7	8	10	6	11	0	35	170	58	57	115	8	293	10	303	58	30	47	22	105	52	0	157	460	9	102
HU64	228.31	227.95	505	3	0	4	7	5	9	5	0	26	185	51	59	110	4	299	5	304	68	32	52	15	120	47	0	167	471	8	109
HU66	228.36	228.00	507	0	0	8	8	5	3	15	0	31	187	51	55	106	4	297	7	304	64	32	52	14	116	46	0	162	466	10	107
HU68	228.41	228.05	537	1	1	9	11	11	9	14	0	45	164	66	60	126	5	295	6	301	74	40	47	19	121	59	0	180	481	11	100
HU70	228.46	228.10	514	1	1	7	9	5	7	15	0	36	162	48	61	109	8	279	9	288	63	41	55	22	118	63	0	181	469	9	102
HU72	228.51	228.15	515	0	0	3	3	7	5	13	0	28	183	68	42	110	5	298	9	307	65	36	58	17	123	53	0	176	483	4	103

An example of the data excel worksheets. This contains raw palcile counts for the Bed 44 interval, point sampled every 5cm.

TOC %, Carbonate %, Remainder % Weight, Bed 44 Interval

Sample No.	Driller's Depth (m)	Down Hole Depth (m)	TOC	Carbonate	Remainder	CaCO3-Free TOC	Estimated TPOM	Estimated Clastics
HU2	226.77	226.46	1.85	37.37	60.78	2.96	3.31	65.94
HU4	226.82	226.51	1.68	38.34	59.98	2.72	2.99	64.65
HU6	226.87	226.56	1.74	34.28	63.99	2.64	3.10	68.82
HU8	226.92	226.61	1.75	33.10	65.15	2.61	3.12	70.01
HU10	226.97	226.65	1.58	33.42	65.00	2.37	2.82	69.40
HU12	227.02	226.70	1.44	34.23	64.33	2.19	2.57	68.34
HU14	227.07	226.75	1.42	35.84	62.75	2.21	2.53	66.70
HU16	227.12	226.80	1.32	38.70	59.98	2.16	2.36	63.66
HU18	227.17	226.85	1.37	39.65	58.98	2.27	2.45	62.79
HU20	227.22	226.90	1.51	36.96	61.53	2.40	2.70	65.74
HU22	227.27	226.95	1.33	42.79	55.88	2.33	2.38	59.59
HU24	227.32	226.99	1.36	41.16	57.48	2.31	2.43	61.27
HU26	227.37	227.04	1.23	44.56	54.21	2.22	2.20	57.64
HU28	227.42	227.09	1.30	42.34	56.36	2.25	2.32	59.98
HU30	227.47	227.14	1.23	47.60	51.18	2.34	2.19	54.59
HU32	227.52	227.19	1.54	38.90	59.56	2.52	2.75	63.84
HU34	227.57	227.24	1.62	34.01	64.37	2.45	2.89	68.87
HU36	227.62	227.28	1.46	33.52	65.02	2.19	2.60	69.08
HU38	227.67	227.33	1.38	32.51	66.11	2.04	2.46	69.94
HU40	227.72	227.38	1.35	34.25	64.40	2.05	2.41	68.15
HU42	227.77	227.43	1.16	47.88	50.96	2.23	2.08	54.20
HU44	227.82	227.48	1.26	47.02	51.73	2.37	2.24	55.23
HU46	227.87	227.53	1.18	49.00	49.83	2.31	2.10	53.11
HU48	227.92	227.58	1.25	49.92	48.83	2.49	2.23	52.30
HU50	227.97	227.62	1.24	51.40	47.36	2.55	2.21	50.81
HU52	228.02	227.67	1.32	49.76	48.92	2.62	2.35	52.59
HU54	228.07	227.72	1.30	47.15	51.55	2.46	2.32	55.18
HU56	228.12	227.77	1.22	50.50	48.28	2.46	2.17	51.68
HU58	228.16	227.81	1.28	49.87	48.85	2.56	2.29	52.42
HU60	228.21	227.86	1.23	49.92	48.85	2.45	2.19	52.27
HU62	228.26	227.91	1.52	47.07	51.41	2.87	2.71	55.64
HU64	228.31	227.95	1.39	46.42	52.20	2.59	2.48	56.06
HU66	228.36	228.00	1.33	46.97	51.70	2.51	2.38	55.40
HU68	228.41	228.05	1.34	45.94	52.73	2.47	2.38	56.45
HU70	228.46	228.10	1.20	49.40	49.40	2.37	2.14	52.74
HU72	228.51	228.15	1.22	46.12	52.65	2.27	2.18	56.06

A data sheet example of the TOC %, carbonate %, and remainder % weights for the Bed 44 Interval. Also calculated are carbonate-free TOC % and estimated TPOM (total organic matter and pyrite organic matter) and estimated clastic % weight.

REFERENCES

Ager, D.V. (1975) *The Jurassic world ocean, (with special reference to the North Atlantic).* Jurassic Northern North Sea Symposium, Oslo, P. R. Assistance: 18-20

Aigner, T. (1980) Biofacies and stratonomy of the Lower Kimmeridge Clay (Upper Jurassic, Dorset, England). *Neues Jarhb. Geol. Palaontol. Abh.* **159**: 324-338.

Al-Ameri, T.K., Al-Musawi, F.S. and Batten, D.J. (1999) Palynofacies indications of depositional environments and source potential for hydrocarbons: uppermost Jurassic-basal Cretaceous Sulaiy Formation, southern Iraq. *Cretaceous Research* **20**: 359-363.

Alldredge, A.L. and Silver, M.W. (1988) Characteristics, dynamics and significance of marine snow. *Progress in Oceanography*, **20**, 41-82.

Allen, P. (1998) Purbeck-Wealden (early Cretaceous) climates. *Proceedings of the Geologists' Association* **109**: 197 - 236.

Allison, P.A., Wignall, P.B. and Brett, C.E. (1995) Palaeo-oxygenation: effects and recognition, in *Marine palaeoenvironmental analysis from fossils. Geological Society Special Publication No. 83*, (eds D. W. J. Bosence and P. A. Allison). London, Geological Society: 97–112. 262pp

Alve, E. (1991) Foraminifera, climatic change, and pollution: a study of late Holocene sediments in Drammensfjord, southeast Norway. *The Holocene*, **1**, 243-61

Andersen, F.O. and Kristensen, E. (1992) The importance of benthic macrofauna in decomposition of microalgae in a coastal marine sediment. *Liminology and Oceanography*, **37**, 1392-403.

Arkell, W.J. (1933) *The Jurassic system in Great Britain.* Oxford, Clarendon Press.

Arkell, W.J. (1947) *The geology of the country around Weymouth, Swanage, Corfe and Lulworth.* Edinburgh, Oliver and Boyd Ltd.

Arntz, W.E., Tarazona, J., Gallardon, A., Flores, L.A. and Salwedel, H. (1991) Benthos communities in oxygen deficient shelf and upper slope areas of the Permian and Chilean Pacific coast and changes caused by El Nino, in *Modern and ancient continental shelf anoxia,* (eds R. V. Tyson and T. H. Pearson). London, Geological Society of London: 131-154.

Arthur, M.A., Dean, W.E., Neff, E.D., Hay, B.J., King, J. and Jones, G. (1994) Varve calibrated records of carbonate and organic carbon accumulation over the last 2000 years in the Black Sea. *Global Biogeochemical Cycles*, **8**, 195-217.

Asper, V.L., Deuser, W.G., Knauer, A. and Lohrenz, S.E. (1992) Rapid coupling of sinking particle fluxes between surface and deep ocean waters. *Nature*, **357**, 670-672.

Axelrod, D.I. (1984) An interpretation of Cretaceous and Tertiary biota in polar regions. *Palaeogeography, Palaeoclimatology, Palaeoecology*, **45**, 105-147.

Ayers, G.P., Ivey, J.P. and Gillett, R. (1991) Coherence between seasonal cycles of dimethyl sulphide, methanesulphonate and sulphate in marine air. *Nature*, **349**, 404-406.

Bailey, D., Milner, P. and Varney, T. (1997) Some dinoflagellate cysts from the Kimmeridge Clay Formation in North Yorkshire and Dorset, U.K. *Proceedings of the Yorkshire Geological Society* **51**(3): 235-243.

Baird, R.A. (1986) Maturation and Source Rock Evaluation of Kimmeridge Clay, Norwegian North Sea. *The American Association of Petroleum Geologists Bulletin* **70**(1): 1-10.

Balch, W.M., Holligan, P.M., Ackelson, S.G. amd Voss, K.J. (1991) Biological and optical properties of mesoscale coccolithophore blooms in the Gulf of Maine. *Limnology and Oceanography*, **36**, 629-43.

Balch, W.M., Kilpatrick, K., Holligan, P.M. and Cucci, T. (1993) Coccolith production and detachment by *Emiliania huxleyi* (Prymnesiophyceae). *Journal of Phycology*, **29**, 566-575.

Banse, K. (1995) Zooplankton: Pivotal role in the control of ocean production. *ICES Journal of Marine Science*, **52**, 265-277.

Barnard, P.D.W. (1973) Mesozoic floras. *Organisms and Continents Through Time.* (ed N.F.Hughes). **12:** 175-188.

Barnard, P.C. and Cooper, B.S. (1981) Oils and source rocks of the North Sea area, in *Petroleum Geology of the Continental Shelf of North-West Europe* (eds L.V. Illing and G.D. Hobson), Heydon, London, pp. 169-175.

Barnard, P. C., Collins, A.G., and Cooper, B. S. (1981) Indentification and distribution of kerogen facies in a source rock horizon - examples from the North Sea Basin, in *Organic Maturation Studies and Fossil Fuel Exploration* (ed. J. Brooks) Academic Press, London, pp. 271–82.

Barron, H.F. (1989) Dinoflagellate cyst biostratigraphy and palaeoenvironments of the Upper Jurassic (Kimmeridgian to Portlandian) of the Helmsdale region, east Sutherland, Scotland, in *North West European micropalaeontology and palynology*, (eds D. J. Batten and M. C. Keen). London, Ellis Harwood Ltd: pp298
Ch 8: 192-211.

Batten, D.J. (1974) Wealden palaeoecology from the distribution of plant fossils. *Proceedings of the Geologists' Association*, **85**, 433-58.

Batten, D.J. (1982). Palynofacies, palaeoenvironments and petroleum. *Journal of Micropalaeontology* **1**: 107-114.

Baudin, F. (1995) Depositional controls on Mesozoic source rocks in the Tethys. *Palaeogeography, palaeoclimatology and source rocks. AAPG Studies in Geology No. 40.* A. Y. Huc. Oklahoma, U.S.A., AAPG: pp347; 191-213.

Baudin, F., Cecca, F., Fourcade, E. and Azema, J. (1992) Paleoenvironments et facies organiques du Kimmeridgien inferieur de la Tethys (Palaeoenvirnoments and Organic Facies of the Early Kimmeridgian in Tethys). *C. R. Acad. Sci. Paris*, **314**(11): 373-379.

Baudin, F., Monod, O., Begouen, V. Laggoun-Defarge, F. and Person, A. (1994) Caracterisation et diagenese de la matiere organicque du Jurassique superieur du Taurus oceidental (Turquie meridionale). Reconstruction paleoenvironmentale et consequences tectoniques. *Bull. Soc. Geol. Fr* **2**: 135-145.

Belin, S., (1992) Application of backscattered electron imagery to the study of source rock microtextures. *Organic Geochemistry* **18**(3): 333-346.

Bellamy, J. R. W. (1980) Carbonate within bituminous shales of the British Jurassic - their petrology and diagenesis. Unpublished PhD Thesis, University of Southampton.

Berggren, W.A. and Hollister, C.D. (1974) Palaeogeography, palaeobiogeography and the history of circulation in the Atlantic Ocean. *Studies in palaeo-oceanography.*
Spec. publ., Soc econ. paleont. Min. W. W. Hay. **20:** 126-186.

Berner, R.A. (1982) Burial of organic carbon and pyrite sulphur in the modern ocean: its geochemical and environmental significance. *American Journal of Science*, **282**, 451-73.

Berner, R. A. (1985) Sulphate reduction, organic matter decomposition and pyrite formation. *Philosophical Transaction of the Royal Society of London*, **A315**, 25–38.

Bertrand, P. and Lallier-Verges, E. (1993) Past sedimentary organic matter accumulation and degradation controlled by productivity. *Nature* **364**: 786-788.

Bertrand, P., Lallier-Verges, E., Martines, L., Pradier, B., Tremblay, P., Huc, A.Y., Jouhannel, R. and Tricart, J.P. (1989) Examples of spatial relationships between organic matter and mineral groundmass in the microstructure of the organic-rich Dorset Formation rocks, Great Britain. *Organic Geochemistry* **16**(4): 661-675.

Billen, G. (1982) Modelling the processes of organic matter degradation and nutrients recycling in sedimentary systems, in *Sediment Microbiology* (eds. D.B. Nedwell and C.M. Brown), Academic Press, London, 15-52.

Bishop, A.N., Kearsley, A.T. and Patience, R.L.,(1992) Analysis of sedimentary organic materials by scanning electron microscopy: The application of backscattered electron imagery and light element x-ray microanalysis. *Organic Geochemistry* **18**(4): 431-446.

Bouloubassi, I., Rullkotter, J. and Meyers, P.A. (1999) Origin and transformation of organic matter in Pliocene-Pleistocene Mediterranean sapropels: organic geochemical evidence review. *Marine Geology* **153** (1-4): 177-197.

Bouma, A.G. (1969) *Methods for the study of sedimentary structures*. New York, Wiley.

Boussafir, M., Gelin, F., Lallier-Verges, E., Derenne, S., Bertrand, P. and Cargean, C., (1995a) Electron microscopy and pyrolsis of kerogens from the Kimmeridge Clay Formation, UK :- Source organisms, preservation processes and origin of microcycles. *Geochimica et Cosmochimica Acta* **59**: 3731-3740.

Boussafir, M., Lallier-Verges, E., Bertrand, P. and Badaut-Trauth, D. (1995) SEM and TEM studies on isolated organic matter and rock microfacies from a short term organic cycle of the Kimmeridge Clay Formation (Yorkshire, Great Britian), in *Organic Matter Accumulation : The organic cyclicities of the Kimmeridge Clay Formation (Yorkshire, Great Britain) and recent Maar sediments (Lac du Bochet, France)*. (eds E. Lallier-Verges, N. P. Tribovillard and P. Bertrand). Lecture notes in Earth Sciences 57. New York, Springer Publishing. pp 187: 15-30

Braarud, T. (1962) Species distribution in marine phytoplankton. *Journal of the Oceanography Society of Japan*, **20**, 628-49.

Brand, L.E. (1994) Physiological ecology of marine coccolithophores, in *Coccolithophores*, (eds A. Winter and W. G. Siesser). Cambridge, Cambridge University Press: 39-49.

Brand, L.E. and Guillard, R.R.L. (1981) The effects of continuous light and light intensity for the biogeochemical control of new production. *Limnology and Oceanography*, **36**, 1756-71.

Brand, L.E., Sunda, W.G. and Guillard, R.R.L. (1983) Limitation of marine phytoplankton reproductive rates by zinc, manganese, and iron. *Limnology and Oceanography*, **28**, 1182-98.

Brandt, K. (1986) Glacioeustatic cycles in the Early Jurassic? *N. Jb. Geol. Palaont. Mh.*: 257-274.

Brasier, M.D. (1995) Fossil indicators of nutrient levels. 1: Eutrophication and climate change, in *Marine Palaeoenvironmental Analysis from Fossils*. (eds D. W. J. Bosence and P. A. Allison). London, Geological Society, London: 113-132.

Brass, G.W., Southam, J.R. and Peterson, W.H. (1982) Warm saline bottom water in the ancient ocean. *Nature* **296**: 620-623.

Brown, S. (1990) The Jurassic, *in Introduction to Petroleum Geology of the North Sea*. (ed K.W.Glennie). Oxford, Blackwell Scientific Publishers, 3rd edition. pp402: 219-254.

Brown, C.W. and Yoder, J.A. (1994b) Coccolithophorid blooms in the global ocean. *Journal of Geophysical Research*, **99**, 7467-7482.

Brush, G.S. and Brush, L.M. Jr (1972) Transport of pollen in a sediment-laden channel; a laboratory study. *American Journal of Science*, **272**, 359-81.

Buesseler, K.D. and Benitee, C.R. (1994) Determination of mass accumulation rates and sediment radio nuclide inventones in the deep Black Sea. *Deep Sea Research I*, **41** (11/12), 1605-1615.

Burky, D. (1974) Coccoliths as paleosalinity indicators - evidence from the Black Sea. *Memoirs of the American Association of Petroleum Geologists*, **20**, 353-63.

Butterfield, B.G. and Meylan, B.A. (1980) *Three-Dimensional Structure of Wood: An Ultrastructural Approach*, 2nd ed, Chapman & Hall, London, 103 pp.

Calvert, S.E. (1987) Oceanographic control on accumulation of organic matter in marine sediments, in *Marine Petroleum Source Rocks* (eds J. Brooks and A. J. Fleet). London, Blackwell Scientific: pp444: 137-151.

Calvert, S.E. and Veevers, J.J. (1962) Minor structures of unconsolidated marine sediments revealed by x-radiography. *Sedimentology* **1**: 287-295.

Calvert, S.E., Korlin, R.E., Toolin, L.J., Donalme, D.J., Southan, J.R. and Vogel., J.S. (1991) Low organic carbon accumulation rates in the Black Sea sediments. *Nature*, **350**, 692-695.

Campbell, I.D. (1991) Experimental mechanical degradation of pollen grains. *Palynology*, **15**, 29-34.

Canfield, D.E. (1989) Sulphate reduction and oxic respiration in marine sediments. Implications for organic carbon preservation. *Deep Sea Research* **36**: 121-138.

Canfield, D.E. (1993) Organic matter oxidation in marine sediments, in *Interactions of C, N, P and S Biogeochemical Cycles and Global Change* (eds R. Wollast, F.T. MacKenzie and L. Chou), *NATO Advanced Studies Institute Series*, **14**, Springer-Verlag, Berlin, 333 - 63.

Carney, R.S. (1989) Examining relationships between organic carbon flux and deep-sea deposit feeding, in *Ecology of Marine Deposit Feeders* (eds G. Lopez, G. Tachon and J. Levinton), Lecture Notes on *Coastal and Estuarine Studies*, **31**, 24-58.

Cecca, F., Azema, J., Fourcade, E., Baudin, F., Guirand, R., Bonneau, M. and Wever, P.d. (1993) Early Kimmeridgian palaeoenvironments and palaeogeographies of the Tethys realm, in *Atlas Tethys palaeoenvironmental maps,* (eds J. Dercourt, L. E. ricou and B. Vrielynch).

Chaloner, W.G. and Muir, M. (1968) Spores and floras, in *Coal and Coal-Bearing Strata* (eds D. Murchison and T.S. Westoll), Oliver & Boyd, Edinburgh, pp. 127-46.

Chadwick, R.A. (1986) Extension tectonics in the Wessex Basin, southern England. *Journal of the Geological Society, London*, **143**, 465-488.

Chaloner, W.G. (1989) Fossil charcoal as an indicator of palaeoatmospheric oxygen level. *Journal of the Geological Society of London*, **146**, 171-4.

Chambers, M.H. (2000) A high resolution chemostratigraphy and mineralogical study of the UK onshore Kimmeridge Clay, Unpublished PhD Thesis, University of Reading.

Charlson, R.J., Lovelock, J.E., Andreae, M.O. and Warren, S. G. (1987) Oceanic phytoplankton, atmospheric sulphur, cloud albedo and climate. *Nature*, **326**, 655-61.

Christensen, J.P. (1989) Biological enhancment of solute exchange between sediment and bottom waters. *Continental Shelf Research*, **9**, 223-246.

Clark, R.L. (1986) Pollen as a chronometer and sediment tracer, Burrinjack Reservoir, Australia, *Hydrobiologia*, **143**, 63-9.

Clark, J.S. (1988) Particle motion and theory of charcoal analysis : Source area, transport, deposition and sampling. *Quaternary Research* **30**: 67-80.

Colbert, E.H. (1964) Climatic zonation and terrestrial faunas, in *Problems of Palaeoclimatology,* (ed A. E. M. Nairn). New York, Wiley: 617–637

Combaz, A. (1964) Les Palynofacies. *Revue Micropaleontology.*, Paris, **7**, 205–218.

Cooke, R.C. and Rayner, A.D.M. (1984) *Ecology of Saprotrophic Fungi*, Longman, Harlow, 415 pp.

Cope, J.C.W. (1978) The ammonite faunas and stratigraphy of the upper part of the Upper Kimmeridge Clay of Dorset. *Palaeontology* **21**: 469-533.

Cope, J.C.W., Getty, T.A., Howarth, M.K., Morton, N. and Torrens, H.S. (1980). *A correlation of Jurassic rocks in the British Isles. Part 2, Middle and Upper Jurassic.* Oxford, Blackwell scientific Publishers.

Cope, M.J. (1980) Physical and chemical properties of coalified and charcoalified phytoclasts from some British Mesozoic sedimets: an organic geochemical approach to palaeobotany. *Physics and Chemistry of the Earth*, **12**, 663-77.

Cope, M.J. (1981) Products of natural burning as a component of the dispersed organic matter in sedimentary rocks, in *Organic Maturation Studies and Fossil Fuel Exploration* (ed. J. Brooks), Academic Press, London, 89-110.

Correia, M. (1971) Diagenesis of sporopollenin and other comparable organic substances: application to hydrocarbon research, in *Sporopollenin*, (eds J. Brooks, P. Grant, M.D. Muir, G. Shaw and P. Van Gijzel), Academic Press, London, pp. 569-620.

Cox, B.M. and Gallois, R.W. (1981). *The stratigraphy of the Kimmeridge Clay of the Dorset type area and its correlation with some other Kimmeridgian sequences.* London, Institute of Geological Sciences.

Creany, S. (1980) The organic petrology of the Upper Cretaceous Boundary Creek Formation, Beaufort-Mackenzie Basin, *Bulletin of Canadian Petroleum Geology*, **28**, 112-29.

Creber, G.J. and Chalonar, W.G. (1984) Influence of environmental factors on wood structure of living and fossil trees. *Botanical Review* **50**: 357-448.

Curtis, C. (1987). Mineralogocal consequences of organic matter degradation in sediments : Inorganic / oragnic diagenesis, in *Marine Clastic Sedimentology*, (eds J. K. Leggett and G. G. Zuffa) : 108-123.

Curtis, C.D. (1980) Diagenetic alteration in black shales. *Journal of the Geological Society of London* **137**: 189-194.

Dale, B. (1976) Cyst formation, sedimentation, and preservation: factors affecting dinoflagellate assemblages in Recent sediments from Trondheimsfjord, Norway. *Review of Palaeobotany and Palynology*, **22**, 39-60.

Davies, R.B (1967) Pollen studies of near-surface sediments in Maine lakes, in *Quaternary Palaeoecology* (eds E.J. Cushing and H.E. Wright Jr), Yale University Press, New Haven, pp. 143-73.

Deconick, J-F. (1986) Clay minerals of Purbeckian facies: Swiss and French Jura, Dorset (England) and Boulonnais (France). *Annales De La Societe Geologique Du Nord,* **CVI (3)**, 285–297.

De la Cruz, A.A. and Gabriel, B.C. (1974) Caloric, elemental, and nutritive changes in decomposing *Juncus roemerianus* leaves. *Ecology*, **55**, 882-6.

Demaison, G.J. and Moore, G.T. (1980) Anoxic environments and oil source bed genesis. *American Association of Petroleum Geologists, Bulletin.* **64**(8): 1179-1209.

Desprairies, A., Bachaoui, M., Ramdani, A. and Tribovillard, N. (1995) Clay diagenesis in organic-rich cycles from the Kimmeridge Clay Formation of Yorkshire (G.B): Implication for palaeoclimatic interpretations, in *Organic Matter Accumulation:- the organic cyclicities of the Kimmeridge Clay Formation (Yorkshire, Great Britain) and the Recent Maar sediments (Lac du Bochet, France)*, (eds E. Lallier-Verges, N. P. Tribovillard and P. Bertrand). New York, Springer Publishing: 63-91.

Deuser, W.G., Ross, E.H. and Anderson, R.F. (1981) Seasonality in the supply of sediment to the deep Sargasso Sea and implications fro the rapid transfer of matter to the deep ocean. *Deep Sea Research*, **28**, 495-505.

Dickman, M. and Artuz, I. (1978) Mass mortality of photosynthectic bacteria as a mechanism for dark lamina formation in sediments of the Black Sea. *Nature* **275**: 191-195.

Dimeter, A. and Smelror, M. (1990) Callovian (Middle Jurassic) marine microplankton from southwestern Germany: biostratigraphy and palaeoenvironmental interpretations. *Palaeogeography, Palaeoclimatology, Palaeoecology*, **80**, 173-95

Disnar, J.R. and Ramanampisoa, L. (1995) Palaeoproduction control on anoxia and organic matter preservation and accumulation in Kimmeridge Clay Formation of Yorkshire: Molecular assessment, in *Organic Matter Accumulation:- the organic cyclicities of the Kimmeridge Clay Formation (Yorkshire, Great Britain) and the Recent Maar sediments (Lac du Bochet, France)*, (eds E. Lallier-Verges, N. P. Tribovillard and P. Bertrand). New York, Springer Publishing: 49 - 61.

Dodge, J.D. and Harland, R. (1991) The distribution of planktonic dinoflagellates and their cysts in the eastern and northeastern Atlantic Ocean. *New Phytologist*, **118**, 593-603.

Donn, W. L. (1987) Terrestrial climate change from the Triassic to Recent, in *Climate, History, Periodicity and Predictability*, (eds Rampino *et al*): 343–352.

Dore, A.G. (1991) The structural foundation and evolution of Mesozoic Seaways between Europe and the Artic. *Palaeogeography, Palaeoclimatology, Palaeoecology* **87**: 441-492.

Douglas, R.G. (1981) Palaeoeocology of continental margin basins margin basins: a modern case history from Borderland of Southern California, in *Depositional Systems of Active Continental Margin Basins* (eds R.G. Douglas, I.P, Colburn and D.S. Gorsline), Short Course Notes, Pacific Section of the Society of Economic Paleontologists and Mineralogists, Los Angeles, pp. 121-56.

Downie, C. (1984) Acritarchs in British stratigraphy. *Geological Society of London, Special Report*, **17**, 26 pp.

Dybkaer, K. (1991) Palynological zonation and palynofacies investigation of Fjerritslev Formation (Lower Jurassic - basal Middle Jurassic) in the Danish Subbasin. *Danmarks Geologiske Undersogelse*, **A30**, 150 pp

Dring, M.J. (1990) Light harvesting and pigment composition in marine phytoplankton and macroalgae. *In Light and Life in the Sea* (eds P.J. Herring, A.K. Campbell, M. Whitfield and L. Maddock) Cambridge University Press, Cambridge. pp. 89 - 103.

Eaton, R.A. and Hale, M.D.C. (1993) *Wood: Decay, Pests and Protection*, Chapman & Hall, London, 546 pp.

Ebukanson, E.J. and Kinghorn, R.R.F. (1985) Kerogen facies in the major Jurassic mudrock formations of southern England and the implications on the depositional environments of their precursors. *Journal of Petroleum Geology* **8**(4): 435-462.

Emerson, S and Hedges, J.I. (1988) Processes controlling the organic carbon content of open ocean sediments. *Paleoceanography*, **3**, 621-34.

Eppley, R.W. and Peterson, B.J. (1979) Particulate organic matter flux and planktonic new production in the deep ocean. *Nature*, **282**, 677-80.

Epshteyn, O.G. (1978) Mesozoic - Cenozoic climates of northern Asia and glacial-marine deposits. *Int. geol. Rev.* **20**: 49-58.

Erkmen, U. and Sarjeant, W.A.S. (1980) Dinoflagellate cysts, acritarchs, and tasmanitids from the uppermost Callovian of England and Scotland: with a reconsideration of the 'Xanthidium pilosum' problem. *Geobeois*, **13**, 45-99.

Evitt, W.R. (1963b) A discussion and proposals concerning fossil dinoflagellates, hystrichospheres, and acritarchs, I & II. *Proceedings of the National Academy of Sciences, Washington*, **49**, 158 - 64; 298-302.

Evitt, W.R. (1985) *Sporopollenin dinoflagellate cysts - Their morphology and interpretation.* U. S. A., AASP.

Farnimond, P., Connet, P., Eglinton, G., Evershed, R.P., Hall, M.A., Pork, D.W. and Wardropper, A.M.K. (1984) Organic geochemical study of the Upper Kimmeridge Clay of Dorset type area. *Marine Petroleum Geology* **1**: 340-354.

Feistner, K.W.A. (1989) Petrographic examination and re-interpretation of concretionary carbonate horizons from the Kimmeridge Clay, Dorset. *Journal of the Geological Society of London.* **146**: 345-350.

Fernandez, E., Boyd, P., Holligan, P.M. and Harbour, D.S. (1993) Production of organic and inorganic carbon within a large scale coccolithophore bloom in the Northeast Atlantic Ocean. *Marine Ecology*, **97**, 271-285.

Fisher, M.J. and Miles, J.A. (1983) Kerogen types, organic maturation and hydrocarbon occurrences in the Moray Firth and south Viking Graben, North Sea basin, *in Petroleum Geochemistry and Exploration of Europe* (ed. J.Brooks), *Geological Society of London Special Publication*, **12**, 195-201.

Fisher, N.S. and Honjo, S. (1991) Intraspecific differences in temperature and salinity responses in the coccolithophore *Emiliania huxleyi. Biological Oceanography*, **6**, 35- 61.

Fourcade, E., Azema, J., Bassoullet, J.P., Cecca, F., Dercourt, J., Enay, R. and Guirand, R. (1996) Palaeogeography and palaeoenvironment of the Tethyan Realm during the Jurassic breakup of Pangea, in *The Ocean Basins and Margins, Volume 8 - The Tethys Ocean,* (eds A. E. M. Nairn, L. Ricou, B. Vrielynck and J. Decourt). New York, Plenum Press: 191-211.

Frakes, L.A. (1979) *Climates Throughout Geologic Time.* Oxford, Elsevier.

Frakes, L.A. and Francis, J.E. (1988) A guide to Phranerozoic cold polar climates from high latitude ice rafting in the Cretaceous. *Nature* **333**: 547-549.

Frakes, L.A., Francis, J.E. and Syktus, J.I. (1992) *Climate modes of the Phanerozoic: the history of the earth's climate for the past 600 million years.* Cambridge, Cambridge University Press.

Francis, J.E. (1983) The dominant conifer of the Jurassic Purbeck Formation, England. *Palaeontology* **26**(2): 277-294.

Francis, J.E. (1984) The seasonal environment of the Purbeck (Upper Jurassic) fossil forests. *Palaeogeography, Palaeoclimatology, Palaeoecology* **48**: 485-307.

Frederiksen, N.O. (1980) Significance of monosulcate pollen abundance in Mesozoic sediments. *Lethia*, **13**, 1-20.

Gagan, M.K., Chivas, A.R. and Herczeg, A.L. (1990) Shelf-wide erosion, deposition and suspended sediment transport during cyclone Winifred, Central Great Barrier Reef, Australia. *Journal of Sedimentary Petrology*, **60** (30), 456-470.

Gallois, R.W. (1976) Coccolith blooms in the Kimmeridge Clay and origin of North Sea oil. *Nature* **259**: 473-475.

Gallois, R.W. and Medd, A.W. (1979) Coccolith rich marker bands in the English Kimmeridge Clay. *Geological Magazine* **116**: 247-260.

Garber, J.H. (1984) Laboratory study of nitrogen and phosphorus remineralization during the decomposition of coastal plankton and seston. *Estuarine, Coastal and Shelf Science*, **18**, 685-702.

Gastaldo, R.A., Bearce, S.C., Degges, C.W., Hunt, R.J., Peebles, M.W. and Violette, D.L. (1989) Biostratinomy of a Holocene oxbow lake: a backswamp to mid-channel transect. *Review of Palaeobotany and Palynology*, **58**, 47-59.

Glenn, C.R. and Arthur, M.A. (1985) Sedimentary and geochemical indicators of productivity and oxygen contents in modern and ancient basins: the Holocene Black Sea as the 'type' anoxic basin. *Chemical Geology*, **48**, 325-54.

Gitmez, G.U. and Sarjeant, W.A.S. (1972) Dinoflagellate cysts and acritarchs from the Kimmeridgian (Upper Jurassic) of England, Scotland and France. *Bulletin of the British Museum of Natural History*, 21; 171–257.

Goldberg, E.D. (1985) *Black Carbon in the Environment: Properties and Distribution*, Wiley, New York, 198 pp.

Goldstein, J.I., Newbury, D.E., Romig, A.D., Lyman, C.E., Echlin, P., Fiori, C., Joy, D.C. and Lifshin, E. (1992) *Scanning electron microscopy and x-ray microanalysis. A text for biologists, materials scientists and geologists.* London, Plenum Press.

Gorin, G. and Monteil, E. (1990) Preliminary note on organic facies of Lower to Middle Jurassic sediments in the Jura Mountains, Switzerland. *Review of Palaeobotany and Palynology*, **65**, 349-55.

Gorin, G. and Steffen, D. (1991) Organic facies as a tool for recording eustatic variations in marine fine-grained carbonates - example of the Berriasian stratotype at Berrias (Ardeche, SE France). *Palaeogeography, Palaeoclimatology, Palaeoecology*, **85**, 303-20.

Graff, G., Martens, V., Queisser, W., Weinholz, P. and Altenbach, A. (1988) A multicalorimeter for the srudy of biological activity in marine sediments. *Marine Ecology – Progress Series*, **45**: 201–204.

Griffin, J.J. and Goldberg, E.D. (1975) The fluxes of elemental carbon in coastal marine sediments. *Limnology and Oceanography*, **20**, 456-63.

Groot, J.J., Groot, C.R., Ewing, M., Burkle, L. and Conooly, J.R. (1967) Spores, pollen, diatoms and provenance of the Argentine Basin sediments. *Progress in Oceanography*, **4**, 179-217.

Habib, D. (1983) Sedimentation rate dependent distribution of organic matter in the North Atlantic Jurassic-Cretaceous, in *Initial Reports of the Deep Sea Drilling Project* (eds R.E. Sheridan, F.M. Gradstein et al.), U.S. Government Printing Office, Washington, DC, **76**, 781-94.

Hallam, A. (1967b) The depth significance of shales with bituminous laminae. *Marine Geology* **5**: 473-480.

Hallam, A. (1975) *Jurassic environments.* Cambridge, Cambridge University Press.

Hallam, A. (1984) Continental humid and arid zones during the Jurassic and Cretaceous. *Palaeogeography, Palaeoclimatology, Palaeoecology.* **47**: 195-223.

Hallam, A. (1985) A review of Mesozoic climates. *Journal of Geological Society, London.* **142**: 433-445.

Hallam, A. (1988) A re-evaluation of Jurassic eustasy in the light of new data and the revised Exxon curve, in *Sea level Changes: an integrated approach,* (eds C. K. Wilgus, B. S. Hastings, C. G. S. C. Kendallet al. Tusla) : 261-273.

Hallam, A. (1992) *Phanerozoic Sea Level Changes.* New York, Cambridge Univeristy Press.

Hallam, A. (1994) Jurassic climate as inferred from the sedimentary and fossil records, in *Palaeoclimates and their modelling: with special reference to the Mesozoic Era,* (eds J. R. L. Allen, B. J. Hoskins, B. W. Sellwood, R. A. Spicer and P. J. Valdes). London, Chapman & Hall: 79-88.

Hallam, A. (1996) Major Bio-events in the Triassic and Jurassic, in *Global events and event stratigraphy in the Phanerozoi,*. (ed O. H. Walliser). Berlin, Springer: 265-278.

Hallam, A. and Bradshaw, M.J. (1979) Bituminous shales and oolitic ironstones as indicators of transgressions and regressions. *Journal of the Geological Society, London* **136**: 157-164.

Hallam, A. and Sellwood, B.W. (1976) Middle Mesozoic sedimentation in relation to tectonics in the British Area. *Journal of Geology* **84**: 301-321.

Hamblin, W.M.K. (1962) X-ray radiography in the study of structures in lamogeneous sediments. *Journal of Sedimentary Petrology* **32**(2): 201-210.

Hancock, N. J. and Fisher, M. J. (1981) Middle Jurassic North Sea deltas with particular refernce to Yorkshire, in *Petroleum Geology of the Continental Shelf of North-West Europe* (eds L.V. Illing and G.D. Hobson), Heydon, London, pp. 186–95.

Haq, B.U., Hardenbol, J. and Vail, P.R. (1987) Chronology of fluctuating sea levels since the Triassic. *Science* **235**(4793): 1156-1166.

Haq, B.U., Hardernbol, J., Vail, P.R. and Baum, G.R. (1988) Mesozoic and Cenozoic chronostratigraphy and eustatic cycles, in *Sea level changes : an intergrated approac,* (eds C. K. Wilgus, B. S. Hastings, C. G. S. C. Kendallet al. Tusla), Society of Economic Paleontologists and Mineralogists Special Publication No. 42: 71-108.

Hargrave, B.T (1985) Particle sedimentation in the ocean. *Ecological Modelling*, **30**, 229-46.

Harmon, M.E., Franklin, J.K., Swanson, F.J., Sollins, P., Gregory, S.V., Lattin, J.D., Anderson, N.H., Cline, S.P., Aumen, N.G., Sedell, J.R., Lienlaemper, G.W., Cromack., F. Jr and Cummins, K.W. (1986) Ecology of coarse woody debris in temperate ecosystems. *Advances in Ecological Research*, **15**, 133-302.

Hart, M.B. and Fitzpatrick, M.E.J. (1995) Kimmeridgian Palaeoenvironments; A micropalaeontological perspective. *Proceedings of the Ussher Society* **8**(4): 433-436.

Harvey, G. R. and Lang, R. F. (1986) Dimethylsulfoxide and Dimethylsulpone in the marine atmosphere. *Geophysical Research Letters*, **13(1)**; 49-51

Havinga, A.J. (1964) Investigation into the differential corrosion susceptibility of pollen and spores. *Pollen et Spores*, **6**, 621-35.

Hay, B. and Honjo, S. (1989) Particle deposition in the present and Holocene Black Sea. *Oceanography* **2**(1): 26 - 31.

Hay, B.J. (1988) Sediment accumulation in central western Black Sea over the past 5000 years. *Paleoceanography*, **3**, 491-508.

Hay, B.J., Honjo, S., Kempe, S., Ittekkot, V.A., Degens, E.T., Konuk, T. and Izdar, E. (1990) Interannual variability in particle flux in south western Black Sea. *Deep Sea Research* **37**(6): 911-928.

Hedges, J.I. Clark, W.A. and Cowie, G.L. (1988) Organic matter sources to the water column and surfical sediments of a marine bay. *Limnology and Oceanography*, **33**, 1116-1136.

Henrichs, S.M and Reeburgh, W.S. (1987) Anaerobic mineralization of marine sediment organic matter: rates and the role of anaerobic processes in the oceanic carbon economy. *Geomicrobiology Journal*, **5**, 191-38.

Herbin, J.P. and Geyssant, J.R. (1993) "Ceintures organiques" au Kimmeridgien / Tithonien en Angleterre (Yorkshire, Dorset et en France, Boulannais). *C. R. Acad. Sci. Paris* **317**(2): 1309-1316.

Herbin, J.P., Muller, C., Geyssant, J.R., Melieres, F. and Penn, I.E. (1993) Variation of the distribution of organic matter within a transgressive system tract:- Kimmeridge Clay Formation (Jurassic), England. *in, AAPG Studies in Geology. Petroleum source rocks in stratigraphy framework.* (eds B.Katz and L.Pratt): 67-99

Herbrin, J.P., Fernanfez-Martinez, J.L., Geyssant, J.R., Albani, E.L., Deconinck, J.F., Proust, J.N., Colbeaux, J.P. and Vidier, J.P. (1995) Sequence stratigraphy of source rocks applied to the study of the Kimmeridgian/Tithonian in the north-west European shelf (Dorset/UK, Yorkshire/UK, Boulonnais/France). *Marine and Petroleum Geology* **12**(2): 177-194.

Heusser, L.E. (1983) Pollen distribution in the bottom sediments of the western North Atlantic Ocean. *Marine Micropalaeontology*, **8**, 77-88.

Heusser, L.E. (1988) Pollen distribution in marine sediments in the continental margin off northern California. *Marine Geology*, **80**, 131-47.

Heusser, L.E. and Balsam, W.L (1977) Pollen sedimentation in the northeast Pacific Ocean. *Quaternary Research*, 7, 45-62.

Heusser, L.E. and Balsam, W.L. (1985) Pollen sedimentation in the northwest Atlantic: effects of the Western Boundary Undercurrent. *Marine Geology*, **69**, 149-53.

Holligan, P.M (1989) Primary productivity in the shelf seas of north-west Europe. *Advances in Botanical Research*, **16**, 193-252.

Holligan, P. M., Violler, M., Harbour, PD. S., Camus, P. and Champagne-Philippe, M. (1983) Satellite and ship studies of coccolithophore production along side a continental shelf edge. *Nature* **304**: 339–342.

Holmes, P. L. (1994) The sorting of spores and pollen by water: experimental and field evidence, in *Sedimentation of Organic Particles,* (ed A. Traverse): 9–32.

Honjo, S. (1975) Dissolution of suspended coccoliths in the deep-sea water column and sedimentation of coccolith ooze. In *Dissolution of Deep-Sea Carbonates.* (eds. W. Silter, A.W.H. Be, and W.H. Berger). Cushman Foundation Foraminiferal Research Special Publication No. **13**, pp. 115-128.

Honjo, S. (1976) Coccoliths: Production, Transportation and Sedimentation. *Marine Micropalaeontology* **1**: 65-79.

Honjo, S. (1978) Sedimentation of materials in the Sargasso Sea at a 5367m deep station. *Journal of Marine Research*, **36(3)**, 469-92.

Honjo, S. and Roman, M.R. (1978) Marine copepod fecal pellets: production, preservation and sedimentation. *Journal of Marine Research*, **36(1)**, 45-57.

Honjo, S., Manganini, S. J., and Cole, J. J. (1982) Sedimentation of biogenic matter in the deep ocean. *Deep-Sea Research*, **29(5A)**; 609–625.

Hooghiemstra, H., Agwu, C.O.C. and Beug, H.J. (1986) Pollen and spore distribution in Recent marine sediments: a record of NW-African seasonal wind patterns and vegetation belts. *'Meteor' Forchungsergebnisse*, **C40**, 87-135.

House, M.R. (1989) *Geology of the Dorset coast.* London, Geologists' Association.

House, M.R. (1995) Orbital forcing timescales: an introduction, in *Orbital forcing timescales and cyclostratigraphy,* . (eds M. R. House and A. S. Gale). Oxford: 1-18.

Hughes, N.F. and Moddy-Stuart, J.C. (1967) Palynological facies and correlation in the English Wealden. *Review of Palaeobotany and Palynology*, **1**, 259-68.

Ioannides, N.S., Stavrinos, G.N. and Downie, C. (1976) Kimmeridgian microplankton from Clavell's Hard, Dorset, England. *Micropaleontology* **22**: 443-478.

Irwin, H. (1979) On an environmental model for the type Kimmeridge Clay. *Nature* **279**: 819.

Irwin, H. (1980) Early diagenetic carbonate precipitation and pore fluid migration in the Kimmeridge Clay of Dorset, England. *Sedimentology* **27**: 577-591.

Irwin, H. (1981) On calcic dolomite-ankerite from the Kimmeridge Clay. *Minerological Magazine* **44**: 105 - 107.

Irwin, H., Curtis, C. and Coleman, M. L. (1977) Isotopic evidence for source of diagenetic carbonates formed during burial of organic-rich sediments. *Nature*, **269**: 209–213.

Ittekot, V. and Arain, R. (1986) Nature of particulate organic matter in the River Indus, Pakistan. *Geochimica et Cosmochimica Acta*, **50**, 1643-53.

Ivanov, M.V., Lein, Y.U., Reeburgh, M.S. and Skyring, G.W. (1989) Interaction of sulphur and carbon cycles in marine sediments, in *Evolution of the Global Biogeochemical Sulphur Cycle* (eds P. Brimblecombe and Y.A. Lein), Wiley, Chichester, pp. 125-79.

Janofshe, D. (1996) Ultrastructure types in recent "calcispheres". *Bulletin de l'Institut Oceanographique (Monaco), Special Issue* **14(4)**, 295-303.

Joint, I.R., Pomroy, A.J., Savidge, G. and Boyd, P. (1993) Size fractionated primary production in the northeast Atlantic in May-June 1989. *Deep Sea Reasearch I*, **40**, 423-440.

Jorgensen, B.B. (1982b) Mineralization of organic matter in the sea bed - the role of sulphate reduction. *Nature*, **296**, 643-5.

Jorgensen, B.B. (1983a) The microbial sulphur cycle, in *Microbial Geochemistry* (ed W.E. Krumbein), Blackwell Scientific, Oxford, pp. 91-124.

Karl, D.M and Knauer, G.A. (1991) Microbial production in the upper 350m of Black Sea, in *Black Sea Oceanography: Results From the 1988 Black Sea Expedition, Deep-Sea Research*, **38** *Suppl. 2A*, S921-S942.

Kohlmeyer, J. and Kohlmeyer, E. (1979) *Marine Mycology, The Higher Fungi*, Academic Press, New York, 690 pp.

Knappertsbusch, M. and Brummer, G.J.A. (1995) A sediment trap investigation of sinking coccolithophorids in the North Atlantic. *Deep Sea Reasearch I*, **42**(7), 1083-1109.

Krassilov, V.A. (1981) Changes in Mesozoic vegetation and the extinction of dinosaurs. *Palaeogeography, Palaeoclimatology, Palaeoecology* **34**: 207-224.

Krinsley, D.H., Pye, K., Boggs, S. and Tovey, N.K. (1998) *Backscattered Scanning Electron Microscopy and Image Anaylsis of Sediments and Sedimentary Rocks*. Cambridge, Cambridge University Press.

Kristensen, E., Andersen, F.O. and Blackburn, T.H. (1992) Effects of benthic macrofauna and temperature on degradation of macroalgal detritus: the fate of organic carbon. *Limnology and Oceanography*, **37**, 1404-19.

Lallier-Verges, E., Bertrand, P., Huc, A.Y., Buckel, D. and Tremblay, P. (1993) Control of the preservation of organic matter productivity and sulphate reduction in Kimmeridgian shales from Dorset (UK). *Marine and Petroleum Geology* **10**: 600-605.

Lallier-Verges, E., Bertrand, P., Tribovillard, N.P. and Desprairies, A. (1995) Short term organic cyclicities from the Kimmeridge Clay Formation of Yorkshire: combined accumulation and degradation of organic carbon under control of primary production variations, in *Organic matter accumulation : the organic cyclcities of the Kimmeridge Clay Formation (Yorkshire, GB) and the recent Maar sediments (Lac du Bochet, France)*, (eds E. Lallier-Verges, N. P. Tribovillard and P. Bertrand). New York, Springer Publisher: 3-13.

Lallier-Verges, E., Hayes, I.M., Boussafir, M., Zabak, D.A., Tribovillard, N.P., Connan, J. and Bertrand, P. (1997) Productivity induced sulphur enrichment of hydrocarbon rich sediments from the Kimmeridge Clay Formation. *Chemical Geology* **134**: 277-288.

Lampitt, R.S (1996) Snow falls in the Open Ocean. In *Oceanography: An Illustrated Guide*. (eds C.P. Summerhayes and S.A. Thorpe). Manson Publishing, London, pp. 96-111.

Leckie, D.A., Singh, C., Goodarzi, F and Wall, J.H. (1990) Organic-rich, radioactive marine shale: a case study of a shallow-water condensed section, Cretaceous Shaftesbury Formation, Alberta, Canada. *Journal of Sedimentary Petrology*, **60**, 101-117.

Lee, C. (1992) Controls on organic carbon preservation: the use of stratified water bodies to compare intrinsic rates of decomposition in oxic and anoxic systems. *Geochimica et Cosmochimica Acta*, **56**, 33323-33335.

Leventhal, J. S. (1983) An interpretation of carbon and sulfur relationships in the Black Sea sediments as indicators of environments of deposition. *Geochimica et Cosmochimica Acta*, **47**: 133–137.

Lyons, T.W. (1991) Upper Holocene sediments of the Black Sea: Summary of Leg 4 Box cores (1988 Black Sea Oceanographic Expedition). *In: Black Sea Oceanography*. (eds E.Izdar and J.W.Murray), Kluwer, Boston, 401-441.

Lyons, T. W. and Berner, R. A. (1992) Carbon-sulphur-iron systematics of the uppermost deep-water sediments of the Black Sea. *Chemical Geology*, **99**: 1-27

MacIsacc, J. J. and Dugdale, R. C. (1972) Interactions of light and inorganic nitrogen in controlling nitrogen uptake in the sea. *Deep-Sea Research*, **19**: 209-232.

Macquaker, J.H.S. and Gawthorpe, R.L. (1993) Mudstone lithofacies in the Kimmeridge Clay Formation, Wessex Basin, Southern England: Implications for the origin and controls of the distribution of mudstones. *Journal of Sedimentary Petrology*. **63**(6): 1129-1143.

Macquaker, J.H.S., Curtis, C.D. and Coleman, M.L. (1997) The role of iron in mudstone diagenesis: comparison of Kimmeridge Clay Formation mudstones from onshore and offshore (UKCS) localities. *Journal of Sedimentary Research* **67**(5): 871-878.

Macquaker, J.H.S., Gawthorpe, R.L., Taylor, K.G. and Oates, M.J. (1998) Heterogeneity staching patterns and sequence stratigraphic interpretation in distal mudstone successions: examples from the Kimmeridge Clay Formation, U.K. *Shales and Mudstones*. J. Schieber, W. Zimmerle and P. Sethi. Stuttgart, Schuveizerbart Sche Verlagsbuchandlung: 163-186.

Mann, K.H. (1972) Macrophyte production and detritus food chains in coastal waters, in *Detritus and its Role in Aquatic Ecosystems* (eds U. Melchiorri-Santolini and J. W Hepton), Memorie Dell'Istituto Italiano di Idrobiologia, Supplement, **29**, 353-83.

McMahon, N.A. and Turner, J. (1998) The documentation of a latest Jurassic – earliest Cretaceous uplift throughout southern England and adjacent offshore areas, in *Development, Evolution and Petroleum Geology of the Wessex Basin*, (ed J. R. Underhill). Geological Society Special Publication No. **133**: 215–240.

Melia, M.B. (1984) The distribution and relationship between palynomorphs in aerosols and deep-sea sediments off the coast of northwest Africa. *Marine Geology*, **58**, 345-71.

Miller, R.G. (1990) A palaeoceanographic approach to the Kimmeridge Clay Formation, in *Deposition of organic facies*, (ed A. Y. Huc) : 13-27.

Moore, G.T., Hayashida, D.N., Ross, C.A. and Jacobson, S.R. (1992) Palaeoclimate of the Kimmeridgian/Tithonian (Late Jurassic) world:I. Results using a general circulation model. *Palaeogeography, Palaeoclimatology, Palaeoecology*. **93**: 113-150.

Moore, G.T., Barron, E.J. and Hayashida, D.N. (1995) Kimmeridgian (Late Jurassic) general lithostratigraphy and source rock quality for the Western Tethys Sea inferred from palaeoclimatie results using a general circulation model, in *Palaeogeography, palaeoclimate and source rocks*, (ed A. Y. Huc). Oklahoma, AAPG: pp347

Mudie, P.J. (1982) Pollen distribution in Recent marine sediments, eastern Canada. *Canadian Journal of Earth Sciences*, **19**, 729-47.

Muir, M.D. (1964) *The Palaeoecology of the Small Spores of the Middle Jurassic of Yorkshire.* Unpublished PhD Thesis, University of London, 234 pp. Cited from Tyson, 1995.

Muller, J. (1959) Palynology of Recent Orinoco Delta and shelf sediments. *Micropaleontology*, **5**: 1–32.

Muramoto, J.A., Honjo, S., Fry, B., Hay, B.J., Howarth, R.W and Cisne, L. (1991) Sulfur, iron and organic carbon fluxes in the Black Sea: sulfur isotopic evidence for origin of sulfur fluxes, in *Black Sea Oceanography: Results From the 1988 Black Sea Expedition* (ed. J.W. Murray), *Deep-Sea Research*, **38**, *Suppl. 2A*, S1151-87.

Myers, K. and Wignall, P. (1987) Understanding Jurassic organic-rich mudrocks - New concepts using gamma-ray spectrometry and palaeoecology: Examples from the Kimmeridge Clay of Dorset and the Jet Rock of Yorkshire. *Marine Clastic Sedimentology*. J. K. Leggett and G. G. Zuffa: 172-189.

Naiman, R.J. (1982) Characteristics of sediment and organic carbon export from pristine boreal forest watersheds. *Canadian Journal of Fisheries and Aquatic Sciences*, **39**, 1699-718.

Newell, R.C., Lucas, M.I. and Linley, E.A.S. (1981) Rate of degradation and efficency of conversion of phytoplankton debris by marine microrganisms. *Marine Ecology Progress Series*, **6**, 123-36.

Newell, A. J. (2000) Fault activity abd sedimentation in a marine rift basin (Upper Jurassic, Wessex Basin, UK). *Journal of the Geological Society of London*, **157**: 83–92.

Nohr-Hansen, H. (1989) Visual and chemical kerogen analysis of the Lower Kimmeridge Clay, Westbury, England. *North West European Micropalaeontology and Palynology*. D. J. Batten and M. C. Kean. Chichester, Ellis Harwood Ltd: 118-134.

Noji, T.T. (1991) The influence of macrozooplankton on vertical flux. *Sarisa*, **76**, 1-9.

Opdyke, N.D. and Runcorn, S.K. (1960) Wind direction in the western United States in the Late Paleozoic. *Bulletin of the Geological Society of America* **71**: 959-972.

Oschmann, W. (1988a) Upper Kimmeridgian and Portlandian marine macrobenthic associations from southern England and northern France. *Facies* **18**: 49-82.

Oschmann, W. (1988b) Kimmeridge Clay sedimentation - A new cyclic model. *Palaeogeography, Palaeoclimatology, Palaeoecology* **65**: 217-251.

Oschmann, W. (1990) Environmental cycles in the late Jurassic northwest European epeiric basin: interaction with atmospheric and hydrospheric circulations. *Journal of Sedimentary Geology* **69**: 313-332.

Oschmann, W. (1993) Environmental oxygen fluctuations and the adaptive response of marine benthic organisms. *Journal of the Geological Society, London* **150**: 187-191.

Oschmann, W. (1994) Adaptive pathways of benthic organisms in marine oxygen controlled environments. *Neues Jahrbuch fur Geologie und Palaontogie Abhandlungen* **191**(3): 393-444.

Paasche, E. (1962) Coccolith formation, *Nature*, **193**, 1094-1095.

Paasche, E. (1968) Biology and physiology of coccolithophores. *Annual Review of Microbiology*, **22**, 71-86.

Parrish, J.T. and Curtis, R.L. (1982) Atmospheric circulation, upwelling, and organic-rich rocks in the Mesozoic and Cenozoic eras. *Palaeogeography, Palaeoclimatology, Palaeoecology* **40**: 3-66.

Parrish, J.T., Zeigler, A.M. and Scotese, C.R. (1982) Rainfall patterns and the distribution of coals and evaporites in the Mesozoic and Cenozoic. *Palaeogeography, Palaeoclimatology, Palaeoecology*. **40**: 67-101.

Parry, C. C., Whitley, P. K. J. and Simpson, R. D. H. (1981) Integration of palynological and sedimentological methods in facies analysis of the Brent Formation, in *Petroleum Geology of the Continental Shelf of North West Europe* (eds L. V. Illing and G. D. Hobson), Heyden, London: 205–15.

Patterson, W.A. III, Edwards, K.J. and Maguire, D.J. (1987) Microscopic charcoal as a fossil indicator of fire. *Quaternary Science Reviews*, **6**, 3-23.

Patterson, W.P. (1999) Oldest isotopically characterized fish otoliths provide insight to Jurassic continental climate of Europe. *Geology*, **27(3):** 193–288.

Pedersen, T.F. and Calvert, S.E. (1990) Anoxia vs. productivity: What controls the formation of organic-carbon-rich sediments and sedimentary rocks. *AAPG Bulletin* **74**(4): 454-466.

Peinert, R., von Bodungen, B. and Smetacek, V. (1989) Food web structure and loss rates, in *Productivity of the Ocean: Present and Past.* (eds W. Berger, V. Smetacek and G. Wefer), Wiley, New York. pp. 34-48.

Pelet, R. (1983) Preservation and alteration of present-day sedimentary organic matter, in *Advances in Organic Geochemistry 1981* (eds M. Bjojroy *et al.*), Wiley, Chichester, pp.241-50.

Penn, I. E., Chadwick, R. A., Holloway, S., Roberts, G., Pharaoh, T. C., Allsop, J. M., Hulbert, A. G. and Burns, I. M. (1987) Principle features of the hydrocarbon prospectivity of the Wessex Channel Basin, UK, in *Petroleum Geology of North West Europe* (ed J. Brooks and K. W. Glennie), London. : 109–118.

Philippe, H., Sorhannus, U., Baroin, A., Perasso, R., Gasse, F. and Adoutte, A. (1994) Comparison of molecular and palentological date in diatoms suggests a major gap in the fossil record. *Journal of Evolutionary Biology* 7: 247 - 265.

Piasecki, S., Christiansen, F.G. and Stemmerik, L. (1990) Depositional history of an Upper Carboniferous organic-rich lacustrine shale from East Greenland. *Bullentin of Canadian Petroleum Geology*, **38**, 273-87.

Piasecki, S. and Stemmerik, L. (1991) Late Permian anoxia in East Greenland, in *Modern and Ancient Continental Shelf Anoxia* (eds R.V. Tyson and T.H. Pearson), *Geological Society of London Special Publication*, **58**, 275-90.

Pike, J. and Kemp, A.E.S. (1996) Silt aggregates in laminated marine sediment produced by agglutinated foraminifera. *Journal of Sedimentary Research* **66**(3): 625- 631.

Pilskaln, C.H. and Pike, J. in Press. Holocene sedimentary laminae formation in the Black Sea and the role of the "Fluff" layer. Submitted to *Palaeoceanography*.

Pinet, P.R. (2000) *Invitation to Oceanography*, 2nd edition, London, pp555.

Pocock, S.J. and Jansonius, J. (1961) The pollen genus Classopollis Pflug, 1953. *Micropaleontology* **7**: 439-449.

Prauss, M. and Riegel, W. (1989) Evidence from phytoplankton associations for causes of black shale formation in epicontinetal seas. *Neues Jahrbuck fur Geologie und Palaontologie* **11**: 67 682.

Price, G.D., Sellwood, B.W. and Valdes, P.J. (1995) Sedimentological evidence of general circulation model simulations for the "greenhouse" Earth: Cretaceous and Jurassic case studies. *Sedimentary Geology* **100**: 159-180.

Prospero, J. M., Savoie, D. L., Saltzman, E.S. and Larsen, R. (1991) Impact of oceanic sources of biogenic sulphur and sulphate aerosol concentration at Mawson, Anatartica. *Nature*, **350**: 221–223.

Purdie, D.A. (1996) Marine phytoplankton blooms. In *Oceanography: An Illustrated Guide*. (eds C.P. Summerhayes and S.A. Thorpe). Manson Publishing, London, pp. 89-95

Raiswell, R. (1987) Chemical model for the origin of minor limestone - shale cycles by anaerobic methane oxidation. *Geology* **16**: 641-644.

Ramanampisoa, L. and Disnar, J.R. (1994) Primary control of palaeoproduction on organic matter preservation and accumulation in the Kimmeridgian rocks of Yorkshire, UK. *Organic Geochemistry* **21**: 1153-1167.

Rayner, A.D.M. and Boddy, L. (1988) *Fungal Decomposition of Wood; Its Biology and Ecology*, Wiley, Chichester, 587 pp.

Reynolds, C.S., White, M.L., Clarke, R.T. and Marker, A.F. (1990) Suspension and sinking of particles in flowing water; comparison of the effect of varying water depth and velocity in circulating channels. *Freshwater Biology*, **24**, 23-34.

Reynolds, S. and Gorslin, D. S (1992) Clay microfabric of deep sea, detrital mudstones, California Continental Borderland. *Journal of Sedimentary Petrology*, **62(1):** 41–53.

Reyre, Y. (1973) Palynologie du Mesozoique Saharien. Traitment des donnes par l'Informatique et applications a la Stratigraphie et a la Sedimentologie. *Memoires du Museum National d'Histoire Naturelle*, Paris, **C27**, 284 pp.

Riding, J.B. and Thomas, J.E. (1988) Dinoflagellate cyst stratigraphy of the Kimmeridge Clay (Upper Jurassic) from the Dorset coast, southern England. *Palynology* **12**: 65-88.

Rudnick, D.T. and Oviatt, C.A. (1986) Seasonal lags between organic carbon deposition and mineralization in marine sediments. *Journal of Marine Research*, **44**, 815-37.

Saelen, G., Tyson, R.V., Talbot, M.R. and Telnaes, N. (1998) Evidence of recycling of isotopically light CO_2 (aq) in stratified black shale basins: contrast between the WhitbyMudstone and the Kimmeridge Clay Formation, U.K. *Geology* **26**(8): 747-750.

Sarjeant, W.A.S., Lacalli, T., and Gaines, G. (1987) The cysts and skeletal elements of dinoflagellates; speculations on the ecological causes for their morphology and development. *Micropaleotology*, **33**, 1-36.

Savrda, C.E., Bottjer, D.J. and Gorsline, D.S. (1984) Development of a comprehensive oxygen-deficient marine biofacies model: evidence from Santa Monica, San Pedro, and Santa Barbara Basins, California Continental Borderland. *American Association of Petroleum Geologists Bulletin*, **68**, 1179-92.

Scotchman, I.C. (1987) Clay diagenesis in the Kimmeridge Clay Formation, onshore UK, and its relation to organic maturation. *Mineralogical Magazine* **51**: 535-551.

Scotchman, I.C. (1989) Diagenesis of the Kimmeridge Clay Formation, onshore UK. *Journal of the Geological Society of London* **146**: 285-303.

Scotchman, I.C. (1991) Kerogen facies and maturity of Kimmeridge Clay Formation in southern and eastern England. *Marine Petroleum Geology* **8**: 278-295.

Scotese, C.R. (1991) Jurassic and Creataceous plate tectonic reconstructions. *Palaeogeography, Palaeoclimatology, Palaeoecology* **87**: 493-501.

Sellwood, B.W. and Price, G.D. (1994) Sedimentary facies as indicators of Mesozoic palaeoclimate. *Palaeoclimates and their modelling: with special reference to the Mesozoic era.* J. R. L. Allen, B. J. Hoskins, B. W. Sellwood, R. A. Spicer and P. J. Valdes. London, Chapman & Hall.: 17-25.

Sellwood, B.W. and Valdes, P.J. (1997) Geological evaluation of climate General Circulation Models and model implications for Mesozoic cloud cover. *Terra Nova* **19**(2): 75-78.

Shaw, H.F. and Primmer, T.J. (1991) Diagenesis of mudrocks from the Kimmeridge Clay Formation of the Brae Area, UK North Sea. *Marine Petroluem Geology* **8**: 271-277.

Shotton, F.W. (1937) The Lower Bunter Sandstone of North Worcestershire and East Shropshire. *Geological Magazine* **74**: 534-553.

Silverberg, N., Edenborn, H.M. and Belzile, N. (1985) Sediment response to seasonal variations in organic matter input, in *Marine and Estuarine Geochemistry* (eds A.C. Sigleo and A. Hattori), Lewis, Chelsea (Michigan), 69-80.

Sladen, C.P. and Batten, D.J. (1980) Source-area environments of Late Jurassic and Early Cretaceous sediments in Southeast England. *Proceedings of the Geological Association.* **95**: 149-163.

Smith, D.M., Griffin, J.J. and Golberg, E.D. (1973) Elemental carbon in marine sediments: a baseline for burning. *Nature*, *241*, 268-70.

Snedden, J.W., Nummedal, D. and Amos, A.F. (1986) Storm- and fair weather combined flow on the central Texas continental shelf. *Journal of Sedimentary Petrology*, **58**, 580-595.

Soutar, A. and Crill, P.A. (1977) Sedimentation and climatic patterns in the Sanata Barabara basin during the 19th and 20th centuries. *Geol. Soc. of America Bulletin* **88**: 1161-1172.

Soutar, A., Johnson, S.R. and Baumgartner, T.R. (1981) In search of modern analoges to the Monterey Formation, in *The Monterey Formation and Related Siliceous Rocks of California* (eds R.E Garrison and R.G. Douglas), Pacific Section, Society of Economic Mineralogists and Paleontologists, Los Angeles, pp. 123-47.

Srivastava, S.K. (1976) The fossil pollen genus Classopollis. *Lethaia* **9**: 437-457.

Stancliffe, R.P.W. (1989) Microforaminiferal linings: Their classification, biostratigraphy and palaeoecology, with special reference to specimens from British Oxfordian sediments. *Micropaleontology* **35**: 337-352.

Steinmetz, J.C. (1994) Sedimentation of coccolithophores, in *Coccolithophores*, (eds A. Winter and W. G. Siesser). Cambridge, Cambridge University Press: 179-197.

Stockmarr, J. (1971) Tablets with spores used in absolute pollen analysis. *Pollen et Spores* **13**(4): 615-621.

Stover, L.E., *et al.*, (1996) Mesozoic - Tertiary dinoflagellates, acritarchs and prasinophytes. *Palynology : Principles and appliactions*. J. Jansonius and D. C. McGregor. Salt Lake City, Utah, Publishers press. **2:** 641-750.

Summerhayes, C.P. and Marsan, T.H. (1983) Organic facies of Cretaceous and Jurassic sediments from DSDP site 534 in the Blake Bahama Basin, western North Atlantic, in *Initial Reports of the Deep Sea Drilling Project* (eds R.E. Sheridan, F. Gradstein et al.), YS Government Printing Office, Washington, DC, **76**, 469-80.

Swift, D.J.P. and Nummedal, D. (1987) Hummocky cross-stratification, tropical hurricans and intense winter storms: discussion. *Sedimentology*, **34**, 338-344.

Tappan, H. (1980) *The Paleobiology of Plant Protists*, Freeman, San Francisco, 1028 pp.

Tarutis, W.J.Jr (1992) Temperature dependence of rate constants derived from the power model of organic matter decomposition. *Geochimica et Cosmochimica Acta*, **56**, 1387-90.

Taylor, F.J.R. (1987) Ecology of dinoflagellates: A General and marine ecosystems, in *The Biology of Dinoflagellates* (ed. F.J.R. Taylor), *Botanical Monographs*, **21**, 399-502

Tillman, U. and Hesse, K.J. (1998) On the quantitative importance of heterotrophic microplankton in the Northern German Wadden Sea. *Estuaries*, **21**(4A), 585-596.

Toth, D.J. and Lerman, A. (1977) Organic matter reactivity and sedimentation rates in the ocean. *American Journal of Science*, **277**, 465-85.

Traverse, A. (1988) *Paleopalynology*. London, Unwin Hyman.

Traverse, A. (1994) *Sedimentation of Organic Particles*. Cambridge, Cambridge University Press.

Traverse, A. and Ginsburg, R.N. (1966) Palynology of the surface sediments of Great Bahama Bank, as related to water movement and sedimentation. Marine Geology, 4, 417-59.

Tribovillard, N.P., Desprairies, A., Lallier-Verges, E., Bertrand, P., Moureau, N., Ramdani, A. and Ramanampisoa, L. (1994) Geochemical study of organic matter rich cycles from the Kimmeridge Clay Formation of Yorkshire (UK): productivity versus anoxia. *Palaeogeography, Palaeoclimatology, Palaeoecology* **108**: 165-181.

Turley, C.M. and Lochte, K. (1990) Microbial responses to the input of fresh detritus to the deep-sea bed. *Palaeogeography, Palaeoclimatology, Palaeoecology (Global and Planetary Change Section)*, **89**, 3-23.

Tyson, R.V. (1984) Palynofacies investigation of Callovian (Middle Jurassic) sediments from DSDP site 534, Blake-Bahama Basin, western Central Atlantic. *Marine and Petroleum Geology*, **1**, 3-13.

Tyson, R.V. (1985) *Palynofacies and sedimentology of some Late Jurassic sediments from the British Isles and northern North Sea.* Unpublished PhD thesis, The Open University, Milton Keynes, 623 pp. Cited in Tyson 1995.

Tyson, R.V. (1987) The genesis and palynofacies characteristics of marine petroleum source rocks, in *Marine petroleum source rocks,* (eds J. Brooks and A. J. Fleet). London, Blackwell Scientific: 47-67.

Tyson, R.V. (1989) Late Jurassic palynofacies trends, Piper and Kimmeridge Clay formations, U.K. onshore and northern North Sea, in *Northwest European Micropalaeontology and Palynology*, (eds D. J. Batten and M. C. Keen). Chichester, Ellis Harwood Ltd: 135-172.

Tyson, R.V. (1995). *Sedimentary Organic Matter*. London, Chapman & Hall. pp 615.

Tyson, R.V. (1996) Sequence stratigraphical interpretation of organic facies variations in marine siliclastic systems: general principles and applications to onshore Kimmeridge Clay Formation, UK, in *Sequence stratigraphy in British geology*, (eds S. P. Hesselbo and D. N. Parkinson) : 75-96.

Tyson, R.V. and Pearson, T.H. (1991). *Modern and ancient continental shelf anoxia*. Geological Society of London Special Publication No. 58. Pp 470.

Tyson, R.V., Wilson, R.C.L. and Downie, C. (1979) A stratified water column environmental model for the type Kimmeridge Clay. *Nature* **277**: 377-380.

Vail, P.R., Hardenbol, J. and Todd, R.G. (1984) Jurassic unconformities, chronostratigraphy and sea level changes from seismic stratigraphy and biostratigraphy. *American Association of Petroleum Gelogists Memoir* **36**: 129-144.

Vail, P.R. and Todd, R.G. (1981). Northern North Sea Jurassic unconformities, chronostratigraphy and sea level changes from seismic stratigraphy. *Petroleum Geology of the continental shelf of north-west Europe*. L. V. Illing and G. Hobson. London: 216-235.

Vairavamurthy, A., Andreae, M.O. and Iverson, R.L. (1985) Biosynthesis of dimethylsulfide and dimethylpropiothetm by *Hymenomonas corterae* in relation to sulfur source and salinity variations. *Limnology and Oceanography*, **30**, 59-70

Vakhrameev, V.A. (1964) Jurassic and Early Cretaceous floras of Eurasia and the palaeoflorissic provinces of this period. *Trans. geol. Inst. Moscow* **102**: 1-263 (In Russian).

Vakhrameev, V.A. (1981) Pollen Classopollis, indicator of Jurassic and Cretaceous climates. *Palaeobotanist.* **28**: 301-307.

Vakhrameev, V.A. (1991) *Jurassic and Cretaceous floras and climates of the Earth*. Cambridge, Cambridge University Press.

Valdes, P.J. (1994) Atmospheric general circulation models of the Jurassic, in *Palaeoclimates and thier modelling: with special reference to the Mesozoic era.* (eds J.R.L.Allen, B.J.Hoskins, B.W.Sellwood, R.A.Spicer and P.J.Valdes). London, Chapman & Hall: 109-118.

Valdes, P.J. and Sellwood, B.W. (1992) A palaeoclimate model for the Kimmeridgian. *Palaeogeography, Palaeoclimatology, Palaeoecology*. **95**: 47-72.

Van Kaam-Peters, H.M.E., Schouten, S., Koster, J. and Damste, J.S.S. (1998) Controls on the molecular and carbon isotopic composition of organic matter deposited in a Kimmeridgian euxinic shelf sea: Evidence for preservation of carbohydrates through sulfurisation. *Geochimica et Cosmochimica Acta*. **62**(19/20): 3259-3283.

Van Waveren, I.M. (1989a) Pattern analysis of organic component abundances from deltaic and open marine deposits: palynofacies distribution (East Java, Indonesia). *Netherlands Journal of Sea Research*, **23**, 441-7.

Voss, K.J., Balch, W.M. and Kilpatrick, K.A. (1998) Scattering and attenuation properties of Emiliania huxleyi cells and their detached coccoliths. *Limnology and Oceanography*, **43(5)**, 870-876.

Walker, G.B. and Walker, G. (1976) Upper Jurassic pyroclastic rocks in Skye, west Scotland. *Nature* **265**: 323 - 324..

Wall, D. and Dale, B (1974) Dinoflagellates in late Quaternary deep-water sediments of Black Sea, in The Black Sea - Geology, Chemistry and Biology, (eds E.T. Degens and D.A. Ross), *American Association of Petroleum Geologist Memoir*, **20**, 364-80.

Wallace, J.B., Ross, D.H. and Meyer, J.L. (1982) Seston and dissolved organic carbon dynamics in a southern Appalachain stream. *Ecology*, **63**, 824-38.

Wassmann, P. (1998) Rentention versus export food chains: processes controlling sinking loss from marine pelagic systems. *Hydrobiologia*, **363**, 85-109.

Wassmann, P. and Slagstad, D. (1993) Seasonal and interannual dynamics of carbon flux in the Barents Sea: a model approach. *Polar Research*, **13**, 363-372.

Waterhouse, H.K. (1992). Quantitative palynofacies analysis of Jurassic climate cycles. *PhD Thesis, Department of Geology*. Southampton, University of Southampton.

Waterhouse, H.K., (1995) High resolution palynofacies investigation of Kimmeridgian sedimentary cycles. *Orbital forcing timescales and cyclostratigraphy*. M. R. House and A. S. Gale. London, Geological Society of London.

Waterhouse, H.K. (1999) Orbital forcing of palynofacies in the Jurassic of France and the United Kingdom. *Geology* **27**(6): 511-514.

Weedon, G.P., Jenkyns, H.C., Coe, A.L. and Hesselbo, S.P. (1999) Astronomical calibration of the Jurassic time-scale from cyclostratigraphy in British mudrock formations. *Phil. Trans. R. Soc. London, A.* **357**: 1787-1813.

Wells, J.T., Park, Y.A. and Choi, J.H. (1985) Strom-induced fine sedimenta transport, west coast of South Korea. *Geomarine Letters*, **4**, 177-180.

Whitaker, M.F. (1984) The usage of palynology in definition of Troll Field geology, in *Reduction of Uncertainities in Innivative Reservoir Geomodelling*, 6th Offshore Northern Seas Conference and Exhibition, Stavanger 1984, Norsk Petroleumsforening, Paper G6, 44 pp.

Wignall, P.B. (1989) Sedimentary dynamics of the Kimmeridge Clay: tempests and earthquakes. *Journal of the Geological Society, London* **146**: 273-284.

Wignall, P.B. (1990) *Benthic palaecology of the Late Jurassic Kimmeridge Clay of England*, The Palaeontological Association.

Wignall, P.B. (1991) Model for transgressive black shales? *Geology* **19**: 167-170.

Wignall, P.B. (1991) Test of the concepts of sequence stratigraphy in the Kimmeridgian (Late Jurassic) of England and northern France. *Marine and Petroleum Geology* **8**: 430-441.

Wignall, P.B. (1994) *Black Shales*. New York, Claredon Press.

Wignall, P.B. and Hallam, A. (1991) Biofacies, stratigraphic distribution and depositional models of British onshore Jurassic black shales, in *Modern and ancient continental shelf anoxia*. (eds R. V. Tyson and T. H. Pearson) : 291-309.

Wignall, P.B. and Newton, R. (1998) Pyrite framboid diameter as a measure of oxygen deficiency in ancient mudrocks. *American Journal of Science* **298**: 537-552.

Wignall, P.B. and Ruffell, A.H. (1990) The influence of a sudden climatic change on marine deposition in the Kimmeridgian of northwestern Europe. *Journal of the Geological Society, London* **147**: 365-371.

Wilkin, R.T., Barnes, H.L. and Brantley, S.L. (1996) The size distribution of framboidal pyrite in modern sediments: An indicator of redox conditions. *Geochimica et Cosmochimica Acta* **60**(20): 3897-3912.

Wilkin, R.T., Arthur, M.A. and Dean, W.E. (1997) History of water-column anoxia in the Black Sea indicated by pyrite framboid size distributions. *Earth and Planetary Science Letters*, **148**, 517-525.

Williams, P.F.V. (1986) Petroleum geochemistry of the Kimmeridge Clay onshore southern and eastern England. *Marine and Petroleum Geology* **3**: 258-281.

Williams, G.L. (1992) Palynology as a palaeoenvironmental indicator in the Brent Group, northern North Sea, in Geology of the Brent Group (eds A.C. Morton, R.S. Haszeldine, M.R. Giles and S. Brown), *Geological Society of London Special Publication*, **61**, 203-12.

Winter, A., Reiss, Z. and Luz, B. (1979) Distribution of living coccolithophore assemblages in the Gulf of Elat (Aquaba). *Marine Micropalaeontology*, **4** : 197-223.

Wishner, K., Levin, L., Gowing, M. and Mullineaux, L. (1990) Involvement of the oxygen minimum in benthic zonation on a deep seamount. *Nature*, **346**, 57-9.

Young, J. R. (1994) Functions of coccoliths, in *Coccolithophores*, (eds A. Winter and W, G. Siesser) Cambridge University Press : 63–82.

Ziegler, A.M., Parrish, J.M., Jiping, Y., Gyllenhaal, E.D., Rowley, D.B., Parrish, J.T., Shangyou, N., Bekher, A. and Hulver, M.L. (1994) Early Mesozoic phytogeography and climate, in *Paleoclimates and thier modelling: with special refernce to the Mesozoic era.* (eds J. R. L. Allen, B. J. Hoskins, B. W. Sellwood, R. A. Spicer and P. J. Valdes). London, Chapman & Hall.: 89-97.

Ziegler, P.A. (1978) Northwestern Europe: tectonics and basin development. *Geol. Mijnbouw* **57**: 598-626.

SOUTHAMPTON UNIVERSITY LIBRARY

USER'S DECLARATION

AUTHOR: PEARSON, SARAH JANE TITLE: HIGH-RESOLUTION ENVIRONMENTAL CHANGE IN THE LATE JURASSIC KIMMERIDGE CLAY FORMATION

DATE: 2000

I undertake not to reproduce this thesis, or any substantial portion of it, or to quote extensively from it without first obtaining the permission, in writing, of the Librarian of the University of Southampton.

To be signed by each user of this thesis

DATE	SIGNATURE	ADDRESS